SEDIMENTARY ENVIRONMENTS FROM WIRELINE LOGS

O. SERRA

Text reviewed by **M. Bett, J.R. Desparmet, R.L. Langley** and **B.F. Mair.**

with the contribution of examples from Schlumberger's geologists :

J.R. Desparmet, A. de La Cruz, S. Jorgensen, J. Loiseau, S. Luthi, B.F. Mair, R. Nurmi, T. Pilenko, G. Pirie, K. Saito, J. Vasquez, R. Widdicombe.

TABLE OF CONTENTS

* Mark of Schlumberger

Chapter 1

INTRODUCTION

Our modern society has a constant need for raw materials and energy. An on-going effort in exploration and research is necessary, therefore, to discover and develop them. And, in this effort, it is better to appeal to geology than to rely on chance.

Geology is by definition *"the study of the planet Earth. It is concerned with the origin of the planet, the material and morphology of the Earth, and its history and the processes that acted (and act) upon it to affect its historic and present forms"* (Glossary of Geology, 1980).

This study, even when it includes fundamental research, is aimed at a better understanding of the influences that have formed, transformed and modelled our planet, of the laws ruling the formation of rocks, their distribution, their transformation, their deformation, and of the laws governing the accumulation of those raw materials which are of economic interest. This scientific guidance is available to help us discover the low cost minerals and energy resources that humanity needs so much.

The work of the geologist (Table 1-1) consists of :

- the complete and objective observation and description of rocks and geological phenomena;
- the interpretation of these observations by comparing them with :
  . those made on recent series or phenomena (existing models),
  . those coming from the study of reconstructed models or from laboratory experiments,
  . observations made on ancient formations which have been studied in detail and are well understood (ancient models and application of theories of *actualism* or *uniformitarianism* as developed by Hutton, 1788).

In the case of the study of sedimentary rocks, this interpretation must lead to a reconstitution of

Table 1-1
A general approach for the analysis of sedimentary rocks.

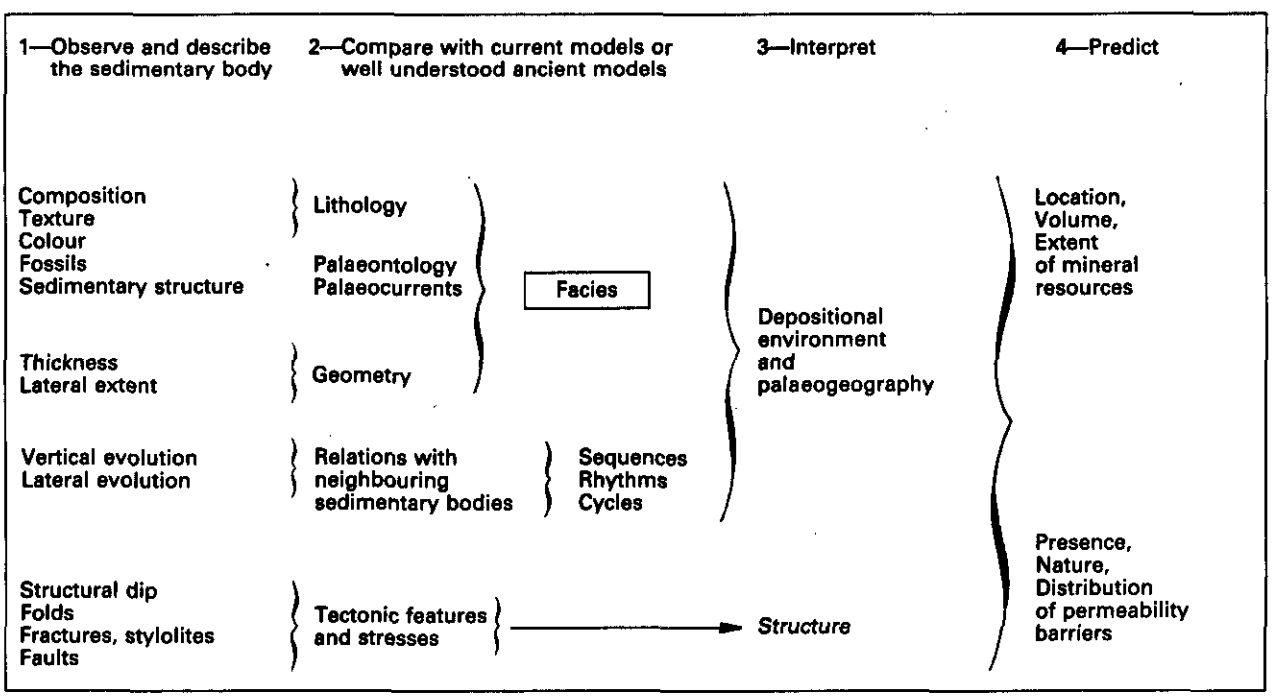

the geographic and climatic frame and, consequently, to the understanding of conditions under which the rocks are formed. From this reconstitution the geologist will try :

- to predict those zones most favourable for the accumulation of mineral resources,
- to specify the extent of the resources,
- to evaluate their volume from the estimation of the content of these mineral resources in rocks.

ORIGIN OF GEOLOGICAL DATA

To proceed with study and research, the geologist utilises three sources of information.

Outcrops (Quarries, trenches, ditches, tunnels, mines)

In certain types of research, natural or man-made outcrops are still the essential source of geological information (Fig. 1-1); in others (petroleum, coal, geothermal resources) outcrop information has been progressively replaced by drilling data or completed by surface geophysics (gravimetry, seismic surveying, magnetism), or borehole geophysics (well logging).

Fig. 1-1. - Photograph of an outcrop in Peira-Cava, South of France, showing several sequences of massive sandstones interbedded with laminated shales, in a deep marine environment (photograph taken by Serra).

This is because in modern exploration, drilling and geophysical techniques are more often used, not only in the petroleum industry, but also in subsurface storage, or to discover coal, uranium or metallic minerals, and in geothermal resources. With deeper targets, outcrops, as a source of information, are less frequently used because extrapolations established from them are less reliable. Moreover, the geological complexity of targets increases (stratigraphic traps,, fluid permeabilit ybarriers, size and depth of structures, ...).

As a result, at the present time, most knowledge concerning geological sedimentary basins (especially deep basins) comes from drilling and geophysics. As stated by Illing (1946) "... if geology has contributed greatly to the growth of the oil industry the debt is not a one-sided one. Geology owes a great deal to the oil industry in the expansion of its knowledge and the increased efficiency of its methods ...".

Surface Geophysics

Two and often three dimensional pictures of subsurface can be obtained by today's surface geophysical techniques. They are extremely important tools for the exploration of subsurface, since it gives direct information, not only on the shape and arrangement of beds, but also on their nature, their petrophysical properties and even sometimes their fluid content (seismofacies, "bright spot", ...). The hypotheses drawn by the interpretation of this information must be verified by drilling. The translation of surface geophysical data into a geological interpretation will be considerably easier and more reliable if it is supported by well log measurements. The former has thus to be correlated with the latter. In other words, wireline log data provide the link between geophysics and geology :

- *wireline logs are the only means for providing an accurate transfer of time data to depth data. They allow for the transfer of amplitude and signal frequency data to sedimentological or economic data (facies, porosity, fluid content, ...).*

In fact, measurements of the density and the travel-time of acoustic sound derived from boreholes with well logging tools, make it possible, after corrections, to determine the accurate acoustic impedence and reflection coefficient for each boundary in formations. A reflectivity log made from acoustic and density data provides a basic document for the establishment of a theoretical seismic section through the GEOGRAM *, program, which, when correlated with real seismic

* Mark of Schlumberger.

sections, permits its conversion into depth and makes a composite log possible.

The Vertical Seismic Profile (VSP) obtained in a well provides the best vision and exact depth of each reflector, its signature and the effect over the underlying reflectors. It enables the transformation to be made from reflectors to beds, providing a precise measurement to go from depth to time and vice versa. For example, it is possible to « see" the beds which underlie formations with strong reflectance (anhydrite, halite, compact dolomite or limestone), or with strong attenuation (undercompacted shales), or formations below the bottom well depth. It also makes it possible to remove the multiples that often complicate the interpretation of seismic sections. VSP can also be used to analyse the rock properties through the study of seismic waves (Direct Signal Analysis DSA * method).

A graphic display of logs versus time instead of depth can also be easily obtained and reproduced alongside VSP and GEOGRAM (Fig. 1-2).

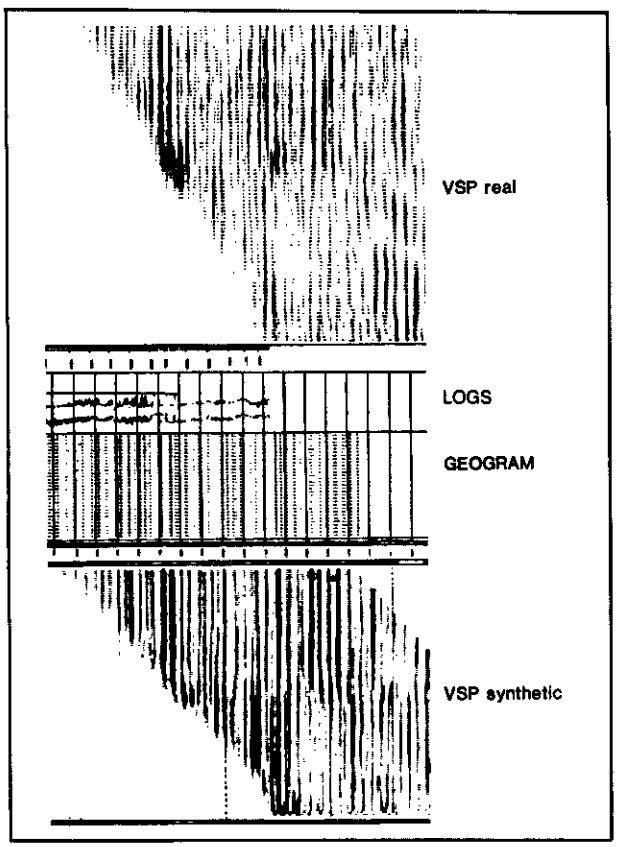

Fig. 1-2. - Composite display of the different geophysical answer products; the logs, in time scale, are reproduced on the side of the GEOGRAM. VSP and synthetic VSP are also shown alongside (from Mons & Babour, 1981).

* Mark of Schlumberger.

Drilling

Two kinds of data are obtained during drilling :

- those linked to rock samples (full diameter cores or sidewall cores, cuttings), and to fluid samples;
- those provided by physical measurements made in drilled holes essentially by wireline logging tools.

Standard cores, if they are continuous, constitute a sampling of good quality that will give abundant data. Unfortunately, for economic and technical reasons, coring can be a rare operation, particularly under certain drilling conditions or in certain types of formations. Therefore, often the only rock sample available consists of the cuttings obtained during drilling, or sidewall cores cut with the help of a bullet core barrel which runs with a wireline.

In some cases, there is considerable uncertainty over the depth of a given cuttings sampling and furthermore it can be difficult to restore the constituents and thickness of the lithological column from cuttings alone. This is due to mud swirling, caving, the loss of some constituents (silt size grains, salts) during washing or by total lost circulation events. The reduced dimension of this type of rock sample does not generally allow a full analysis, and makes an observation incomplete.

Cores may also have drawbacks such as partial recovery or none at all, sample damages (mechanical fracturation, depth matching, ...).

The geologist is therefore often short of, or deprived of representative or good quality samples. Sidewall cores can partly compensate for this shortcoming but, because of their small size, observations or measurements may still be inaccurate compared to those carried out on larger samples. As a result of these limitations, the second type of information (obtained from wireline logs) has become increasingly important, especially as the quality and diversity of tools and methods of interpretation have been developed. It has not only proved its complementarity to the preceding geological data, but also the invaluable and essential aid it provides in synthesis of data.

Wireline logs are of special interest in that they :

- provide the only source of data to give accurate information on the depth and the apparent, and even real, thickness of beds if a dipmeter has been recorded.
- give a nearly continuous analysis of the formations (one sampling every 15 cm for traditional open hole logs; this frequency can be increased to one sample every 3 cm if required, and one sampling every 5 mm or even 2.5 mm for dipmeter tools). In contrast, information extracted from cores is more discontinuous, and often scattered in depth. Even in the case of continuous coring, all analyses are not systematically made on each plug taken from the cores.

- generally analyse a volume of rock that is much greater than the one represented by a core or plug, and consequently than a cutting. Consequently, they are more representative of the mean properties of the rock, especially in heterogeneous rocks.

- measure rock properties at depth conditions.

- The information logs provide is :

. quantitative and, consequently, it allows us to think about geological objects represented by wireline measurements by using the full the computer's capacity to process the information;

. precise, even if, sometimes, errors are present;

. objective and repetitive;

. permanent; whereas the cores are destroyed for analysis, preventing any further study, log data can be reinterpreted with new ideas, new techniques, or new parameters;

. obtained rapidly, even on the well site;

. economic, coring and analysis of cores are expensive and time consuming, and the desired information is obtained only several weeks later.

- The measurements made with wireline tools are strongly dependent on geological parameters. Consequently, the information they provide is of the utmost interest for geologists.

Table 1-2 attempts to establish a hierarchy in the influence on each tool of the three principal geological parameters : composition, texture and structure. The influence of fluids is also indicated because fluids are indissociable from rocks, in subsurface, and can influence certain measurements.

One can reasonably conclude that wireline logs "photograph" the drilled formations. They provide a spectral picture, albeit particular and incomplete, which is practically continous and always permanent, objective and quantified. It is easily understood that the "picture" will be clearer when the number and the diversity of the log measurements are greatest. One can say that logging tools are to subsurface rock description what the eyes and geological instruments (hammer, magnifying glass, ...) are to the surface outcrop. Thus, the logs can be considered as the "signature" of the rocks since they depend on their physical properties. Log data must be treated like geological data and any log interpretation is in itself a geological interpretation, whether we are aware of it or not.

Wireline logging tools measure the physical characteristics of drilled formations. These characteristics in fact result on the one hand, from physical, chemical and biological (hence also geographical and climatic) conditions that existed in the deposits and which characterize environment (Table 1-3), and on the other hand from the evolution that these formations were subjected to during their geological history.

It is necessary, therefore, to *observe, describe, analyse and interpret the wireline "objects" as we would any other geological object.* In the following pages we will try to explain and to demonstrate this point.

It must be noted that a clear interpretation of wireline logs has not only to be supported by an accurate and detailed analysis of obtained log data, but must also be based on a solid knowledge of tool principles and serious geological concepts.

It is important not only to understand how the measurements of physical parameters are obtained, but also to know to which geological reality they correspond.

Table 1-2
Comparative response of well logs to the four main geological parameters
(from Serra & Abbott, 1980).

LOG TYPE	COMPOSITION	TEXTURE	SEDIMENTARY STRUCTURE	FLUID
RESISTIVITY	**	***	**	***
SP	*	**	***	***
EPT (Propagation Time)	**	*	*	***
EPT (Attenuation)	**	*	*	***
GR	**	*	*	*
NGS	***	*	*	*
CNL	**	**	*	**
FDC. LDT (ρb)	***	**	*	***
LDT (Pe)	***	*	*	*
TDT (Σ)	**	**	*	***
BHC (Δt)	**	***	*	**
BHC (Attenuation)	*	**	**	***
GST, GLT	***	***	*	***
HDT or SHDT, FMS	*	***	***	*
CAL	*	**	*	*
HRT	**	***	***	**

Log interpretation consists, thus, of a data "translation" from log parameters to geological data. To do this we need a good "dictionary" or an "interpreter" who knows the two "languages" well.

In fact, to determine if wireline logs are capable of giving information concerning mineralogical or elementary composition, texture, sedimentary or tectonic structures, facies, stratigraphy, ..., we need first to define what these geological terms cover.

Only then we will be able to specify how and in what proportion these geological parameters affect tool responses and, through this, by inverse reasoning, to deduce the geological parameters.

As

- a depositional environment is characterized by a typical facies association,

and

- a facies is itself defined by the following parameters : composition, texture, colour, fossils, sedimentary structure and geometry,

it seems obvious to start by showing how well logs can provide information related to these parameters before describing the electrofacies model corresponding to each principal environment.

Table 1-3
Relation between geometry, facies, sequences, and environment
(adapted from Krumbein & Sloss, 1963).

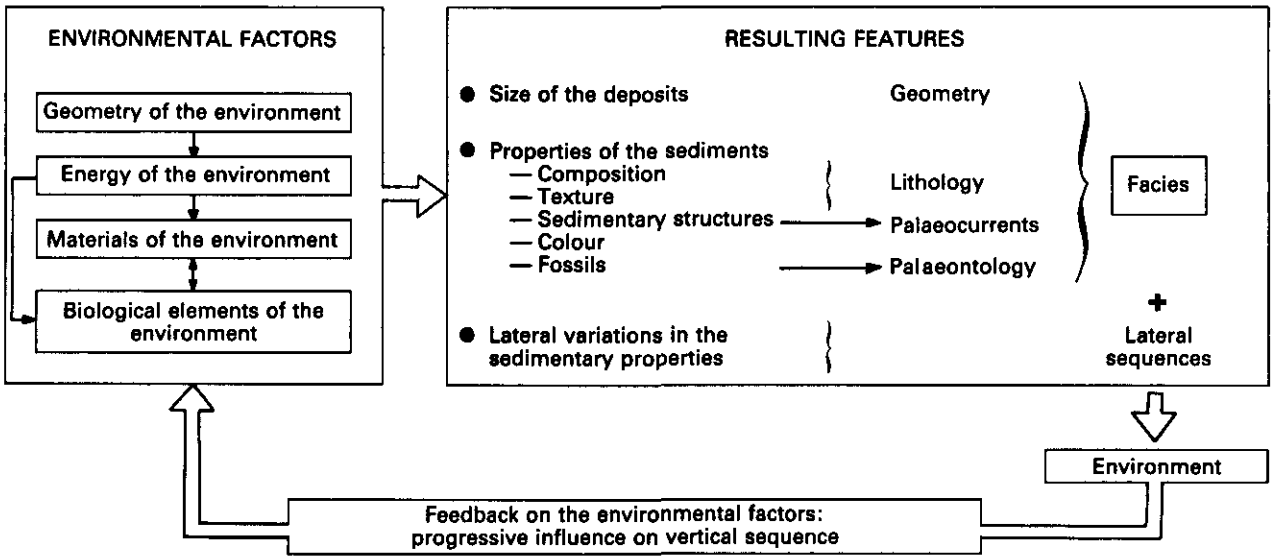

Chapter 2

INFORMATION ON ROCK COMPOSITION

(Rock description)

The nature of a rock and its composition are the first characteristics which the geologist attempts to determine, and a knowledge of these enables him to name the rock. This is also his first concern in the study of well logs.

He will therefore attempt to reconstruct the vertical lithological profile from an analysis of the well logs. This reconstruction is aimed at defining :

- the apparent thickness and the real thickness of each *electrofacies* or *electrosequence*[1] :
- the type of rock and the mineralogical composition of each electrofacies or electrosequence.

In order to obtain the most reliable reconstruction possible, the interpreter, or *log analyst*, must first of all procure a suite of logs which is as complete as possible, and in addition, a good description of cores and cuttings from the drilling process. Secondly, he must possess the basic concepts which are necessary for a good understanding of the problems involved in analysing the logs, and the implications that these will have in the choice of a quantitative interpretation model, be it manual or automatic.

Clearly, the interpretation of a volcanic or granitic rock will proceed differently, and therefore require a different model, from the interpretation of a sedimentary rock such as an argillaceous sand made up of a mixture of quartz, feldspar, kaolinite, illite and montmorillonite. Moreover, taking account of the frequently limited availability of data and recorded logs, it is not always possible to simultaneously determine the nature of the minerals present and their proportions, especially in the case of complex composition.

It is often necessary, therefore, to obtain additional information from examinations of cuttings, core analysis and local geological knowledge to establish the mineralogy model, and thereafter to restrict the investigation to determining the percentages of each of the principal minerals assumed to be present in the rock.

2.1. COMPOSITION OF ROCKS

The *composition* is "the make-up of a rock in terms of the species and numbers of minerals present" (Glossary of Geology).

The composition of a rock can be expressed in two different ways.

2.1.1. Elemental and Chemical Composition

This is provided by a chemical analysis in the laboratory using X-ray diffraction or neutron activation, the latter being the most precise and accurate. The results can be expressed either in terms of percentages of elements present, or in terms of oxides of these elements, the oxygen being strongly bonded to each of the abundant elements.

An examination of the relative abundances of the elements will reveal that only 8 of the 103 known elements account for 99 % of the total mass (Fig. 2-1).

2.1.2. Mineralogical Composition

In spite of its usefulness — we shall see later the application of new tools such as the Natural Gamma Ray Spectroscopy (NGS *), or induced

[1] The prefix *electro* has been added to the purely geological nomenclatures to avoid any confusion with them, and to indicate that the term relates to log measurements. There is, however, no implication that the term applies only to electrical measurements.

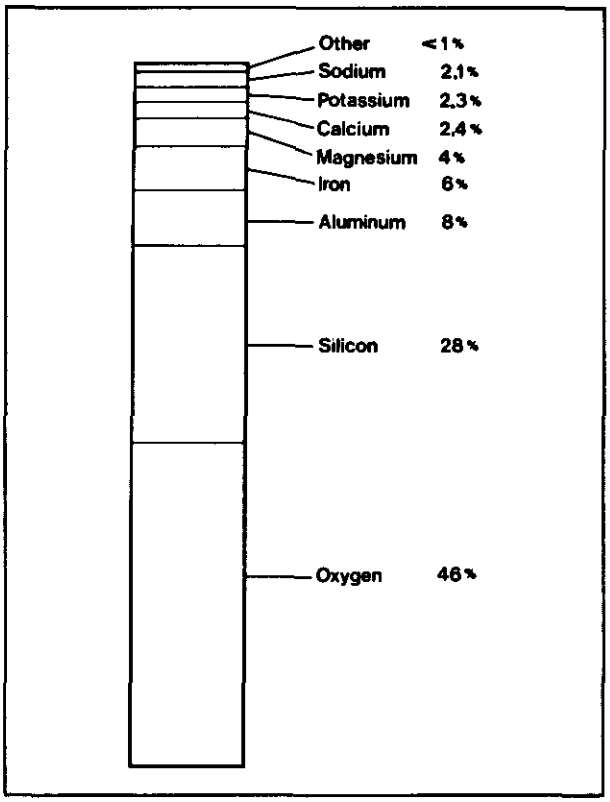

Fig. 2-1. - Relative abundance of elements in the earth's crust (from Press & Siever, 1978, fig. 1-12).

spectroscopy (GST *) tools for this — the elemental composition of a rock is not the best expression of rock composition, either from a sedimentological or from a log analysis standpoint. In fact, a rock is a *mixture of minerals*. These are what give it its petrophysical characteristics, which are generally those measured by the logging tools— density, resistivity, sonic travel time, compressibility, etc. These properties therefore depend on :

- the individual characteristics of each of the constituent minerals forming the rock,
- the relative percentages of each mineral,
- their distribution and bonding.

For this reason, it is preferable to express the composition of a rock in mineralogical terms.

More than 2,200 minerals have been identified, but the vast majority are rare and only found either as trace minerals or occasionally.

The various rock types are made up of a reduced number of minerals.

According to Krynine (1948), only twenty minerals are needed to be able to constitute 99 % of all the sedimentary rocks. These minerals are listed in Table 2-1.

The important point is that *sedimentary rocks are usually composed of a mixture of at most four minerals or major contituents*, that is, having a

* Mark of Schlumberger.

Table 2-1

The principal minerals found in sedimentary rocks (from Krynine, 1948).

	Major Constituents		Accessory Minerals (Less than 1 Per Cent of Rock)
	Over 10 Per Cent of Rock	Less than 10 Per Cent of Rock	
Detrital Minerals	QUARTZ Microcline CLAY MINERALS (kaolin-bauxite) FINE-GRAINED MICAS (illite, sericite muscovite)	DETRITAL CHERT Sodic plagioclase (albite-oligoclase) Coarse-grained micas: muscovite biotite chlorite Hematite Limonite	"IRON ORES": MAGNETITE, ilmenite, DETRITAL LEUCOXENE STABLE GROUP: ZIRCON TOURMALINE, rutile UNSTABLE GROUP: APATITE, EPIDOTE GARNET, HORNBLENDE kyanite, sillimanite, staurolite, titanite, zoisite MICAS: frequently occur as accessories rather than as major constituents
Chemical and Authigenic Minerals	CALCITE DOLOMITE ANKERITE	CHERT and opal "SECONDARY" QUARTZ GYPSUM and anhydrite, halite Some hydromicas of the illite-sericite-chlorite series Phosphates and glauconite, Siderite and some iron ores	ANATASE; authigenic rutile and leucoxene

* Minerals printed in capitals are the relatively more common ones within each group.

content of more than 5 %. The concept of *"end-members"*, or major constituents, introduced by Krynine (1948) and extended by Pettijohn (1949) to describe the composition of a rock is based on this observation.

The extended form of the concept proposes that the composition of any sedimentary rock in terms of minerals can be represented by a point within a triangle or tetrahedron whose apexes correspond to the *end-members* in a pure state (Fig. 2-2).

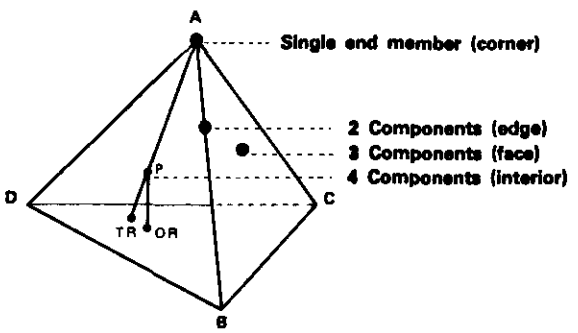

Fig. 2-2. - Representation of rock composition by means of a tetrahedron (from Krumbein, 1954).

2.2. ROCK COMPOSITION FROM WELL LOGS

There are many different log measurements which respond to the rock composition. As a result, an adequate logging suite will make the determination of rock composition much easier.

Two approaches are possible in using well logs to determine composition.

2.2.1. Determination of elemental composition

The recently introduced gamma ray spectrometry tools (natural and induced gamma ray) allow

the detection and, in favorable cases, measurement of the proportions of the following elements :

- potassium (K), thorium (Th), and uranium (U) in the case of natural gamma ray spectrometry, using the NGS * tool (Fig. 2-12a);
- carbon (C), oxygen (O), silicon (Si), iron (Fe), calcium (Ca), sulphur (S), chlorine (Cl), hydrogen (H), and aluminium (Al), in the case of induced gamma ray spectrometry, either by inelastic neutron-nucleus interaction or by thermal neutron absorption using the GST * tool, or by activation with the new Aluminium Clay Tool (ACT *) [1].

Examination of the above list will reveal that, with only two exceptions (Mg and Na), these tools enable the percentages of the most common elements to be determined. Hence their interest for the direct determination of the content of certain elements, and above all for a better analysis of composition in conjunction with the other tools, in particular hydrogen index and photoelectric index. Neutron-based tools provide a breakdown either in terms of light elements (H, C, O and Si) which have a slowing effect (seen by the epithermal tool), or in terms of thermal neutron absorbers (Gd, B, Li, Cl, Fe) seen by the thermal tool. The litho-density tool (LDT *) provides a measure of the mean atomic number of the rock components.

2.2.2. - Determination of Mineralogical Composition

As we have seen, rocks are made up of a mixture of minerals. Consequently, it is the physical properties of these minerals, and ultimately the atomic properties of their constituent elements which influence the log responses.

In fact, the responses are a function of the characteristics of each mineral present in the rock and of their relative percentages in the zone of investigation on the one hand, and on the nature and percentages of the fluids occupying the pore spaces on the other. (Table 2-2).

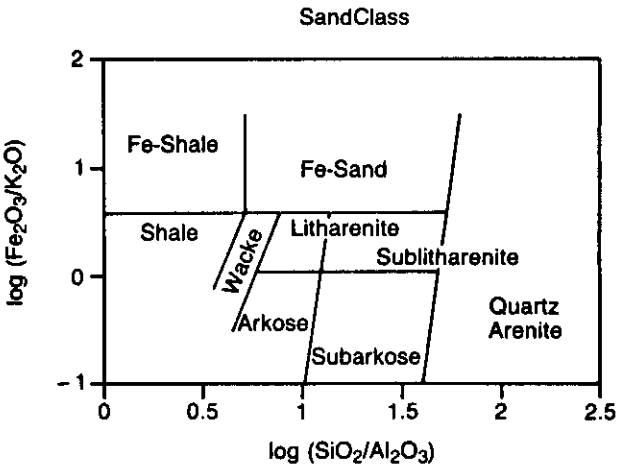

Fig. 2-3. - Sandclassification derived from the geochemical log (from Herron, 1987).

If we accept the fact that rocks rarely contain more than four different major minerals, it is only necessary to have a preliminary knowledge of their types and their characteristic log parameters (density, neutron hydrogen index, photoelectric cross-section, and natural gamma activity or potassium content, for example) to be in a position to compute their relative percentages from a combination of LDT, CNL, and GR (or NGS) tools.

Naturally, the rock composition can be more complex, in which case further independent log measurements are required, along with a good knowledge of the types of minerals present. In the case of porous rocks, it is also necessary to know the nature of the fluids present in the pores, and to determine their percentages in the rock (i.e. porosity) and in the pores (i.e. saturation) to decide which components of the response are attributable to each.

The correct determination of the mineralogical composition of a rock will ensure on the one hand the correct choice of mineralogical model and log response parameters, and on the other hand will provide a solution to a system of equations, usually linear, which relate the response of each tool to the parameters and volumetric percentages of each constituent (mineral or fluid).

The choice of mineralogy model is made partly by analysis of the logs themselves (using cross-plots of two, three (Z-plots) or even four dimensions using colour; dipmeter analysis; use of electrofacies, etc.), and partly from auxiliary information, such as examination of cuttings, core analysis, and previous knowledge of regional geology or formations. The latter speeds the choice of model adapted to each formation. But in the absence of such data, or alternatively, as a means of cross-checking, it is possible to quickly determine the rock type from log data alone, and hence to arrive at a choice of the mineralogical model itself.

---

* Mark of Schlumberger.

[1] Schlumberger's new ACT is a nuclear tool, which enables determination of the aluminium content of the formation. The formation is irradiated by a ^{252}Californium (Cf) source which emits 10^8 neutrons per second with an average energy of 2.3 MeV. This source is prefered to an Am-Be (4.5 MeV) source because the number of interactions between fast neutrons and silicon is reduced. The aluminium activation is the result of neutron capture by ^{27}Al (natural abundance 100 %), resulting in ^{28}Al which decays by β emission with a half life of 2.27 minutes. The decay product is ^{28}Si which emits a 1.779 MeV gamma ray. The induced gamma rays are recorded with the help of a NaI detector (similar to the one used in the NGS tool). The recording speed is 600 ft/h. The tool has two detectors. One above the source records the natural gamma ray, while one below the source records both natural and induced gamma ray. The difference between the two (before and after irradiation) gives the gamma ray yield related to the aluminium activation. It is proportional to the aluminium content of the formation. This measurement, combined with the thorium and potassium content measured by the NGS service, and with the silicon and iron contents determined by the GST tool, enables determination of the clay types and classification of sandstones (Fig. 2-3).

Table 2-2. *Relationship between composition of a rock and well logging parameters* (from Serra, 1984, Table 1-4a)

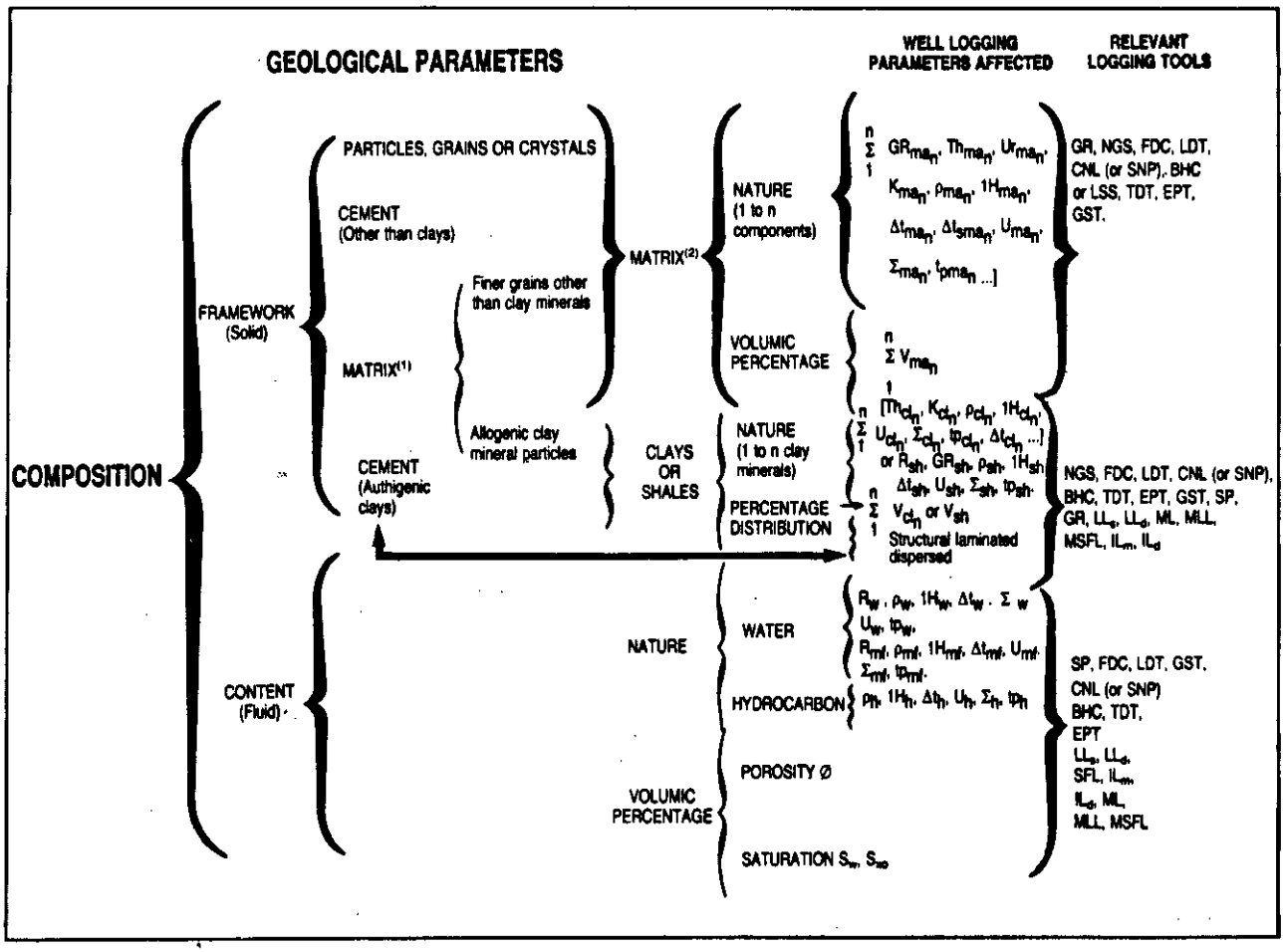

2.3. AUTOMATIC LITHOLOGY DETERMINATION — GEOCOLUMN * THE LITHO PROGRAM

Since each rock is composed of a certain number of minerals in known proportions, and whose log parameters are usually well-known, it can be represented by an electrofacies (excluding dipmeter data), and hence by a *lithofacies*. An electro-lithofacies corresponds to a volume (a hyper-ellipsoid) in the space of *n* dimensions represented by the *n* log measurements. It can be defined empirically from actual log responses to the various rock types. Theoretically, it can be determined from a knowledge of the mean mineralogical composition of the rock determined statistically from laboratory core analysis, and from a knowledge of the log response to each of the minerals or elements constituting the rock.

* Mark of Schlumberger.

The LITHO method, then, consists initially of establishing a *"lithofacies library"*

2.3.1. Establishment of the Lithofacies Database

The technique employed for defining the lithofacies, and therefore for constituting the database, consists of *dividing a n-dimensional space into hypervolumes*, each of which corresponds to a major lithology type. Put more simply, it involves *defining on each plot the limits of the area occupied by this type of lithology*. This area depends on several factors :

- the composition of the rock type in terms of major minerals (allowing for a certain amount of variation in content), and in terms of secondary minerals which could affect tool responses (radioactivity, capture cross-section, or hydrogen index). This may even be necessary for trace minerals such as zircon, pyrite, uranium, boron or gadolinium;

- the texture, which in turn affects porosity and its distribution, as well as permeability, and hence all the effects which depend on them, such as invasion and tortuosity;
- the internal structure of the rock (homogeneity, bedding and vertical sorting);
- the response equations of each tool;
- the uncertainties on the measurements. These volumes and surfaces must be determined both practically and theoretically : *theoretically* from a knowledge of the mineralogical composition of each rock and the log responses to these minerals, and *practically* by comparing crossplots of log responses to each rock with laboratory core analyses.

A discriminant function is defined for each lithofacies which is maximal at the centre of the hypervolume, and zero on its boundaries.

2.3.2. Comparison, Selection and Establishment of the Lithological Profile

The allocation of a reading level or a bed to a lithofacies is based on the position of the selected point in the n-dimensional space relative to the hypervolumes defining each lithofacies. The procedure is statistical and is known as the *Bayes*

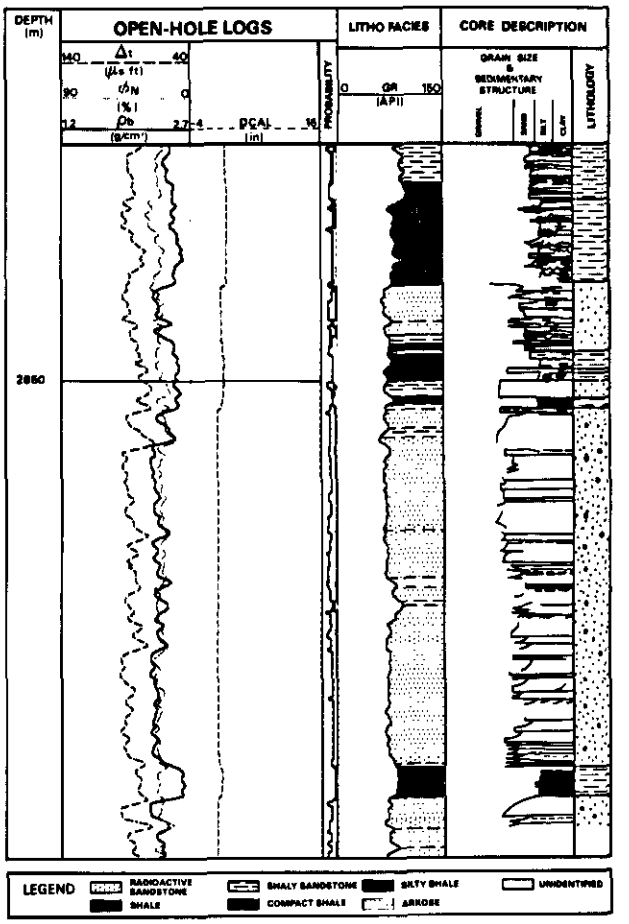

Fig. 2-4. - Example of a lithological description obtained with the LITHO program in a detrital sequence.

Fig. 2-5. - Example of a lithological description obtained with the LITHO program in carbonate and evaporite sequences. A comparison with core data in included (from Delfiner *et al.*, 1984). ▼

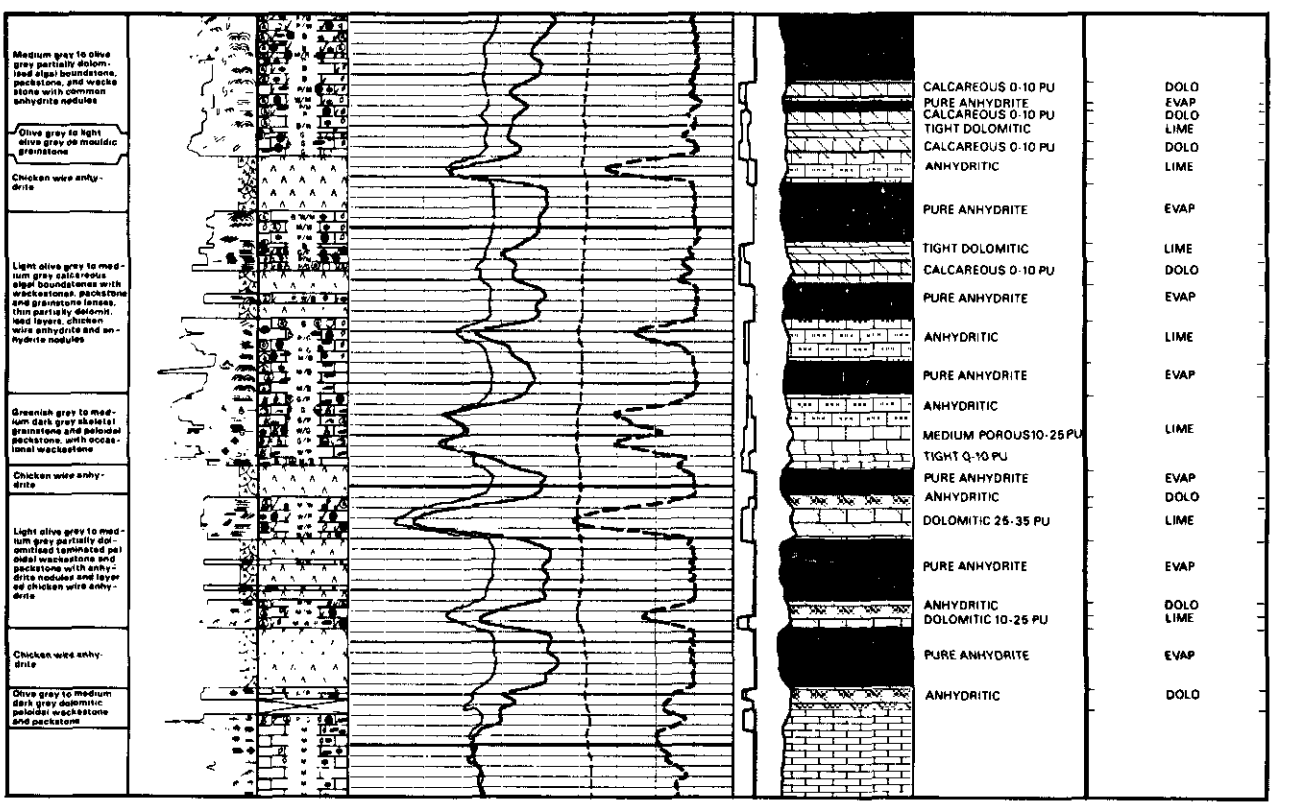

Criterion. The principle is to define a probability distribution of log values for each lithofacies, and to decide to which population the set of log readings is closest. Several variants are possible :

- the point falls inside a single hypervolume. In this case there is no ambiguity, and the selection of lithofacies is clear;
- the point is shared by two or three hypervolumes. The lithofacies with the highest discriminant function is selected. In effect, a discriminant probability is calculated;
- the point is not inside any of the hypervolumes. Several explanations are possible : poor depth-matching of logs; badly calibrated or faulty tool (e.g. cycle skips on the sonic); effect of drilling fluid on one of the tools (e.g. barite on the LDT or potassium on the NGS); effect of hole washouts on one or more tools; incomplete lithofacies database. All that is required in the last case is to create the appropriate hypervolume.

Special logic is used to cope with these situations and with thin beds. On the other hand, the selection program can be guided by specifying the principal lithology in a given interval, with a view to removing certain lithofacies from the database and hence avoiding possible confusion. This guidance can be provided by analysis of other logs (e.g. caliper, SP, resistivity), by local geological knowledge or by adding information to a geological database which can be consulted using artificial intelligence techniques.

Figs. 2-4 & 2-5 show two examples of results obtained with the LITHO program developed by Schlumberger. The usefulness of such an analysis for obtaining a quick description of the vertical lithological profile of the well, and ultimately for choosing the mineralogical model for a quantitative interpretation is clear. Results can also be used for mapping purposes.

2.4. REFERENCES

ADAMS, J.A.S. & GASPARINI, P. (1970). -Gamma-ray spectrometry of rocks. *Elsevier Publ. Co., Amsterdam.*

ADAMS, J.A.S. & WEAVER, R. (1958). - Thorium to Uranium ratio as indicator of Sedimentary Processes: examples of concept of Geochemical facies. *Bull. amer. Assoc. Petroleum Geol.,* **42** *, 2.*

BARTH, T.F.W. (1952). - Theoretical Petrology. *John Wiley & Sons, Inc., New York.*

BLATT, H., MIDDLETON, G. & MURRAY, R. (1980). - Origin of Sedimentary Rocks. 2d ed. *Prentice-Hall Inc., Englewood Cliffs, New Jersey.*

CAILLERE, S. & HENIN, S. (1963). — Minéralogie des argiles. *Masson, Paris.*

CLAVIER, C. & RUST, D.H. (1976). - MID-Plot: A new Lithology Technique. *The Log Analyst,* **17,** *6, p. 16.*

DEER, W.A., HOWIE, R.A. & ZUSSMAN, J. (1962). — Rock-forming Minerals. Vol. 3. Sheet Silicates. *Longwan, London.*

DELFINER, P., PEYRET, O., & SERRA, O. (1984). - Automatic determination of lithology from well logs. *59th ann. Techn. Conf. of SPE of AIME, Houston, paper SPE 13290.*

EDMUNDSON, H. & RAYMER, L.L. (1979). -Radioactive parameters for Common Minerals. *SPWLA, 20th Ann. Log. Symp. Trans., paper O.*

FELDER, B. & BOYELDIEU, C. (1979). - The Lithodensity Log. *SPWLA, 6th Europ. Symp. Trans., paper O.*

FRIEDMAN, G.M. & SANDERS, J.E. (1978). -Principles of Sedimentology. *John Wiley & Sons, New York.*

GARRELS, R.M. & MACKENSIE, F.T. (1971). -Evolution of Sedimentary rocks. *Norton, W.W. & Co, New York.*

GRIM, R.E. (1968). — Clay Mineralogy. McGraw-Hill Co., New York.

HERRON, M.M. (1987). - Sand Class : Geochemical Classification of terrigenous Sands and Shales from Core or Log Data. *Journ. Sedim. Petrology.*

KRUMBEIN, W.C. (1959). - The tetrahedron as a facies mapping device. *J. Sed. Petrol.,* **24** *, 1, p. 3-19.*

KRUMBEIN, W.C. & SLOSS, L.L. (1963). -Stratigraphy and Sedimentation. 2d ed.*W.H. Freeman & Co, San Francisco.*

KRYNINE, P.D. (1948). - The megascopic study and field classification of sedimentary rocks. *J. Geology,* **56** *, p. 130-165.*

MAYER, C. & SIBBIT, A. (1980). - GLOBAL, a new Approach to Computer-processed Log Interpretation. *SPE of AIME, Fall Mtg., Dallas, SPE 9341.*

PETTIJOHN, F.J. (1975). - Sedimentary Rocks. 3d ed. *Harper & Row, Publishers, New York.*

PETTIJOHN, F.J., POTTER, P.E. & SIEVER, R. (1972). - Sand and Sandstone. *Springer, New York.*

PRESS, F. & SIEVER, R. (1978). - Earth. 2d ed. *W.H. Freeman & Co, San Francisco.*

Schlumberger Technical Services, Inc. (1982). -Essentials of NGS Interpretation.

SERRA, O. (1984). - Fundamentals of well-log Interpretation. 1. The acquisition of logging data. Developments in Petroleum Science 15 A, Elsevier, Amsterdam.

Chapter 3

INFORMATION ON TEXTURE

(Rock description)

3.1. REVIEW OF PETROGRAPHIC CONCEPTS

Before explaining how to extract textural information from wireline logs it is important to review some concepts which will help in the understanding of the links between well logging data and textural parameters.

3.1.1. Definition

The texture covers the geometrical aspects of the constituent components of rocks : grains or particles and crystals, i.e. their size, shape, appearance, their arrangements and sorting; also the grain-grain, grain-matrix or grain-cement boundings.

Texture plays a very important part in sedimentary rocks, because the **petrophysical properties of a rock**, hence its **porosity** and **permeability, depend essentially on texture**.

According to the origin of the rocks, Krumbein & Sloss (1963) distinguish :

- fragmental texture, more specific to detrital rocks;
- crystalline texture, more specific to chemical or eruptive rocks.

3.1.2. Components of texture

Regardless of the type of texture, sedimentary rocks are marked by the textural characteristics of three components :

- *grains*, or *particles*, and *crystals*;
- *matrix*, that corresponds to the finest materials filling interstices, or holes, between the grains;
- *cement*, binding the grains and the matrix.

These components may have different mineralogical compositions. Figure 3-1 shows the constituent minerals of the different textural components, depending on the type of detrital rocks.

These components are not necessarily present all together in the same rock. For example in medium-grained and very well-sorted sand there will be neither matrix nor cement. A consolidated, medium-grained, well-sorted sandstone has no matrix, but contains a cement that can be siliceous, calcitic or dolomitic, sideritic, or halitic ...

The grains and matrix are generally associated, because they are most often deposited together (sand grains in an argillaceous matrix, or pebbles in a sandy matrix). As for cement, it is always post-depositional, being the result of chemical precipitation in the pore space.

As shown by Krumbein & Sloss (1963), the study of texture must be subdivided into three categories depending on the nature of sedimentary rocks :

- purely chemical rocks, such as halite, gypsum, anhydrite... The texture of these rocks is characterized only by the crystalline system, the size and imbrication of crystals;
- partly chemical or biochemical and partly detrital rocks, such as carbonates, for which the three textural components play, in turn or simultaneously, a very important part;
- detrital rocks, for which the three components play a very important part.

Detrital rocks will be discussed first.

3.2. TEXTURE OF DETRITAL ROCKS

According to Krumbein & Sloss (1963), the final texture of a sediment is influenced by six fundamental properties :

- *grain size* and its variation that will control the *sorting*;
- *shape* (or *sphericity*) of grains (Fig. 3-2);
- *roundness*;
- *surface texture*;
- *grain orientation* or *fabric*;
- mineralogical composition. This is not, pro-

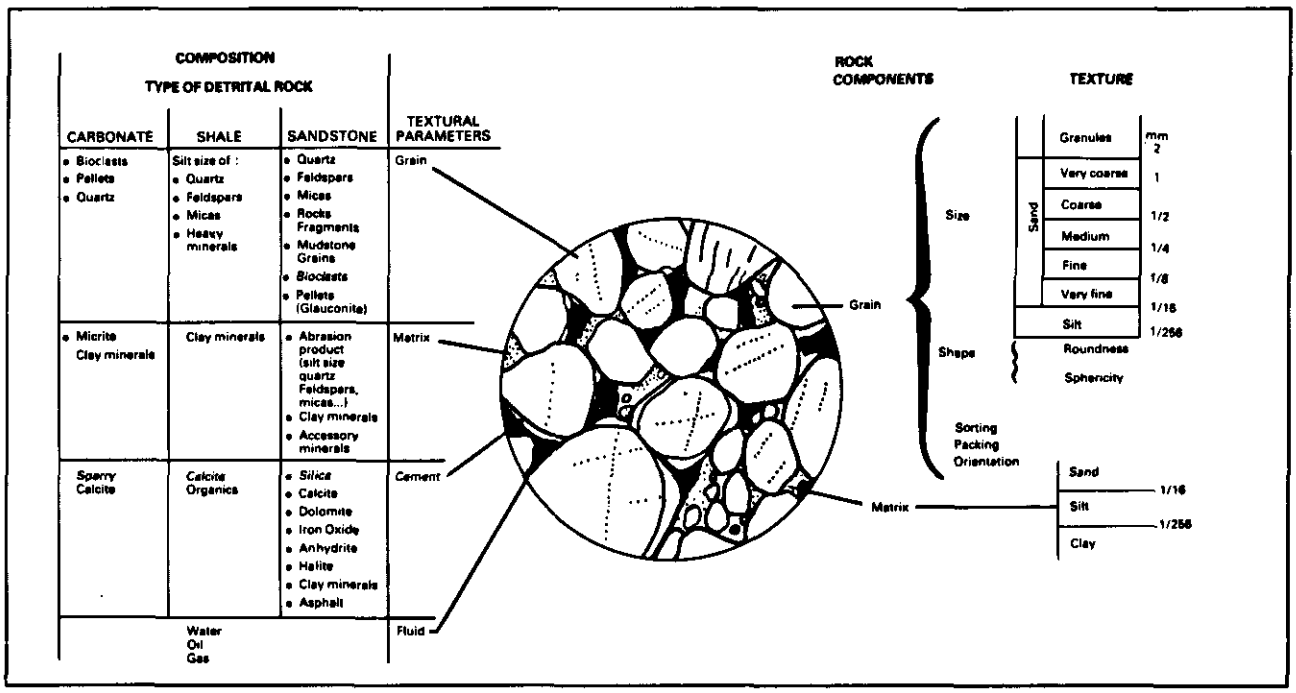

Fig. 3-1. - Textural components of rock.

perly speaking, a textural parameter, but depends upon :

. density, hence the rate of sedimentation of each component;

. possibility of dissolution (solubility) or of alteration, consequently the ulterior formation of cement;

. wettability of rock.

These different properties affect reservoir characteristics. Their influences will be studied in detail in the next sections.

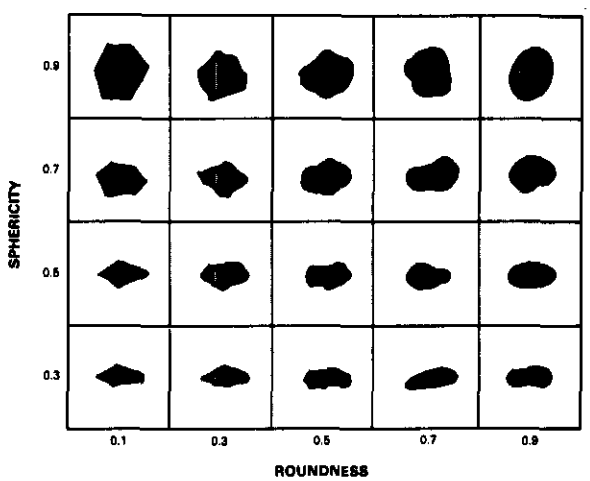

Fig. 3-2. - Sphericity and roundness of particles (from Krumbein & Sloss, 1963, fig. 4-10).

3.2.1. Influence of Grain Properties on Reservoir Characteristics

Porosity and permeability are the main petrophysical characteristics of a reservoir.

Beard & Weyl (1973) showed that the primary porosity and permeability of a detrital sediment, which has just been deposited, depend on five variables : size, sorting, shape, roundness, orientation and arrangement of grains.

3.2.1.1. *Influence of grain size*

Porosity is theoretically independent of grain size. An arrangement of spheres with uniform size, which present the same organization, will have the same porosity, regardless of size. This ideal situation, which corresponds to a maximum sorting rarely occurs in nature. It can sometimes be observed in washed or winnowed sands, and more frequently in oolitic sands. Figure 3-3 from Dodge *et al.* (1971), seems to confirm that, above a certain level of porosity reflecting the best sorting and the absence of cement, the porosity is independant of grain size.

In fact, Lee (1919), Von Engelhardt (1960) (Fig. 3-4) discussing ancient sedimentary rocks, and Rogers & Head (1961) (Fig. 3-5), and Pryor (1973), on the subject of contemporary sands, show that porosity decreases slightly, when grain size increases. This evolution is probably due to a number of factors which have only an indirect connection to grain size. Finer sands have a tendency to be more angular and are likely to be

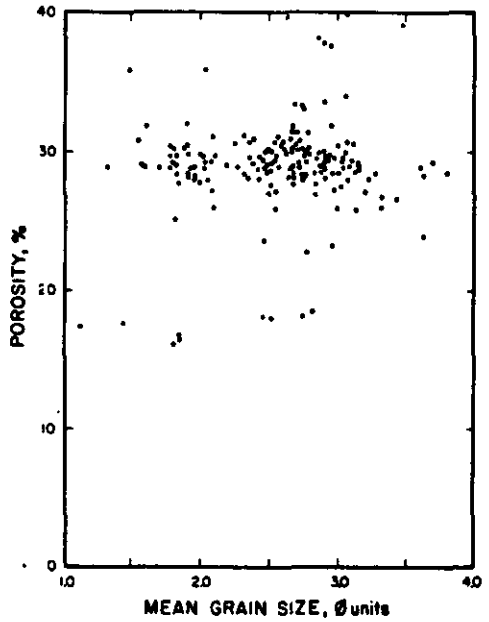

Fig. 3-3. - Relationship between porosity and mean grain size for all samples coming from sandstones of Paluxy Formation, Texas (from Dodge *et al.*, 1971).

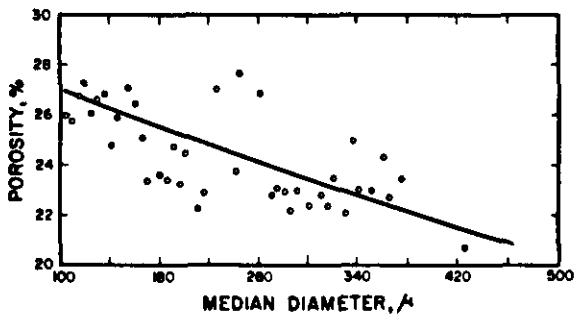

Fig. 3-4. - Relationship between porosity and mean diameter of grains in Bentheimer sandstones (from von Engelhardt, 1960).

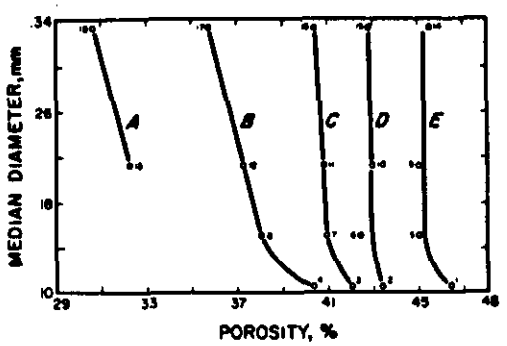

Fig. 3-5. - Relationship between porosity and mean diameter of sand grains for several different sorting coefficients. A : So = 2.086; B : So = 1.625; C : So = 1.279; D : So = 1.128; E : So = 1.061 (from Rogers & Head, 1961).

organized according to a less dense arrangement. Thus, they present a higher porosity than sands with coarser grains.

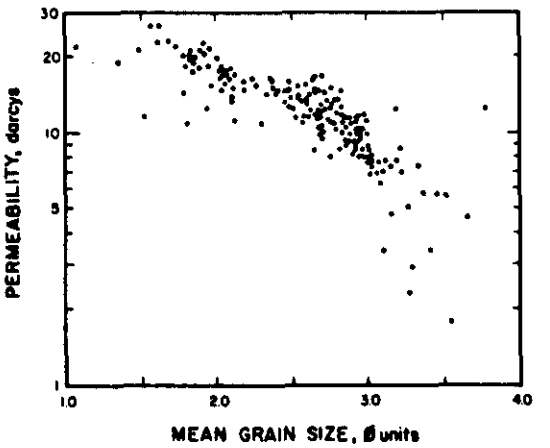

Fig. 3-6. - Relationship between permeability and mean grain size for all the samples coming from sandstones of Paluxy Formation, Texas (from Dodge *et al.*, 1971).

Contrarily, as demonstrated by Dodge *et al.*, (1971) (Fig. 3-6), in a well-calibrated sand permeability increases when the size of the grain increases. This is easily understood because the size of pores and the canals (throats) which connect the pores to one another are governed by grain size : the smaller the grains, the smaller the pores and the section of the canals will be. Thus, capillary attraction will be stronger and permeability will be less (Fig. 3-6).

3.2.1.2. *Influence of sorting*

As investigated by Rogers & Head (1961) porosity and permeability increase when sorting increases (Fig. 3-7). In fact, in a poorly-sorted sand, the small grains (matrix) are set in interstices left by the coarser grains. Thus, the matrix invades the large pores and fills up the big canals.

The combined influence of grain size and sorting on porosity and permeability has been studied by Beard & Weyl (1973). It is illustrated by Fig. 3-8.

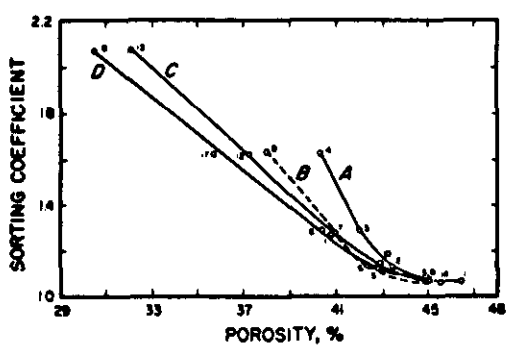

Fig. 3-7. - Relationship between porosity and sorting coefficient of sands for different grain sizes. A : median diameter md = 0.106 mm; B : md = 0.151 mm; C : md = 0.213 mm; D : md = 0.335 mm (from Rogers & Head, 1961).

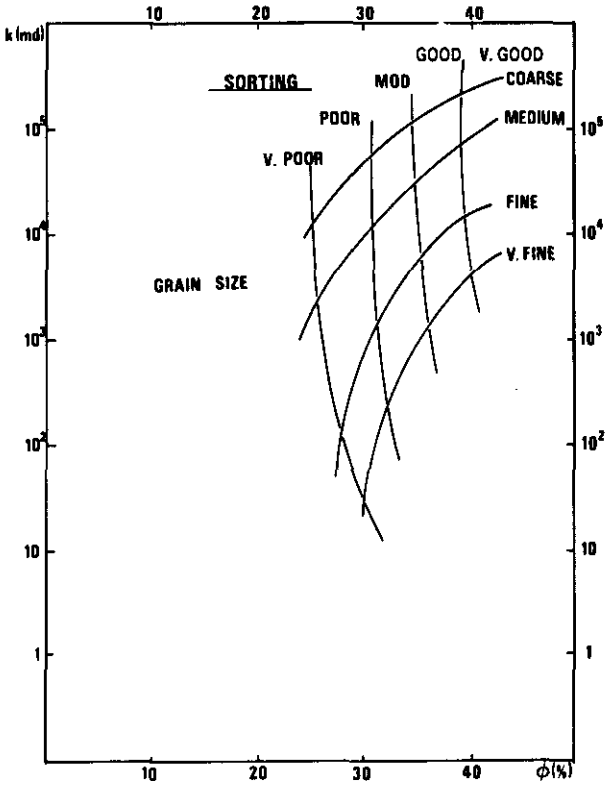

Fig. 3-8. - Relationship between porosity and permeability for different grain size and sorting (from Beard & Weyl, 1973).

3.2.1.3. *Influence of shape and roundness of grains*

It seems that shape and roundness affect intergranular porosity. Fraser (1935) came to the conclusion that sediments composed of spherical grains have lower porosity than those formed by grains with less sphericity [1]. He attributed this to the fact that in the first type the grains tend to settle according to a denser arrangement than in the second type. Less spherical grains can pack together in a way that creates wider volumes between them.

The influence of shape and roundness on permeability is not still well known, but we observe that permeability follows the fluctuations of porosity in connection with variations in shape and roundness.

3.2.1.4. *Influence of the orientation of grains*

The orientation of particles is defined by reference to a horizontal plane and to the direction of current.

The orientation of pebbles is generally well-defined, because their size makes observation relatively easy (Fig. 3-9). The measurement and

[1] Grains with natural shapes are considered. A packing of bricks - no sphericity - would generate a rock without any porosity.

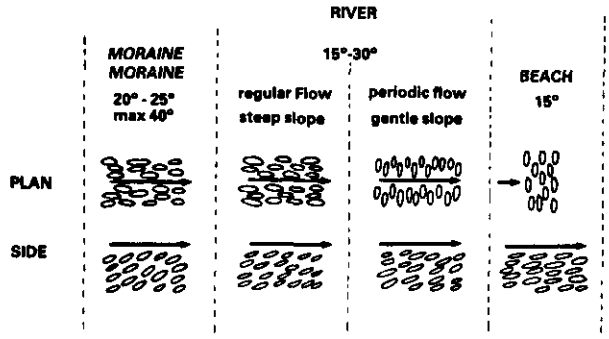

Fig. 3-9. - Schematic representation of the pebble orientation in different environments (from Rukhin, 1958).

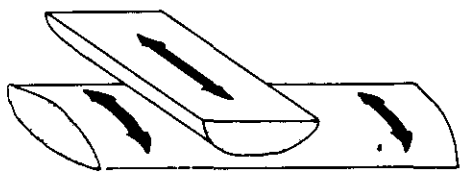

Fig. 3-10. - Grain orientation and directions of maximum permeability in channel and bar sand bodies, upper and lower respectively (from Pryor, 1973, in Selley, 1976, fig. 15).

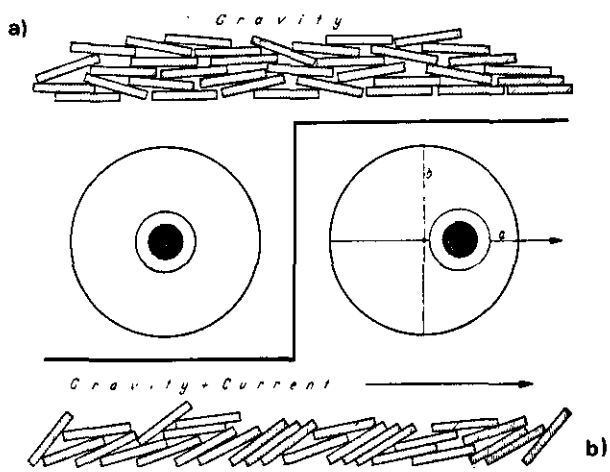

Fig. 3-11. - Orientation of flakes. a) : flakes deposited under gravity action; b) : flakes deposited under combined action of gravity and current (from Potter & Pettijohn, 1971, fig. 3-2).

quantification of the orientation of small sized grains (sand, silt...) is much more difficult. However, for non-spherical grains it is generally observed that the orientation of grains is the same as the orientation of their axis of maximum elongation and is parallel to the direction of current. On the whole, the orientation of non-phyllitic (non-shaly) grains has no influence on porosity. On the contrary, it has a very strong influence on permeability or more precisely on anisotropy or the direction of highest permeability. Thus, in channel sands, the direction of maximum permeability is parallel to the axis of the elongation of sand

bodies. In a littoral bar sands, maximum permeability is perpendicular to the axis of elongation of sand bodies, but is parallel to the dominant direction of currents (Fig. 3-10). The orientation of phyllitic particles (shales) will be the same as the orientation of their large sides that are parallel to the plane of stratification (Fig. 3-11).

3.2.1.5. *Influence of packing*

According to Graton & Fraser (1935), simple geometrical packing of equal-sized spheres are made in six different manners (Fig. 3-12). They proved that porosity varies according to packing from 47.64 % for the most « open » arrangement to 25.95 % for the most compact or « closed ».

Allen (1984) made a complete review of several types of packing (ordered, random or haphazard) of particles of different shapes (spheres, prolate and oblate spheroids). He concluded that « regular particles ... may form packing of all three kinds, whereas natural particles, which are irregular, can

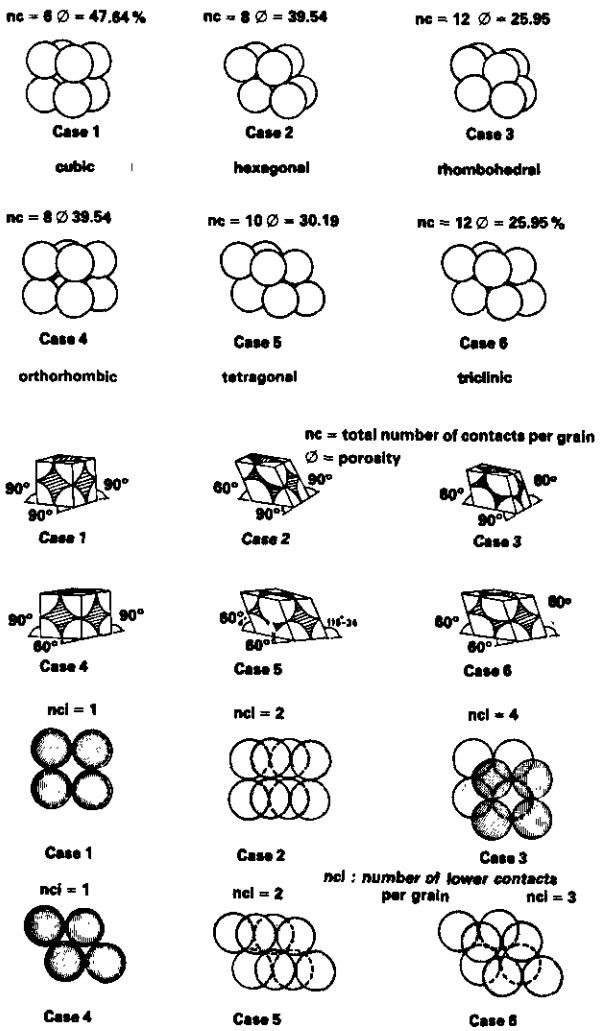

Fig. 3-12. - The six possible geometric arrangements of equal size spheres (from Graton & Fraser, 1935).

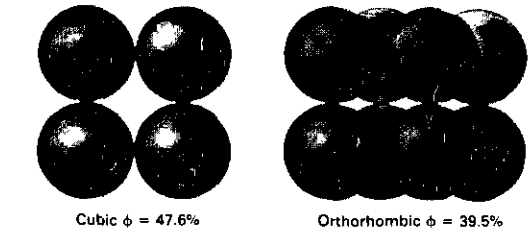

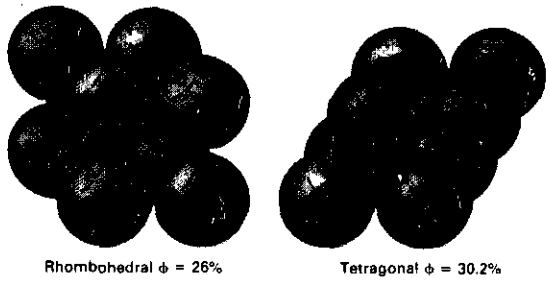

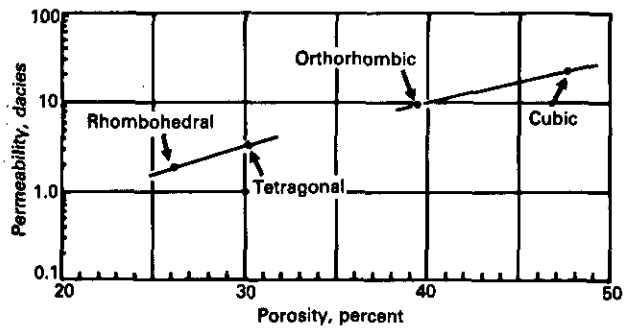

Fig. 3-13. - Porosity vs permeability for some ideal geometric packings of 500 µm-diameter spheres (courtesy of R. Nurmi).

only form packings of random or haphazard kinds. » In fact, regular particles can exist in nature. They correspond to oolites. He also concluded that porosity is decreased by a « widening of the range of particles sizes present in mixture », but is increased « by an increase of particule angularity and surface roundness, and by the inclusion of strongly anisometric particles ».

It seems obvious that permeability must follow a comparable evolution, because the section of pores and capillaries in compact arrangement is smaller than in others. Figure 3-13 shows the theoretical variations in permeability for ideal geometric packings of 500 µm-diameter spheres.

Naturally, the most « open » arrangements do not, in fact, ever occur in ancient formations; very soon under the influence of compaction the grains are organized according to the most « closed » arrangement. The influence of compaction will be studied in chapter 8 as it also affects the form of grains.

3.2.1.6. *Influence of the mineralogical composition of grains*

Grains composed of heavy and denser minerals will be deposited with the minerals of the same weight, i.e. with less density, but with bigger size.

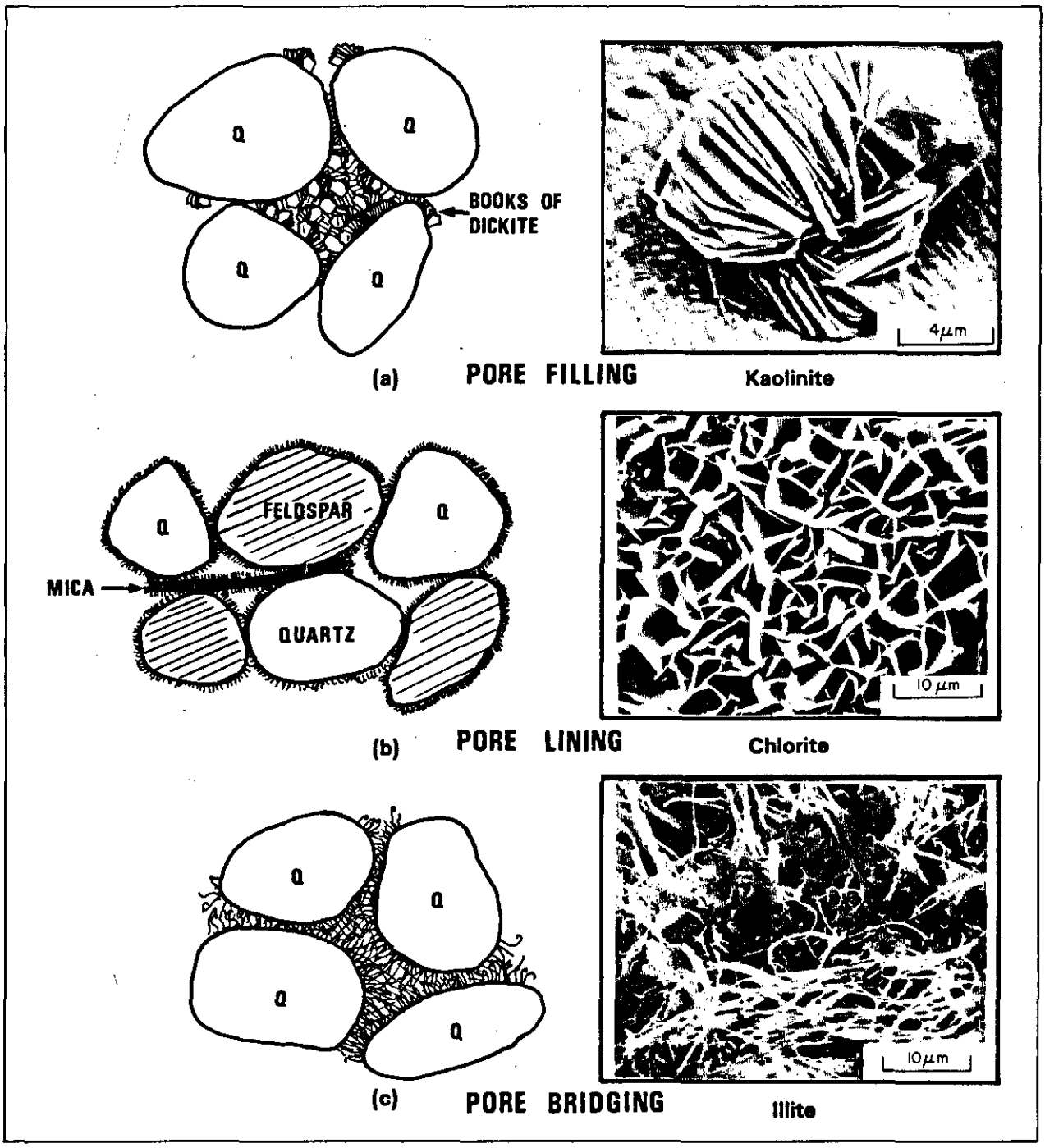

Fig. 3-14. - The three types and distributions of dispersed authigenic clay minerals in pore space (from Neasham, 1977).

This situation will lead to a decreasing of sorting, therefore of porosity and permeability.

Grains composed of unstable or chemically immature minerals (pyroxene, amphibole, mica, feldspar,...) will influence porosity of the sediments in which they occur. Their ulterior alteration will cause the formation of authigenic clay minerals (kaolinite, montmorillonite, illite, chlorite,...) which will surround the grains or invade the pore space, ı us, causing major reductions in porosity and permeability (Fig. 3-14). But the type and distribution of authigenic clay minerals must also be considered because they affect the permeability in a different way (Fig. 3-15). Their influence has been studied by Neasham (1977).

Discrete-particule or *pore-filling* clay minerals

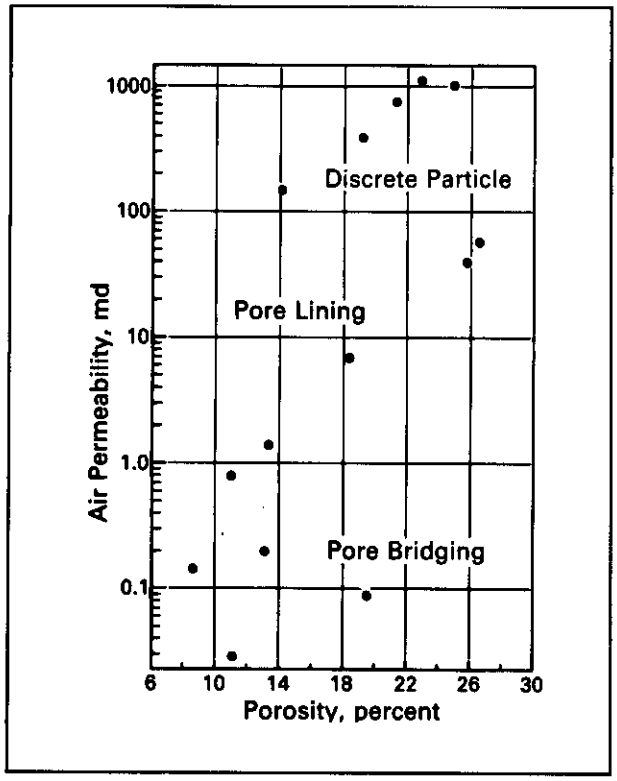

Fig. 3-15. - Influences on porosity and permeability of the distribution type of authigenic clay minerals. Data from Neasham's study of 14 sandstones (from Neasham, 1977).

(for example kaolinite « books ») are characterized by uneven distribution in the pore space. Crystals can reach large size (more than 10 μm). As crystals grow, pore space and permeability decrease, although there is always a small amount of microporosity between individual plates.

Pore-lining clay minerals, essentially illite, chlorite and montmorillonite, coat the pore walls with a thin layer of flakes that are parallel or perpendicular to the pore wall (Fig. 3-14b), but the growth does not reach far into the pore space. A large amount of microporosity can be present between flakes, although these pores are less than μm in diameter. This type of authigenic clay greatly reduces permeability and also influences many of the rock's electrical properties because it can considerably increases the surface area.

Pore-bridging clays, fundamentally illite fibers (Fig. 3-14c), are connected across the pore space. This type causes major reductions in permeability, since bridging is most easily attained across the throats, and also it reduces the size of the pores. Porosity is less affected because microporosity is preserved between the very fine fibers.

From the previous remarks, it seems obvious that the knowledge of the type of distribution (laminated, structural or dispersed), and of the nature of the clay minerals is of the utmost importance to predict the permeability range and the existence and distribution of permeability barriers.

Particles composed of soluble minerals (calcite, dolomite,...) lead to the creation of a secondary porosity by their ulterior dissolution and the elimination of the solution by hydrodynamism. They can also obliterate porosity and consequently permeability by solution and formation of cement by precipitation of new crystals in the pore space. The diagenetic influences will be analysed later in Chapter 7.

3.2.2. Influence of other Textural Components on Reservoir Characteristics

The other textural components, matrix and cement also have an important influence on the petrophysical characteristics of detrital reservoirs.

When the percentage of matrix and/or cement increases, the porosity and permeability diminish, since the fine particles, that make up the matrix, and the cement tend to occupy the pore space between the coarser elements.

The matrix is really an important component only in conglomerates, whereas in sands it is present only in very poorly sorted sand bodies.

Cement is developed after deposition either by chemical interaction between unstable grains and formation water, or by circulation in the pore space of solutions under hydrodynamic forces.

These different influences are synthesized in Table 3-1.

Table 3-1

Influence of textural parameters on porosity and permeability of detrital rocks.

TEXTURAL PARAMETERS		POROSITY ϕ	PERMEABILITY k
PARTICLES OR GRAINS	Grain size ↗	→	↗↗
	Sphericity ↗	↘	?
	Roudness ↗	↘	?
	Sorting ↗	↗↗	↗↗
	Packing (effect of compaction) ↗	↘	↘
MATRIX	percentage ↗	↘	↘
CEMENT	percentage ↗	↘	↘

3.3. TEXTURE OF CARBONATE ROCKS

The texture of carbonate rocks depends on the relative percentage of three components (particles, matrix and cement), and on the type of distribution of pores (Fig. 3-16).

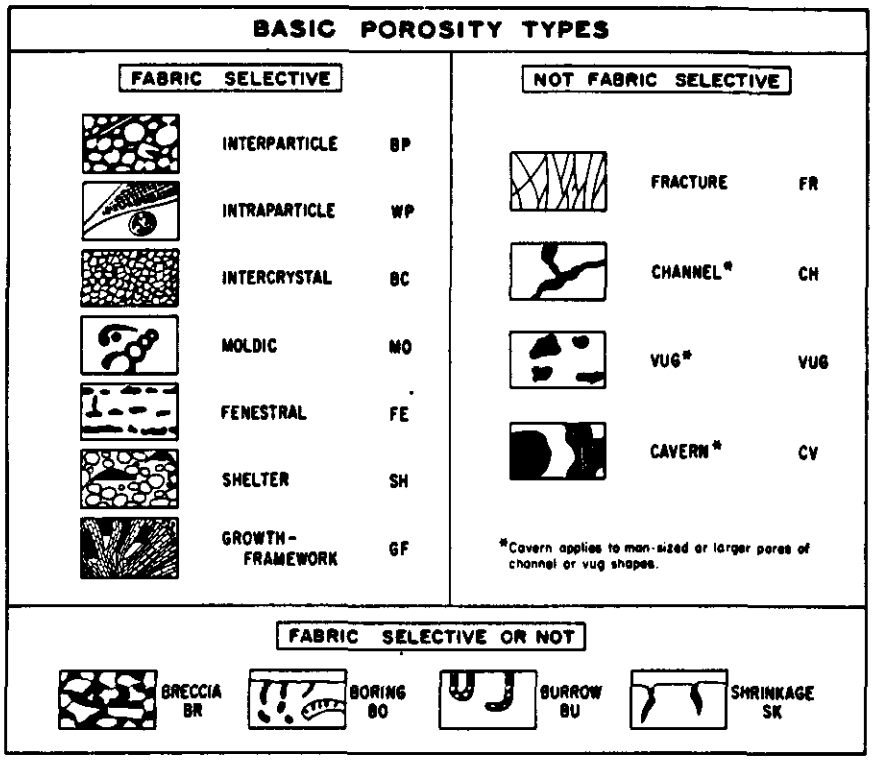

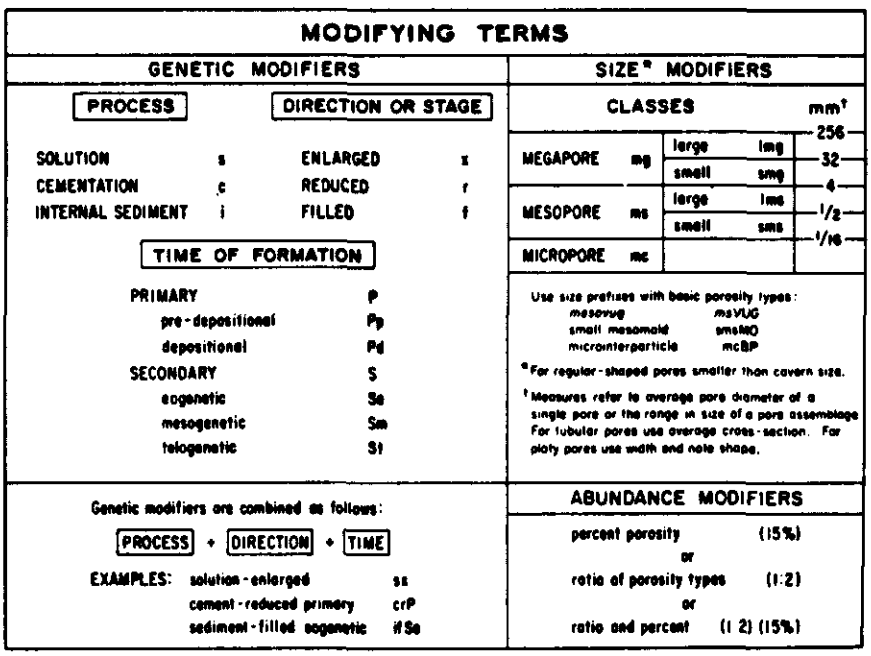

Fig. 3-16. - Porosity types in carbonates (from Choquette & Pray, 1970, fig. 2).

These different parameters are used to classify the carbonate rocks (Fig. 3-17 and Table 3-2).

It is obvious that porosity and permeability depend on texture as illustrated by Fig. 3-18 which shows their dependence on the texture of the carbonate rocks.

But, in these rocks we have to distinguish the original characteristics, i.e. those existing at the time of deposition, from present characteristics. In fact, the original texture may have been deeply modified as a result of diagenetic phenomena that are often precocious and more important in these formations than in detrital series. These modifications in texture consequently bring about a change in the reservoir characteristics themselves.

This is why these characteristics arise more from diagenetic phenomena that from texture, and why the study of porosity is so essential.

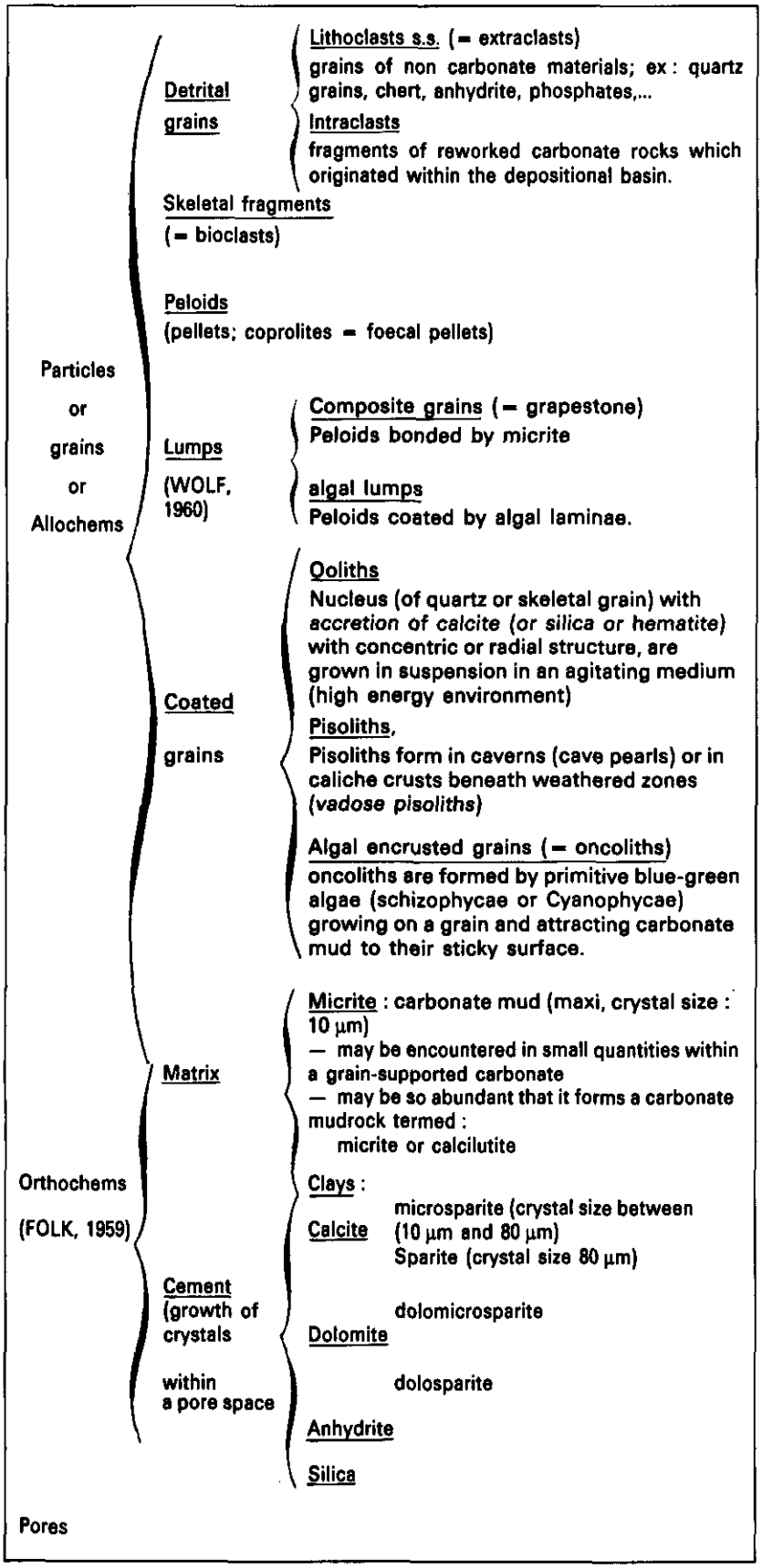

Fig. 3-17. - The textural components of carbonates.

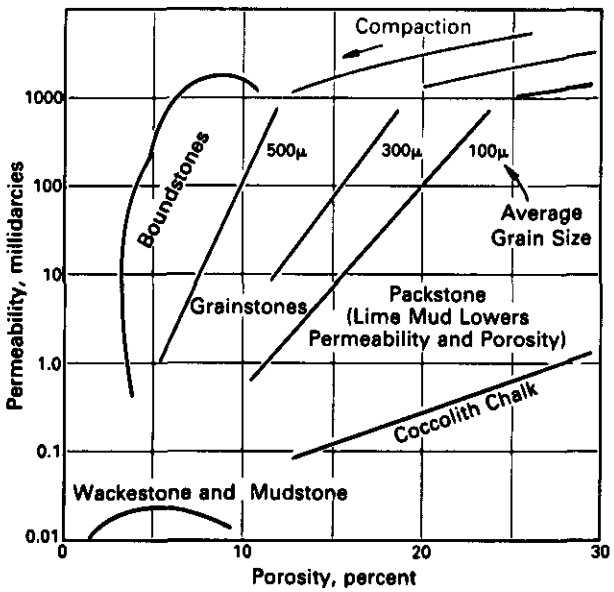

Table 3-2
The Dunham's classification of carbonate rocks based on depositional texture
(from Dunham, 1962).

Boundstone – Original components bound together in life, i.e. biogenic reefs

Mudstone <10% grains	Mud supported	Contain mud	Original constituents not bound together during life
Wackestone >10% grains			
Packstone	Grain supported		
Grainstone <10% micrite			

Crystalline carbonate – Primary depositional fabric destroyed by recrystallization

◀ Fig. 3-18. - Relationship between porosity and permeability for the five Dunham limestone classification (from Nurmi & Frisinger, 1983).

Table 3-3
Different types of porosity in carbonate rocks.

Time	Type	Illustration	Origin	
Predepositional	Intraparticle (1)			
Depositional	Interparticle or Intergranular		Sorting and packing	Fabric selective
	Shelter			
	Growth–framework		Framework accretion	
Post depositional	Intercrystalline		Replacement	
	Fenestral (2) *Laminated*		Organic or physical disruption	
	(= Bird's eye) *Irregular*			
	Moldic		Solution	not fabric selective
	Channel (3)			
	Vug (3)			
	Cavern (3)			
	Fracture		Physical or organic disruption	Fabric selective or not
	Breccia			
	Boring		Organic disruption	
	Burrow			
	Shrinkage		Dehydration	

Table 3-4
Comparison between porosity in sandstones and limestones
(from Choquette & Pray, 1970).

Aspect	*Sandstone*	*Carbonate*
Amount of primary porosity in sediments	Commonly 25–40%	Commonly 40–70%
Amount of ultimate porosity in rocks	Commonly half or more of initial porosity; 15–30% common	Commonly none or only small fraction of initial porosity; 5–15% common in reservoir facies
Type(s) of primary porosity	Almost exclusively interparticle	Interparticle commonly predominates, but intraparticle and other types are important
Type(s) of ultimate porosity	Almost exclusively primary interparticle	Widely varied because of postdepositional modifications
Sizes of pores	Diameter and throat sizes closely related to sedimentary particle size and sorting	Diameter and throat sizes commonly show little relation to sedimentary particle size or sorting
Shape of pores	Strong dependence on particle shape—a "negative" of particles	Greatly varied, ranges from strongly dependent "positive" or "negative" of particles to form completely independent of shapes of depositional or diagenetic components
Uniformity of size, shape, and distribution	Commonly fairly uniform within homogeneous body	Variable, ranging from fairly uniform to extremely heterogeneous, even within body made up of single rock type
Influence of diagenesis	Minor; usually minor reduction of primary porosity by compaction and cementation	Major; can create, obliterate, or completely modify porosity; cementation and solution important
Influence of fracturing	Generally not of major importance in reservoir properties if present	Of major importance in reservoir properties
Visual evaluation of porosity and permeability	Semiquantitative visual estimates commonly relatively easy	Variable; semiquantitative visual estimates range from easy to virtually impossible; instrument measurements of porosity, permeability and capillary pressure commonly needed
Adequacy of core analysis for reservoir evaluation	Core plugs of 1-in. diameter commonly adequate for "matrix" porosity	Core plugs commonly inadequate; even whole cores (~3-in. diameter) may be inadequate for large pores
Permeability-porosity interrelations	Relatively consistent; commonly dependent on particle size and sorting	Greatly varied; commonly independent of particle size and sorting

Table 3-3 illustrates the different types of porosity, and links them with original phenomenon and with time of pore formation. Table 3-4, from Choquette & Pray (1970), illustrates the differences between porosity in carbonate rocks and that in detrital rocks.

3.4. HOW TO OBTAIN INFORMATION ON TEXTURE FROM WELL LOGGING

The influence of textural components on log parameters is summarized in Table 3-5.

Thus, it clearly appears that some log measurements contain within themselves textural information. But it is not always simple to determine the origin of influence because several textural parameters may have similar effects. However, if we reexamine the problem, according to type of rock, it is sometimes possible to perceive the privileged influence of certain parameters. This is what we are going to analyse now.

3.4.1. Poorly-Consolidated Clastic Formation (Sand-Shale)

In this type of rock, texture is fundamentally linked to the properties of grains, whereas the matrix and cement, in particular, are the minor components. In this special case the purpose of log study will be to obtain, if possible, information on the size of grains, their sorting, arrangement, and orientation.

3.4.1.1. *Grain Size*

There is no general universal relation between the grain size and a log measurement. Nevertheless, in a number of cases we often observe, regionally, a very clear correction between the log and the size of grains.

Different authors (Sarma *et al.*, 1963; Alger, 1966) showed the existence of a correlation between resistivity, or the factor of formation, and the size of grains (Fig. 3-19).

Remark

In the example of this figure for the same value of R_w the formation factor increases when the size of grains increases. This seems to contradict the commonly accepted relation. This situation is undoubtedly due to the fact that in fresh water formations the importance of surface's conductance increases when the size of grains reduces.

Other authors have observed relations between a well logging parameter and grain size.

In the examples of Fig. 3-20 it is obvious that a correlation exists between gamma-ray and grain size measured on core samples. Gamma-ray increases when grain size decreases, because radioactivity is linked with the finest grains. These fine grains consist of clay minerals. Further analysis shows that these minerals are fundamentally of detrital (or allogenic) origin and are of structural or laminated type. Indeed, it is hardly conceivable that authigenic clays occupying the pore space would show such evolution, because in this case the percentage in the rock does not significantly evolve with granulometry.

Table 3-5
Relationship between textural parameters and well log responses
(from Serra, 1984).

TEXTURAL PARAMETERS			RESERVOIR CHARACTERISTICS DEPENDING ON TEXTURAL PARAMETERS		WELL LOGGING PARAMETERS AFFECTED	RELEVANT LOGGING TOOLS
TEXTURE	PARTICLES OR GRAINS	SIZE	• POROSITY	ϕ	$R, \rho b, I_{xo}, \Delta t, \Sigma, tpl, P_e$	LL_s, LL_d, SFL, IL_m $IL_d, ML, MLL, MSFL$
		SHAPE (ROUNDNESS, SPHERICITY)	TOTAL POROSITY	ϕ_t		FDC, LDT, CNL (or SNP), BHC, TDT, EPT, GST
		SORTING PACKING ORIENTATION	PRIMARY POROSITY	ϕ_i		
			EFFECTIVE POROSITY	ϕ_e		
			• TORTUOSITY OR *CEMENTATION FACTOR*	m	R, F, Δt, tpl	LL_s, LL_d, SFL, IL_m $IL_d, ML, MLL, MSFL$, BHC, EPT
	MATRIX	PERCENTAGE	• SIZE OF PORES AND THROATS WHICH CONTROL			
		NATURE	PERMEABILITY	k	• $(Sw)_{irr}$ • di • k, k_{xo}, k_{xo}	LL_s, LL_d, SFL, IL_m $IL_d, ML, MLL, MSFL$ SP
			HORIZONTAL	k_H		
			VERTICAL	k_V	• SP curve shape	SP
			• *WETTABILITY*			
	CEMENT	PERCENTAGE	• ANISOTROPY		• λ	LL_s, LL_d, SFL, IL_m $IL_d, MLL, MSFL$
		NATURE				

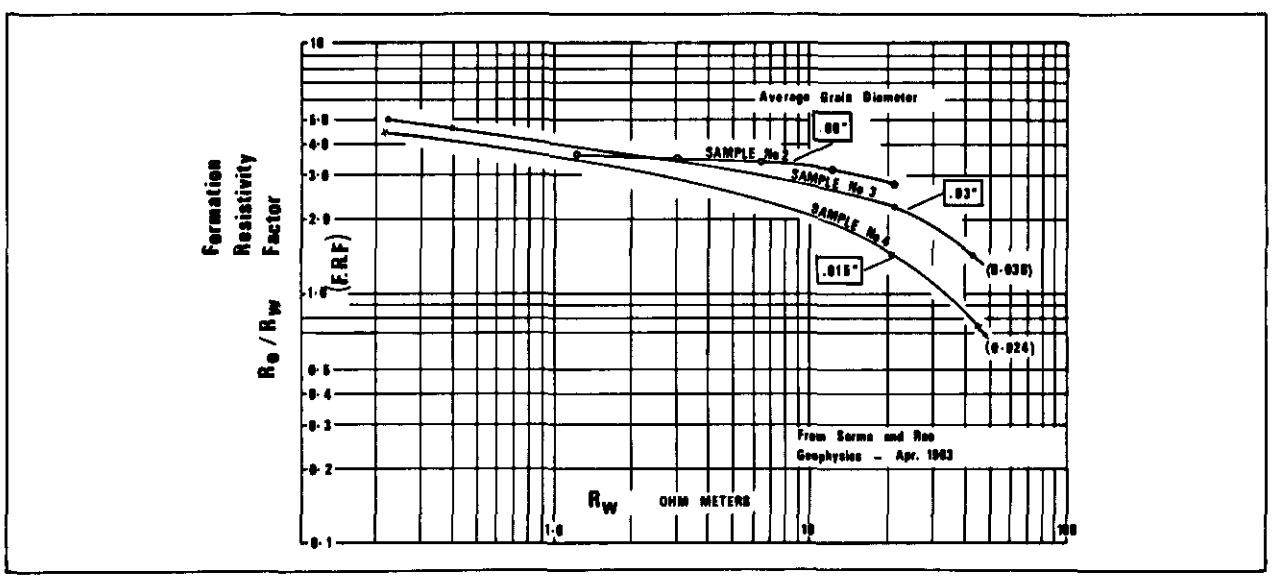

Fig. 3-19. - Relationship between formation factor, resistivity and grain size (from Sarma & Rao, 1963).

The « bell » or « funnel » shapes of spontaneous potential, gamma-ray, or resistivity curves (Fig. 3-21) introduced by SHELL geologists around 1956, are another application of this relation between a curve and a textural parameter.

In these cases if we cannot precisely define the absolute grain size without preliminary calibration, we are nevertheless always able to determine a relative size. These shapes (Fig. 3-22), in fact, explain the normal graded-bedding (« fining upward ») or reverse graded-bedding (« coarsening upward »). In other words we can conclude that distribution of the shales is essentially of structural and/or laminated type.

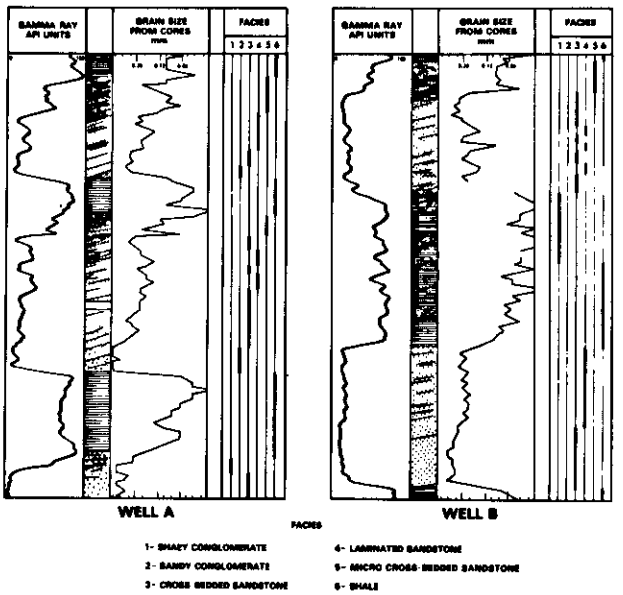

Fig. 3-20. - Correlation between natural radioactivity and grain size (from Serra & Sulpice, 1975).

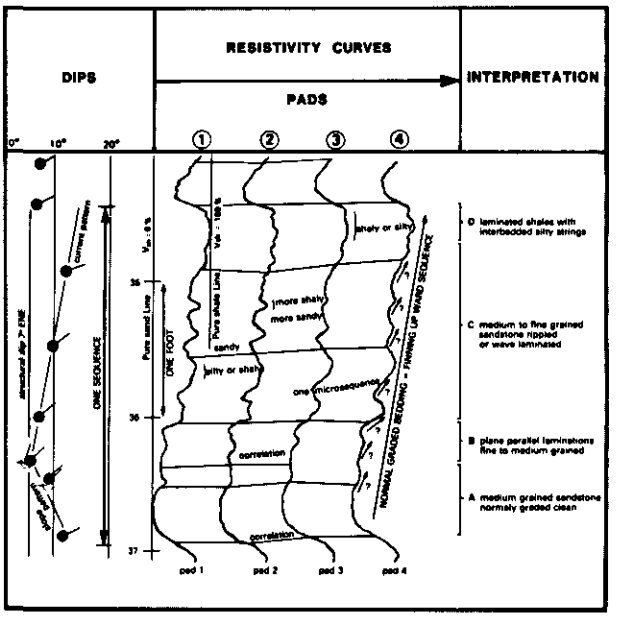

Fig. 3-22. - Example of structural and partly laminated shales as they can be recognized on dipmeter resistivity curves. This *figure is an enlargement of one sequence of Fig. 3-27 (between* 34.5 and 37 ft).

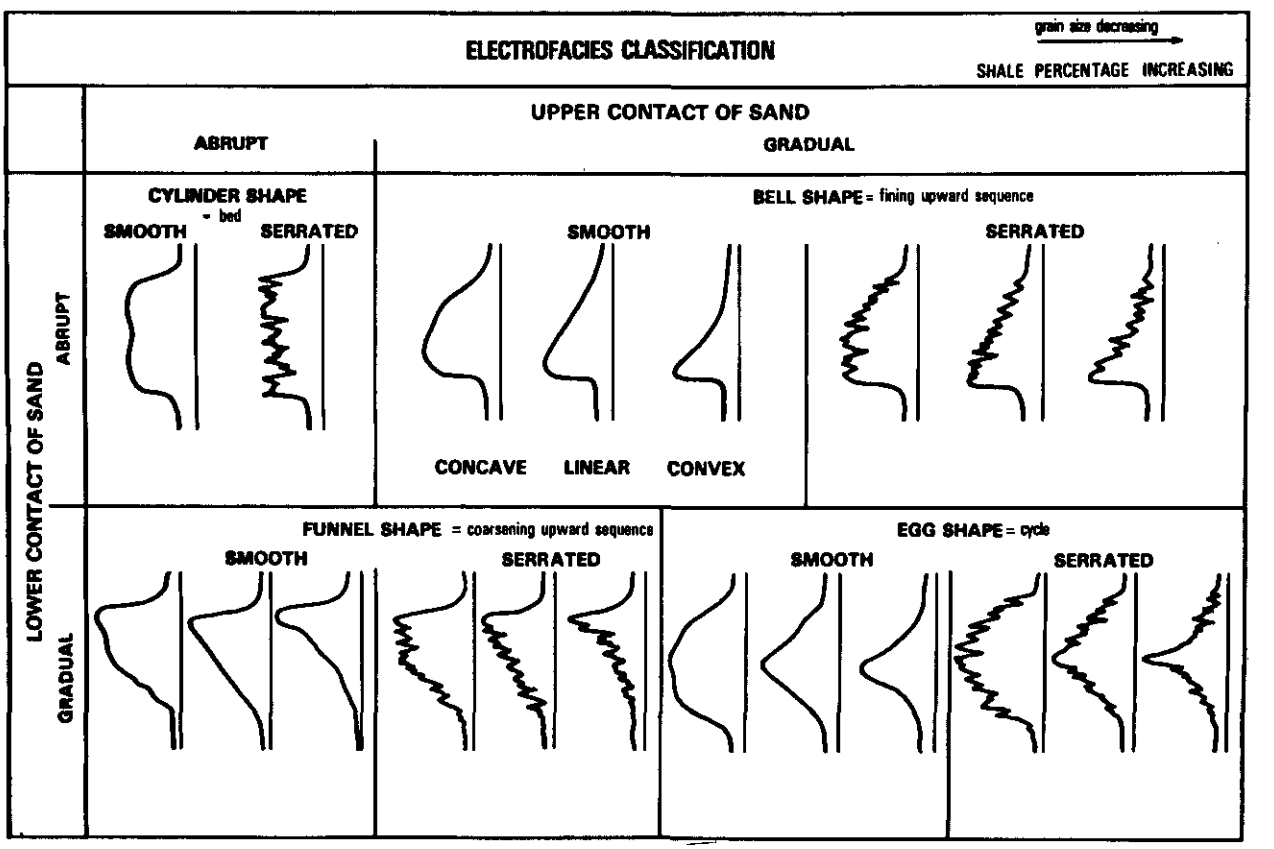

Fig. 3-21. - Relationship between SP curve shape and grain size or shaliness (adapted from SHELL's documents).

We can also convert these curves into shale percentage and into permeability if a preliminary calibration was done with the help of core measurements (Fig. 3-23).

The relation between radioactivity and granulometry is not always proved. It may happen that the silty levels are more radioactive than shales (Fig. 3-24). In this case it is necessary to have

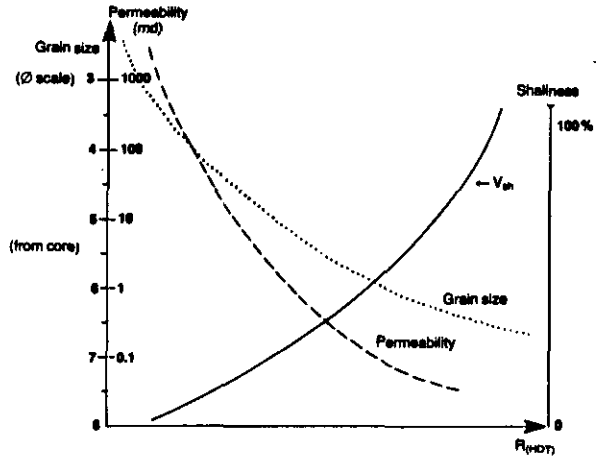

Fig. 3-23. - Schematic relationships between dipmeter resistivity on one hand, and grain size, shaliness and permeability on the other hand. These relationships are applicable to the case illustrated by Fig. 3-27.

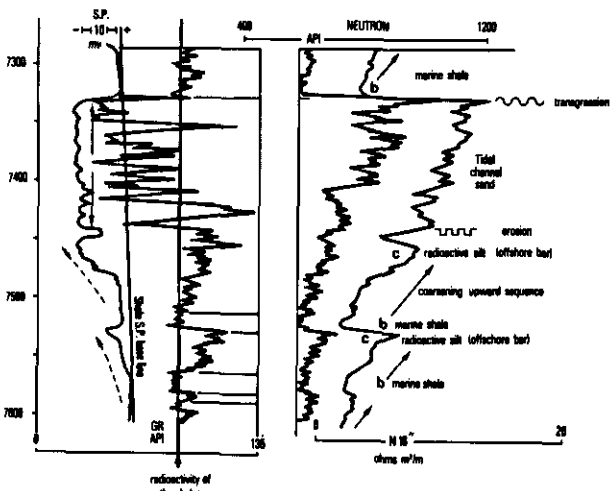

Fig. 3-24. - Example of silts being more radioactive than shales. The grain size evolution can still be detected on resistivity, SP and neutron curves (from Serra & Sulpice, 1975).

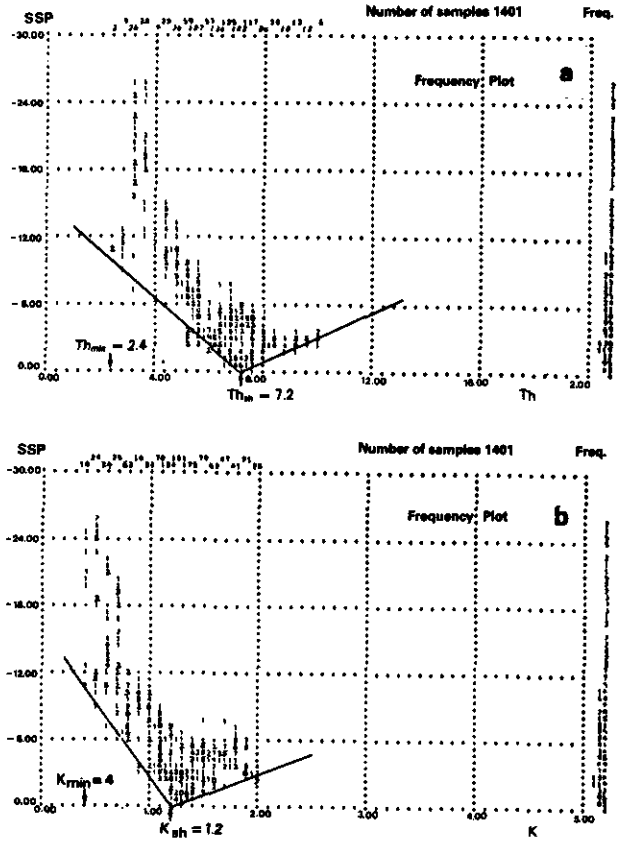

Fig. 3-25. - Examples of crossplots of SSP vs thorium (a), and potassium (b) contents. They define the Th_{sh} and K_{sh} for shales. The thorium and potassium contents of « clean » sands suggest the presence of radioactive minerals such as feldspars, micas and zircon. They show the existence of silts more radioactive than shales.

several log recordings, enabling the determination of grain size. The *« crossplot »* combining two logs, such as gamma ray and spontaneous potential (Fig. 3-25) help in this analysis, particularly if the technique of *« Z-plots »* is used. This technique presents the plotting of the value of a third, parameter such as GR (gamma ray) Th or K (amount of thorium or potassium obtained from a spectrometry of natural gamma radiation), ρ_b, ϕ_N, or SP (Fig. 3-26b), at the intersection point of the two other values on the cross-plot.

If the thickness of each granulometric sequence is very small the logging macrodevices cannot detect these grain size evolutions.

Fig. 3-26a. - Composite-log in sandstones rich in heavy thorium and uranium bearing radioactive minerals . Observe around 200 ft the increase in GR, thorium, uranium and ρ_b, and the more or less constant value of neutron and sonic at the same time. ▶

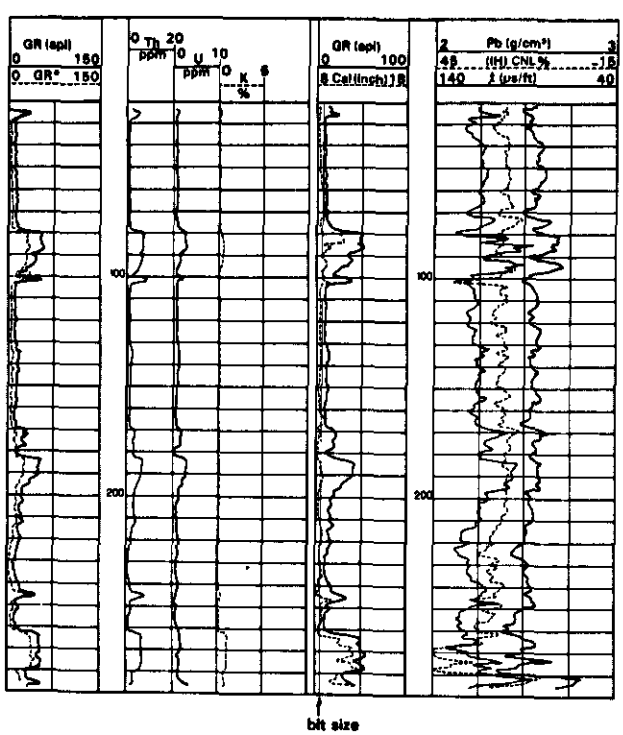

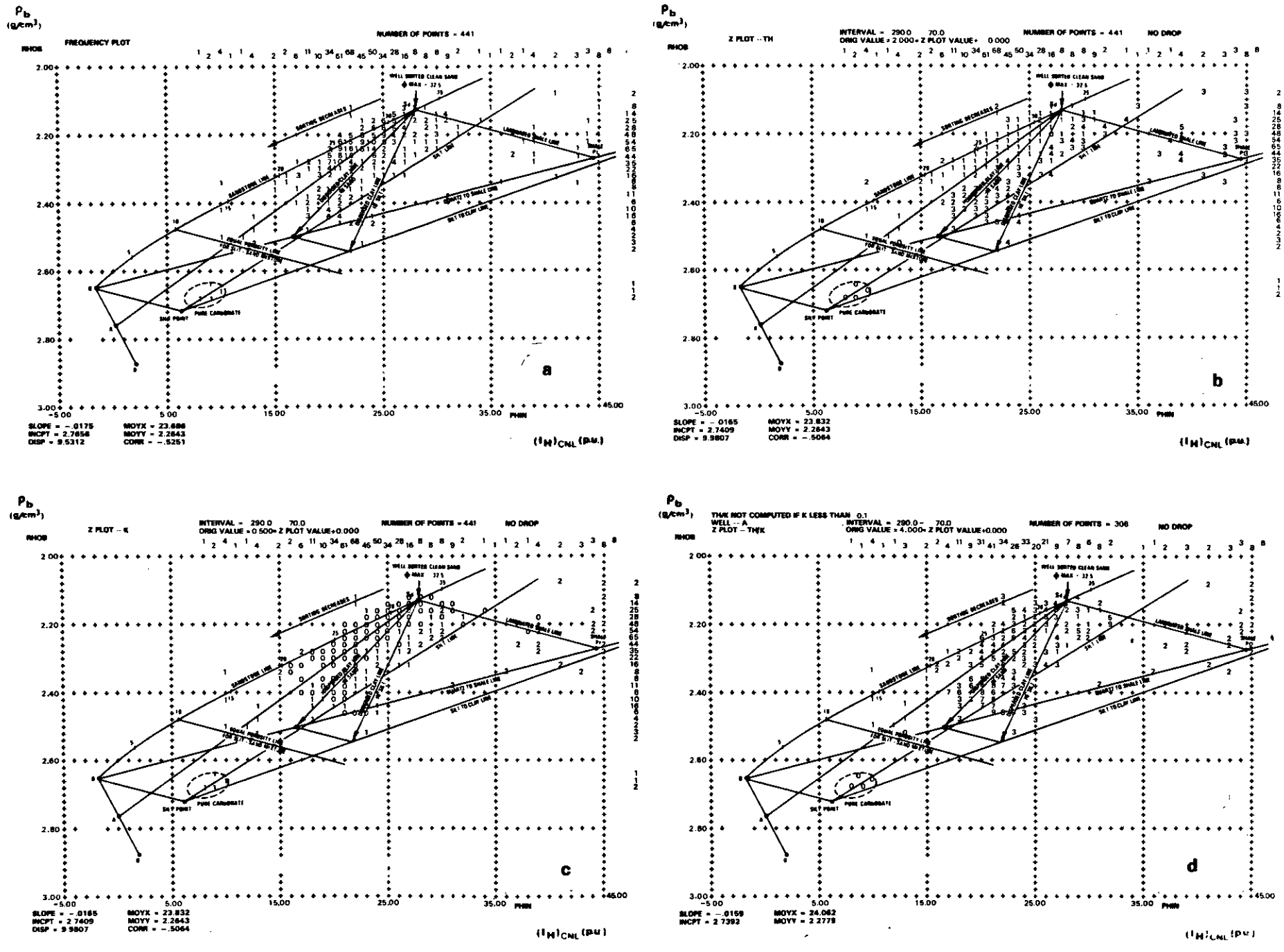

Fig. 3-26b. - Crossplots of ρ_b vs ϕ_N, with frequency (a), thorium content (b), potassium content (c), and thorium-potassium ratio (d), on the same interval than Fig. 3-26a, and their interpretation.

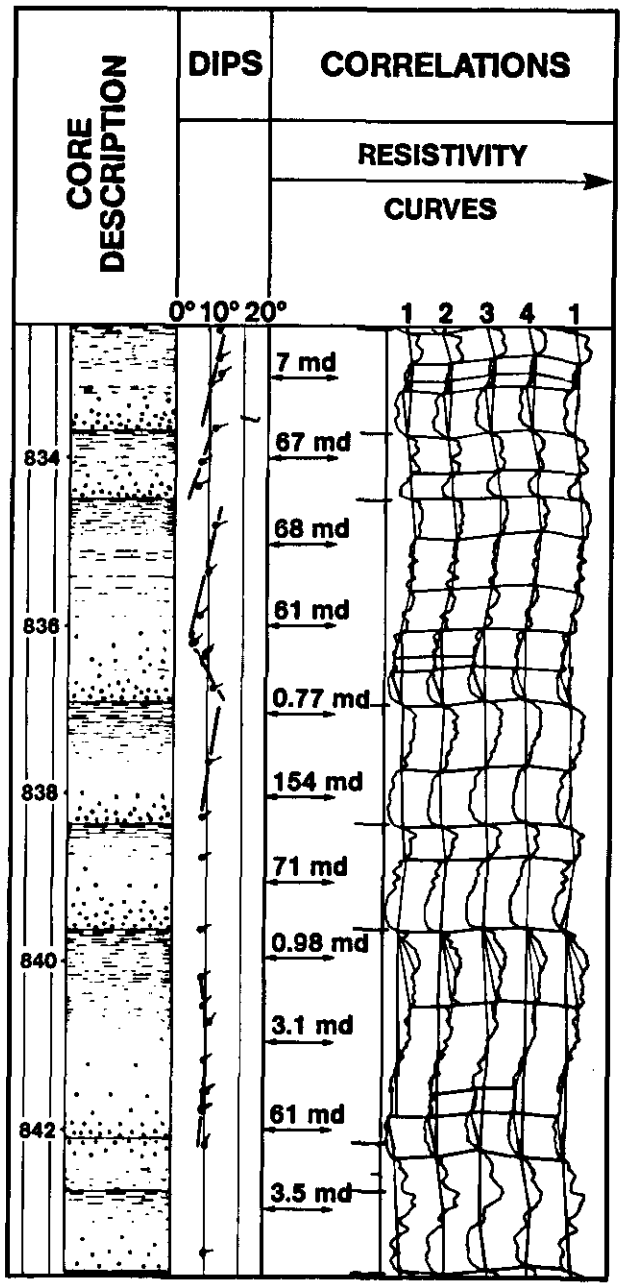

Fig. 3-27. - Example of grain size evolutions very well detected on dipmeter resistivity curves, even in thin sequences (1 to 2 feet thick). These evolutions are confirmed by the core description reproduced alongside.

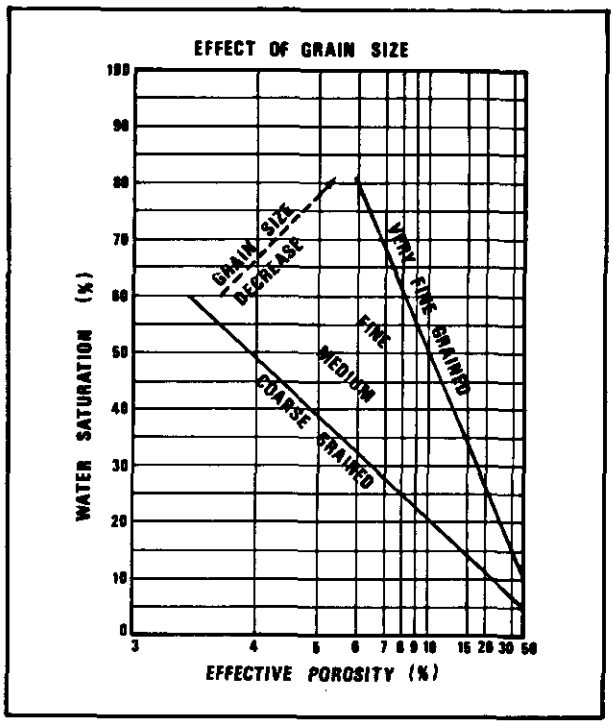

Fig. 3-28. - Relationship between irreducible water saturation, porosity and grain size.

It is better, then, to use the resistivity curves of dipmeter tools HDT * or SHDT *. Their high resolution allows to detect sequences of a few centimetres (Fig. 3-27).

If a poorly-consolidated detrital reservoir contains hydrocarbons, we can observe the existence of a good correlation between grain size and irreducible water-saturation (Fig. 3-28). The latter depends, in fact, on permeability that depends, in turn, on grain size (Fig. 3-29).

Lastly, the invasion diameter, as it can be deduced from a microlog, may constitute a good indicator of grain size. The example of Fig. 3-30 shows an evolution of microlog resistivity curves which can be correlated with changes in grain size (normal graded-bedding in this case), - the porosity being the same in this interval - , these changes affecting the diameter of invasion.

3.4.1.2. *Sorting*

One can approach this parameter with a study of porosity evolution. In fact in sandy formation, at a given depth, we can reasonably assume that arrangement and packing are the same for all grain sizes, the porosity generally decreasing when sorting decreases.

Fig. 3-31 gives an example of the change in sorting. Levels 9 and 10 present an average porosity close to 35 %. Taking into account their depth (7000 feet) this high porosity is certainly due to a good sorting. The low radioactivity of these levels combined with a strong deflection of spontaneous potential seems to indicate the presence of radioactive minerals other than shales. Granulometry of these levels must be fine to very fine. Level 11 shows a lower porosity (25 %) with less radioactivity and an identical spontaneous potential. This drop in porosity, seems, therefore to indicate a poorly sorted sand (coarse to fine grained).

Again, the best way to analyse this phenomenon is to make a crossplot (type Z-plot), combining the hydrogen-neutron index and the density with

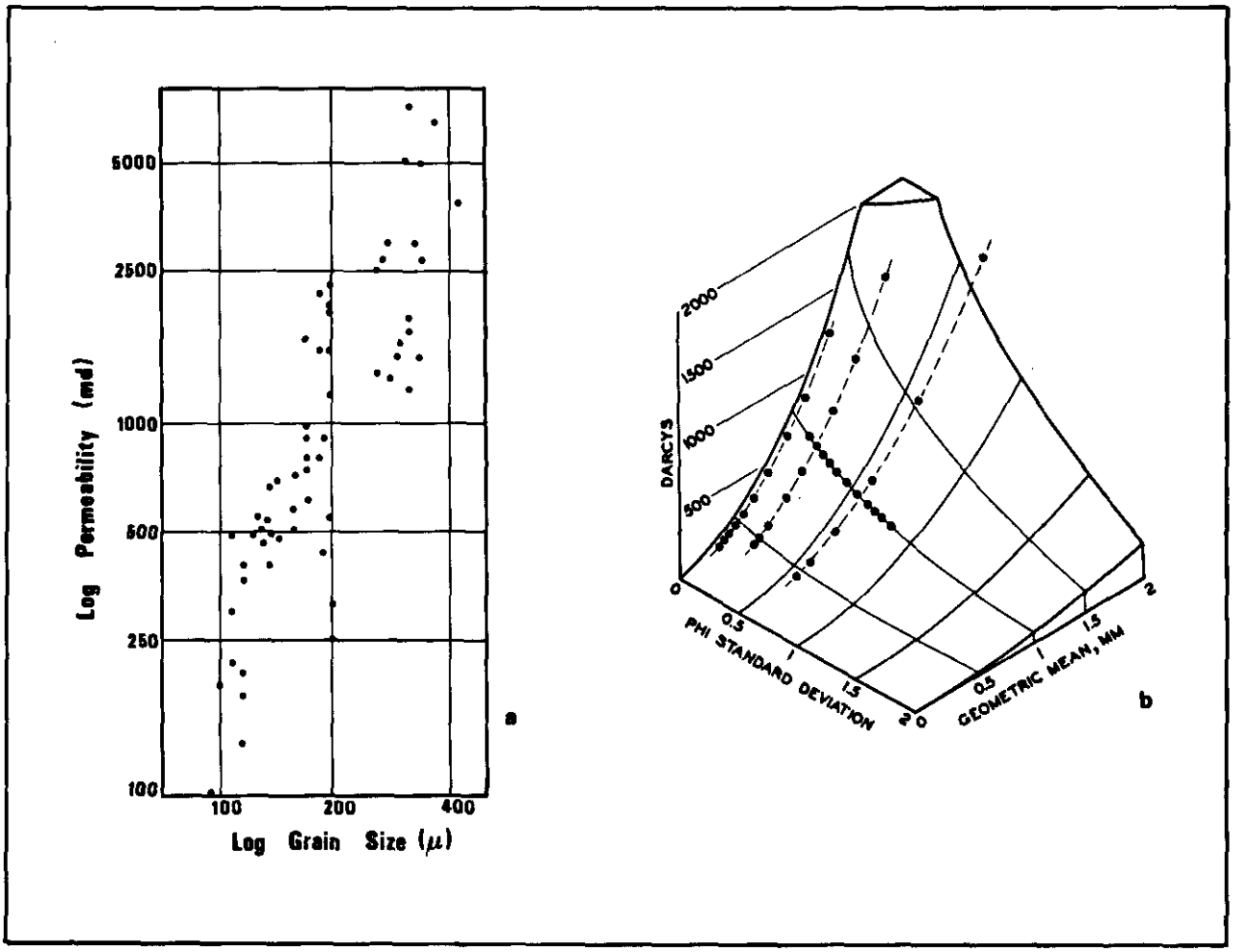

Fig. 3-29. - a) : Relationship between permeability and grain size (from von Engelhardt, 1960). b) : Relationship between permeability, mean grain size and the phi standard deviation (from Krumbein & Monk, 1942).

radioactivity, spontaneous potential values, or the amount of thorium or potassium. On such a crossplot (Fig. 3-32), from the point defining the maximum porosity for a given interval (corresponding to the best sorting), a drop in porosity along the sand line (not less than 15 %), represents decrease in the level of sorting.

Remark

This porosity drop could correspond to a cementation by precipitation of silica. Even if this hypothesis cannot be totally rejected, it is however unlikely if we consider the existing high porosity.

3.4.1.3. *Grain orientation*

A preferential orientation of grains must theoretically be indicated by an anisotropy in resistivity reflecting an anisotropy in the permeability from which it is derived. But, the contrast between vertical and horizontal resistivities being small (around 1.5), it seems tenuous to attribute any variation in the two horizontal axes to anisotropy because other explanations can be responsible of this variation (pad contact, mud thickness...).

It does not seem possible at the present time to approach this phenomenon quantitatively. However, we can approach it by means of relative deflections or, more specifically, by directions of currents determined from dip measurements and from « red » or « blue » patterns on arrow plots.

3.4.1.4. *Arrangement or Packing*

This parameter is not accessible, because we can reasonably admit that after a burying of several hundred metres, packing of sediment is such that arrangement of grains becomes more compact (or closed).

The study of porosity within a short interval, or even more understandably at any given point, cannot reveal information on packing. All porosity variations can be explained, in a plausible manner, by a change in sorting or by diagenetic effects.

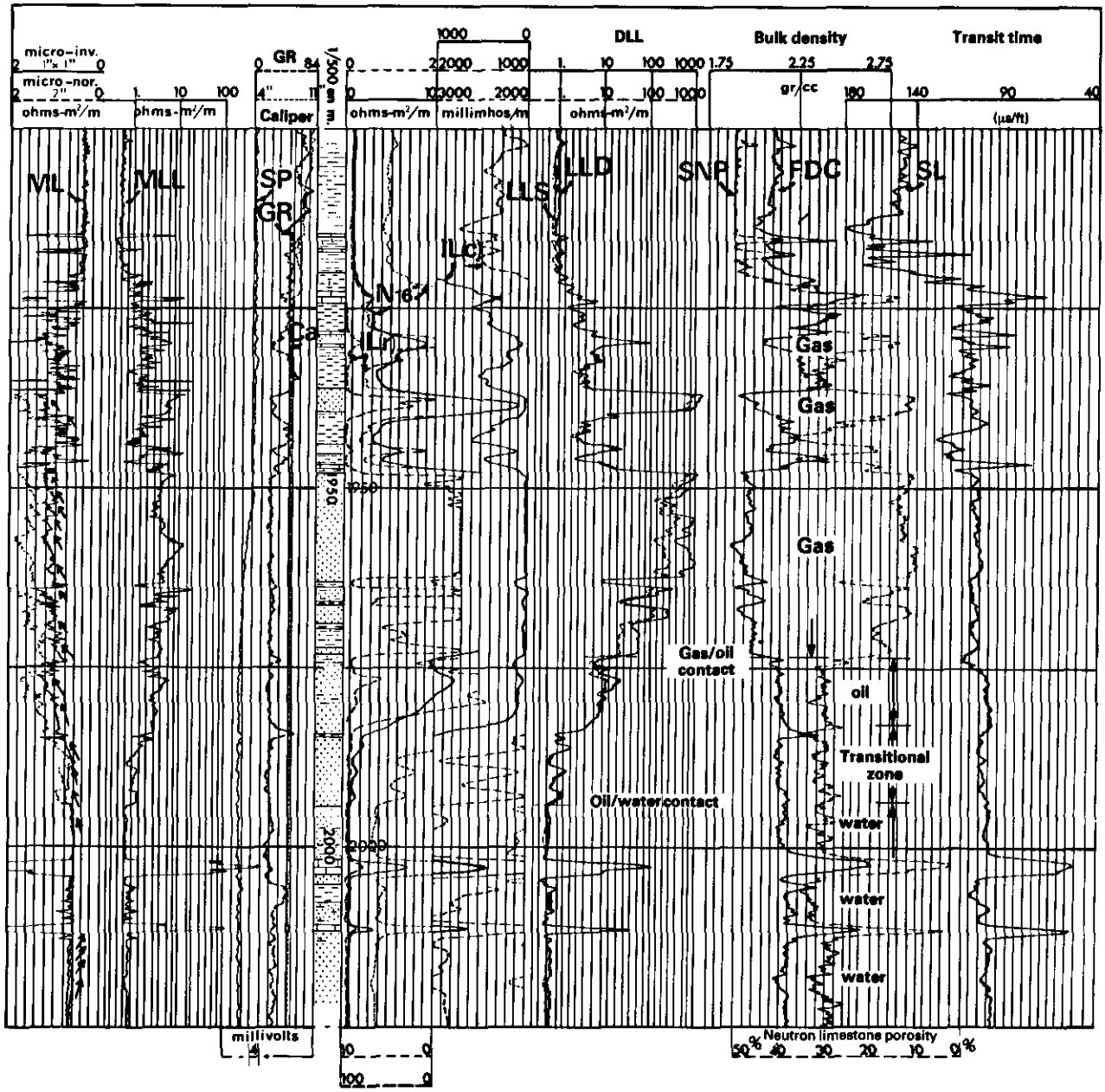

Fig. 3-30. - Observe microlog resistivity curves. Their evolution reflects changes in the diameter of invasion, possibly in relation with grain size decrease. Observe also the number of sequences which can be detected in this massive sand reservoir thanks to the microlog.

On the other hand the evolution of porosity with depth on a long interval will explain the modification of packing under the effect of compaction, and/or of diagenesis. This aspect will be analysed with the study of compaction.

3.4.1.5. *Grain shape*

If the sandy formation is chemically immature and, therefore rich in feldspars, mica etc..., shown by recordings of density and by natural gamma ray radiation (relatively high amounts of potassium), we can deduce the existence of a textural immaturity and consequently of angular grains. On the other hand, if the sand appears to be very clean, with a very low radioactivity and high porosity, we can suppose the existence of a chemically and texturally mature sand, hence probably well-washed or winnowed and well-sorted sand with round spherical grains.

From Sen (1980, 1981), the grain shape has a strong influence when the electromagnetic field is applied perpendicularly to the flakes (micas). Thus, sands rich in mica flakes should show a higher

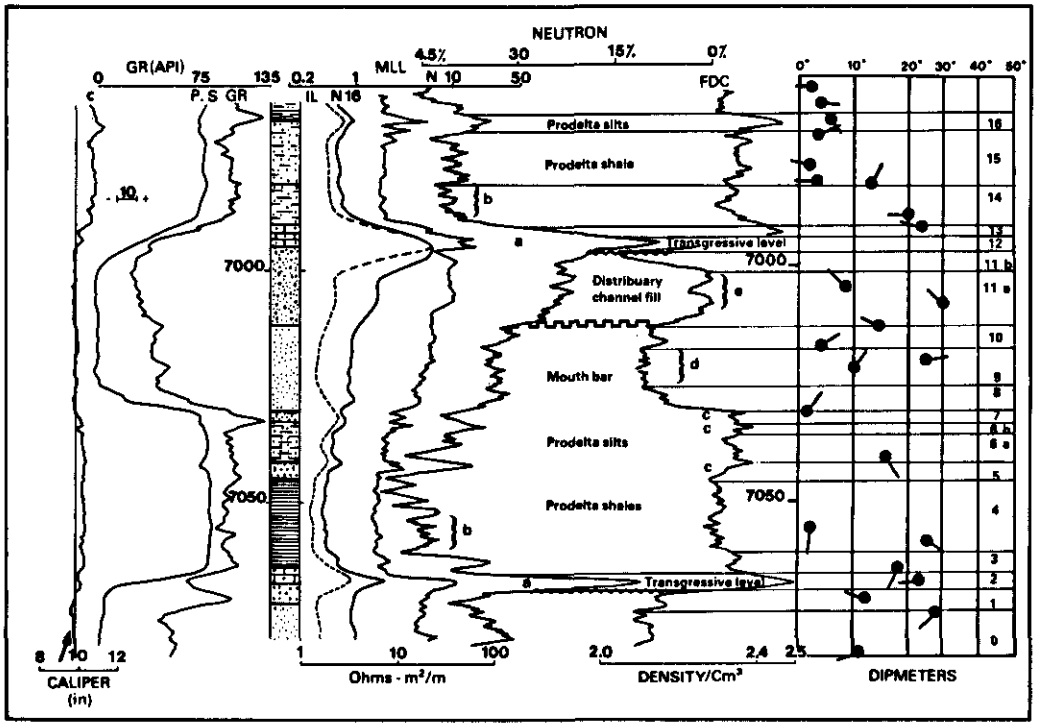

Fig. 3-31. - Observe the change in porosity from levels 9 and 10 and 11. It corresponds to a change in sorting. The two lower sands are fine, clean, well sorted, slightly radioactive; the upper sand is coarser and badly sorted (from Serra & Sulpice, 1975).

dielectric constant than the one expected from the measured values for quartz and mica. The analysis of the data recorded by the EPT tool should enable determination of the orientation of mica flakes and consequently give an indication of the existence of horizontal or vertical permeability barriers in a micaceous sand.

3.4.2. Detrital Consolidated Formations (Sandstones)

The cement proportion in this case is more important. Porosity is lower, so it is not therefore always easy to draw certain obvious conclusions concerning the grains. However, for the same content of cement, a decrease in porosity must be attributed to a diminution of sorting.

The type of cement can be determined from the mineralogical composition of the rock, obtained from log analysis. In the case of ambiguity (calcitic or dolomitic cement ?), we have to remember that because cementation is always a postdepositional phenomenon, the volume of cement added to the porosity value cannot exceed the maximum porosity value that existed at the beginning of the cementation process.

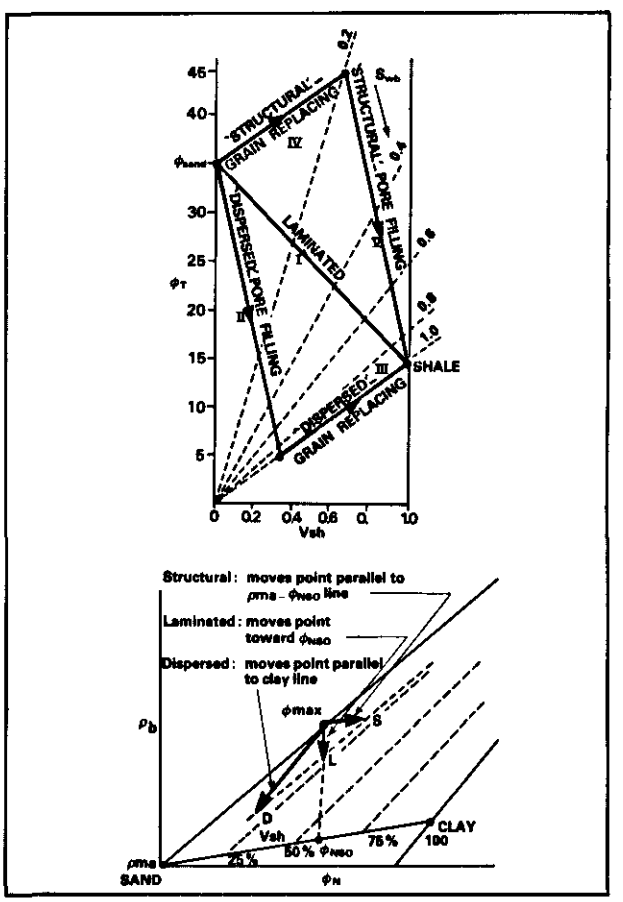

Fig. 3-32. - Sorting decrease, grain size evolution and type of shale distribution can be predicted from crossplot analysis. ▶

Thus, if we compute from crossplots a percentage of calcite cement which is higher than usual, either a hypothesis of dolomitic cement must be accepted, or, if the existence of calcitic cement is confirmed from other data (Pe from lithodensity tool LDT, cutting analysis), the presence of detrital limestone particles (bioclasts, oolites...), associated with grains of quartz or feldspars must be considered.

3.4.3. Conglomerates

When the pebbles are larger than the electrodes they can be detected by dipmeter tools or by the formation microscanner tool (FMS * [2]). The pebbles are generally more resistive than the surrounding matrix in which they are embedded. Consequently, each pebble is distinguished by a peak of resistivity whose shape varies with the size, the proportion and the arrangement of the pebbles. This gives a heterogeneous aspect to the curves with a practically total absence of correlations between them (Fig. 3-33). When the pebbles touch each other (« grain supported conglomerate »), the peaks are very close; where the pebbles are isolated in a sandy or shaly-sandy matrix (« mud supported conglomerate »), the peaks are isolated (Fig. 3-34). The other open-hole logs may indicate a detritic formation dominated by quartz and often feldspars and micas, or by pebbles originating from igneous rocks. The NGS tool may be very useful to determine the type of radioactive minerals.

With the FMS image one can even determine the average size of the pebbles and sometimes their orientation (Fig. 3-35) if they have a diameter greater than the diameter of the buttons (5 mm).

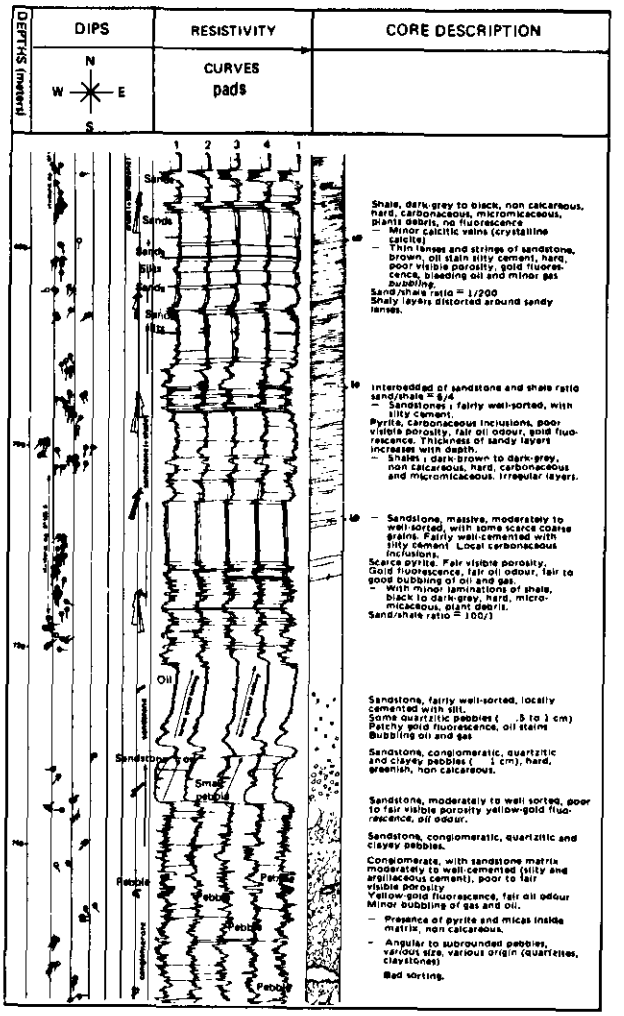

Fig. 3-33. - Example of grain-supported conglomerate.

3.4.4. Carbonate Formations

We know that in this type of formation the precocious diagenetic effects have a tendency to completely modify the initial texture. Therefore, in this particular case, it will, exceptionally, be possible to obtain information on texture.

The dipmeter resistivity curves after correlation with cores, may indicate some types of texture. Fig. 3-36 shows that calcirudites or boundstones, calcarenites or grainstones and calcilutites or mudstones can be recognized from the shape of resistivity curves.

As shown by Fig. 3-37 an excellent agreement between the core description given in terms of constituent percentages and one resistivity curve is obvious. It allows a very detailed description of the formation (Fig. 3-38) in terms of mudstone, wackestone, packstone, grainstone and even boundstone. It is of considerable interest for the

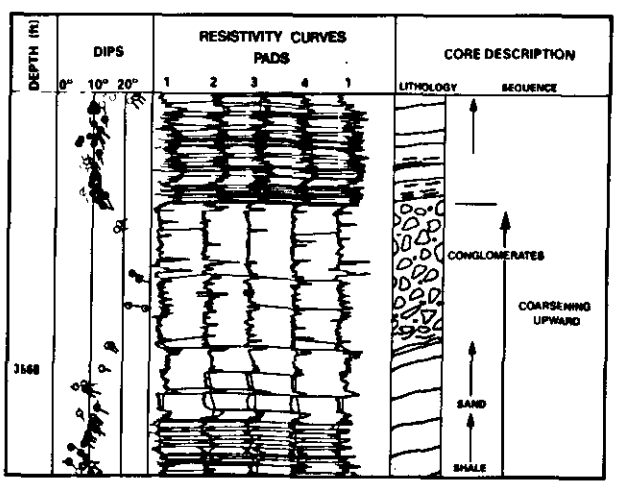

Fig. 3-34. - Example of mud-supported conglomerate. Observe isolated peaks on resistivity curves.

palaeogeographic reconstruction of a reefal environment, especially if natural gamma ray spectrometry (NGS tool) data, the photoelectric index

[2] The tool will be presented in the next chapter.

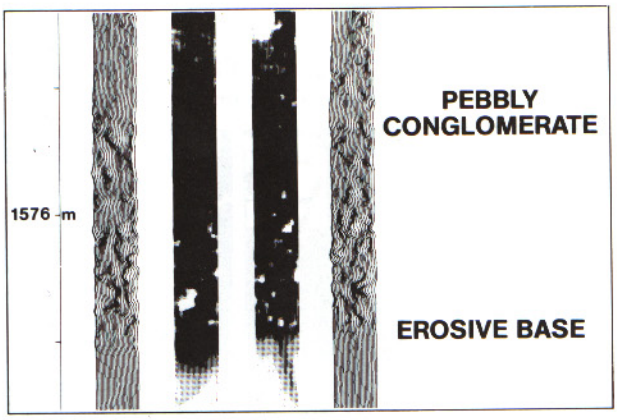

Fig. 3-35. - Example of pebbles as they can be recognized on FMS images (courtesy of Schlumberger).

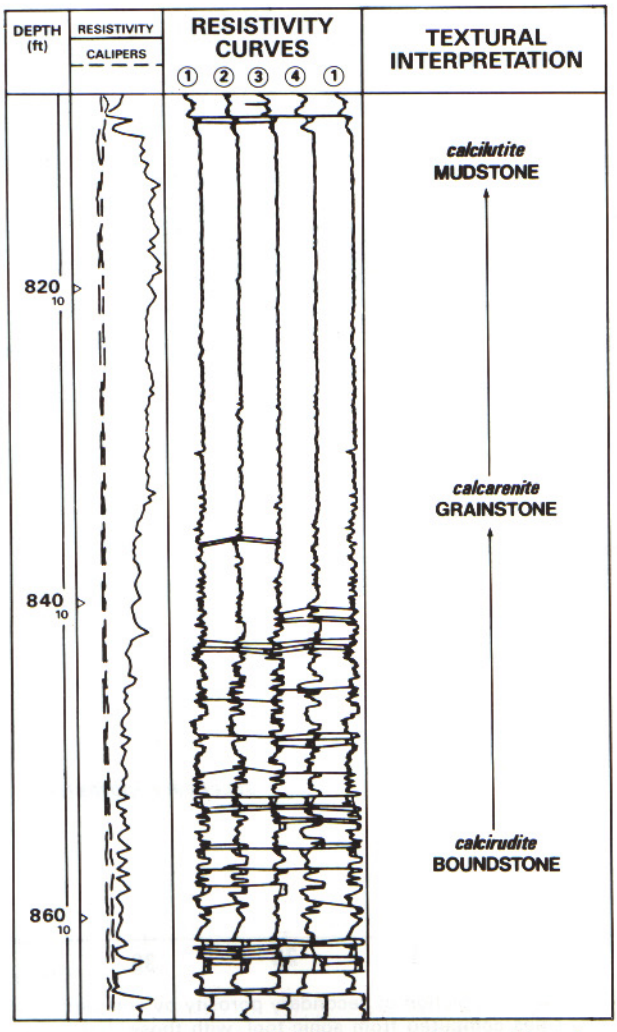

Fig. 3-36. - Example of GEODIP response in a reefal environment. Note that the aspect of the dipmeter resistivity curves (HDT tool) enables separation of boundstone or calcirudite, grainstone or calcarenite, and mudstone or calcilutite following terms used by Dunham (1962), or Grabau (1903).

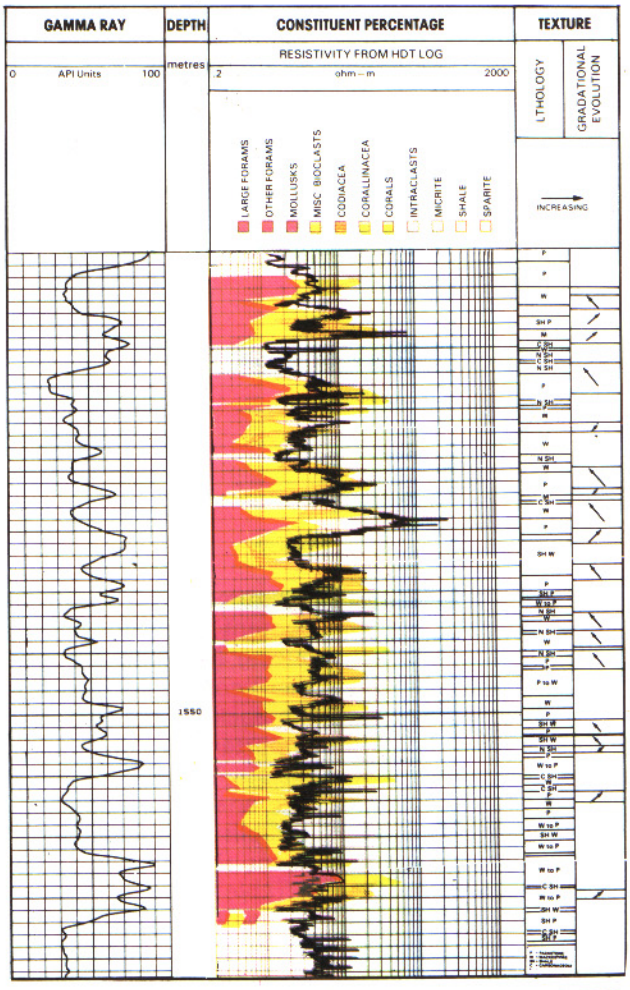

Fig. 3-37. - Comparison of textural interpretation of HDT micro-resistivity curves with core description (from Schlumberger, Well Evaluation Conference, India, 1983).

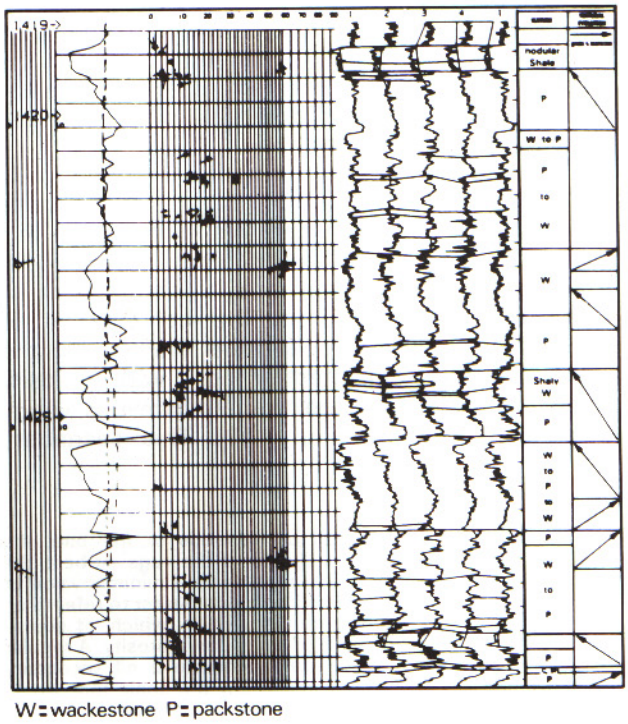

Fig. 3-38. - Very detailed interpretation of dipmeter curves in a carbonate formation of India (from Schlumberger, Well Evaluation Conference, India, 1983). ▶

W = wackestone P = packstone

Table 3-6
Relationship between dipmeter signatures and lithofacies in carbonates
(from Theys *et al.*, 1983).

GEODIP OR LOCDIP SIGNATURE					FACIES
ACTIVITY OF THE CURVES	DENSITY OF CORRELATIONS	DIP MAGNITUDE	DIP PATTERNS	MODE	
VERY LOW	LOW TO NIL	-	-	-	CALCILUTITE, MUDSTONE, CHALK
MEDIUM	MEDIUM TO LOW	-	-	-	CALCARENITE OR WACKESTONE, PACKSTONE OR GRAINSTONE NEAR REEF
MEDIUM	MEDIUM	MEDIUM	BLUE SOMETIMES RED	UNI	FORESET BEDDING OOLITIC OR BIOCLASTIC SHOALS DIP AZIMUTH INDICATES THE MAIN CURRENT DIRECTION
		VARIABLE		SCATTER	CROSS-BEDDING
MEDIUM	HIGH	LOW	GREEN	UNI	LAMINATED MUDSTONES OR MARLS OR SHALES
			RED	UNI	STRUCTURAL DIP MUST BE READ HERE DRAPPING OF A PREVIOUS HIGH (REEF, BAR, ..)
HIGH	LOW		SCATTER	-	CALCIRUDITE, WACKESTONE (REEF TALUS) OR BOUNSTONE (REEF) OR ANHYDRITIC NODULES (SUPRATIDAL FLATS) (see ϕ_s for recognition) or bioturbation

(Pe), and the density measurement (LDT tool) are available. The uranium content measured by the NGS tool will reflect reducing (uranium present), or oxidizing (uranium absent) conditions, which in turn may help to locate the back- or the fore-reef. The Pe will indicate the importance of dolomitization.

By comparison with core analysis an empirical relationship has been established between (a) curve and dip parameters, and (b) facies in carbonates. It is reproduced in Table 3-6.

A high porosity accompanied by shallow invasion, if it is continuous along a certain interval, can explain the presence of chalk. Of course, the other open-hole logs must indicate a limestone composition.

The existence of vugs is sometimes easier to determine. With the help of the formation microscanner tool (FMS), the vugs can be even seen (Fig. 3-39). They correspond to conductive peaks on the resistivity curves, or to dark irregular spots on the images. The other open-hole logs will confirm the carbonate nature of the rock.

The vugs are connected to secondary porosity due to the dissolution of calcite or dolomite crystals by water circulation. We know that, in this case, the sonic tool does not « see » this secondary porosity[3]. Consequently, a comparison of porosity determined from the combination of density and neutron tools (tools that « see » the total porosity connected or not), with porosity deduced from sonic tool will indicate this vuggy secondary porosity (Fig. 3-40). This secondary

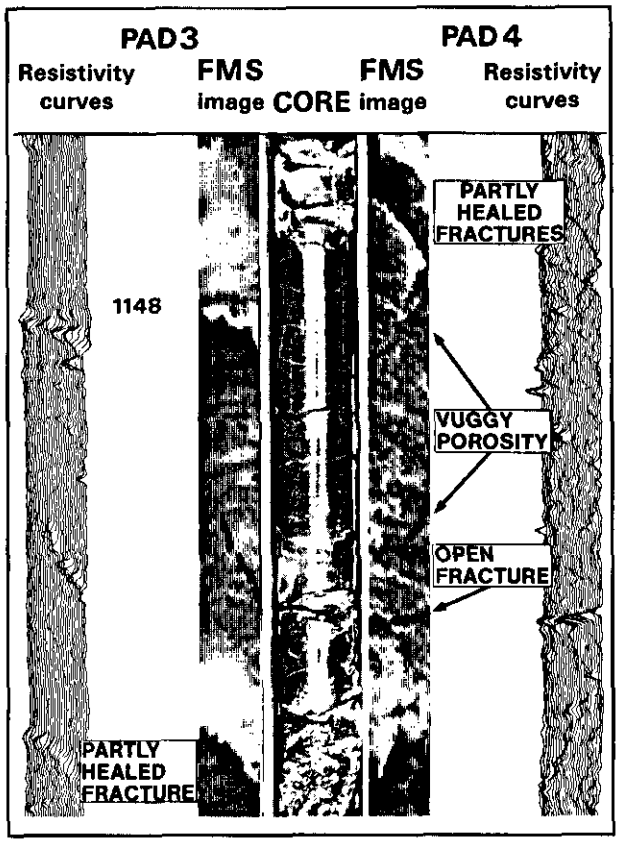

Fig. 3-39. - Examples of vugs as they appear on FMS images (courtesy of Schlumberger).

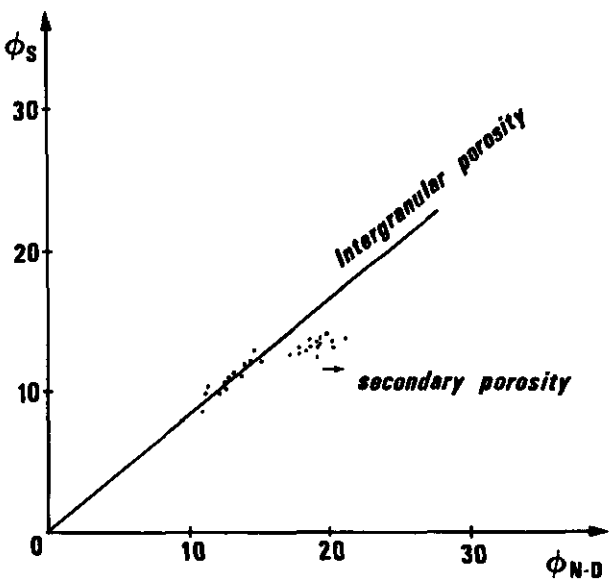

Fig. 3-40. - Detection of secondary porosity by comparison of porosities computed from sonic tool, with those deduced of the neutron-density combination.

[3] In fact, the first arrival corresponds to the one, the trajectory of which, has missed most of the vugs. At best, the secondary porosity index (SPI) represents a minimal value of the secondary porosity. It would be more correct to refer to an index of heterogeneity of pore distribution, which, of course is dependent on the presence of secondary porosity. A regular distribution of small vugs would generate a nil secondary porosity index which would mean that the sonic tool would see the total porosity.

porosity index (SPI) is computed and reproduced alongside the left track in computational result display (Fig. 3-41). For this purpose we can also use the M-N-plot, or the MID-plot techniques (Fig. 3-42).

Similarly to the sonic travel time, the resistivity is also affected by the distribution of the pores in

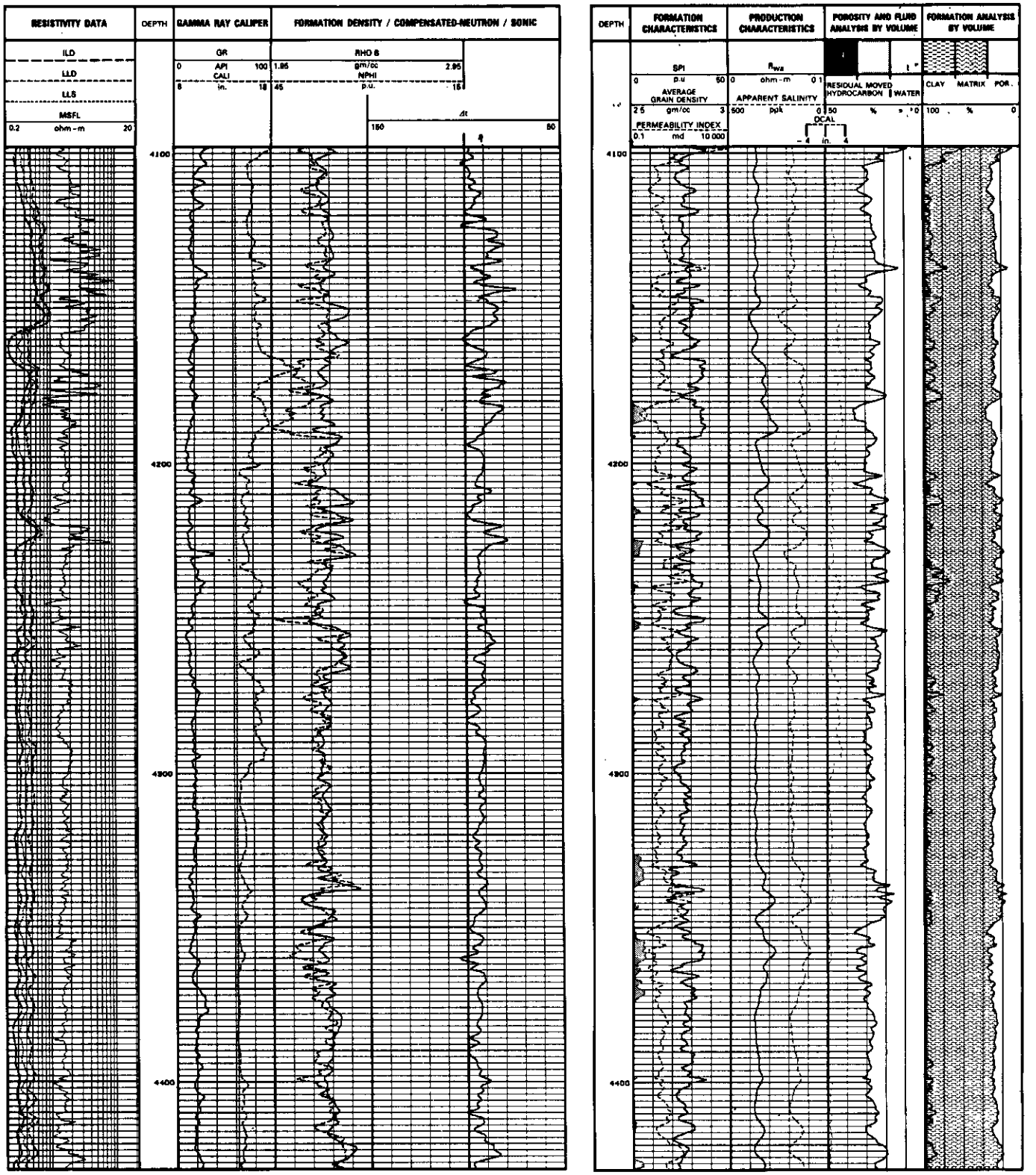

Fig. 3-41. - Composite-display of open-hole logs and computation results with secondary porosity index reproduced alongside (from Schlumberger, Well Evaluation Conference, Emirats/Qatar, 1981).

the rocks. The resistivity does not « see » the isolated or not connected pores (Fig. 3-43). Neither is it influenced by the size of the pores, but only by the network of the capillaries which connect them.

Brie *et al.*, (1985) developed a method of analysis of acoustic and electric measurements, based on Kuster-Toksoz model for acoustic velocities, and the Maxwell-Garnett model for resistivity, that

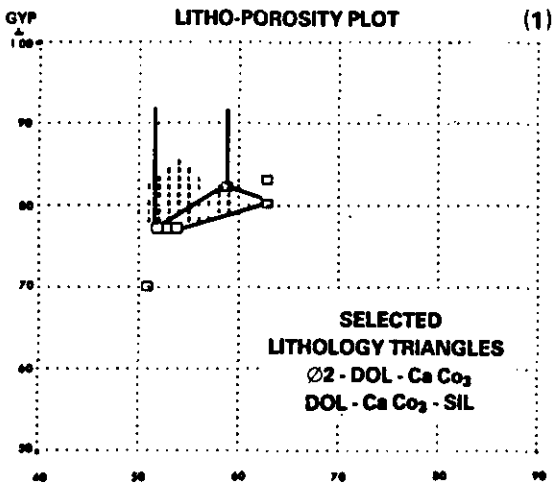

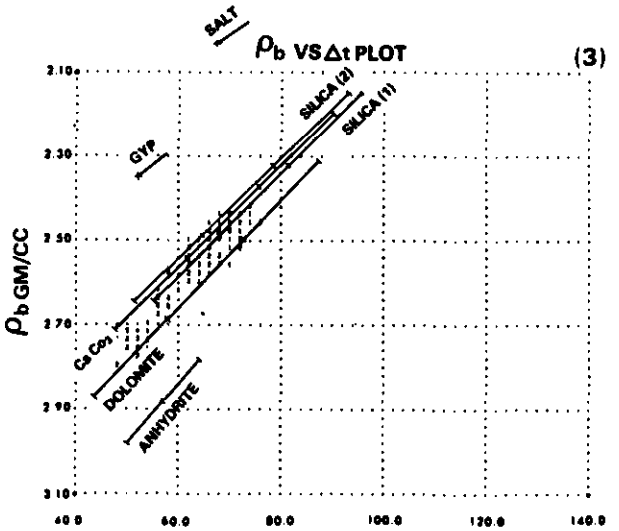

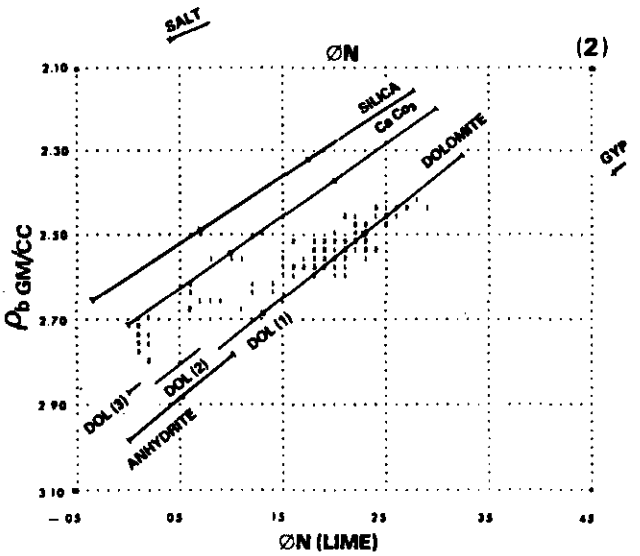

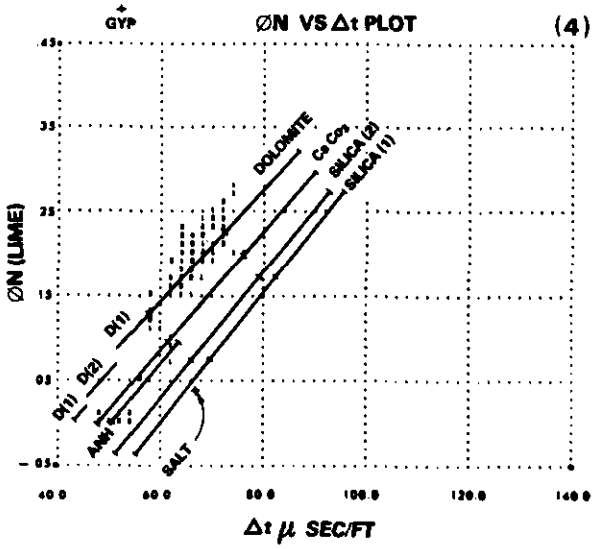

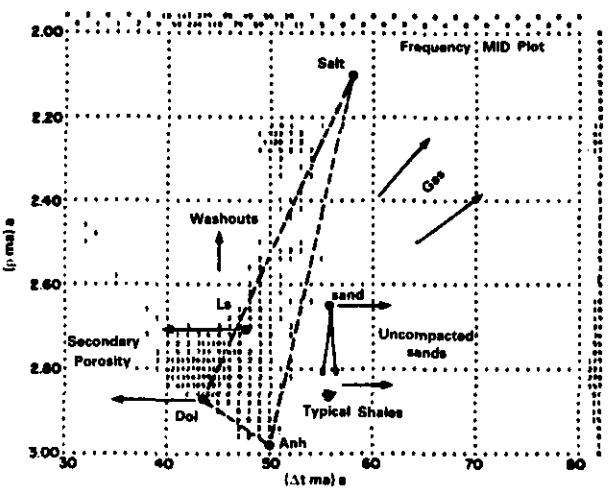

Fig. 3-42. - Several crossplots allowing to detect secondary porosity (from Clavier *et al.*, 1976).

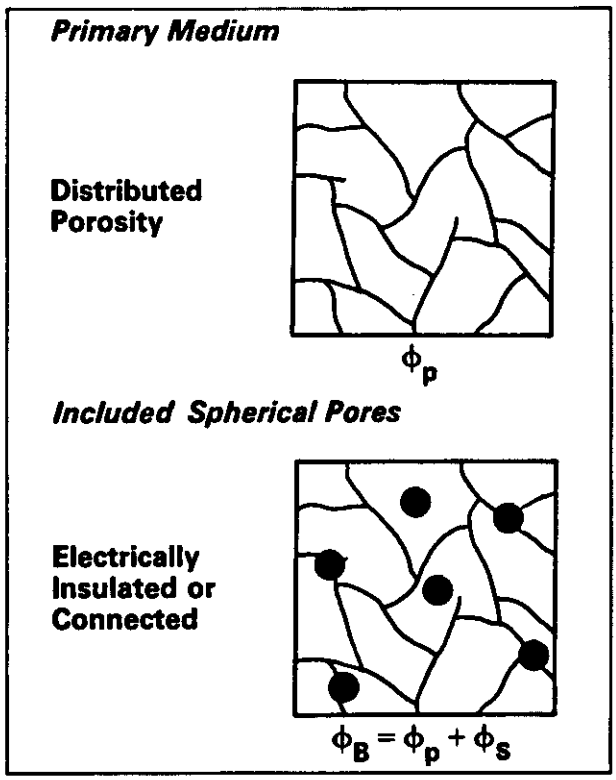

Fig. 3-43. - Schematic representation of the effect of vugs (supposed to be more or less spherical or oomoldic) on the electric properties (from Brie *et al.*, 1985).

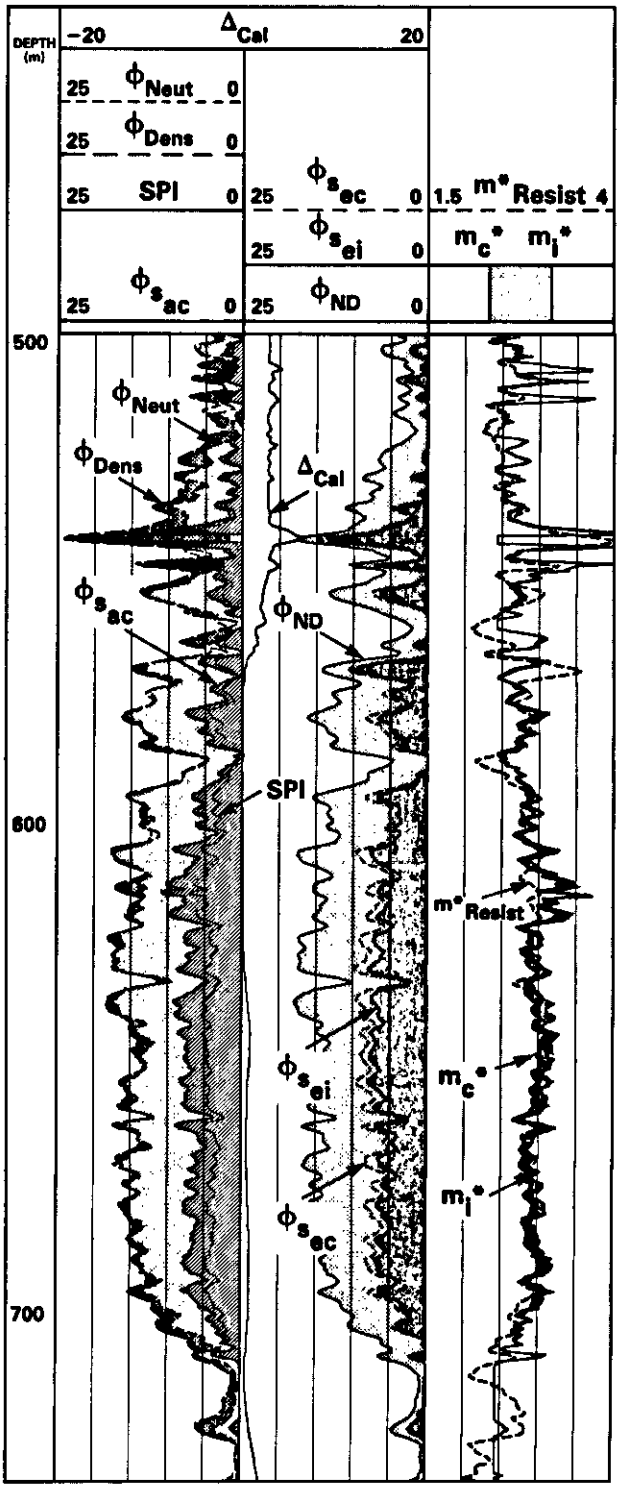

Fig. 3-44. - Example of results of spherical porosity computation (from Brie *et al.*, 1985).

determines the amount of spherical (oomoldic) porosity in carbonate rocks. In addition, they proposed a way of evaluating the cementation factor level by level from the sonic indication of spherical porosity (Fig. 3-44). This value can be used to obtain a more accurate value of the water saturation in such reservoirs. They also mentioned that the accuracy of the model could be increased by combining it with other texture sensitive measurements such as dielectric permittivity.

From recent works it seems that dielectric measurements made by the electromagnetic propagation tool (EPT tool), combined with data extracted from microresistivity devices, can help to determine the microgeometry of a carbonate rock.

Kenyon (1984), Kenyon & Baker (1984) demonstrated the need to introduce a « bimodal model » taking into account the microgeometry of the rock (shape of pores and grains) to explain the EPT tool response. They advocate an interpretation method of the measurement and extract an evolution of the microgeometry and of the cementation factor with depth in carbonate series.

Rasmus & Kenyon (1985) developed a technique for estimating separately the amounts of intergranular and oomoldic water. They used the results to predict the presence of oil and its flow rate in carbonates.

In conclusion, one can emphasize the importance of the knowledge of the texture for permeability estimation and for a more accurate saturation computation, especially in carbonate reservoirs. This knowledge will also help in the quantitative interpretation by favouring the m factor choice.

3.5. REFERENCES

ALGER, R.P. (1966). - Interpretation of Electric Logs in Fresh Water Wells in Unconsolidated Formations. *SPWLA, 7th Ann. Log. Symp. Trans., Tulsa.*

ALLEN, J.R.L. (1984). - Sedimentary structures. Their character and physical basis. *Developments in Sedimentology,* **30.** *Elsevier, Amsterdam.*

BEARD, D.C., & WEYL, P.K. (1973). - Influence of texture on porosity and permeability of unconsolidated sand. *Bull. Amer. Assoc. Petroleum Geol.,* **57,** *p. 349-369.*

BLATT, H., MIDDLETON, G., & MURRAY, R. (1972, 1980). - Origin of Sedimentary Rocks. 1st and 2nd ed. *Prentice-Hall Inc., Englewood Cliffs, New Jersey.*

BRIE, A., JOHNSON, D.L., & NURMI, R.D. (1985). - Effect of spherical pores on sonic and resistivity measurements. *SPWLA, 26th Ann. Log. Symp. Trans., paper W.*

CAROZZI, A.V. (Ed.) (1975). - Sedimentary Rocks. *Benchmark Papers in Geology,* **15,** *Dowden, Hutchinson, & Ross, Inc., Stroudsburg, Pennsylvania.*

CHOQUETTE, P.W., & PRAY, L.C. (1970). -Geological nomenclature and classification of porosity in sedimentary carbonates. *Bull. Amer. Assoc. Petroleum Geol.,* **54,** *p. 207-250.*

CLAVIER, C., & RUST, D.H. (1976). - MID-PLOT : a new Lithology Technique. *The Log Analyst,* **17,** *6.*

DICKEY, P.A. (1979). - Petroleum Development Geology. *Petroleum Publishing Co., Tulsa.*

DODGE, C.F., HOLLER, D.P., & MEYER, R.L. (1971). - Reservoir heterogeneities of some Cretaceous sandstones. *Bull. amer. Assoc. Petroleum Geol.,* **55,** *p. 1814-1828.*

DUNHAM, R.J. (1962). - Classification of Carbonate Rocks according to Depositional Texture. *Amer. Assoc. Petroleum Geol., Mem.* **1,** *p. 108-121.*

ENGELHARDT, W.V. von (1960). - Der porenraum der sedimente. *Springer, Berlin, 207 p.*

FOLK, R.L. (1959). - Practical Petrographic Classification of Limestones. *Bull. Amer. Assoc. Petroleum Geol.,* **43,** *p. 1-38.*

FOLK, R.L. (1962). - Spectral subdivision of Limestone Types. *Amer. Assoc. Petroleum Geol., Mem.* **1,** *p. 62-84.*

FRASER, H.J. (1935). - Experimental study of porosity and permeability of clastic sediments. *J. Geol.,* **43,** *p. 910-1010.*

FRIEDMAN, G.M., & SANDERS, J.E. (1978). -Principles of Sedimentology. *John Wiley & Sons, New York.*

GRATON, L.C., & FRASER, H.J. (1935). - Systematic packing of spheres with particular relation to porosity and permeability. *J. Geol.,* **43,** *p. 785-909.*

GRABAU, A.W. (1903). - Paleozoic coral reefs. *Bull. Geol. Soc. Amer.,* **14,** *p.337-352.*

HOBSON, G.D., & TIRATSOO, E.N. (1975). -Introduction to Petroleum Geology. *Scientific Press Ltd, Beaconsfield, England.*

KENYON, W.E. (1984). - Texture effects on megahertz dielectric properties of calcite rock samples. *J. Appl. Phys.,* **55,** *8, p. 31533159.*

KENYON, W.E., & BAKER, P.L. (1984). - EPT interpretation in Carbonates drilled with salty muds. *59th Ann. Tech. Conf. SPE of AIME, paper SPE 13192.*

KRUMBEIN, W.C., & MONK, G.D. (1943). -Permeability as a function of the size parameters of unconsolidated sand. *Petroleum Technol., AIME Techn. Publ. 1492,* **5,** *p.1-11.*

KRUMBEIN, W.C., & SLOSS, L.L. (1963). -Stratigraphy and Sedimentation. 2nd ed. *W.H. Freeman, & Co., San Francisco.*

KUSTER, G.T., & TOKSOZ, M.N. (1974). - Velocity and Attenuation of Seismic Waves in Two-Phase Media : Part I, Theoretical Formulations; Part II, Experimental results. *Geophysics,* **39,** *5.*

LANDES, K.K. (1951). - Petroleum Geology. *John Wiley, & Sons, New York.*

LEE, C.H. (1919). - Geology and groundwaters of the western part of San Diego County, California. *Wat.-Supply Irrig. Pap. Wash.,* **446,** *121 p.*

LEET, L.Don, JUDSON, S., & KAUFFMAN, M.E. (1978). - Physical Geology. 5th ed. *Prentice-Hall Inc., Englewood Cliffs, New Jersey.*

LINK, P.K. (1982). - Basic Petroleum Geology. *OGCI Publications, Tulsa.*

LOMBARD, A. (1956). - Géologie Sédimentaire. Les séries marines. *Masson, Paris.*

LOMBARD, A. (1972). - Séries sédimentaires. Genèse - Evolution. *Masson, Paris.*

LONGMAN, M.W. (1980). - Carbonate diagenetic textures from nearsurface diagenetic environments. *Bull. Amer. Assoc. Petroleum Geol.,* **64,** *p. 461-487.*

MAXWELL-GARNETT, J.C. (1904). - Transactions of the Royal Society, **203,** *p. 385, London.*

MIDDLETON, G.V. (1976). - Hydraulic interpretation of sand size distributions. *J. Geology,* **84,** *p. 405-426.*

NEASHAM, J.W. (1977). - The morphology of dispersed clays in sandstone reservoirs and its effect on sandstone shaliness, pore space and fluid flow properties. *52nd Ann Fall Meet SPE of AIME, paper SPE* **6858.**

NURMI, R.D., & FRISINGER, M.R. (1983). — Synergy of Core petrophysical measurements, log data, and rock examination in carbonate reservoir studies. *58th Ann. Fall Mtg. and Techn. Conf. of SPE of AIME, paper SPE* **11969.**

PETTIJOHN, F.J. (1930). - Imbricate arrangement of pebbles in a pre-Cambrian conglomerate. *Jour. Geol.,* **38,** *p. 568-573.*

PETTIJOHN, F.J. (1975). - Sedimentary Rocks. 3rd ed. *Harper, & Row, Publishers, New York.*

PETTIJOHN, F.J., POTTER, P.E., & SIEVER, R. (1972). - Sand and Sandstone. *Springer, New York.*

PICKETT, G.R. (1960). - The use of acoustic logs in the evaluation of sandstone reservoirs. *Geophysics,* **25**, *1, p. 250-274.*

PICKETT, G.R. (1963). - Acoustic Character Logs and their Applications in Formation Evaluation. *J. Pet. Technol.,* **15**, *6.*

POTTER, P.E., & PETTIJOHN, F.J. (1977). -Paleocurrents and Basin Analysis. 2nd ed. *Springer, New York.*

PRYOR, W.A. (1973). - Permeability-porosity patterns and variations in some Holocene sand bodies. *Bull. amer. Assoc. Petroleum Geol.,* **57**, *p. 162-189.*

RASMUS, J.C., & KENYON, W.E. (1985). - An improved petrophysical evaluation of oomoldic Lansing-Kansas City Formation utilizing conductivity and dielectric log measurements. *SPWLA, 26th Ann. Log. Symp. Trans., paper V.*

REINECK, H.E., & SINGH, I.B. (1975, 1980). -Depositional Sedimentary Environments. 1st and 2nd ed. *Springer, New York.*

ROGERS, W.F., & HEAD, W.B. (1961). - Relationships between porosity, median size, and sorting coefficients of synthetic sands. *J. Sediment. Petrol.,* **31**, *p. 467-470.*

RUKHIN, L.B. (1958). - Grundzüge des Lithologie. *Akademie-Verlag, Berlin.*

RUSSELL, W.L. (1951). - Principles of Petroleum Geology. *McGraw-Hill Book Co., New York.*

SARMA, V.V.J., & RAO, V.B. (1963). - Variation of Electrical Resistivity of River Sands, Calcite and Quartz Powders with Water Content. *Geophysics, April.*

Schlumberger (1979). - Well Evaluation Conference. Algeria.

Schlumberger Middle East S.A. (1981). - Well Evaluation Conference. United Arab Emirates/ Qatar.

Schlumberger Technical Services, Inc. (1982). -Essentials of Natural Gamma ray Spectrometry Interpretation.

Schlumberger Technical Services, Inc. (1983). -Well Evaluation Conference. India.

SELLEY, R.C. (1970, 1978, 1985). - Ancient Sedimentary Environments. 1st, 2nd and 3rd ed. *Chapman & Hall, London.*

SELLEY, R.C. (1976). - An Introduction to Sedimentology. *Academic Press, London.*

SEN, P.N. (1980). - Dielectric and conductivity response of sedimentary rocks. *SPE of AIME, paper 9379.*

SEN, P.N. (1981). - Relation of certain geometrical features to the dielectric anomaly of rocks. *Geophysics,* **46**, *p. 1714-1720.*

SERRA, O. (1972). - Diagraphies & Stratigraphie. In : *Mém. B.R.G.M.,* **77**, *p. 775-832.*

SERRA, O. (1973). - Interprétation Géologique des diagraphies en Séries Carbonatées. *Bull. Centre Rech. Pau - SNPA,* **7**, *1, p. 265-284.*

SERRA, O. (1974). - Interprétation géologique des Séries deltaïques à partir des diagraphies différées. *Rev. A.F.T.P.,* **227**, *Oct., p. 9-17.*

SERRA, O., & ABBOTT, H. (1980). - The Contribution of Logging data to Sedimentology and Stratigraphy. *55th Ann. Fall Techn. conf. SPE of AIME, paper SPE 9270, and in SPE J., Feb. 1982.*

SERRA, O., & SULPICE, L. (1975). - Sedimentological Analysis of shale-sand series from well logs. *SPWLA, 16th Ann. Log. Symp. Trans., paper W.*

SERRA, O., & SULPICE, L. (1975). - Apports des diagraphies différées aux études sédimentologiques des séries argilo-sableuses traversées en sondage. *9th Cong. Intern. Sédiment., Nice, thème 3, p. 86-95.*

THEYS, P., LUTHI, S., & SERRA, O. (1983). - Use of dipmeter in Carbonates for detailed sedimentology and reservoir engineering studies.

VATAN, A. (1954). - Pétrographie sédimentaire. *Ed. Technip, Paris.*

VISHER, G.S. (1965). - Use of vertical profile in environmental reconstruction. *Bull. Amer. Assoc. Petroleum Geol.,* **49**, *p. 41-61.*

Chapter 4

INFORMATION ON SEDIMENTARY STRUCTURE

(Rock description)

4.1. REVIEW OF GENERAL CONCEPTS

4.1.1. Definition

According to Pettijohn & Potter (1964) « the *structure* is an inherent property of a rock and a guide to its origin. Whereas the texture deals with the grain to grain relations in a rock, structure has to do with discontinuities and major inhomogeneities. The structure is concerned with the organization of the deposit - the way in which it is put together - . Hence structures are the larger features that, in general, are best studied in the outcrop rather than in the hand specimen or thin section ».

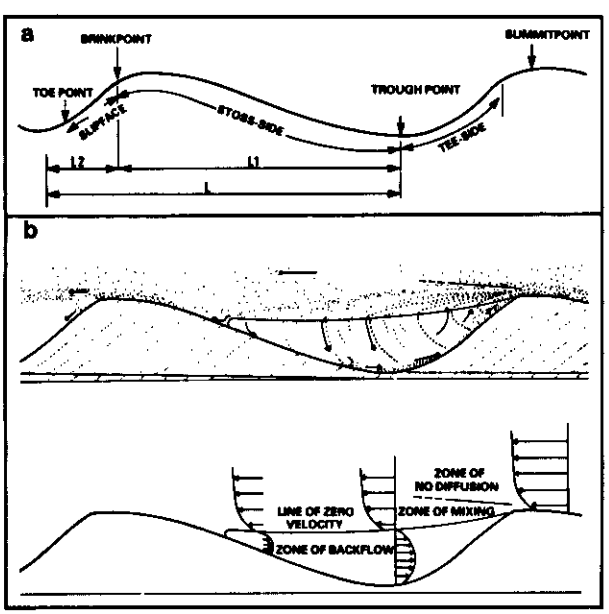

Fig. 4-1. - (a) Terms used in ripple description. L - ripple length. H - ripple height. l_1 - horizontal projection of stoss side. l_2 -horizontal projection of lee side. (b) Dynamic mechanism for ripple formation
(adapted from Reineck & Singh, 1975).

They explain the local variations of the composition or texture.

A sedimentary structure refers to megascopic morphological features. These features have been studied for some time, as they are often visible to the naked eye. They include the thickness and the shape of beds, their internal organization, the nature of their surfaces, joints, concretions, cleavages, and fossil content.

Primary sedimentary structures are generated by either current velocity, impeding the action of the gravity, and its evolution, (scour and erosional marks, ripple marks (Fig. 4-1 to 4-3), cross-bedding, wavy-bedding, graded bedding (Fig. 4-4),...), or biogenic activity (tracks, trails, burrows, rootlets,...), or action of climatic or physical agents (mud cracks, pits, load casts, dikes, convolute bedding, slump structures).

« Some structures are texture dependent. Ripples marks and cross-bedding for example, characterize only those sediments which have a grain size in the sand range » (Pettijohn *et al.*, 1964).

4.1.2. Importance of Sedimentary Structures

The primary sedimentary structures are particularly important because they will reflect the hydrodynamic conditions at the time of deposition (e.g. energy, type of current,...). They constitute an important element of the facies of a sedimentary unit (Fig. 4-5) and will lead to a better definition of the depositional environment (Table 4-2).

As mentioned by Selley (1970), structures « unlike lithology and fossils are undoubtedly generated in place and can never have been brought in from outside ».

Consequently, it is essential to detect them by analysing open-hole logs and specifically dipmeter and Formation MicroScanner * tool data.

* Mark of Schlumberger.

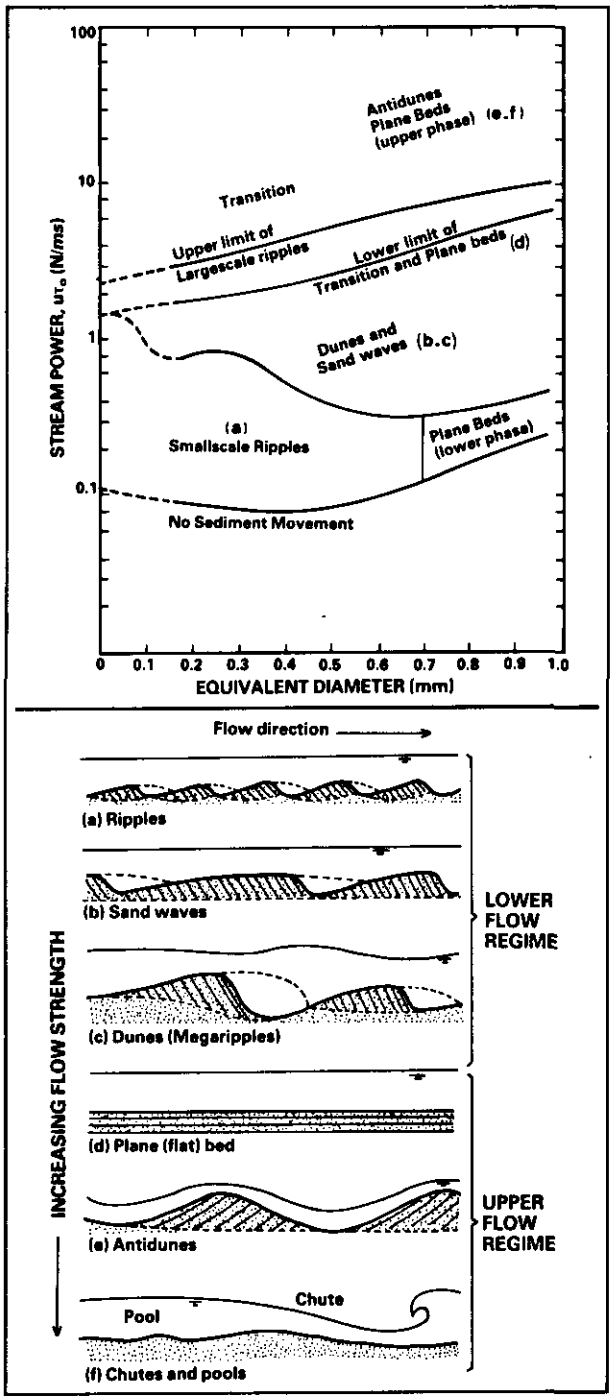

Fig. 4-2. - Relationship between current energy and bed forms (from Allen, 1968, and Blatt *et al.*, 1980).

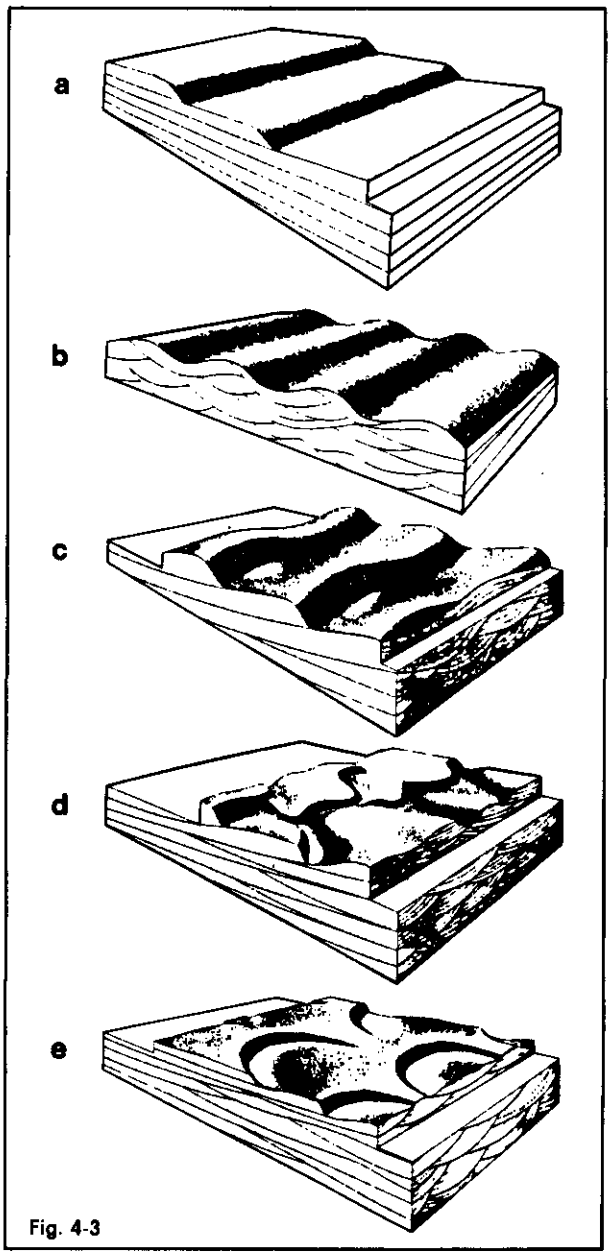

Fig. 4-3

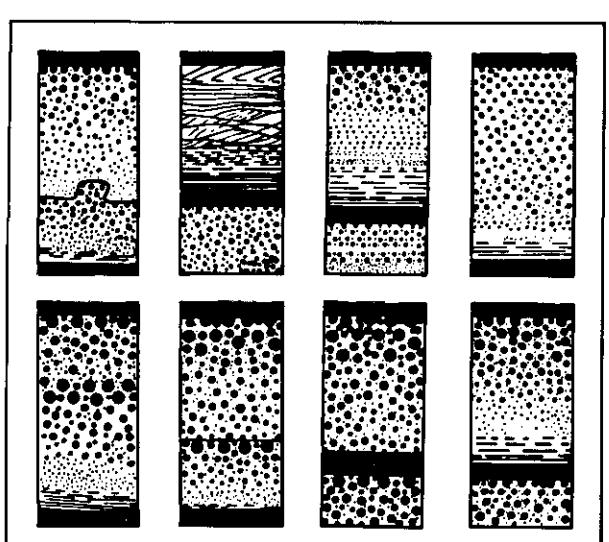

Fig. 4-3. - Different types of ripple marks. (a) Straight-crested small-current ripples. The cross-bedded units are planar. (b) Asymmetrical wavy ripples and resulting wave ripple cross-bedding. (c) Undulatory small ripples. The cross-bedded units are weakly festoon-shaped. In the front view lower units are strongly trough-shaped. d) Migrating lingoid small ripples. Cross-bedded units are strongly festoon-shaped. e) Lunate megaripples. Cross-bedded units present trough spoon-shaped scours. (from Reineck & Singh, 1975).

Fig. 4-4. - Varieties of graded bedding (from Kuenen, 1953). ▶

Table 4-1
Genetic classification of ripples
(from Reineck *et al.*, 1971).

a) Current ripples (transverse)

Name	Nature of crest	Size parameters	Ripple index L.H.	Symmetry	Internal structure
Small-current ripples	Straight Undulatory Lingoid Rhomboid	L = 4-60 cm (11, 13) H = upto 6 cm (11, 13)	> 5 (11, 13) Mostly 8-15	Asymmetrical	Form-concordant Form-discordant Climbing
Megacurrent ripples[a]	Straight Undulatory Lunate Lingoid Rhomboid	L = 0.6-30 m (9, 13) H = 0.06-1.5 m (9, 13)	Mostly > 15	Asymmetrical	Form-concordant Form-discordant
Giant-current ripples[b]	Straight Undulatory Bifurcating	L = 30-1 000 m (rarely 20-30 m) H = 1.5-15 m (2, 9, 10)	Mostly > 30 Upto about 100 (2, 9)	Asymmetrical and symmetrical	Known only as form-discordant (2, 9)
Antidunes	Straight	L = 0.01-6 m (7, 10) H = 0.01-0.45 m (7, 10)		Almost symmetrical	Form-concordant (8) Form-discordant (9)

[a] An active megaripple field can be covered by small ripples.
[b] An active giant ripple field can be covered by megaripples.

b) Wave ripples

Name	Nature of crest	Size parameters	Ripple index L.H.	Symmetry	Internal structure
Symmetrical wave ripples	Straight, partly bifurcating	L = 0.9-200 cm (4, 5, 11, 15) H = 0.3-22.5 cm (4, 11)	4-13 Mostly 6-7 (4, 11)	Symmetrical	Form-concordant Form-discordant Climbing
Asymmetrical wave ripples	Straight, partly bifurcating	L = 1.5-105 cm H = 0.3-19.5 cm (4, 11)	5-16 Mostly 6-8 (4, 11)	Asymmetrical R.S.I. = 1.1-3.8 (11)	Form-concordant Form-discordant Climbing

c) Isolated (incomplete) ripples. (Formed on the foreign substratum by sediment paucity)

Name	Nature of crest	Size parameters	Symmetry	Internal structure
Isolated small-current ripples	Like small-current ripples	Like small-current ripples, but lesser in height	Asymmetrical	Form-concordant Form-discordant
Isolated mega-current ripples	Straight (6, 7) Curved (6) Sichel-shaped (10)	Like megacurrent ripples, but lesser in height	Asymmetrical	Form-concordant Form-discordant (6, 10)
Isolated giant-current ripples (16)	Like current ripples	Similar to giant-current ripples	Asymmetrical Symmetrical	Form-discordant
Isolated wave ripples	Straight Curved	Like wave ripples, but lesser in height	Symmetrical Asymmetrical	Form-Concordant Form-discordant

d) Combined current / wave ripples

Name	Nature of crest	Size parameters	Symmetry	Internal structure
Longitudinal current/ wave ripples (direction of wave propagation at right angles to current direction)	Straight, unbranched crests parallel to the current direction: also known to occur in mud	L = 2.6p5 cm (16)	Symmetrical and asymmetrical	Form-discordant (10, 14)
Transverse current/ wave small ripples (wave direction parallel to current direction)	Mostly rounded crests, transverse to current direction (3)		Asymmetrical	Form-concordant Form-discordant

e) Wind ripples

Name	Nature of crest	Size parameters	Ripple index L.H.	Symmetry	Internal structure
Wind sand ripples	Straight, partly bifurcating	L = 2.5-25 cm H = 0.3-1.0 cm (1, 12)	10-70 and more (1, 12)	Asymmetrical	Laminated sand; rarely few foreset laminae. Concentration of coarse sand near the crest.
Wind granule ripples	Straight, cuspate, barchan-like	L = 2.5 cm-20 m H = 2.5-60 m (1, 12)	12-20 (12)	Asymmetrical	Foreset laminae in opposing directions. On the crest enrichment of granules.

Legend: Longitudinal = ripple crest parallel to current direction, transverse = ripple crest at right angles to current direction. L = Ripple lenght; H = Ripple height.
(1) = Bagnold (1954b), (2) = Coleman (1969), (3) = Harms (1969), (4) = Inman (1957), (5) = Inman (1958), (6) = Newton and Werner (1969), (7) = Nordinn (1964), (8) = Panin and Panin (1967), (9) = Reineck (1963 a), (10) = Reineck and Singh (unpublished), (11) = Reineck and Wunderlich (1968 a), (12) = Sharp (1963), (13) = Simons et al. (1965), (14) = Van Straaten (1951), (15) = Werner (1963), (16) = Wunderlich (1969).

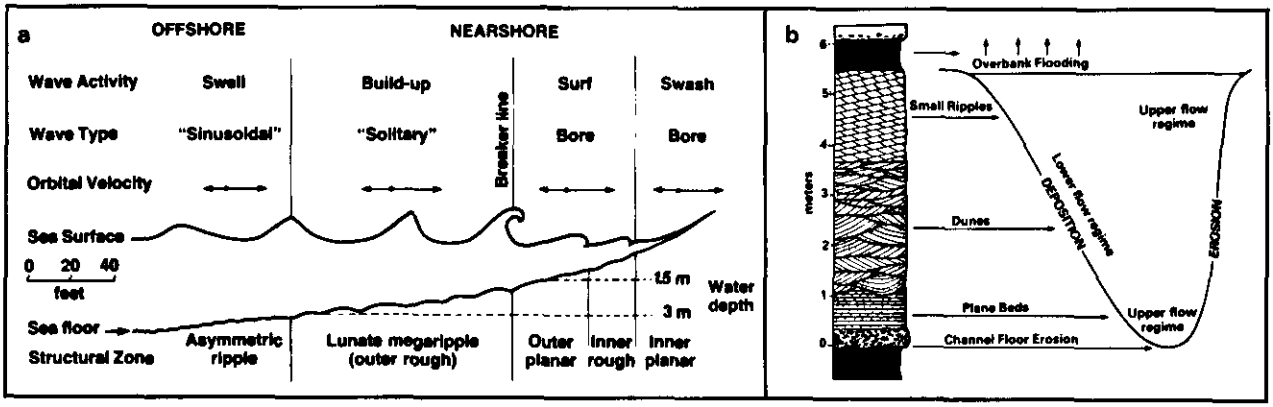

Fig. 4-5. - (a) Relationship between present day environment and structures (in : Blatt *et al.*, 1980). (b) Interpretation by Allen, 1963, of a British Old Red Sandstone cyclothem in terms of flow regimes in a meandering channel model.

Table 4-2
Occurrence of ripples in various depositional environments
(from Reineck & Singh, 1975).

	Mega-current ripples	Small-current ripples	Wave ripples	Climbing ripple lamination	Rhom-bo-hedral ripples	Anti-dunes
River	++	++	0	++	0	0
Lake	–	0	+	–	–	–
Lake beach	–	+	++	–	0	0
Lagoon	–	0	+	0[a]	–	–
Intertidal flat	+	++	++	0	0	0
Tidal channel and inlet	++	++	–	0	–	–
Backshore and foreshore	+	+	++	0	+	+
Upper shoreface	+	+	+	–	–	–
Lower shoreface	–	0	+	–	–	–
Transition zone	–	0	+	–	–	–
Muddy shelf	–	–	*0*	–	–	–
Sandy shelf	+	+	0	–	–	–
Continental slope and rise	–	0	–	–	–	–
Deep sea	–	–	–	–	–	–
Sandy deep sea	–	+	?	–	–	–
Turbidite	0	+	–	+	–	0
Seamounts	–	+	0	–	–	–

[a] Climbing ripple lamination of only wave ripple origin.

++ abundant + common 0 rare – absent

4.1.3. Classification of Sedimentary Structures

The classification of structures can be based on the *time* of their formation. They are defined as :

. *predepositional*, (formed before the deposition of a bed). They correspond to features observed on the surface of a preceeding bed such erosion or impressions;

. *syngenetic or primary or syndepositional*, (contemporaneous with deposits). These structures contain information on physical, chemical or biological conditions, existing in a depositional environment during sedimentation. They are subdivided into inorganic and organic structures, depending on their origin; inorganic structures are a result of physical agents; organic structures are

Table 4-3
Classification of sedimentary structures
(from Pettijohn & Potter, 1964).

BEDDING EXTERNAL FORM

1. Beds *equal* or *subequal* in thickness: beds laterally uniform in thickness: beds *continuous*
2. Beds *unequal* in thickness: beds laterally uniform in thickness: beds continuous
3. Beds *unequal* in thickness: beds laterally variable in thickness: beds continuous
4. Beds *unequal* in thickness: beds laterally variable in thickness: beds discontinuous

BEDDING INTERNAL ORGANIZATION AND STRUCTURE

1. Massive (structureless)
2. Laminated (horizontally-laminated; crosslaminated)
3. Graded
4. Imbricated and other oriented internal fabrics
5. Growth structures (stromatolites, etc.)

BEDDING PLANE MARKINGS AND IRREGULARITIES

1. On base of bed
   (a) Load structures (load casts)
   (b) Current structures (scour marks and tool marks)
   (c) Organic markings (ichnofossils)
2. Within the bed
   (a) Parting lineation
   (b) Organic markings
3. On top of the bed
   (a) Ripple marks
   (b) Erosional marks (rill marks: current crescents)
   (c) Pits and small impressions (bubble and rain prints)
   (d) Mud cracks, mud-crack casts, ice-crystal casts, salt-crystal casts
   (e) Organic markings (ichnofossils)

BEDDING DEFORMED BY PENECONTEMPORANEOUS PROCESSES

1. *Founder and load structures (ball-and-pillow structures, load casts)*
2. Convolute bedding
3. Slump structures (folds, faults, and breccias)
4. Injection structures (sandstone dikes, etc)
5. Organic structures (burrows, "churned" beds, etc)

formed in connection with an animal or plant organic activity (burrow; impressions; root traces);

. *epigenetic or secondary or postdepositional*, (formed after sedimentation). These are often of chemical origin and their occurrence reflects diagenetic phenomena; or of physical origin resulting from tectonic deformation.

A second classification can also be suggested which is based on the *agents* or *processes*, which have created the sedimentary structures :

. *physical* such as action of gravity, influences of current or stress (ripple marks, tool marks, convolute bedding, slumping, mud cracks,...),

. *chemical* such as dissolution, concretions;

. *biological* such as burrows, tracks, trails, foot impressions, root traces,...

A third classification of sedimentary structures based on their *location* can be suggested :

. *external structures*, that cover the size and the shape of beds, thus the nature of their boundaries and the shapes of the lower and upper bedding planes;

. *internal structures*, relative to internal organization of the bed : i.e. massive, laminated, graded bedding, growth structures (stromatolitic limestones,...).

Table 4-4
Relationship between sedimentary features and well logging parameters
(from Serra, 1984).

STRUCTURAL FEATURES (SEDIMENTARY AND TECTONIC)				LOG TO USE FOR DETECTING THE PHENOMENON
EXTERNAL FORM OF BED	SIZE: VERTICAL THICKNESS	APPARENT		ALL LOGS BUT ESPECIALLY MICRODEVICES AND HDT, SHDT, FMS
		REAL		HDT, SHDT, FMS
	SHAPE: LATERAL VARIATIONS IN THICKNESS			CORRELATIONS : HDT, SHDT, FMS (CURVES AND DIPS)
	ARRANGEMENT OR SEQUENCE OF BEDS			ALL LOGS
	BOUNDARIES — ASPECT	ABRUPT		ALL LOGS (SHAPE OF CURVES: BELL, FUNNEL, CYLINDER)
		PROGRESSIVE CONFORMABLE		
	BOUNDARIES — NATURE	UNCONFORMABLE		HDT, SHDT, FMS (CURVES AND DIPS) CORRELATIONS
BEDDING PLANE FEATURES	ON BASE (LOWER BOUNDARY) — PHYSICAL ORIGIN	LOAD		HDT, SHDT (CURVES AND DIPS), FMS
		EROSIONAL (SCOUR MARKS)		HDT, SHDT (CURVES AND DIPS), FMS
		TOOL MARKS		
	ON BASE (LOWER BOUNDARY) — ORGANIC ORIGIN	TRAILS		
		BURROWS		FMS
	ON TOP (UPPER BOUNDARY) — PHYSICAL ORIGIN	CURRENT (RIPPLES)		HDT, SHDT (CURVES AND DIPS), FMS
		EROSIONAL		HDT, SHDT (CURVES AND DIPS), FMS
		MUD CRACKS		FMS
	ON TOP (UPPER BOUNDARY) — ORGANIC ORIGIN	TRACKS		
		TRAILS		
		BURROWS		
INTERNAL ORGANIZATION	MASSIVE OR HOMOGENEOUS HETEROGENEOUS			ALL LOGS AND HDT, SHDT (CURVES), FMS
	LAMINATED	HORIZONTAL LAMINATIONS		HDT, SHDT (CURVES AND DIPS), FMS
		PORESETTS		HDT, SHDT (CURVES AND DIPS), FMS
		CROSS BEDDING		HDT, SHDT (CURVES AND DIPS), FMS
	GRADED BEDDING ORIENTED INTERNAL FABRIC GROWTH STRUCTURE			ALL LOGS BUT ESPECIALLY HDT, SHDT, FMS (CURVE EVOLUTION) FMS ?
POST DEPOSITIONAL DEFORMATION	PHYSICAL ORIGIN — VERTICAL MOVEMENT	LOAD MARKS		HDT, SHDT (DIPS AND CURVES), FMS
		CONVOLUTE		FMS
		INJECTION		FMS
		FRACTURES		ALL LOGS AND HDT, SHDT (CURVES, ROTATION OF THE TOOL...), FMS
		FAULTS		HDT, SHDT (DIP EVOLUTION): CORRELATIONS : FMS
	PHYSICAL ORIGIN — HORIZONTAL MOVEMENT	SLUMP		RGS
		SLIDE		FMS
		FALLING		FMS
	ORGANIC ORIGIN: BURROWS CHEMICAL ORIGIN: STYLOLITES			HETEROGENEOUS CURVES ON HDT, SHDT, FMS HDT, SHDT WITH GAMMA-RAY OR NGS : FMS

The classifications proposed by Krumbein & Sloss (1963), by Selley (1976), essentially combine the time period and the agent, whereas the classification of Pettijohn & Potter (1964), and Blatt et al., (1979) are based more on the location of features (Table 4-3). We have retained the classification of Table 4-4, derived from Pettijohn & Potter, because it adapts more closely to log analysis and illustration. The relationship of features with well logging parameters, especially dipmeters, is mentioned.

4.2. SEDIMENTARY FEATURES EXTRACTED FROM LOGS

It is quite obvious that open-hole logs can reflect sedimentary features (texture and structure) such as thickness, sometimes heterogeneity, or sequences (lithology or grain size evolution). In general, however, for most of the open hole logging tools, the vertical resolution is not sufficient to detect thin events or sequences, and give a detailed picture of the formations crossed by a well.

By comparison, high resolution dipmeters (HDT and SHDT tools) have the advantage that they are capable of detecting very thin events which can be related to sedimentary features (textural and structural).

Due to their very small electrodes (1 cm thick) and a very short sampling interval (every 2.5 or 5 mm instead of 15 cm or exceptionally 4 cm for other tools), they have the best vertical resolution, among the open-hole tools. They measure the apparent thickness of events (more than 1 cm thick), and detect very thin events or laminations (less than 1 cm thick) as long as they are conductive in a resistive environment (Fig. 4-6);

. Dipmeter tools record four or eight curves in the direction of four pads 90 degrees apart, giving better coverage of the borehole wall and, consequently, a better idea on the lateral variations;

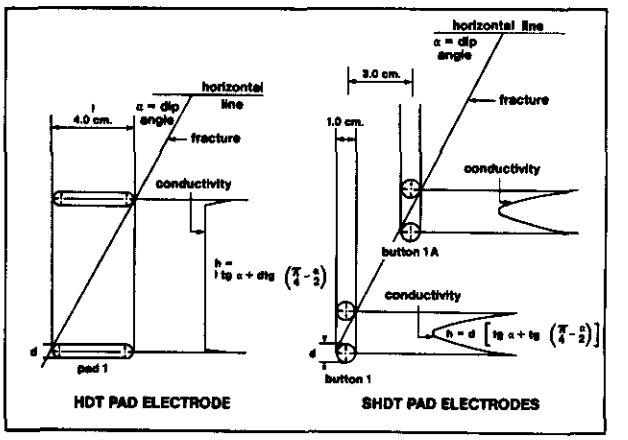

Fig. 4-6. - Detection of very fine conductive events by HDT or SHDT curves.

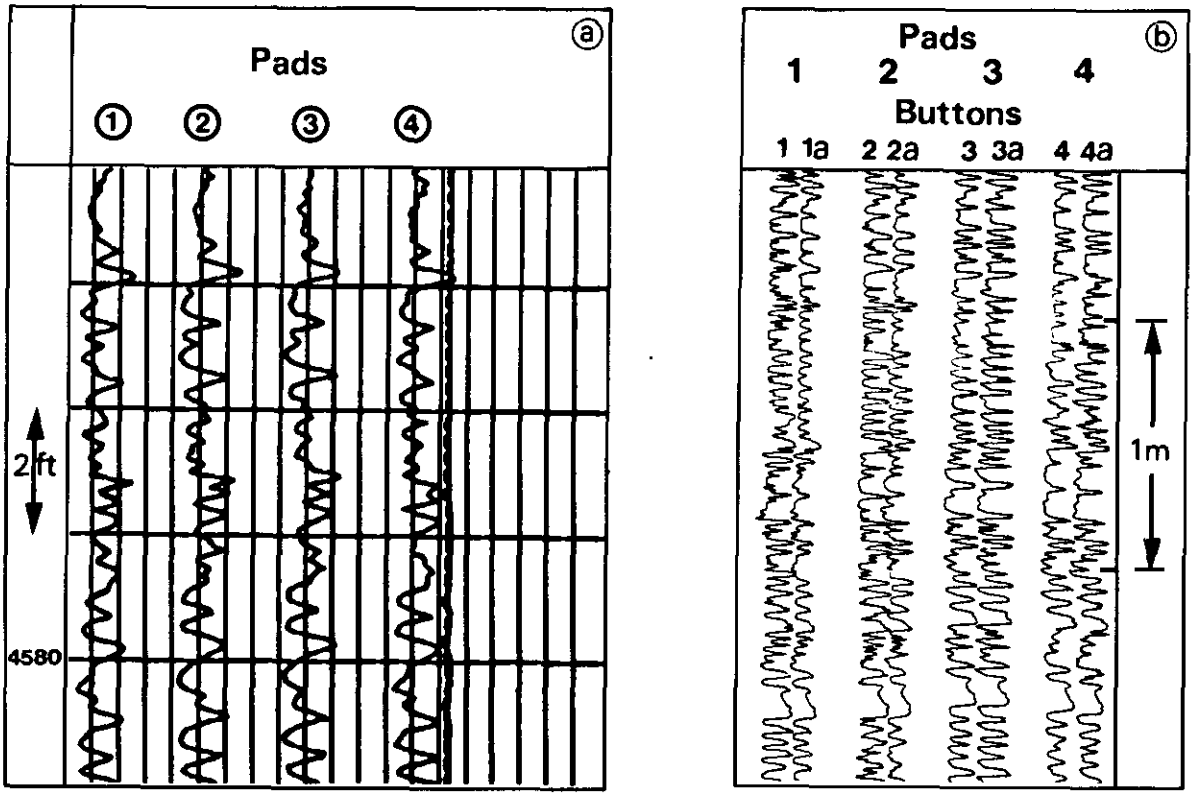

Fig. 4-8. - Examples showing the details detected by the dipmeter tools. (a) : HDT curves; (b) : SHDT curves.

. Curves allow for dips to be computed, which are indicative of current energy and direction, and, consequently, of the type of bedding.

To be convinced of the detail attained by these tools, it is sufficient to compare the dipmeter resistivity curves at 1/40, or 1/20 scales (Figs. 4-7 and 4-19) with the other open-hole logs. One is surprised by the density of the finely-detailed curve events which sometimes can be easily correlated with other similar events on the other curves. Every detected contrast of resistivity explains a change in one characteristic or another of the rock such as mineralogical change (e.g. layers of shale in a sand), or textural change (e.g. granulometry, sorting, porosity or tortuosity factor), or possible fluid change.

A close study of dipmeter curves shows that many curve features are identifiable from curve to curve. These features have varying thickness (from less than one inch to several feet), amplitude, and shape. Each feature may be considered to be the signature of a geological event in the depositional sequence of the formation or its evolution by diagenesis. The inflection points of these curve features correspond to the upper and lower limits of geological events or to the bed boundaries. Moreover, the dip of the bedding is not necessarily constant, and may sometimes vary rapidly. All this information is needed for recognition of sedimentary features. This is why Schlumberger developed programs to obtain this information.

For the HDT tool the program is known as GEODIP *. It uses a method of correlation by pattern recognition. This method is best adapted to automatically detect these curve features, to recognize them from curve to curve, and to derive dips at the boundaries of each individual feature. The GEODIP program mimics the process of correlation by eye, looking for the most prominent features, and then working up and down the curves to confirm the initial tentative picks. The GEODIP program examines a curve, and then applies the methods of pattern recognition to identify features on it which may be matched to features of the other curves.

But the different curve features are often similar and easy to confuse. The human correlator avoids this ambiguity by constant eye movements to confirm or reject hypothetical correlations. In so doing, he implicity, often unconsciously, applies some logic rules which are integrated into his perception process. The GEODIP program uses equivalents of such rules. Safeguards are also integrated, as far as they have been recognized. In particular, the method is constructed around a basic law which is justified by geological conditions of deposition, the rule of noncrossing correlations (Vincent *et al.*, 1979).

For the SHDT tool, an event-association program is used. It is known as LOCDIP * (Localdip).

* Mark of Schlumberger.

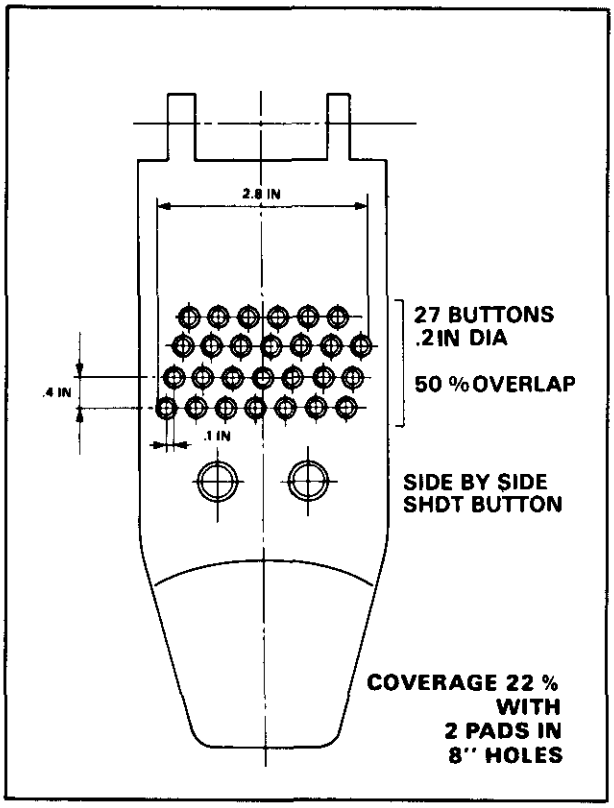

Fig. 4-9. - Formation MicroScanner tool pad configuration (courtesy of Schlumberger).

Derivatives of all eight curves are produced, and the maxima of the derivatives of each curve are used to compute the displacement between curves and the dips.

In the corresponding arrow-plot displays the correlation lines found by the programs are drawn across the dip resistivity curves. This allows quality control of the correlation and consequently of the dip measurement.

In these kinds of processing a constant link can be established between the dip and the event which generated its computation. One can reason on both curve features and dips.

More recently (1985) Schlumberger has introduced a new tool which is a kind of microelectrical scanner, the Formation MicroScanner * tool. The size of the electrodes (5 mm), their number (27 per pad), and their arrangement (Fig. 4-9), provide a continuous electrical survey of the borehole wall accross two bands 7 cm wide, corresponding to the paths of two adjacent pads 90 degrees apart. The recorded conductivity curves, after depth matching, speed correction and equalization, can be converted into images in which the gray density depends on conductivity (Fig. 4-10). The images are comparable to black and white core photographs. They show a lot of very interesting features related to texture and sedimentary structure as it will be illustrated later.

* Mark of Schlumberger.

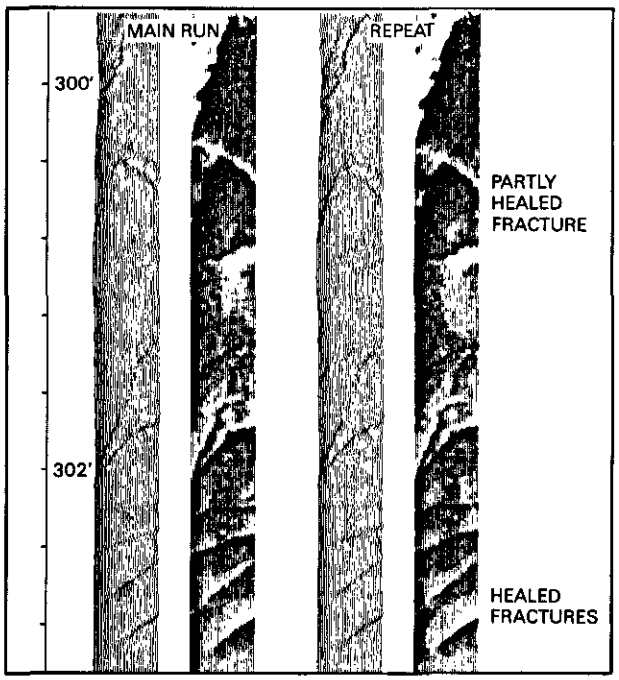

Fig. 4-10 . - Example of curves and images obtained with the Formation MicroScanner tool (courtesy of Schlumberger).

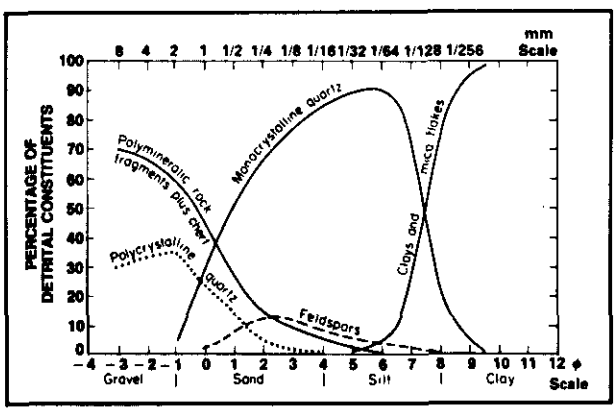

Fig. 4-11 - Relationship between grain size and composition of the detrital fraction in clastic silicate rocks (from Blatt *et al.*, 1980).

It can be stated that the dipmeters and the Formation MicroScanner tool principally give information on the texture and the sedimentary structure of the rock and only through this information can the dip be obtained.

Three types of information can be extracted from analysis of dipmeter and Formation MicroScanner data :

- information deduced from dip computation -coming from correlation of events detected on each curve -, and dip evolution with depth (sedimentary features, folds, faults, unconformities);
- information deduced from conductivity curve analysis. For instance, a resistive change reflects variations in :

. mineralogy (percentage of clay minerals, micas and heavy minerals, cement);

texture (presence of vugs, nodules, or crystals of sulfides, size of particles, size of vugs and throats,); and other textural parameters such as :

- grain size, which partly controls the mineralogy (silt- and clay-size mineral content, Fig. 4-11), the diameter of the pore throats, and the shape of the grains; and on which depends the permeability which, in turn, controls the depth of invasion and the irreducible water saturation;
- sorting, which is also dependent on grain size (sorting decreases when grain size decreases), and which controls the porosity and the tortuosity (*m* factor);
- packing (arrangement of the grains), which affects porosity, tortuosity and permeability;

. structure (homogeneity, heterogeneity, graded bedding, lenticular bedding, flaser bedding, cross-bedding,...); fractures;

. percentage of fluids which depends on the previous parameters or on a fluid change;

- information deduced from the evolution of thickness of beds with depth.

4.3. INFORMATION ON STRUCTURE EXTRACTED FROM DIPMETERS AND FORMATION MICROSCANNER

4.3.1. Bed Shape

One must stress that a single bed, or *sedimentation unit,* is « that thickness of sediment which was deposited under essentially constant physical conditions » (Otto, 1938), separated from other under- and over-lying beds by physically and visually more or less well-defined bedding planes, « ... made evident because of the unlike texture or composition » (Pettijohn & Potter, 1964).

The parameters defining the shape of a bed are :

. thickness;
. bedding planes;
. lateral dimensions.

4.3.1.1. *Bed thickness*

Bed thickness can vary from a few millimetres to several metres (Campbell, 1967). A bed can be massive or internally finely stratified, formed by a succession of finer units (laminations). A lamination results from minor fluctuations in the physical conditions, which prevailed in the depositional environment. They are particularly expressed by changes in grain size (sand to silt) and sometimes in composition (quartz to clay mineral). The thickness of a lamination is measured in millimetres and generally does not exceed several centimetres (Fig. 4-12).

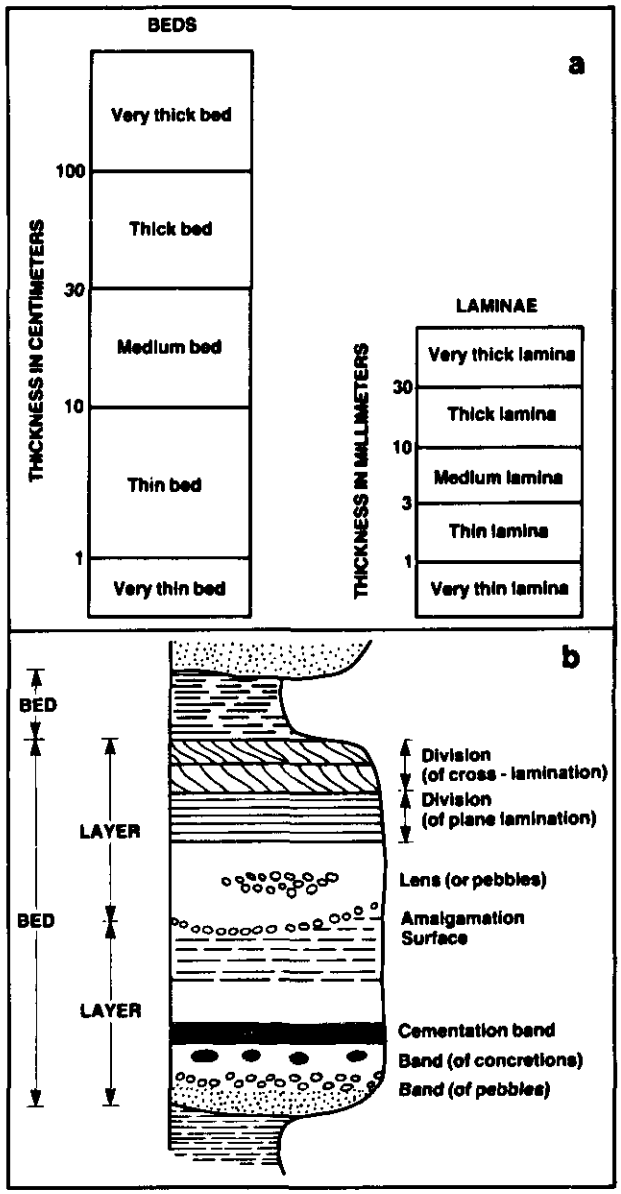

Fig. 4-12. - (a) Terminology for thickness of beds and laminae (modified after Ingram, 1954, and Campbell, 1967; in Reineck & Singh, 1975). (b) Terms for description of beds with internal structures (from Blatt *et al.,* 1980).

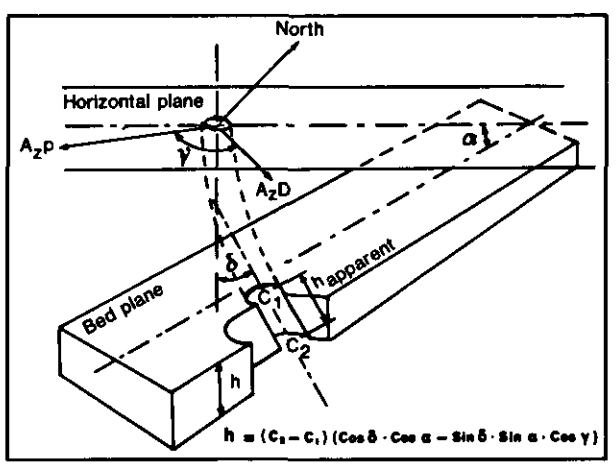

Fig. 4-13. - Computation of the real thickness of a bed.

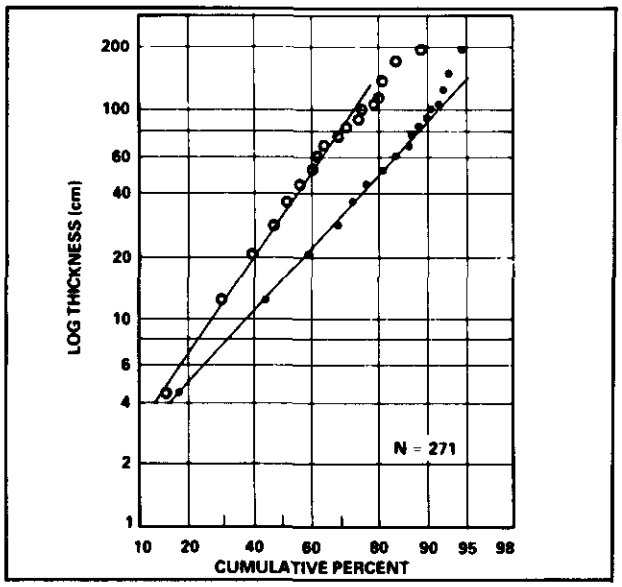

Fig. 4-14. - Approach to lognormality of thickness of turbidite sandstone beds (from Scott, 1966).

In general, bed thickness is easily detectable with most logs, especially with dipmeters and the Formation MicroScanner tool. These tools permit the determination of not only the apparent thickness of beds exceeding 1 cm, but also their true thickness (for isopach maps) because the dip of

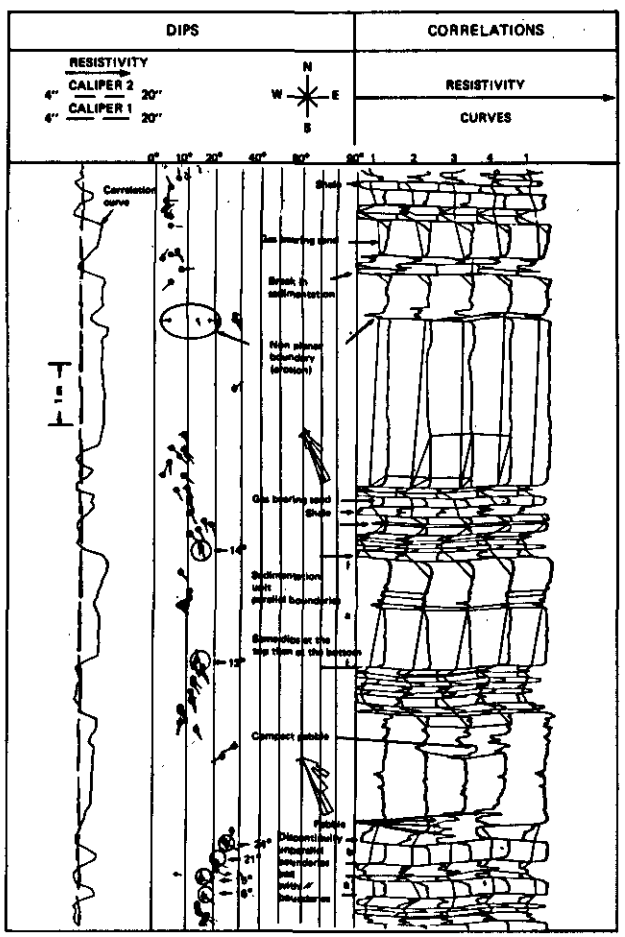

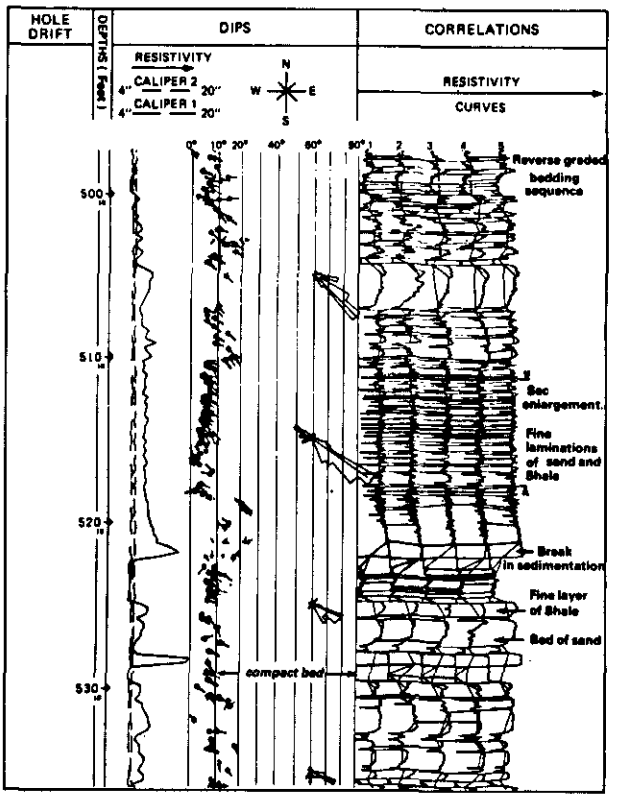

Fig. 4-16. - Very fine beds detected by HDT, showing wavy bedding.

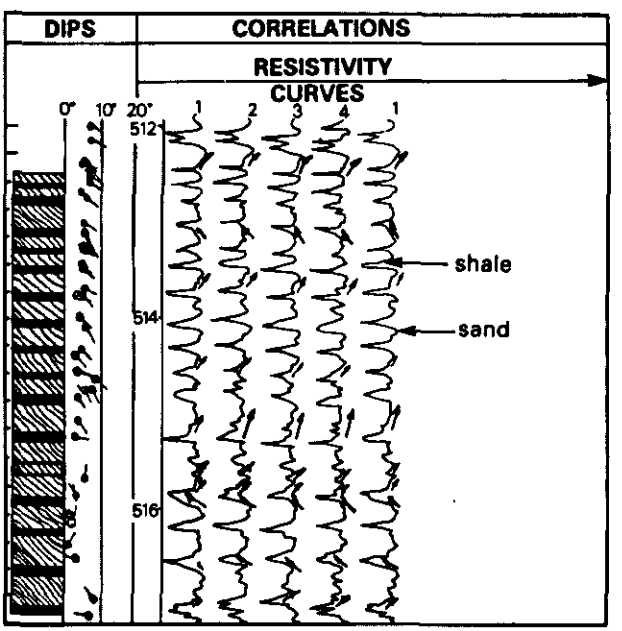

Fig. 4-17. - Enlargement of Fig. 4-16 showing details of beds and dip variations.

the upper and lower boundaries of the beds, their azimuth, and the dip and azimuth of the hole deviation are known (Fig. 4-13). These tools also

◀ Fig. 4-15. - Variations of bed thickness as illustrated by a GEODIP * display.

* Mark of Schlumberger.

allow computation of the most accurate and precise bed thickness because the tool speed variations are corrected. The other open-hole logs should be depth-matched and thickness corrected by reference to the dipmeter data.

Knowledge of the thickness of beds is important because it is sometimes related to the granulometry or to the depositional mode. For example, in sandy turbidites and volcanic ashes the thickness of the beds and the size of the grains are related and decrease in the direction of flow (Scheidegger & Potter, 1971). This is therefore a means to distinguish proximal from distal deposits. In another way Scott (1966), after Schwarzacher (1953), points out that the thickness of individual beds pertaining to the same kind of deposit are distributed following a straight line on a probability - logarithmic grid (Fig. 4-14).

According to Pettijohn (1975) the existence of laminations in marine environments is either the indication of very fast deposits, below the zone of wave action, or of reduction conditions at the sea floor explaining the absence of the benthonic fauna and related bioturbation.

The analysis of the vertical evolution of bed thicknesses within the same lithology can indicate a change in rhythm of sedimentation. These changes can be used as time-markers. Fig. 4-15 illustrates the thickness variations of beds just as they appear on a dipmeter, and Fig. 4-17, (an enlargement of part of Fig. 4-16), gives a clear picture of what can be achieved with this tool.

4.3.1.2. *Bedding planes*

As Campbell (1967) has correctly analysed, the surface of a bed represents a surface of non-deposition, or corresponds either to a rapid change in the condition of sedimentation (variation in the energy of environment) or to a surface of erosion. Usually the upper surface of a bed constitutes the lower surface of the following upper layer. A bedding plane has no thickness, but has a lateral extension that is equivalent to those layers, which they limit. Hence the characterization of beds depends on the recognition of their surfaces. The geometry of a layer depends on the relative disposition of its two boundaries.

Campbell, (1967), defined the different shapes of layers, according to the nature of their surfaces as shown in Fig. 4-18.

Fig. 4-19 illustrates the layers with even or planar, parallel, and continuous surfaces, whereas Fig. 4-20 shows discontinuous events (that appear only on 1, 2, or 3 pads).

Surfaces, which may be flat, but non-parallel, at the scale of the borehole are shown in Fig. 4-21. They will probably remain non parallel at the scale of the layers. The upper and lower boundaries of each bed can show different dips and sometimes

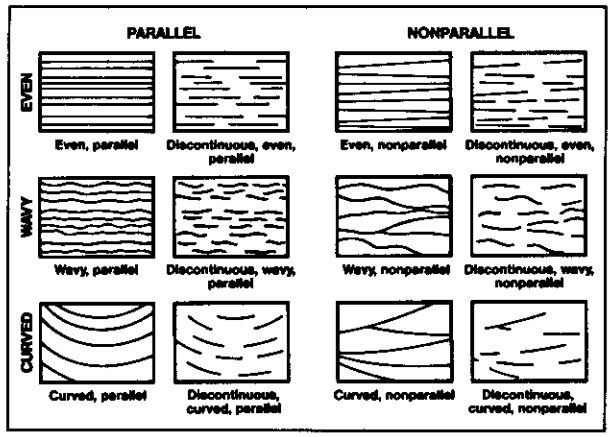

Fig. 4-18. - Diagram showing different shapes that can be acquired by beds and laminae, and the corresponding descriptive terms (from Campbell, 1967).

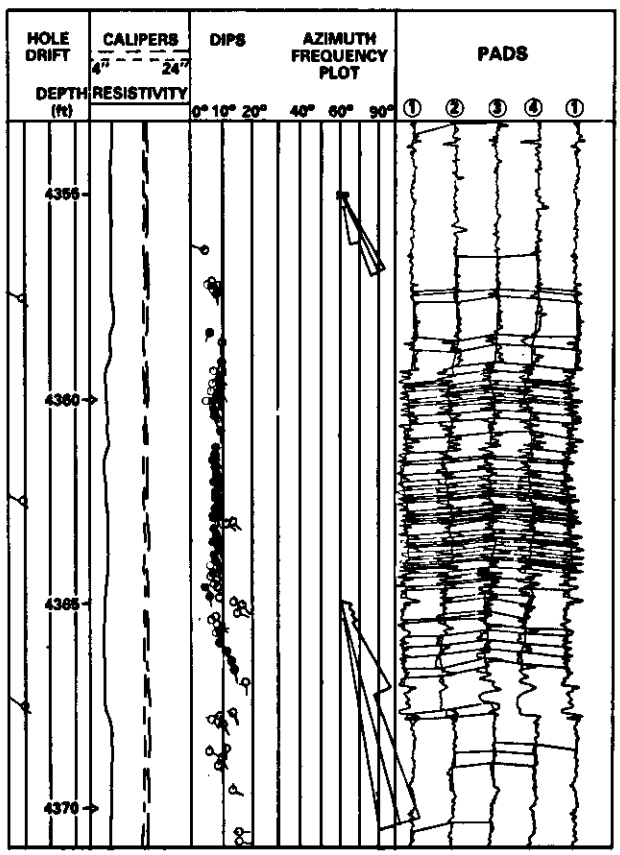

Fig. 4-19. - Example of even, parallel, continuous surface boundaries. Observe the very good consistency of dips.

different azimuth magnitudes suggesting non parallel boundaries. Examples of wavy non-planar surfaces are given by Fig. 4-22. In the GEODIP presentation they correspond to the computation of four planes by combination of the resistivity curves three by three (1-2-3, 2-3-4, 3-4-1, 4-1-2). Fig. 4-15 and 4-16 show other such examples. In the LOCDIP or SYNDIP programs presentation they are emphasized by a wavy symbol.

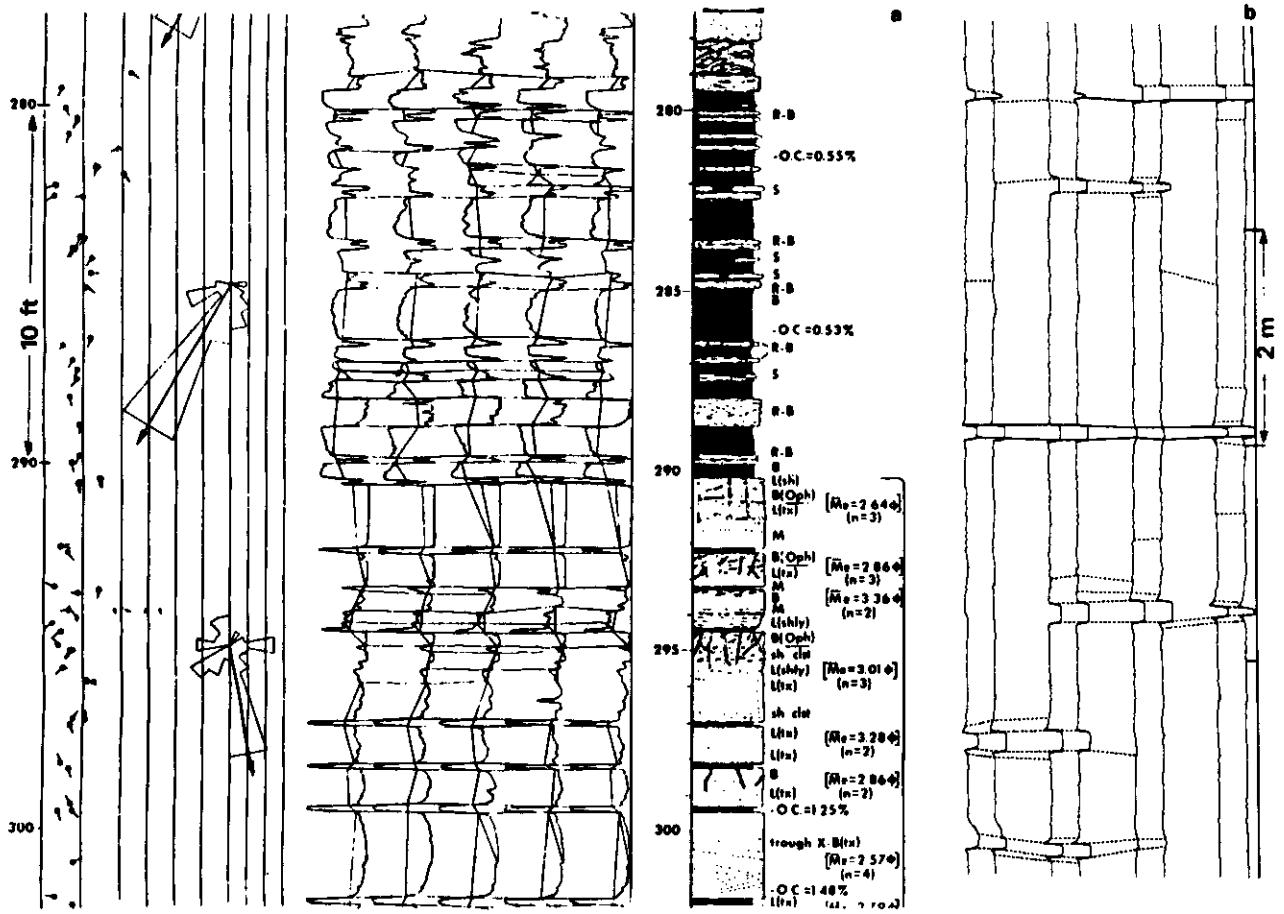

Fig. 4-20. - Examples of discontinuous, wavy beds; (a) on GEODIP display; (b) on LOCDIP display.

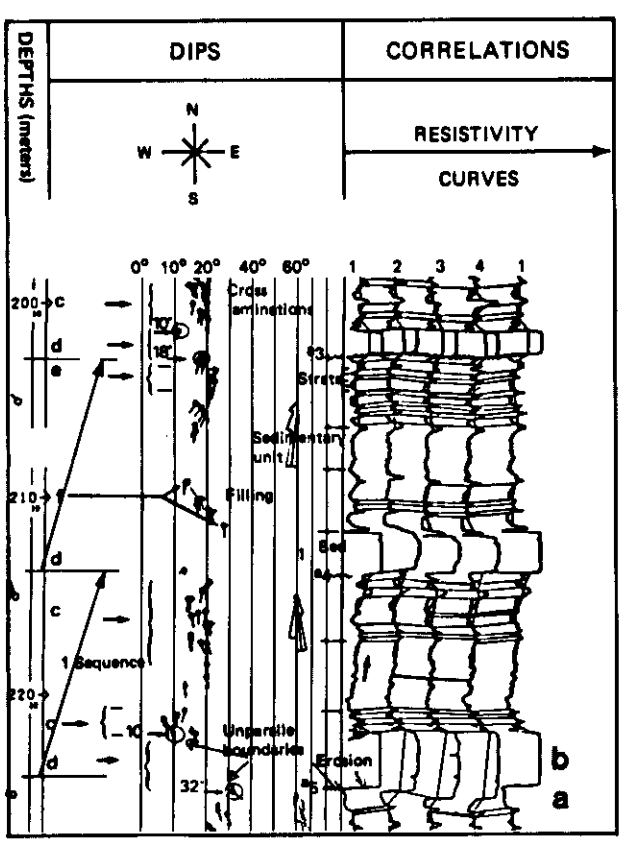

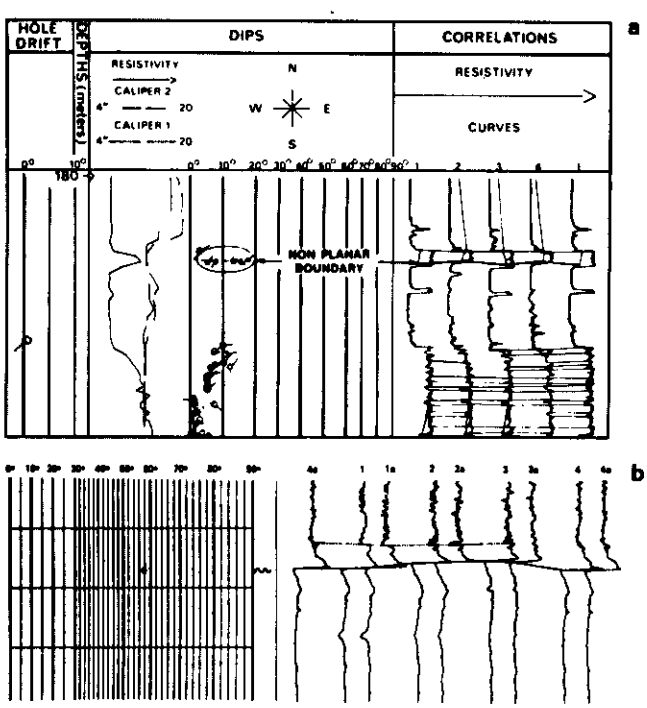

Fig. 4-22. - Examples of non planar boundary. (a) : in GEODIP presentation; (b) : in LOCDIP presentation.

◀Fig. 4-21. - Example of even, non parallel, continuous boundaries.

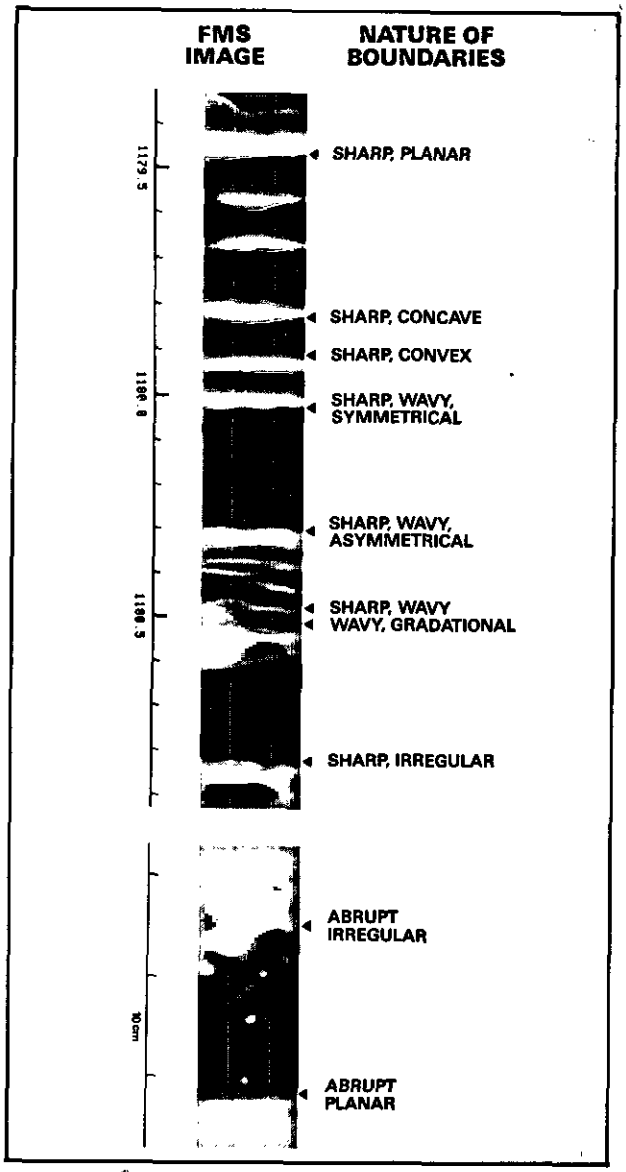

Fig. 4-23. - Several examples of bed boundaries can be observed on Formation MicroScanner images

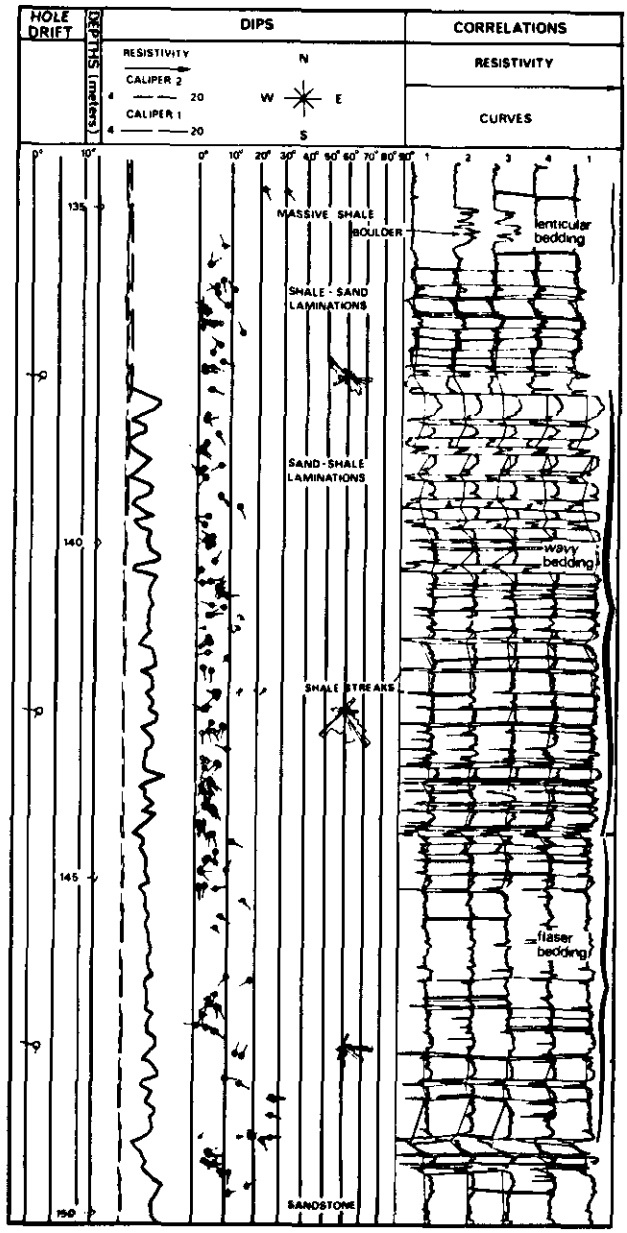

Fig. 4-24. - Example of flaser, wavy and lenticular bedding.

Fig. 4-16 and 4-24 illustrate a sedimentation cycle corresponding to an alternation of sand and clay beds (flaser, wavy and lenticular bedding) with wavy surfaces, detected by variations in the dip magnitude and azimuth. These kinds of features are better seen on Formation MicroScanner images (Fig. 4-25). They correspond to dark crescent-like or lenticular features appearing in sandstones.

Fig. 4-23 illustrates several types of bed boundaries as they can be observed on a Formation MicroScanner image. One can imagine the interest to recognize these features for facies definition and reconstruction of the environment.

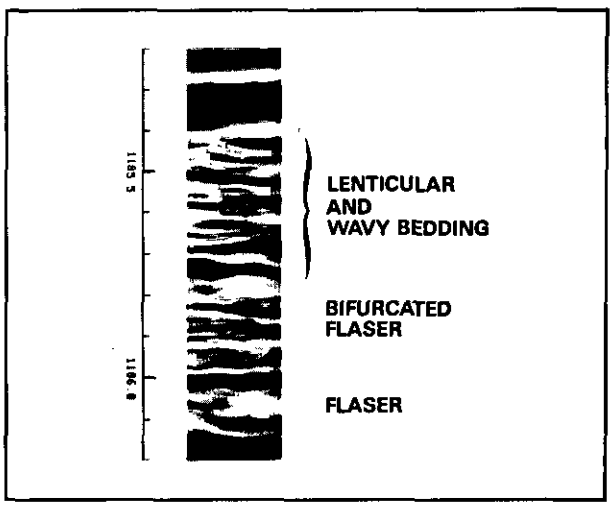

Fig. 4-25. - Example of flaser, wavy and lenticular bedding as seen on a Formation MicroScanner image

4.3.1.3. *Lateral dimension of beds*

The dipmeter tools respond to resistivity variations near the well bore and, therefore, the depth of investigation of a dipmeter is limited and does not allow to determine the precise lateral extension of any penetrated bed. However, it is possible to obtain some idea if the following factors are taken into consideration.

. *Thickness*

The thicker the bed with parallel boundaries, the higher will be the probability of a larger lateral extension (Fig. 4-15).

. *The bedding planes*

If these planes are planar and parallel, the probability of a larger extension will be higher (Figs. 4-19 and 4-26); contrarily, if both lower and upper boundaries are planar but at an angle it can lead to thinning, and to a thickening in the opposite direction. If the dip of two surfaces is known, it is possible to define the direction of thinning and the distance to the pinching out point. Even if the direction of thickening is known, the shape of the bed cannot be determined (Fig. 4-21).

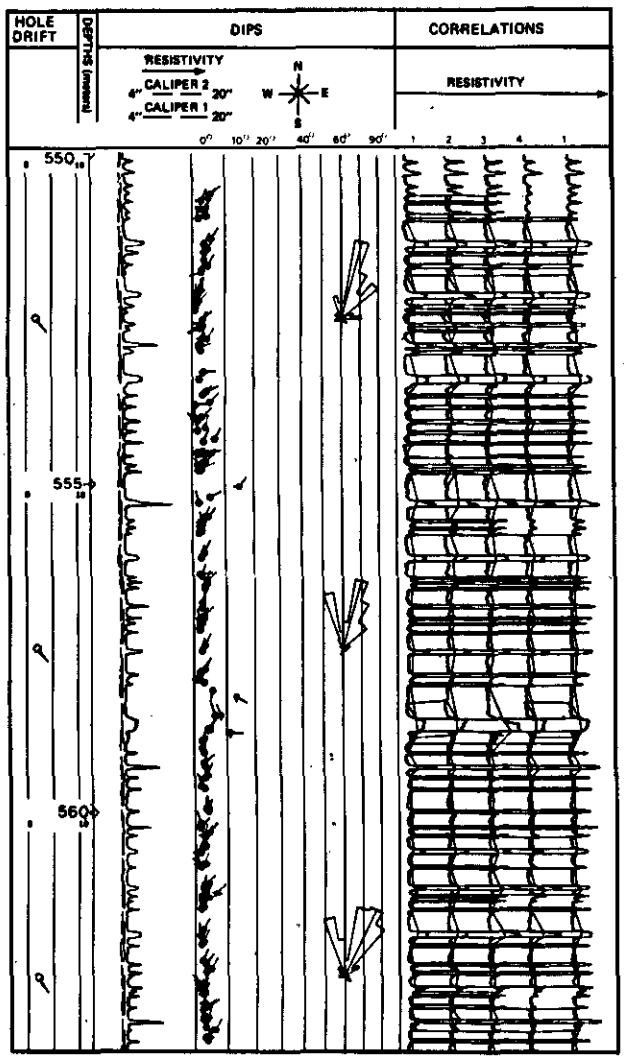

Fig. 4-26. - Example of numerous beds with good consistency of dips suggesting a quite important lateral extension.

. *Frequency of the beds*

If numbers of beds, (even thin ones), with a good dip azimuth and magnitude consistency, follow each other over a certain interval, an important lateral extension of those beds can be inferred (Figs. 4-19 and 4-26).

4.3.2. Nature of Bed Boundaries

The transition from one layer to another can either be abrupt or gradual. In the first case the boundary is well defined and agrees with the bedding planes. The boundary is conformable if it corresponds to a short break in sedimentation

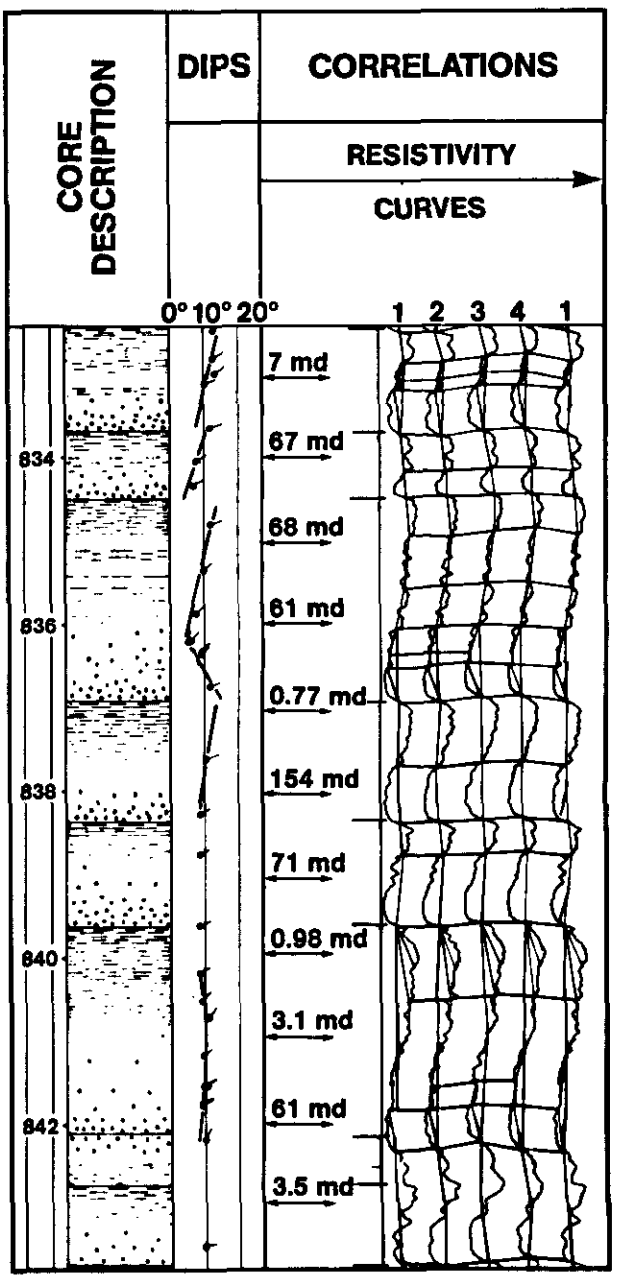

Fig. 4-27. - Example of gradational transition corresponding to sequences.

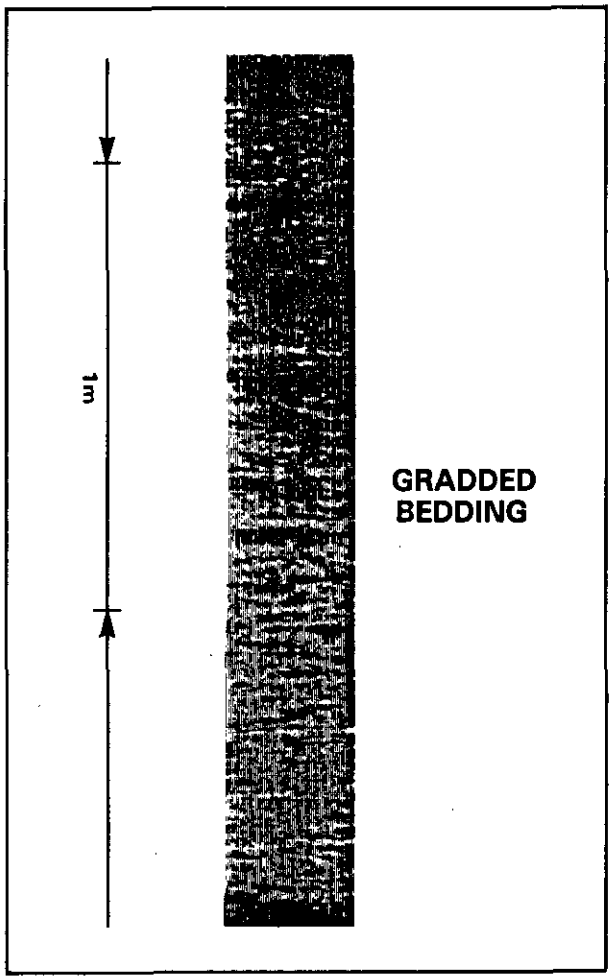

Fig. 4-28. - Example of gradational transition as seen on a Formation MicroScanner image (courtesy of Schlumberger).

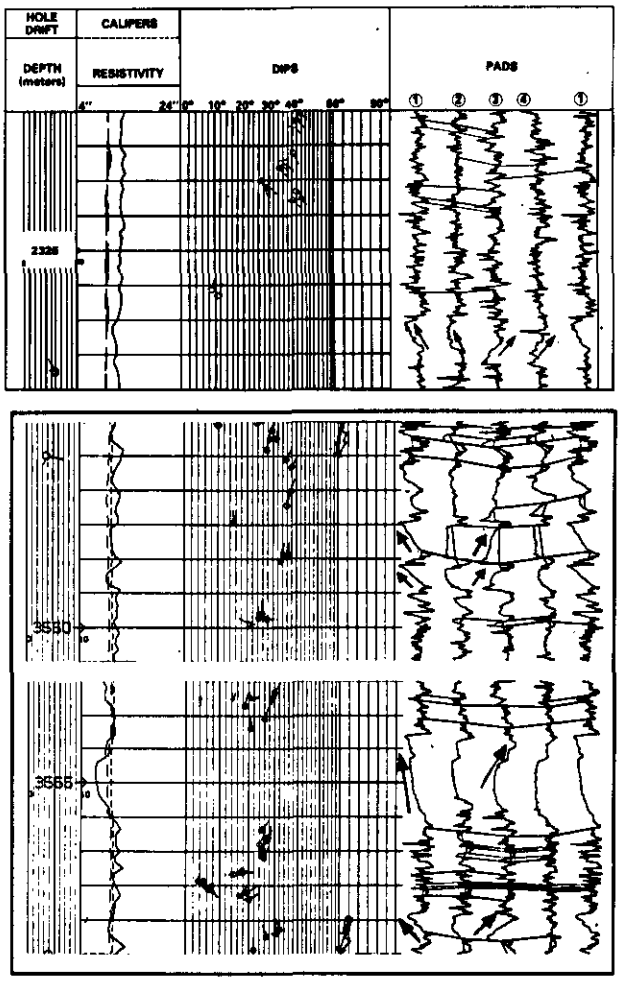

Fig. 4-29. - Example of pseudo-ramps due to low apparent angle between hole deviation and bed dips.

without modification of the depositional sequence or without erosion, and the beds remain parallel (Fig. 4-24). The boundary will be unconformable if it corresponds to a break in sedimentation, followed by a change in the sequence of deposition underlined either by an erosional or by a lateritized surface (if continental), and possibly by a change in dip (Fig. 4-21, level b). In this last example we can clearly observe : the erosion of the underlying sand bed on the resistivity curves of pads 3 and 4; the dip 32° N 120° of the lower boundary, compared to the average regional dip 20° N 180°; the filling-up of the erosional topography by a very consolidated and cemented rock (observe the thickest bed overlying the thinest one on pad 3), the upper surface of which has a dip of 10° N 180° with a draping effect. Another example of erosion with filling-up of the palaeotopography of erosion is given in Fig. 4-36 (above 495 m).

In the case of a gradational transition the boundary is not clearly defined and thus not visible. It then agrees with a sequence, which is either granulometric (normal or reverse), or mineralogic, or both (sand to shale, Fig. 4-27). Such transition is clearly seen on a Formation MicroScanner image by a vertical decrease, or increase, of gray density (Fig. 4-28) which is easier to detect at a compressed scale.

However, in the case of dipmeter data, this must not be mistaken with that related to a low apparent angle between the hole deviation (here 3°) and dip of beds, 30° to 40° which produces the pseudo-ramps on the opposite pads (Fig. 4-29).

4.3.3. Internal Organization of Beds

Several types of internal organization can be recognized.

4.3.3.1. *Massive bedding*

A bed can be *homogeneous*, (i.e. without any resistivity variation due to textural changes or sedimentary features). This corresponds to a constant condition of sedimentation, without apparent stratification either due to the absence of current ripples, or to an intensive bioturbation, or

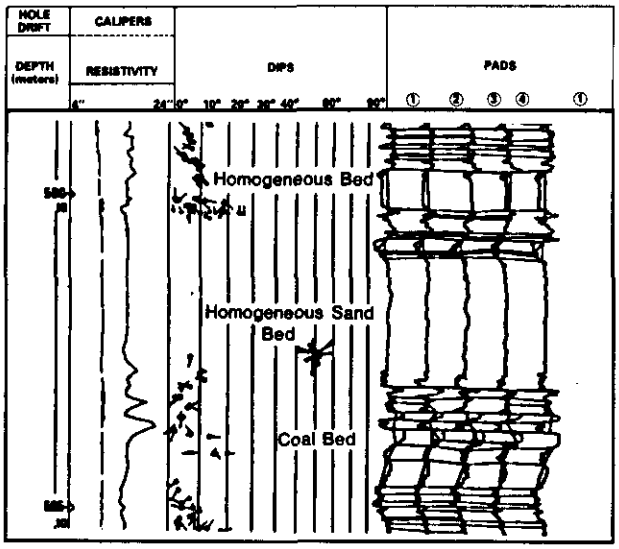

Fig. 4-30. - Example of homogeneous beds.

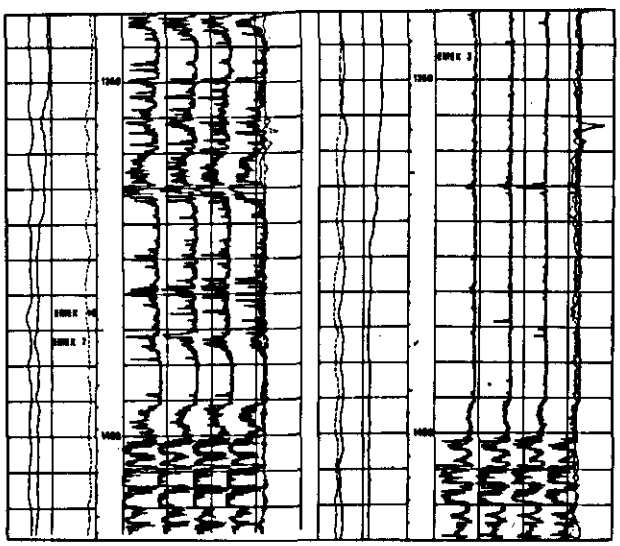

Fig. 4-31. - Example of change of curve appearence due to change of the EMEX current. According to the choice of the EMEX, the curves are saturated in low or high resistivities.

even to a massive sudden sedimentation which has completely destroyed all traces of stratification (Fig. 4-30).

Remark

A homogeneous bed must not be confused with an interval without curve activity due to poor choice of EMEX[1] current. In this case the resistivity curve is saturated in the very high or the very low resistivity region (compare the logs in Fig. 4-31 recorded on same interval, but with two different EMEX).

[1] The EMEX current is the current emitted by the whole sonde. It focusses the current emitted by the button electrodes. It is generally chosen to have the best contrast either in low or in high resistivity environments. In the SHDT tool it can be automatically adjusted.

4.3.3.2. *Laminated bedding*

A bed can be finely layered and therefore with stratifications either parallel, oblique or cross-bedded. Fig. 4-32 shows an example of stratification in an aeolian sand (large scale cross-bedding in the Rotliegendes from the North Sea). It is possible to recognize each sequence of deposition and to follow the variation in wind direction. Fig. 4-32b shows the result of a dip computation by the CLUSTER program for the same interval. Comparing Figs. 4-32a and 4-32b, one can see the great

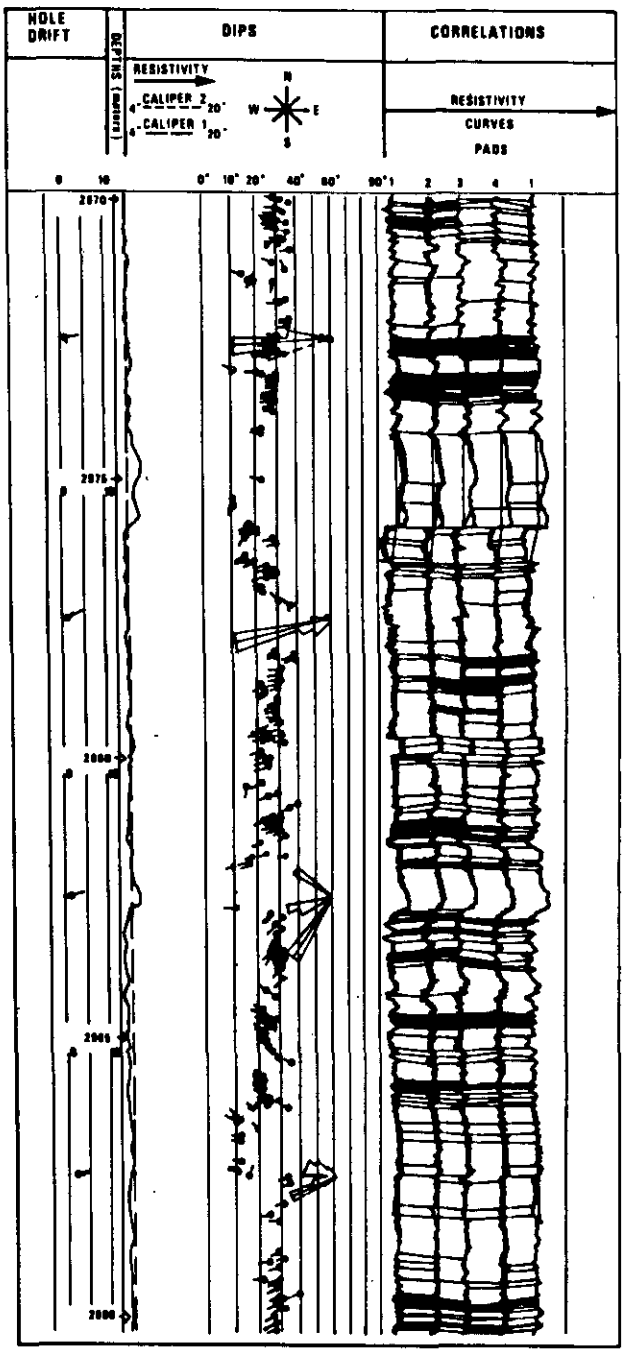

Fig. 4-32a. - Example of GEODIP response in an aeolian sand.

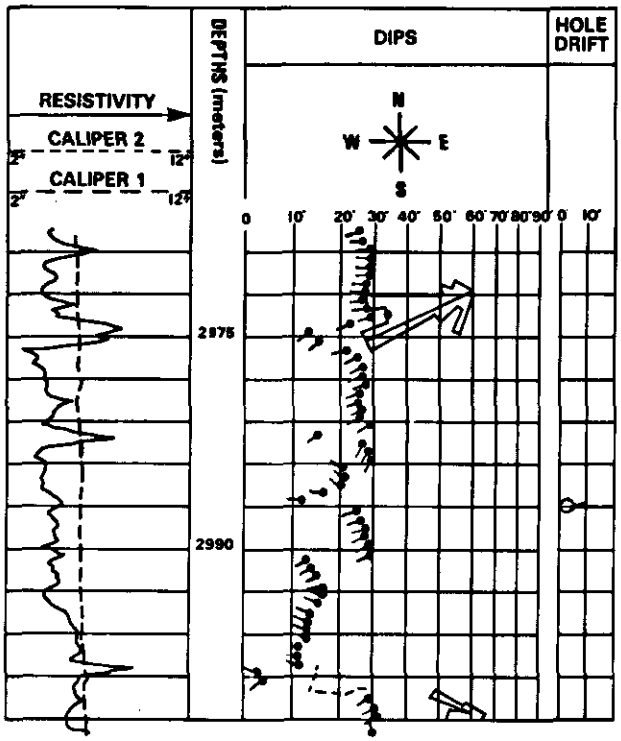

amount of additional information provided by the GEODIP program. Fig. 4-33 illustrates the kind of image obtained with the Formation MicroScanner tool in such an environment and its comparison with core photograph. The foresets are very clearly seen in this last case.

4.3.3.3. *Ripples and cross-bedding*

These features are better recognized with the aid of the Formation MicroScanner tool images as illustrated by Figs. 4-34 and 4-35.

But, oblique (cross-bedded) stratifications of a fluvial sand can also be detected with dipmeters as shown in Fig. 4-36. In this specific case the dip of each stratum cannot be conclusively determined but the dip corresponding to each boundary of a set (McKee & Weir, 1953) can be defined (Fig. 4-37).

◀ Fig. 4-32b. - Example of CLUSTER results on the same interval than Fig. 4-32a.

Fig. 4-33. - Formation MicroScanner image in aeolian sands and comparison with core photograph ▼

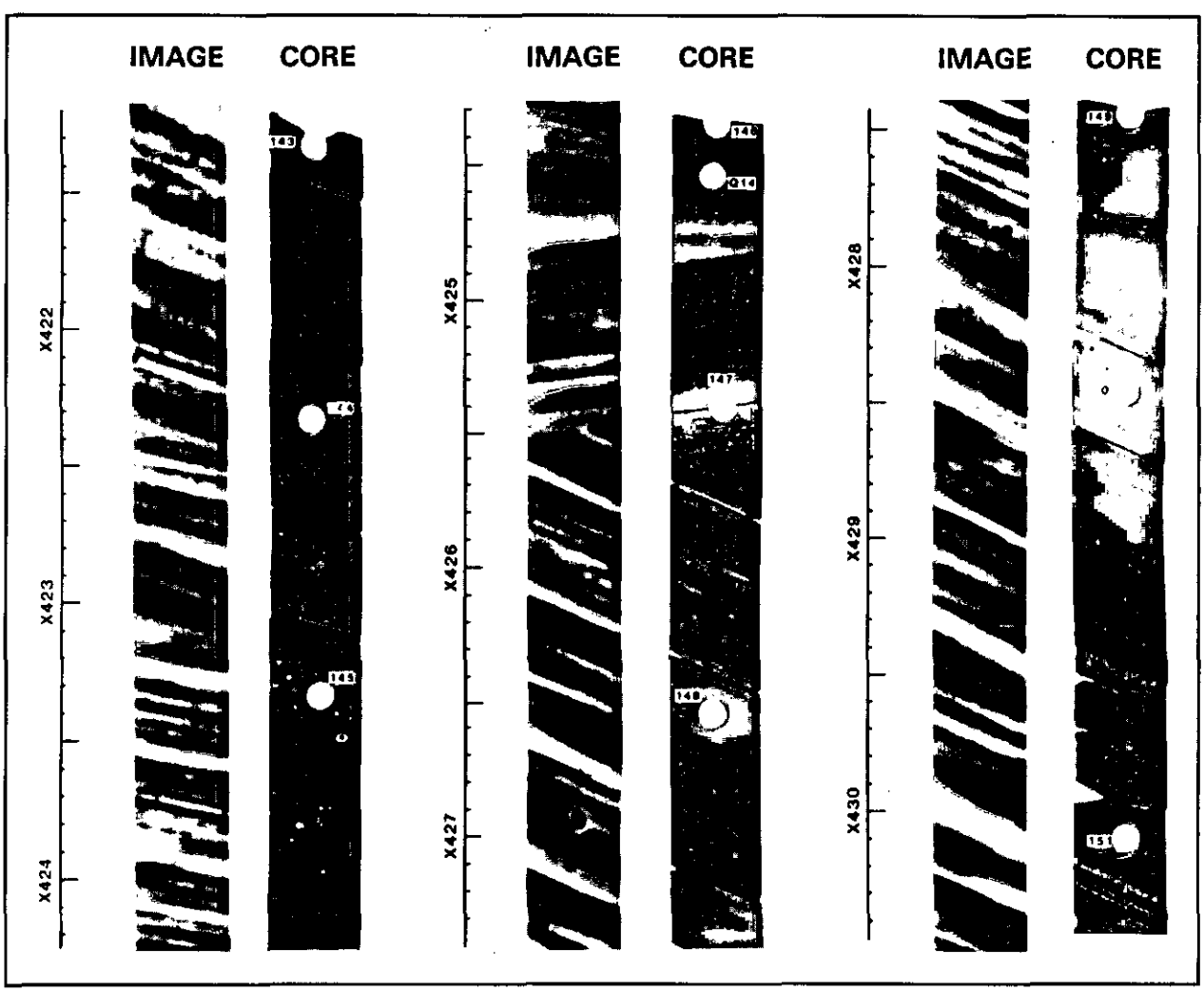

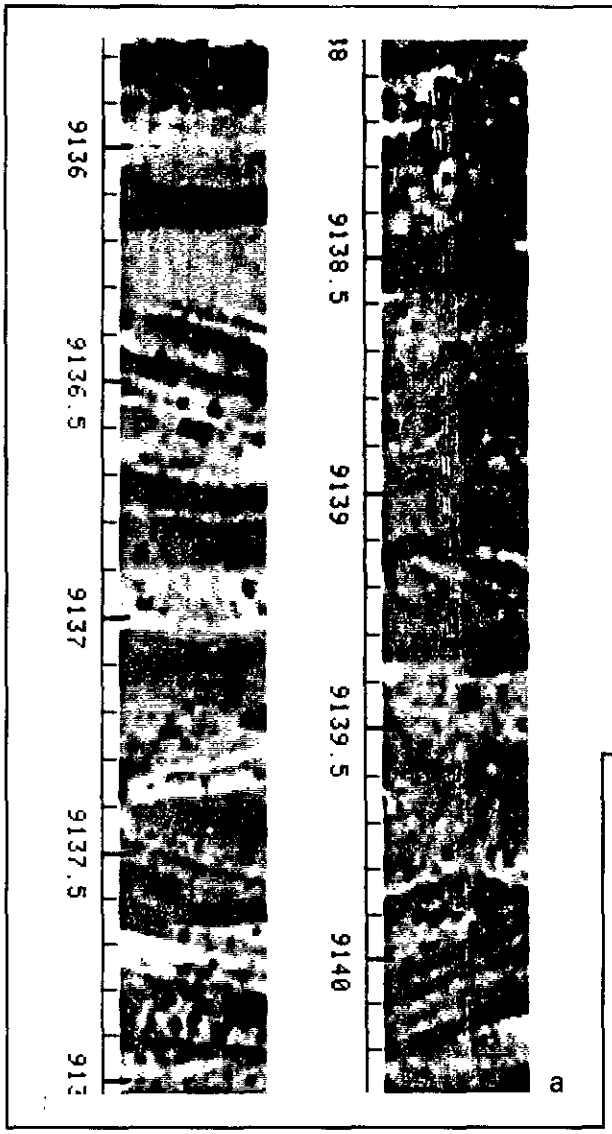

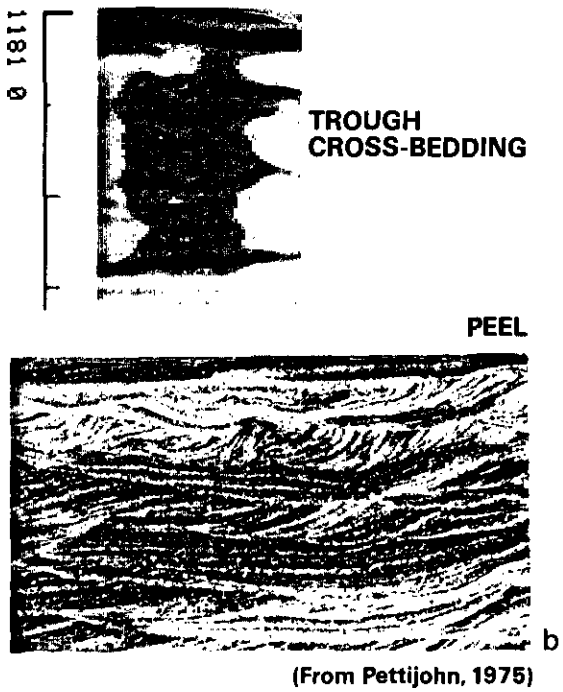

Fig. 4-34. - a) Example of herringbone. b) Example of cross-bedding well seen on a Formation MicroScanner image and comparison with peel. As can be observed, even cross-strata are detectable

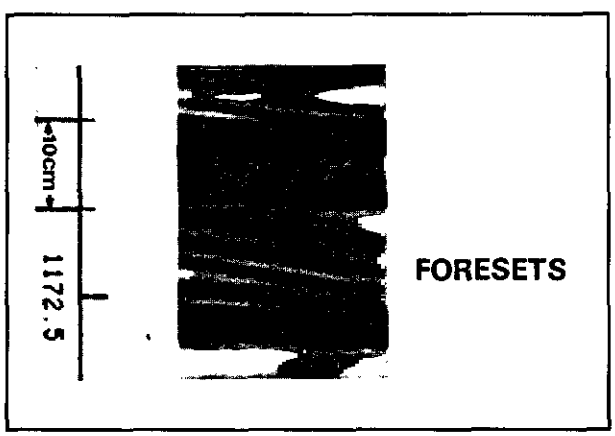

Fig. 4-35. - Example of tangential cross-bedding very well observed on a Formation MicroScanner image

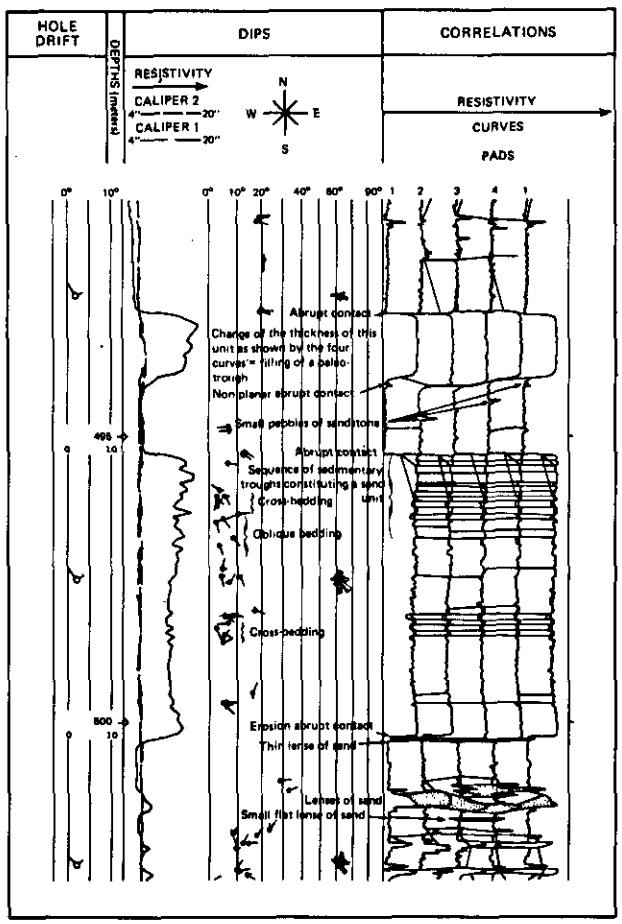

Fig. 4-36. - Example of cross-bedding in fluvial sand detected on GEODIP display by variations of dip magnitude and azimuth.

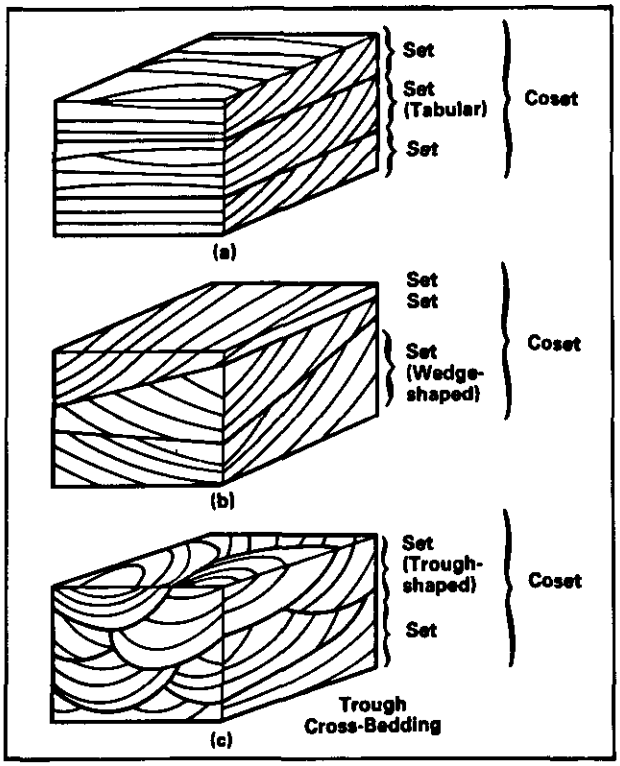

Fig. 4-37. - Terminology for cross-bedding. In (a) and (b) the cross-strata have tangential to angular contact with the lower set boundary. In (a) the sets are tabular, but in (b) they are wedge-shaped. In (c) both cross-strata and sets are trough shaped (Terminology after McKee & Weir, 1953).

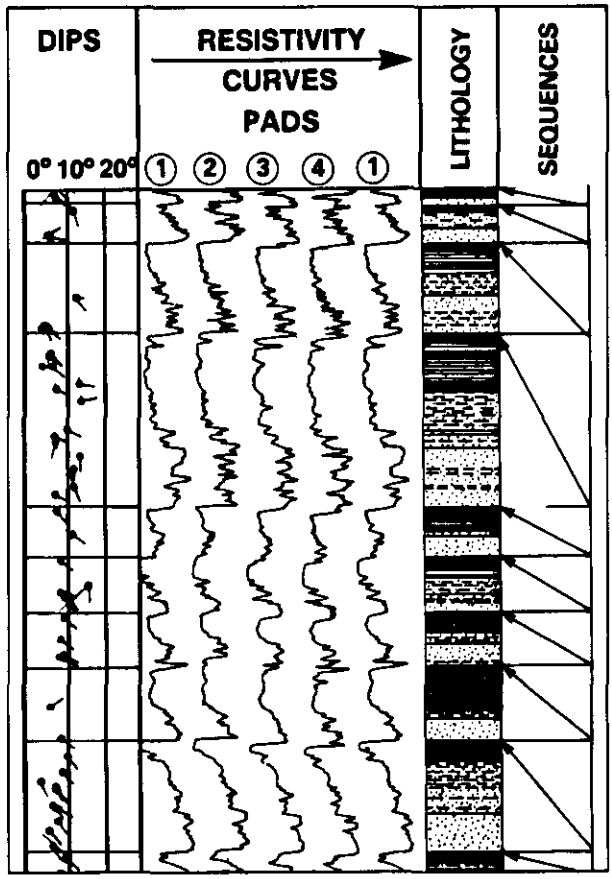

Fig. 4-38. - A series of fining upward sequences. At the bottom of each sequence is an oil-bearing coarse-grained sandstone, about one foot thick. Note that the raw dipmeter resistivities decrease upward in a normally graded bed as the permeable zones are oil-bearing.

4.3.3.4. *Graded bedding*

There are two types of vertical evolution of grain size in a bed : namely normal (fining upward) or reversed (coarsening upward) graded beddings. Normal graded bedding is generally underlined by an abrupt contact at the base (Fig. 4-27) and can be defined on the resistivity curves of a dipmeter. In this example the coarse sands of the base of the sequence are less resistive than the silts or shales of the top. This can be related, on the one hand to the fluid content (saline water), on the other hand to tortuosity variations (*m* factor), to permeability changes (less fluid mobility, different invasion depths), or possibly to porosity evolution. This last factor increases with the sorting, which in turn decreases as grain size decreases. The contrary can naturally exist when the sand contains a resistive fluid : gas, oil, fresh water (Fig. 4-38). The graded bedding can be reversed : the grain size increases upward (« coarsening upward »). Fig. 4-27 gives several examples of reversed sequences interbedded between normal sequences.

On Formation MicroScanner images graded bedding is generally better detected using a compressed scale rather than the traditional 1/5 scale (Fig. 4-39).

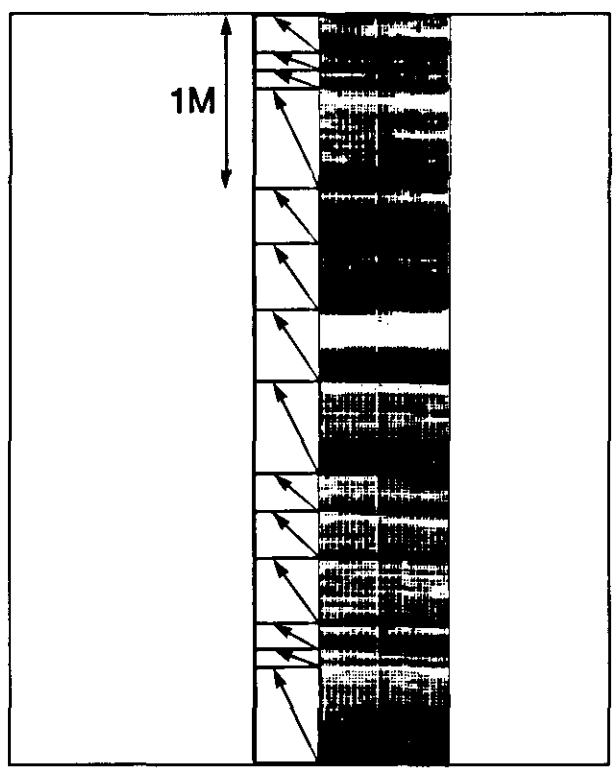

Fig. 4-39. - Example of graded bedding very well observed on Formation MicroScanner images ▶

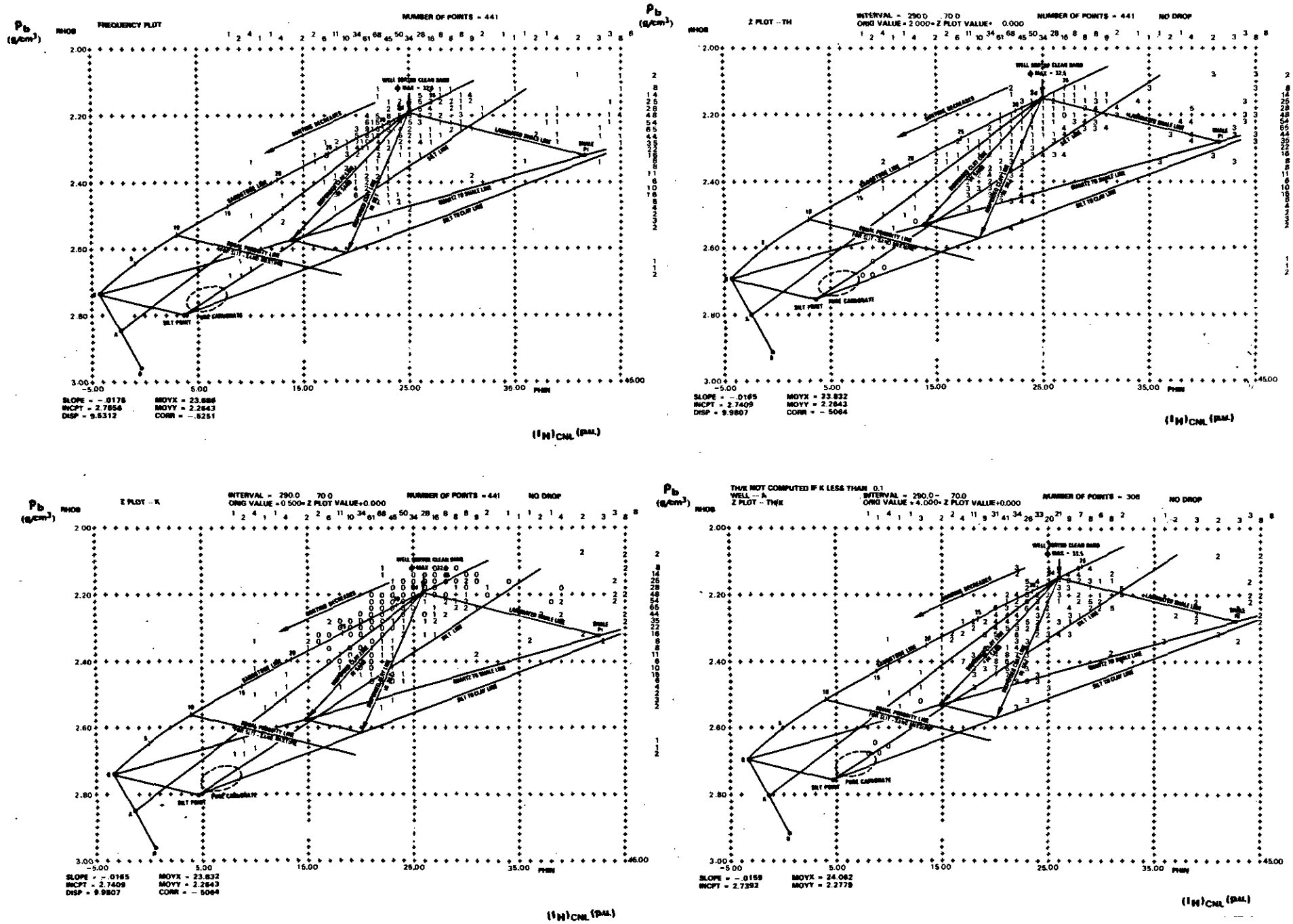

Fig. 4-40. - ρ_b vs ϕ_N crossplots with SP, K and Th on Z, showing clearly the grain size evolution (from Schlumberger, Well Evaluation Conference. India, 1983).

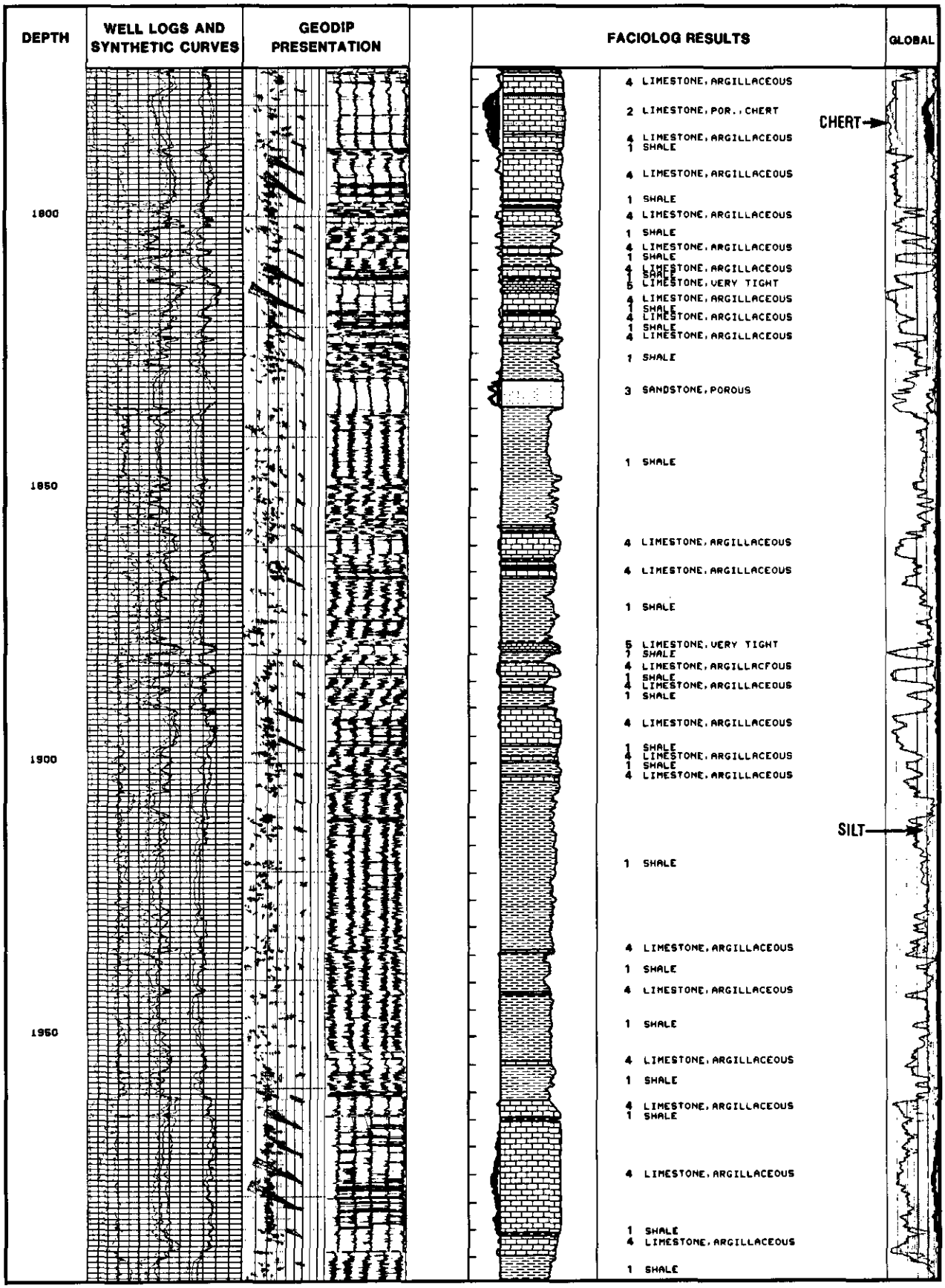

Fig. 4-41. - Composite-log including GEODIP results (from Schlumberger, Well Evaluation Conference. Egypt, 1984).

Graded bedding can be also recognised on ρ_b vs ϕ_N crossplots using Z-plot techniques as illustrated by Fig. 4-40 .

To accurately define the evolution of a sequence it is necessary to depth match the dipmeter with other logs (e.g. gamma-ray, density, neutron, resistivity,...) and with the lithological column. For this purpose a 1/200 scale composite display of either GEODIP or LOCDIP results together with other log data or the result of a processing giving lithology (Fig. 4-41) is necessary.

4.3.3.5. *Imbricated bedding (heterogeneous beds)*

A simple look at the dipmeter resistivity curves may sometimes reveal very heterogeneous beds. Numerous events are observed on each curve but they are either not correlatable or the correlations found by the program are erroneous. This situation generally corresponds with one of the following cases :

Conglomeratic intervals

When pebbles are larger (longest section wider than 1 cm for SHDT, or 5 mm for Formation MicroScanner tool) than the electrodes, they are detected as generally more resistive events than the surrounding matrix. The shape of the event varies with the size of the pebbles or their proportion in the rock. This gives a heterogeneous aspect to the curves with practically total absence of correlations between them (Fig. 4-42). When the pebbles touch each other (« grain supported ») the peaks are very close; where the pebbles are isolated in a sandy or shaly-sandy matrix (« mud supported ») the peaks are isolated (Fig. 4-42 and 4-43). The other open-hole logs may indicate a detritic formation predominated by quartz and often feldspars and micas, or by pebbles originated from igneous rocks. The natural gamma-ray spectrometry (NGS) may be very useful to determine the type of radioactive minerals.

Heterogeneous shales with inclusions (i.e chert, pebbles, anhydrite or carbonate nodules, lignitic fragments,...)

These inclusions in a more conductive matrix are generally very resistive and appear consequently as a series of resistive peaks (Fig. 4-44a). The other logs (gamma-ray, neutron, density) together, indicate the shaly nature of the matrix. Such inclusions may indicate a specific depositional environment (continental, aerial clay dessication,...).

Very finely laminated shale

Since the lamination is too thin to be detected by each electrode, the amplitudes of deflection are weak compared to the previous case and the resistivity curves appears to be « noisy » (Fig. 4-44b, lower section). The events are also rarely correlatable. This situation corresponds to laminations, veins or streaks of silt or sand, lignite fragments, having a thin thickness, and very short

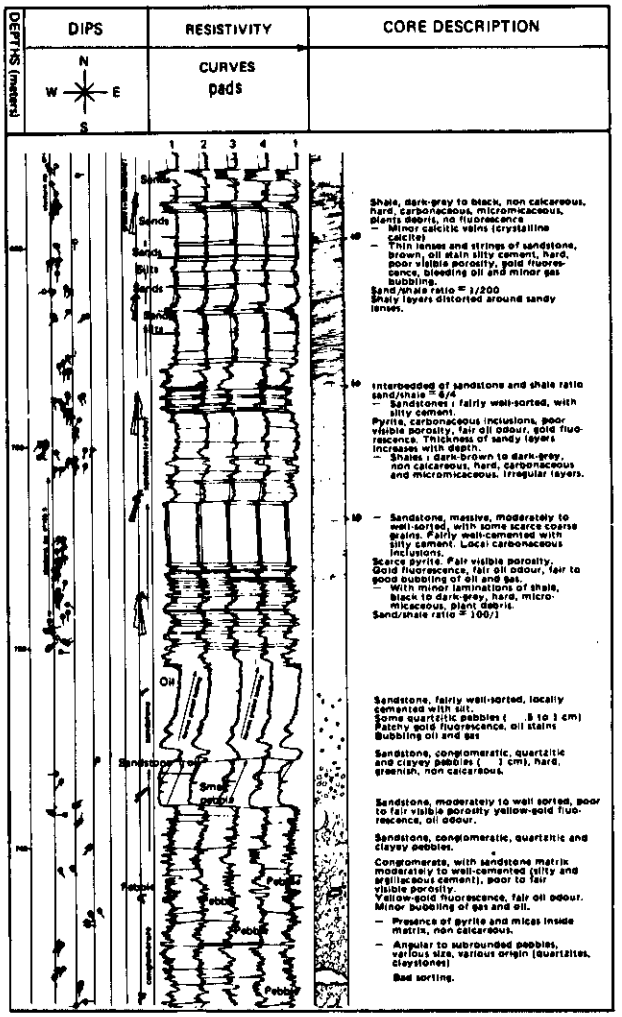

Fig. 4-42. - Example of a general fining upward sequence starting with a grain-supported conglomerate.

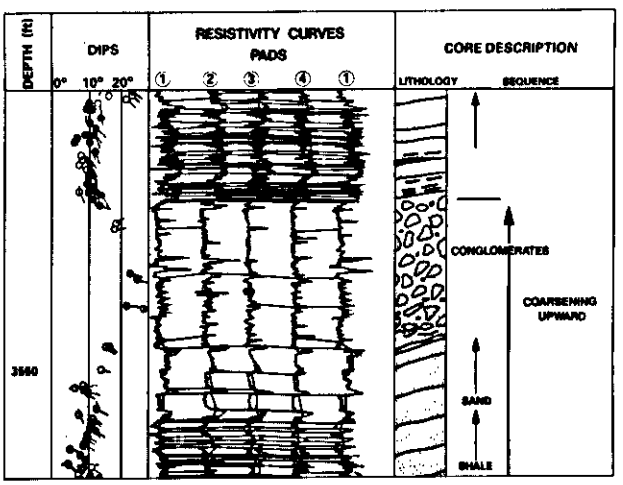

Fig. 4-43. - Example of a mud-supported conglomerate.

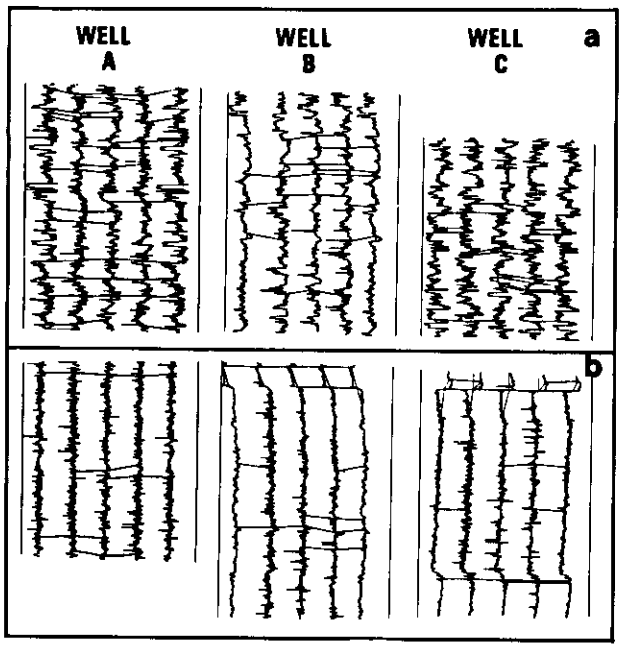

Fig. 4-44. - Examples of heterogeneous shales easily recognized and correlated from well to well. (a) : shales with nodules of anhydrite; (b) : shales with very thin veins or streaks of silt or sand.

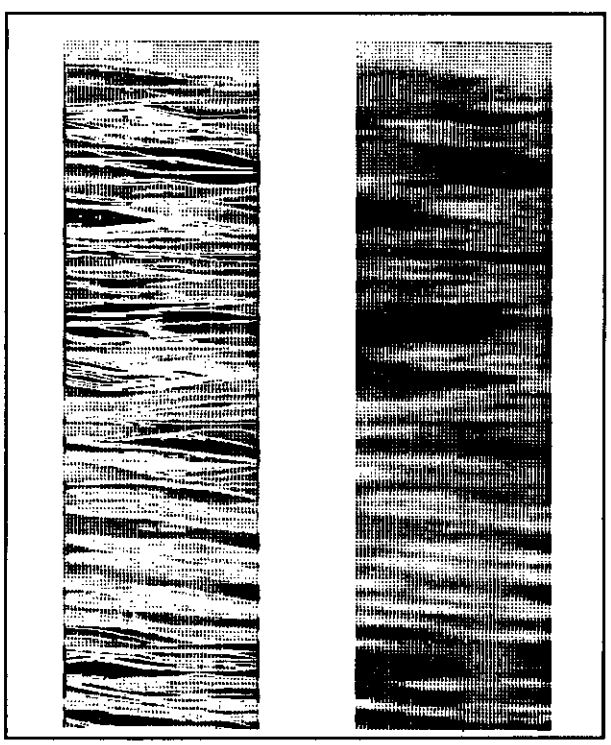

Fig. 4-45. - Shales with very fine discontinuous layers of silt as they can be seen on a Formation MicroScanner image (courtesy of Schlumberger).

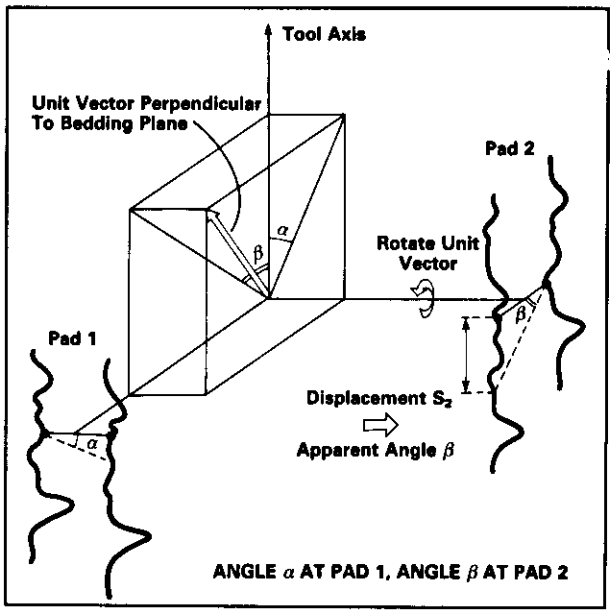

Fig. 4-46. - Dip computation method by association of two vectors (courtesy of Schlumberger).

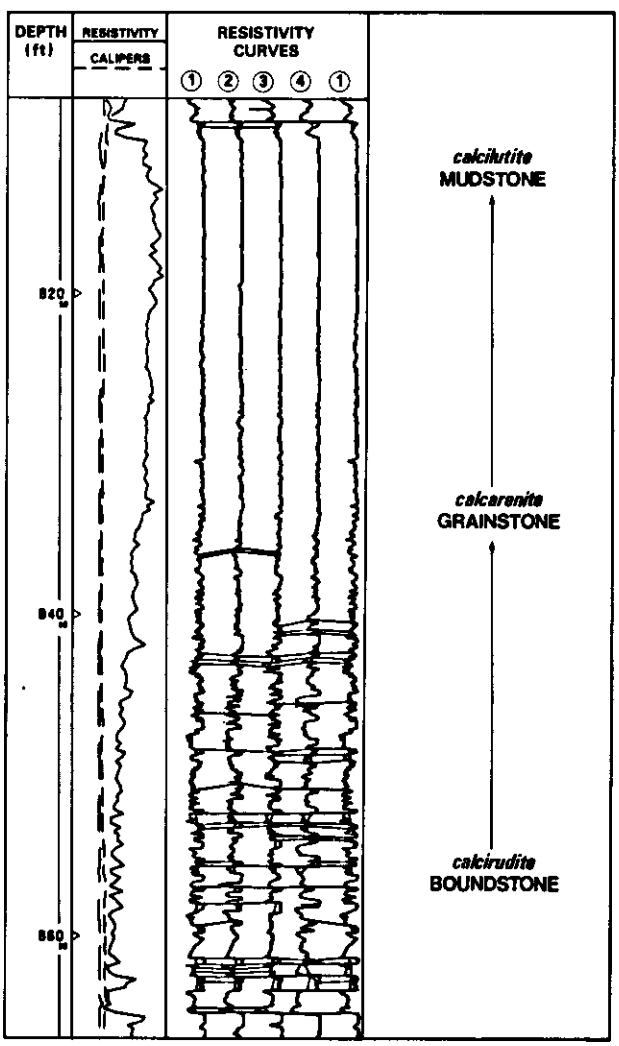

Fig. 4-47. - Example of GEODIP response in a reefal environment. Note that the aspect of the curves allows differentiation between boundstone or calcirudite, grainstone or calcarenite, and mudstone or calcilutite following the terms used by Dunham (1962) or Grabau (1903).

lateral extension. The Formation MicroScanner tool gives a clearer picture of this kind of shale (Fig. 4-45). On such images, even when the streaks are discontinuous, a general apparent slope can be deduced on each pad and associated to compute a dip (Fig. 4-46).

Reef formation

The resistivity curves show a heterogeneous aspect, due to the texture and the specific internal structure typical of these formations (i.e. coral fragments, or very resistive calcitized shells in micritic matrix, presence of conductive vugs,... (Fig. 4-47). The other logs provide lithological information to differenciate this from the previous cases : mineralogy essentially being composed of calcite or dolomite. In reefs the resistivity curves are much more indicative of the rock texture than its sedimentary structure (see chapter 3).

The Formation MicroScanner image clearly indicates the vuggy textural type : dark spots with irregular shapes (Fig. 4-48).

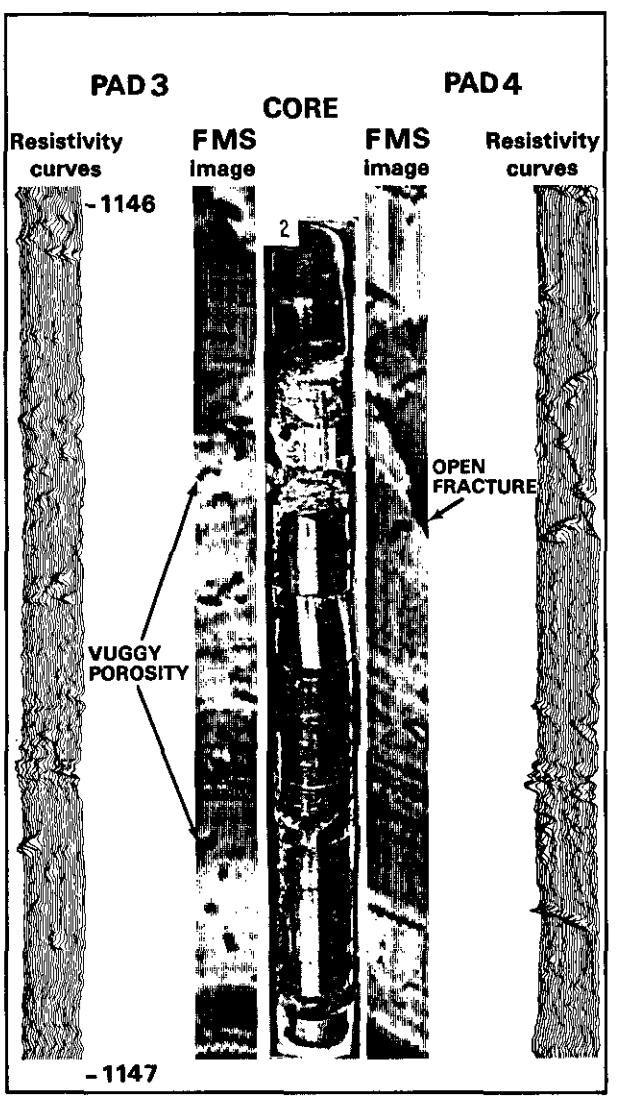

Phosphatic nodules

Resistive dots seen on Formation MicroScanner image above a break on conductivity curves can correspond to phosphatic nodules if these dots are associated with uranium peaks observed on a NGS log.

Sulfide crystals

Very conductive spikes seen on the Formation MicroScanner curves (black dots on images) can correspond to sulfide crystals (pyrite or galena) if they are associated with an increase of density or Pe index (Fig. 4-49).

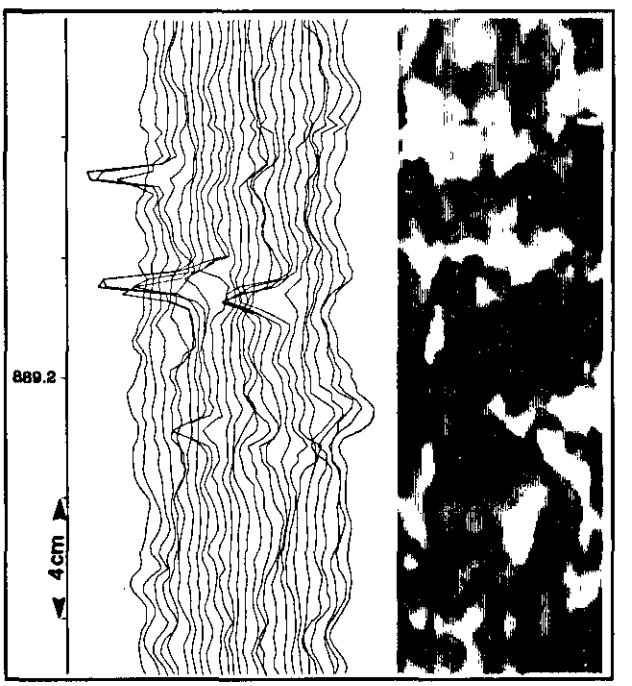

Fig. 4-49. - Example of pyrite crystals seen on a Formation MicroScanner image

Anhydritic nodules

Very resistive peaks on few resistivity curves, or irregular white spots on Formation MicroScanner images, can correspond to anhydrite nodules if at the same depth the other open-hole logs indicate limestones or dolomites with local increase of ρ_b (Fig. 4-50).

◀ Fig. 4-48. - Example of Formation MicroScanner images in a vuggy limestone

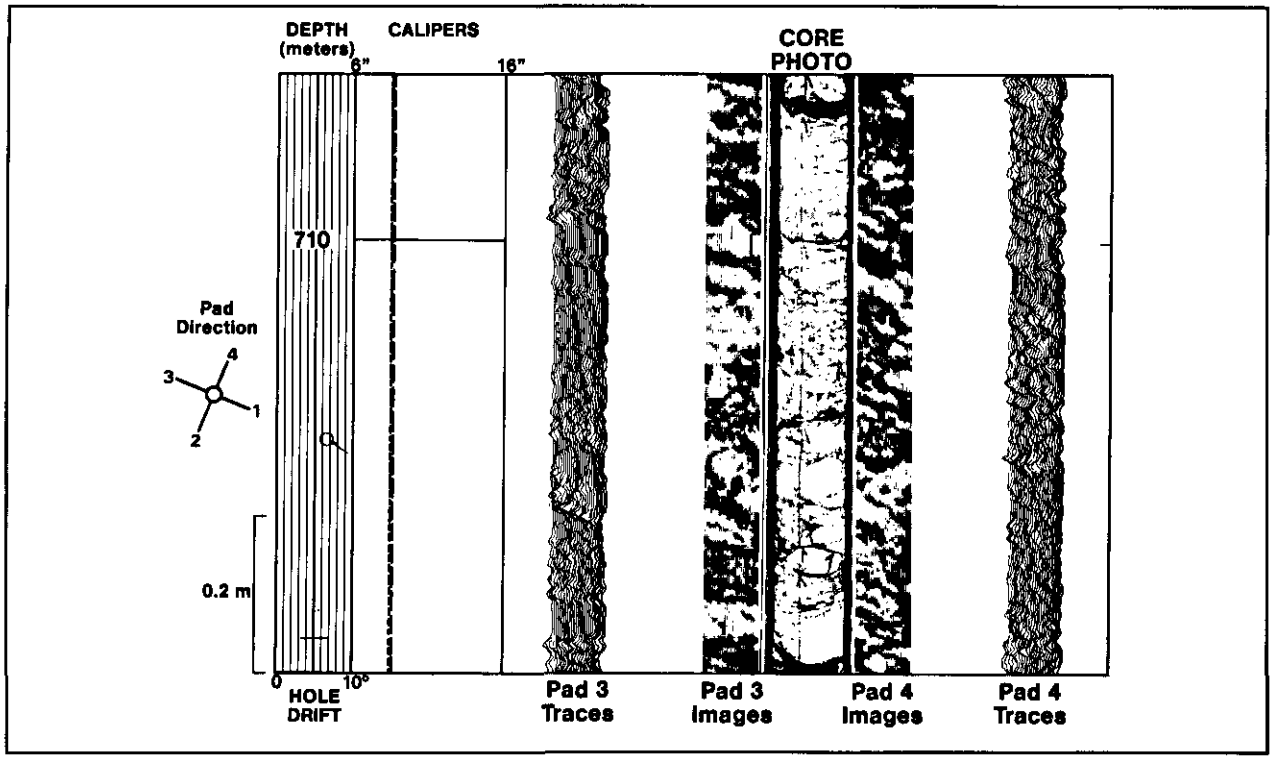

Fig. 4-50. - Example of nodules of anhydrite clearly observed on a Formation MicroScanner image

4.3.3.6. *Organic activity*

Sometimes, the Formation MicroScanner images can clearly show features which correspond to organic activity. For example, in Fig. 4-51 one can recognise a section of an oyster shell with its concavity upward. Presence of such oysters is confirmed by the core photograph. In Fig. 4-52 a burrow is detectable. It corresponds to the black vertical feature penetrating the whity substratum. The core photograph on the same interval confirms its existence.

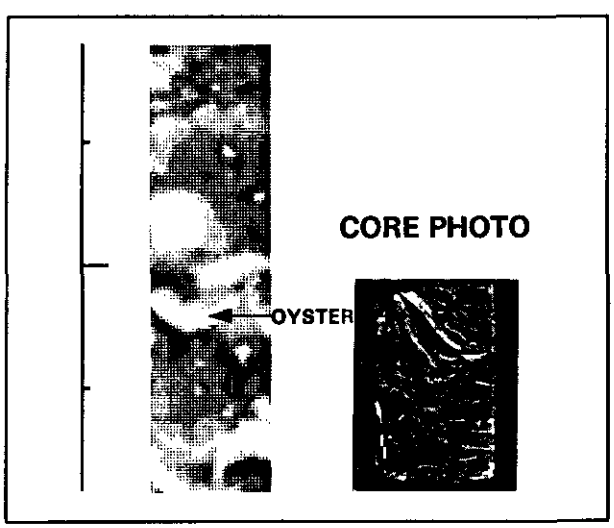

Fig. 4-51. - Example of oyster shell detected on a Formation MicroScanner image confirmed by core photograph

4.3.3.7. *Deformations*

Features such as *slumps,* convolutes, fractures, and stylolites can easily be recognised on Formation MicroScanner images as illustrated by Figs. 4-53 to 4-55. This recognition will be of considerable interest in determining the depositional environment more accurately, as well as the effects of diagenesis.

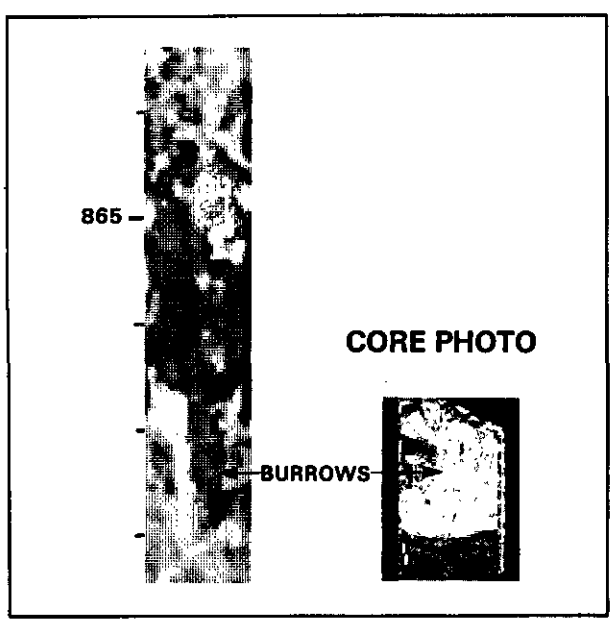

Fig. 4-52. - Example of burrow detected on a Formation MicroScanner image confirmed by core photograph

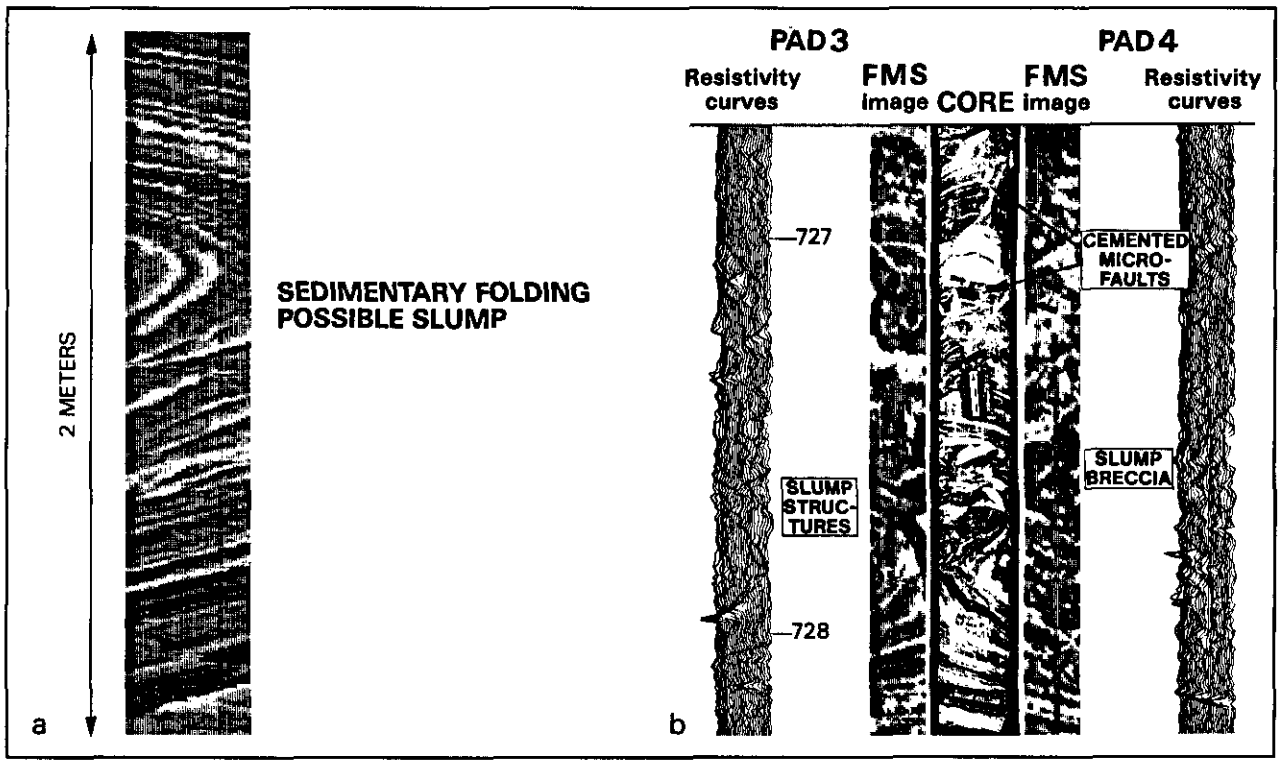

Fig. 4-53. - Examples of slumps very well seen on Formation MicroScanner images

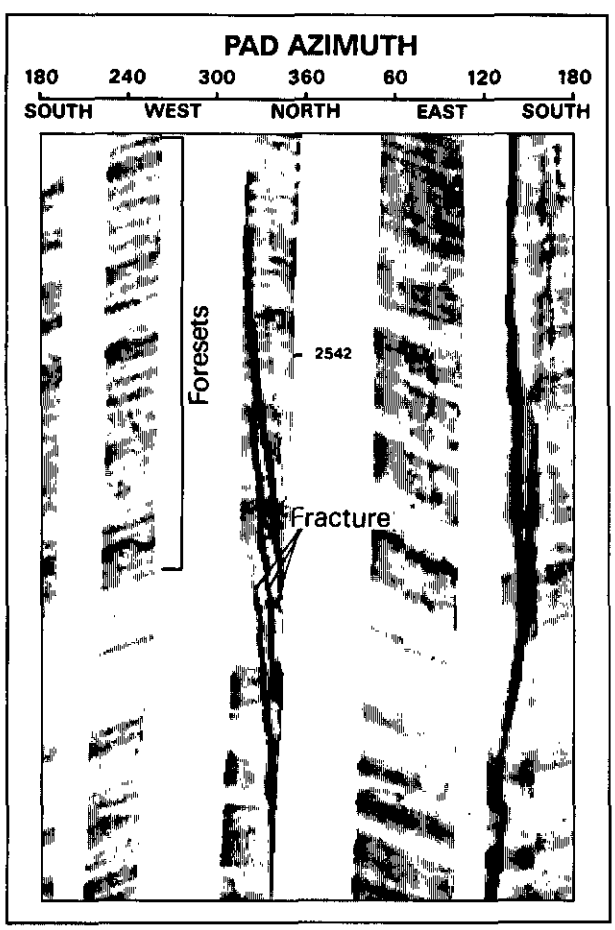

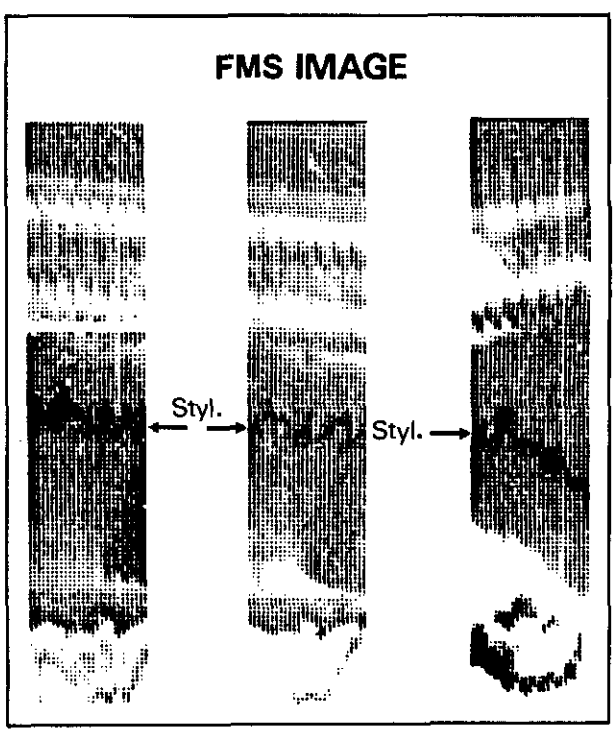

Fig. 4-55. - Example of stylolites very well observed on a Formation MicroScanner image

◄ Fig. 4-54. - Example of fractures detected on a Formation MicroScanner image. One can separate between open or healed fractures

4.3.4. Groups of Beds ("Bedset")

McKee & Weir (1953) have defined a group of beds as a succession of layers or laminae, essentially conformable, separated from adjacent sedimentary units by a surface of erosion or by a break in deposition, or a sudden change of charateristics.

The group of beds is called *simple* if it consists of two or more superimposed beds, having the same general characteristics (mineralogy, texture, internal structure) and surrounded by other beds of a different nature.

A sequence of beds is called *composite* if it consists of a group of layers, having different composition, texture, and internal structure (Fig. 4-56).

Groups of composite beds made of an alternation of parallel sand and shale layers, are shown in Figs. 4-19 and 4-26.

The case of a group of composite beds having a « wavy bedding » is illustrated in Figs. 4-16 and 4-24.

On this last figure are represented nearly all the intermediary cases between the « flaser bedding » and the « lenticular bedding », according to Reineck & Singh's classification, 1975, (Figs. 4-57 and 4-58).

Similar features are more easily observed on a Formation MicroScanner image (Fig. 4-59).

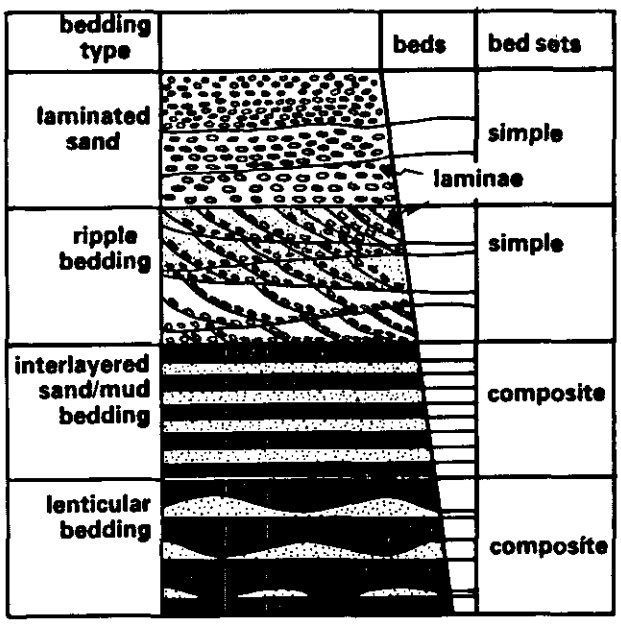

Fig. 4-56. - Schematic illustration of bedding terminology : lamina, bed, simple bed set, composite bed set, and bedding type (from Reineck & Singh, 1975).

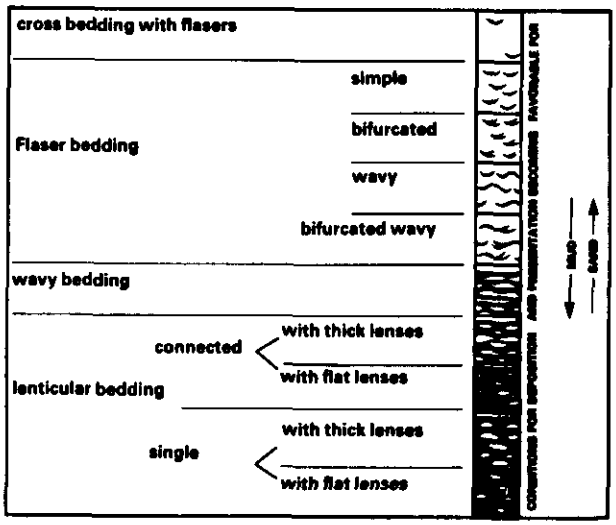

Fig. 4-57. - Schematic classification of flaser and lenticular bedding. Black = mud, white = sand (from Reineck & Singh, 1975).

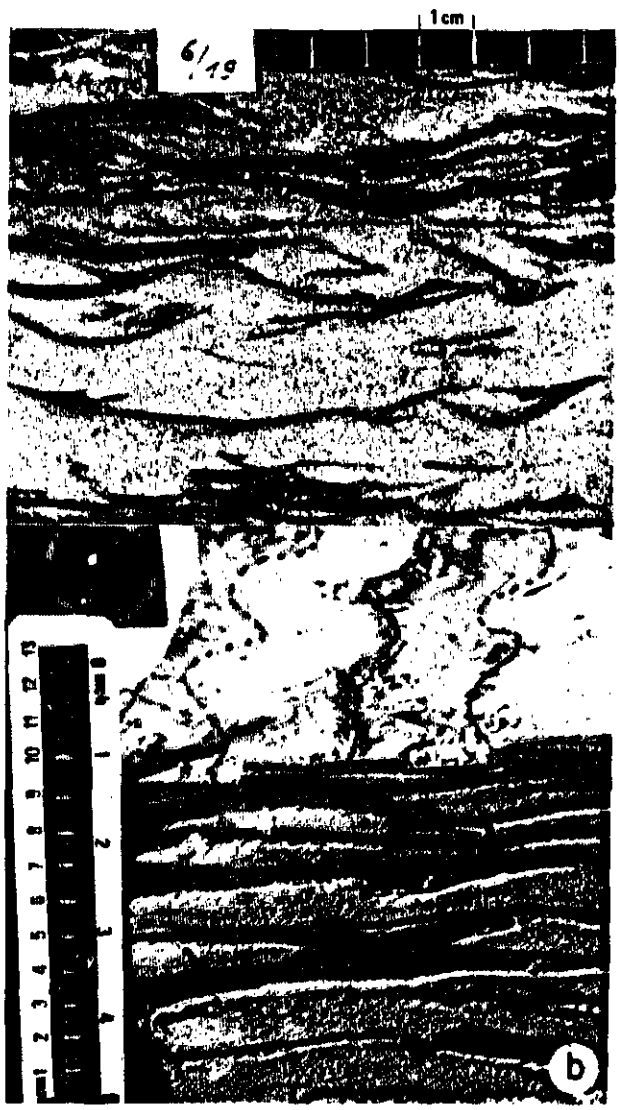

Fig. 4-58. - Photographs of (a) : flaser bedding, and (b) : lenticular bedding, on a section normal to the ripple crests (from Reineck & Singh, 1975). ▶

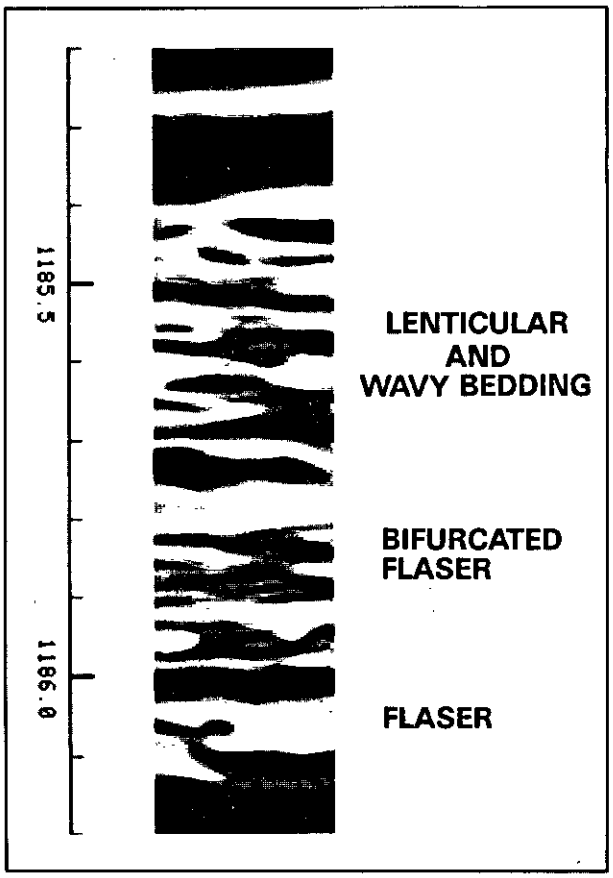

Fig. 4-59. - Examples of flaser and lenticular bedding very well seen on a Formation MicroScanner image

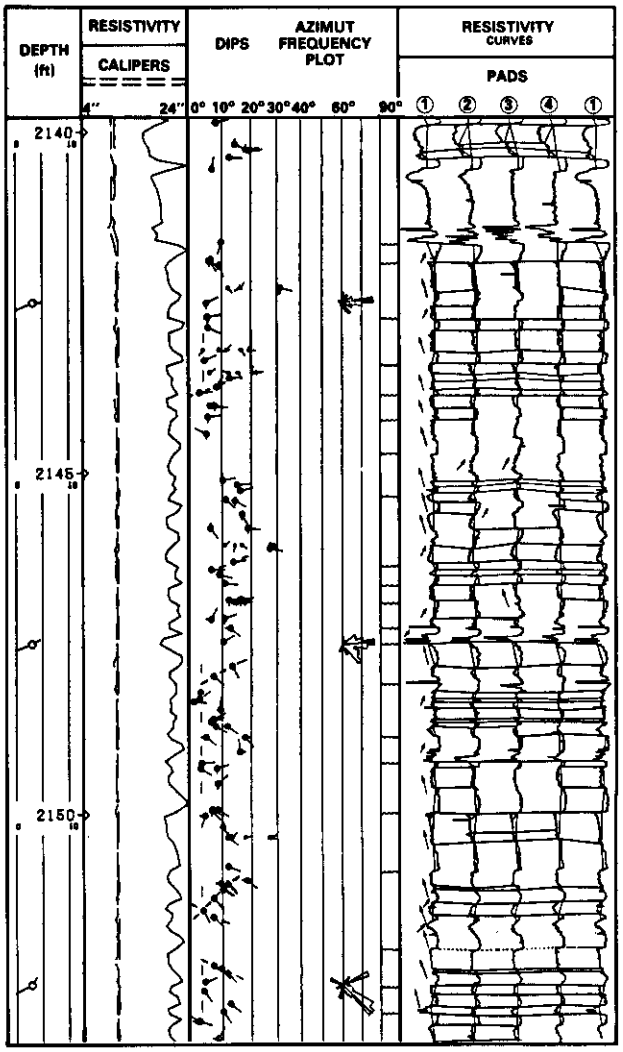

Fig. 4-60. - Example of thin sequences in a flysch series as seen by GEODIP (from Payre & Serra, 1979).

4.3.5. Sequences, Rhythms and Cycles

The great importance of sedimentological parameters for the reconstitution of a depositional environment is well established and a complete chapter is dedicated to this subject (see Chapter 6). The recognition of sequences, rhythms, or cycles in fact uses all available logs and most often passes through a preliminary period involving facies analysis. However, it may happen that the sequences, rhythms, or cycles are so thin that only the dipmeter or Formation MicroScanner tool is able to detect them due to their high vertical resolution. Such granulometric and lithologic sequences are shown (Fig. 4-27) and two other examples of such cases in « flysch » series and in carbonate turbidites are illustrated (Figs. 4-60 and 4-61).

4.3.6. Precise Definition of Structural Dip

Thanks to the possibility of analysing the geological origin of the dip, intervals which show dips with constant magnitude and azimuth in a low energy environment can be selected. They correspond to the groups of beds, whose bedding planes have not undergone any biogenic, sliding or slumping alteration. It can reasonably be assumed that these beds were deposited on nearly horizontal surfaces and that their present dips are the result of tectonic stresses (Figs. 4-19 and 4-26).

Once structural dip has been identified it is important that the amount of structural dip be removed before analysing the dip patterns.

4.3.7. Palaeocurrent Patterns and Direction of Transport

Dips computed by GEODIP or LOCDIP programs are associated with well-defined events on the curves and thus in the formation. Consequently, the origin of these events can be determined by the simultaneous examination of the resistivity curves. Dips related to current features can be selected and their evolution with depth analysed.

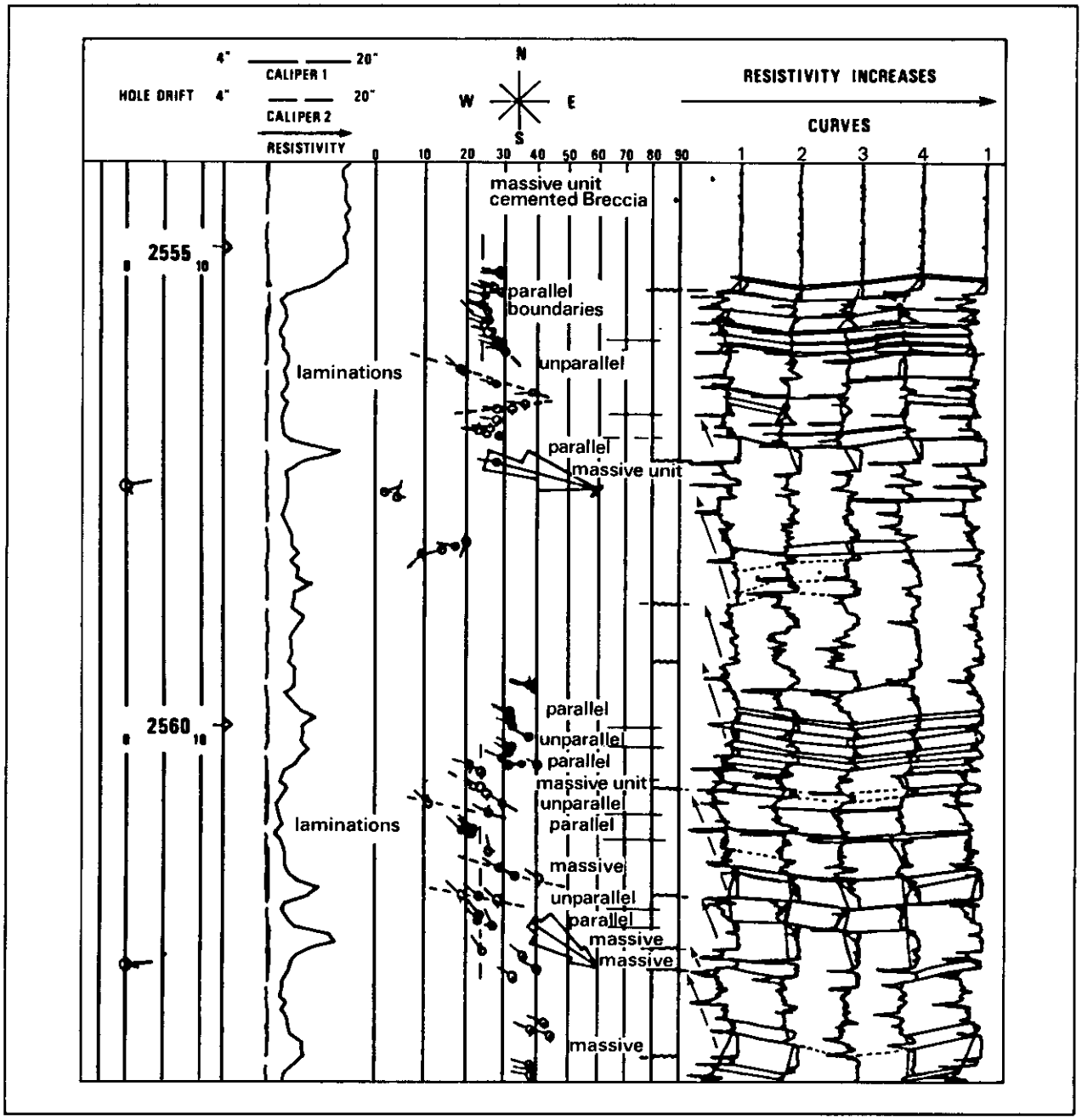

Fig. 4-61. - Example of thin sequences in a carbonate turbidite, as seen by GEODIP (from Payre & Serra, 1979).

The study of sedimentary structures can thus be completed by the definition of the direction of transport. Prior to the reconstruction of the original conditions it is necessary to subtract the structural dip or the dip evolutions related to differential compaction. Thereafter it is possible to determine whether the direction of the current is uni-, bi-, or poly-modal and identify the amplitude of the dip variation. These results will then help to specify the dynamic regime prevailing in the depositional basin (energy of current, change of direction with time,...), and obtain a better idea of the depositional environment (Table 4-5).

The dip grouping (« colour pattern ») technique introduced by Gilreath *et al.* (1964) can be used for this purpose (Fig. 4-62) if it is applied on the sedimentary unit. A succession of dips with the same azimuth, but magnitude increasing upwards within the same sedimentary unit defines a group called « blue pattern ». This pattern characterizes a sequence of foresets related to current ridges that are associated with an accretion or a progradation (Fig. 4-63). These foresets are sometimes very well observed on Formation MicroScanner images and consequently the direction of transport current can easily be defined (Fig. 4-64). If the dips

Table 4-5

Listing of current bedding characteristics in terms of dip spread and dip sequences versus depth and current bedding orientation related to palaeoslope and sand body geometry for several depositional environments.

DEPOSITIONAL ENVIRONMENT	CURRENT BEDDING CHARACTERISTICS	CURRENT BEDDING ORIENTATION
BRAIDED STREAM ALLUVIUM	- FESTOON (TROUGH) TYPE - LARGE DIP SPREAD	- UNIMODAL LARGE SCATTER (90°) - GENERALLY DOWN PALEOSLOPE - DIRECTION OF SAND ELONGATION
MEANDERING STREAM POINT BARS	- FESTOON (TROUGH) TYPE - LARGE DIP SPREAD - HIGHER ANGLE AT BASE - LOW ANGLE TABULAR AT TOP	- UNIMODAL,SEVERE SCATTER (180°) - GENERALLY DOWN PALEOSLOPE - DIRECTION OF MEANDER SELT & SAND BODY ALIGNMENT
EOLIAN DUNES	- TABULAR HIGH ANGLE (30°) EXTREMELY CONSISTENT - DECREASING ANGLE AT BASE	- UNIMODAL-LITTLE SCATTER - NO RELATION TO PALEOSLOPE - NORMAL TO SAND ELONGATION
DELTA DISTRIBUTARY CHANNELS	- FESTOON TABULAR - HIGHER ANGLE AT BASE - MODERATE SPREAD	- UNIMODAL MODERATE SCATTER - IN SEAWARD DIRECTION - DIRECTION OF SAND ELONGATION
DISTRIBUTARY MOUTH BARS	- TABULAR MODERATE ANGLE (> 10°) - HIGHER ANGLE AT TOP - MODERATE SPREAD	- UNIMODAL RADIATING - SEAWARD DIRECTION BUT INFLUENCED BY LONGSHORE CURRENTS - DIRECTION OF SAND ELONGATION (LOBATE)
ESTUARINE & TIDAL CHANNELS	- TABULAR LOW ANGLE (10°) - HIGHER ANGLE AT BASE - FLATTER AT TOP	- SIMODAL (180°) SCATTERED - NORMAL TO COASTLINE - DIRECTION OF SAND ELONGATION
BEACHES & BARS	- TABULAR - LOW ANGLE ON SEAWARD SIDE (< 10°) - HIGH ANGLE ON LAGOONAL SIDE (> 20°)	- UNIMODAL POSSIBLY SIMODAL - USUALLY DOWN PALEOSLOPE BUT POSSIBLY REVERSED - NORMAL TO SAND ELONGATION
MARINE SHELF SANDS	- TABULAR - VERY LOW ANGLE TROUGHOUT	- POLYMODAL-RANDOM
TURBIDITES	- TABULAR OR ABSENT - VERY LOW ANGLE TROUGHOUT - RARELY OBSERVABLE	- UNIMODAL - DOWN PALEOSLOPE - DIRECTION OF SAND ELONGATION

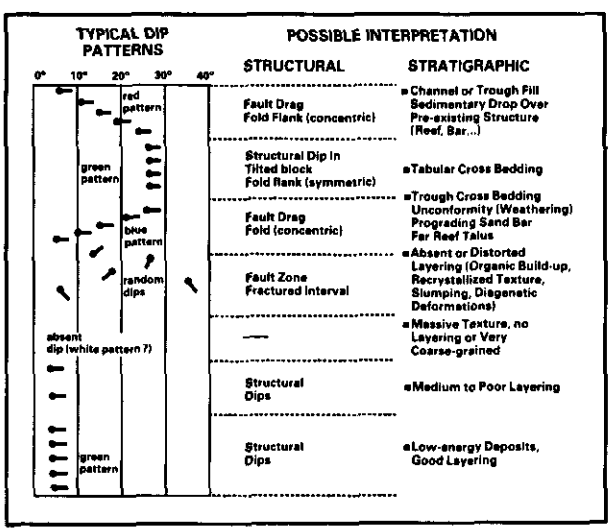

Fig. 4-62. - Coloured dip patterns and the geological events commonly associated with them (from Gilreath *et al.*, 1964).

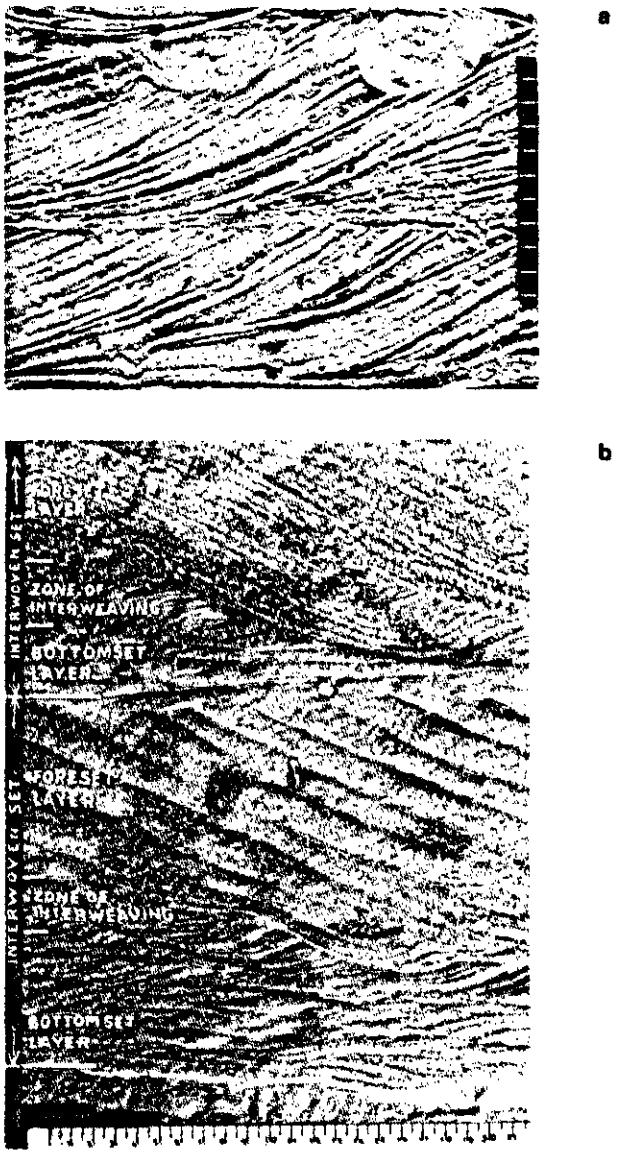

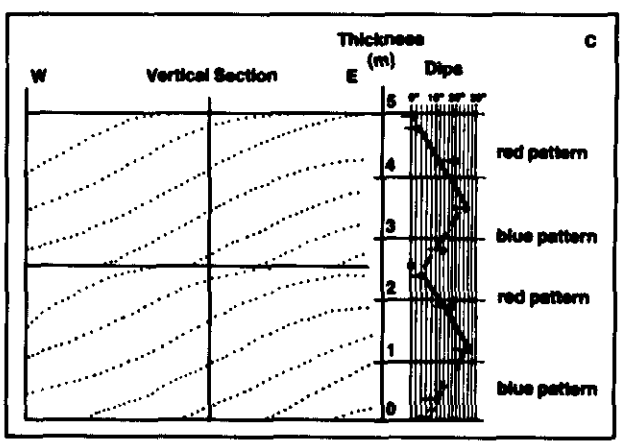

Fig. 4-63. - (a) Megaripple bedding. Inclined foreset laminae of two units of megaripple bedding are clearly visible (from Reineck & Singh, 1975). (b) Megaripple bedding showing well-developed backflow ripple bedding at the base of foreset laminae of megaripple bedding (from Boersma *et al.*, 1968, in Reineck & Singh, 1975). (c) Example of blue and red patterns in foreset beds.

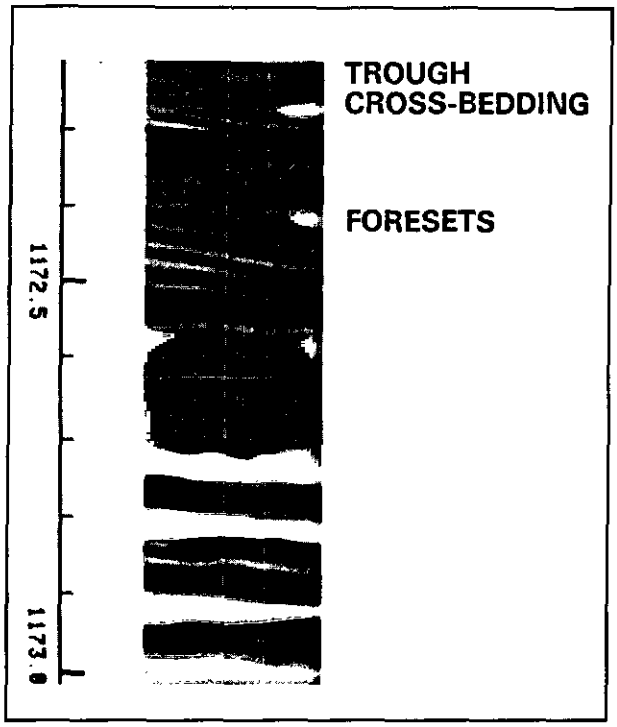

Fig. 4-64. - Example of foreset beds seen on a Formation MicroScanner image, from which the direction of transport can be infered

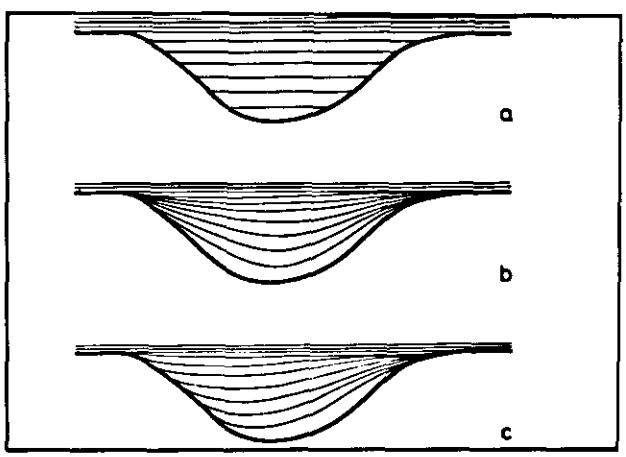

Fig. 4-65. - Three modes of channel fill. (a) Channel filled by horizontally layered sediments. (b) Channel filled by layers conforming roughly to the channel shape, and, near the top, laminae become horizontal. (c) Channel filled asymmetricaly by steeply inclined layers (based on McKee, 1957).

decrease in magnitude upwards (Fig. 4-62) *a « red* pattern » group is defined. This group signals either the filling of a trough (Fig. 4-65b, 4-65c); the convex part of a foreset (Fig. 4-63); a draping over a previous deposit, which forms a topographic relief; barrier bar (Fig. 4-66); reef (Fig. 4-67), or a draping over a diapir salt or shale domes (Fig. 4-68). In such cases the red patterns will be *observed over a thicker interval.*

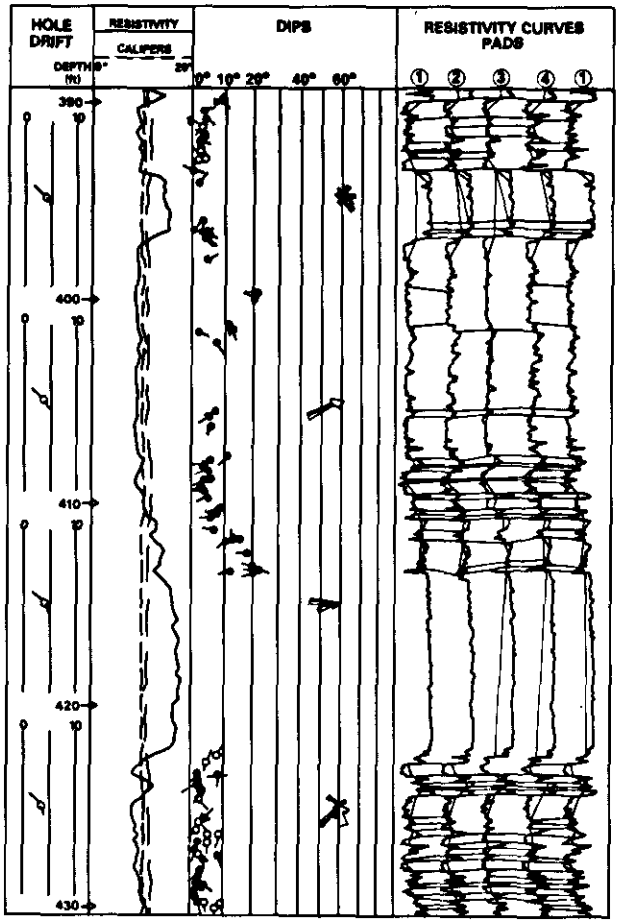

Fig. 4-66. - Example of red pattern above a sand bed (barrier bar).

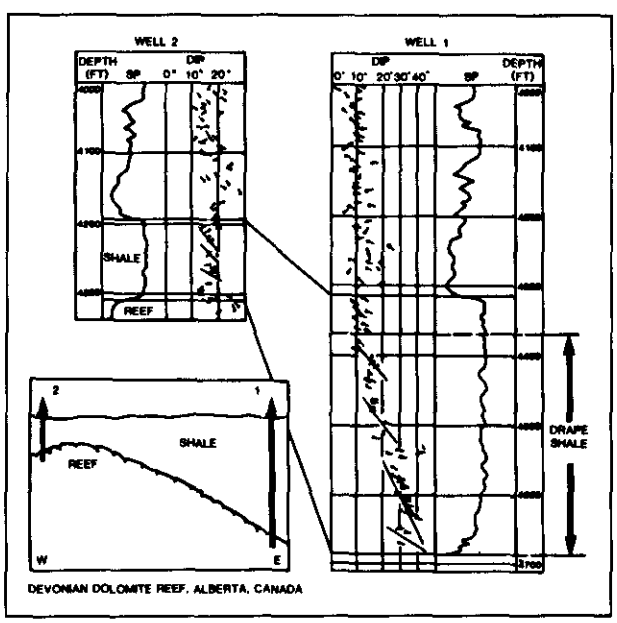

Fig. 4-67. - Example of red patterns above a reef.

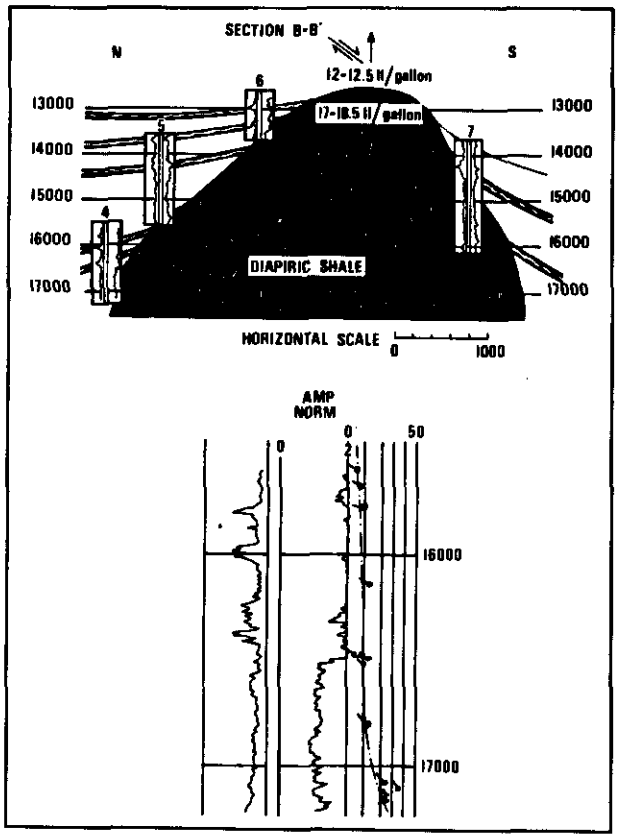

Fig. 4-68. - Example of red pattern above a diapiric shale (from Gilreath, 1968).

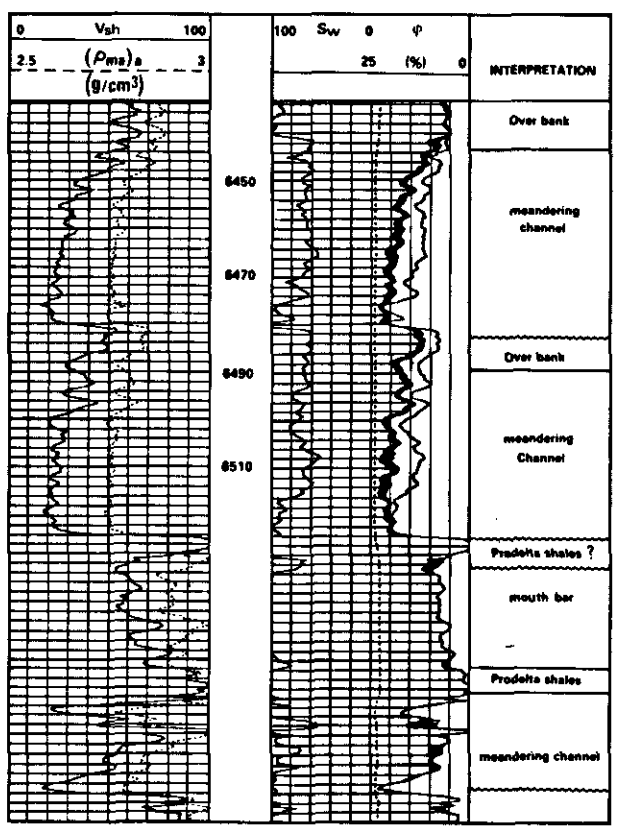

Fig. 4-69a. - A composite-log showing two fluvial sands superposed.

On the dipmeter log of the sand dune (Fig. 4-32), each boundary of foreset lamination is more or less inclined as generally observed on outcrop. The direction of wind for each deposit can also be defined. See also the Formation MicroScanner image of Fig. 4-33.

A fluvial deposit is illustrated in Fig. 4-69. The interpretation of an isolated blue pattern (at 6452) suggests a direction of transport to the North; the interpretation of another isolated red pattern seems to indicate a fill-up of troughs in the channel with the axis seemingly in a N-S direction; and the groups of blue and red patterns (above 6450) seem to correspond to the development of front bars or chute bars. The axis of the channel that also seems to be in N-S direction is situated more easterly. At the base of the sand the numerous cross-bedding, and at the top an increase in sedimentary dip magnitudes in connection with a decrease of current energy and of grain size can also be established. The top of the interval comprises flood plain deposits. This example resembles that shown by Fig. 4-61. It can be also compared to the point bar system (Fig. 4-70) that shows dip and grain size measurements as seen in outcrop.

4.4. COMPUTERIZED ANALYSIS OF DIPMETERS. THE SYNDIP PROGRAM

4.4.1. History

As demonstrated in the previous chapter and in the first part of this one, the interest of the dipmeter data to extract information on the texture and the sedimentary structure of rocks is obvious. This information is very important for a better and more accurate definition of the electrofacies, consequently of the facies and the sedimentary environnements, and cannot be ignored.

But this information is qualitative by nature : character of the dipmeter resistivity curves, type of the bed boundaries, dip evolution with depth, ... Consequently, its utilization for the automatic determination of electrofacies is only possible if the data, extracted from the dipmeters and their processing by GEODIP or LOCDIP programs, are quantified. On the other hand, to be used those data must be assigned to the electrobed or electrosequence, or averaged in a given window and sampled with the same rate as the open-hole logs. As known, fast channel dipmeter data are sampled each 5 mm for HDT tool, or 2.5 mm for SHDT or Formation MicroScanner tools instead of each half-foot (15 cm) or exceptionally each 1.2 inch for open-hole tools.

To achieve these goals, dipmeter resistivity curves and dip computation results were initially described by a series of parameters :

- the variability or activity of the curves (VAR), which reflects the homogeneity (very low va-

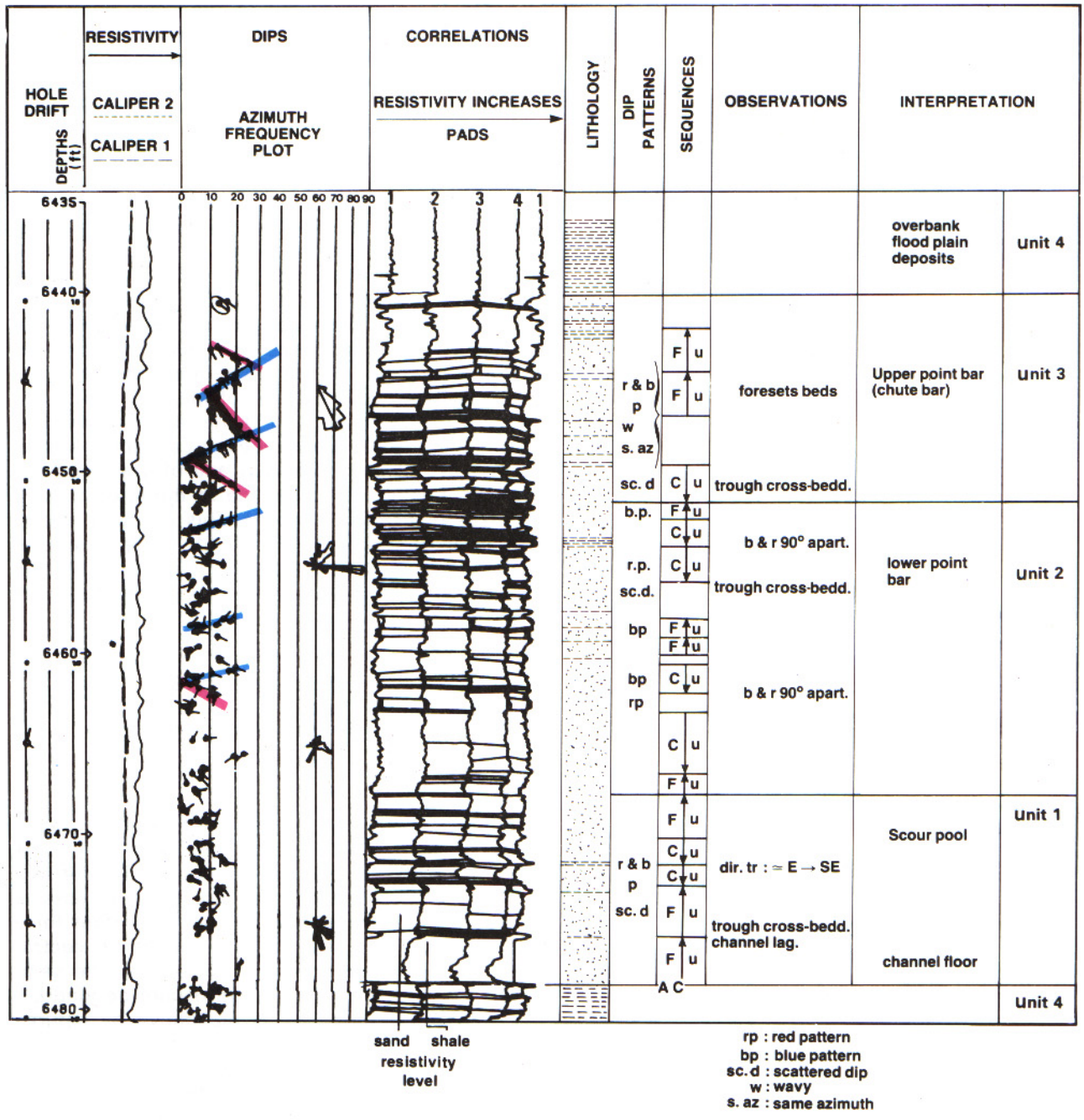

Fig. 4-69b. - The GEODIP arrow plot corresponding to the upper sequence.

riance), or the heterogeneity (high variance) of the formation,

- the frequency of events (peaks or troughs) per curve (FRE) over a given interval (6 in) as recognized by the GEODIP program,
- the average event thickness per curve (ALT) (P_9, parameter of pattern vector computed during the GEODIP processing),
- the balance of positive to negative excursions of the resistivity curves or, in other words, the ratio of the average thickness of the peaks over the average thickness of the troughs in the interval (BAL). If these peaks and troughs correspond to sand and shale beds, this parameter is used to compute a sand-shale ratio (Fig. 4-71),
- the density of correlations found by the GEODIP program (DEN), the frequency of events (FRE) can be high and the density of correlation (DEN) can be low if these events are not similar and consequently not easily correlated (case of conglomerates, or recifal boundstones),
- the sharpness of the curve events (averaging from the four resistivity curves) (SHA),
- the average resistivity of the interval (SRES).

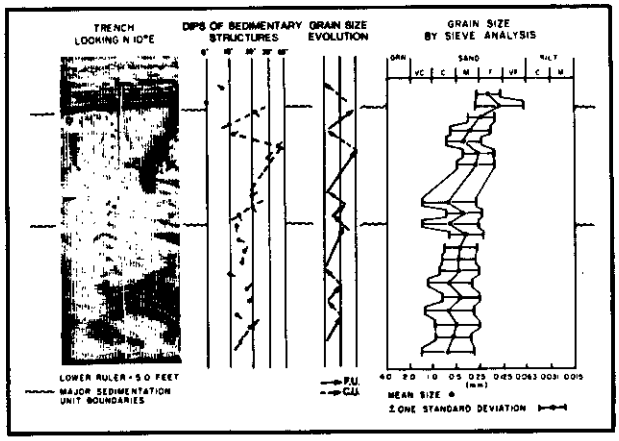

Fig. 4-70. - Vertical variation in grain size, true dip angle and dip direction in the deposit of a single flood (from Steinmetz, 1967, in Reineck & Singh, 1975).

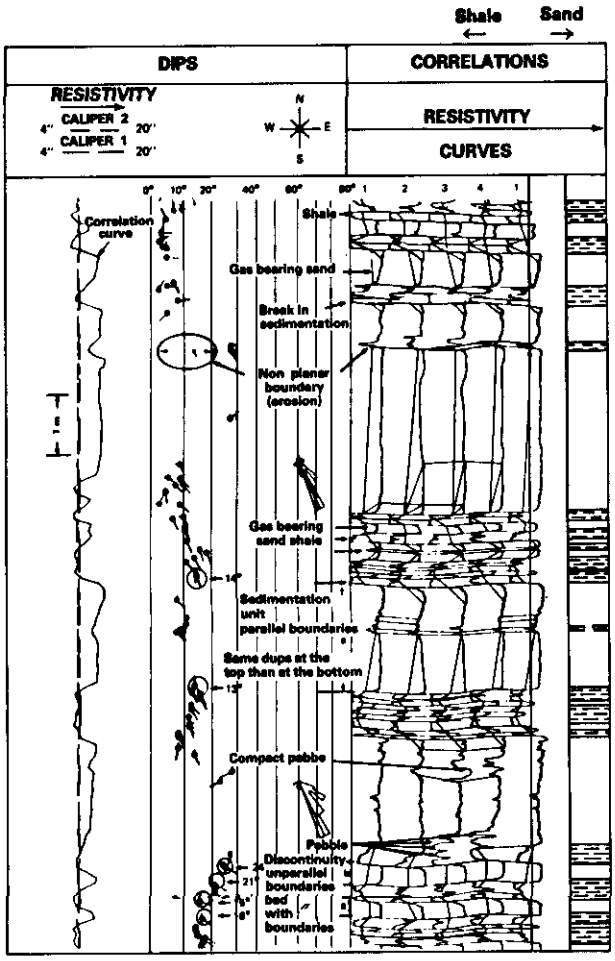

Fig. 4-71. - Example of sand-shale ratio easily computed from the dipmeter data (parameter BAL).

These parameters were computed for each 6-in. interval corresponding to 30 samples. They represented an attempt to convert the information included in the curve shape to a quantitative form

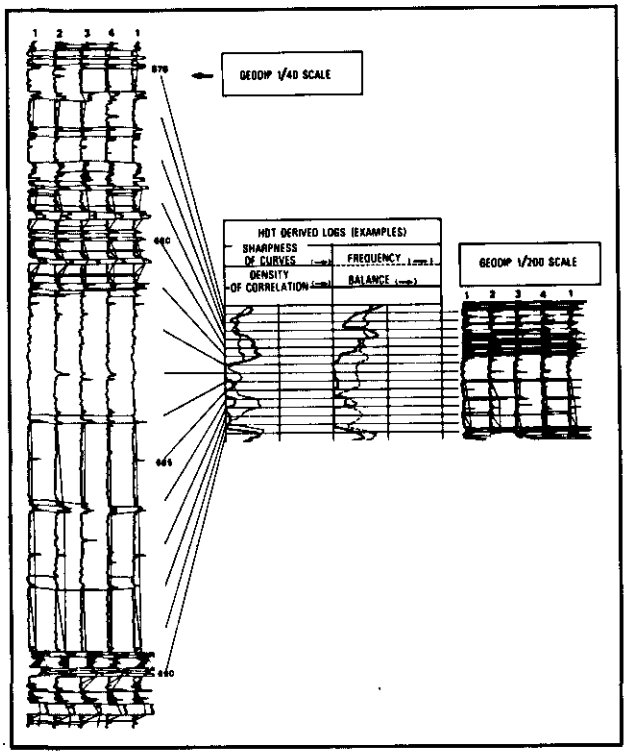

Fig. 4-72. - Some HDT-derived curves and GEODIP display alongside (from Serra & Abbott, 1982).

useable in the definition of electrofacies similar to a log. It is for that reason that the name of « synthetic logs » was given to these computed curves.

Fig. 4-72 shows some of the HDT-derived curves, or synthetic logs, compared to the GEODIP display on the same interval.

Since some of the HDT-derived logs can reflect same phenomena (i.e. FRE, DEN, ALT, VAR), and consequently can be highly correlated (Fig. 4-73), a certain amount of redundancy is present. To avoid that, the HDT-derived logs were processed using Principle Component Analysis (PCA) (to be defined in the next chapter). It turns out that generally the first principal component in the derived log space may be an indicator of homogeneity. Fig. 4-74 shows the first principal component in a series of beds with the corresponding GEODIP response. Comparison of the two shows that positive excursions of the new curve indicates heterogeneity (laminations, poor grain sorting, etc.) and the negative side indicates homogeneity (well-sorted sands, etc.). This curve can then be used in the processing as a textural and structural indicator, instead of FRE, DEN, VAR,...

Some of these synthetic logs exhibit a high degree of correlation with open-hole logs such as gamma ray (Fig. 4-75), or spontaneous potential (Fig. 4-76).

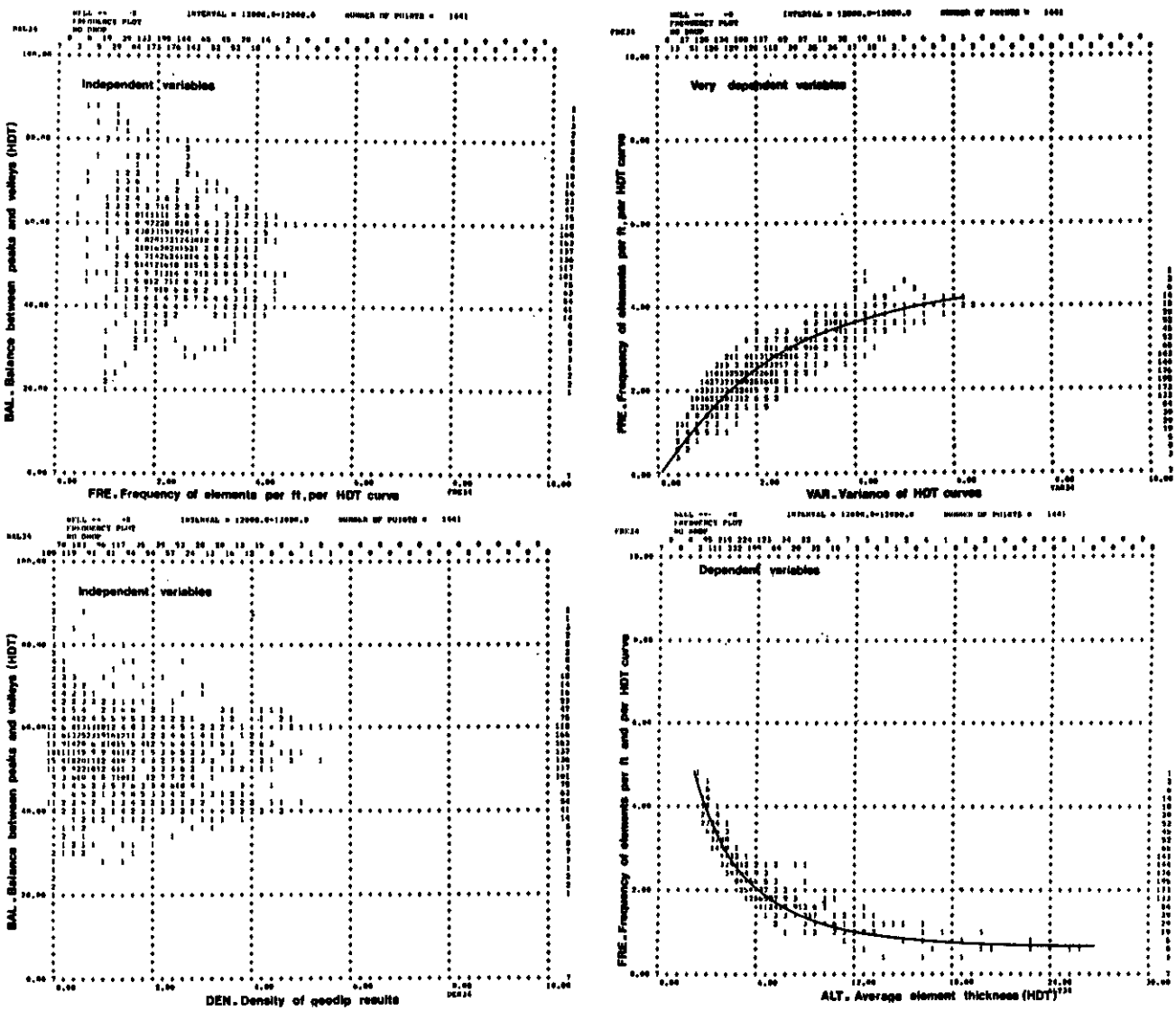

Fig. 4-73. - Correlations between different synthetic logs derived from dipmeter data.

4.4.2. The SYNDIP Program

SYNDIP is a program developed by Schlumberger (Delhomme & Serra, 1984), to replace the previous procedure. It generates dipmeter-derived (or synthetic) logs from HDT or SHDT raw data and computation results. The so-called synthetic logs are based on the features and likeness of the microresistivity curves, and on the evolution versus depth of dips and planarity. SYNDIP can be focused, according to different criteria (dip quality and planarity, size of curve events ...).

In normal use, SYNDIP synthetic logs are output with a half-foot sampling rate; this rate was chosen in order to be consistent with the sampling rate of most open-hole logs. However, for detailed studies, another rate (e.g. 1.2", that is the usual sampling rate for EPT * tool measurements) can be selected.

The frequency of inflexion points, correlated or not, on a single dipmeter resistivity curve is first computed as an indicator of curve activity. The sharpness of this synthetic log is ensured by the fact that no window is used to compute frequency; rather, it is based on the thickness between consecutive inflexion points (ATBR).

A bed, or a lamina, can be defined as the depth interval between two consecutive correlations found by GEODIP or LOCDIP programs. Correlation lines link upper or lower inflexion points of similar events on several dipmeter curves. Layer thicknesses are thus computed between consecutive correlation links (ATCL). When correlation links are closer than the output sampling interval, an average thickness is simply computed, but the resolution is maintained.

* Mark of Schlumberger.

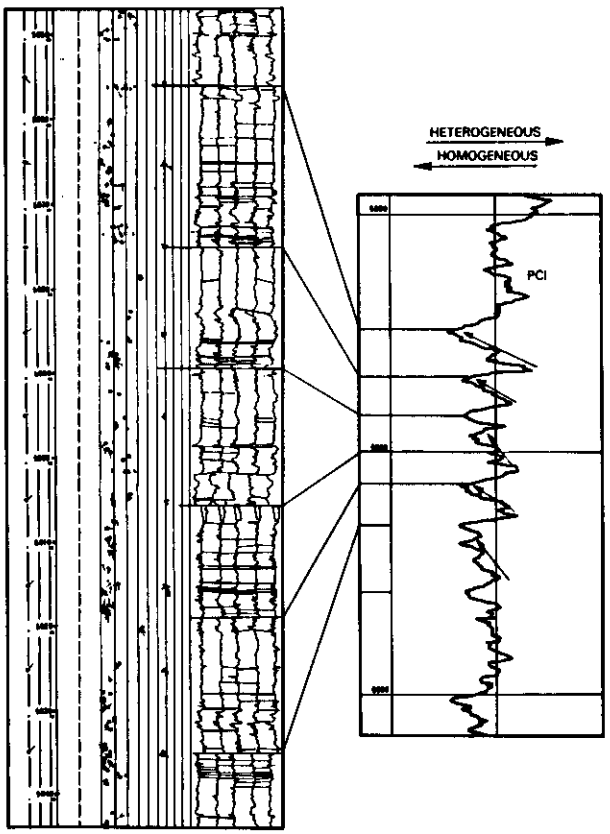

Fig. 4-74. - First principal component derived from PCA on the six HDT-derived logs (from Serra & Abbott, 1980).

An idea of the bed internal organization is obtained by combining curve activity with density of correlations. High activity with no correlations will reflect a coarse heterogeneous bed organisation (conglomerates, flaser bedding, reefs, vuggy limestones ...). Low or no activity with no correlations will reflect either a homogeneous bed or a very finely heterogeneous bed. High activity with high density of correlations will correspond to thinly laminated formations.

As for bed boundaries, a non-planarity flag is output when the GEODIP or LOCDIP planarity coefficient is below a certain threshold. This indicates non planar and possibly erosive surface.

The parallelism between consecutive bed boundaries can be appreciated by comparing the corresponding dipping planes; the angle between a layer's top and bottom is computed and a non-parallelism flag is output if the angle is higher than a certain value (e.g. 10°). Dip dispersion is also computed in a given sliding window (typically 3 m or 10 ft wide); it is an angular standard deviation computed on the unit hemisphere.

Intervals with low dip dispersion, thin beds, small angles between bed tops and bottoms, and with a lithology that corresponds to low energy deposits (shaly-silty or shaly-marly laminations) are those intervals where the structural dip can be picked.

The nature of contacts and transitions is also identified. The high vertical resolution of the dipmeter and its sampling rate allow separation of abrupt changes from gradational ones. This last type corresponds to conductivity ramps, which generally reflect grain size or lithology evolution (sequences). SYNDIP ramp analysis outputs small and large-scale ramps.

Lastly, in SYNDIP, dipmeter data are corrected for EMEX (i.e. for the value of the total current sent out into the formation), rescaled and averaged in conductivity over the output sampling interval since levels appear in parallel.

4.4.3. Description of a SYNDIP Display

An example of the SYNDIP graphic output is given in Fig. 4-77.

The first track reproduces on a logarithmic scale 3 calibrated resistivity curves of dipmeter : the minimum and maximum values recorded by the 4 or 8 buttons in thin lines, and the average value computed from these 4 or 8 resistivity measurements as heavy lines. This presentation enables detection of homogeneous or heterogeneous beds.

The second track displays the internal organization of the beds : small dots represent the homogeneous or massive beds, bubble-like shading correspond to heterogeneous beds, and dark gray with horizontal lines the laminated beds. The limiting curve is the frequency of inflexion points, an indicator of the total curve activity (1/ATBR), and the frequency of correlations (1/ATCL).

On the side, in three columns, are flags indicating detection of non planar surfaces, non parallelism between consecutive bed boundaries, and correlated parallel planes. The following column indicates intervals containing a minimum of five dips with angular spherical dispersion lower then 5°, with the computed average dip. This represents the structural dip if the interval corresponds to a low energy environment (shale, silt or marl).

Sometimes, selected dip results are represented in a third track. The dip, which is taken as representative of a 1.5 ft wide interval, is the one which minimizes the spherical distance to the (n/2)th closest dip result among the n ones found in this interval. The solid curve to the right is the dip spherical standard deviation, and the dashed line is the angle between current layer's top and bottom.

The next track shows a conductivity curve, shaded with a continuous grey scale (or in colour) to reinforce the sand/shale opposition in sand/shale series. Colours are selected by using the histogram of dipmeter resistivity measurements (Fig. 4-78). Sometimes, two scales of conductivity ramps are displayed on the left side.

The last track displays thicknesses of conductive or resistive layers in two mirror logarithmic

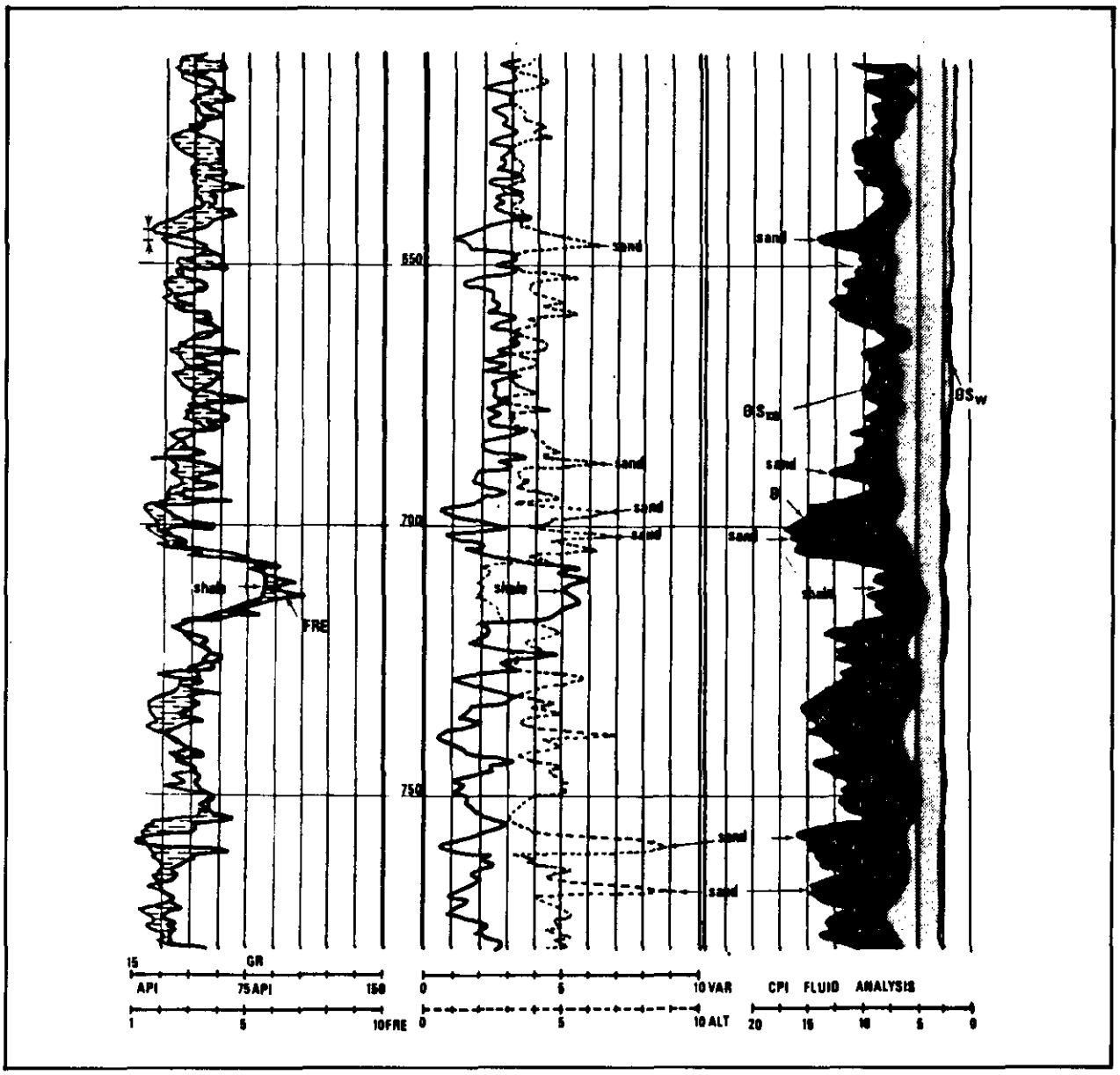

Fig. 4-75. - Correlations between HDT derived synthetic logs (FRE, VAR and ALT) and gamma ray or CPI results.

scales. The thickness is equal to the interval between correlation planes which correspond to important changes in resistivity. The beds are shaded to reinforce the perception of thickening or thinning upwards trends. When conductive and resistive beds correspond respectively to shale and sand, a direct sand-shale ratio can be computed. To help to do so, the sum of resistive layers is indicated on the left side.

In order to zoom on a shaly sand interval, a 1.2" output sampling rate has been used for the synthetic logs instead of the standard 6" rate (Fig. 4-79). Where the standard display shows thicknesses ranging from about 5 cm to 33 cm, the zoom presentation reveals two thin sand beds and gives exactly their thickness : 10 and 22 cm. It also indicates that, apart from these two beds, the thickness of sandstone laminae never exceed 10 cm.

Dipmeter derived synthetic logs can be output at any sampling rate, but the sharpness is always maintained.

Synthetic logs highlight and quantify the sedimentological information included in dipmeter data. They lead to a more comprehensive geological log analysis which will be used for facies recognition and determination of the depositional environment.

Sometimes, an unrolled image of the borehole wall as seen by the SHDT dipmeter is obtained by

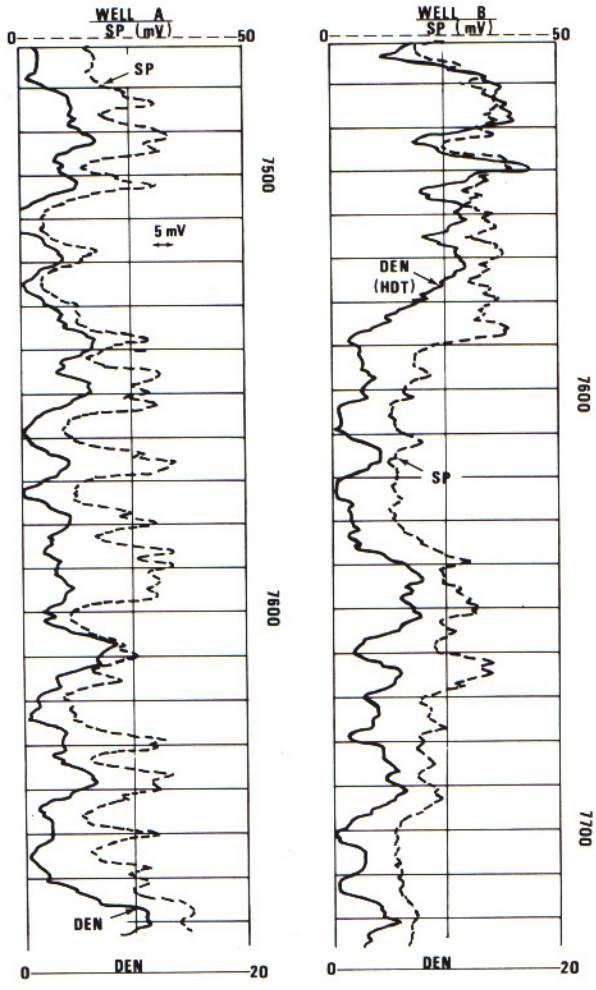

Fig. 4-76. - Correlations between HDT derived synthetic log (DEN) and spontaneous potential.

Fig. 4-77. - Example of SYNDIP display ▶

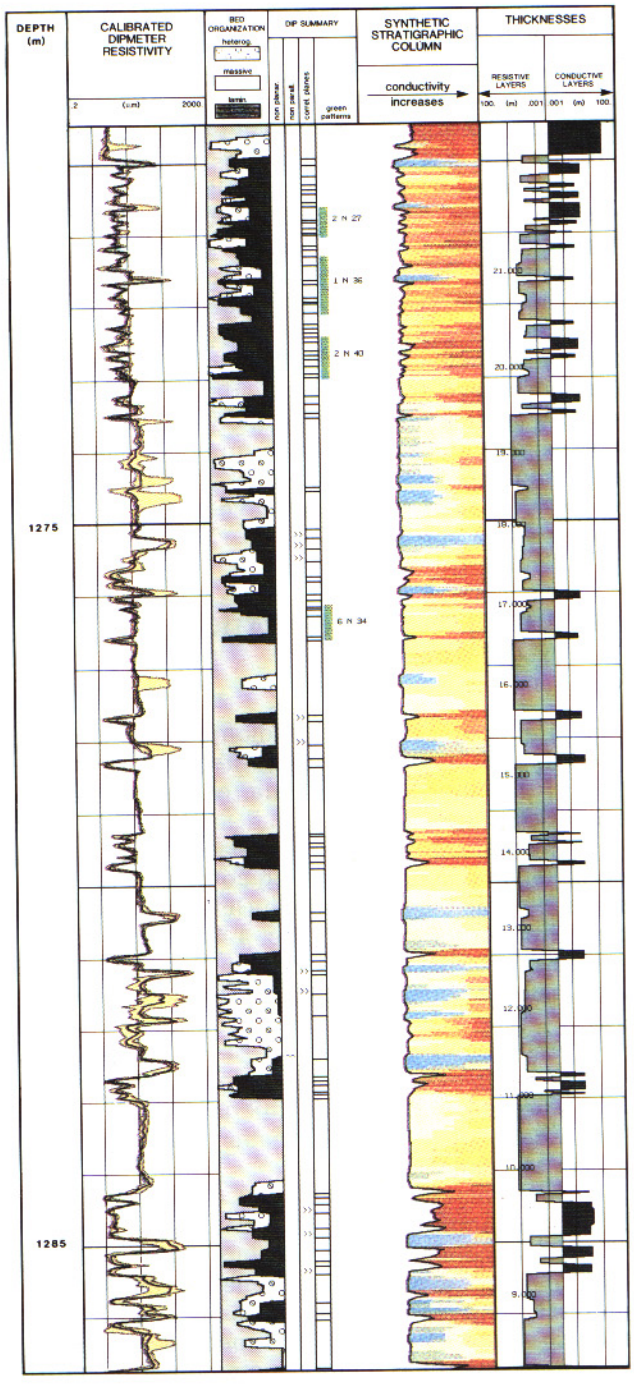

interpolation between the 8 resistivity curves, after equalization, following the dips computed by the LOCDIP program. This display is known as DUADIM or STRATIM * (Fig. 4-80).

4.5. COMPLEMENTARY REMARKS ON FEATURES SEEN BY DIPMETERS

The above-mentioned examples demonstrate that dipmeters and Formation MicroScanner tools provide a mass of information, covering the texture as well as the sedimentary structure of rocks, the direction of transport and the thickness of the beds. The advantages of its integration in all subsurface sedimentological studies can therefore

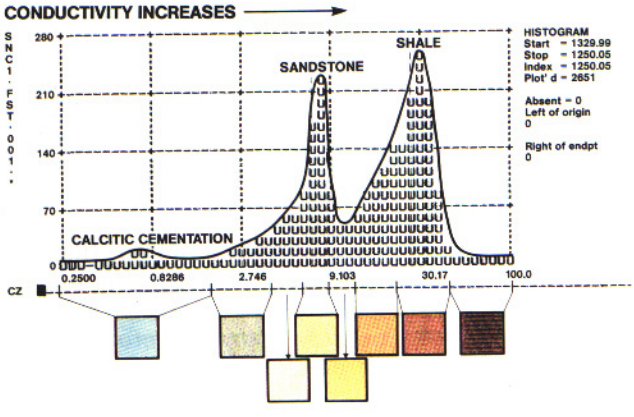

Fig. 4-78. - Histogram of resistivity for the choice of the colours. ▶

* Mark of Schlumberger.

be understood. It is obvious that HDT, SHDT or Formation MicroScanner tools do not see all sedimentary features : *they detect only those presenting a minimum resistivity contrast.* Thus, the figures visible to the naked eye due to a colour change are not detected unless this change is accompanied by a resistivity variation. The features appearing on the surface of a bed without repercusion on a vertical section (tool marks, rain imprints, ...), cannot be recognized because the tool only analyses a cylindrical section.

In general one can admit that all events detected by dipmeter or Formation MicroScanner tool (corresponding to resistivity variations) inevitably explain a change of geological parameters (mineralogy, texture, sedimentary structure, fluids ...) with the condition, of course, that the pad is properly applied to the borehole wall and is the tool working correctly.

4.6. RULES FOR INTERPRETATION OF DIPMETER DATA

The interpretation of a dipmeter arrow-plot should never be implemented without the integration of all other available data, consequently the open-hole logs.

- The first step of the interpretation must be the compilation of a composite log combining at 1/200 scale all available logs and the GEODIP or LOCDIP plot after depth matching (Fig. 4-41). The result of a LITHO, FACIOLOG or CPI lithology output can also help considerably if it is reproduced alongside.

- The second step consists of the *observation* and *description* of the following aspects, by refering if necessary to the GEODIP or LOCDIP plot at 1/40 scale, or to the Formation MicroScanner image at 1/5 scale.

. The investigated interval is subdivided into zones with approximately constant characteristics.

. The mineralogical composition of each zone, and of each event in the zone, is defined as precisely and carefully as possible. To achieve that, the data of other logs, especially litho-density, neutron, sonic, natural gamma-ray spectrometry, ..., or a LITHO display, must be used.

. The nature of the contact (abrupt or gradational, planar or warped, conformable or not) is observed.

. The type of layer succession is described : simple or composite, with or without parallel boundaries, continuous or discontinuous.

. The thickness of each bed type and its evolution with the depth must be noted.

. The existence of current features (flaser, wavy, or lenticular bedding), revealed by the thickness of the events and the dip variations (magnitude and azimuth), or by Formation MicroScanner images, must be extracted and analysed (Figs. 4-16, 4-17 and 4-24).

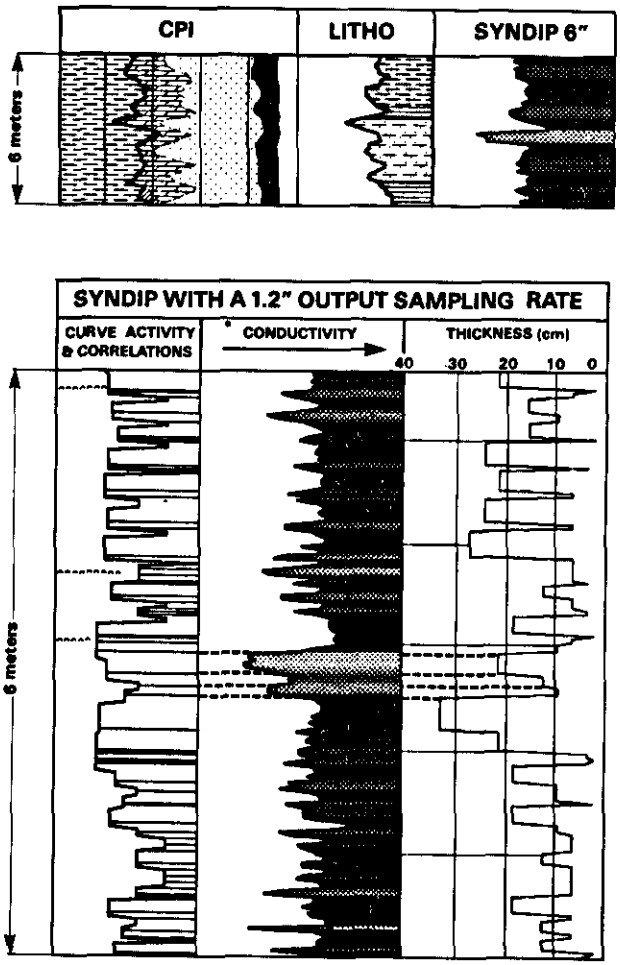

Fig. 4-79. - SYNDIP zooming capability : thin bed precise description with a 1.2" output sampling rate (from Delhomme & Serra, 1984).

. Internal structure of a bed including the curve shape (massive and homogeneous, heterogeneous, resistivity ramp revealing a graded bedding), and dip evolutions (oblique bedding, cross-bedding, foreset, ...) must be added. The amplitude of dip variation is also analysed. The absence of these variations indicate either a low energy, or, on the contrary, a very high energy. The choice between the two hypotheses is derived from the mineralogical nature or the vertical position of this phenomenon in the granulometric sequence, and from the dips. The important variations of the dip magnitude indicate changes of energy in the environment.

. Finally, the sequential evolutions, the rhythms or cycles, the evolution in thickness of each bed and sequence as they are revealed by the dipmeter resistivity curves, are studied.

- The third step corresponds to the direct interpretation. It involves the translation of the observed features into geologically meaningful interpretations. For instance a « blue pattern » (increasing dip magnitude upward) will be interpreted as a foreset (Fig. 4-81).

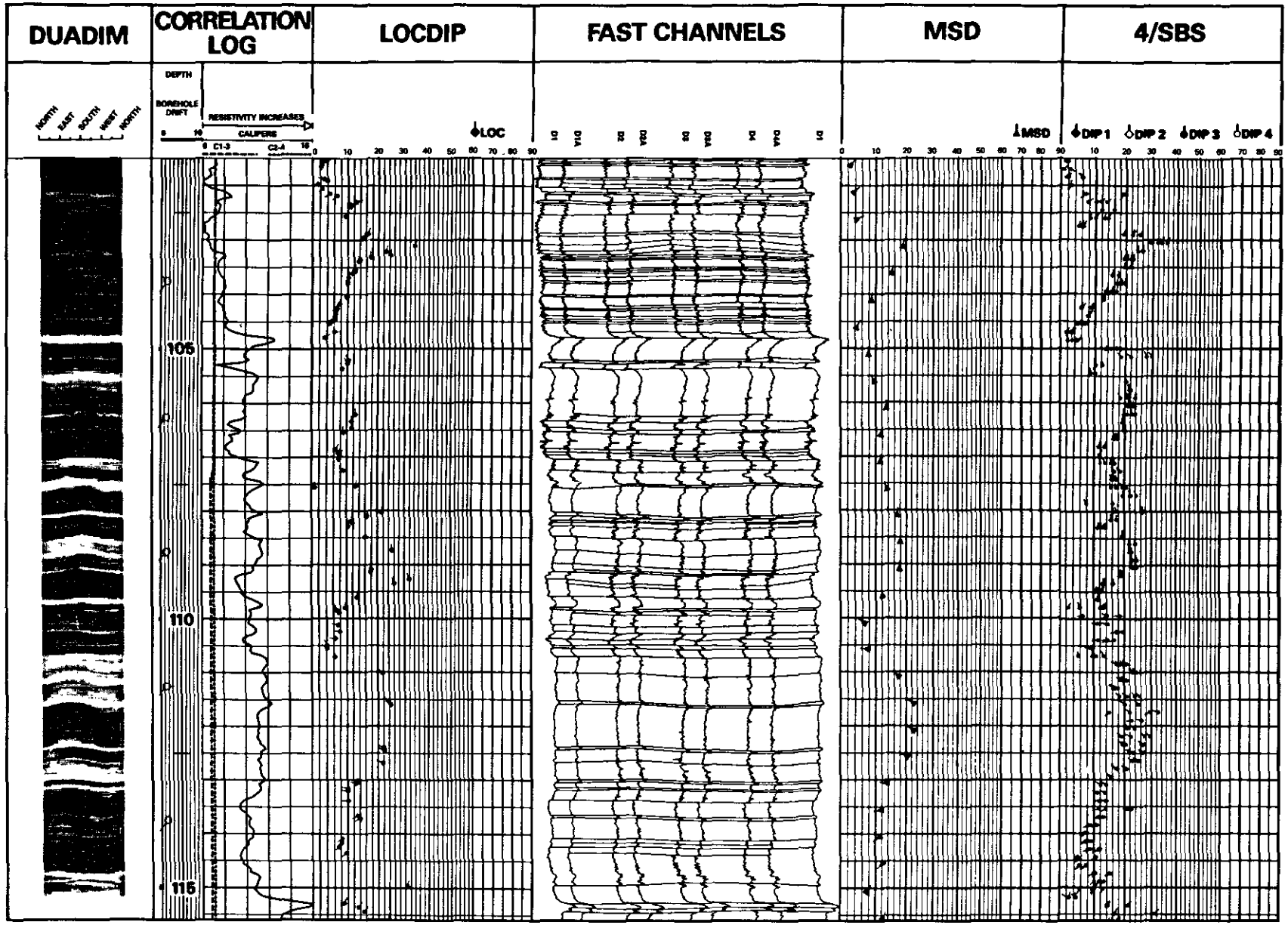

Fig. 4-80. - Example of DUADIM display obtained from SHDT data and interpolation between curves

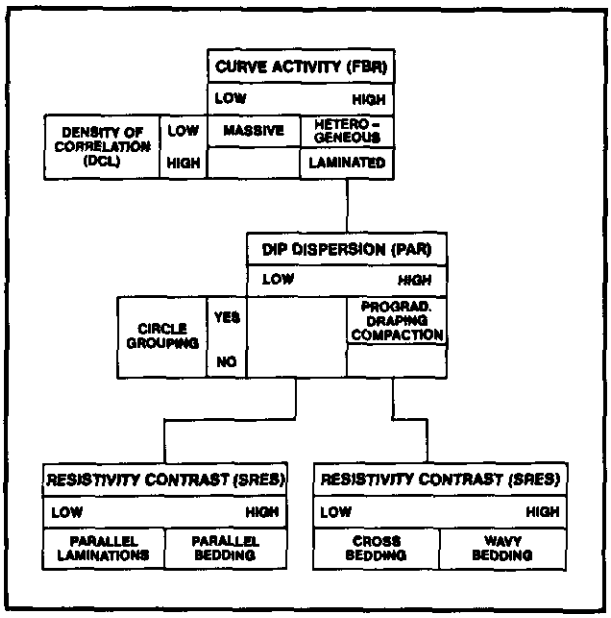

Fig. 4-81. - Bedding type identification from dipmeter.

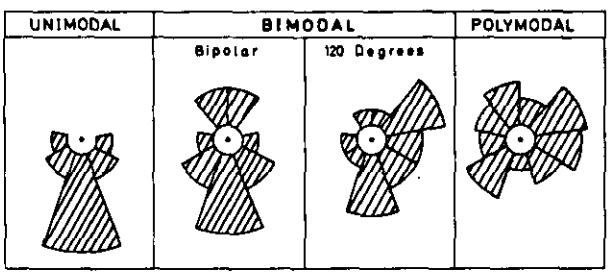

Fig. 4-82. - Classification of azimuth frequency plots (from Selley, 1968, in Pettijohn, 1975).

Table 4-6

Type of cheklist for description of GEODIP or LOCDIP arrow plots.

WELL :...			INTERVAL : Start :... Stop :...		
1	WD Caliper curves	Wash out ☐ Break out ☐ Super-poxed ☐ Separated ☐ Smisoth ☐ Constant ☐ Nominal bit site ☐ Mud-cake ☐ Caved ☐	9	Nature of boundaries	Sharp ☐ Planar ☐ Non planar ☐ (4 dip comp. : GEODIP) /..... Symbol LOCDIP or SYNDIP) diffuse ☐
2	Curve activity	High ☐ Medium ☐ Low ☐ Nil ☐	10	Angle between successive dips (parallelism)	Low ☐ Medium ☐ High ☐
3	Conductivity level	High ☐ Medium ☐ Low ☐ Very low ☐	11	Dip patterns	Green ☐ Blue ☐ Red ☐ Scatter ☐
4	Amplitude of variations	High ☐ Medium ☐ Low ☐	12	Azimuth frequency plot	Unimodal ☐ Bimodal ☐ Scatter ☐
5	Direction of variation from the average value	Less conductive ☐ More conductive ☐	13	Rhythm	Unic ☐ Repetitive ☐ Cyclic ☐
6	Curve shape between breaks	Bell ☐ Funnel ☐ Cylinder ☐	14	Thickness evolution of conductive beds	Thickenning upward ☐ Thinking upward ☐
7	Density of correlations	High ☐ Medium ☐ Low ☐ Nil ☐	15	Thickness evolution of resistive beds	Thickenning upward ☐ Thinning upward ☐
8	Non correlatable events	Present ☐ • More cond. ☐ • Less cond. ☐ • thin ☐ • Medium ☐ • Thick ☐ Absent ☐	16	Hole deviation	Nil ☐ Low ☐ High ☐ • Angle...
			17	Tool rotation	Nil ☐ Slow ☐ Rapid ☐

- The fourth step constitutes the deductive interpretation in terms of a depositional environment. Analysis of azimuth frequency plots established on selected intervals will help to define the uni-, bi- or polymodal nature of the dips (Fig. 4-82).

To achieve this we have to integrate data obtained from the observation of cuttings and cores, such as the presence of glauconite, lignite fragments, phosphate, shells; heavy minerals; grain size, granulometric sorting, nature of cement, shale type, ...

One proceeds by the elimination of the environmental hypotheses which do not fit with the observed features. The final selected solution among the remaining hypotheses, is the one which fits the best with the geological knowledge we have of the formation, the basin and the main tectonic features.

It is suggested to summarize all the observations in a table (Table 4-6) or in several columns put alongside the composite log at 1/200 scale : one column for lithology, one for sedimentary features, one for sequential evolution, one for the direct interpretation and complementary remarks, one for the final interpretation in terms of facies, subenvironments and environment (Fig. 4-83).

In the following chapters several other examples of the procedure will be presented.

4.7. SEDIMENTOLOGICAL APPLICATIONS OF SEDIMENTARY STRUCTURE DETECTION

The main application is the determination of the depositional environment.

Without minimizing the sedimentological interest of the CLUSTER-type program - see the works and papers of Gilreath *et al.* (1964, 1969, 1971), Campbell, (1968), Goetz *et al.* (1977), Selley, (1979) - it should be underlined that this technique does not utilize the very detailed analysis of the dipmeter that is now possible with the newer tool (SHDT) or the Formation MicroScanner tool and

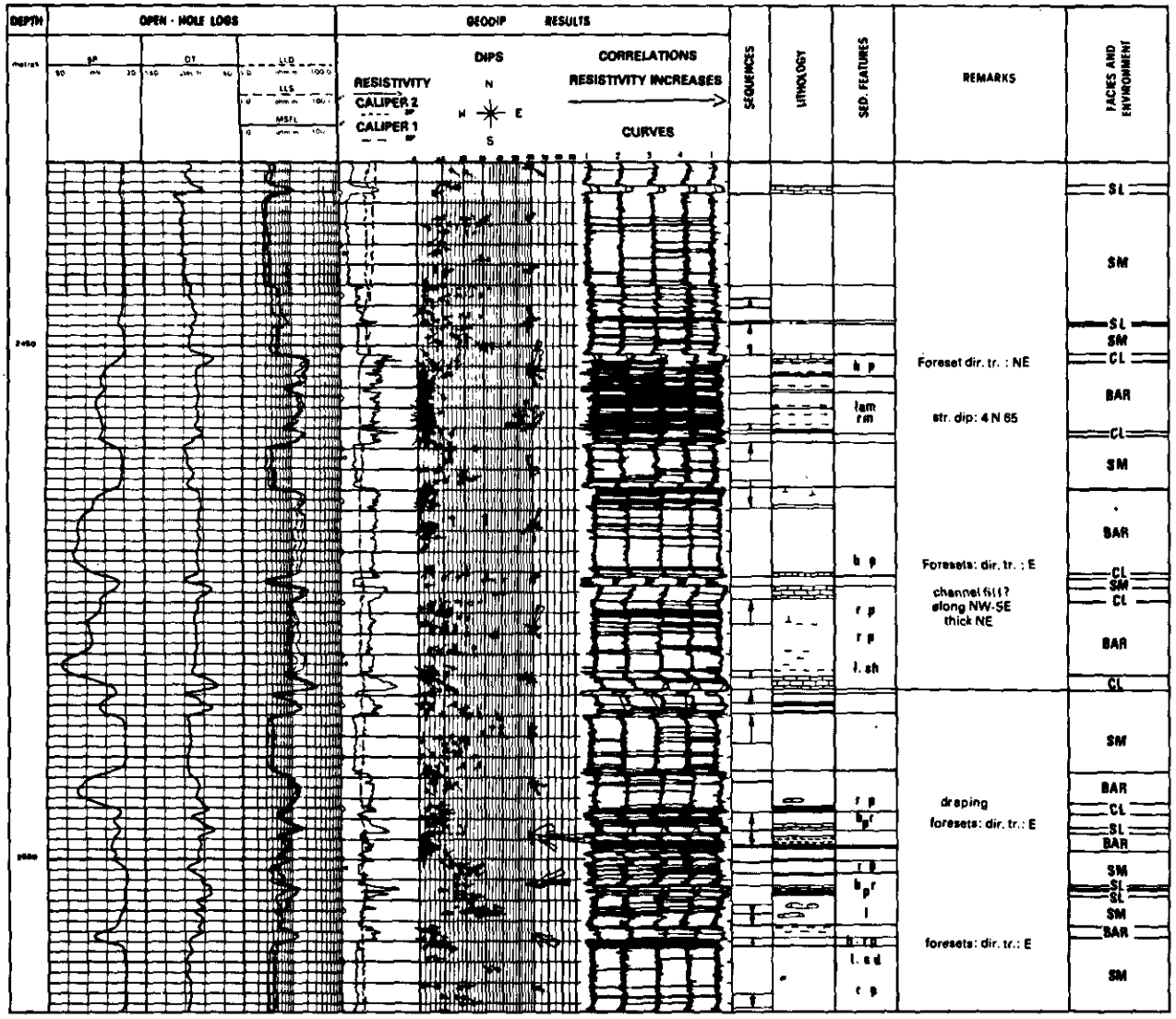

CL= channel lag SL= storm or swell lag SM= shelf mud

Fig. 4-83. - Example of composite-log with GEODIP and its interpretation.

improved processing techniques. The curves are generally not shown and the precise events from which the dips are computed are still unknown. These dips are determined with the help of a correlogram established from a correlation of events in a given interval, without distinction and selection of their origin. The obtained dip is consequently an average dip for an interval which can cover several sedimentary units, each of them possibly having sedimentary features with different dips. For these reasons it is highly preferable to use a GEODIP or LOCDIP presentation for sedimentological interpretation.

As previously stated the primary sedimentary structures - which, can be detected on dipmeter logs or on Formation MicroScanner images -are particularly important because they reflect the hydro- (or aero-) dynamic conditions prevailing in the environment at the time of deposition.

Several illustrations of the importance of the dipmeter plot interpretation for the recognition of the depositional environment will be given later.

4.8. REFERENCES

ALLEN, J.R.L. (1963). - The classification of cross-stratified units, with notes on their origin. *Sedimentology*, **2**, *p. 93-114.*

ALLEN, J.R.L. (1968). - Current Ripples. *North-Holland, Amsterdam.*

ALLEN, J.R.L. (1970). - Physical Processes of Sedimentation. *Elsevier, New York.*

BLATT, H., MIDDLETON, G. & MURRAY, R. (1972, 1980). - Origin of Sedimentary Rocks. 1st and 2nd ed. *Prentice-Hall Inc., Englewood Cliffs, New Jersey.*

CAMPBELL, C.V. (1967). - Lamina, Laminaset, Bed and Bedset. *Sedimentology*, **8**, *p. 7-26.*

CAMPBELL, R.L. (1968). - Stratigraphic applications of dipmeter data in Mid-Continent. *Bull. Amer. Assoc. Petroleum Geol.*, **52**, *9, p. 1700-1719.*

CAROZZI, A.V. (Ed.) (1975). - Sedimentary Rocks. *Benchmark Papers in Geology*, **15**, *Dowden, Hutchinson & Ross, Inc., Stroudsburg, Pennsylvania.*

Chambre Syndicale de la Recherche et de la Production du Pétrole et du Gaz naturel (1966). -Essai de nomenclature & caractérisation des principales structures sédimentaires. *Ed. Technip, Paris.*

Chambre Syndicale de la Recherche et de la Production du Pétrole et du Gaz naturel (1974). -Méthodes modernes de géologie de terrain. 1 -Principes d'analyses sédimentologiques. *Ed. Technip, Paris.*

COLLINSON J.D. & THOMPSON, D.B. (1982). -Sedimentary Structures. *George Allen & Unwin Publ. Ltd., London.*

CROSBY, E.J. (1972). - Classification of Sedimentary Environments. In : *« Recognition of Ancient Sedimentary Environments », edited by RIGBY, J.K. & HAMBLIN, W.K., SEPM, special publication* **16**.

DELFINER, P., PEYRET, O. & SERRA, O. (1984). -Automatic determination of Lithology from Well Logs. *59th Ann. Techn. Conf. SPE of AIME, Houston, Texas; paper n° SPE 13290.*

DELHOMME, J.P. & SERRA, O. (1984). - Dipmeter-derived Logs for Sedimentological Analysis. *SPWLA, 9th Europ. Intern. Format. Eval. Trans., paper 50.*

DICKEY, P.A. (1979). - Petroleum Development Geology. *Petroleum Publishing Co., Tulsa.*

DUNHAM, R.J. (1962). - Classification of Carbonate Rocks according to Depositional Texture. *Amer. Assoc. Petroleum Geol., Mem.* **1**, *p. 108-121.*

EKSTROM, M.P., CHEN, M.Y., ROSSI, D.J., LOCKE, S. & ARON, J. (1986). - High Resolution Microelectrical Borehole Wall Imaging. *SPWLA, 10th Europ. Symp. Trans., Aberdeen.*

EKSTROM, M.P., DAHAN, C.A., CHEN, M.Y., LLOYD, P.M. & ROSSI, D.J. (1986). - Formation Imaging with Microelectrical Scanning Arrays. *SPWLA, 27th Ann. Log. Symp. Trans., Houston.*

FONS, L. Sr. (1969). - Geological application of well logs. *SPWLA, 10th Ann. Log. Symp. Trans.*

FRIEDMAN, G.M. & SANDERS, J.E. (1978). -Principles of Sedimentology. *John Wiley & Sons, New York.*

GARY, M., McAFEE, R.Jr. & WOLF, C.L. (1972). -Glossary of Geology. *Amer. Geol. Institute, Washington, D.C.*

GILREATH, J.A. & MARICELLI, J.J. (1964). -Detailed Stratigraphic Control through dip Computations. *Bull. Amer. Assoc. Petroleum Geol.*, **48**, *12, p. 1902-1910.*

GILREATH, J.A., HEALY, J.S. & YELVERTON, J.N. (1969). - Depositional Environments Defined by Dipmeter Interpretation. *Gulf Coast Assoc. Geol. Soc. Trans.*, **19**, *p. 101-111.*

GILREATH, J.A. & STEPHENS, R.W. (1971). -Distributary Front Deposits Interpreted from Dipmeter Patterns. *Gulf Coast Assoc. Geol. Soc. Trans.*, **21**, *p. 233-243.*

GILREATH, J.A. & STEPHENS, R.W. (1975). -Interpretation of Log Responses in a Deltaic Environment. *Amer. Assoc. Petroleum Geol. Marine Geology Workshop, Dallas, Texas.*

GOETZ, J.I., PRINS, W.J. & LOGAR, J.F. (1977). -Reservoir Delineation by Wireline Techniques. *paper presented at 6th Ann. Conv. Indonesia Petroleum Assoc., Jakarta, May 1977.*

HEPP, V. & DUMESTRE, A.C. (1975). - CLUSTER -A method for selecting the most probable dip results from dipmeter survey. *SPE of AIME, 50th Ann. Fall Mtg., Dallas, Paper SPE 5543.*

HOBSON, G.D. & TIRATSOO, E.N. (1975). -Introduction to Petroleum Geology. *Scientific Press Ltd, Beaconsfield, England.*

INGRAM, R.L. (1954). - Terminology for the thickness of stratification and parting units in sedimentary rocks. *Bull. Geol. Soc. Amer.*, **65**, *p. 937-938.*

JUNG, J. (1958). - Précis de pétrographie. *Masson, Paris.*

KRUMBEIN, W.C. & SLOSS, L.L. (1963). -Stratigraphy and Sedimentation. 2nd ed. *W.H. Freeman & Co., San Francisco.*

KUENEN, Ph. H. (1953). - Significant features of graded bedding. *Bull. Amer. Assoc. Petroleum Geol.*, **37**, *p. 1042-1066.*

LANDES, K.K. (1951). - Petroleum Geology. *John Wiley & Sons, New York.*

LEET, L.Don, JUDSON, S. & KAUFFMAN, M.E. (1978). - Physical Geology. 5th ed. *Prentice-Hall Inc., Englewood Cliffs, New Jersey.*

LINK, P.K. (1982). - Basic Petroleum Geology. *OGCI Publications, Tulsa.*

LLOYD, P.M. (1986). - The Formation MicroScanner : A New Generation High Resolution Logging Technique.

LLOYD, P.M., DAHAN, C.A. & HUTIN, R. (1986). - Formation Imaging from Microelectrical Scanning Arrays : A New Generation of Stratigraphic High Resolution Dipmeter Logging Tool. *SPWLA, 10th Europ. Symp. Trans., Aberdeen.*

LOMBARD, A. (1956). - Géologie Sédimentaire. Les séries marines. *Masson, Paris.*

LOMBARD, A. (1972). - Séries sédimentaires. Genèse - Evolution. *Masson, Paris.*

MATTHEWS, R.K. (1974). - Dynamic Stratigraphy. An introduction to Sedimentation and Stratigraphy. *Prentice-Hall Inc., Englewood Cliffs, New Jersey.*

McGOWEN, J.H. & GARNER, L.E. (1970). -Physiographic features and stratification types of coarse-grained point bars : Modern and ancient examples. *Sedimentology,* **14**, *p. 77-111.*

McKEE, E.D. (1957). - Flume experiments on the production of stratification and cross-stratification. *J. sediment. Petrol.,* **27**, *p. 129-134.*

McKEE, E.D. (1966). - Structures of dunes at White Sands National Monument, New Mexico (and comparison with structures of dunes from other selected areas). *Sedimentology,* **7**, *p. 1-69.*

McKEE, E.D. & WEIR, G.W.(1953). - Terminology for stratification and cross-stratification in sedimentary rocks. *Bull. geol. Soc. Amer.,* **64**, *p. 381-390.*

MIDDLETON, G.V. (ed.) (1965). - Primary sedimentary structures and their hydrodynamic interpretation. *SEPM, Spec. Pub.* **12.**

MIDDLETON, G.V. (1976). - Hydraulic interpretation of sand size distributions. *J. Geology,* **84**, *p. 405-426.*

NURMI, R.D. (1984). - Geological evaluation of stratigraphic high resolution dipmeter data. *SPWLA, 25th Ann. Log. Symp. Trans., New Orleans.*

OTTO, G.H. (1938). - The sedimentation unit and its use in field sampling. *J. Geol.,* **46**, *p. 569-582.*

PAYRE, X. & SERRA, O. (1979). - A case study -Turbidites recognized through dipmeter. *SPWLA, 6th Europ. Log. Symp. Trans., London, paper K.*

PERRIN, G. (1975). - Comparaison entre des structures sédimentaires à l'affleurement et les pendagemétries de sondages. *Bull. Centre Rech. Pau, SNPA,* **9**, *p. 147-181.*

PETTIJOHN, F.J. (1930). - Imbricate arrangement of pebbles in a pre-Cambrian conglomerate. *Jour. Geol.,* **38**, *p. 568-573.*

PETTIJOHN, F.J. (1975). - Sedimentary Rocks. 3rd ed. *Harper & Row, Publishers, New York.*

PETTIJOHN, F.J. & POTTER, P.E. (1964). - Atlas and Glossary of Primary Sedimentary Structures. *Springer, New York.*

PETTIJOHN, F.J., POTTER, P.E. & SIEVER, R. (1972). - Sand and Sandstone. *Springer, New York.*

PIRSON, S.J. (1977). - Geologic Well Log Analysis. 2nd ed. *Gulf Publishing Co., Houston.*

POTTER, P.E. & PETTIJOHN, F.J. (1977). - Paleocurrents and Basin Analysis. 2nd ed. *Springer, New York.*

PRESS, F. & SIEVER, R. (1982). - Earth. 3rd ed. *W.H. Freeman & Co, San Francisco.*

READING, H.G. (Ed.) (1978). - Sedimentary Environments and Facies. *Blackwell Scientific Publications, Oxford.*

REINECK, H.E. & SINGH, I.B. (1975, 1980). -Depositional Sedimentary Environments. 1st and 2nd ed. *Springer, New York.*

REINECK, H.E. & WUNDERLICH, F. (1968). -Classification and origin of flaser and lenticular bedding. *Sedimentology,* **11**, *p. 99-104.*

RUSSELL, W.L. (1951). - Principles of Petroleum Geology. *McGraw-Hill Book Co., New York.*

SCHEIDEGGER, A.E. & POTTER, P.E. (1971). -Downcurrent decline of grain size and thickness of single turbidite beds : a semi-quantitative analysis. *Sedimentology,* **17**, *p. 41-49.*

Schlumberger Ltd (1970). - Fundamentals of Dipmeter Interpretation.

Schlumberger Ltd (1972). - Log Interpretation. Volume I - Principles.

Schlumberger Ltd (1974). - Log Interpretation. Volume II - Applications.

Services Techniques Schlumberger (1974). -Well Evaluation Conference. North Sea.

Schlumberger (1979). - Well Evaluation Conference. Algeria.

Schlumberger Ltd (1981). - Dipmeter Interpretation. Volume 1 - Fundamentals.

Schlumberger Middle East S.A. (1981). - Well Evaluation Conference. United Arab Emirates/ Qatar.

Schlumberger Technical Services, Inc. (1982). -Essentials of Natural Gamma ray Spectrometry Interpretation.

Schlumberger Technical Services, Inc. (1983). -Well Evaluation Conference. India.

SCHOLLE, P.A. & SPEARING, D. (Ed.) (1982). -Sandstone Depositional Environments. *Amer. Assoc. Petroleum Geol., Mem.* **31.**

SCHWARZACHER, W. (1953). - Cross-bedding and grain size in the Lower Cretaceous sands of East Anglia. *Geol. Mag.,* **90**, *p. 322-330.*

SCOTT, K.M. (1966). - Sedimentology and dispersal pattern of a Cretaceous flysch sequence, Patagonian Andes, southern Chile. *Bull. Amer. Assoc. Petroleum Geol.,* **50**, *p. 72-107.*

SELLEY, R.C. (1970, 1978, 1985). - Ancient Sedimentary Environments. 1st, 2nd and 3rd ed. *Chapman & Hall, London.*

SELLEY, R.C. (1976). - An Introduction to Sedimentology. *Academic Press, London.*

SERRA, O. & ABBOTT, H. (1980). - The Contribution of Logging data to Sedimentology and Stratigraphy. *55th Ann. Fall Techn. conf. SPE of AIME, paper SPE 9270, and in SPE J., Feb. 1982.*

STEINMETZ, R. (1967). - Depositional history, primary sedimentary structures, cross-bed dips, and grain size of an Arkansas river point bar at Wekiwa, Oklahoma. *Rep. F67-G-3 (In : REINECK & SINGH, 1975).*

THEYS, P., LUTHI, S. & SERRA, O. (1983). - Use of dipmeter in Carbonates for detailed sedimentology and reservoir engineering studies.

VATAN, A. (1954). - Pétrographie sédimentaire. *Ed. Technip, Paris.*

VINCENT, P., GARTNER, J. & ATTALI, G. (1979). -GEODIP - An approach to detailed dip determination using correlation by pattern recognition. *J. Petroleum Technol., Feb.1979, p. 232-240.*

WALKER, R.G. (Ed.) (1979, 1984). - Facies Models. 1st and 2nd ed. *Geoscience Canada, reprint series 1, published by Geol. Assoc. Canada.*

Chapter 5

INFORMATION ON FACIES AND SEQUENCE

(Rock description)

5.1. REVIEW OF GENERAL CONCEPTS

Since its introduction by Gressly (1838), the term *facies* has been used in many different ways and these uses have been the centre of considerable debate. Usages and definitions have been reviewed by Moore (1949), Weller (1958), Teichert (1958), Krumbein & Sloss (1963), and more recently by Selley (1970), Reading (1978) and Middleton (1978).

Without reopening the debate, the general, almost identical, definitions proposed by the Glossary of Geology (1980) and by several geologists are listed here :

- "The aspect, appearance, and characteristics of a rock unit, usually reflecting the conditions of its origin; esp. as differentiating the unit from adjacent or associated units" (Glossary of Geology, 1980).
- Haug (1907) : "the sum of the lithologic and palaeontologic characteristics of a [sedimentary] deposit at a given place".
- Moore (1949) : "any areally restricted part of a designated stratigraphic unit which exhibits characters significantly different from those of other parts of the unit".
- Selley (1970) : "a mass of sedimentary rock which can be defined and distinguished from others by its geometry, lithology, sedimentary structures, palaeocurrent pattern, and fossils".

It is obvious from such definitions that a facies has a necessarily limited extension, both stratigraphic and geographic, even if it can be found at different levels in the same stratigraphic unit.

Geologists have noticed that a facies observed in a stratigraphic unit can show similar features and characteristics to those described in other units of different ages or coming from other regions of the earth. This is related to the fact that such facies, with the same aspects, were deposited under identical physico-chemical conditions.

Consequently, the term facies can be used with an extended meaning for designating sedimentary rocks with the same aspect, fauna and flora, even if they are different in age, reflecting similar physico-chemical conditions in their environment.

In the following, the term facies will cover the more general meaning given above. But, it will always be *descriptive*, without any genetic or environmental connotation. It will correspond to the general aspect of a sedimentary rock as it results from the sum of lithological, structural and organic characteristics which can be detected in the field, and which distinguish this rock from other surrounding rocks.

These characteristics, on one hand, are the results of the physical, chemical and biological conditions under which the sediment was deposited, and, on the other hand, are derived from its evolution under diagenetic influences since the time of its deposition.

It is from its characteristics and the context in which it is found - vertical and lateral sequential evolutions, time-space relationship with neighbouring facies, regional tectonic control in the period of deposition - that one will be able to determine its origin, its depositional environment and its geological history.

Selley (1970) states "that a facies has five defining parameters, viz. geometry, lithology, palaeontology, sedimentary structures and palaeocurrent pattern".

Generally, a facies is surrounded by other facies which are related to it. This means that in a given environment the facies are not randoml ydistributed, but constitute a predictable association or sequence.

The general meaning of a *sequence* is a "succession of geologic events, processes, or rocks, arranged in chronologic order to show their relative position and age with respect to geologic history as a whole" (Glossary of geology).

Lombard (1956) has introduced the concept of *lithological sequence* that he defines as "a series

of two lithological units, at least, forming a natural succession, without any other important break except for the joints of stratification. The thickness of the bed is not considered". He distinguishes three orders of sequence :

- thin microscopic sequences (i.e. varves);
- medium macroscopic sequences (i.e. cyclothem);
- large megascopic sequences (i.e. stage, system).

Other concepts must be added. A *granulometric sequence* corresponds to a grain size evolution without change in mineralogy (i.e. coarse, medium, fine, very fine sands). It can be *fining upward*, or *coarsening upward*.

A *facies sequence* corresponds to a series of facies which gradually merge into each other. The sequence may be bounded at top and bottom by a sharp or erosive junction, or by a hiatus in deposition. An example is the Bouma's sequence.

Following the order of succession of the facies A, B and C, or terms of the sequence, we have :

- a *rhythm*, which corresponds to ABC, ABC, AB,...; such succession characterizes a *rhythmic sedimentation* and the results are *rhythmites* (e.g. cyclothems, turbidites, varves);
- a *cycle*, which corresponds to the succession of two sequences with opposite evolution : ABCBA; such succession characterizes a *cyclic-sedimentation*.

The first type of succession is more frequent than the second.

A lateral evolution or association of related facies deposited at the same time, in different places in the same environment but forming a continuum, creates a *lateral sequence*, a succession of superposed terms in relation to time corresponds to a *vertical sequence*.

IMPORTANCE OF FACIES AND SEQUENCE ANALYSIS

The study of facies and their arrangement or association in lateral and vertical sequences is the only way to establish the depositional environment, and thus to reconstruct the palaeogeography. The physical, chemical and biological conditions existing in an environment, which define it, can only be determined by its imprints on the sediments. Among these imprints, the primary sedimentary features are more important because they have been formed in-situ. The sequences will reflect the modifications in the conditions both in space and in time. Walker (1976) made a comparison between the results of analysis and *facies models* (established on the basis of modern environments). This comparison allows, by analogy, determination of the depositional environment by application of *uniformitarianism* or *actualism* theories introduced by Hutton (1785) and Lyell (1830) : *"the present is the key to the past"*.

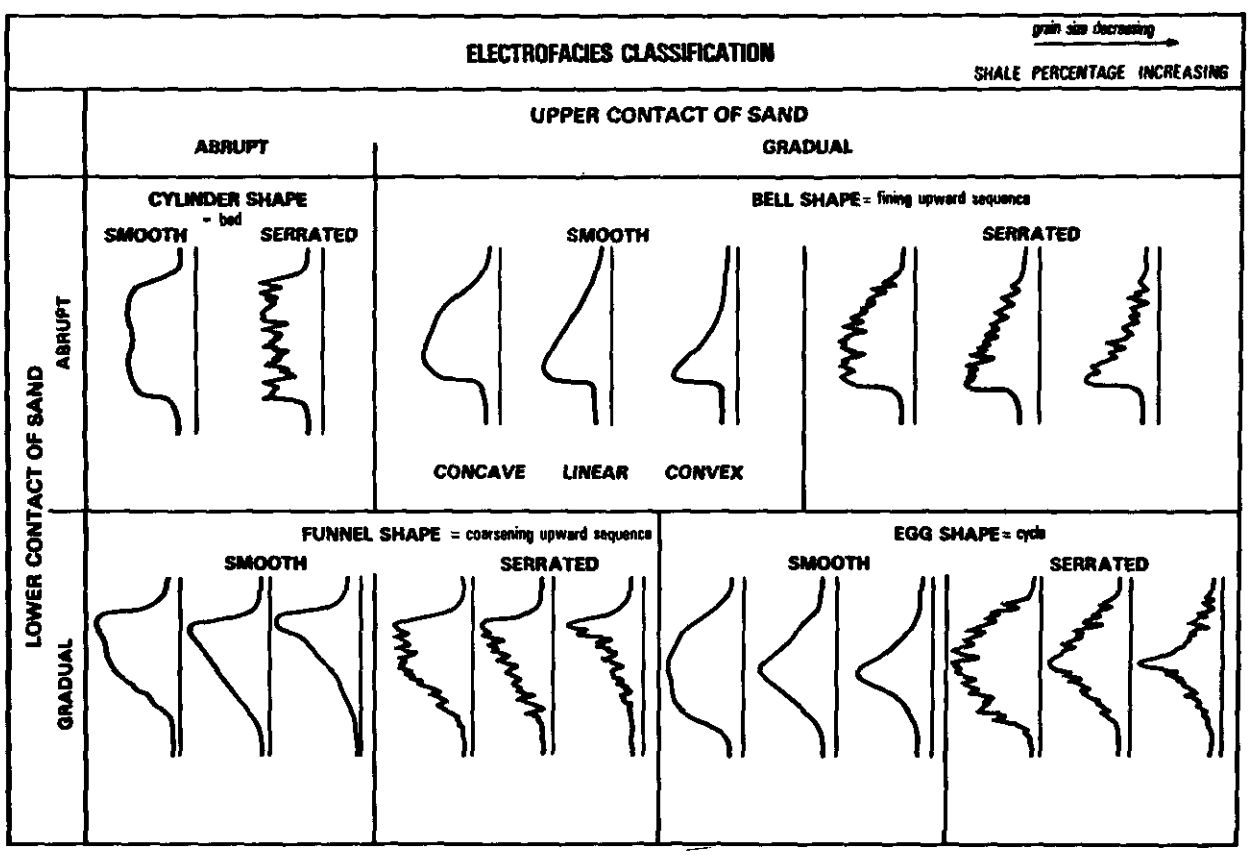

Fig. 5-1. - Classification of electrofacies by shapes of log responses.

5.2. FACIES ANALYSIS FROM WIRELINE LOGS

5.2.1. Historical

It seems that the idea of using wireline logs as sedimentological tools first came in 1956-1957, from engineers working for the SHELL-PECTEN Company in Houston, U.S.A. Studying the Mississippi delta, they stated that the spontaneous potential curve (SP) presented characteristic shapes. Each of these shapes corresponds to a facies of a particular sand body. By analyzing the SP curve, the type of contact (abrupt or progressive) between sands and shales, and the character of the curve (smooth or serrated; concave, rectilinear or convex) one can establish the classifications shown in Fig. 5-1.

Pirson (1970, 1977) associates a facies and a depositional environment to each shape, and he interprets the curvature of the curve as an indicator of the speed of transgression or regression processes (Fig. 5-2).

Several geologists used this very rapid and synthetic method of curve analysis to construct facies maps (Fig. 5-3).

Knowing the fundamental reasons for the choice of the SP curve (other logs often being unavailable, resistivity curves being heavily affected by the presence of hydrocarbons, large number of wells to be studied, etc.) and its real possibilities in detrital sand-shale series (in a majority of cases it reflects shaliness and grain size evolution), we have to acknowledge that the use of SP curve alone is often insufficient to clearly determine a facies and a depositional environment. It may lead to a misreading of the events because of "parasite effects" on SP deflection (influence of R_t, invasion, contrast of R_s/R_m, compact zones, thickness of beds, etc.). Finally, this curve becomes unusable if the contrast of R_{mf}/R_w is insufficient. This is why the shape of a single curve may only exceptionally define the facies and the depositional environment, particularly if we intend to use this method to study other types of sediments such as carbonates and evaporites.

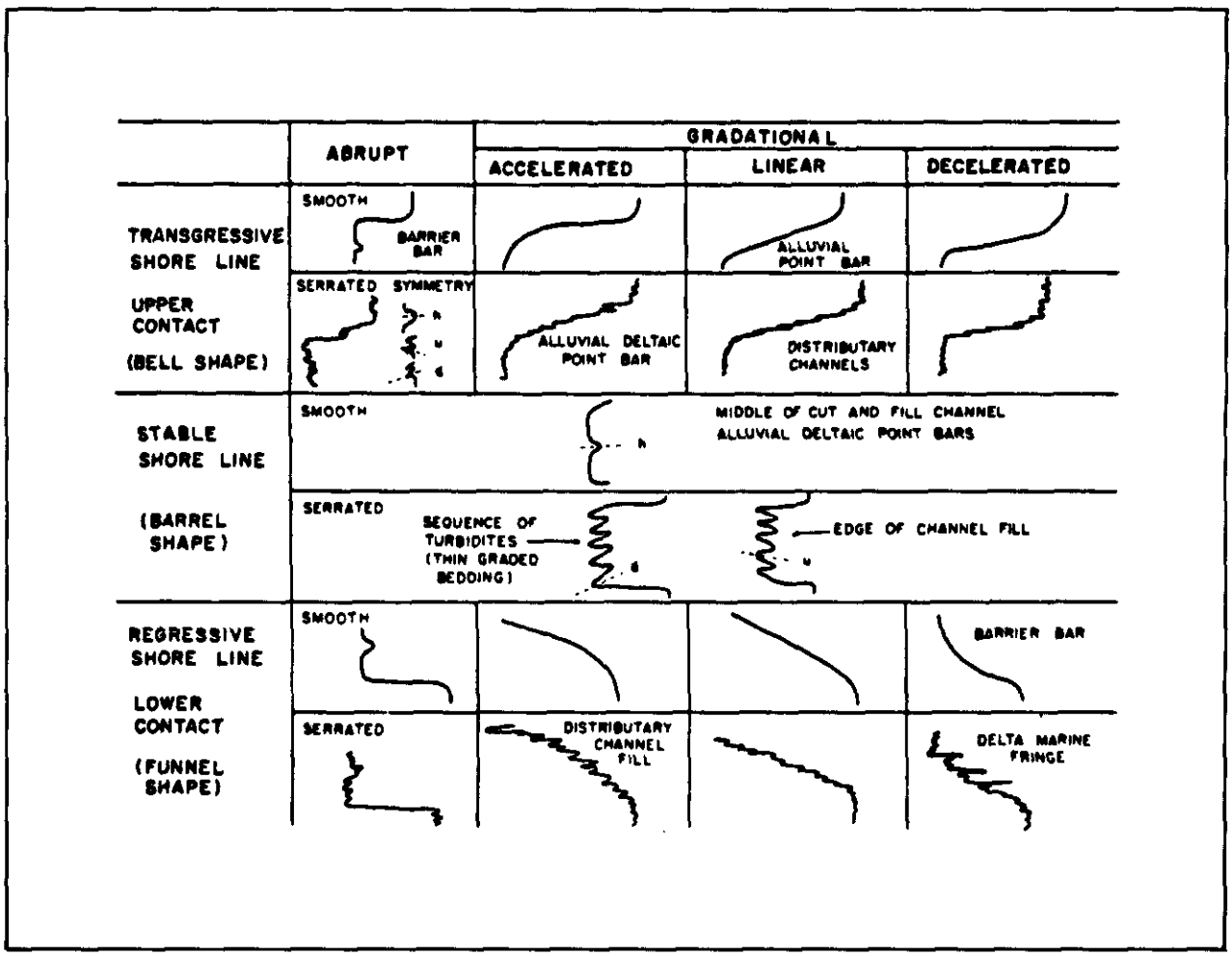

Fig. 5-2. - Classification of SP curve shapes in terms of sedimentary patterns (courtesy of Pirson, 1970, and Gulf Publishing Co., fig. 2-1).

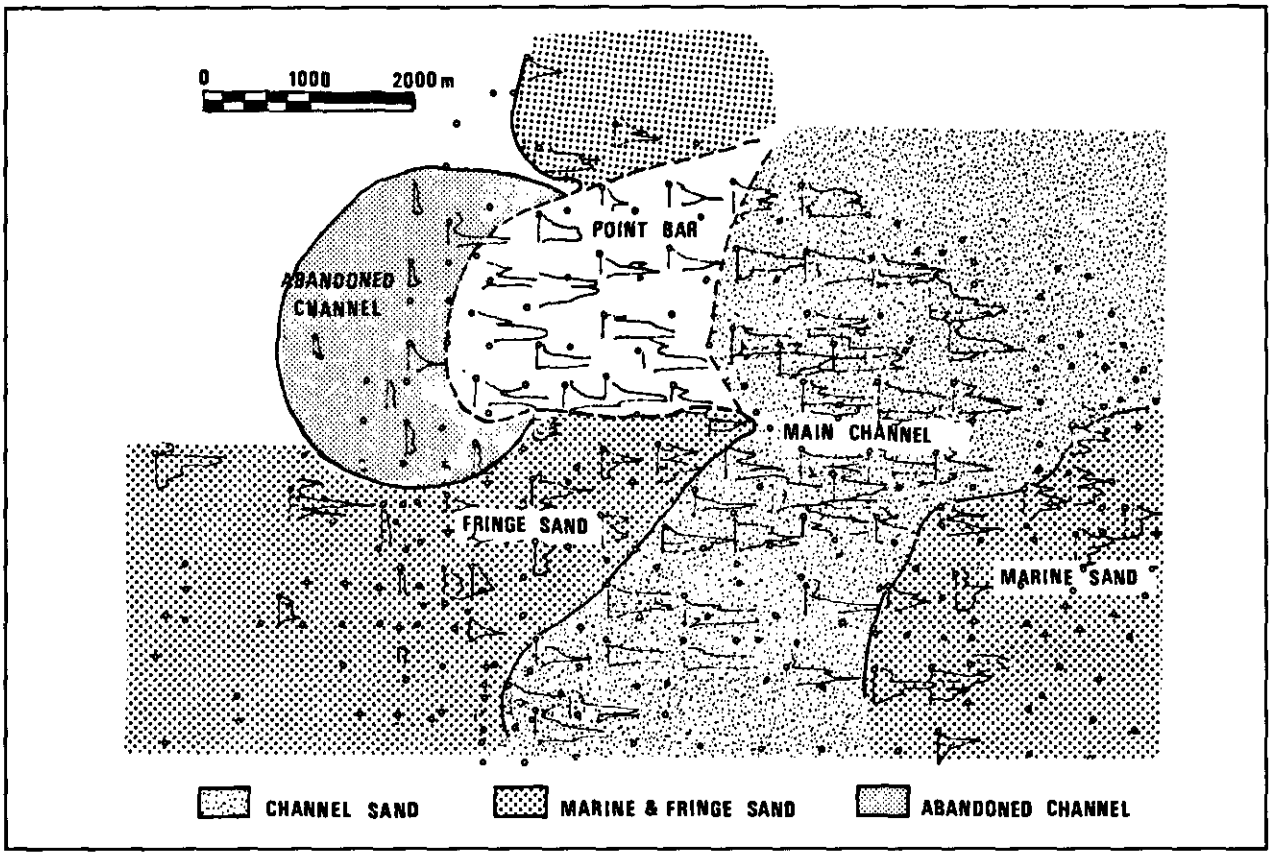

Fig. 5-3. - Distribution of facies from the shape of the resistivity curve (from Lennon, 1976).

5.2.2. The Electrofacies Concept

As we have seen in previous chapters, every wireline log gives, more or less, some information about the mineralogical composition, the texture, and the sedimentary structures, even if this information is sometimes implicit. In other words, each wireline log gives a particular spectral picture of the rock properties.

In certain cases one or two spectral pictures, therefore one or two logs as we have previously noted, are sufficient for the determination of rock characteristics (for instance, the use of the shape of the SP curve in the sand-shale series of the Gulf Coast). But, it is preferable to use all the available log data for interpretation. Their number, their diversity and their complementarity allow, in fact, the establishment of a spectrum of rock characteristics covering their chemical and mineralogical composition their texture and their structure. The higher the number of wireline logs used, the richer the spectrum will be, and the better defined the rock characteristics. Hence there will be less risk of ambiguity and error in their interpretation.

Moreover, dipmeter data processed by GEODIP program for HDT tool, or LOCDIP program for SHDT tool, or FMS data allow, in many cases, the determination of the palaeocurrent pattern and the direction of transport.

Finally, the geometry is defined by both analysis of the true thickness of the beds (only dipmeters give this information), and by the lateral extension of beds. This can only be defined by correlations between several wells and by the drawing of isopach maps based on thickness data (Fig. 5-4 and 5-5).

Most of the parameters defining the facies, or at least the lithofacies in Moore's definition (1949), are directly accessible from logs. The latter, therefore, produce a picture of the present facies. This picture is certainly particular, incomplete, sometimes confused, but alway spermanent and objective. If the set of wireline logs is diversified and rich enough for a better covering of geological parameters, the picture will be sufficiently precise. In other words the spectrum will be sufficiently rich and detailed to permit a new representation of the lithofacies by means of log data.

This *parafacies* was named by Serra (1970) as *electrofacies*, the definition of which is :

"the set of log responses which characterizes a bed and permits it to be distinguished from the others" (Serra, in Schlumberger Well Evaluation Conference, Algeria, 1979).

All log responses (electric, nuclear, acoustic, dipmeter, etc.), that indicate the quantitative (log values) as well as qualitative (characteristics of

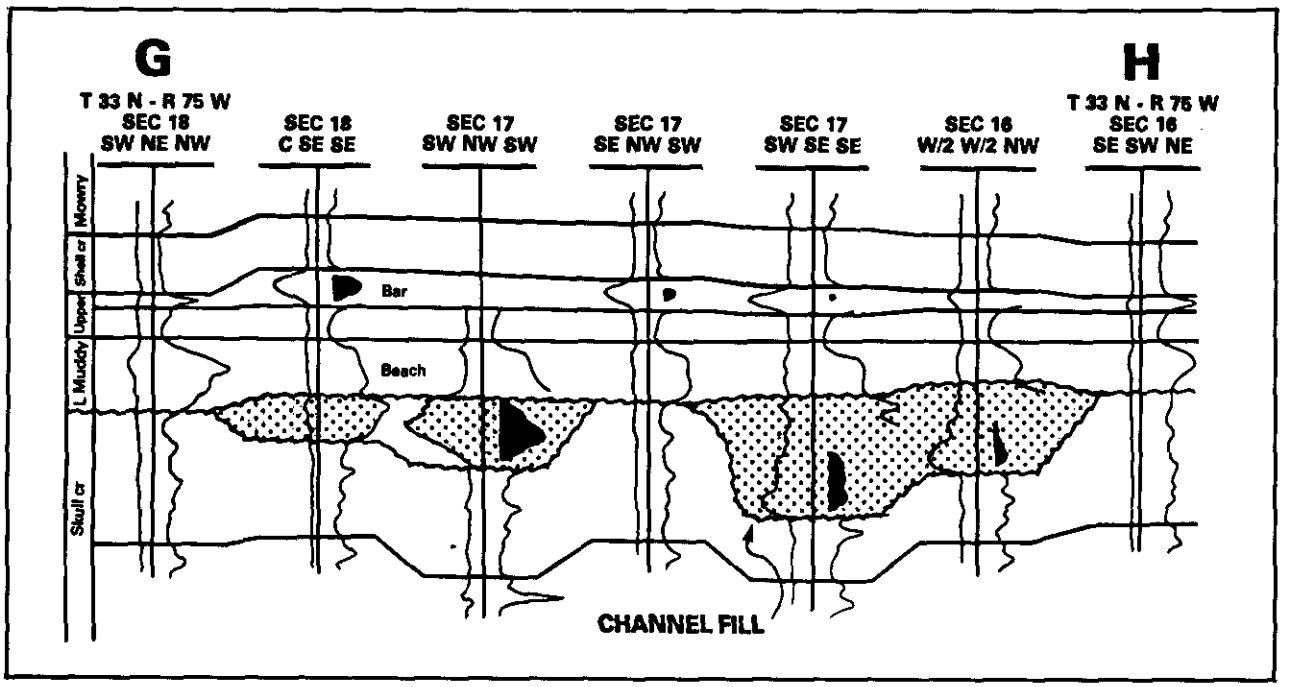

Fig. 5-4. - Log-correlations between wells in the South Glenrock Oilfield, Wyoming. Bar, beach and channel fill are easily recognized (From Curry & Curry, 1972).

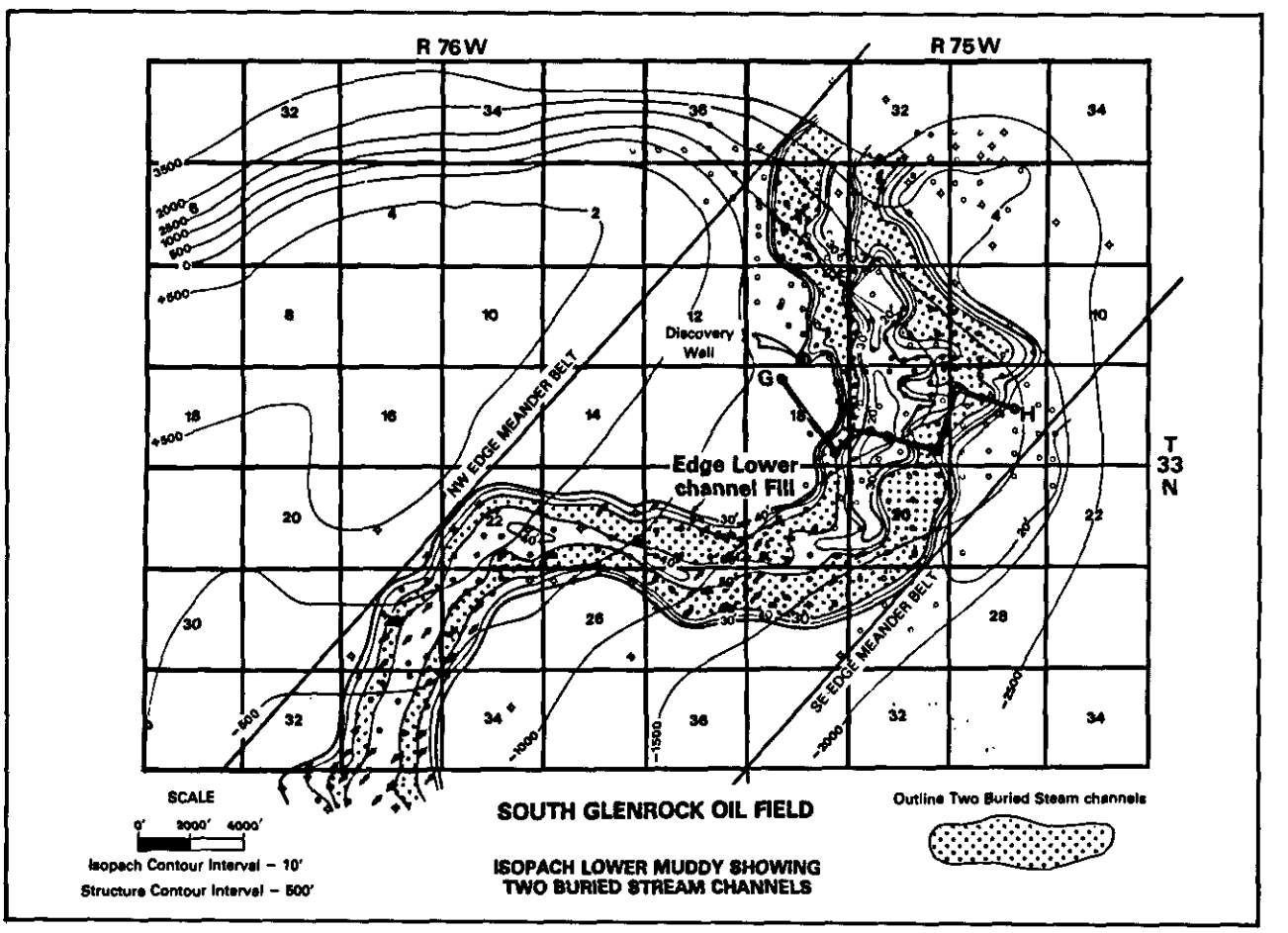

Fig. 5-5. - Isopach map of the lower Muddy in the South Glenrock Oilfield, showing two buried stream channels (from Curry & Curry, 1972).

curves) aspects represent, therefore, the component elements of the electrofacies.

Electrofacies constitutes more than one element of a facies. It is, in fact, its equivalent since it includes in itself the parameters which define the facies.

But we have to realize that there is a parameter which has never been taken into consideration by sedimentologists in their definitions of facies. This parameter is the fluid that occupies the porous space of the rocks. If in surface outcrops it is neglected because it is absent or without significance, it is always present in the subsurface and it influences the response of most logging tools. Therefore, we cannot eliminate it and, in fact, it enters into the definition of electrofacies. Consequently ,several electrofacies, depending on the nature of fluids present in the rocks (gas, oil, fresh or salty water), may correspond to the same geological facies. This situation may be considered, at first sight, as an important disadvantage of the electrofacies concept and of its utilization. In fact, it is not important because the purpose of the electrofacies analysis is, first of all, to *describe* the formations as they are "seen" by logging tools .After all, we can possibly utilize logging tools, and their data, less sensitive to fluids or to porosity (i.e. NGT, LDT, GST), or we can correct the log response for porosity and fluid influence. For all that, in the absence of hydrodynamism, the fluid may be an important factor for the recognition of a depositional environment : fresh water in fluvial or lacustrine environment, briny water in swamp or marsh, salty water in sands deposited in marine environments ...

The objection has often been raised that the electrofacies is only an equivalent of the lithofacies because it does not contain palaeontological information. Without being argumentative, it is necessary to make the followings remarks :

- if the fossils are utilized as indicators of the depositional environment, we have to remember that :

. in many cases the fauna and flora are almost nonexistent and, consequently, the definition of the facies is given without this information;

. the fauna and flora are not always good indicators of the environment (ubiquitous species, mixtures, allochtone species, etc.);

. in many cases the presence of fossils (animal or vegetal) is shown by their influence on log responses, particularly on dipmeters and Formation MicroScanner. Moreover, it is controlled by the physico-chemical conditions existing at the time of deposition, which also determine the other parameters, especially the sedimentary structures;

. other elements of facies (mineralogy, texture, sedimentary features, palaeoccurents and geometry) are often sufficient for a precise definition of the facies, and also for specifying the depositional environment, especially if we use the additional information on sequential evolution (see Chapter 6).

- If the fossils are used to define the geological

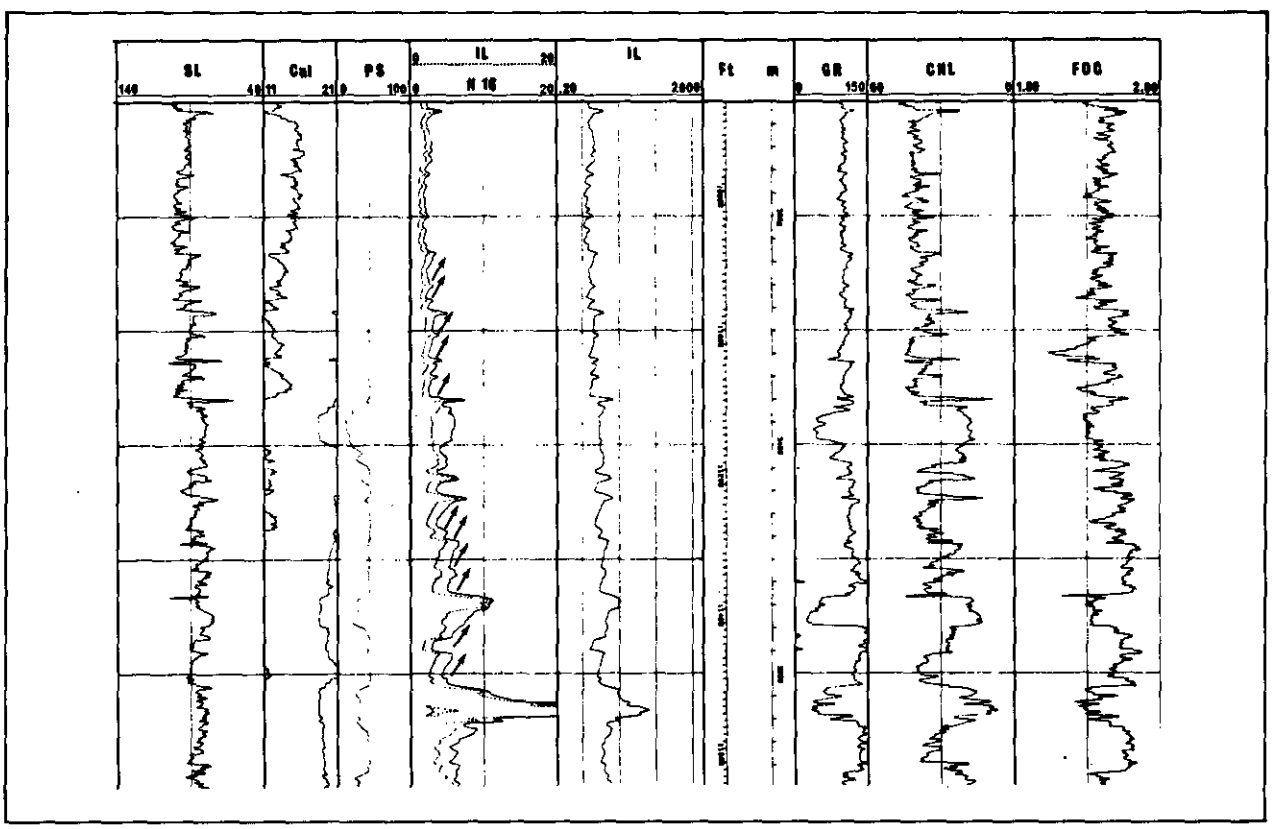

Fig. 5-6. - Examples of electrosequences (ramps) clearly seen on wireline logs.

age, we may note that this information is implicitly included in the subsurface data through the depth data and the position in relation to markers. Besides, at this stage, the logs allow a more precise appraisal of the lapse of time than that defined by fossils.

Hence, we have good reasons to assimilate the electrofacies into the facies. Moreover, the reconstitution of the time-space repartition of the different facies, and the definition of their mutual relations is the final goal of facies and sequence analysis, regardless of the methods used to achieve this goal (traditional method by examination of rocks, or from log data).

Depositional environments will therefore be defined by these analyses, and thus we may forecast more accurately the continuity of a reservoir, the presence, nature and distribution of permeability barriers, and the location of mineral resources in exploitable economic quantities.

5.2.3. The Electrosequence Concept

We sometimes observe, on certain recordings, progressive evolutions of measured parameters (resistivity, gamma ray, spontaneous potential, etc.) in relation to depth (Fig. 5-6). These evolutions, having the shape of ramps, were named *electrosequences* by Serra (1970). The proposed definition of an electrosequence is :

depth interval thicker than the vertical resolution of the measuring tool, presenting a progressive and continuous evolution between two extreme values of measured parameter, tracing a ramp.

This variation may reflect :

- a progressive change in mineralogical composition with depth : percentage evolution of shale in a sand or in a limestone; enrichment of a limestone in dolomite, or of a sand in radioactive heavy minerals (Fig. 5-7);
- the evolution of a textural parameter : grain size change reflecting fining or coarsening upward sequences; sorting decrease, etc.;

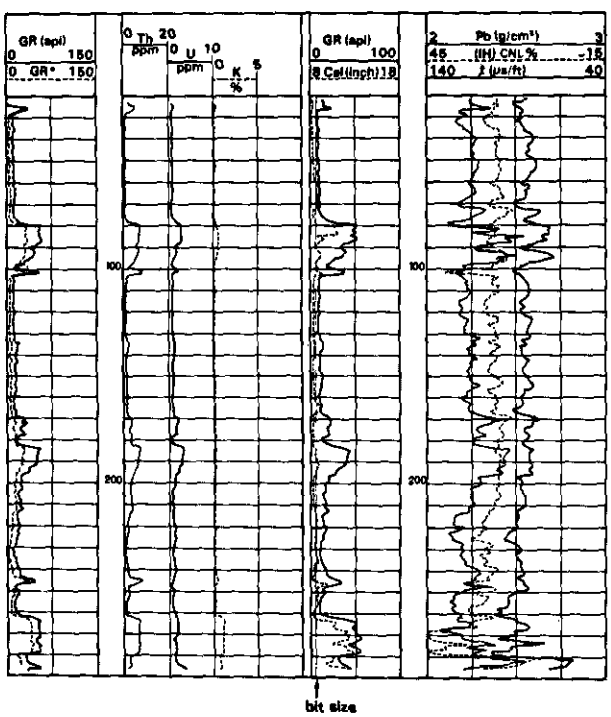

Fig. 5-7. - Example of grain size evolution detected on wireline logs. Observe, between 210 and 182 ft, the progressive evolution of gamma ray (GR), thorium (Th), uranium (U) and density (ρ_b) curves. They suggest a progressive enrichment of the sand with heavy radioactive minerals, thorium -and uranium-bearing, which can be correlated with a decrease in grain size, heavy minerals being more abundant in the silty fraction than in the sandy. Observe the neutron curve (IH_{CNL}) : it does not show significant porosity variations in the same interval. The potassium curve (K) is practically zero, indicating the absence of shale.

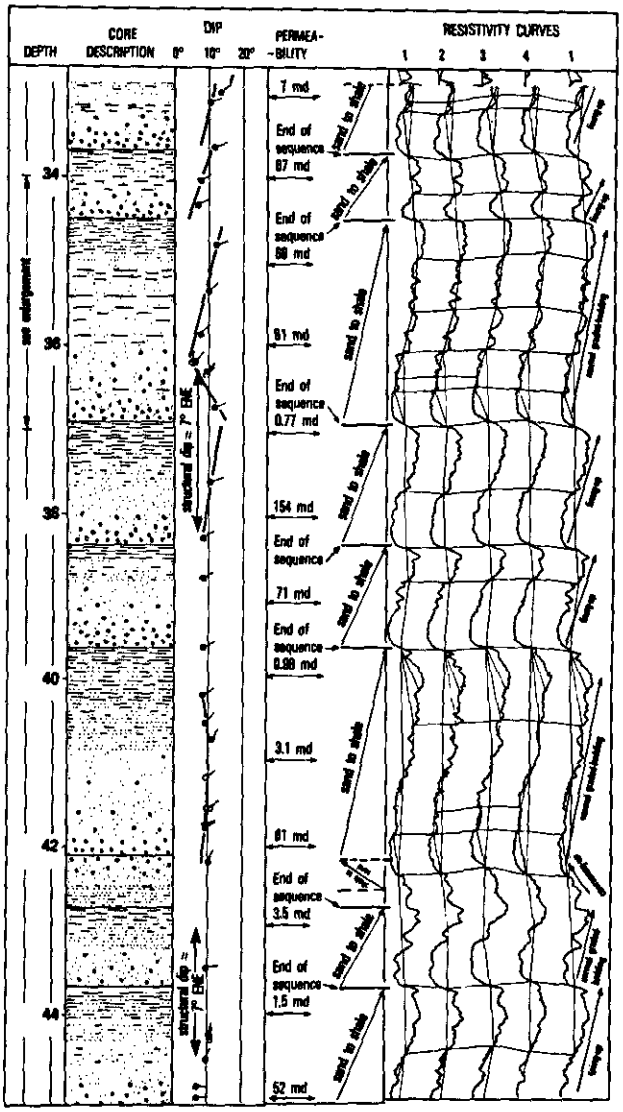

Fig. 5-8. - Example of gradational evolutions or ramps very easily seen on the dipmeter (HDT tool) resistivity curves, corresponding to electrosequences. The thickness of these electrosequences varies between 1 and 3 feet. With such thicknesses these sequences cannot be detected by other tools.

- *a simultaneous variation in mineralogical composition and in texture (conglomerate → sand → shale);*

- *a saturation evolution in the transition zone between oil- and water-bearing reservoirs that appears particularly on resistivity curves.*

This electrosequence is not necessarily observed on all curves and, moreover, if it has a small vertical extension, it will be detectable only by microdevices (dipmeters, FMS tool, microlog, Fig. 5-8).

It corresponds, most often, to a first order sequence (thin or microscopic according to the definition of Lombard 1956), and sometimes to a second order (medium or macroscopic), if detailed study of the curves shows very fine variations in the general trend (Fig. 5-9).

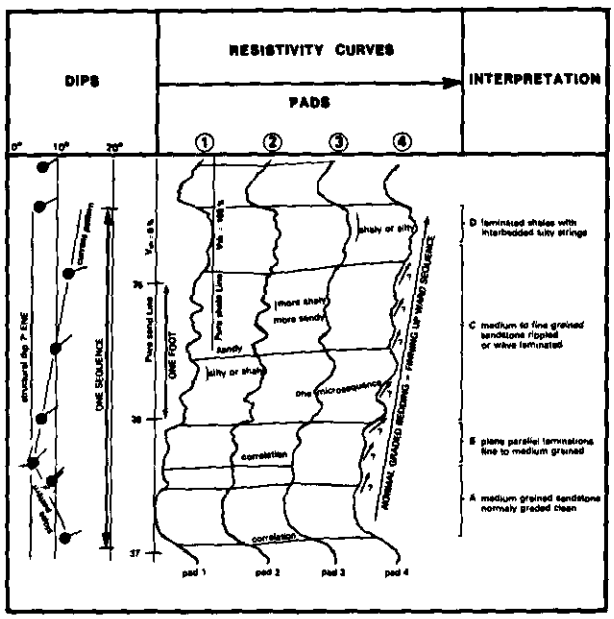

Fig. 5-9. - Enlargement of one electrosequence of the previous example showing thin microsequence within the macrosequence (from Serra & Abbott, 1980).

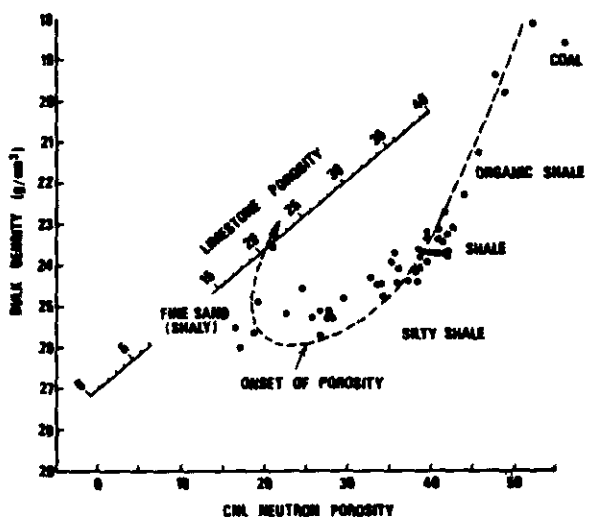

Fig. 5-10. - Plot of one progradational sequence showing the crossplot trend (from Rider & Laurier, 1979).

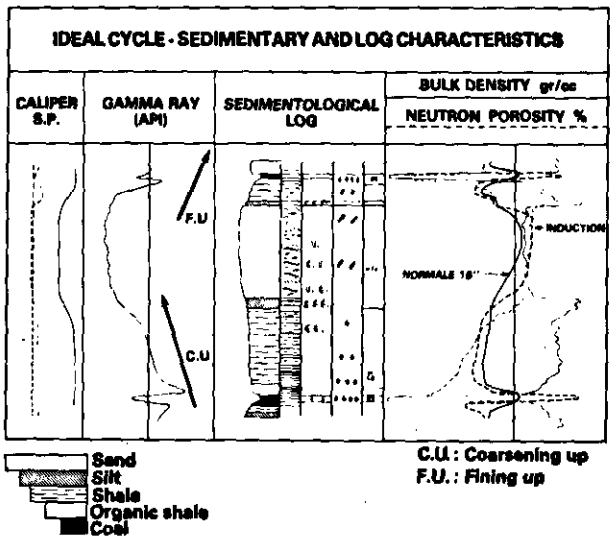

Fig. 5-11. - Log responses of an idealized prograding sedimentary sequence from shale to sand, shale and coal (from Rider & Laurier, 1979).

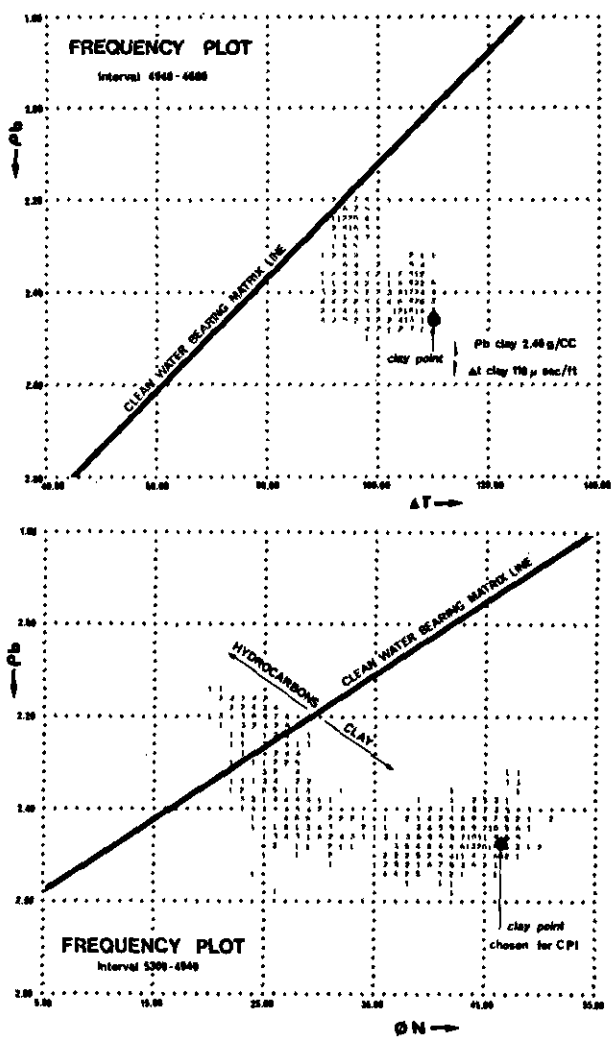

Fig. 5-12. - The "boomerang" shape as it can be observed on neutron-density and sonic-density crossplots in a sand-shale series. It reflects a grain size sequence.

The *"bell"* and *"funnel"* shapes of the SP curve correspond to electrosequences (Fig. 5-1), and not to facies or environment.

It is possible to extend the electrosequence concept to all depth intervals in which the crossplot of two parameters (hydrogen-index and density for instance) shows a continuous form (Fig. 5-10), even if each separate curve (Fig. 5-11) does not clearly show a smooth evolution.

The "boomerang" shape, sometimes observed on density-neutron crossplots and well known by log analysts, is another example of an electrosequence of this type (Fig. 5-12).

5.3. ELECTROFACIES ANALYSIS FROM WIRELINE LOGS

The goal of this analysis is to *describe* objectively the formations penetrated during drilling, through their wireline log responses, and to *recognize all the different fundamental electrofacies present*, in such a way that ultimately it will be possible to *study their association in vertical sequences*, and, consequently, *deduce the lateral evolution* by applying Walther's law. In other words, the first goal is to reconstruct the electrofacies models which will help to define the depositional environments (see Chapter 6). An electrofacies analysis can be carried out manually or automatically. In both cases the basic approach is essentially the same.

5.3.1. Manual Identification of Electrofacies

Originally a sedimentological study from logs involved examining the shapes of various curves for indications of the type of sedimentation and the depositional environment. As previously seen, a ramp or a gradient on a log could indicate an upward-fining or coarsening of grains (Fig. 5-8). Classification of electrofacies by the shape of spontaneous potential response is well known and has been used for many years (Fig. 5-1 and 5-3). Other logs can be used. For example, Serra & Sulpice (1975) correlated gamma ray and grain-size (Fig. 5-13).

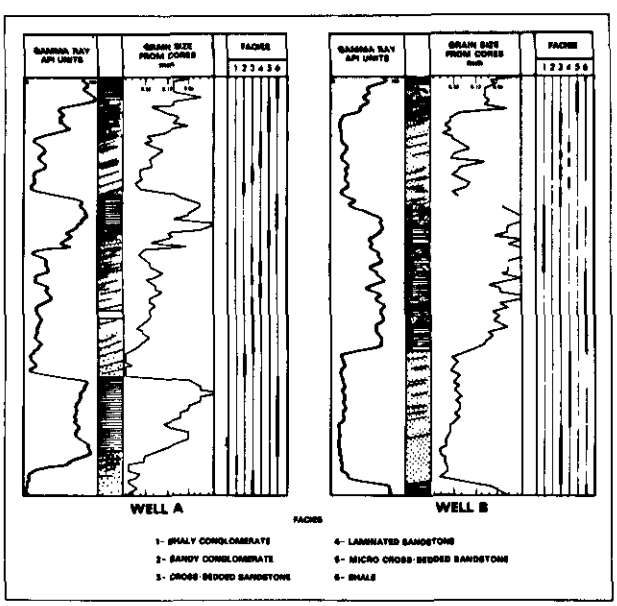

Fig. 5-13. - Correlation between gamma ray and grain size (from Serra & Sulpice, 1975).

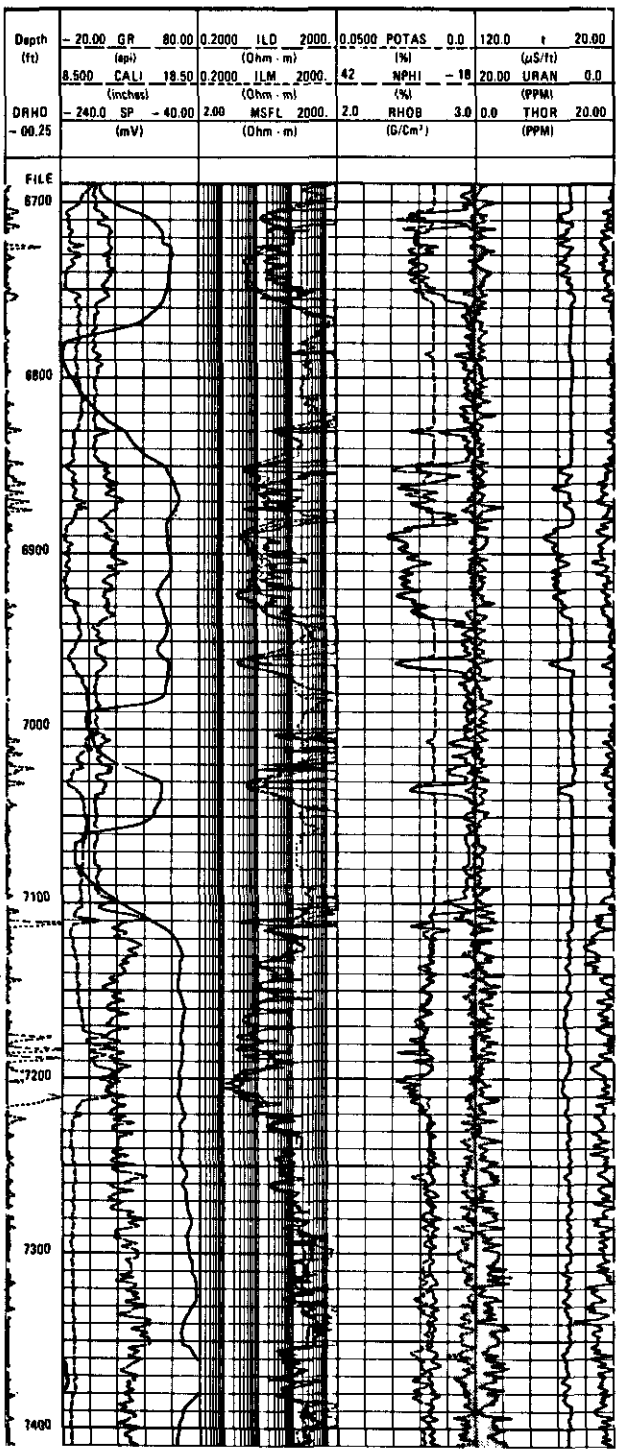

Fig. 5-14. - Example of composite log obtained at the well site

One starts from a contrived document, the composite-log (Fig, 5-14). This document gathers together and depth matches all the log data recorded in a well, including dipmeter data and dip computation results obtained by GEODIP or LOC-DIP processing.

One *divides* the studying interval into *electrobeds* or *electrosequences*. For this purpose the amplitude of the variations on macrodevice curves is analyzed. According to its importance and its shape, it is subjectively decided :

- either it corresponds to an electrobed boundary;
- or it indicates a "noise" that is inherent either to the measurement (statistical variations of nuclear measurements), or to hole conditions (borehole wall rugosity, presence of caves, etc.), or to minor changes in the geological parameters;
- or it reflects a gradual evolution (ramp) with minor variations.

In the following step one determines the electrofacies for each electrobed presenting a thickness greater than the average vertical resolution of most macrodevices (about 2 to 3 feet, or 60 to 90 cm).

As the synthesis of different measurements, corresponding to the same electrobed (especially when it concerns a large amount of data) is not easy, a representation using *rosettes, spider's webs* (Fig. 5-15), or *histograms* has been proposed *to visualize the electrofacies (Serra, in Schlumberger Well Evaluation Conference, Algeria, 1979).* As histograms cannot easily be obtained manually, and a spider's web varies in shape according the number of involved measurements (hence the branches), a ladder diagram presentation (Serra, in Schlumberger Well Evaluation Conference, Algeria 1979) seems to be more usefull because the absence of one log data does not modify the general shape of the figure (Fig. 5-16). In these representations, each branch of the spider's web, or each bar of the ladder, represents a scaled log axis with is range of variation. One plot son these basic documents the minimal, maximal and median values of each log.

When the points on each axis are joined, a characteristic shape is formed. For each electrofacies, there will be an allowed band on each axis; hence, an allowed area is created corresponding to one electrofacies.

Figure 5-17 shows the shapes of two electrofacies. Two shapes need to differ in only one axis to

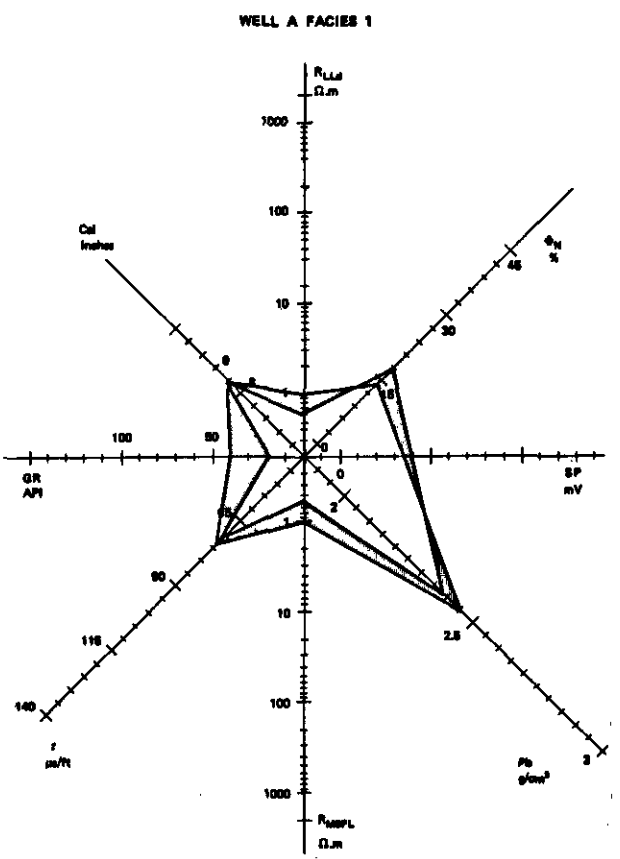

Fig. 5-15. - After logs have been zoned and electrofacies established, the log parameters are plotted on rosette or spider's web diagrams. Comparison of such diagrams facilitates well-to-well correlation (from Serra, in Schlumberger Well Evaluation Conference, Algeria, 1979).

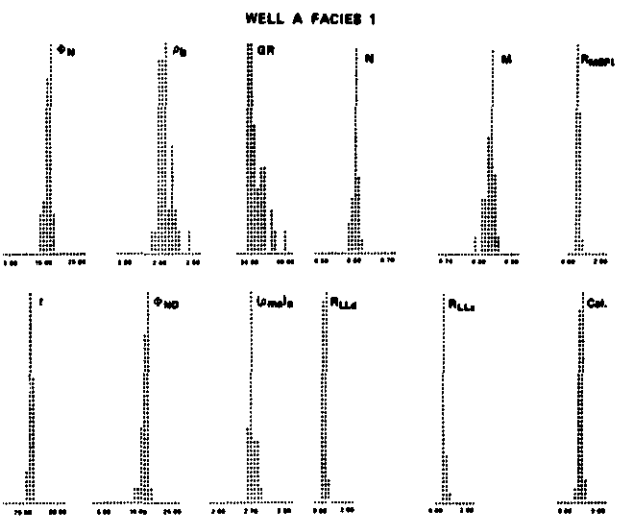

Fig. 5-16. - Representation of the same electrofacies by histograms (from Serra, in Schlumberger Well Evaluation Conference, Algeria, 1979).

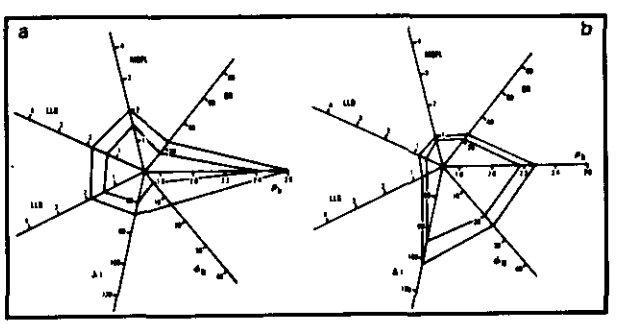

Fig. 5-17. - Spider's web diagrams for (a) a limestone and (b) a sandstone (from Serra & Abbott, 1980).

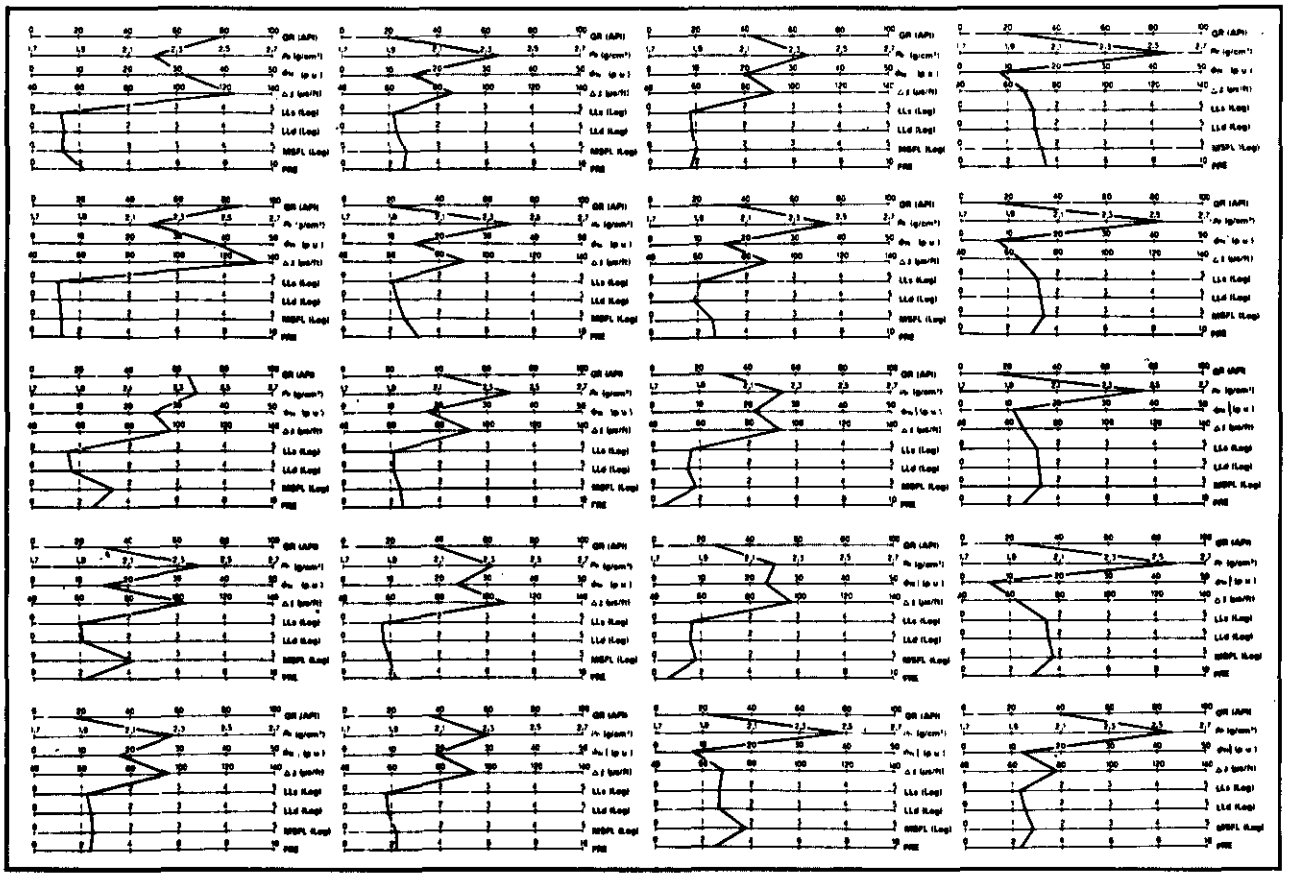

Fig. 5-18. - Comparison of electrofacies (from Serra & Abbott, 1980).

establish the difference between two electrofacies. Essentially, the comparison of shapes allows an analyst to break down a logged interval into some 10 to 15 electrofacies (Fig. 5-18). This last figure shows the progressive change in shapes from one electrofacies to the next. The interval covered is shown in Fig. 5-19. The shallowest depth is at the top left corner, and figures are arranged in columns with depth increasing downward. Correlation with facies defined from core analysis is also made.

A correlation between electrofacies from different wells can also be achieved by this technique (Fig. 5-19).

Determination of the electrofacies in thin beds requires a preliminary step : the correction of the different measurements for the influence of the surrounding beds. For this purpose environmental correction charts are used. But, this is a long and very tedious operation. Therefore, the following empirical method may be preferable. One draws the electrofacies representation of the thin bed and indicate, for each measurement, by an arrow the direction toward which the correction shoul ddisplace the representative point. By comparison with preliminary defined electrofacies, and by using dipmeter resistivity curves, it is possible to estimate the closest electrofacies (Fig. 5-21 & 5-22).

In the case of ramps or electrosequences, one defines the electrofacies of the starting and stopping depths or of the surrounding electrobeds.

This manual analysis is often long and sometimes tedious. Certain traditional geologists may consider it as uninteresting. In this connection we remind these geologists that this method is used by some oil companies in the world, perhaps not in the above mentionned way, but at least in spirit. For example this method allowed the ELF-Aquitaine group to study more than 1000 wells and to have, thus, a synthetic idea of the facies and environments for each well. They were able to draw facies maps. It was done at low cost and in a very short time. Otherwise, it would have been impossible to obtain this information, because cores were rarely cut and the core analyses were often unavailable (exchange wells). This method enabled a more accurate covering of the seismic profiles and a more reliable interpretation in terms of seismofacies. This gave the best possible knowledge of the basins and consequently a more judicious and justified choice of prospects.

But this analysis is subjective, because the results may partly depend on the analyst performing the study. For this reason specialists dreamed for an automatic process using computers. The computer processed method (Serra & Abbott, 1980) described hereafter, was developed by

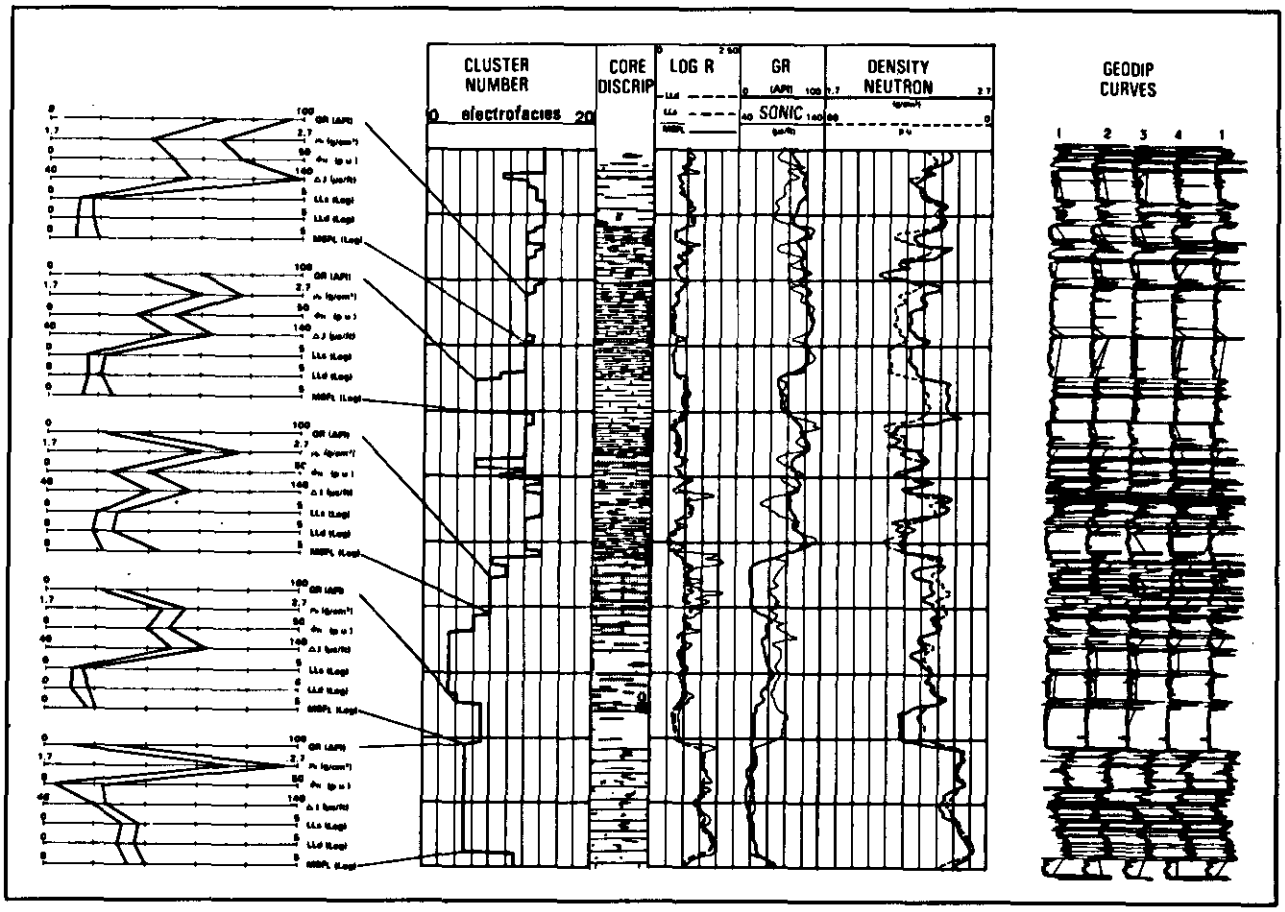

Fig. 5-19. - Correlation of electrofacies with core facies (from Serra & Abbott, 1980).

Schlumberger and commercialized under the mark of FACIOLOG. Its description is destined to explain *the different steps of data processing. Other* approaches could be imagined, and will doubless be developed. They will certainly be inspired by the same general philosophy.

5.3.2. Automatic Electrofacies *Identification* : FACIOLOG

Essentially the same steps are taken as when applying the manual method. We simply try to translate the approach of the analyst into mathematical functions or statistical processing.

The set of n log responses that characterizes an electrobed, or level of reading, may be considered as defining the coordinates of electrofacies (here represented by a point) in a n-dimensional space. Since the same causes produce the same effects, we may think that another bed with same geological facies and containing the same fluids will have the same electrofacies. Consequently, its representative point in n-dimensional space has to be very close to the previous point. Hence, an electrofacies must correspond to a cluster, or to a cloud of points very close to each another in this space. *Contrarily, the distinct electrofacies must correspond* to different and separated clusters. They can possibly overlap in one or several dimensions of the n space.

If we start with "raw", unzoned data, we will observe a certain dispersion of points corresponding to one electrofacies, and it will be more dispersed with a higher number of log measurements. This dispersion is related to the "noise" due to the tool, to hole conditions and even to weak variations of the geological parameters. A preliminary zoning and an analysis of the principal components will, on the one hand, decrease this dispersion, and on the other hand, reduce the dimensionality of the space. Only after this step, can an automatic clustering be carried out.

We can, in certain cases (the absence of ramps and of thin beds), immediately start the analysis of the principal components and carry out a clustering. The results of the processing leads to an automatic zoning (Fig. 5-23).

The use of automatic zoning concentrates the cluster by attempting to eliminate measurement errors. If an n-dimensional histogram is created

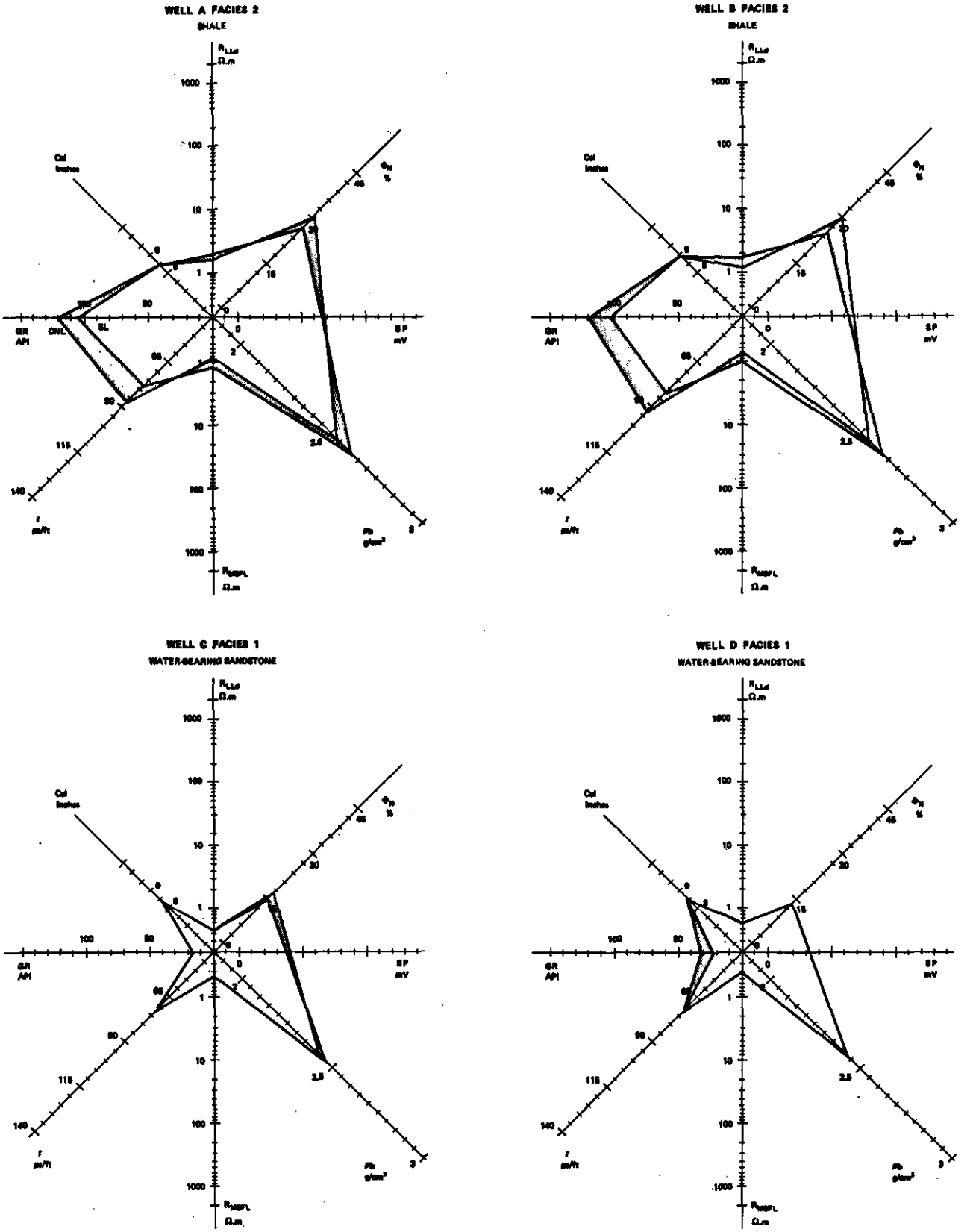

Fig. 5-20. - Electrofacies identification and correlations between different wells (from Serra, in Schlumberger Well Evaluation Conference, Algeria, 1979).

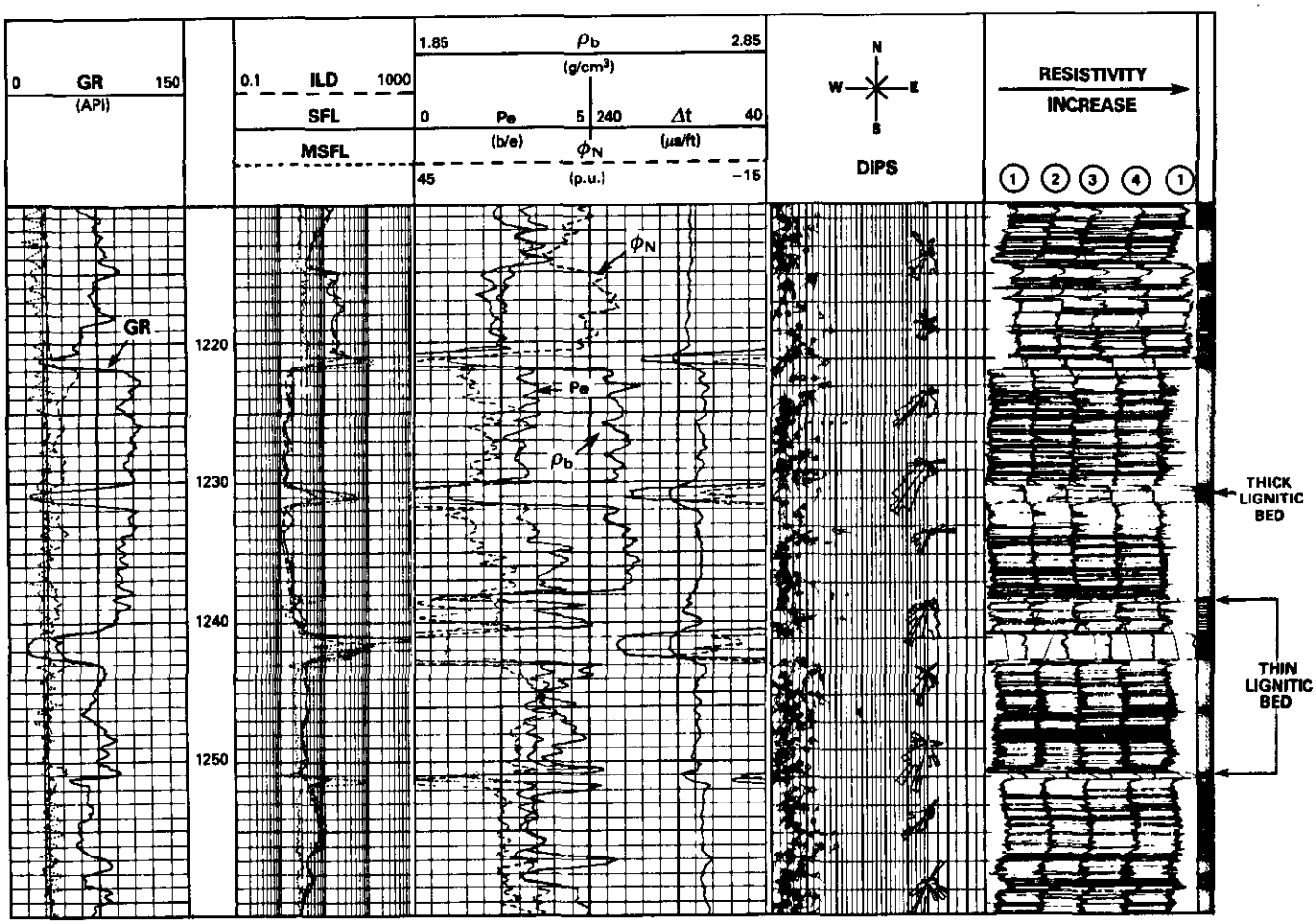

Fig. 5-21. - Composite-log.

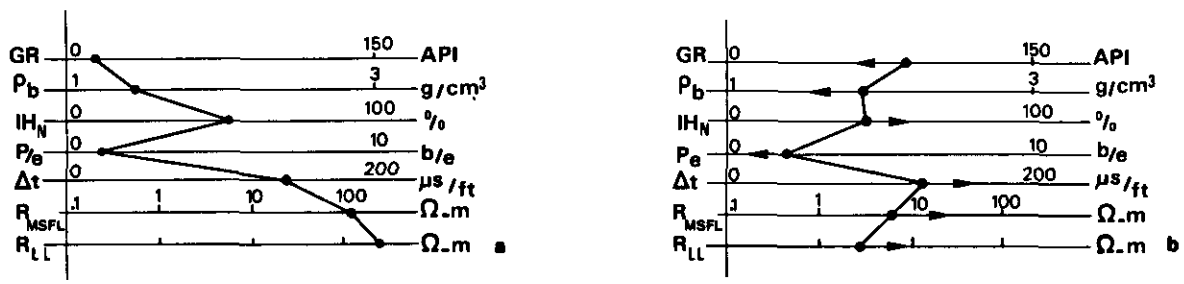

Fig. 5-22. - (a) : Electrofacies of the coal bed at 1241-1243 m. (b) : electrofacies of the thin bed at 1238-1238.5 m which corresponds to a coal as indicated by dipmeter resistivity curves.

and the frequency of each cell analysed, we obtain results as in figure 5-24a. The results on the same interval after zoning are shown in figure 4-23b. Evidently, the data distribution shown in figure 5-24b is easier to handle. Figures 5-25a and 5-25b show the corresponding frequency plots on two selected axes of the interval.

5.3.2.1. *Automatic zoning of logs*

A zoning program has to divide the studied interval into electrobeds and electrosequences (ramps). An electrobed can be defined as a succession of levels with contiguous reading, according to the sampling rate used (6 or 1.2 inches). These levels present essentially the same values .This means that their response variations do not exceed certain limits (allowed variations). These variations correspond to the tool error in the measurement, and to minor acceptable changes in geological parameters (Fig. 5-26).

These changes may be expressed in terms of measurement error or may follow a more complex law.

An electrosequence can be defined as a succession of contiguous readings. The level having an order n, shows a value higher than that of leve lwith order n — 1, but lower than that of level with

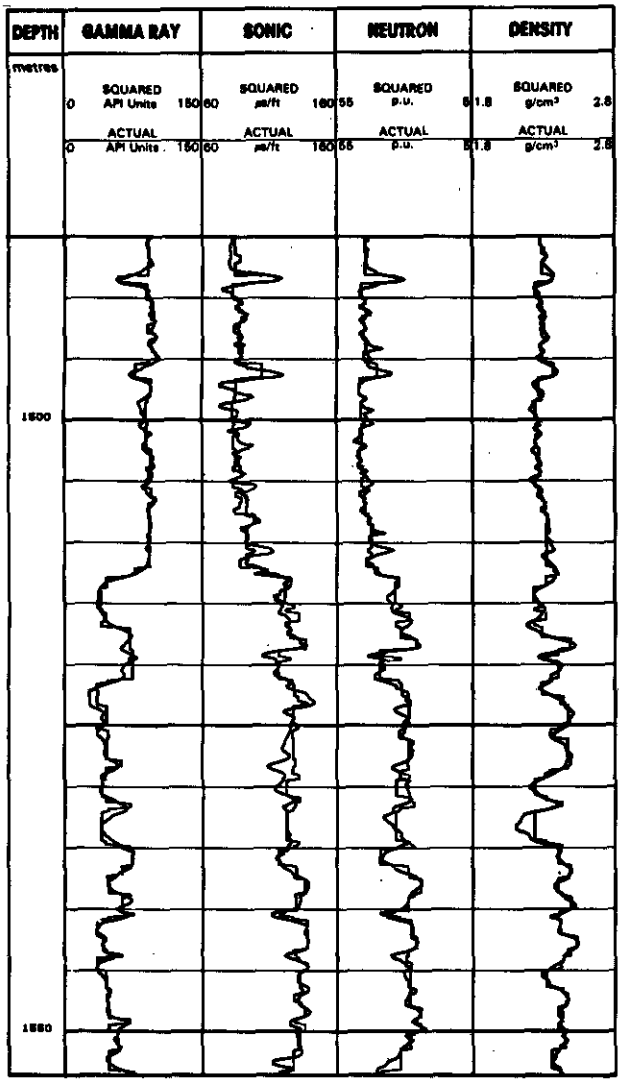

Fig. 5-23. - Example of automatic zoning of logs obtained by clustering techniques and comparison with raw logs (from Serra, in Schlumberger Well Evaluation Conference, India, 1983).

a)

VARIABLE	MIN.	MAX.	STEPS
GR	0.000	100.000	30
LLD	0.000	2.500	30
LMSFL	0.000	2.500	30
RHOB	1.700	2.700	30
NPHI	0.000	60.000	30
FRE	0.000	12.000	24
DT	40.000	240.000	40

NUMBER OF CELLS HAVING 1 ELEMENT	683
NUMBER OF CELLS HAVING 2 ELEMENTS	35
NUMBER OF CELLS HAVING 3 ELEMENTS	5
TOTAL NUMBER OF CELLS	724

b)

VARIABLE	MIN.	MAX.	STEPS
GR	0.000	100.000	30
LLD	0.000	2.500	30
LMSFL	0.000	2.500	30
RHOB	1.700	2.700	30
NPHI	0.000	60.000	30
FRE	0.000	12.000	24
DT	40.000	240.000	40

NUMBER OF CELLS HAVING 1 ELEMENT:	7
NUMBER OF CELLS HAVING 2 ELEMENTS	17
NUMBER OF CELLS HAVING 3 ELEMENTS	17
NUMBER OF CELLS HAVING 4 ELEMENTS.	11
NUMBER OF CELLS HAVING 5 ELEMENTS	5
NUMBER OF CELLS HAVING 6 ELEMENTS	8
NUMBER OF CELLS HAVING 7 ELEMENTS	10
NUMBER OF CELLS HAVING 8 ELEMENTS	5
NUMBER OF CELLS HAVING 9 ELEMENTS	5
NUMBER OF CELLS HAVING 10 ELEMENTS	3
NUMBER OF CELLS HAVING 11 ELEMENTS.	2
NUMBER OF CELLS HAVING 12 ELEMENTS:	1
NUMBER OF CELLS HAVING 13 ELEMENTS.	2
NUMBER OF CELLS HAVING 14 ELEMENTS.	2
NUMBER OF CELLS HAVING 15 ELEMENTS.	2
NUMBER OF CELLS HAVING 16 ELEMENTS	1
NUMBER OF CELLS HAVING 17 ELEMENTS	3
NUMBER OF CELLS HAVING 18 ELEMENTS	3
NUMBER OF CELLS HAVING 19 ELEMENTS.	1
NUMBER OF CELLS HAVING 24 ELEMENTS:	1
NUMBER OF CELLS HAVING 31 ELEMENTS:	1
TOTAL NUMBER OF CELLS.	107

Fig. 5-24. - Electrofacies are distinguished using data generated by a clustering program : (a) unzoned, (b) zoned (from Serra & Abbott, 1980).

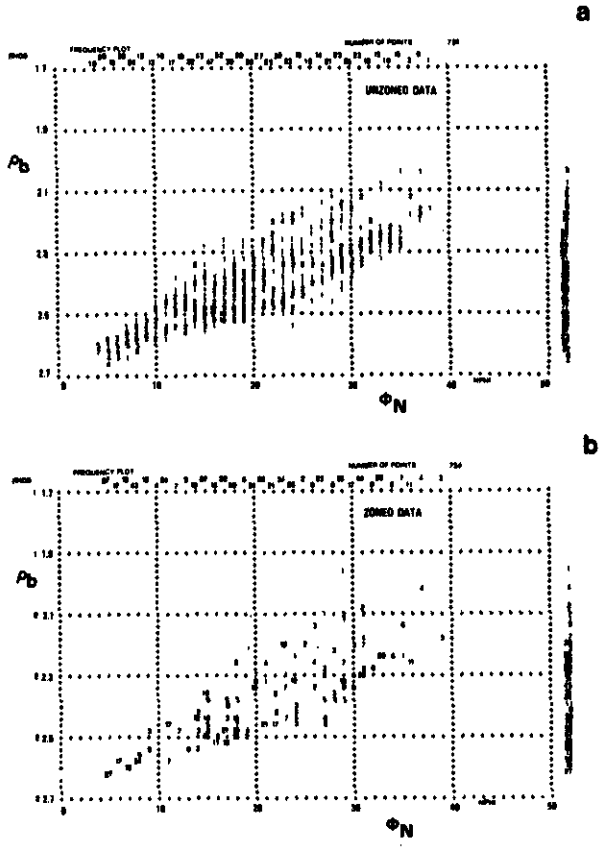

Fig. 5-25. - Frequency plots of the data presented in Fig. 5-24 : (a) unzoned, (b) zoned (from Serra & Abbott, 1980).

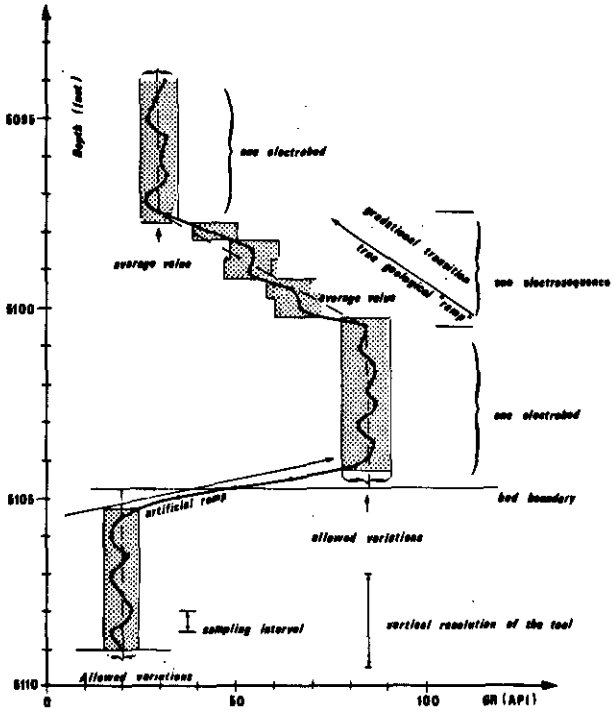

Fig. 5-26. - Principle of the automatic zoning into electrobeds and electrosequences.

order n + 1, or vice-versa. This evolution must constinue in a depth interval thicker than the vertical resolution of the measuring tool, to be considered as representative of an electrosequence. Otherwise , it corresponds to an artificial ramp, due to lack of resolution of measuring tool (Fig. 5-26).

Hence, it is necessary to define for each tool, the vertical resolution and the amplitude of the accepted variations, expressed as a percentage. Figure 5-27 shows the influence of this last parameter on the division into electrobeds and electrosequences for a log (gamma ray). We can state that the effect is minor if we do not exceed a *certain value. Generally, we carry out the zoning* from active logs, on which we rely to determine the limits and the type of evolution. We impose these limits to other so-called passive logs. The type of evolution between these limits defines, for passive logs, either a bed or a sequence. Figure 5-28 gives an example of automatic zoning obtained with the help of three active log sgamma ray, neutron and density.

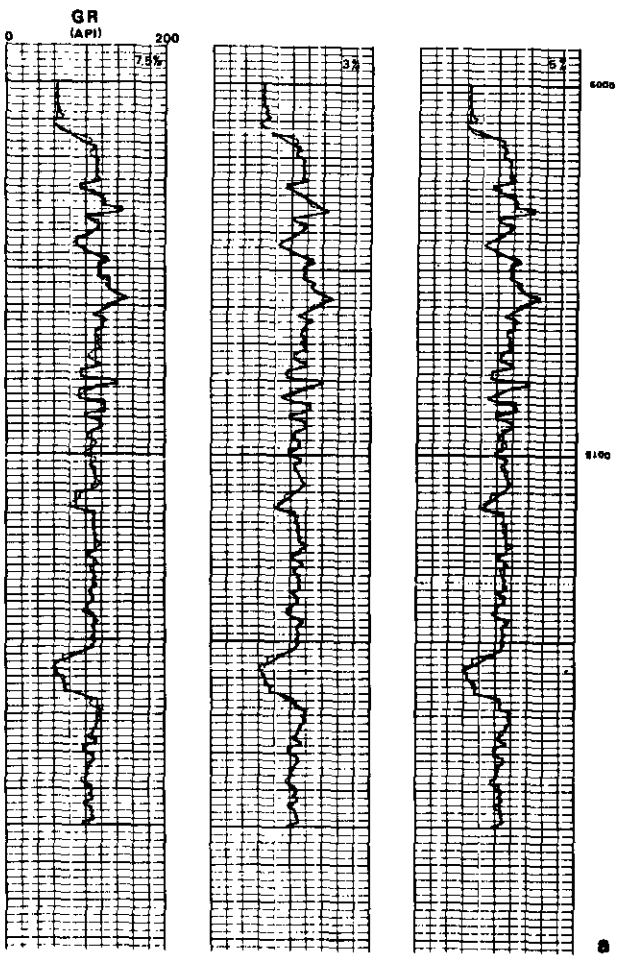

Fig. 5-27. - Influence of the allowed percentage of variation on the zoning of the gamma ray log into electrobeds and electrosequences.

5.3.2.2. ***Dipmeter data processing***

In chapters 3 and 4 we insisted on the interest of dipmeter data as a source of textural and structural information. This information, that is very important for the definition of the electrofacies, and therefore for facies and depositional environment, should not be ignored.

But this information is by nature qualitative : the aspect of resistivity curves, nature of the bed boundaries, dip evolution with depth ... Its use can only be achieved through a quantification of the dipmeter data as done by the SYNDIP program previously described in Chapter 4.

5.3.2.3. ***Automatic clustering techniques***

The method described in the previous section is essentially a way of trying to divide n-dimensional log space (n corresponds to the number of different log data taken into account) into definable *volumes corresponding to each electrofacies* (Fig. 5-29).

Many of the mathematical techniques known as clustering are adaptable to such problems. In more than two dimensions, we can think of the electrofacies points falling into clusters or clouds. (A cluster may be described as a continuous region of the n-dimensional space containing a relatively high density of points, separated from other such regions by regions containing a relatively low density of points). The task of the clustering program is then to distinguish each cloud. For this purpose, we determine, for each level or reading depth, the distance d_k of the k^{th} closest neighbour. It corresponds to the radius of the smallest circle with its center at a known level and *containing k neighbouring points. If any other* level, situated below or above a certain depth window (IBAND) does not have a lower d_k value, and if among these neighbouring k none of them has a lower d_k value, a level will be taken as a cell, or as a *local mode* (Fig. 5-30). Each cell obtained in this manner corresponds to an elementary electrofacies.

The shape of the clusters is difficult to define, as one cannot assume, automatically, that the distribution within each facies, for each log, is normal. A clou dis dispersed in any direction by the effects of log errors, as described, or by changes in the facies itself. Consider, for example, the grain size variation within a sandstone. This will disperse the sandstone points, leading to a *"cloud" with a concentration of points at one end* and a tail. In the case of a gradual change from one facies to another, the actuation is even more complicated since the clouds are not separated. In most cases at facies interfaces the differing vertical resolution of the logs introduces some scatter in the response. For these reasons statistical techniques are needed to establish criteria to separate clusters.

In deciding what kind of clustering technique to

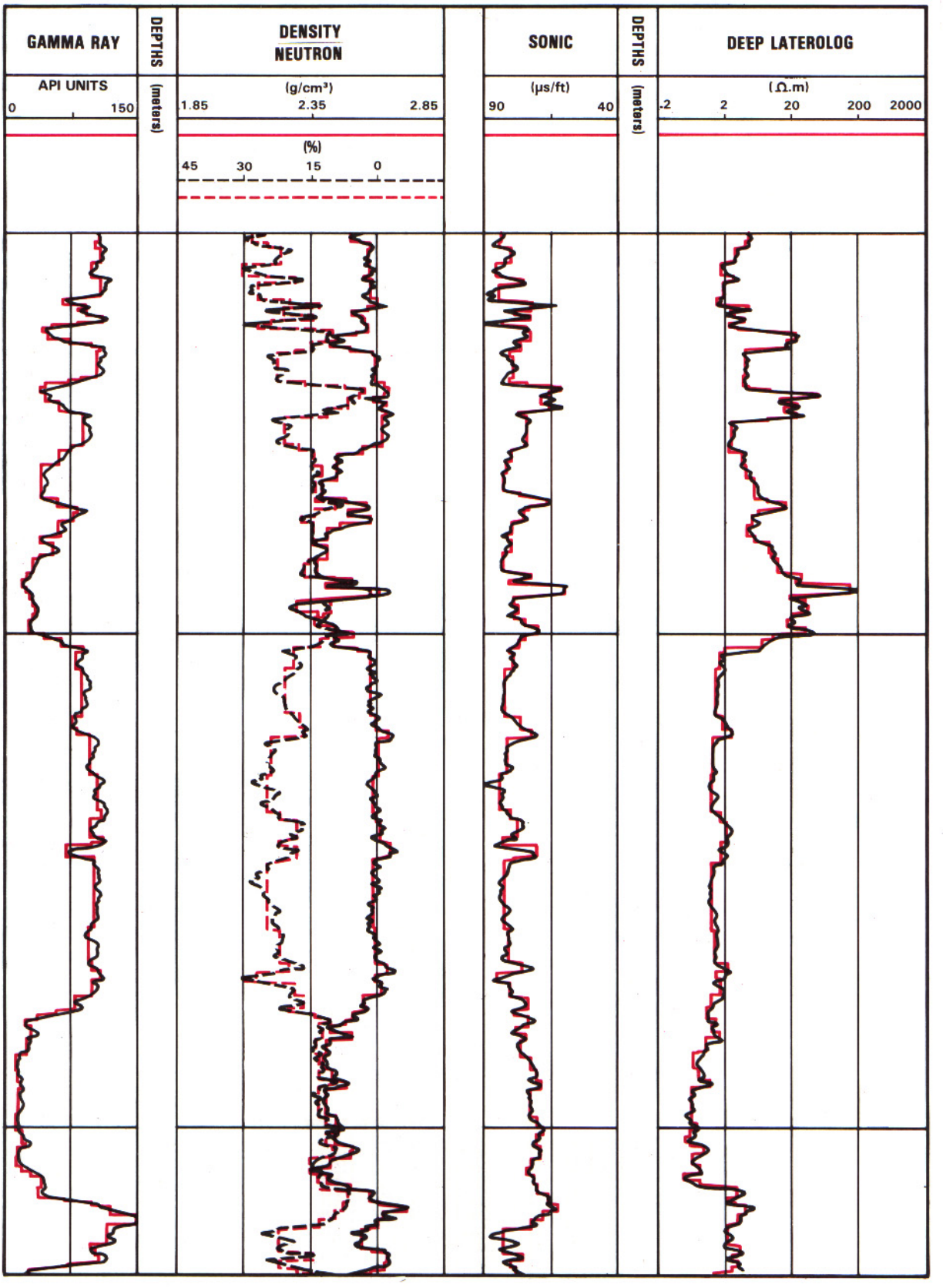

Fig. 5-28. - Example of automatic zoning obtained with three active logs : gamma ray, density and neutron logs (from Schlumberger Well Evaluation Conference, Algeria, 1979).

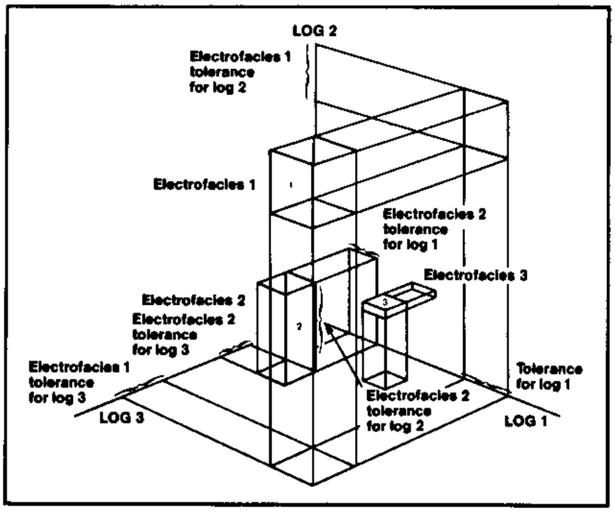

Fig. 5-29. - Three-dimensional case of three electrofacies on a three-log axis (from Serra & Abbott, 1980).

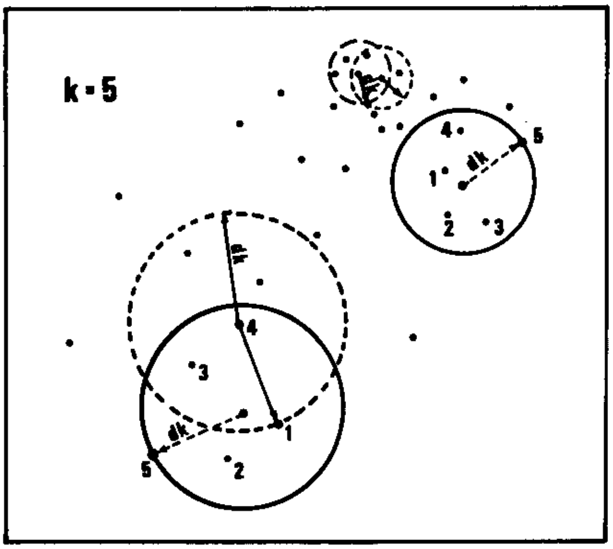

Fig. 5-30. - Determination of local modes or elementary electrofacies.

use, several things are important :

- the number of levels to be examined at any time;
- the number of variables (logs) to be considered;
- the size and distribution of each cluster;
- the occurrence of electrofacies with only limited representation;
- the effects of gradational changes from one cluster to another.

If it is desirable to introduce information provided by a dipmeter, it must be quantified. This is achieved through the dipmeter derived synthetic logs previously described and obtained from the SYNDIP program.

For data where the significance of changes over the range of a log is heavily dependent on the log value, some nonlinear scale changes are necessary. For example, resistivity values that vary from 0.1 to 10000 are transformed to logarithm base 10. This makes the processing easier and allows the use of a metric standard.

5.3.2.4. *Final electrofacies definition*

The previous described method defines a certain number of local modes (or elementary electrofacies) that is much smaller than the original number of levels. A list of the local modes classified following the order of creation is also produced. It indicates the depth of the most representative value, the d_k value, and the link with other modes. The coordinates of the principal components are also given (Table 5-1).

Even if they describe logging reality better and more objectively (compare zoned logs with raw logs of Fig. 5-23), these local modes are often too numerous to be easily correlated to geological facies. The analysis of their proximity to each other can group some elementary modes to reduce the number of final electrofacies to a value close to the number of geological facies (Fig. 5-31). One method is to search within the multidimensional

Table 5-1

List of local modes found by the clustering techniques.

MODE	LEVEL #	DEPTH	DK	LINK	LENGTH	PRINCIPAL COMPONENT COORDINATES				
1	4	1474.47	0.5879E+00	13	1.212190	[illegible]	[illegible]	[illegible]	0.341	[illegible]
2	13	1473.10	0.7013E+00	13	[illegible]	[illegible]	[illegible]	[illegible]	[illegible]	[illegible]
3	23	1471.57	0.9990E+03	6	1.713679	[illegible]	[illegible]	[illegible]	[illegible]	[illegible]
4	38	1469.79	0.5167E+00	10	2.181019	[illegible]	[illegible]	[illegible]	[illegible]	[illegible]
5	56	1466.55	0.5654E+00	4	1.160310	[illegible]	[illegible]	[illegible]	[illegible]	[illegible]
6	70	1464.41	0.9990E+03	18	1.952307	[illegible]	[illegible]	[illegible]	[illegible]	[illegible]
7	83	1460.91	0.5196E+00	24	1.162869	-1.100	[illegible]	[illegible]	[illegible]	[illegible]
8	101	1459.69	0.5406E+00	7	0.915526	[illegible]	[illegible]	[illegible]	[illegible]	[illegible]
9	110	1458.32	0.4411E+00	18	1.169152	[illegible]	[illegible]	[illegible]	[illegible]	[illegible]
10	147	1457.68	0.3762E+00	10		[illegible]	[illegible]	[illegible]	[illegible]	[illegible]
11	157	1451.15	0.9990E+03	18	1.308238	[illegible]	[illegible]	[illegible]	[illegible]	[illegible]
12	164	1450.09	0.5540E+00	17	1.313608	[illegible]	[illegible]	[illegible]	[illegible]	[illegible]
13	197	1445.06	0.4603E+00	10	3.240164	[illegible]	[illegible]	[illegible]	[illegible]	[illegible]
14	209	1443.23	0.4990E+00	13	0.853180	[illegible]	[illegible]	[illegible]	[illegible]	[illegible]
15	214	1442.47	0.6520E+00	17	1.754190	[illegible]	[illegible]	[illegible]	[illegible]	[illegible]
16	227	1440.48	0.9990E+03	18	1.673174	[illegible]	[illegible]	[illegible]	[illegible]	[illegible]
17	245	1437.74	0.8468E+00	10	1.435101	[illegible]	[illegible]	[illegible]	[illegible]	[illegible]
18	251	1436.83	0.9990E+03	20	2.408956	[illegible]	[illegible]	[illegible]	[illegible]	[illegible]
19	271	1433.47	0.3886E+00	10	4.699294	[illegible]	[illegible]	[illegible]	[illegible]	[illegible]
20	303	1428.90	0.1771E+01	10	3.053074	[illegible]	[illegible]	[illegible]	[illegible]	[illegible]
21	325	1425.55	0.6867E+00	4	1.320209	[illegible]	[illegible]	[illegible]	[illegible]	[illegible]
22	335	1424.03	0.1592E+01	10	1.887332	[illegible]	[illegible]	[illegible]	[illegible]	[illegible]
23	346	1422.35	0.7196E+00	4	1.152328	[illegible]	[illegible]	[illegible]	[illegible]	[illegible]
24	354	1421.13	0.4825E+00	19	1.776616	[illegible]	[illegible]	[illegible]	[illegible]	[illegible]
25	378	1417.47	0.5928E+00	4	1.457719	[illegible]	[illegible]	[illegible]	[illegible]	[illegible]
26	386	1416.25	0.8001E+00	4	1.725510	[illegible]	[illegible]	[illegible]	[illegible]	[illegible]
27	408	1412.90	0.6711E+00	24	1.406988	[illegible]	[illegible]	[illegible]	[illegible]	[illegible]
28	542	1397.48	0.9990E+03	19	3.609340	0.810	-0.027	1.740	0.677	-1.803

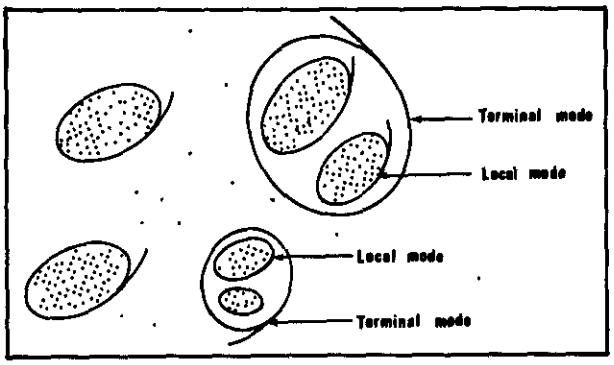

Fig. 5-31. - Schemes explaining the clustering of points into local modes and terminal modes.

histogram for cells of the locally highest frequency (*modes*) and then to construct a dendrogram of similarities between the modes (Fig. 5-32).

The *dendrogram* is a graphic representation of the distance, in n-dimensional space, between each mode and its closest neighbour. Value salong the x-axis of Fig. 5-32 correspond to these distances. They give an idea of the degree of similarity between modes and can be used to justify the grouping of modes into the final electrofacies. The analyst then chooses a reduced list of modes as seed points for a partitioning algorithm, working not on the histogram but on the original data.

Single-link clustering methods on the original data have not been used because of the amount of data and the effects of chaining. However, clustering directly on constant values within zones after zoning gives a reduced data set and works well. This is, in effect, a method of segmentation followed by clustering.

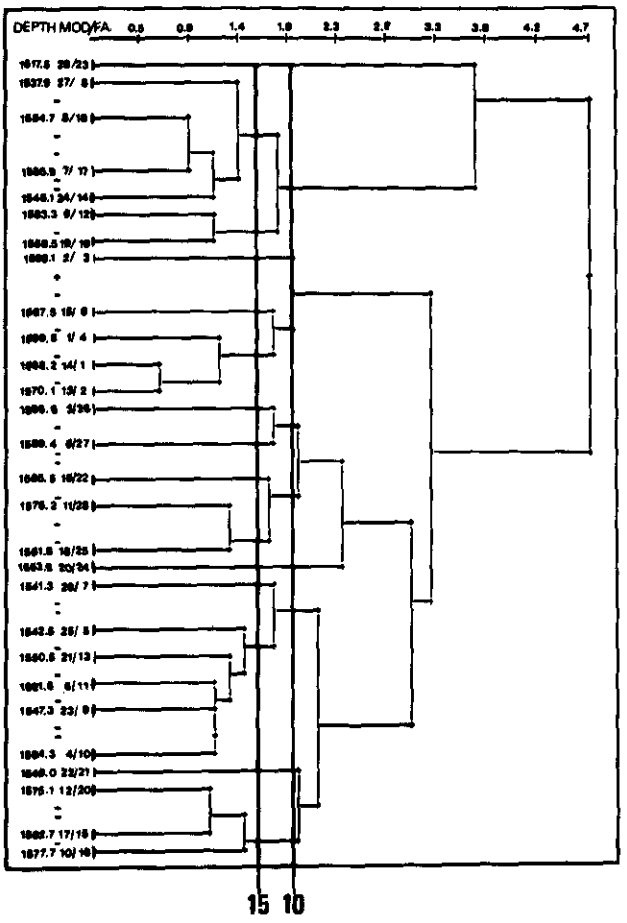

Fig. 5-32. - Example of dendrogram and its use for defining the terminal modes.

5.3.2.5. *Principal Component Analysis*

In fact, the clustering methods are applied on the principal component logs, which are derived from a *Principal Component Analysis (PCA)*.

As we noted previously, each log is influenced, in different degrees, by the geological parameters of the rocks. In combining several logs we have, automatically, a certain redundancy of geological information. This is highly useful for mutual verification of the data quality .The goal of the Principal Component Analysis is to study the correlations between log data, to reduce the number of n variables to a lower number m, by eliminating the insignificant components.

The *Principal Component Analysis*, or PCA, is a statistical study of the logging data over a given interval. From the search of correlations between

Table 5-2
Statistical analysis of logging data.

LOG NAME	MEAN	STND DEV	RANGE	MINIMUM	MAXIMUM	WEIGHT
GR	60.0135	21.4079	85.8293	24.9209	110.7502	2.000
NPHI	0.3261	0.0739	0.3139	0.1726	0.4866	1.000
RHOB	2.5773	0.0931	0.3550	2.3101	2.3651	1.000
DT	100.4467	13.3161	72.3640	74.3620	146.7260	1.000
VAR	1.1471	1.3760	6.1961	0.1059	6.3019	0.350
FRE	1.7566	1.5059	6.1500	0.2500	6.3000	0.350
SAL	47.0103	14.2932	79.8874	9.6139	89.5028	0.000
SHA	2.9793	1.2270	8.3376	0.2996	8.7372	0.350
ALT	6.6620	3.0032	21.9160	2.8018	24.7198	0.350

Table 5-3
Correlation matrix between wireline log.

LOG NAME	GR	NPHI	RHOB	DT	VAR	FRE	SAL	SHA	ALT
GR	1.000	0.870	-0.198	0.750	-0.106	-0.135	-0.095	-0.036	0.056
NPHI	0.870	1.000	-0.514	0.925	-0.286	-0.250	-0.232	-0.147	0.158
RHOB	-0.198	-0.514	1.000	-0.551	0.323	0.242	0.214	0.117	-0.102
DT	0.750	0.925	-0.551	1.000	-0.211	-0.263	-0.209	-0.125	0.133
VAR	-0.106	-0.286	0.323	-0.211	1.000	0.908	0.100	0.826	-0.384
FRE	-0.135	-0.250	0.242	-0.263	0.908	1.000	0.053	0.729	-0.377
SAL	-0.095	-0.232	0.214	-0.209	0.100	0.053	1.000	0.044	-0.063
SHA	-0.036	-0.147	0.117	-0.125	0.826	0.729	0.044	1.000	-0.199
ALT	0.056	0.158	-0.102	0.133	-0.384	-0.377	-0.063	-0.199	1.000

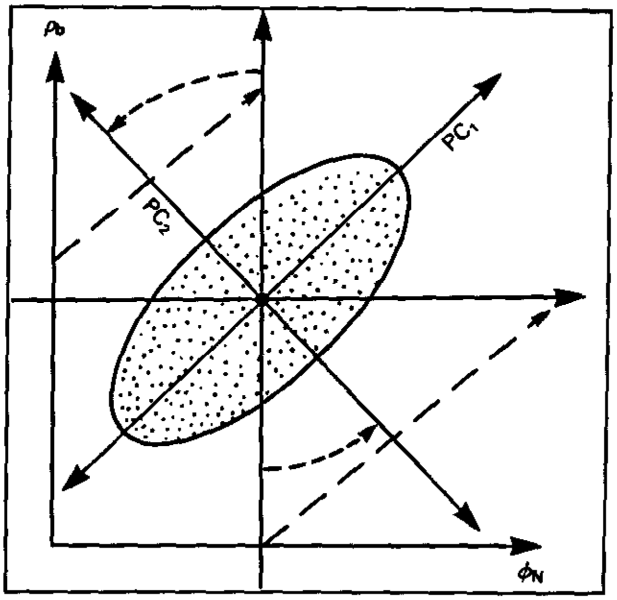

Fig. 5-33. - Principal Component Analysis corresponds to a change of axes.

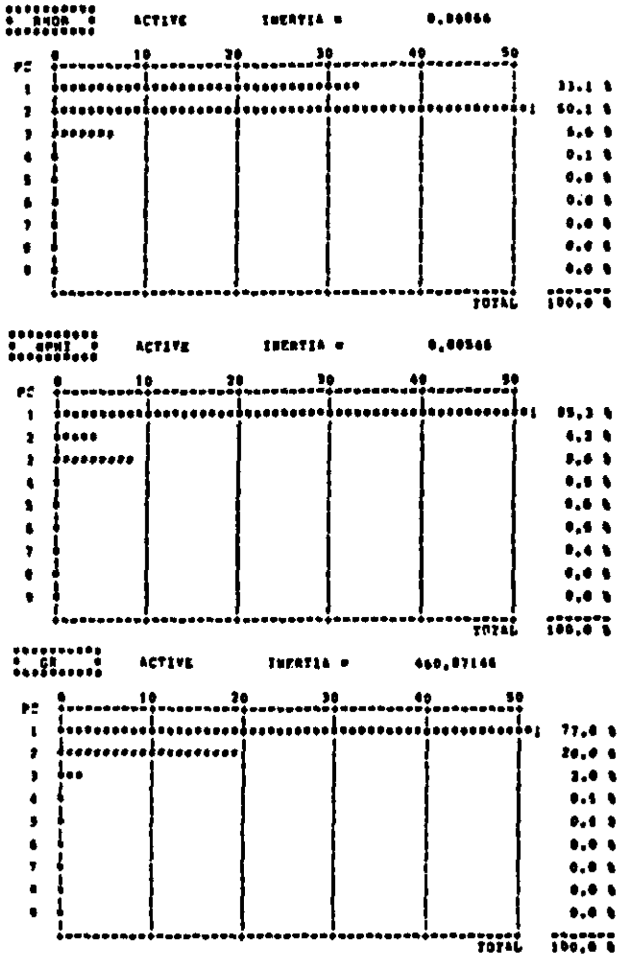

Fig. 5-34. - Histograms illustrating the contribution of the principal components to the reconstruction of the logs.

Table 5-4
Evaluation of the principal axes and rank by amount of original information carried.

AXIS	INERTIA CARRIED	IN PERCENTAGE	CUMULATED PERCENTAGE	NOISE RATIO
1	0.6668D+01	64.617	64.617	-1.003
2	0.2317D+01	22.341	86.958	-2.537
3	0.5081D+00	4.909	91.867	-2.457
4	0.3224D+00	3.115	94.982	-0.709
5	0.2802D+00	2.691	97.673	-0.387
6	0.1008D+00	0.974	98.647	-2.965
7	0.8140D-01	0.786	99.634	-3.605
8	0.3045D-01	0.294	99.928	-3.228
9	0.7478D-02	0.072	100.000	14.320

Table 5-5
Correlations between wireline logs and principal components.

LOG NAME	WEIGHT	PC 1	PC 2	PC 3	PC 4	PC 5	PC 6	PC 7	PC 8	PC 9
GR	2.000	0.882	0.447	0.142	0.033	0.028	0.008	0.010	0.002	0.000
VPHI	1.500	0.926	-0.305	-0.293	-0.070	-0.073	0.072	0.061	-0.002	0.000
RHOB	1.500	-0.575	0.775	-0.258	-0.030	0.017	-0.062	-0.002	0.004	0.000
DT	1.000	0.934	-0.110	-0.207	-0.053	-0.012	-0.193	-0.181	0.001	-0.002
VAR	0.350	-0.269	0.284	0.125	0.213	-0.820	0.188	-0.186	0.094	-0.186
FRE	0.350	-0.241	0.194	0.103	0.238	-0.858	0.040	-0.092	0.273	0.148
BAL	0.600	-0.182	0.215	0.316	-0.090	-0.167	0.000	-0.006	0.007	0.001
SHA	0.350	-0.251	0.412	0.119	0.183	-0.729	0.095	-0.141	-0.408	0.058
ALT	0.350	0.141	-0.161	-0.043	-0.412	0.547	0.613	-0.813	0.021	0.031

logging parameters (Tables 5-2 and 5-3), PCA replaces n measured parameters (or n curves or logs as IL, SP, FDC, CNL, GR, etc.) with n other uncorrelated parameters (or n PC logs). In fact, this results in a change of coordinate axes (Fig. 5-33). The readings of n logs at a given depth can be considered as coordinates of a point (corresponding to the depth) in a n-dimensional space.

Over a given interval, all measurements or levels (or sets of data) define a cloud in n-dimensional space.

This n-dimensional cloud can be described by a set of axes. PCA defines the principal axes of inertia. If each data point has the same weight, the first axis of inertia (or PC 1) will be aligned according to the direction of maximum length. In other words, the first axis is the one having the largest variability. The second (or PC 2) is the second largest but in a perpendicular direction. etc. There is no correlation between PC 1, ... , PC n, so their use eliminates the redundancy between original logs and permits isolation of the elementary effects. The amount of original information that each PC axis contains decreases from PC 1 to PC n (Table 5-4). When the n of them are taken, the total amount of information contained in the original set of logs is restored. PC axes of high order contain little information, which in some

cases can be considered noise. In this case, we can eliminate them in a further treatment. This corresponds to a filtering and reduces the number of parameters to be taken into account (it reduces the dimensionality of the cloud from n to m, m being lower than n).

But if variations observed on a PC of high order, correspond to events that appear on one log and not on the others, these events cannot be considered as noise (i.e. organic material only detected by the uranium content, measured by the NGT tool).

The distribution of the information carried by a log between the PC logs, can be represented by histograms (Fig. 5-34). At the same time correlation between logs and PC is provided (Table 5-5). This can help to understand what type of information is essentially represented by a given PC log.

Once the principal axes of inertia have been calculated from a set of "active"logs, it is also possible to project other logs or curves (i.e., "passive" logs) onto these axes. Thus, one can determine which part of the passive logs can be explained by the information contained in the set of active ones and how much the passive logs are related to each PC log.

PC logs do not carry additional information. It is just another way to present the essential information contained in the original logs. This technique makes clustering somewhat easier, with little or no loss of information. Hence, after the principal component analysis of the standard logs, a reduced set of principal component logs is chosen. PC logs can be drawn as logs (Fig. 5-35).

The definition of the axis is based on the cloud distribution. The latter will depend on the weight given to each data. Hence, if we want to give priority to mineralogy, we can put more weight on those logs that are more sensitive to composition (NGT, LDT, GST, ACT tools). This situation will amplify the variations of parameters measured by these tools, and will diminish the weight given to those logs particularly sensitive to porosity and saturation (FDC, CNL, LL, IL ...). This will naturall ycompress the variations of parameters obtained from the last mentioned tools.

The results of either of these approaches is an affectation of each log sampling level to one electrofacies. Fig. 5-19 shows the results obtained by the partitioning technique. The electrofacies is coded arbitrarily as a number from 0 to 20. Evidently, we expect the n^{th} electrofacies to reappear whenever the core description indicates a repeat of the lithofacies type. The maps from electrofacies to core lithofacies can be made easily by means of the representation of Fig. 5-19. For example, the No. 7 electrofacies is a clea nsand, whereas No. 5 is a limestone. Electrofacies 12 repeats several times, corresponding to the shale intervals.

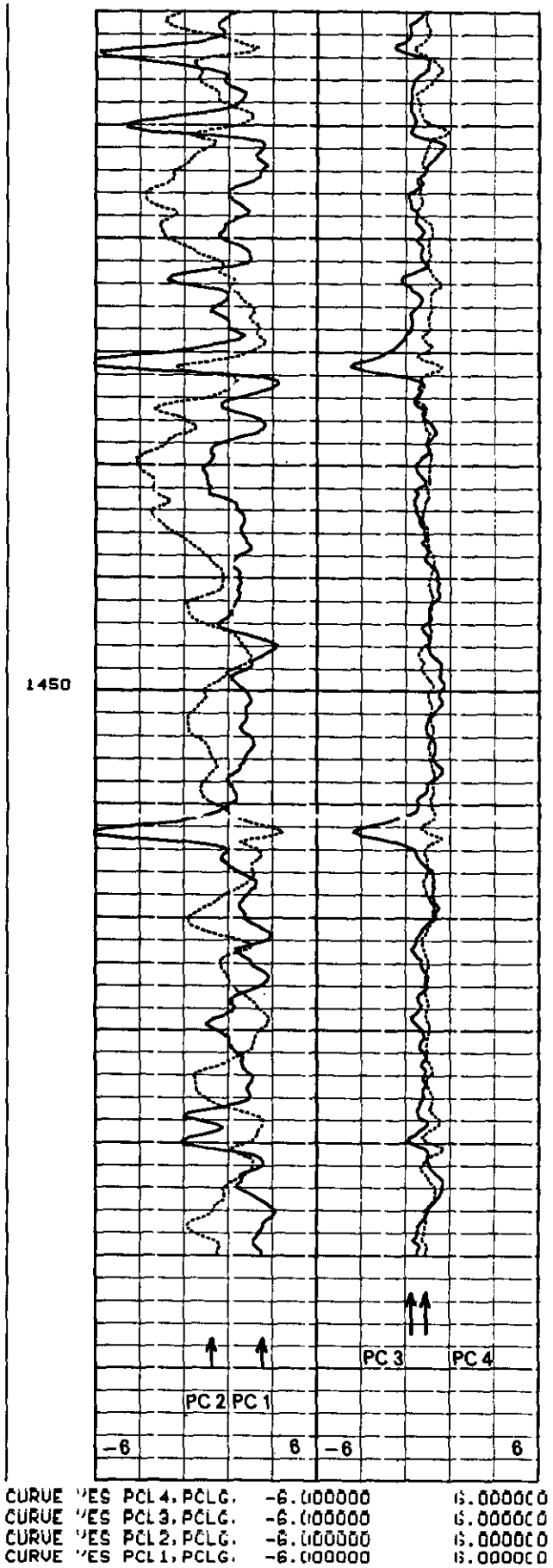

Fig. 5-35. - Example of PC logs. ▶

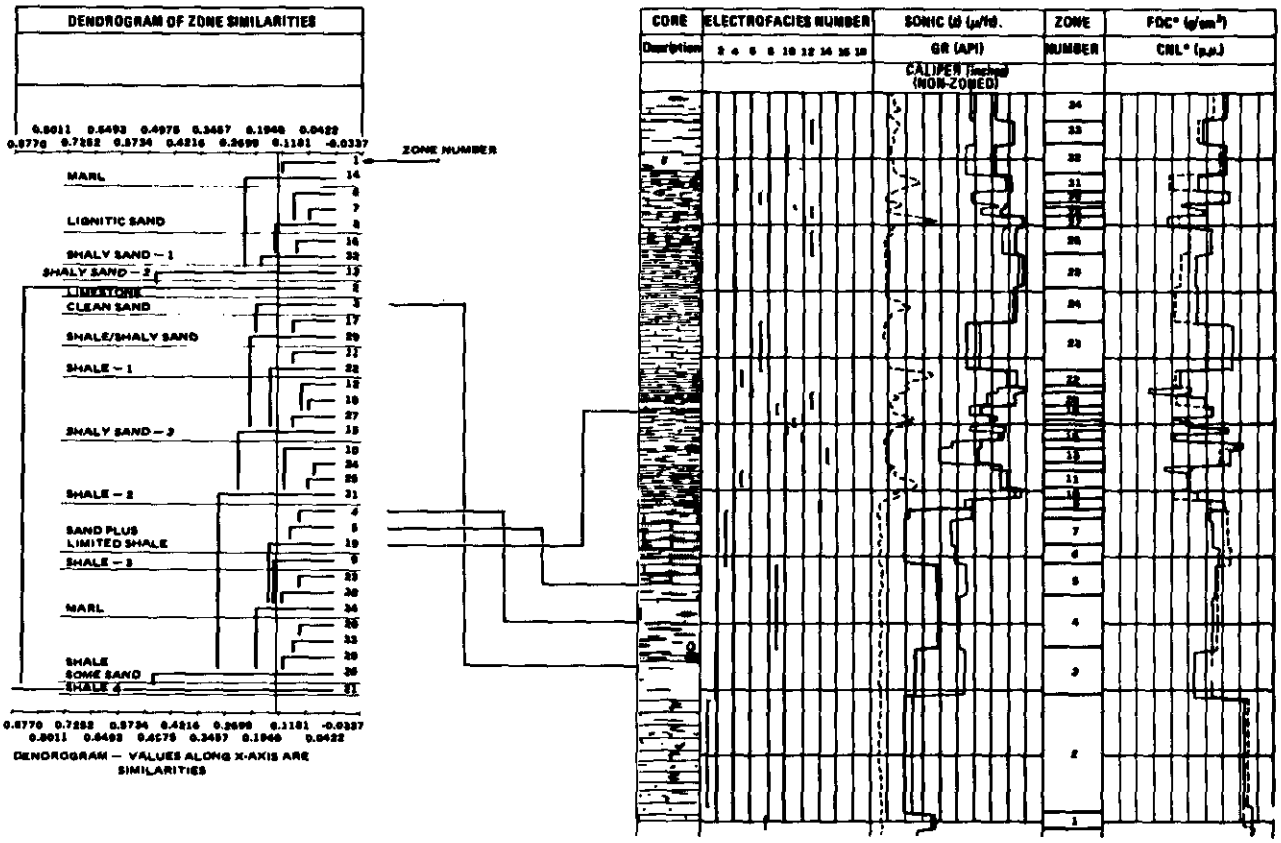

Fig. 5-36. - Direct clustering on zone values (from Serra & Abbott, 1980).

The correspondence with core data is shown. The "ladder" presentation for some of the electrofacies (Nos. 5, 6, 7, 8 and 12) also is shown. A glance at the "ladder" corresponding to No. 12 shows a wide variation on several logs. Furthermore, the GEODIP results shown on the right indicate different response types within electrofacies No. 12. It can be subdivided by establishing subfacies in the shale zones.

Fig. 5-36 illustrates the result of direct clustering on the zone values. In this case, the criteria used in the automatic zoning program have been relaxed to give longer and, hence, fewer zones than in Fig. 5-19. The dendrogram shows the zone "families" grouped in terms of their similarities and distinguished by use of a cutoff level. Each of these families is assigned an electrofacies number, as shown in the appropriate column. We can note immediately that this method gives four different shale and three shaly sand types. With a more detailed definition of the core, we probably would see differences in the composition of each of these shales or shaly sands. The main layers of marl, sand, and limestone are as seen in Fig. 5-19.

An example of electrofacies analysis in carbonates is given by Fig. 5-37. A final selection of 9 terminal electrofacies was made. The superposition of the squared logs obtained from these 9 terminal modes on the actual logs (Fig. 5-38) gives a good quality-control indicator of the selection of terminal electrofacies. The 9 selected electrofacies allow an adequate description of the main geological facies over this interval. At the same time, the representative mean values of the parameters characterizing each final electrofacies are reproduced under the form of a listing (Table 5-6).

At this stage it is necessary to make the following remarks :

- it is not recommended to try to obtain, at any price, the same number of electrofacies as well recognized in the core by facies analysis made by a geologist. Even if the logging tools "substitute the geologist's eyes", it is impossible for them to "see" the formations as a geologist would see them. The tools do not react to the same parameters as the eyes and the brain of geologist do. To define a facies, he will often "filter" the available information, and rely on a feeling that is based on some of the information : composition, colour, certain elements of texture, and more often sedimentary features and faunistic associations. He pays little attention to the precise proportion of each mineral or element, because these are studied on chosen samples, and they may vary appreciably from one point to another. He rarely estimates the porosity and never includes the fluids. The majority of tools are sensitive to minor variations in composition, and the latter is not easily detected in a core except in a very detailed and expensive analysis.

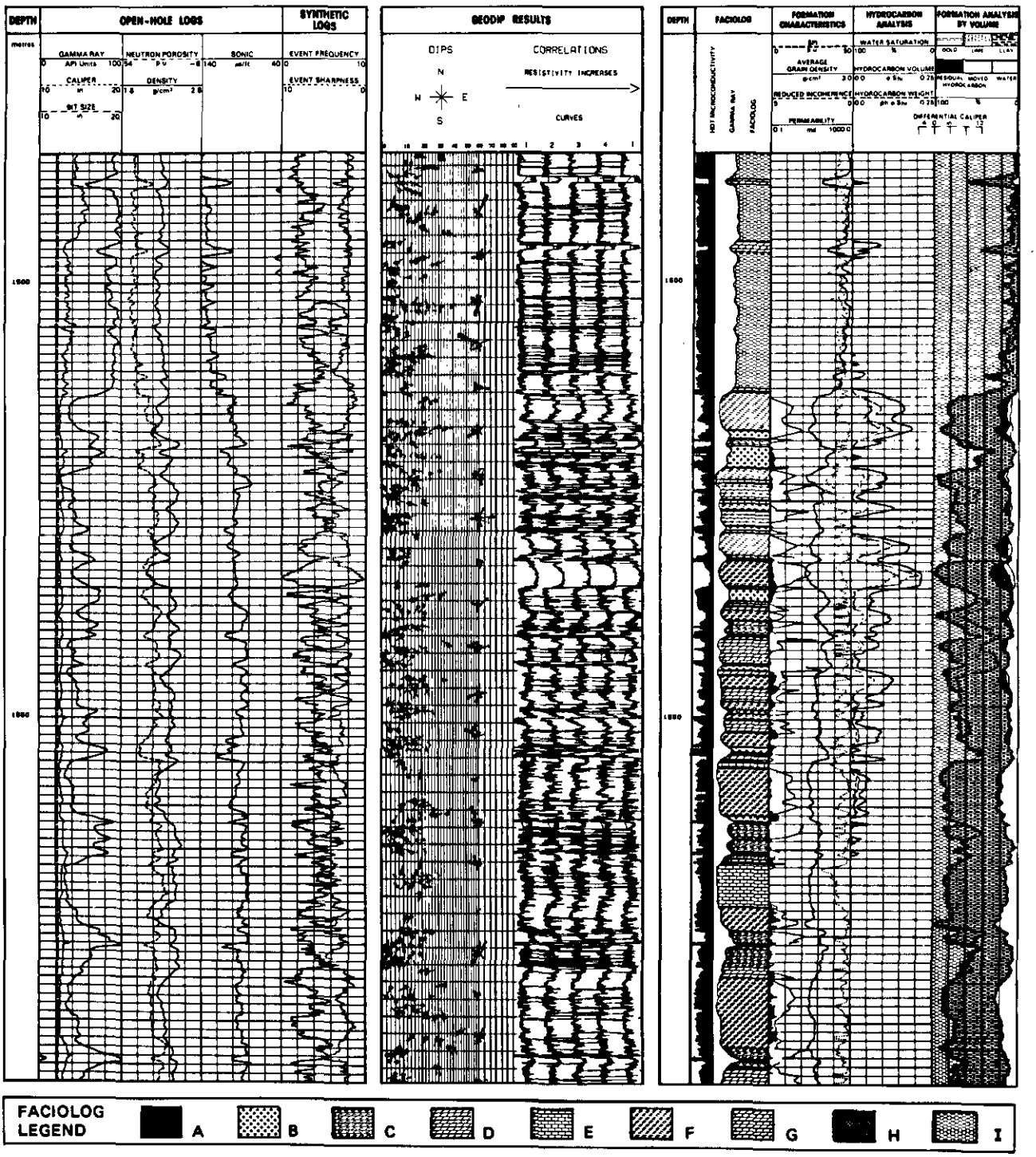

A = carbonaceous shale
B = nodular bedded shale
C = dolomitic mudstone
D = packstone to wackestone with abundant rounded algae
E = packstone to wackestone rich in foraminifers
F = packstone to wackestone rich in large foraminifers
G = bioclastic mudstone to wackestone
H = packstone to wackestone rich in bioclasts
I = upper shale, calcareous

Fig. 5-37. - Open-hole logs, synthetic logs, GEODIP and FACIOLOG results and GLOBAL evaluation of a well (from Schlumberger Well Evaluation Conference, India, 1983).

Table 5-6

Listing of the mean values of the parameters characterizing each terminal mode or electrofacies.

FACIES	< PC1 >	< RAFW >	< GR GAPI >	< NPHI PU >	< RHOB G/C3 >	< DT US/F >	< VAR >	< FRE >	< BAL >	< SHA >	< ALT >
1	-3.407	6.887	33.785	24.328	2.469	84.175	2.771	5.067	41.648	3.759	5.228
2	-3.704	1.589	48.112	18.519	2.542	75.925	2.308	3.750	63.289	3.627	5.830
3	-2.162	16.821	45.792	27.526	2.461	87.531	1.729	3.230	50.698	2.722	6.678
4	-0.992	11.259	67.670	27.281	2.491	87.928	2.418	4.393	54.530	4.107	4.922
5	-1.156	29.801	41.152	30.770	2.309	93.075	1.616	3.581	43.311	2.338	6.802
6	0.933	7.020	70.530	37.164	2.423	101.593	2.627	4.194	37.255	3.825	5.831
7	1.747	2.649	80.276	39.906	2.429	100.284	4.094	5.500	41.979	4.936	5.523

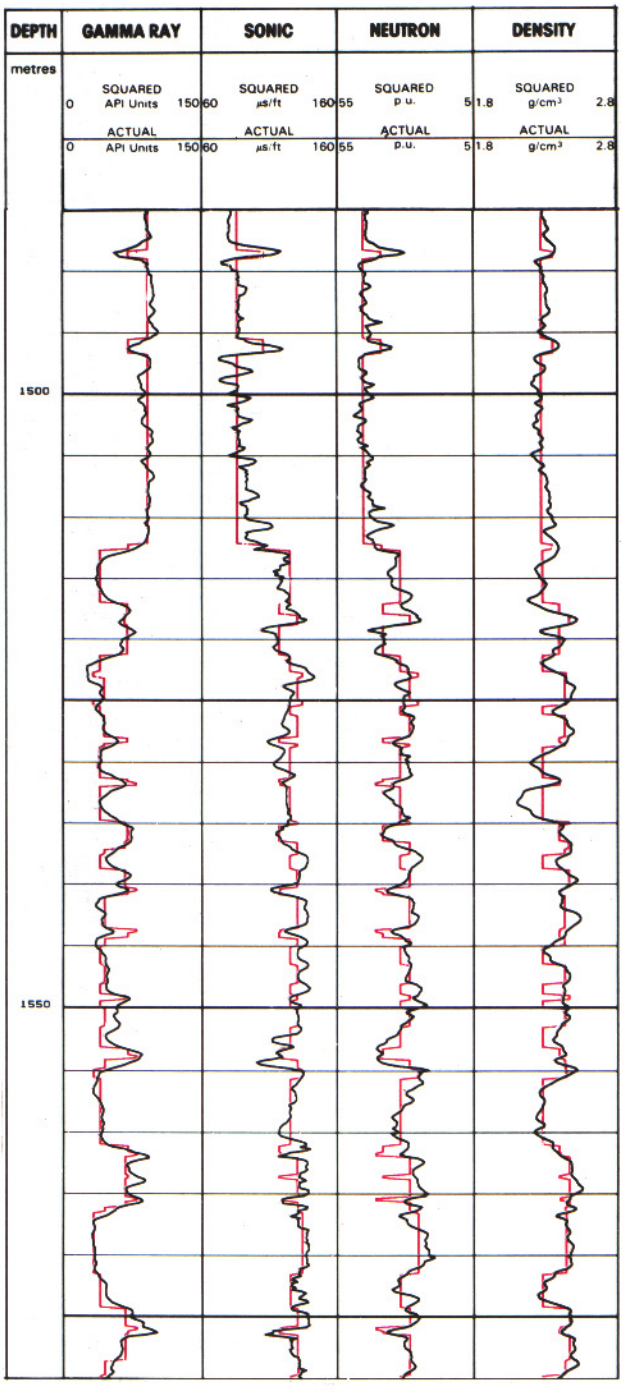

- The purpose of electrofacies analysis is to describe the formations from the tool responses. If we wish to be precise and objective it is necessary that the retained electrofacies reflect, first of all, log parameters. This verification is carried out by superposing the average values, defined for each electrofacies, on the raw data (Fig. 5-38).

- It is important that the geologist gets to know this new concept and learns to exploit the results of this new method of formation analysis. It is necessary that he benefits from its advantages; objectivity, rapidity, quantification, accuracy, and finesse of analysis. However, while maintaining the detail made possible by analysis of the electrofacies, the geologist can cluster several electrofacies under the same shading, representing one lithofacies.

- As it was previously mentionned he can give more weight to those log data particularly sensitive to lithological parameters, or to sedimentary features.

- If the beds are very thin, compared to the vertical resolution of the tools, or if the series are fundamentally composed of thin sequences (i.e. distal turbidites, tempestites), the majority of open-hole logging tools will not recognise the proper electrofacies of each bed or each term of the sequence. The computer processing will thus define an electrofacies corresponding to an average response that combines the influence of two or more beds, and therefore facies. This electrofacies will not give an accurate idea of the real facies. In such a case, it is necessary to use tools with a high vertical resolution (dipmeters, EPT), and a combination of the results obtained by processing of the data with the LITHO and SYNDIP programs. This allows conversion of the dipmeter resistivity curves in terms of lithology and structure (Fig. 5-39), by analyzing dipmeter resistivity histograms (Fig. 5-40) and the nature of the events on the curves.

◀ Fig. 5-38. - Terminal modes or electrofacies : averaged squared logs superposed on actual logs. (from Schlumberger Well Evaluation Conference, India, 1983).

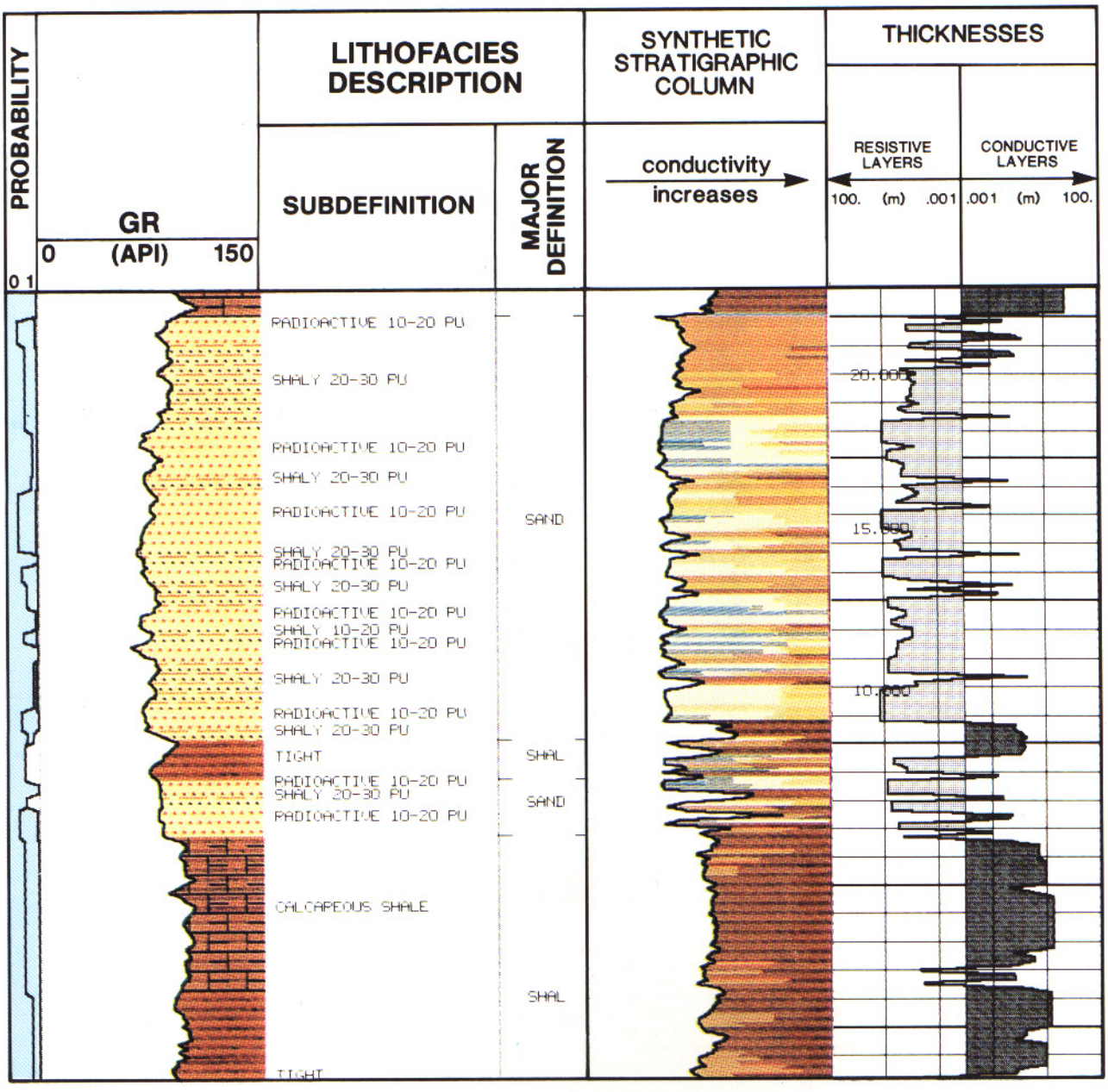

Fig. 5-39. - Example of the lithological interpretation of dipmeter resistivity curves by a combination of LITHO and SYNDIP results.

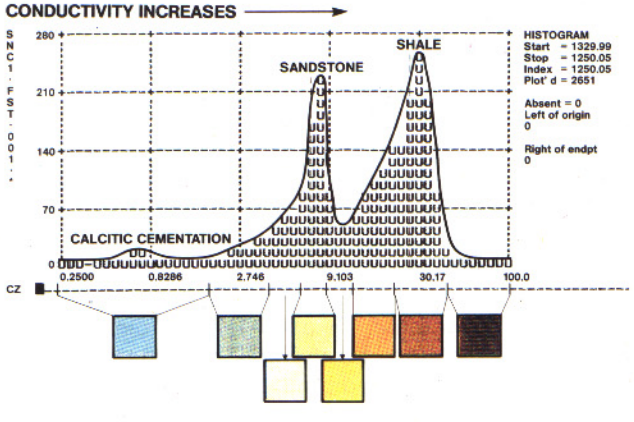

Fig. 5-40. - Example of dipmeter resistivity histogram and its conversion in lithology.

5.3.2.6. *Translation of electrofacies to facies*

An electrofacies is an abstract mathematical concept that needs to be "translated" into geological words to be easily understood and used by geologist. Even if the two approachs are very similar, they differ in language : a set of words and qualitative adjectives for the description of the facies by a geologist, a set of log parameters for characterizing an electrofacies by a log analyst. To pass from one language to the other it is necessary to "bring together the two vocabularies". The most accurate method is to put alongside each other, at the same scale, the two types of analysis, and to attach to each electrofacies the descriptive terms used by the geologist to describe facies.

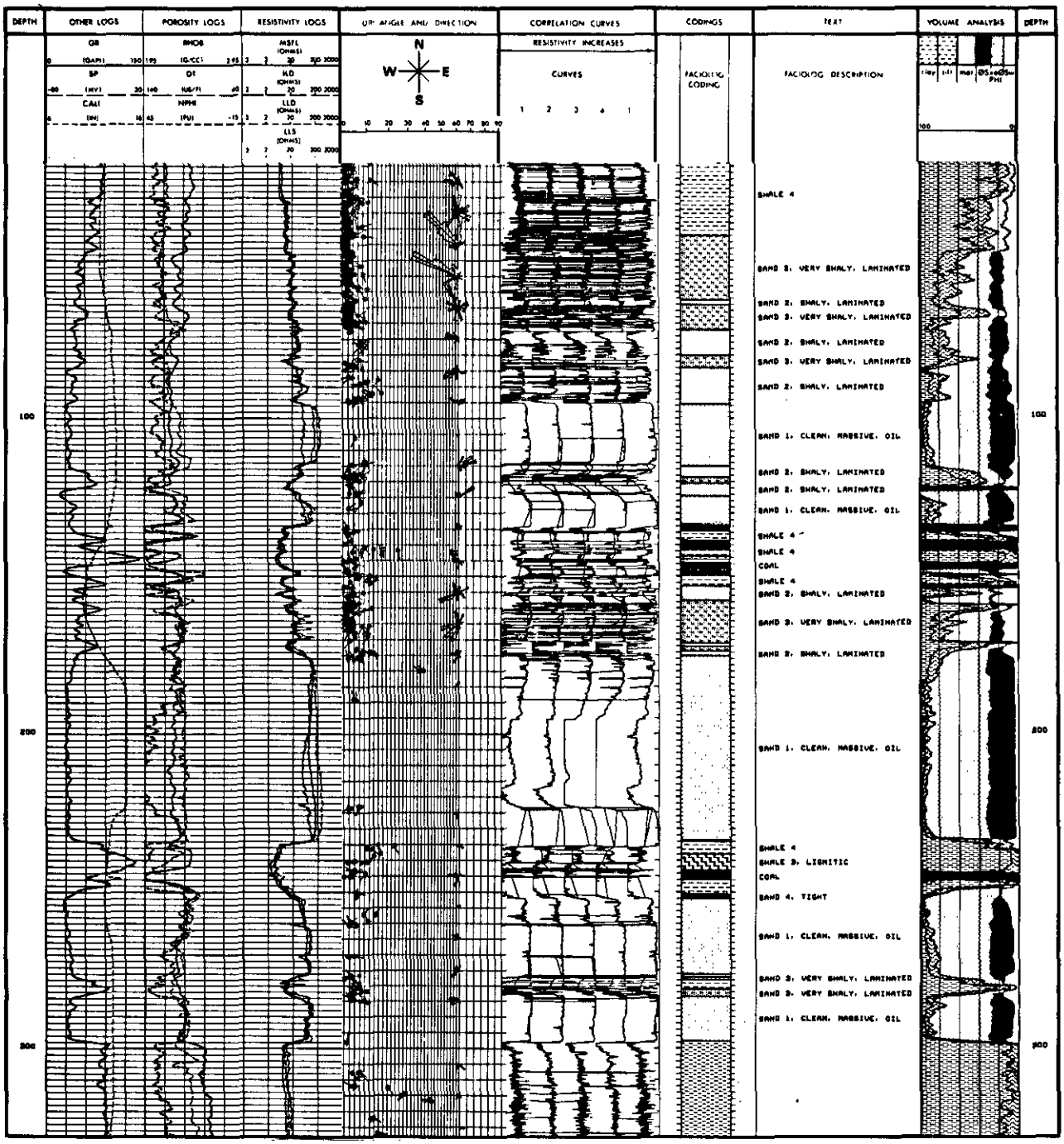

Fig. 5-41. - Composite display of open-hole logs, GEODIP results, FACIOLOG results and GLOBAL results

Attach to the set of log values which characterize an electrofacies (ρ_b, ϕ_N, Δt, GR ...), the set of words and adjectives describing the composition, the texture and the structure of the corresponding bed (e.g. micaceous well sorted sandstone with calcareous cement, cross-bedded, having a porosity between 18 and 23 % , water saturated).

Sometimes the logs recognize an electrofacies that a first core analysis has not differentiated. In this case, if it is not linked to a fluid change, it is better to review and re-analyze the core in a more elaborate manner, and try to explain the origin of this electrofacies (i.e. presence of heavy radioactive minerals, of uranium linked to phosphates or organic matter ...).

If the interval was not cored, we will try to translate the electrofacies into facies using interpretation techniques. To achieve this objective the lithology must first be defined, and the features, extracted from the dipmeter analysis, must be converted into qualifying adjectives.

The conversion of open-hole log responses to

lithology is obtained by crossplot analysis or by using an automatic program based on the construction of a lithofacies data base which itself is done by combining multi crossplot analysis and conversion of the composition of rock lithofacies into log responses. This last program is LITHO and has been described in Chapter 2.

The conversion of the dipmeter data in textural and structural information is explained in Chapter 4 and can be achieved with the SYNDIP program described in the same chapter.

5.3.2.7. *Result presentation*

The presentation of the results of the interpretation by the FACIOLOG program must include the original logs, the dipmeter results provided by a processing of the HDT or SHDT data using GEODIP or LOCDIP programs, and if possible the lithological column obtained from LITHO, as well as a display of the SYNDIP results (Fig. 5-41). Hence, we have the means of verifying the quality of the electrofacies analysis. We may also add the results of a quantitative interpretation provided by the GLOBAL program. It is also possible to superpose on the raw logs the zoning derived from the electrofacies analysis.

5.4. SEQUENCE ANALYSIS FROM WIRELINE LOGS

It consists of analysing, on the one hand, the type of transition from one electrofacies to another (gradational or abrupt contact), and on the other, the arrangement of electrofacies in vertical sequences, at different scales (elementary, meso-and mega-sequences).

5.4.1. Gradational Transition : Elementary Sequence

A gradational transition corresponds to a ramp or an elementary electrosequence, simultaneously detectable on one, two or several curves : most often gamma ray, spontaneous potential, resistivity, but sometimes sonic, density and neutron.

Remark :

It is necessary to remember that a ramp on resistivity curves may correspond to a transition from water-bearing to hydrocarbon-bearing reservoir, and thus may indicate a progressive change in saturation. A look at other logs, less, or not, sensitive to fluids (particularly gamma ray) distinguishes this case from that of a sedimentary sequence.

When the sedimentary sequence is not very thick (few centimetres or decimetres), it is not detectable on macrodevices. In this case the electrosequences often appear more clearly on dipmeter resistivity curves (Fig. 5-8 and 5-9).

It may happen that, following the vertical evolution of thicknesses of each elementary sequence, the macrodevices give a hypothesis for the sequential evolution that does not agree with that given by the dipmeter resistivity curve evolution (Fig. 5-42). In this case, only the data derived from dipmeter is valid.

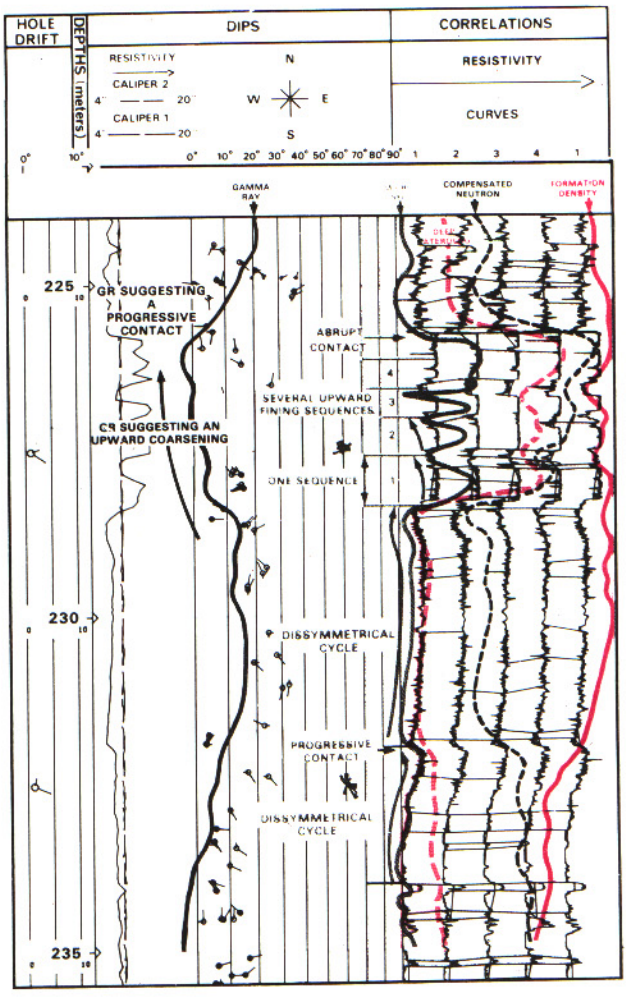

Fig. 5-42. - Example of dipmeter resistivity evolution suggesting thin fining upward sequences contradicting the evolution suggested by the gamma ray log (from Serra, in Schlumberger Well Evaluation Conference, Algeria, 1979).

Remark :

Once more, we must be careful in the interpretation of curve evolution in the case of deviated wells. In fact, some sequences are purely artificial and simply due to the influence of surrounding layers which, because of the apparent low dip between the axis of the hole and the beds, are situated behind the bed immediately in front of the measuring devices (Fig. 5-43).

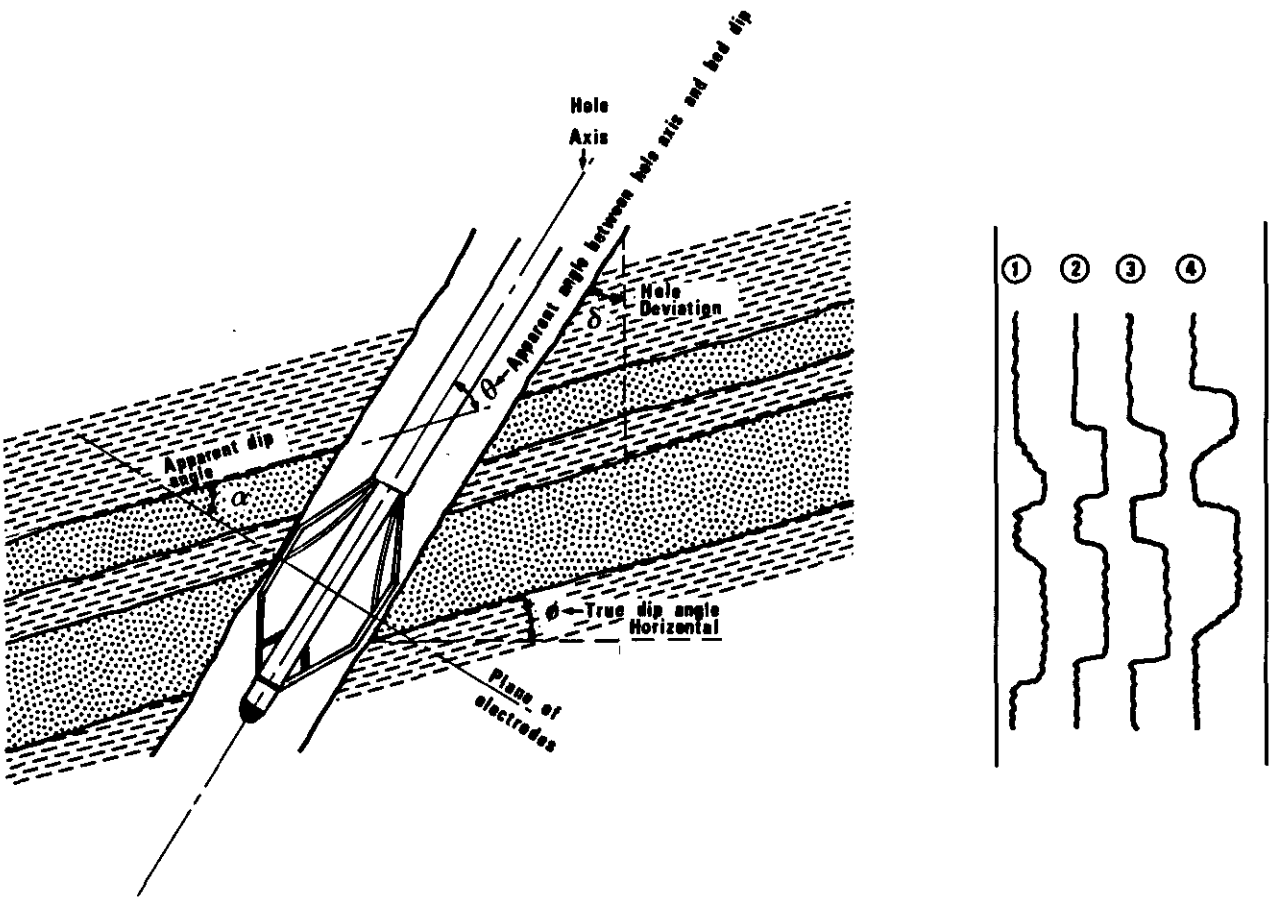

Fig. 5-43. - Scheme explaining the different evolutions observed on dipmeter resistivity curves, related to the apparent low angle between the axis of the hole and the beds.

In a terrigenous detrital series, the elementary electrosequences (cf. Fig. 5-8) indicate evolution both in grain size and in lithology : normal graded bedding (fining upward) or reverse graded bedding (coarsening upward).

In a carbonate series, an elementary electrosequence more often indicates a change in lithology (enrichment in shale or in dolomite), a diagenetic influence, or, sometimes, a textural evolution (transition from grainstone or packstone to wackstone or mudstone Fig. 5-44).

5.4.2. Abrupt Contact

It corresponds to an abrupt and significant change of reading observed at the same depth on one, and more generally, on several logs simultaneously. Its interpretation needs the study of the relationship between electrofacies. From that analysis one should be able either to determine sequences of electrofacies, or the significance of this change : transition from one term of the sequence to the following one, or break in the sedimentological sequence, or fault, unconformity ... For instance, if the abrupt change corresponds to the transition from anhydrite to halite, it only reflects a natural evolution inside the evaporitic sequence from a less to a more resticted environment.

Inversely, the abrupt change from a shale to a sand, or from a sand to a limestone, may indicate a fundamental change in depositional sequence. It marks the beginning of a new cycle of sedimentation, after a break or an erosion even if it does not correspond on the dipmeter to a non planar surface (wavy symbol on LOCDIP display, 4 dip computation on GEODIP display).

Finally, an abrupt change may be linked to a fault or to an unconformity that brings into contact two rocks having different properties. The interpretation of the dipmeter generally allows recognition of these phenomena (see Chapter 13 and 14), and hence determination of the origin of this abrupt change.

5.4.3. Sequences of Electrofacies

The electrofacies, as well as the facies, do not superpose each another randomly, except if there are tectonic accidents, unconformities, erosion, or periods of non deposition.

As we have seen previously some crossplots indicate directly these sequences of electrofacies. Rider & Laurier (1979) used this technique to

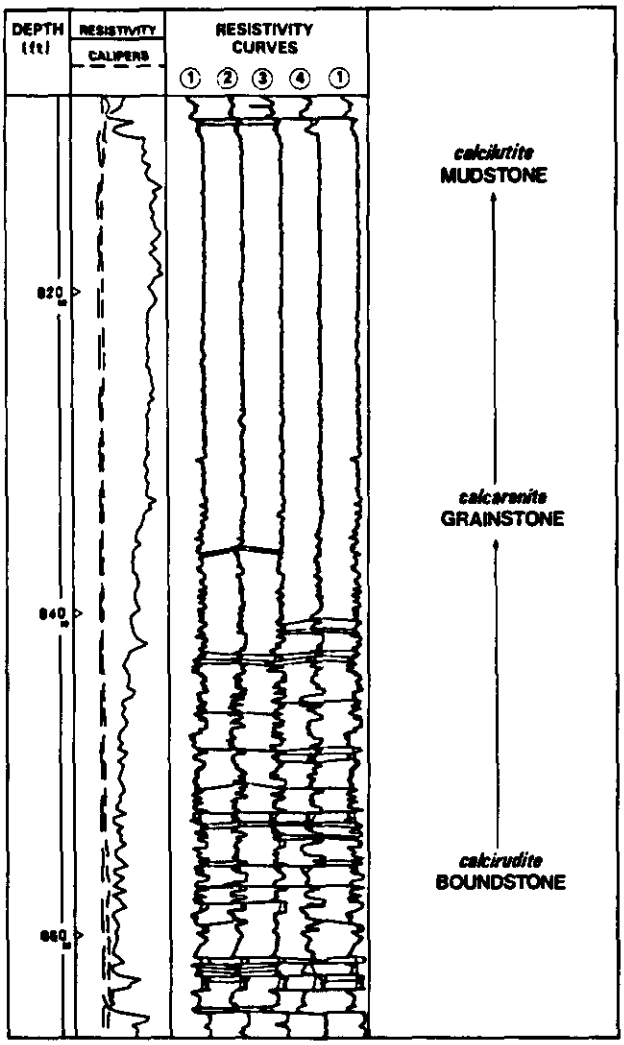

Fig. 5-44. - Example of textural evolution in a limestone. Observe the general trend on the averaged resistivity curve on the leftside.

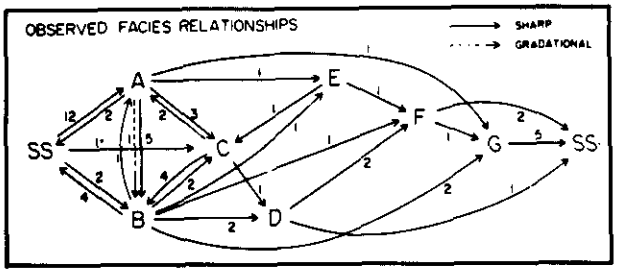

Fig. 5-45. - Example of a Facies Relationship Diagram, showing the observed number of sharp and gradational transitions between facies (from Walker, 1979). SS = scoured surface; A = poorly defined trough cross-bedding; B = well defined cross-bedding; C = large planar tabular cross-bedding; D = small-scale planar tabular cross-bedding; E = isolated scours; F = trough cross laminated fine sandstones and shales; G = low angle stratification.

Table 5-7
Observed minus random transition probabilities for well of Fig. 5-37
(from Serra, in Schlumberger Well Evaluation Conference, India, 1983).

FACIES	1	2	3	4	5	6	7
1	***	18	39	-20	-2	-18	-15
2	-8	***	-19	-19	-20	-17	85
3	-1	-1	***	9	0	3	-9
4	-9	-1	-23	***	16	11	7
5	15	-2	26	-15	***	-13	-9
6	-9	-1	-13	4	11	***	9
7	-9	-1	0	22	-24	12	***
(COUNT)	5	1	12	12	13	11	9

characterize deltaic sequences. They give the log responses for an ideal sedimentary cycle (Fig. 5-11) that consists of a progradation from shale to sand, with occasional coal deposits. Their method uses the location of each facies on crossplots (Fig. 5-10).

But, undoubtedly the best and most accurate method will be the analysis of their arrangement by probability methods. Once the electrofacies have been defined, a study of their vertical organisation can be made following a method proposed by de Raaf *et al.* (1965). Applying a procedure suggested by Selley (1970), the succession of electrofacies has been represented in a diagram resembling a spider's web. An example of what is now referred to as a "Facies Relationship Diagram" (FRD) is given in Fig. 5-45. In this diagram, the probability of transition from one facies to another, as observed in the well, is shown by numbered arrows.

In order to construct a FRD, a computer program tabulates a difference matrix (observed minus random transition probabilities) as shown in Table 5-7. The observed transition probability is the number of observed transitions in the well from one electrofacies to another converted to probabilities. The random transition probability is obtained on the assumption that all facies transitions are random, and depends only on the absolute abundance of the various electrofacies. The difference between the two probabilities gives the difference matrix. It is to be noted that some values are high-positive (transitions much more common than if electrofacies were random) and some are high-negative (transition much less common than random). The last row gives the total number of occurrences of a particular facies (e.g. facies H is observed only once).

Remark :

Walker (1984) mentionned that this method is statistically incorrect. He suggests using a more complex methods of Markov chain analysis.

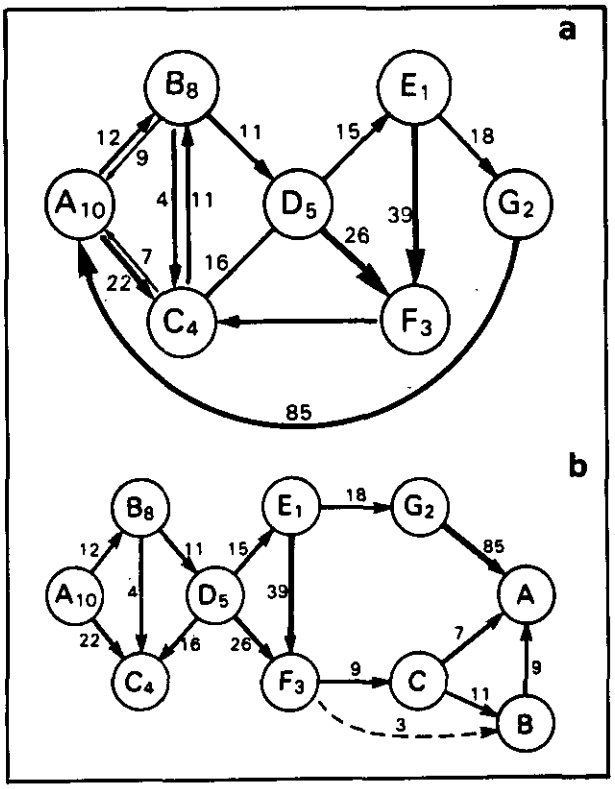

Fig. 5-46. - Spider's web diagram for well of Fig. 5-37 representing the facies relationship as obtained from data of Table 5-7, and its FRD interpretation (from Serra, in Schlumberger Well Evaluation Conference, India, 1983).

The interpretation of the FRD suggests a cycle of deposition as represented by Fig. 5-46.

5.5. APPLICATIONS OF FACIES AND SEQUENCE ANALYSES

Facies and sequence analysis is a fundamental step of the geological study of a formation. So, it is normal that its applications cover a certain number of fields related to sedimentology, and the quantitative interpretation of reservoirs.

5.5.1. Reconstitution of the Depositional Environment

As it was pointed out by Middleton (1978), the final goal of facies and sequence analysis is the reconstitution of the depositional environment. But, Walker (1979) stated "many, if not most, facies defined in the field have ambiguous interpretations - a cross-bedded sandstone facies, for example, could be formed in a meandering or braided river, a tidal channel, an offshore area dominated by alongshore currents, or on an open shelf dominated by tidal currents". In such cases, "the key to interpretation is to analyze all of the facies communally, in context. The sequence in which they occur thus contributes as much information as the facies themselves". Finally, the sequence will usually allow recognition of the depositional environment.

In the same way, we can only reconstruct the depositional environment, from logs, by replacing the electrofacies both in vertical and lateral electrosequences. This is why we cannot be solely interested in the electrofacies of sand bodies. In fact, when we analyze the shape of the SP curve we make this kind of interpretation unconsciously. The "bell" and "funnel" shapes corresponding to electrosequences as previously noted. But, still we cannot be conclusive, because such sequential evolution can belong to several environments. The choice between the several hypotheses will be done by taking into account other information related to the thickness of each electrofacies and electrosequence, and its evolution with depth and in space through well to well correlations.

Considering the importance of this application the following chapter is completely devoted to this topic.

5.5.2. Reconstruction of the Geometry of the Facies

After an electrofacies and electrosequence analysis for each well of a field, or possibly of a permit or even a basin, we can, through the correlations of electrofacies jointly with chronostratigraphic correlations between wells, reconstitute the space-time distribution of the different electrofacies. The application of mapping techniques will define the geometry of each facies or group of facies (see Fig. 5-4 and 5-5). This question will be discussed later in Chapter 15 devoted to the study of several wells.

5.5.3. Mapping of Electrofacies

As seen previously, SP and resistivity curves can be used for mapping purposes, to define the spatial repartition of typical facies. This helps to better define the environment (see Fig. 5-3). We can generalise this application by the realization of isopach or percentage maps of one typical electrofacies or group of electrofacies. One can also generate maps of sand-shale ratios computed from FACIOLOG, LITHO or SYNDIP. For instance, the ratio of the cumulative thickness of resistivity peaks to the cumulative thickness of conductive troughs computed in a given interval, leads to an accurate sand-shale ratio map if the peaks correspond to sand beds and the troughs to shale beds. These maps describe objectively, precisely and quantitatively, the lateral evolution of the facies. This type of application will be developed in the Chapter 15.

5.5.4. Constitution of a Data base of Electrofacies

By combining the results of electrofacies analysis processed on several wells of a field or a basin, we can constitute an electrofacies data base which can be used as reference for the study of any new wells in the field or the basin. Each set of log data will be cross checked with this data base for attribution. If not attributed a new electrofacies must be introduced into the data base for its completeness.

By applying methods suggested by Walker (1979), the analysis or the "distillation" of the electrofacies and electrosequences, belonging to the same depositional environment will allow the extraction of the logging responses and features which characterize a depositional environment. Thus, we can constitute an equivalent of what Walker (1979) calls a *facies model* which will "act as :

- a *norm* to which each new example will be compared;
- a *framework* and a *guide* for future observations;
- a *predictor* in new geological situations;
- an integrated *basis for interpretation* of the environment or system that it represents."

This application is very important. It will later enable definition of the depositional environment directly from wireline logs using programs involving "expert systems". This will be developed in the following chapter.

5.5.5. Quantitative Interpretation

The electrofacies analysis leading to a reconstitution of facies and depositional environment, we are able to attribute to each electrofacies, or group of electrofacies, the most probable mineralogical model for quantitative interpretation (i.e. quartz, potassium feldspar, plagioclase, kaolinite as principal minerals entering into the composition of a sand). This limits the number of unknowns for each electrofacies and optimises the interpretation by a GLOBAL * or ELAN * type program as suggested by Suau *et al.* (1982).

Moreover, the texture and the sedimentary structure indicated by dipmeters or Formation MicroScanner images enable definition of the types of distribution of shales and, consequently, a better choice of the response equations (for the computation of shaliness and saturation), and the parameters a, m and n that relate porosity to the formation factor and saturation (textural and structural models, see Chapter 9).

* Mark of Schlumberger.

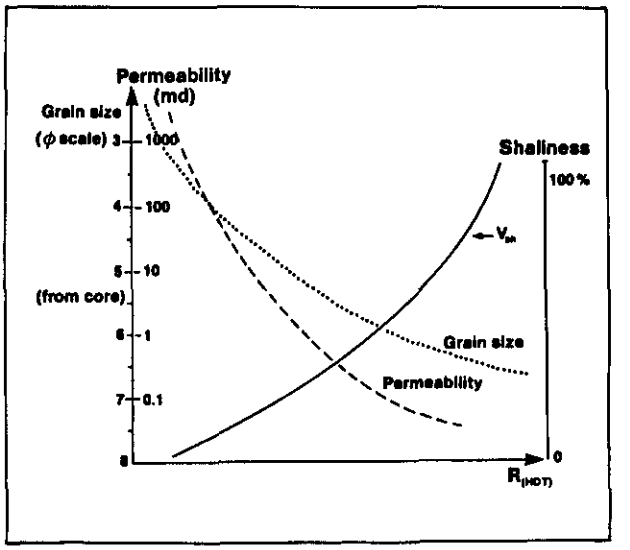

Fig. 5-47. - Calibration of the dipmeter resistivity curve in terms of grain size, shaliness and permeability.

One can also better specify the constraints and determine for each electrofacies the functions that permit an approach to permeability. Finally, one can reduce the computation time and thus carry out a higher number of tests by working with local modes or electrofacies instead of level by level. All these aspects will be developed in Chapter 9.

5.5.6. Choice of a More Judicious Core Sampling for Analysis

This aspect is often neglected. In bringing together the cores and the results of electrofacies analysis, or at least the open-hole logs and more precisely the dipmeters and FMS images, we are able to select in a more reasonable manner the sampling intervals and rates for detailed laboratory analysis. This way to sample allows both a saving on expense and time, and a clarification of certain lo gresponses not clearly understood and interpreted.

Thus, if we refer to the example of Fig. 5-8, if the sampling and the analysis were concentrated on one, two or even three electrosequences with a sampling interval of 5 cm, we should be able to calibrate the dipmeter resistivity curves (Fig. 5-47) in terms of grain size, shaliness and permeability. We should also be able to precise the facies and the depositional environment (turbidite). In this way, all uncored intervals, and even all the wells of the same field, representing the same characteristics, would be easily, rapidly and economically interpreted.

5.6. REFERENCES

BLATT, H., MIDDLETON, G. & MURRAY, R. (1972, 1980). - Origin of Sedimentary Rocks. 1st and 2nd ed. *Prentice-Hall Inc., Englewood Cliffs, New Jersey.*

BOUMA, A.H. & BROUWER, A. (eds) (1964). -Turbidites. *Elsevier, Amsterdam.*

CURRY, W.H. & CURRY, W.H. III (1972). - South Glenrock Oilfield, Wyoming : Prediscovery, Thinking and Post-Discovery Description. *In Stratigraphic Oil and Gas Fields - Classification, Exploration Methods, and Case Histories, Amer. Assoc. Petroleum Geol., Memoir* **16**, *p. 415-427.*

DELFINER, P., PEYRET, O. & SERRA, O. (1984). -Automatic determination of Lithology from Well Logs. *59th Ann. Techn. Conf. SPE of AIME, Houston, Texas; paper nº SPE 13290.*

DELHOMME, J.P. & SERRA, O. (1984). - Dipmeter-derived Logs for Sedimentological Analysis. *SPWLA, 9th Europ. Intern. Format. Eval. Trans., paper 50.*

FISCHER, A.G. (1964). - The Lofer cyclothems of the Alpine Triassic. *In : Symposium on Cyclic Sedimentation (Ed. by MERRIAM, D.F.), p. 107-149. Bull. geol. Surv. Kansas,* **169**.

FISHER, W.L. (1969). - Facies characterization of Gulf Coast basin delta systems, with some Holocene analogues. *Gulf Coast Assoc. Geol. Soc. Trans.,* **19**, *p. 239-261.*

FISHER, W.L. & McGOWEN, J.H. (1969). - Depositional systems in Wilcox Group (Eocene) of Texas and their Relation to Occurrence of Oil and Gas. *Bull. Amer. Assoc. Petroleum Geol.,* **53**, *p. 30-54.*

FISHER, W.L. & BROWN, L.F. Jr. (1972). - Clastic depositional systems -A genetic approach to facies analysis. *University of Texas, Austin, Texas Bureau of Econ. Geol.*

FISHER, W.L., BROWN, L.F., SCOTT, A.J. & McGOWEN, J.H. (1969). -Delta systems in the exploration for oil and gas. - A research colloquium *University of Texas, Austin, Texas Bureau of Econ. Geol.*

FONS, L. Sr. (1969). - Geological application of well logs. *SPWLA, 10th Ann. Log. Symp. Trans.*

GALLOWAY, W.E. & HOBDAY, D.K. (1983). -Terrigenous Clastic Depositional Systems. *Springer, New York.*

GILREATH, J.A. & STEPHENS, R.W. (1971). -Distributary Front Deposits Interpreted from Dipmeter Patterns. *Gulf Coast Assoc. Geol. Soc. Trans.,* **21**, *p. 233-243.*

GILREATH, J.A. & STEPHENS, R.W. (1975). -Interpretation of Log Responses in a Deltaic Environment. *Amer. Assoc. Petroleum Geol. Marine Geology Workshop, Dallas, Texas.*

GOETZ, J.I., PRINS, W.J. & LOGAR, J.F. (1977). -Reservoir Delineation by Wireline Techniques. *paper presented at 6th Ann. Conv. Indonesia Petroleum Assoc., Jakarta, May 1977.*

GRESSLY, A (1838). - Observations géologiques sur le Jura Soleurois. *Neue Denkschr. allg. Schweiz. Ges. ges. Naturw.,* **2**, *p. 1-112.*

HAUG, E. (1907). - Traité de géologie. *Armand Colin, Paris.*

KRUMBEIN, W.C. & SLOSS, L.L. (1963). - Stratigraphy and Sedimentation. 2nd ed.*W.H. Freeman & Co., San Francisco.*

LENNON, R.B. (1976). - Geological factors in steam-soak projects on the west side of the San Joaquin Basin. *J. Petroleum Technol., July, p. 741-748.*

LOMBARD, A. (1956). - Géologie Sédimentaire. Les séries marines. *Masson, Paris.*

LOMBARD, A. (1972). - Séries sédimentaires. Genèse - Evolution. *Masson, Paris.*

MIALL, A.D. (1984). - Principles of Sedimentary Basin Analysis. *Springer, New York.*

MIDDLETON, G.V. (1973). - Johannes Walther's Law of the correlation of facies. *Geol. Soc. America Bull.,* **84**, *p. 979-988.*

MIDDLETON, G.V. (1978). - Facies. In : *FAIRBRIDGE, R.W., & BOURGEOIS, J., eds. Encyclopedia of sedimentology. Stroudsburg, Pa., Dowden, Hutchinson & Ross, p. 323-325.*

MOORE, R.C. (1949). - Meaning of facies. *Geol. Soc. Amer., Mem.* **39**, *p. 1-34.*

NORWOOD, E.M. Jr., & HOLLAND, D.S. (1974). -Lithofacies mapping. A descriptive tool for ancient delta systems of the Louisiana outer continental shelf. *Trans. Gulf Coast Assoc. Geol. Soc.,* **24**.

PIRSON, S.J. (1977). - Geologic Well Log Analysis. 2nd ed. *Gulf Publishing Co., Houston.*

RAAF, J.F.M. de (1968). - Turbidites et associations sédimentaires apparentées, I and II. *Kon. Ned. Akad. Wetensch., Amsterdam, Verh., series B,* **71**, *p. 1-23.*

RAAF, J.F.M. de, READING, H.G. & WALKER, R.G. (1965). - Cyclic sedimentation in the Lower Westphalian of north Devon, England. *Sedimentology,* **4**, *p. 1-52.*

READING, H.G. (Ed.) (1978). - Sedimentary Environments and Facies. *Blackwell Scientific Publications, Oxford.*

RIDER, M.H. & LAURIER, D. (1979). - Sedimentology using a computer treatment of well logs. *SPWLA, 6th Europ. Symp. Trans., paper J.*

Schlumberger (1979). - Well Evaluation Conference. Algeria.

Schlumberger Technical Services, Inc. (1983). -Well Evaluation Conference. India.

Schlumberger Middle East S.A. (1984). - Well Evaluation Conference. Egypt.

SELLEY, R.C. (1970). - Studies of sequence in sediments using a simpl emathematical device. *J. geol. Soc. London, Quart. Jour.,* **125**, *p. 557-581.*

SELLEY, R.C. (1970, 1978). - Ancient Sedimentary Environments. 1st and 2nd ed. *Chapman & Hall, London.*

SELLEY, R.C. (1976). - An Introduction to Sedimentology. *Academic Press, London.*

SELLEY, R.C. (1978). - Concepts and methods of subsurface facies analysis. *Amer. Assoc. Petroleum Geol., Continuing Education Course Note Series* **9**.

SELLEY, R.C. (1979). - Dipmeter and log motifs in North Sea submarine-fan sands. *Bull. Amer. Assoc. Petroleum Geol.,* **63**, *6, p. 905-917.*

SERRA, O. (1972). - Diagraphies & Stratigraphie. In : *Mém. B.R.G.M.,* **77**, *p. 775-832.*

SERRA, O. (1973). - Interprétation Géologique des diagraphies en Séries Carbonatées. *Bull. Centre Rech. Pau - SNPA,* **7** *, 1, p. 265-284.*

SERRA, O. (1974). - Interprétation géologique des Séries deltaï ques à partir des diagraphies différées. *Rev. A.F.T.P.,* **227**, *Oct., p. 9-17.*

SERRA, O. (1977). - Méthode rapide d'analyse faciologique par diagraphies différées. *SPWLA, 5th Europ. Symp. Trans., Paris, paper 9.*

SERRA, O. (1984). - Fundamentals of Well-Log Interpretation. Volume 1 : The Acquisition of Logging Data. *Developments in Petroleum Science,* **15A**, *440 p., Elsevier, Amsterdam.*

SERRA, O. & ABBOTT, H. (1980). - The Contribution of Logging data to Sedimentology and Stratigraphy. *55th Ann. Fall Techn. conf. SPE of AIME, paper SPE 9270, and in SPE J., Feb. 1982.*

SERRA, O. & SULPICE, L. (1975). - Sedimentological Analysis of shale-sand series from well logs. *SPWLA, 16th Ann. Log. Symp. Trans., paper W.*

SERRA, O. & SULPICE, L. (1975). - Apports des diagraphies différées aux études sédimentologiques des séries argilo-sableuses traversées en sondage. *9th Cong. Intern. Sédiment., Nice, thème 3, p. 86-95.*

SHROCK, R.R. (1948). - Sequence in Layered Rocks. *McGraw-Hill Book Co., Inc., New York.*

TEICHERT, C. (1958). - Concepts of facies. *Bull amer. Assoc. Petroleum Geol.,* **42**, *p. 2718-2744.*

VINCENT, P., GARTNER, J. & ATTALI, G. (1979). -GEODIP - An approach to detailed dip determination using correlation by pattern recognition. *J. Petroleum Technol., Feb.1979, p. 232-240.*

VISHER, G.S. (1965). - Use of vertical profile in environmental reconstruction. *Bull. Amer. Assoc. Petroleum Geol.,* **49**, *p. 41-61.*

WALKER, R.G. (1975). - Generalized facies models for resedimented conglomerates of turbidite association. *Bull. geol. Soc. Amer.,* **86**, *p. 737-748.*

WALKER, R.G. (1976). - Facies Models. Turbidites and associated coarse clastic deposits. *Geoscience Canada,* **3**, *p. 25-36.*

WALKER, R.G. (Ed.) (1979, 1984). - Facies Models. 1st and 2nd ed. *Geoscience Canada, reprint series 1, published by Geol. Assoc. Canada.*

WALKER, R.G. & MUTTI, E. (1973). - Turbidite facies and facies association. *SEPM, Pacific Section, Short Course, Anaheim.*

WALTHER, J. (1893-4). - Einleitung in die Geologie als historische Wisssenschaft. *Fischer, Jena.*

WIDDICOMBE, R.E. & NOON, P. (1984). - Multiwell FACIOLOG evaluation, Hartzog Draw Field,Powder River Basin, Wyoming. *SPWLA, 25th Ann. Log. Symp. Trans., New Orleans.*

WILLIAMS, P.F. & RUST, B.R. (1969). - The sedimentology of a braided river. *J. sediment. Petrol.,* **39**, *2, p. 649-679.*

YAPAUDJIAN, L. (1972). - Une approche actualiste en géologie sédimentaire (quelques données d'interprétation des séquences de plateforme). In : *Mém. BRGM,* **77**, *p.715-744.*

Chapter 6

INFORMATION ON DEPOSITIONAL SEDIMENTARY ENVIRONMENTS

(Formation of sedimentary rocks)

DEFINITION
REVIEW OF GENERAL CONCEPTS

An *environment* is a general term used by geomorphologists or oceanographers to characterize physiographic or morphologic units (mountain ranges, desert, deltas, continental shelves, abyssal plains ... A *sedimentary depositional environment* is *a geographically restricted part of the earth's surface, which can be easily distinguished from its adjacent areas by the complex of physical, chemical and biological conditions, influences or forces under which a sediment accumulates. This complex largely characterises the environment and determines the properties of the sediments deposited within it* (Krumbein & Sloss, 1963; Selley, 1970; Reineck & Singh, 1975; Blatt *et al.*, 1980).

The physical conditions which act on and control an environment are numerous. They include :

- the climate : the weather and its components :
  . temperature variations (diurnal, nocturnal, seasonal);
  . importance and frequency of rainfalls, snowfalls;
  . humidity;
  . wind regime (dominant direction, velocity, and their variations);
  . all these factors acting on the vegetal cover;
- the altitude and the topographic profile : nature, size, shape and slope of the mountains or of the receiving basin, the energy of the flow, the water depth, which will control the hydraulic regime; in marine environments : the bathymetry, the amplitude of the tides, the waves, the current system of the water mass, the wind regime, the Coriolis forces.

The chemical conditions which operate within an environment include the geochemistry of the rocks at the surface, and of the waters (river, lake, sea, ocean) : salinity (nature and percentage of salts in solution), *pH, Eh,* gas in solution.

The biological conditions comprise both fauna and flora, terrestrial or aquatic, and bacteria present in the environment.

These three conditions or factors are not independant but, to the contrary, are strongly linked. Any change in one of them has immediate repercussions on the others.

Following the medium (air, ice, water) and the relative importance of each condition, factor and process, an environment can be depositional, erosional or non depositional (equilibrium). As a broad generalization, subaerial environments are essentially erosional, while sub-aqueous environments are mostly depositional.

In the study of ancient deposits, because we analyze sedimentary rocks, we will always refer to *depositional environments.* However, it must be kept in mind that depositional sequences can be interrupted by periods of non deposition or even erosion, which of course have no associated sediments. It will be important to detect and localize them, both in time and space, because they will enable a better definition of the environment and the geological history of a sedimentary basin. They can also be used for correlation purposes.

The determination of the depositional environment will only be possible through the description of the imprints, or responses, that the physical, chemical, biological and geomorphological conditions characterizing the environment left in the deposit.

Those imprints define a facies which is, as previously seen, the *"sum of the physical, chemical and biological characteristics which differentiate a sedimentary body from another".*

As pointed out by Krumbein & Sloss (1963), "the study of any sedimentary environment includes

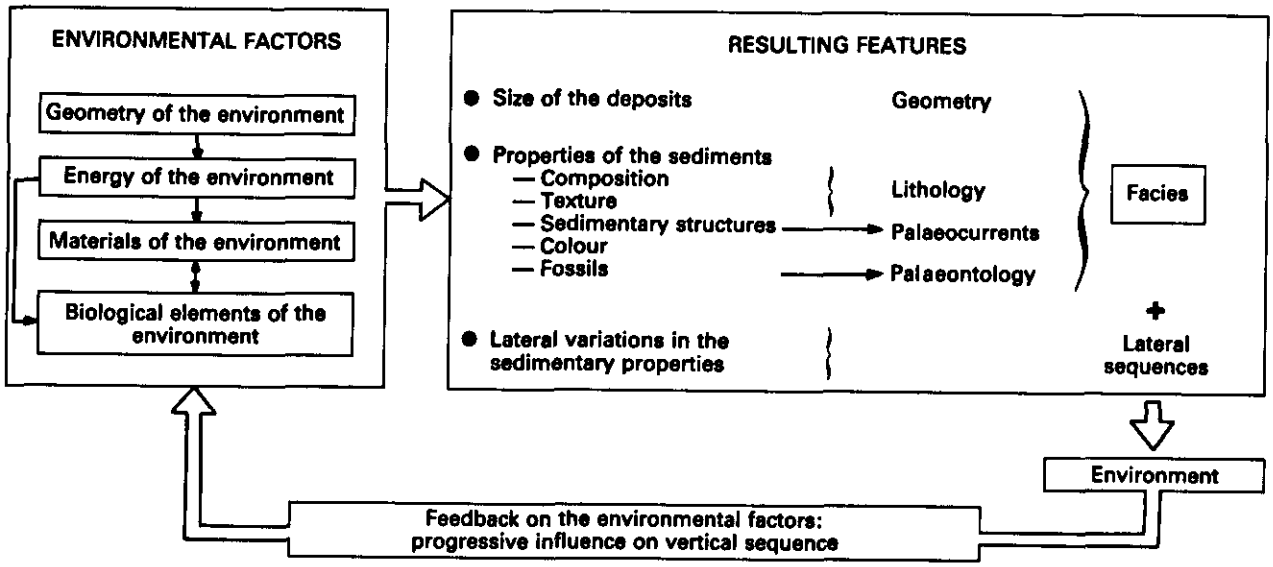

Fig. 6-1. - A generalized sedimentary environment process-response model (from Krumbein & Sloss, 1963).

considerations of the four basic *environmental elements*" listed in Fig. 6-1. To each element are attached several factors. "The relative influence of environmental elements varies with the nature of the environment. Similarly, the factors in any element vary in their importance within different environments".

The *material factors* include the medium (air, fresh or salty water, ice), the *pH*, the *Eh*, the temperature, the dissolved salts (Ca^{2+}, Na^{+}, CO_3^{2-}, SO_4^{2-}, Cl^{-}), and gases (CO_2, O_2, SH_2), and the solids. "Each of the material factors may have some effect on sediments being deposited, but the importance of the effect is controlled, in part, by factors of other elements". For instance in a high energy environment (zone of breaking waves), the solids (sand and gravel) are dominant, salts and gases have very little influence. On the contrary, in a low energy environment (quiet water), they become dominant in controlling organisms, and hence play a part in the deposition of carbonate.

"*Boundary and energy factors* include water depth, distance from shore, topography of the bottom, and, in a general way, the geography of the depositional area". The energy controls the quantity of particles in suspension, and the size of the settling grains. It also controls the current type (laminar or turbulent) and consequently the nature of sedimentary features.

The energy and material factors control, in turn, the *biological factors*. "In clear warm seas, well oxygenated and mildly alkaline, organisms may thrive and produce abundant carbonate sediment" (Krumbein & Sloss, 1963). On the contrary, turbid medium, or reducing conditions, may restrict living conditions for some organisms.

The areal variations of the elements and factors within an environment, called the *environmental pattern* by Krumbein & Sloss, (1963), induce progressive evolution of the nature and properties of the sediments creating a *lateral sequence* of facies.

But, the accumulation of sediments in an environment can modify its elements and factors sufficiently to create new conditions and consequently new properties. "This sort of interlocked relation between process and response is called *feedback*". These continuous modifications at any given geographical point contribute to create a *vertical sequence of facies*.

Consequently, an environment will be characterized by a typical sequence of facies both in space and time. Following the Walther's law[1] these sequences are similar.

So, the knowledge of the vertical sequence, which can be obtained from wireline logs, helps to predict the type of lateral sequence and the depositional environment.

By considering all the possible combinations of the physical, chemical and biological processes or all elements and factors which characterize an environment, one could guess that there should be an infinite number of environments. In fact, due to the strong interdependance of all these processes and factors, a finite number of environments has been recognized. This is also related to the fact that there are a finite number of physiographic types. It is for this reason that, even if two environments or morphologic units are never totally identical, the number of major environments is reduced if one considers the dominant

[1] Walther's Law : "The various deposits of the same facies area, and similarly, the sum of the rocks of different facies area, were formed beside each other in space, but in a crustal profile, we see them lying on top of each other. It is a basic statement of far-reaching significance that only those facies and facies area can be superimposed, primarily, that can be observed beside each other at the present time" (Blatt *et al.*, 1972 , p. 187-188).

Table 6-1
A classification of depositional sedimentary environments
(from Selley, 1970).

Continental	Fanglomerate Fluviatile Lacustrine Eolian		Braided Meandering
Shorelines	Lobate (deltaic) Linear (barrier)		Terrigenous Mixed carbonate-terrigenous
Marine	Reef Shelf Turbidite Pelagic	Terrigeneous Carbonate	Carbonate

This Table tabulates only those environments which have generated large volumes of ancient sediments.

factors. They are listed in Table 6-1. Of course, especially when we study modern deposits, several sub- or even sub-sub-environments can be added to take into account small variations. But, for the ancient sediments the separation between them is not an easy task. It is for that reason that we will limit the illustration of their recognition by wireline logs to the major environments.

INTEREST OF THE RECONSTITUTION OF THE DEPOSITIONAL ENVIRONMENT

The reconstitution of the depositional environment is not a pure academic objective. It is a necessity in the search for mineral natural resources such as hydrocarbons, coal, phosphates, potassium salts, uranium... because these resources are, most commonly, strongly associated to specific depositional environments.

In petroleum exploration, one of the essential objectives is the evaluation of the hydrocarbon potential of a basin. This requests the determination of the quality, the thickness and lateral extension (the volume) of the different facies which represent *source rocks* in which will be generated hydrocarbons, *reservoir rocks* in which hydrocarbons will accumulate by migration from the previous rocks, and *cap rocks* which will constitute impermeable traps avoiding any dismigration of the hydrocarbons from reservoirs.

In reservoir study, only the reconstitution of the depositional environment gives a correct idea of the lateral evolution of the facies and consequently of the petrophysical properties of the reservoirs, and to enable prediction of the existence, nature, importance and distribution of permeability barriers. This information is of the utmost importance to evaluate the production potential of a field and to locate extraction and injection wells for a better oil recovery.

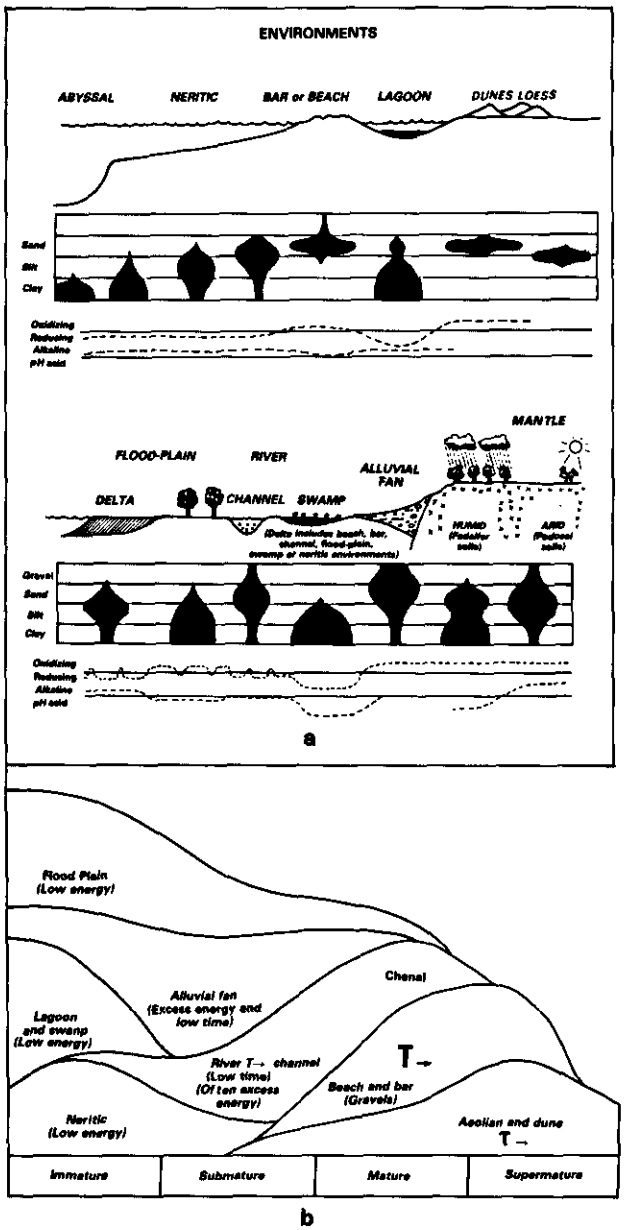

Fig. 6-2. - a) : Distribution of the grain size as a function of the environment. b) : Relationship between the textural maturity and the depositional environment.

RECOGNITION OF THE MAJOR DEPOSITIONAL ENVIRONMENTS FROM WIRELINE LOGS

In the study of ancient deposits, the traditional approach of geologists consists of analysing rock samples by defining their facies through the mineralogical, textural and structural characteristics of the rocks.

The knowledge of the lithology and the mineralogy is important, but it is necessary to control if diagenesis has modified the original rock type.

The grain size and the textural maturity can help to recognize the depositional environment as illustrated by Fig. 6-2.

As previously seen, sedimentary features constitute a fundamental information for the recognition of the facies and the environment.

But, the facies knowledge is not sufficient to identify an environment. As pointed out by Walker (1979), "a cross-bedded sandstone facies, for example, could be formed in a meandering or braided river, a tidal channel, an offshore area dominated by alongshore currents, or on an open shelf dominated by tidal currents." Additional information related to the thickness of each facies, or sequence of facies, and to its evolution with time, and consequently with depth, will often allow discrimination between two or three possible environments (Fig. 6-3).

In a multi-well study the facies and the environments will be more accurately recognized using correlation techniques (Fig. 6-4), and facies mapping (isoliths or isopachs, Fig. 6-5), the geometry of sedimentary bodies being an important parameter for facies and environment recognition. For example, the meandering channel fill system is easily recognized from the isopach map of the lower Muddy in the South Glenrock Oilfield, Wyoming (Fig. 6-5 from Curry & Curry, 1972).

Correlations (Fig. 6-6) and isopach of total sands (Fig. 6-7) in the Bisti Oilfield show the barrier bar nature of the reservoir (from Sabins, 1972).

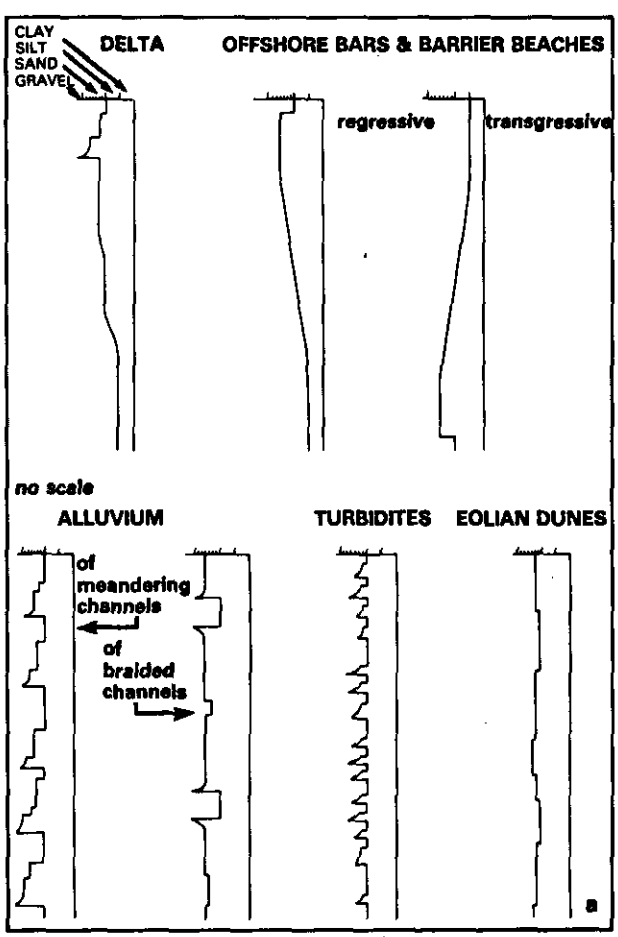

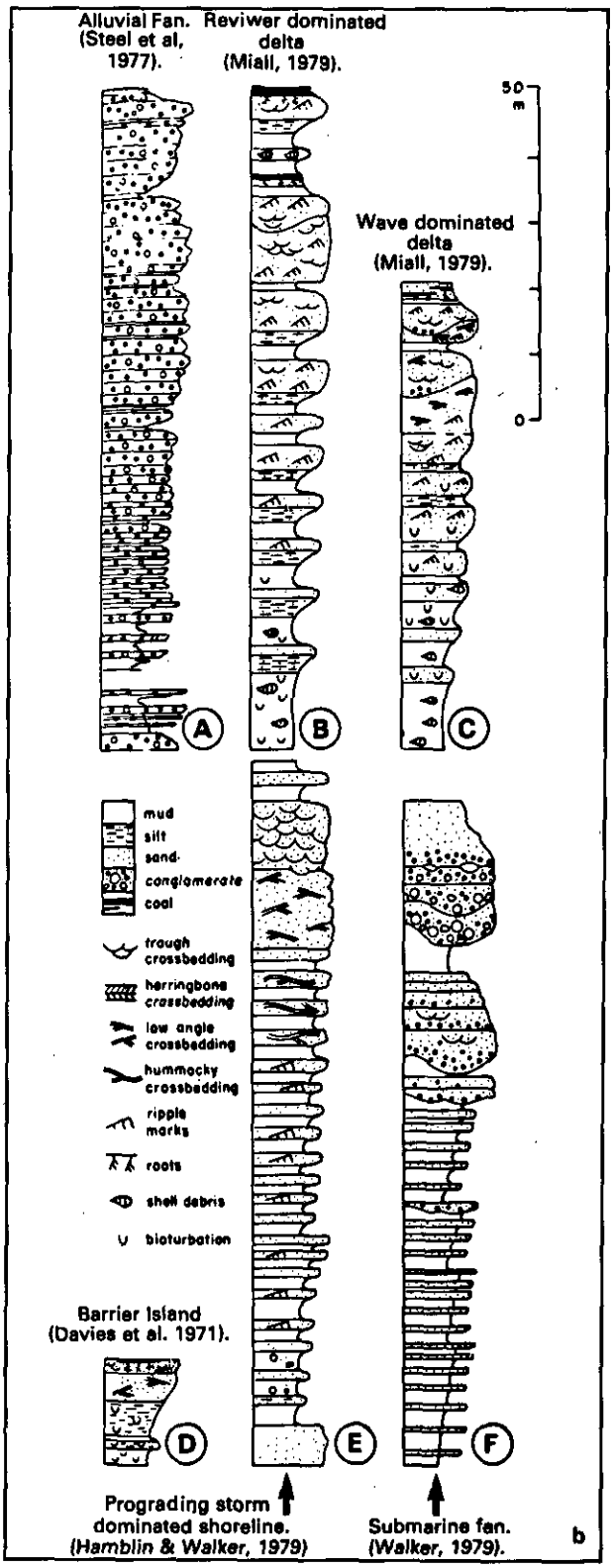

Fig. 6-3. - Typical examples of thickness and grain size evolution related to typical depositional environments. (a) : from Selley (1970); (b) : from Miall (1984).

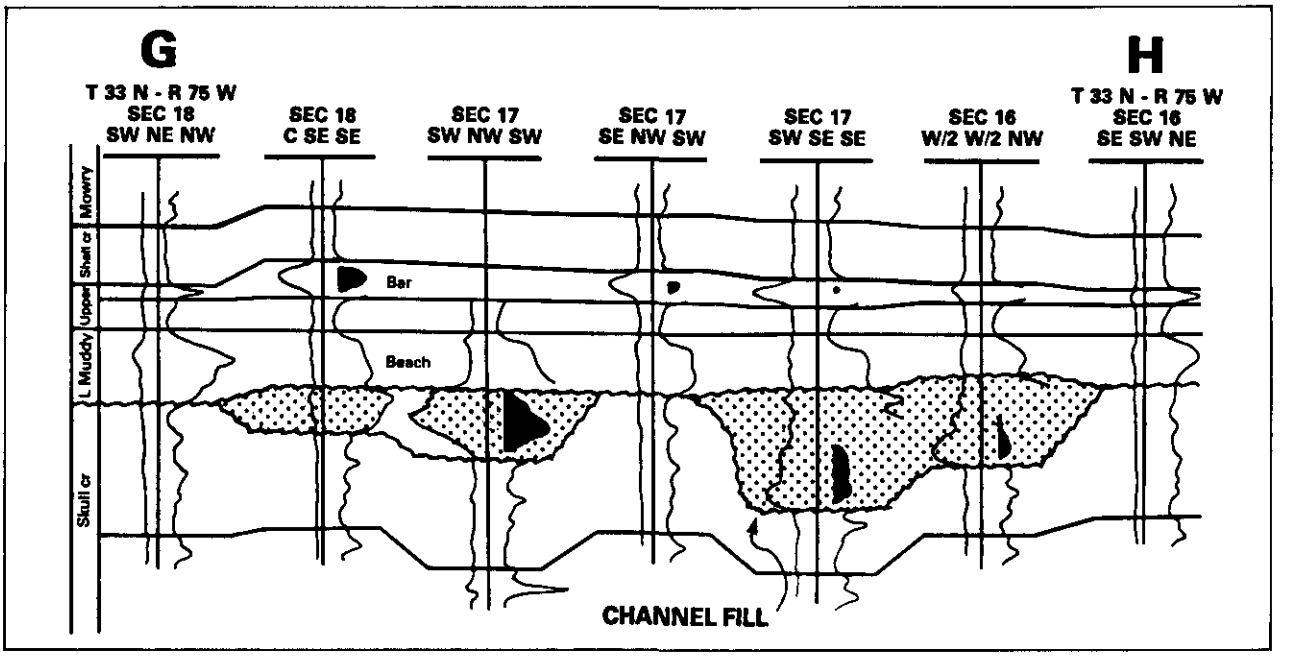

Fig. 6-4. - Log-correlations between wells in the South Glenrock Oilfield, Wyoming. Bar, beach and channel fill are easily recognized (from Curry & Curry, 1972).

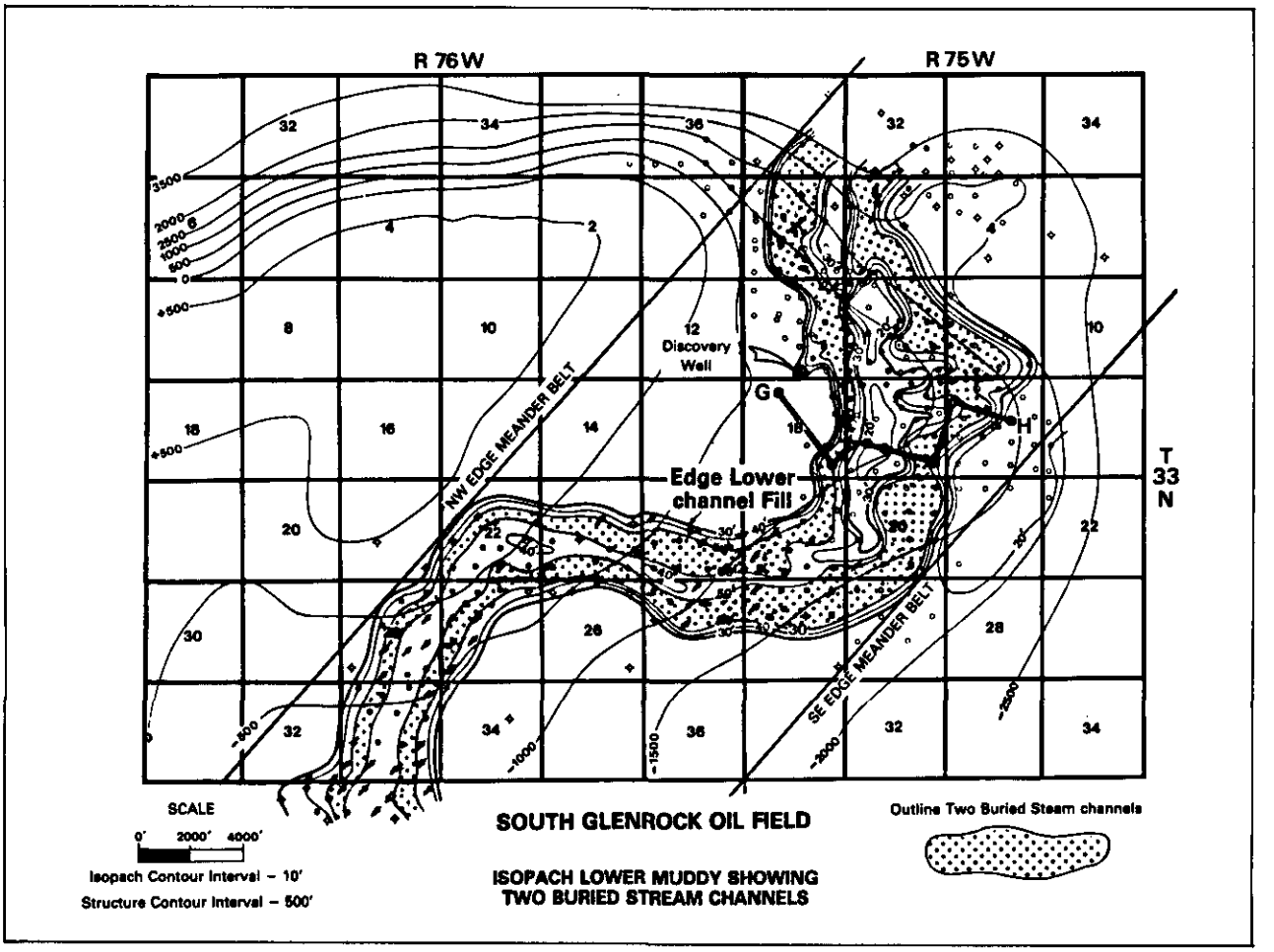

Fig. 6-5. - Isopach map of the lower Muddy showing two buried stream channels (from Curry & Curry, 1972).

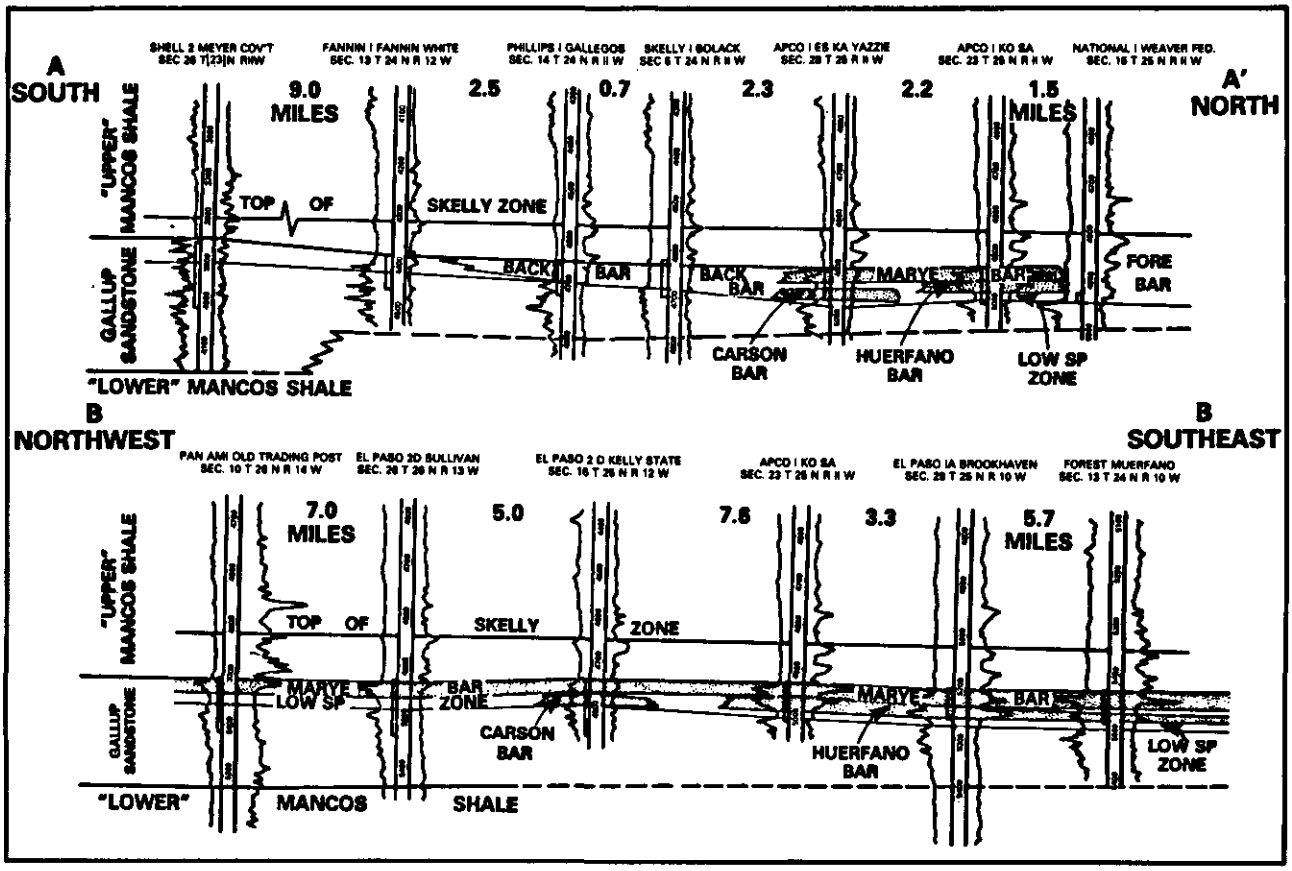

Fig. 6-6. - Log-correlations between wells in the Bisti Oilfield, New Mexico (from Sabins, 1972).

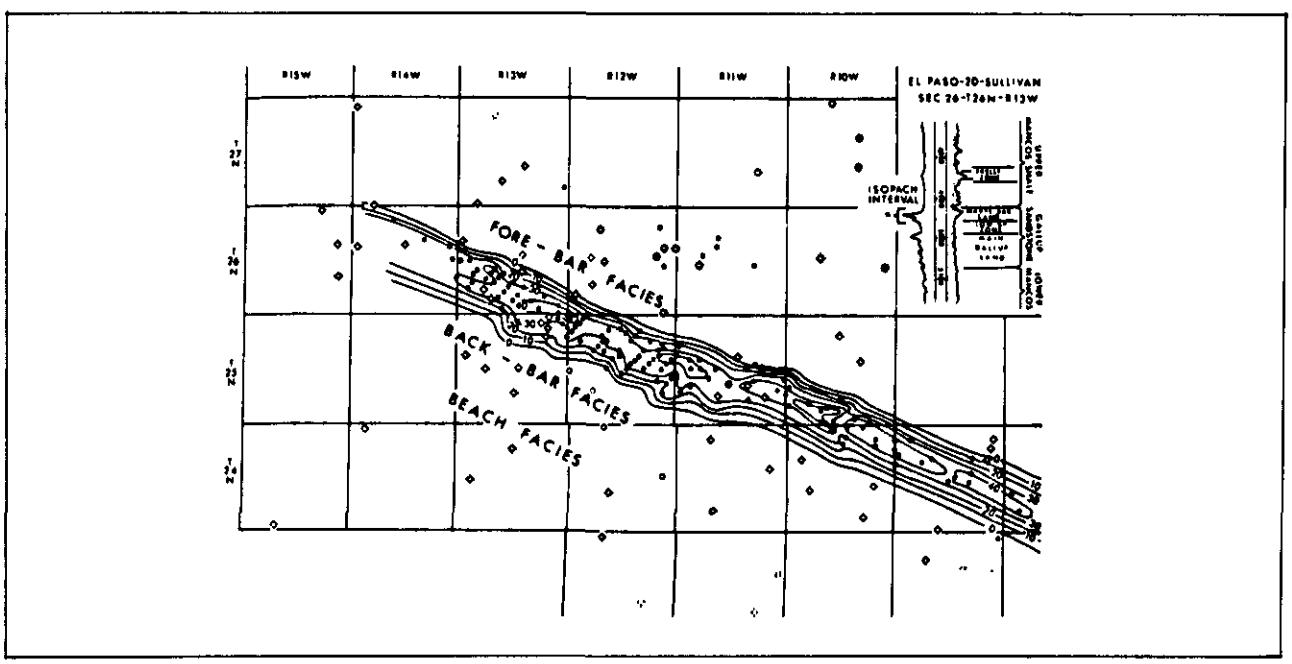

Fig. 6-7. - Isopach map of total sands in the Bisti Oilfield, New Mexico (from Sabins, 1972).

In fact, the depositional environment will be better and more accurately defined by integrating all the information on facies and sequences of facies. "The key to interpretation is to analyze all of the facies communally, in context. The sequence in which they occur thus contributes as much information as the facies themselves" (Walker, 1984).

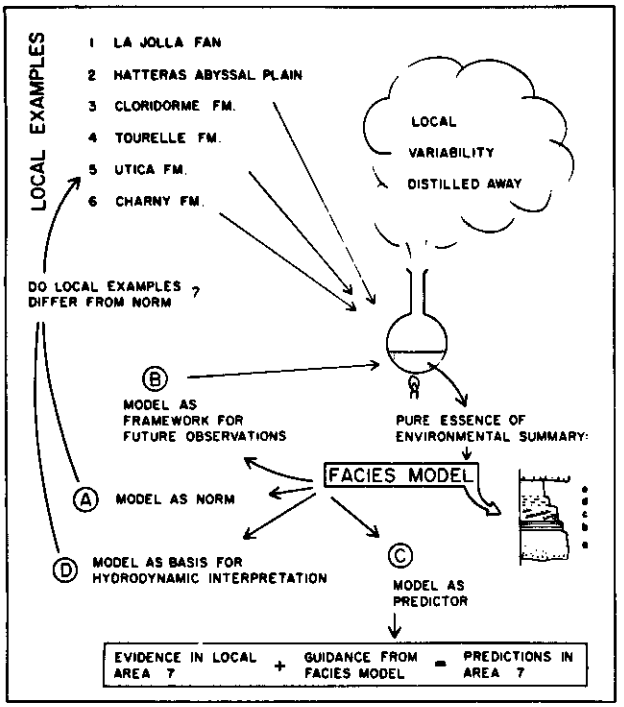

Fig. 6-8. - Distillation of a general facies model from various local examples to extract pure essence of environmental summary (from Walker, 1979).

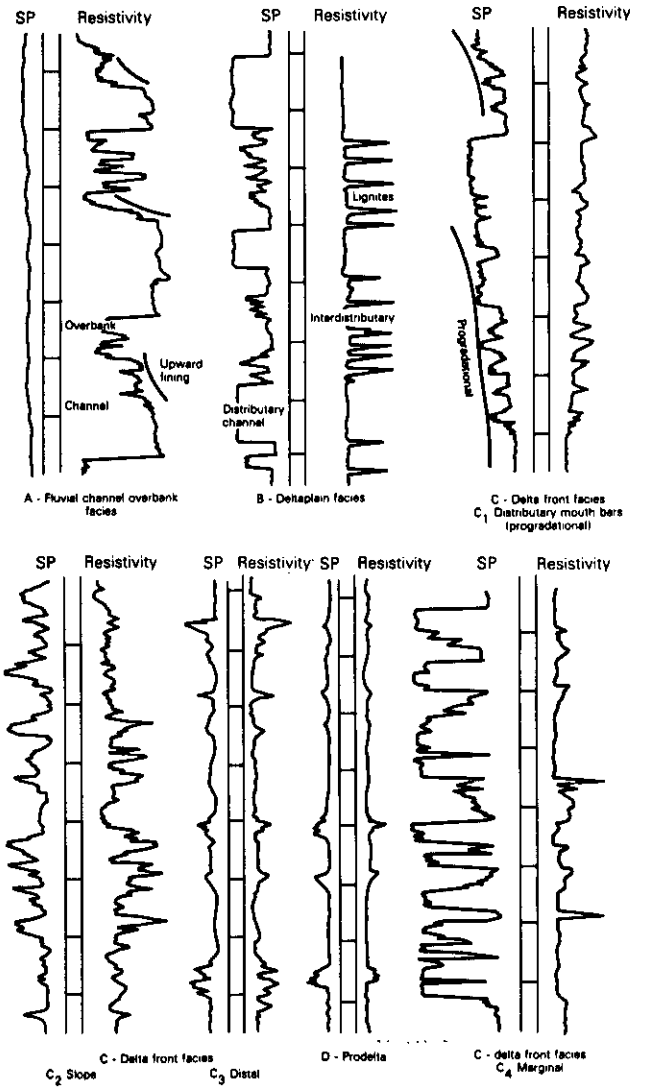

Fig. 6-9. - Examples of vertical SP and resistivity profiles in high-constructive lobate delta systems, Gulf Coast Basin (from Fisher, 1969).

These sequences can be described, as suggested by Visher (1965), by a *vertical profile*, or, in other terms introduced by Walker (1976), by a *facies model*. As illustrated by Fig. 6-8 from Walker, the facies model is obtained by "distilling and concentrating the important features that" several similar environments "have in common".

As Walker explained "a facies model could be defined as a general summary of a specific sedimentary environment, written in terms that make the summary useable in at least four different ways".

For Walker a facies model must "act as :

- a *norm*, for purpose of comparison;
- a *framework and guide* for future observations;
- a *predictor* in new geological situations;
- a *basis* for hydrodynamic interpretation of the environment or system that it represents".

In a subsurface study involving well logs, the equivalent of the facies model will be the concept of an *electrofacies model*. As seen in previous chapters, wireline logs enable determination of all the components of facies (mineralogy, texture, sedimentary features, geometry). One can also define the organisation of facies in sequences. Many authors (Fisher, Visher, Pirson, Coleman, Galloway ...) have used the SP-resistivity curve shapes to determine facies and environments. An illustration is given by the small sketches of Fig. 6-9 and 6-10 from Fisher (1969) which quickly determine the different facies and sub-environments of two delta systems.

But, as previously mentioned, SP and resistivity curves are not always sufficient to correctly determine the facies. The other logs, especially the dipmeter or FMS, bring information which help to be more accurate and precise. It is the reason why I suggest they be introduced, when available, in any sedimentological study.

ILLUSTRATION OF DEPOSITIONAL ENVIRONMENTS BY WIRELINE LOGS

In the following pages, the main geological characteristics of each major environment, on a single vertical profile, are described, through the geological facies-model concept.

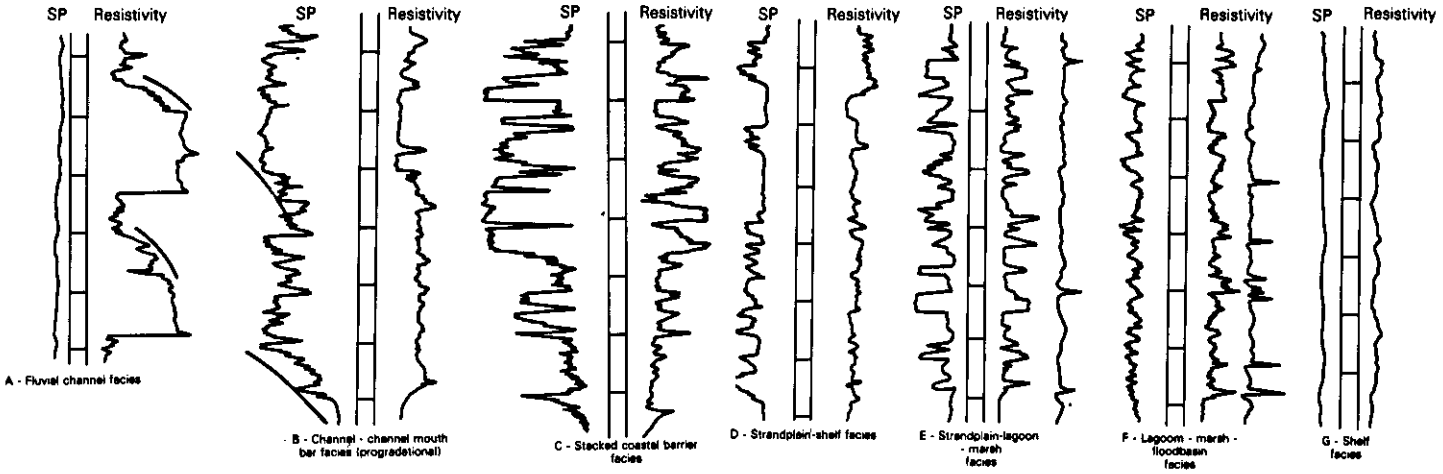

Fig. 6-10. - Examples of vertical SP and resistivity profiles in high-destructive, wave-dominated delta systems, Delta Coast Basin (from Fisher, 1969).

The geological parameters are then "translated" into well-log responses, both open-hole logs and dipmeter data, the validity of which is in turn controlled and illustrated by examples in which GEODIP or LOCDIP arrow-plots have been interpreted with the help of the other open-hole logs. In each case the most important logging features which allow their recognition are indicated. As suggested by Walker (1976), such an electrofacies model will act as a *norm* to which any actual example will be compared, and as a *guide* for future observations and enrichment of the model.

Remarks

GEODIP or LOCDIP arrow-plots have been prefered to CLUSTER or MSD and CSB displays because on a GEODIP or LOCDIP presentation one can easily control the correlations and consequently the dip validity, and one can base the interpretation on real facts and features (it is known that CLUSTER, MSD or CSB processing can sometimes compute wrong dips or generate artificial patterns). One can also analyse the curves, thus helping to interpret the dips or understand why they are missing.

6.1. GLACIAL ENVIRONMENT

6.1.1. DEFINITION

Environments characterized by deposits on continents, in lakes or in seas (Fig. 6.1-1), resulting from the melting of ice masses (*glaciers, inlandis*) which carried along detrital materials landslided, avalanched or pulled out from bed rocks by erosion and abrasion of the glacier floor during their movement. A present day aerial view of a valley glacier is given Fig. 6.1-2.

6.1.2. GEOLOGICAL FACIES MODEL

6.1.2.1. Lithology

Two parameters must be considered separately.

6.1.2.1.1. *Composition*

Glacial deposits are commonly known as *drift*. They show a wide type of lithology from rock fragments (i.e. igneous, metamorphic or even sedimentary rocks) to clay minerals. This variety of lithology is controlled by several factors (Kukal, 1970) :

- the character of bed rock on which the glacier moves,
- the morphological characteristics and flow velocity of the glacier,
- position of the transported material in relation to the glacier,
- mode of deposition,
- subsequent reworking by melt water.

Drift can be divided into two general categories : *unstratified* and *stratified*.

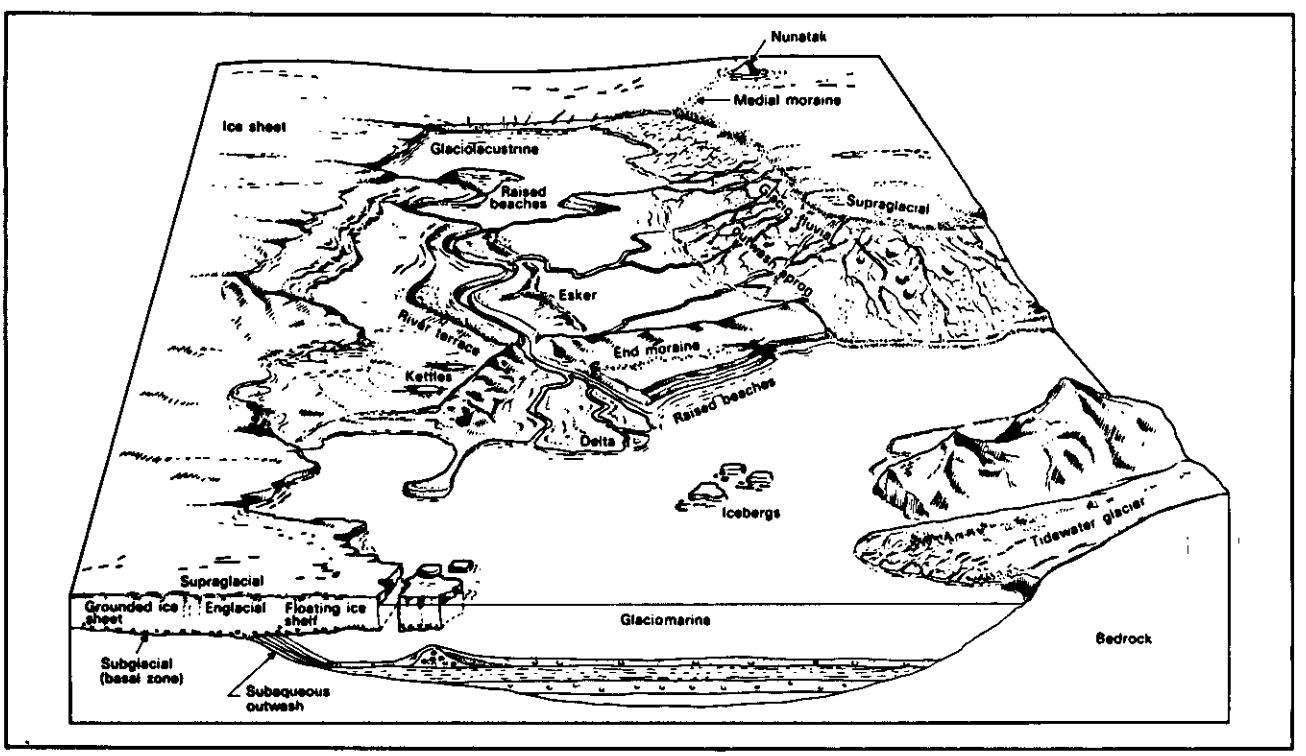

Fig. 6.1-1. - Glacial environments and associated landforms typical of glacial areas (from Edwards, in Reading, 1978).

- *Unstratified glacial drift* is laid down directly by glacier ice. It is called a *till* or a *mixtite* which is found in *moraines* and *drumlins*. It is characterized by the constant presence of a certain amount of gravel fraction and by the equilibrium among the sand, silt and clay fractions (Kukal, 1970). Larger sediment particles are scattered irregularly in the fine-grained matrix (Fig. 6.1-3). An important feature of glacial sediments is the presence of

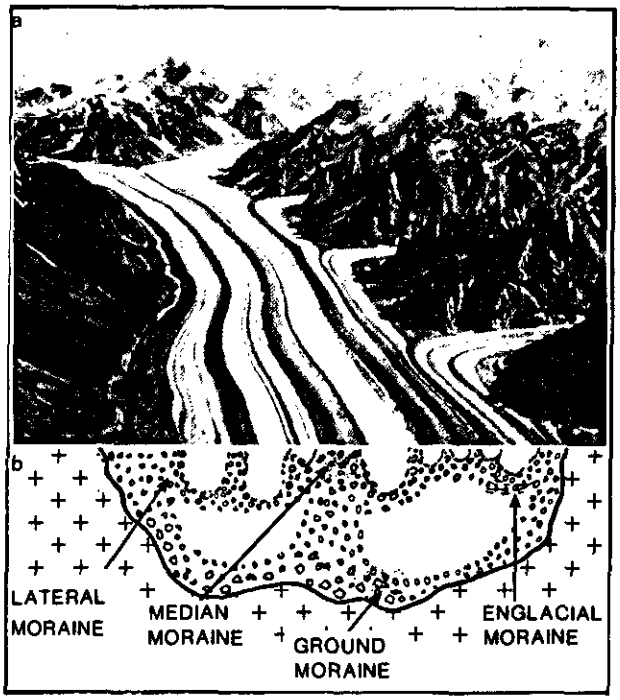

Fig. 6.1-2. - a) Photograph of a compound valley glacier fed by many tributary ice streams with moraines. b) Cross-section illustrating various modes of transport and types of sediment load (adapted from Sharp, 1960).

Fig. 6.1-3. - Example of till (photograph by Holmes, in Pettijohn, 1976.)

Fig. 6.1-4. - Example of varves (from Pettijohn, 1975).

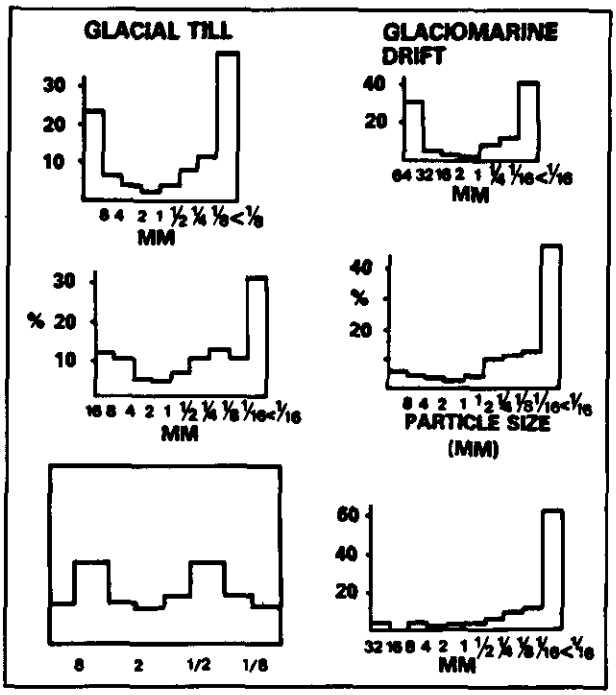

Fig. 6.1-5. - Examples of grain size distribution (histograms) in a till (from Pettijohn, 1975, and Easterbrook, 1982).

numerous labile minerals, e.g., feldspars, ferromagnesian minerals as unalterated, angular grains even in silt and clay-size fractions.

- *Stratified glacial drift* is ice-transported sediment that has been washed and sorted by glacial melt waters according to particle size. Sediments of stratified drift are laid down in recognizable layers. They occur in *outwash* and *kettle* plains, in *eskers*, *kames*, and *varves* or *laminites* formed in glacial lakes (Fig. 6.1-4).

6.1.2.1.2. *Texture*

The sorting is very poor in unstratified deposits (Fig. 6.1-5), the size of particles ranging from boulders or large blocks (erratic), weighing several tonnes, to silt or clay, or even colloids. The shape

Fig. 6.1-6. - Example of scour and fill structure in sandur deposits (after Augustinus & Riezebos, 1971, in Reineck & Singh, 1980).

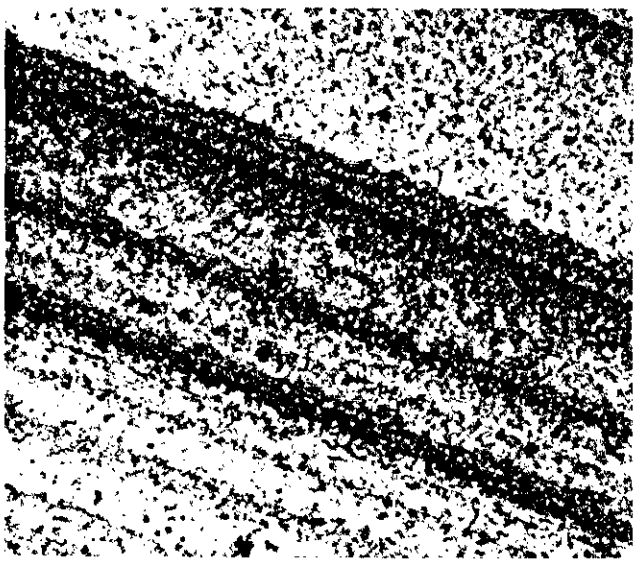

Fig. 6.1-7. - Photograph of a varve, magnified 75 ×, to show laminations of silt, mainly angular quartz and feldspar, interbedded with layers of finer materials (dark) of similar composition but much richer in chlorite (from Pettijohn, 1975).

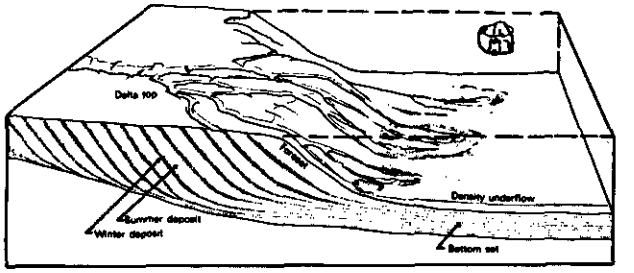

Fig. 6.1-8. - Sedimentation in a glacial lake. During the summer, mainly climbing ripple-laminated sand is deposited on a prograding delta, while thin silt layers are deposited by a density under flow on the lake bed. During the winter, lake surfaces are frozen and suspended clay material can settle down and drape the previous deposits. Icebergs (shore and river ice) may raft coarse sediment into the lake during the spring thaw and summer (from Edwards, in Reading, 1978).

is angular, especially in the sand fraction. Pebbles and boulders are better rounded and show striations on their surface. The outwash sediments are better sorted.

6.1.2.2. Structure

In unstratified sediments a lack of sedimentary structures is generally observed and they comprise a mass of heterogeneous materials with no regular bedding planes, except when pebbles are imbricated. In stratified sediments, cross-bedding, foresets, and scour and fill structures (Fig. 6.1-6) are observed in outwash deposits (*sandurs*), and laminations in varves (Fig. 6.1-7).

6.1.2.3. Boundaries

Generally a sharp, erosional lower boundary is present. A gradational upper boundary can be

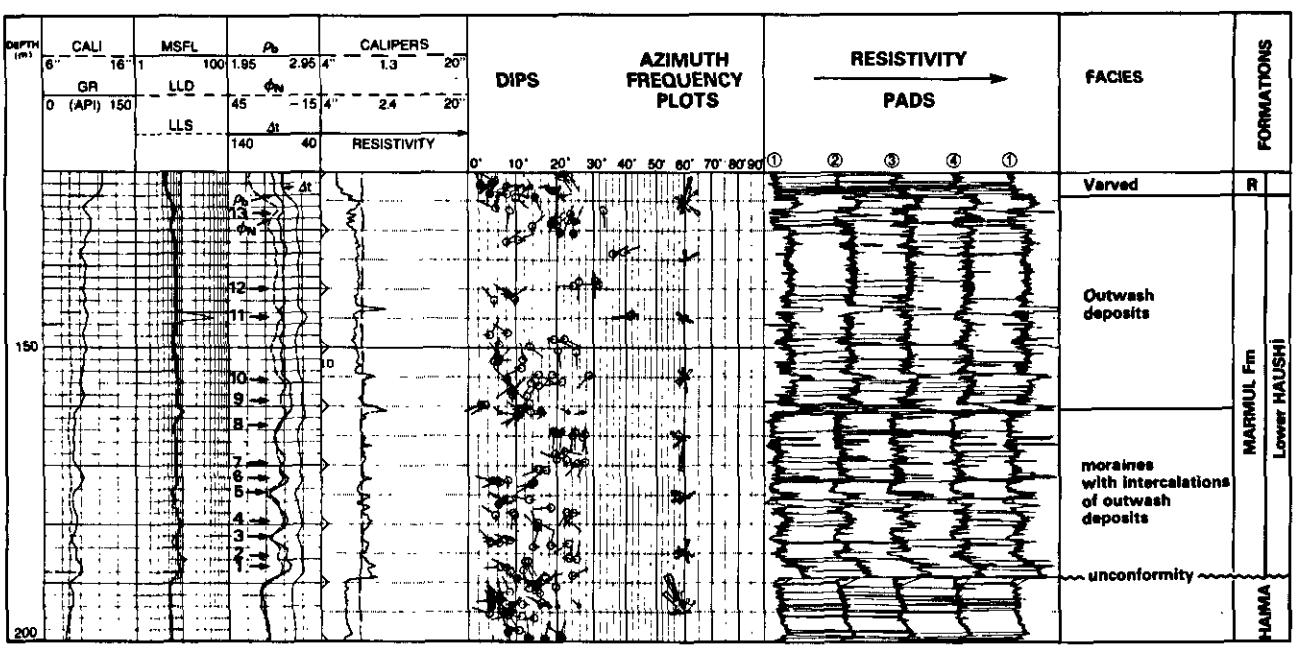

Fig. 6.1-9. - Composite log illustrating typical well-log responses in a glacial drift.

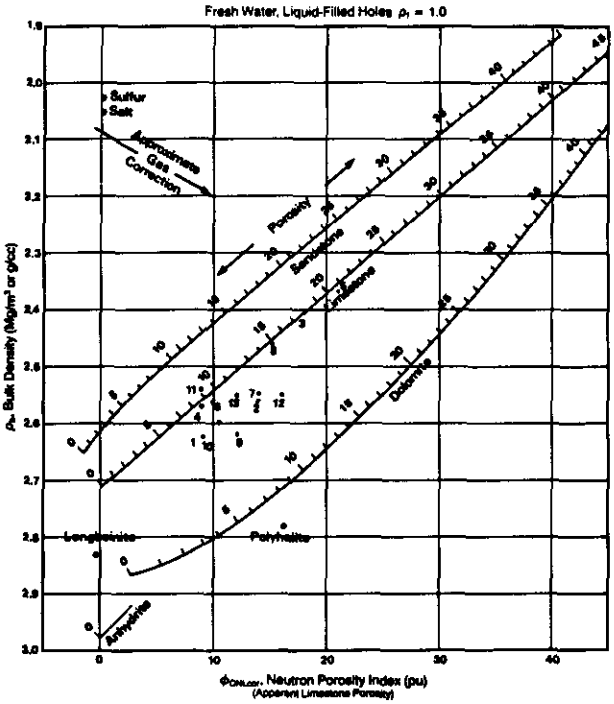

Fig. 6.1-10. - Typical ρ_b vs ϕ_N cross-plot in a glacial drift.

observed in outwash sediments with conformable sharp lower and upper contacts in varves.

6.1.2.4. Sequences

A fining upward sequence can be observed in *outwash deposits and in varves (coarse grains* deposited during the summer period, finer materials during the winter).

6.1.2.5. Geometry of bodies and directional flow model

Tills can be accumulated in mounds or ridges (*moraines*) of various sizes and shapes (crescent, loop), or in smooth, elongated hills (*drumlins*). A drumlin can be from 8 to 60 m thick, 0.5 to 1 km long and several times longer than wide. Drumlins can occur in clusters or in fields with their long axis parallel to the ice flow. Varves, typical of glacio lacustrine deposits (Fig. 6.1-8) are on average 6 to 10 cm thick. Each annual varve is itself composed of 0.2 to 1 mm thick laminae, ranging in number from 75 to 150. They indicate seasonal fluctuation in the rate of supply of sediment and can accumulate in very thick sheets exceeding several tens of metres.

6.1.2.6. Surrounding facies

Generally glacial deposits grade into braided fluvial deposits. If a glacier terminates in a water body, delta-like features are produced and they grade to lake or marine sediments.

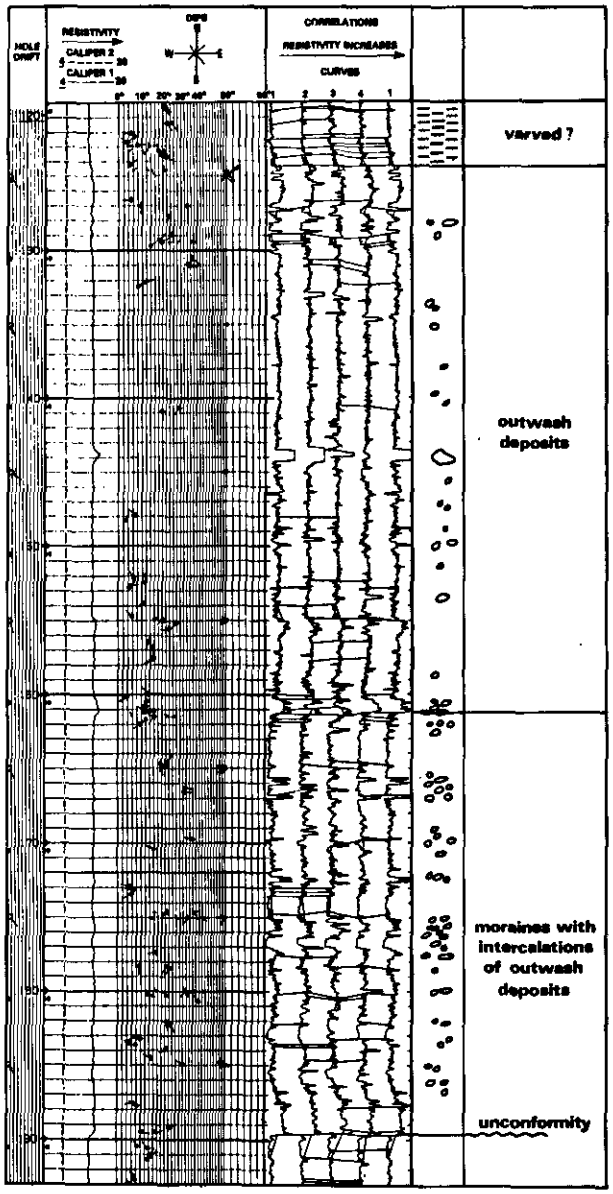

Fig. 6.1-11. - Typical results obtained by the GEODIP program applied to the HDT dipmeter data.

6.1.2.7. Reservoir characteristics

Glacial deposits do not constitute potentially good reservoir rocks. This is related to the, generally, high amount of fine materials (silt sand clays) present in the deposits.

6.1.3. WELL-LOG RESPONSES AND CHARACTERISTICS

6.1.3.1. Electro-Lithofacies

The natural radioactivity (thorium and potassium content) can vary significantly, depending on the source rock type, reflecting the chemical

immaturity of the material. In the example of Fig. 6.1-9, from Oman, the gamma ray is between 45 and 75 API indicating a relatively immature material of metamorphic and sedimentary origin (de la Grandville, 1982). On a ρ_b vs ϕ_N crossplot the representative points fall between sandstone and dolomite lines suggesting the presence of heavy minerals (feldspars, plagioclases, amphiboles), and clay. Porosities range from 5 to 20 % (Fig. 6.1-10).

6.1.3.2. Dipmeter response and dip patterns

In general, tills and outwash deposits are characterized by very "noisy" dipmeter resistivity curves. Those curves show erratic peaks of different sizes which are not or wrongly correlatable giving no, or few and scarce, dips, with variable magnitudes and azimuths (Fig. 6.1-11). The thickness of the events varies considerably from curve to curve (cf. Fig. 6.1-11 at 144 m : the event on pad 2 is approximately 1 m thick. It disappears on pad 4. This suggests a block with an angular shape, since a rounded boulder with a diameter close to 1 metre should extend beyond pad 4). The angular shape of the blocks should be easy to see on FMS images. Outwash deposits can probably be recognized by a generally lower amplitude of the resistivity peaks with fewer thick events. Varved deposits should be characterized by numerous dips with the same azimuth and magnitude, if a sufficient resistivity contrast between summer and winter deposits exists.

6.1.3.3. Boundaries

On most of the well logs the bed boundaries cannot be detected in tills. Sometimes they can be recognized in outwash deposits.

6.1.3.4. Electro-Sequences

Some ramps can be observed on well logs (i.e. Fig. 6.1-9 between samples 4 and 5). They reflect changes in porosity which can correspond to a better sorting in a coarse to medium grain size grade.

6.1.3.5. Confusion with other environments

Tills and outwash deposits can be confused with alluvial fan and debris flow turbidite deposits. However, the angular shape of the resistive events can possibly be used to avoid this confusion.

6.2. ALLUVIAL FAN ENVIRONMENT

6.2.1. DEFINITION

A continental environment characterized by coarse sediments, shaped like an open fan or a segment of a cone, deposited by an emerging mountain stream at the outlet of a narrow valley upon a plain or a broad valley. An aerial view of a modern alluvial fan is reproduced Fig. 6.2-1 and a general vertical lithology column shown in Fig. 6.2-2.

Fig. 6.2-1. - Alluvial fans in the Mohave desert, California. Each cone-shaped fan has been deposited where the slope changes abruptly at the base of the mountains (photo by J.R. Balsley, U.S. Geological Survey; in Press & Siever, 1978).

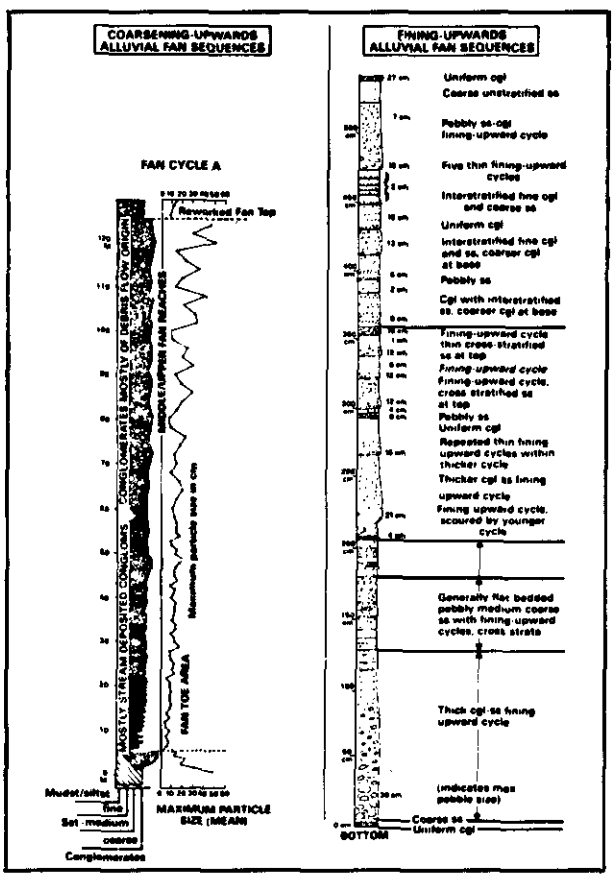

Fig. 6.2-2. - Examples of coarsening upward (Devonian alluvial fan cycle in the Hornelen Basin, Norway from Steel *et al.*, 1977), and fining upward (Devonian, western Norway, from Nilsen, 1969), showing cyclic deposition.

6.2.2. GEOLOGICAL FACIES MODEL

6.2.2.1. Lithology

Two parameters must be considered separately.

6.2.2.1.1. *Composition*

Alluvial fan deposits are essentially composed of rock fragments, the mineral composition of which depends on the geological source. The abundance of rock fragments decreases down fan as a result of abrasion during transport.The matrix of fan gravels is sand or mud of primary or secondary origin with a filling of intergranular porosity by finer material deposited by an overlying braided river on the previous fan. In keeping with their typically chemical immaturity, alluvial fan deposits range from arkoses to lithic quartzoses. Plant fragments may be present. Clay occurs as films around sand grains or as a partial filling in intergranular voids.

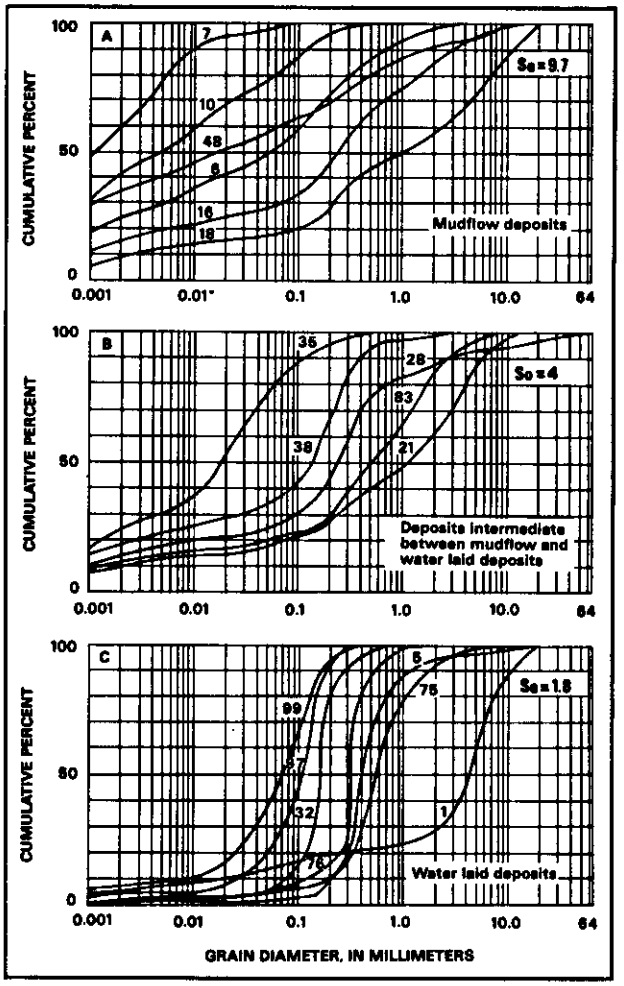

Fig. 6.2-3. - Grain size distribution curves and sorting coefficients for the three main types of alluvial fan deposits (from Bull, 1963).

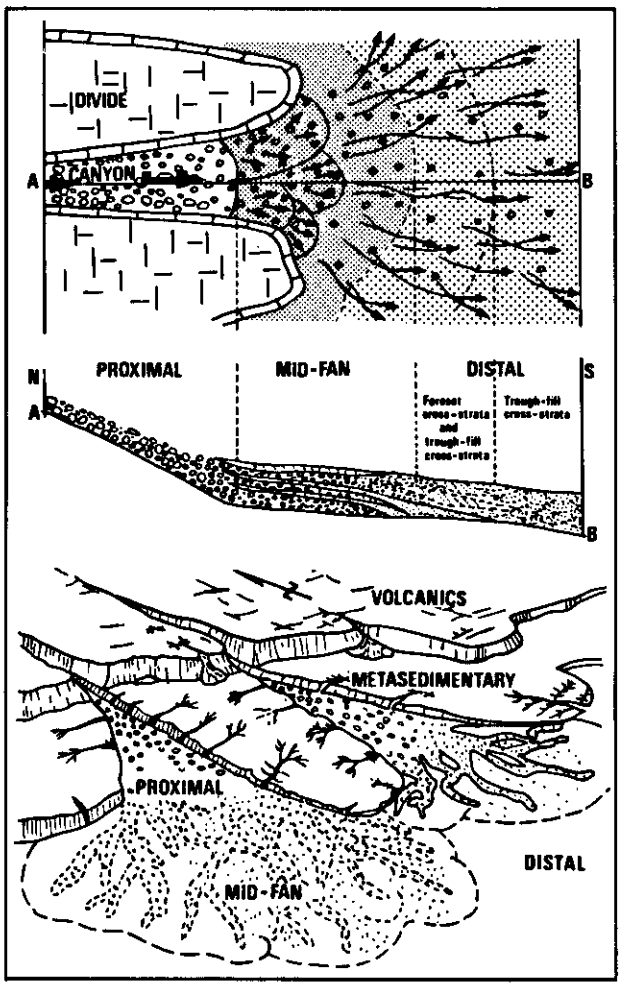

Fig. 6.2-4. - Block diagram, plan view and cross-section of Van Horn fan, West Texas. Widths of arrows, in plan view, indicate relative competency of stream flow. Profile and section show down fan decrease of slope and particle size and the types of stratification : proximal fan = massive conglomerate; mid-fan = interbedded conglomerate and cross-stratified sandstone; distal fan = cross-stratified sandstone (from McGowen & Groat, 1971).

6.2.2.1.2. *Texture*

Particles range from boulder to clay size, and 50 % or more of particles are coarser than 2 mm in diameter. Sand and silt grade sediments are commonly subordinate (Fig. 6.2-3), with clay content increasing in debris or mud flows.

Abrupt changes in maximum or mean particle size and roundness are characteristic. Particle shapes vary from angular to very well rounded. Particle size generally decreases from fan head or proximal fan to fan base or distal fan (Fig. 6.2-4). But in sieve deposits, down slope of the intersection point (Fig. 6.2-5), where water will transport no further, coarser material can accumulate at the base and act as strainers or sieves holding back finer material. Clast roundness increases down fan. Bed thickness typically decreases down fan. Sorting of debris flow and mudflow deposits is generally poor. Stream flow deposits are better sorted.

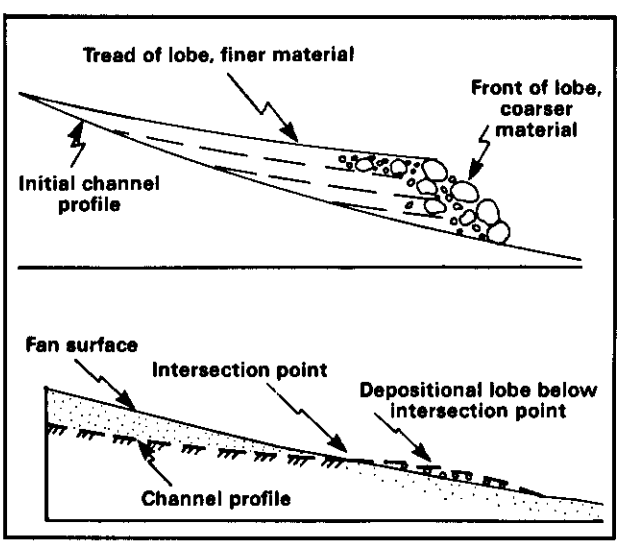

Fig. 6.2-5. - Schematic sketch of a sieve lobe (from Hooke, 1967).

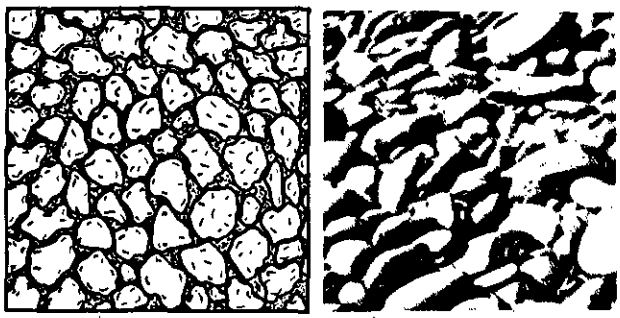

GRAIN SUPPORTED

Fig. 6.2-6. - Example of grain-supported conglomerate.

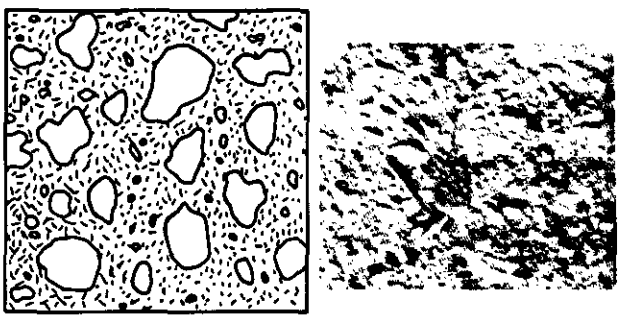

MATRIX SUPPORTED

Fig. 6.2-7. - Example of matrix supported conglomerate.

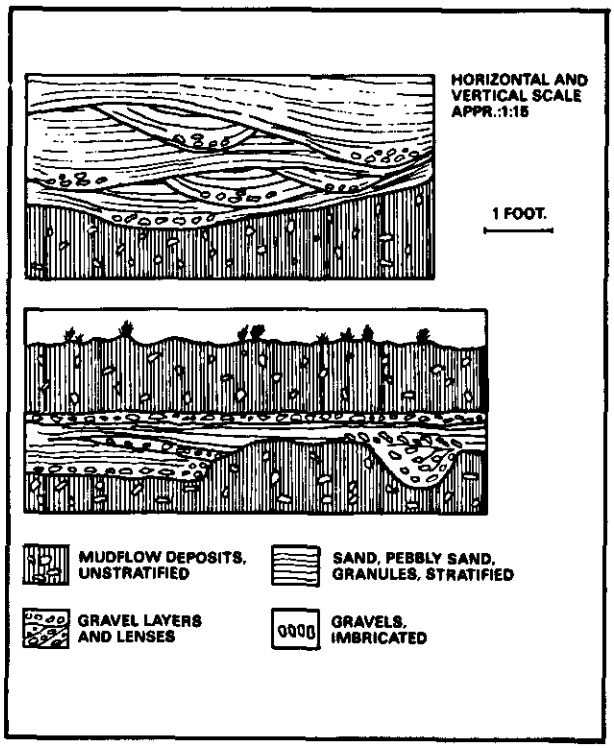

Fig. 6.2-8. - Characteristic sedimentary structures in an alluvial fan (from Blissenbach, 1954; in Spearing, 1971).

Distinction must be made between grain- (or clast-) supported (Fig. 6.2-6), and matrix-supported conglomerates (Fig. 6.2-7).

Grain-supported conglomerates are the predominant facies of stream flow or water-laid deposits within a proximal fan, while matrix-supported conglomerates are more characteristic of debris flow or mudflow deposits. They are also found in distal fans of water-laid deposits. According to Bull (1977), debris flows form on steep slopes (more than 10°), with a lack of vegetation, during short periods of very abundant water supply (heavy rains in dry regions, or rapid thaw). Water-laid deposits are characteristic of wet regions with permanent water supply (perennial stream).

6.2.2.2. Structure

Trough cross-bedded grain-supported gravel is the major structure and planar cross-bedded gravel, trough and planar cross-stratified sands are the minor structures present in the environment (Fig. 6.2-8). Graded bedding is frequent, fundamentally fining upward, but coarsening upward may be present if tectonic uplifts occur (Steel *et al.*, 1977).

6.2.2.3. Boundaries

The lower contact is generally irregular and erosional. There is a gradational contact toward the top.

6.2.2.4. Sequences

Rhythmic sedimentation with each sequence thickness ranging from few centimetres to few metres. Several tens or hundreds of superposed sequences are generally observed. The lateral facies sequence is alluvial fan deposits evolving to proximal braided river and flood plain deposits.

6.2.2.5. Geometry of Bodies

Alluvial fans are usually cone-shaped. Each sequence is a long narrow tongue-shaped body extending radially down slope from the fan apex. The depositional area from a single flood may be several kilometres long, but only 150 to 500 m wide (Fig. 6.2-9). Surface ranges from 1 to 900 km^2. Thickness ranges from several hundred metres up to 10 000 m (Southern California). On a cross-fan profile the shape is convex upward, on a radial profile the general shape is concave upward (Fig. 6.2-10). Fan surface slopes vary greatly, but are generally less than 10°.

6.2.2.6. Directional current flow model

The general direction of flow is radial and can be deduced from the imbrication of gravels (Fig. 6.2-11).

6.2.2.7. Surrounding Facies

Fans may interfinger with talus deposits toward the source area. Fan margins may coalesce or

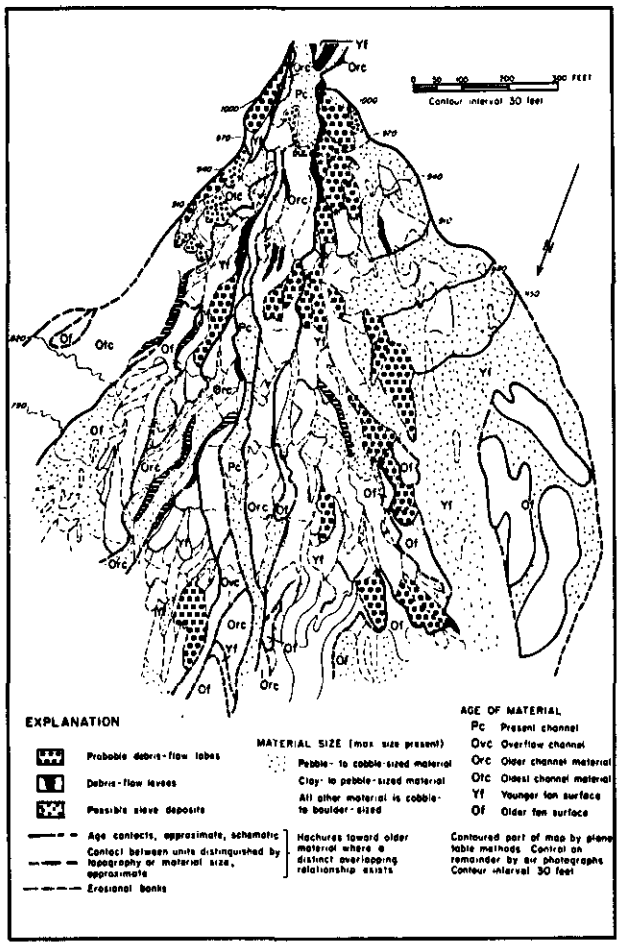

Fig. 6.2-9. - Distribution of various types of sediments in the Trollheim alluvial fan (from Hooke, 1967).

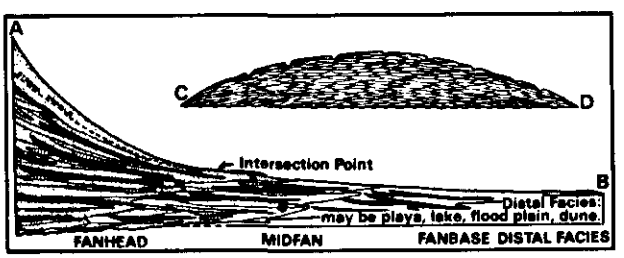

Fig. 6.2-10. - Schematic cross-sections in an alluvial fan (from Spearing, 1971).

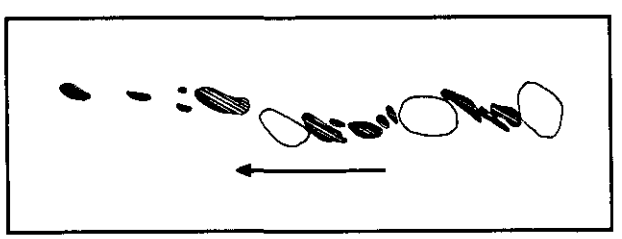

Fig. 6.2-11. - Sketch showing the imbricate arrangements in a single pebble band. Archean conglomerate, Little Vermilion Lake, Ontario, Canada. The arrow gives the direction of the flow (from Pettijohn, 1930).

interfinger with deposits of playa, flood plain, aeolian dunes, and fluvial sands. Playa lake deposits are easily distinguished by their dominant clay size and chemical deposits (carbonates, evaporites). Flood plain deposits have better stratification than alluvial fans. Aeolian sands are recognized by their dip pattern (see chapter 6.3).

6.2.2.8. Reservoir Characteristics

"Alluvial fan deposits are not generally reservoir rocks for petroleum because they fail to connect laterally to source rocks, are not sufficiently extensive laterally, do not have proper seals, have low permeability and porosities following diagenesis, and generally do not contain facies that are good source rocks" (Nilsen, 1982).

6.2.3. WELL-LOG RESPONSES AND CHARACTERISTICS

6.2.3.1. Electro-Lithofacies

The radioactivity (potassium and thorium content) is generally medium to high, reflecting chemical immaturity and presence of feldspars, micas, and rock fragments from igneous, metamorphic or even sedimentary origin. Because of oxidizing conditions uranium is present only if the source-rock contains uranium bearing minerals (i.e. granite). On a ρ_b vs ϕ_N crossplot representative points fall between the sand (quartz) line and the shale "region" according to the rock fragment composition and the percentage of matrix. Pe ranges generally between 2 and 3 b/e. Fig. 6.2-12 shows typical open-hole log responses in such facies.

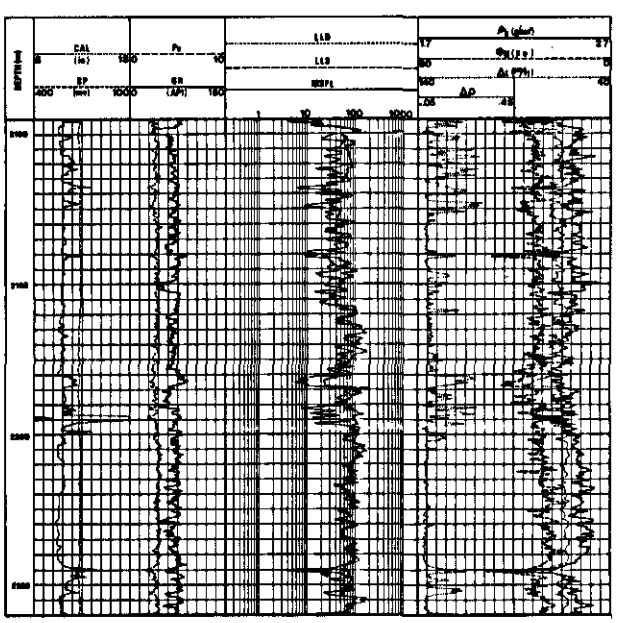

Fig. 6.2-12. - Typical log responses in an alluvial fan deposit as shown by this composite-log. Logs reflect a certain heterogeneity continuing on a thick interval.

6.2.3.2. Dip patterns

Fig. 6.2-13 represents a typical GEODIP result in an alluvial fan (part of Fig. 6.2-12). Grain-supported conglomerates are characterized by high resistivity with low amplitude activity on the curves, no or erroneous correlations, and scarce and scattered dips. Matrix (or mud) supported conglomerates are characterized by higher amplitude activity, lower resistivity intervals with isolated resistivity peaks corresponding to compact indurated pebbles embedded in a more conductive matrix. Layers of pebbles can sometimes be interbedded with sand layers, generating correlations and dip computations (water-laid deposits). Some very consistent and high dips may correspond either to aeolian sand deposits, if the green dip pattern does not correspond to structural dip, or to water-laid (braided fluvial) deposits, if the green pattern can be related to structural dip. Pebbles can be detected on, and their orientation sometimes determined from FMS images.

6.2.3.3. Boundaries

The lower sharp erosional contact, as theoretically expected, is not frequently observed as a result of the coalescence of pebbles with the previous unit. This abrupt contact can occur only on one or two curves.The upper gradational contact is better seen on the averaged resistivity curve.

6.2.3.4. Electro-Sequences

The sequential grain size evolution appears more clearly on the averaged resistivity curve than on the raw curve because of the small resistivity peaks occurring randomly and obscuring the general trend.

6.2.3.5. Direction of flow

The direction of flow is not easily extracted from the dipmeter data. It can be determined from isopach maps of alluvial deposits.

6.2.3.6. Thickness

The above mentioned characteristics persist over several tens or hundreds of metres.

6.2.3.7. Confusion with other environments

Alluvial fan deposits can sometimes be confused with glacial deposits, or with debris flow turbidite deposits. The angular shape of the resistive events can help to differentiate these deposits from the tills. The position of the deposits in the megasequence should distinguish alluvial fan deposits (general fining upward megasequence) from debris flow turbidite deposits (general coarsening upward megasequence).

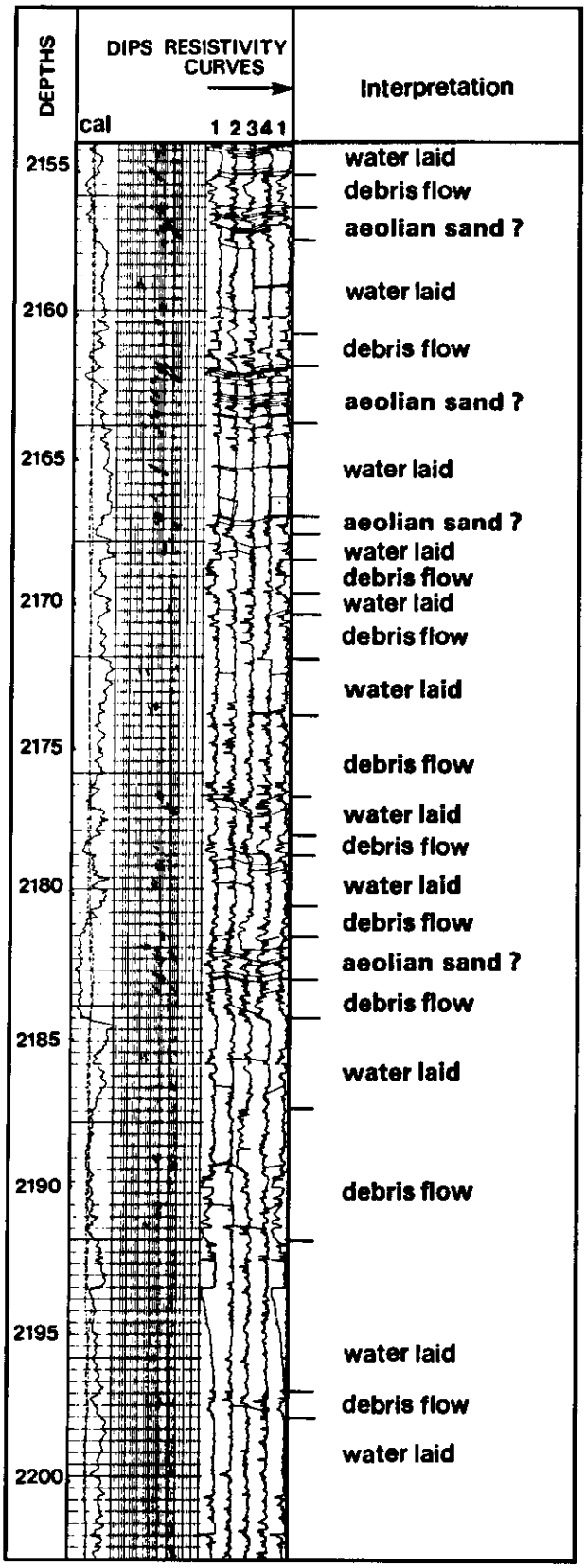

Fig. 6.2-13. - Typical GEODIP response in an alluvial fan, and its interpretation. It corresponds to a short interval of the previous composite log.

6.3. AEOLIAN ENVIRONMENT

6.3.1. DEFINITION

A continental environment characterized by deposits resulting from wind action,often mixed with fluvial or sabkha facies. An aerial view of modern dunes is given in Fig. 6.3-1, and a vertical lithology column in Fig. 6.3-2. Three aeolian subenvironments have been distinguished by Ahlbrandt *et al.* (1982) : dune, interdune and sand sheet.

Fig. 6.3-1. - Aerial photograph of a sand dune in the Saudi Arabian desert (from ARAMCO, in Press & Siever, 1978, Fig. 8-16).

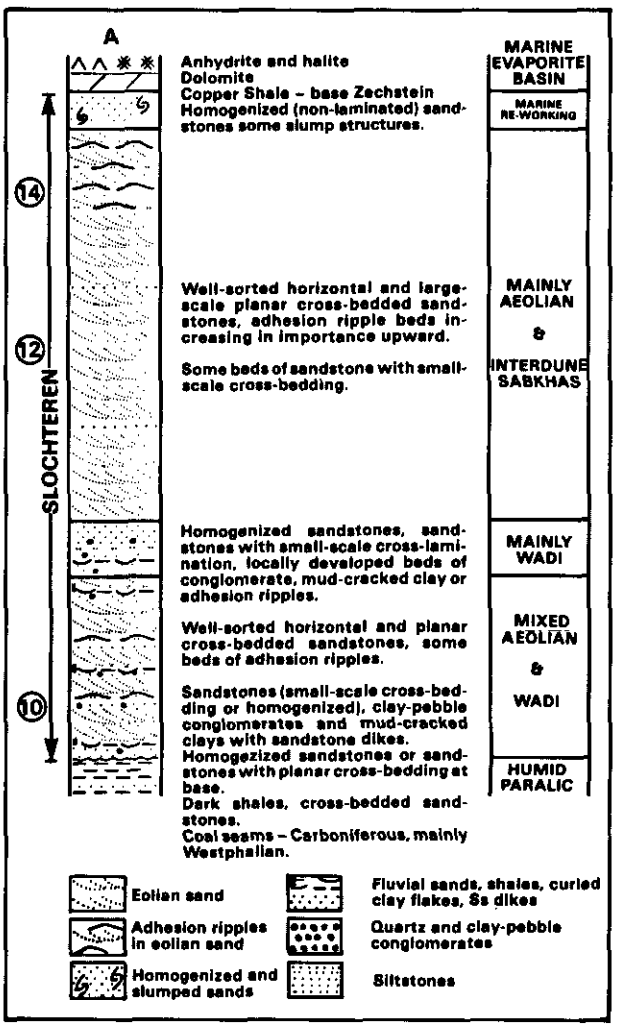

Fig. 6.3-2. - Vertical cross-section in aeolian deposits in northwest Europe, southcentral part of Rotliegendes basin (from Glennie, 1970).

6.3.2. GEOLOGICAL FACIES MODEL

6.3.2.1. Lithology

Two parameters must be considered separately.

6.3.2.1.1. *Composition*

The typical dunes are made of protoquartzite to quartzite sands (more than 85 % quartz grains); but depending on clastic source and transport distance, marine calcareous sand dunes (Bahamas), oolitic dunes of Abu Dhabi, and loess-gypsum sand dunes (White Sands, New Mexico) have been described. Heavy minerals may be present, but iron-bearing minerals tend to be chemically alterated. According to their composition, sand dunes are considered to be chemically mature deposits. Clays are minor components in an aeolian environment, occurring only in wadi deposits, interdune or coastal sabkhas, in inland sabkhas and

playa lakes, or as post depositional authigenic minerals. Cement may be calcitic or dolomitic and due often to the rise of the water table (phreatic level). Nodules of gypsum or anhydrite may be present in intertongue wadi or sabkha deposits.

6.3.2.1.2. *Texture*

Aeolian sand generally consists of fine-to-medium sand grains (0.2 to 0.5 mm), well rounded, well sorted (Fig. 6.3-3), frosted and positively skewed. But Ahlbrandt (1979) recognized three textural groups :

- moderately to well sorted, fine- to medium-grained inland dune sands;
- well sorted fine-grained coastal dune sands;
- moderately to very poorly sorted interdune or serir sands.

Grains are commonly coarser on ripple tops than in adjacent swales, but lag grains in swales may be coarser than grains in adjacent large dunes. The absence of fines (clays) and micaceous minerals, due to aeolian winnowing, give a high grain/matrix ratio. Flat deflation surfaces (serirs) may have characteristic lag deposits of coarser grains. These grains are very evenly spaced due to deflation and saltation of sand across the surface.

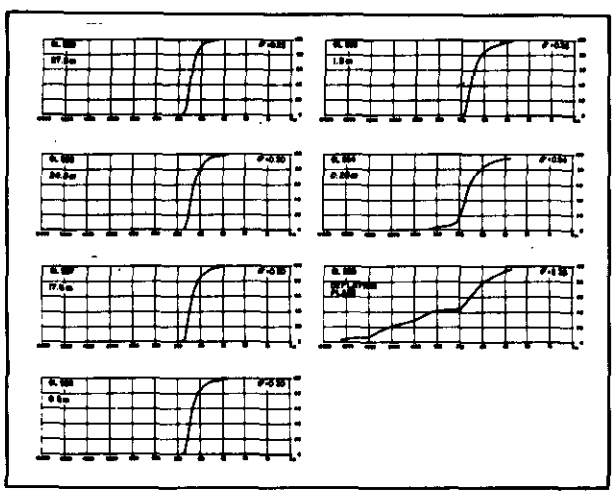

Fig. 6.3-3. - Grain size distribution curves and sorting coefficients (from Glennie, 1970).

6.3.2.2. Structure

Dunes commonly contain the following internal structures (Fig. 6.3-6, 6.3-8, 6.3-10 and 6.3-12) : (1) large-scale, moderate to high angle (up to 34°) cross-strata, facing downwind, commonly wedge planar to tabular planar sets and laminae within sets are, generally, tangential to the lower bounding surface; (2) successive boundaries separating individual cross-sets horizontal or downwind at a low angle of dip; (3) cross-sets become progressively thinner toward the top of dunes, as the dunes grow upward, winds more frequently truncate the upper laminae, producing the thinning-upward pattern of sets; (4) dipping foresets are progressively larger in a downwind direction; (5) contorted bedding; (6) rare ripple laminae.

6.3.2.3. Boundaries

Sharp, abrupt contacts are developed for each unit. It may even be undulated because of interdune blowouts, making nicklines and serirs (Fig. 6.3-4). This boundary is related to phreatic control over deflation processes (Reineck *et al.*, 1975). Surfacing of phreatic levels produces interdunal deposits (oasis, intracontinental sabkhas). Flash flood deposits (wadis) are also responsible for scoured boundaries.

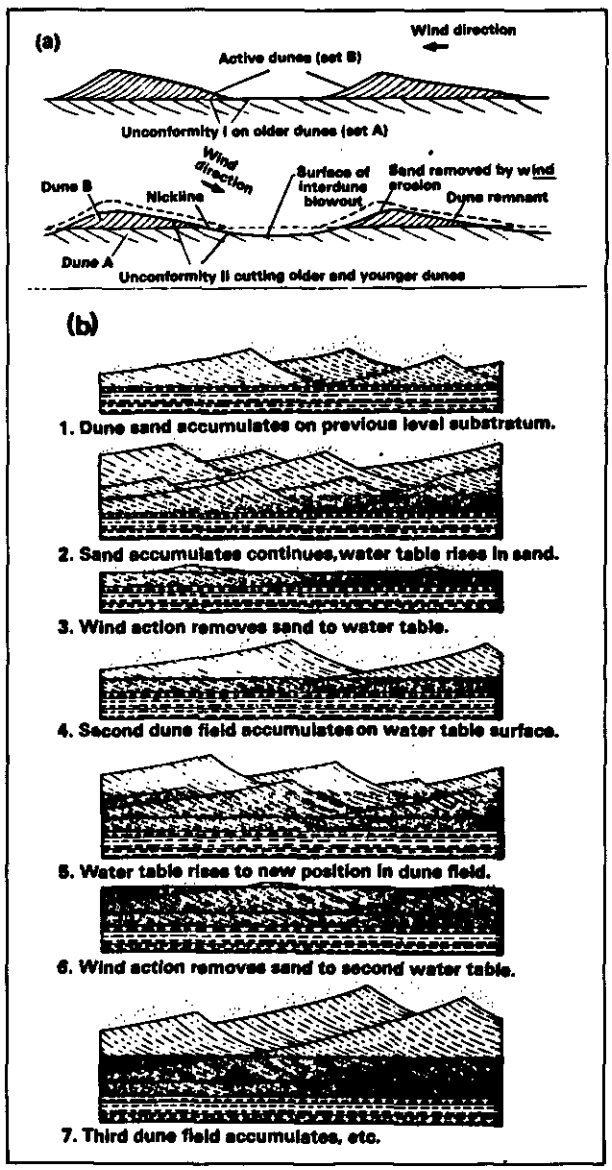

Fig. 6.3-4. - (a) Development of scoop-like erosion surfaces and nicklines within aeolian dune sands by the development of a interdune blowout (from Walker & Harms, 1972). (b) Schemes showing horizontal truncation surfaces and the role of phreatic level (from Stokes, 1968).

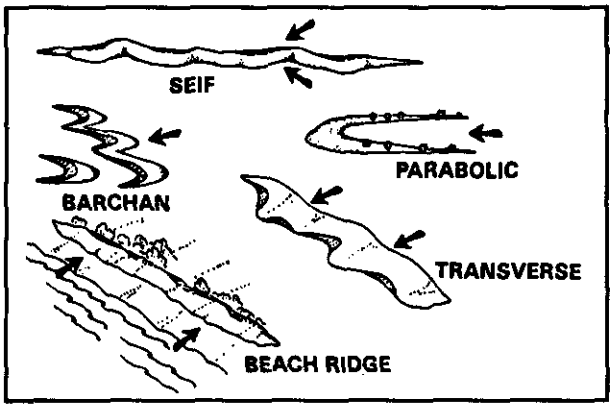

Fig. 6.3-5. - Major dune types, showing orientation with respect to dominant wind direction (arrows) (from Spearing, 1971).

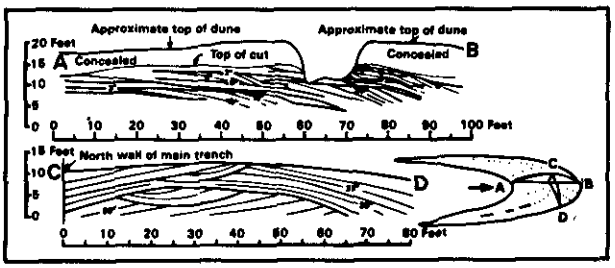

Fig. 6.3-6. - Internal stratification of parabolic dune, White Sands, New Mexico (McKee, 1966).

6.3.2.4. Sequences

A well defined fining-upward sequence is sometimes described for dunes (Fig. 6.3-2 and 6.3-14). The type of dune, persistence of winds and fluvial or marine influences will also affect their sequential arrangement. Sedimentary structures also show a vertical organization with thinning-upward units. Bottomset beds develop over sharp lower contacts, followed by planar cross-bedding, covered by sediments affected by variations of the phreatic level. The sequence may be interrupted by wadi channels or fluvial systems.

6.3.2.5. Geometry of Bodies and Directional flow model

As the flow model defines the dune geometry, without any other influence of slopes, it is impossible to separate dune geometries from directional flow models. They will be discussed together as more comprehensive items.

Several dune types are recognized in modern dune fields (Fig. 6.3-5).

Each dune type can be characterized by the dip pattern and the shape of the azimuth frequency plot. The following figures illustrate both internal stratification and dips plus their azimuth patterns.

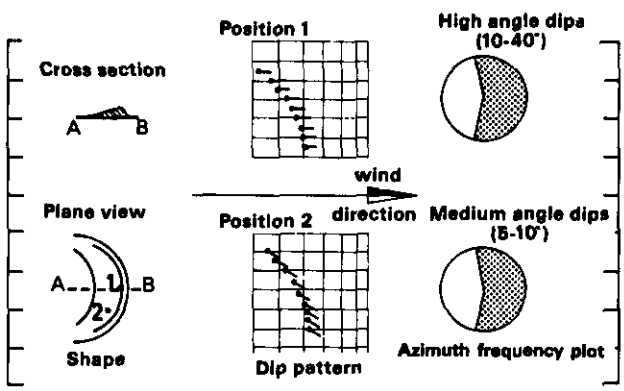

Fig. 6.3-7. - Shape, dip pattern and azimuth frequency plot of a parabolic dune.

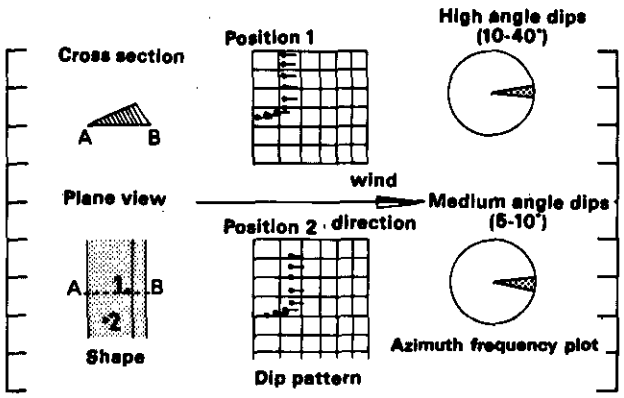

Fig. 6.3-9. - Shape, dip pattern and azimuth frequency plot of a transverse dune.

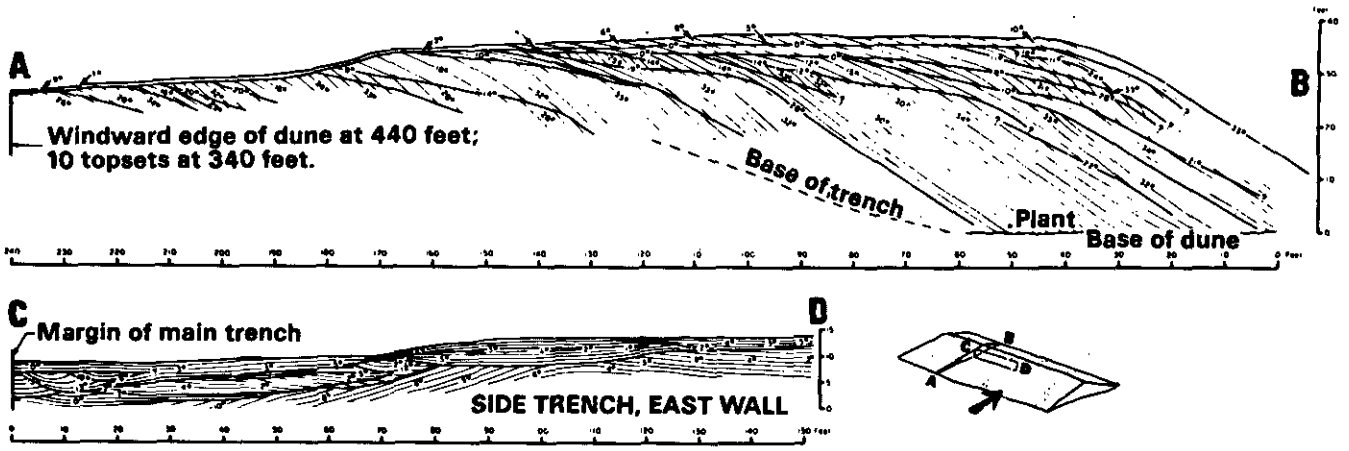

Fig. 6.3-8. - Internal stratification of transverse dune, White Sands, New Mexico (McKee, 1966).

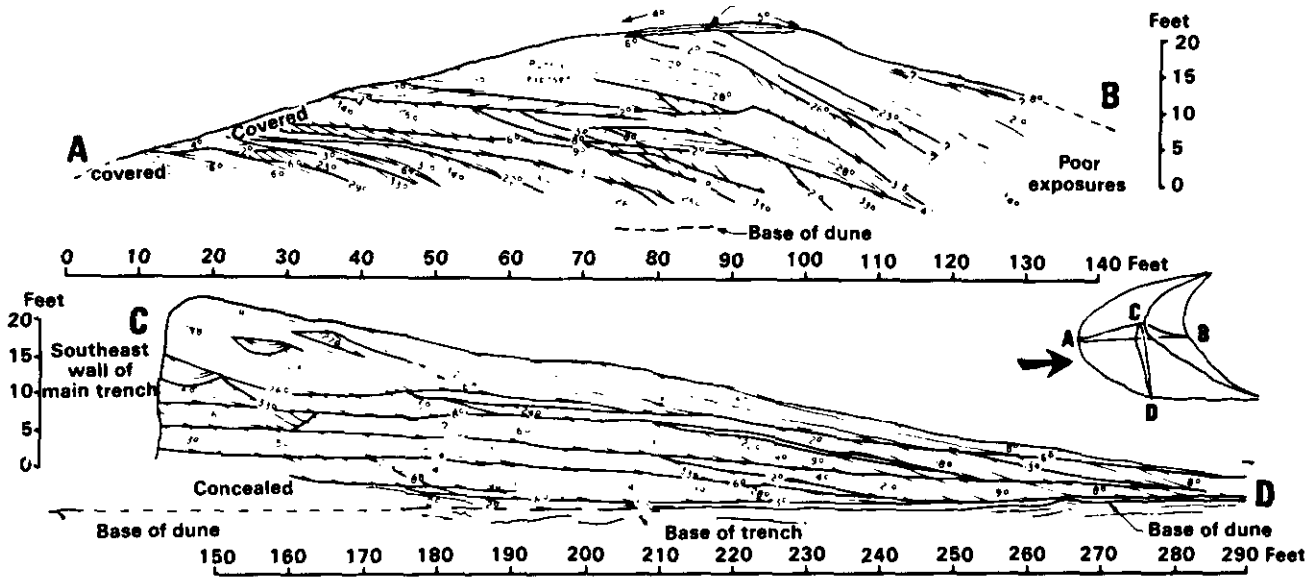

Fig. 6.3-10. - Internal stratification of barchan dune, White Sands, New Mexico (McKee, 1966).

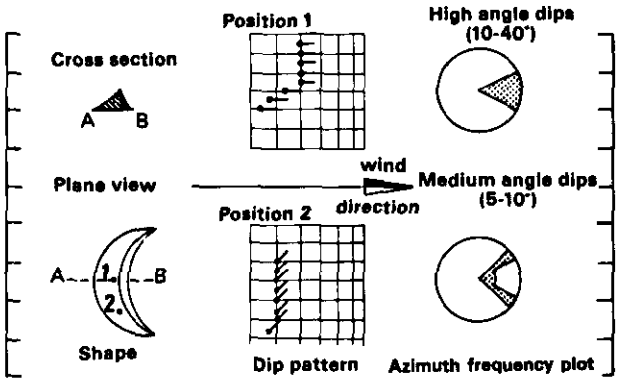

Fig. 6.3-11. - Shape, dip pattern and azimuth frequency plot of a barchan dune.

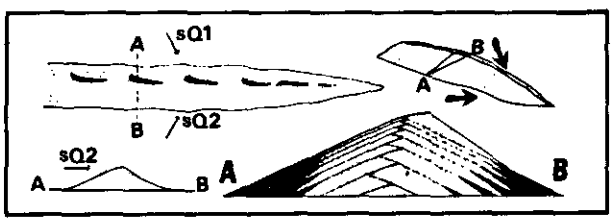

Fig. 6.3-12. - Internal stratification of seif dune, North Africa (Bagnold, 1941).

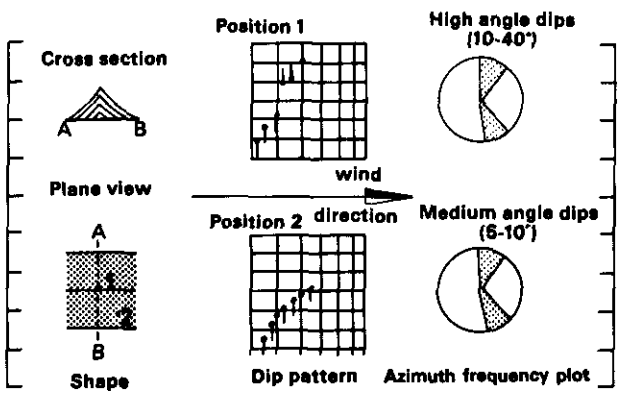

Fig. 6.3-14. - Lacquer peel and "core" from a seif dune. Dubai, *Trucial Coast* (from Glennie, 1970).

6.3.2.6. Surrounding Facies

Aeolian dunes are found in dry deserts, along rivers, and along coastlines. Consequently, aeolian sands may grade laterally or intertongue with nearshore marine sands, silts or clays, fluvial overbank silts and clays, or alluvial fan, playa and evaporite deposits of the desert setting (Fig. 6.3-15).

◀ Fig. 6.3-13. - Shape, dip pattern and azimuth frequency plot of a seif dune.

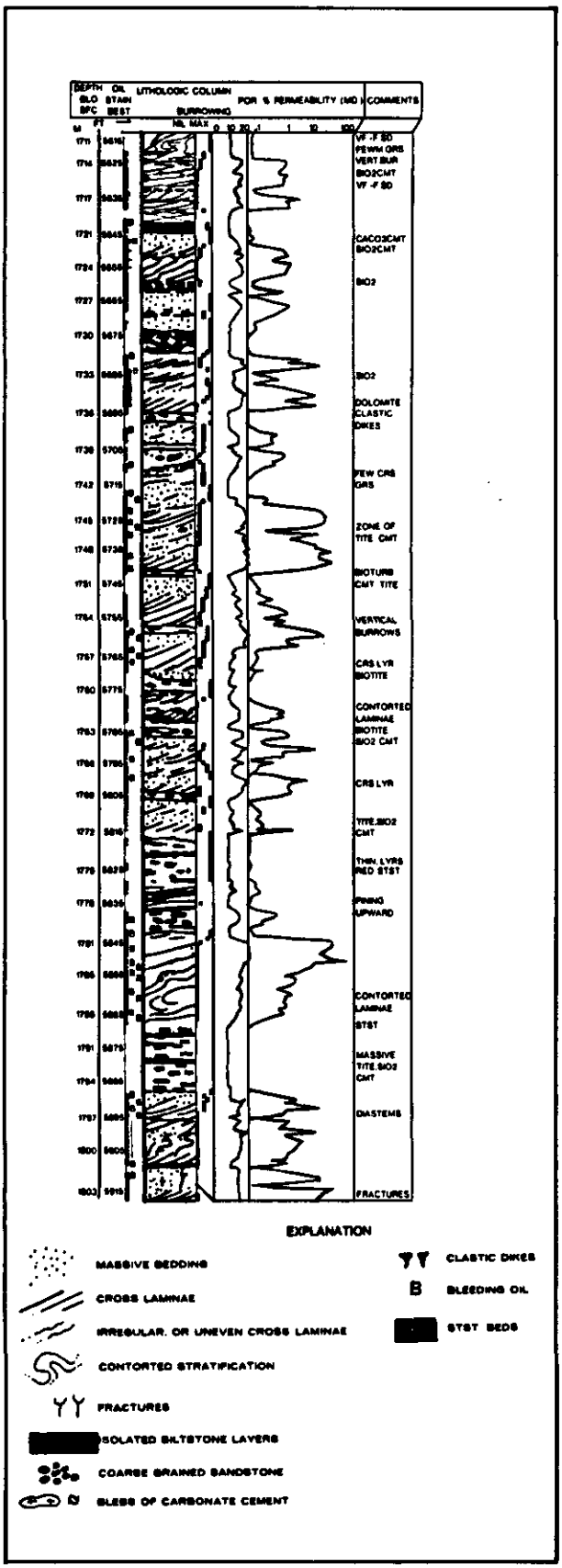

Fig. 6.3-15. - Example of aeolian deposits in Colorado, U.S.A. Subsurface core description of Weber Sandstone (Pennsylvanian-Permian) in Chevron well Larson B-15 (from Fryberger, 1979).

6.3.2.7. Reservoir Characteristics

Aeolian deposits are complex, heterogeneous reservoirs due to : "(1) lateral discontinuity of reservoir zones; (2) impermeable or less permeable carbonate or flat-bedded units interspersed with more permeable cross-bedded units; (3) anisotropic permeabilities and related textural changes and cementation along individual laminae causing low transmissivity across laminae - anhydrite cement is the most common, but calcite, dolomite, and silica cement are problems in well log interpretation; (4) secondary and tertiary recovery problems related to isolated reservoirs causing reduced well spacing, commonly to 10 or 20 acres" (Ahlbrandt & Fryberger, 1982).

6.3.3. WELL-LOG RESPONSES AND CHARACTERISTICS

6.3.3.1. Electro-Lithofacies

As shown by Fig. 6.3-16 and 6.3-17, the general radioactivity of dune sands is low. On the ρ_b vs ϕ_N crossplot representative points of massive dunes fall very close to the sandstone line (if no gas influence) clearly indicating quartz as the main component. The increase of radioactivity corresponds to interdune deposits (wadi or sabkha), which are also reflected by density and neutron responses. Pe values are close to 1.8 and increase when calcitic or dolomitic cement or anhydrite nodules are present. Dolomite and anhydrite (or gypsum) are common in interdune sabkhas or bottomsets.

Porosities are often high and range from 10 to 30 %. When the porosity decreases the representative points slightly move toward the limestone line reflecting the presence of cement (calcite, dolomite or anhydrite).

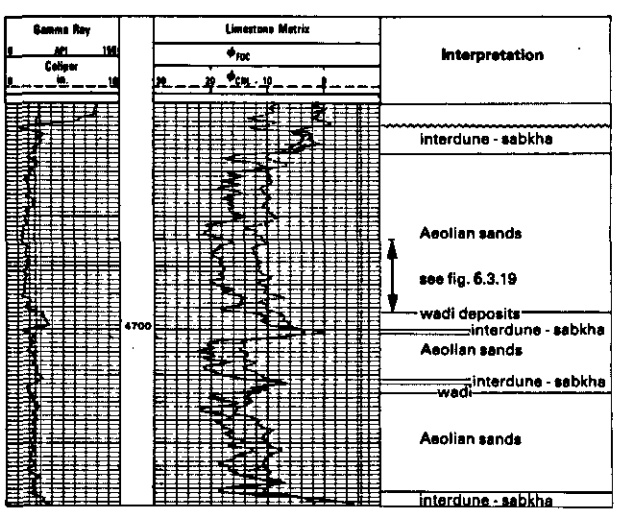

Fig. 6.3-16. - FDC-CNL-GR logs show typical responses in dune sands.

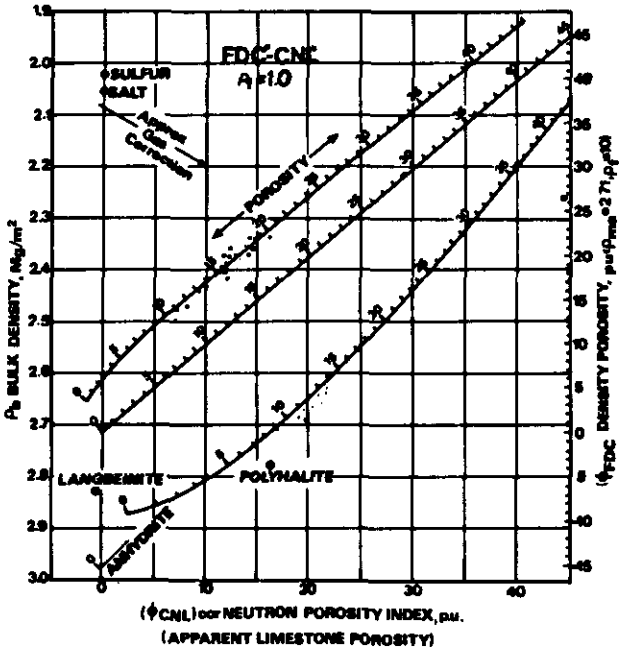

Fig. 6.3-17. - Density-neutron porosity crossplot showing the lithology (quartz sandstone) of the aeolian sands represented by Fig. 6.3-16.

6.3.3.2. Dip Patterns

As well known by log analysts and geologists and as mentionned by Ahlbrandt *et al.* (1982), "the dipmeter is an extremely useful device for recognizing and interpreting eolianites in the subsurface". Fig. 6.3-18 represents the results of a CLUSTER on Rotliegendes in North Sea. It shows, very clearly, a succession of green patterns (foreset beds), generally superposed on blue patterns (toeset or bottomset beds), which can in turn cover wadi deposits represented by scattered dips, or interdune clays, represented by a green pattern if they are not mud-cracked. Very low dips consistent in azimuth, may correspond to sabkha deposits. All these features can easily be extracted from CLUSTER processing due to the vertical and lateral extension of the sedimentary features.

Fig. 6.3-19 represents the results of a GEODIP processing on a 35 feet section of the well illustrated by Fig. 6.3-16. GEODIP gives a very high density of correlations allowing a very precise study of the formation and the recognition of the sedimentary features generally observed in dunes. Low changes in dip magnitude generate small blue and red patterns which represent foreset beds. The longer blue pattern (at 4686 ft) corresponds to a bottomset bed with a sharp contact at its base. This resistivity evolution can correspond to a decrease of cement percentage from the water

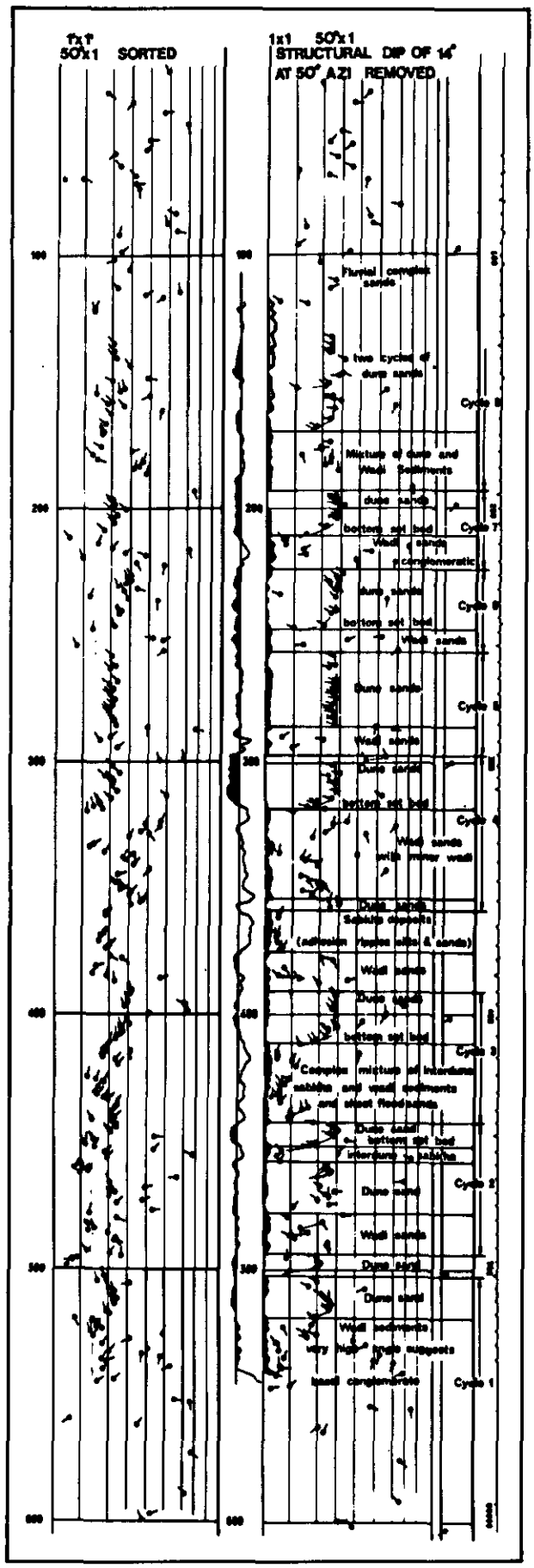

Fig. 6.3-18. - Example of CLUSTER results in aeolian deposits (Rotliegendes in North Sea) and its interpretation in terms of facies. ▶

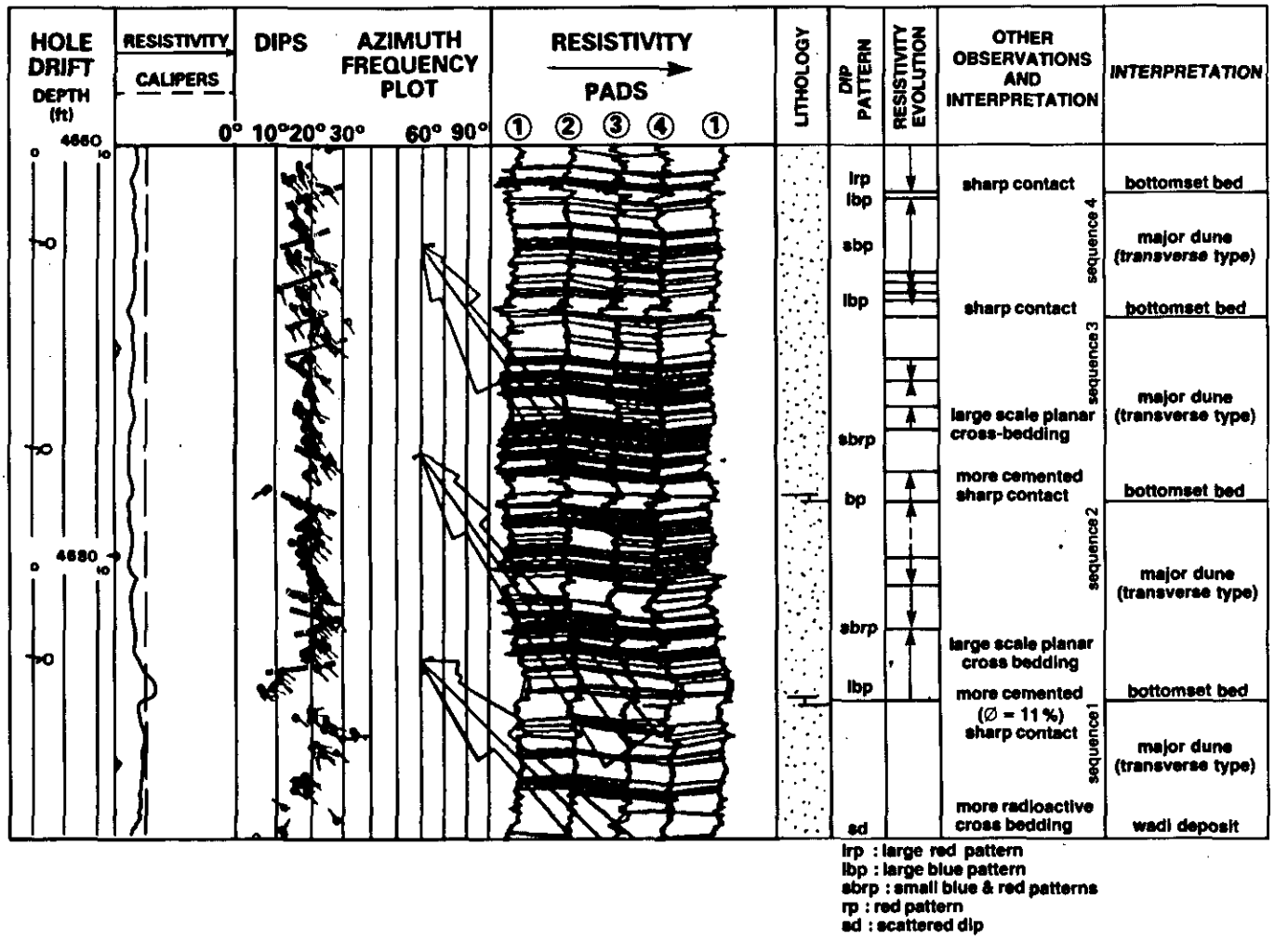

Fig. 6.3-19. - GEODIP results over 35 feet of the aeolian sands shown on Fig. 6.3-16, and its interpretation.

table toward the top of the dune. Other small resistivity evolutions can reflect fining upward sequences. Azimuth frequency plots show a very narrow dispersion, possibly indicating a transverse dune. The direction of the wind was toward SE. Sometimes red patterns are present at the top, indicating avalanche scars on steep unstable foresets. In general, azimuth frequency plots show uni-or bi-modal distribution with narrow to large scatter depending on the dune type.

Fig. 6.3-20 is another example of GEODIP interpretation in sand dunes. All the observations and their interpretation are listed on the side.

In aeolian environments FMS images (Fig. 6.3-21) show, very well, the foreset beds, the sharpness of the erosional surface (at × 425.5), the more cemented sandstones, the changes in wind direction, and the change in dip magnitude. The comparison of FMS images with core photographs in this aeolian environment shows the perfect fit between the two types of data. In such cases FMS images indicate more clearly the cemented intervals (white bands) than the core photographs. They can be used to define the permeability barriers.

6.3.3.3. Boundaries

The sharpness of the lower boundary is clearly seen on the dipmeter resistivity curves (Fig. 6.3-19 and 6.3-20), as the progressive evolution toward the top of each cycle.

6.3.3.4. Electro-Sequences

The dipmeter resistivity evolution and the dip patterns reflect the sequences. Small resistivity evolutions can reflect either changes in cement percentage, or fining upward sequences, if they do not correspond to variations on density and neutron responses, and consequently to changes in porosity by cementation.

6.3.3.5. Surrounding Facies

Sabkha deposits can be recognized. They correspond to intertongue dolomitic or anhydritic

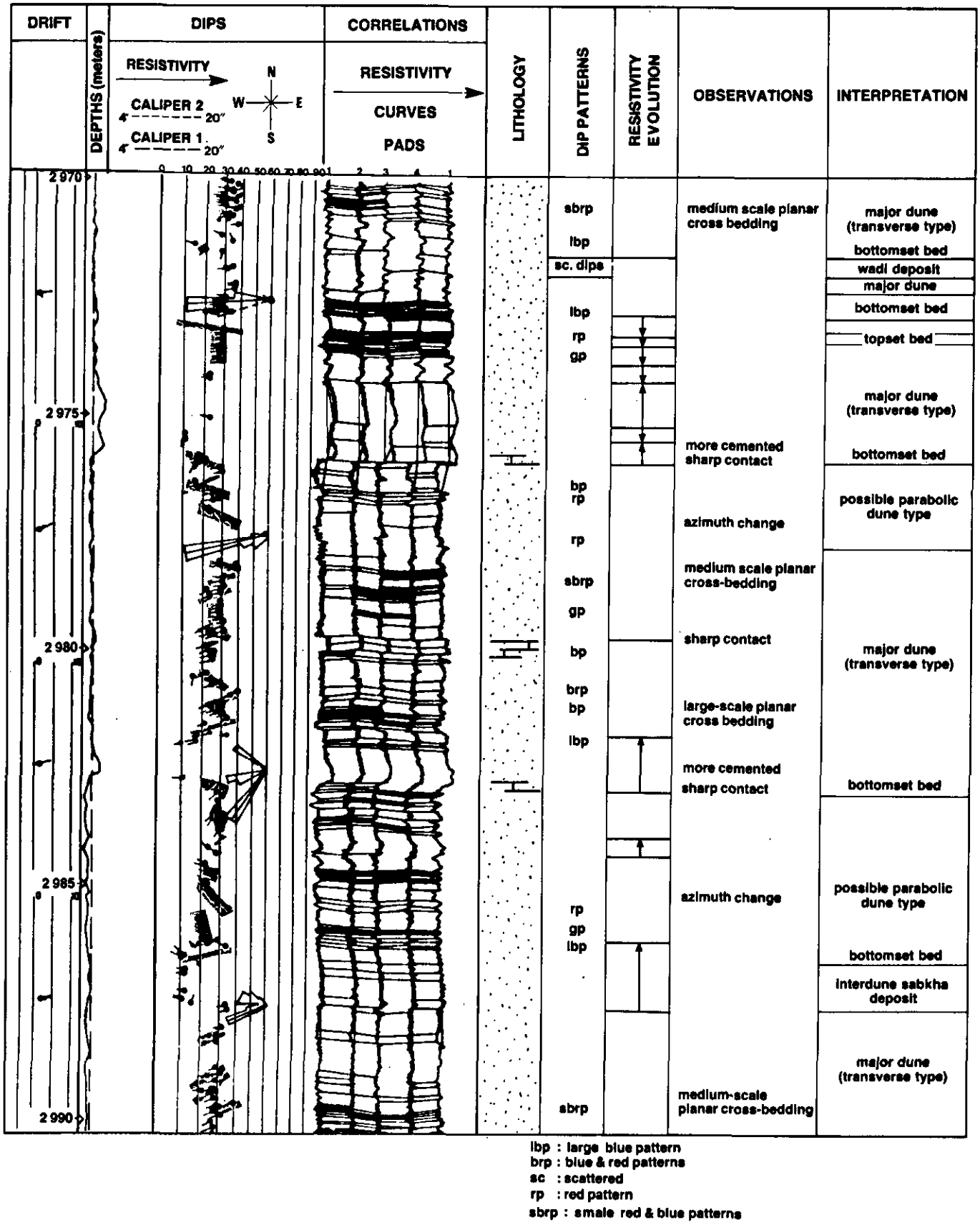

Fig. 6.3-20. - Example of GEODIP results and its interpretation indicating an aeolian environment.

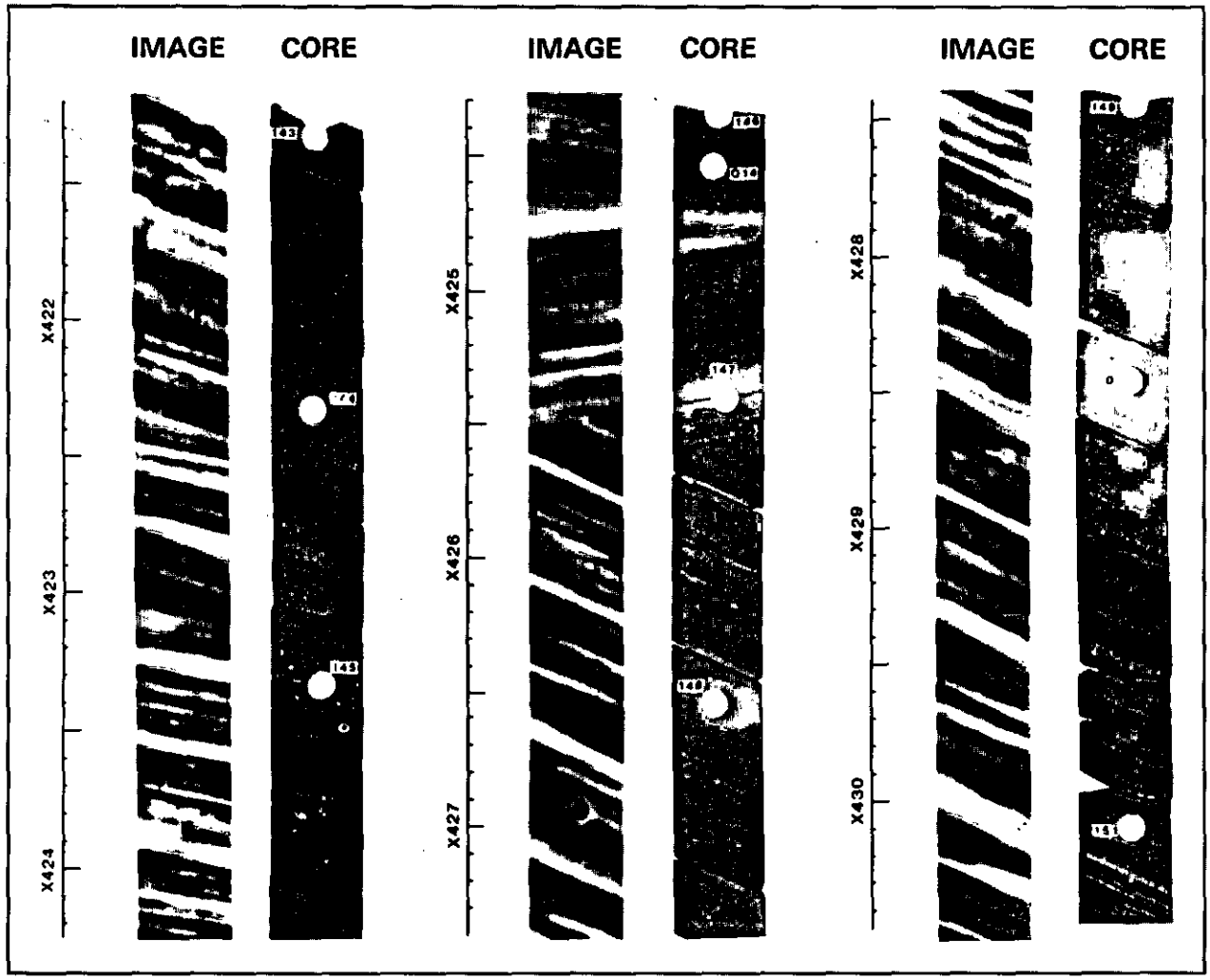

Fig. 6.3-21. - Comparison of core photographs and FMS images in an aeolian environment (courtesy of Schlumberger).

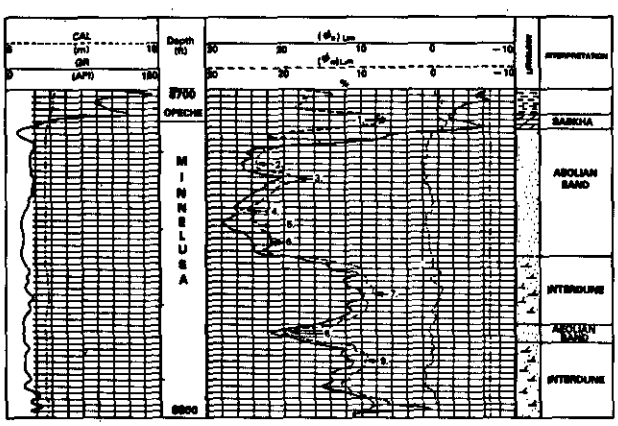

Fig. 6.3-22. - Composite-log showing sabkha, aeolian and interdune deposits in the Minnelusa, Powder River Basin, U.S.A.

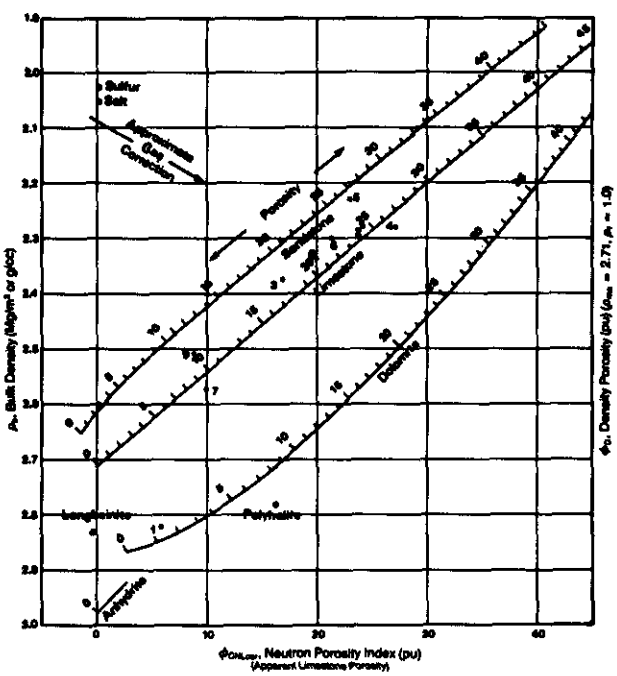

Fig. 6.3-23. - Density-neutron crossplots indicating the main lithology of Fig. 6.3-22.

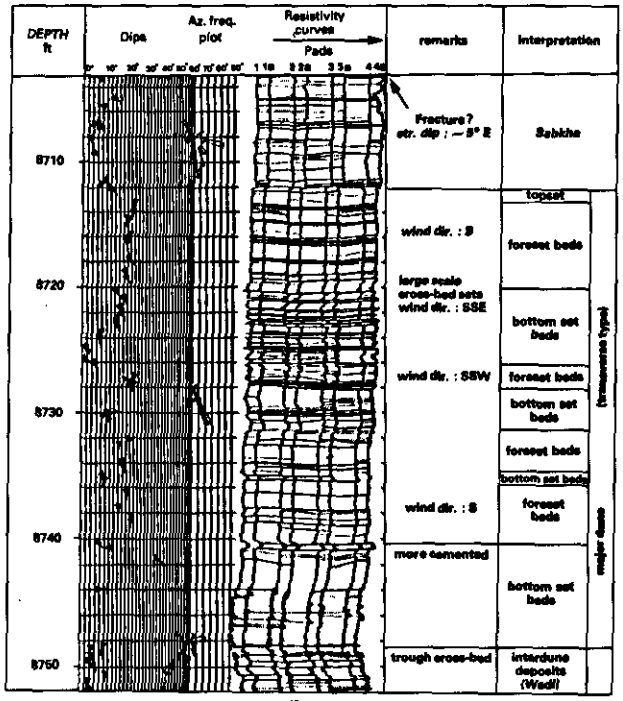

silty-shaly deposits. Wadi deposits can be also observed. They are characterized by coarser, poorly sorted sediments richer in clay material and consequently a little more radioactive. They show scattered dips (through cross-bedding), or even no dip (conglomeratic levels or mud-cracked clays). Another example of an aeolian environment with interdune and sabkha deposits is illustrated by Fig. 6.3-22 to 6.3-24. It comes from the Minnelusa Formation, Powder River Basin, U.S.A.

6.3.3.6. Confusion with other Environments

The log responses, especially dipmeter, are so characteristic that confusion with other environments is unlikely.

◀ Fig. 6.3-24. - LOCDIP presentation on the same interval and its interpretation.

6.4. FLUVIAL ENVIRONMENT : BRAIDED SYSTEM

6.4.1. DEFINITION

A continental environment characterized by deposits resulting from a river system of an interlaced network of low sinuosity channels. The style of a braided system is shown in Fig. 6.4-1, and representative vertical sections in Fig. 6.4-2.

6.4.2. GEOLOGICAL FACIES MODEL

6.4.2.1. Lithology

Two parameters must be considered separately.

6.4.2.1.1. *Composition*

Braided river deposits are typically composed of texturally and chemically immature gravels and sands with a sand-shale ratio greater than 1. They can be classified as *lithic arenites to lithic wackes* (Pettijohn *et al.*, 1972). Only minor amounts (some 10 %) of silt are found and correspond to abandoned channel deposits (Selley, 1976). Gravels and pebbles are rock fragments, the composition of which depends on the source areas. Shale pebbles and reworked clay-ironstone concretions may be present. Common mineral constituents are quartz, feldspars, micas. Glauconite is absent (non marine deposit). Carbonaceous organic matter is very rare, due to the oxidizing nature of the environment (Selley, 1976). Alteration of iron-rich minerals to haematite or limonite is frequent. Uranium bearing minerals may accumulate along with gold as placer deposits (e.g. Blind River in Canada and Witwatersand basin in South Africa). These minerals concentrate at the bases of channels (Minter, 1978).

Fig. 6.4-1. - Aerial photograph of a braided stream choked with erosional debris, near the edge of a melting glacier (Photo by B. Washburn, in Press & Siever, 1978, Fig. 7-25).

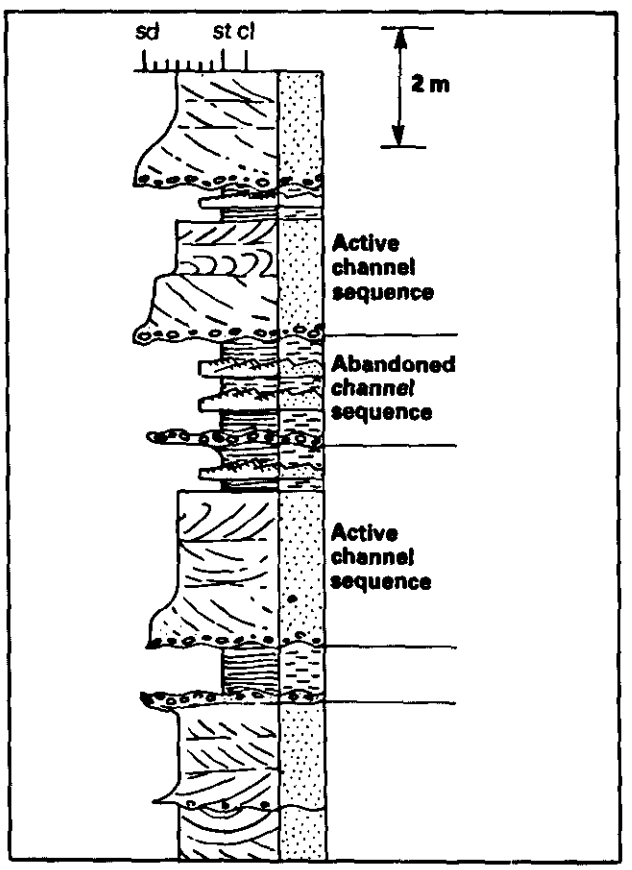

Fig. 6.4-2a. - Theoretical vertical cross-section of a braided *alluvial channel system deposits. Sedimentation occurs almost* entirely in the rapidly shifting complex of channels. A flood plain is absent (from Selley, 1976, Fig. 101).

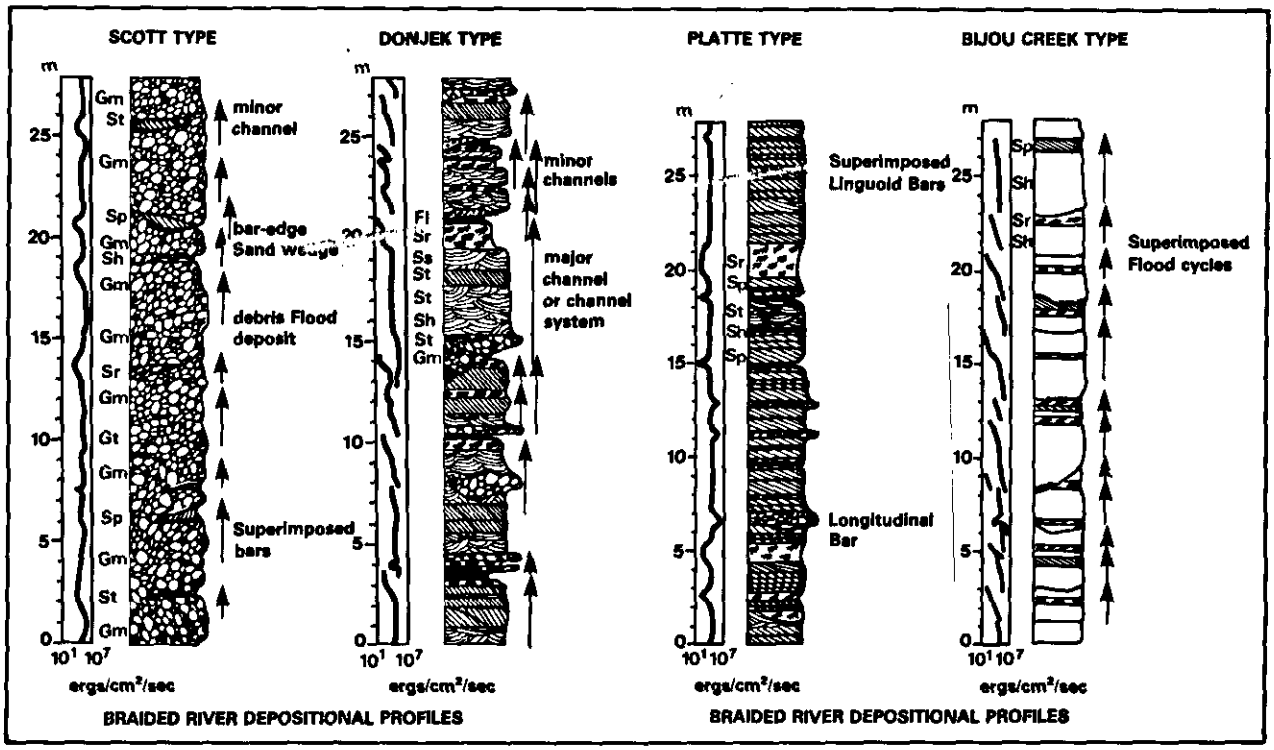

Fig. 6.4-2b. - Four braided river depositional profiles representing the four models of braided river systems related to the energy involved during deposition, and consequently to the proximity to the apex (from Miall, 1977).

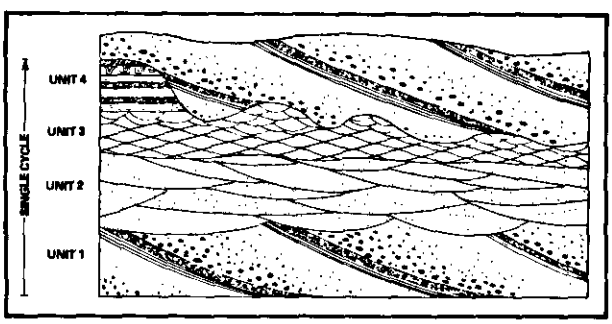

Fig. 6.4-3. - Schematic vertical sequence of a braided river deposit. Unit 1 : large scale cross-bedding with pebbles. Unit 2 : medium sand megaripple bedding. Unit 3 : fine sand small ripple bedding. Unit 4 : fine sand and mud horizontal bedding, occasional convolute bedding (from Reineck & Singh, 1975, based on data of Doeglas, 1962).

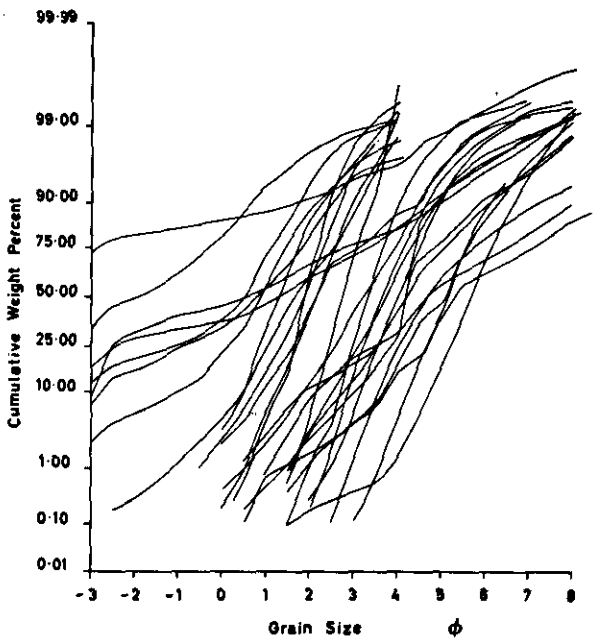

Fig. 6.4-4. - Cumulative size frequency curves of samples from braided river systems (from Williams & Rust, 1969, Fig. 4). For a given sample the range of grain size reflects the poor sorting.

6.4.2.1.2. *Texture*

Poor to moderate sorting (gravel to sand) with low sphericity and with moderate to low grain-matrix ratio is observed; abundant silt in fine end tail (Pettijohn *et al.*, 1972). Conglomerates range from clast-supported matrix-free, through clast-supported with interstitial sandy matrix, on to sandy conglomerates with dispersed clasts. Matrix-free conglomerates are reasonably well sorted and unimodal; conglomerates with sandy matrix show a bimodal distribution; matrix-supported conglomerates are unimodal with poor sorting.

6.4.2.2. Structure

Table 6.4-1 summarizes the principal sedimentary structures and their abundance found in a braided river deposit. Asymmetrical small scale

Table 6.4-1
Principal sedimentary structures and their relative abundances
(from Williams & Rust, 1969, Table 1).

Level/ Stream Channel	Lamination, Cross-Lamination				Ripples							Bedding		Large-Scale Structures				Small-Scale Structures													
					Small-Scale					Large-Scale				Erosional		Depositional		Surface								Cross Section					
	Parallel	Lenticular	Small Scale X-L	Large Scale X-L	Straight	Sinuous	Lunate	Linguoid	Wave	Lunate	Linguoid	Massive	Graded	Scour Hollows	Channels	Bar, Avalanche Face	Bars	Rill Markings	Current Crescents	Grain Lineation	Plant Lineation	Rain Pits	Desiccation Cracks	Silt Volcanoes	Tracks and Trails	Bedded Organics	Color Banding	Bioturbation	Imbrication	Bank Slippage
4	O	R										O		R	C		C								R	A	C	A		
3	C	O	A	O			A			O		O	O	C	A	O	A	R	C	R	R	O	C		C	C	C	C	O	
2	C	R	A	C			A			R		O	O	C	A	R	A	R	A	O	R	C	O	O	C	R		R	O	R
1	O	R	A	C			A			R		O	R	C	A	O	A	R	A	O	R	C	O	O	R	R		R	O	O
Overall (1-4)	C-O	O-R	A	C	O	A	A	A	C	R	R	O	O-R	C-R	A	O-R	A	R	A	O-R	R	C-O	C-O	O	C-R	A-R	C-R	A-R	O	O-R

A = Abundant, C = Common, O = Occasional, R = Rare.

ripples and abundant well oriented cross-bedding, commonly unimodal, are observed, as well as small scale cross-laminations. The bedding may be either massive or graded. Beds tend to be lenticular with erosional scour; infrequent tracks and trails. Depositional bars are abundant.

6.4.2.3. Boundaries

Lower contact of the sand is erosional. Upper contact is also frequently abrupt.

6.4.2.4. Sequences

Four units or facies can be distinguished. They are arranged as shown in Fig. 6.4-3 to compose a theoretical vertical sequence.

Unit 1: large scale cross-bedding mostly coarse-grained with pebbles, with erosional lower contact. Discontinuous lenses of sand, silt and clay can be present. This unit is related to lateral and downstream advance of channel bars.

Unit 2: megaripple bedding in medium sand; large and small scale cross-stratifications and ripples. They correspond to migrations of channel sand bars.

Unit 3: small ripple bedding in fine sand composed of banded sands and silts. Ripple laminated or massive. Small scale ripples, microbars and scours. They may be related to recently abandoned channel deposits.

Unit 4: fine sand and mud showing horizontal or convolute bedding. This unit corresponds to abandoned channels.

Such fining upward sequences are best developed in channel fill sediments. The grain size gradually decreases upward and the sorting improves upward. Coarse- and fine-grained units may be interbedded. Small grain size reversals can occur. They are due to fluctuating river stages.

In relation to the energy involved during deposition, Miall (1977) proposed four models of braided river sediments, which are shown in Fig. 6.4-2b.

6.4.2.5. Geometry of the Body

"Braided channel systems are characterized by a network of constantly shifting low-sinuosity anastomozing courses" (Selley, 1976).

Both sandy and gravelly braided rivers migrate laterally leaving sheet-like or wedge-shaped deposits of channel and bar complexes preserving only minor amounts of floodplain material (Cant, 1982).

In detail, three main geomorphological bodies are recognized : channels, bars and islands (Williams & Rust, 1969) (Fig. 6.4-5).

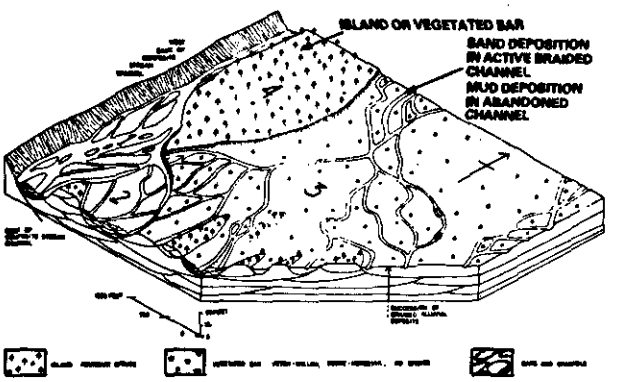

Fig. 6.4-5. - Composite model of a braided river deposit (from Williams & Rust, 1969, Fig. 27).

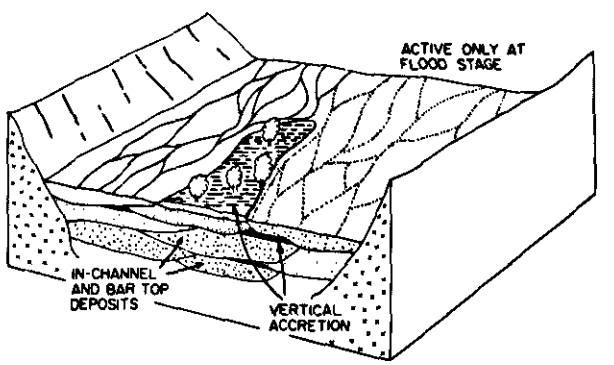

Fig. 6.4-6. - Block diagram of a braided sandy system with low sinuosity channels. Vertical accretion can occur during flood stage (from Walker, 1969).

Channels vary considerably in size and are arranged in five hierarchical orders. *A composite stream channel* is straight with an average width of one mile (1.6 km). *Stream channel* is characterized by a braided network of three finer order channels. These smaller channels - width up to hundreds of feet - are generally of low sinuosity. The basic sedimentary fill succession is fining-upward. In cross-section the channels are erosional, occurring in a very high frequency association. The main channel is divided into several channels which meet and redivide (Fig. 6.4-5 to 6.4-7). Channel bars, which divide the stream into several channels at low flow, are often submerged during high flow. They are commonly composed of coarse-grained lag deposits of the stream (often gravels) which could not be carried by the flow.

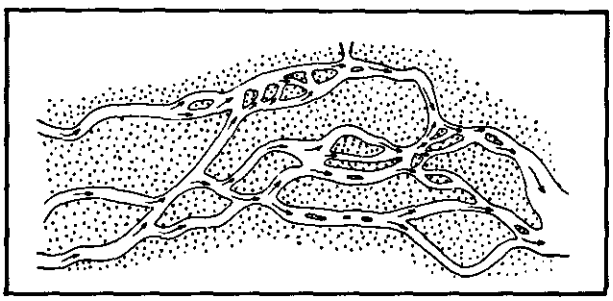

Fig. 6.4-7. - Aerial distribution of a braided system showing hierarchical organization of channels and bars (from Allen, 1965).

Once such a channel bar is formed, it may stabilize by the deposition of fine-grained sediment on its top during high flows and may later be colonised by vegetation forming an island.

Three types of *bar are present*: longitudinal, transverse, and point bars. Longitudinal bars are the most abundant (95 %) and occur as lateral bars along channel sides and central bars in mid-channel areas. They are invariably elongate downstream. Maximum length and width vary from a few feet to hundreds of feet. The surface of the bar is *never smooth, including a very wide range of* large- and small-scale structures. They are composed of gravel, sand, and silt-mud admixtures. Bars tend to be built up by lateral accretion down stream. The upstream end is partly eroded.

Islands are the most permanent features on the valley floor within a braided system. They are elongate downstream. Root evidence or carbonaceous material can be present.

Braided rivers are characterized by wide channels of changing position, and rapid and continuous shifting of the sediment. Consequently, an *individual unit may be between . 5 and 8 km wide.* Their length may commonly range from 10s to 100s km. The thickness of an individual unit ranges from several decimetres to 30 metres. The width-depth ratio is high. The area occupied by braided *rivers may be very wide (100s km) and coalescing* bars and sand-flats will result in a laterally continuous and extensive sand sheet, unconfined by shales (Walker, 1979).

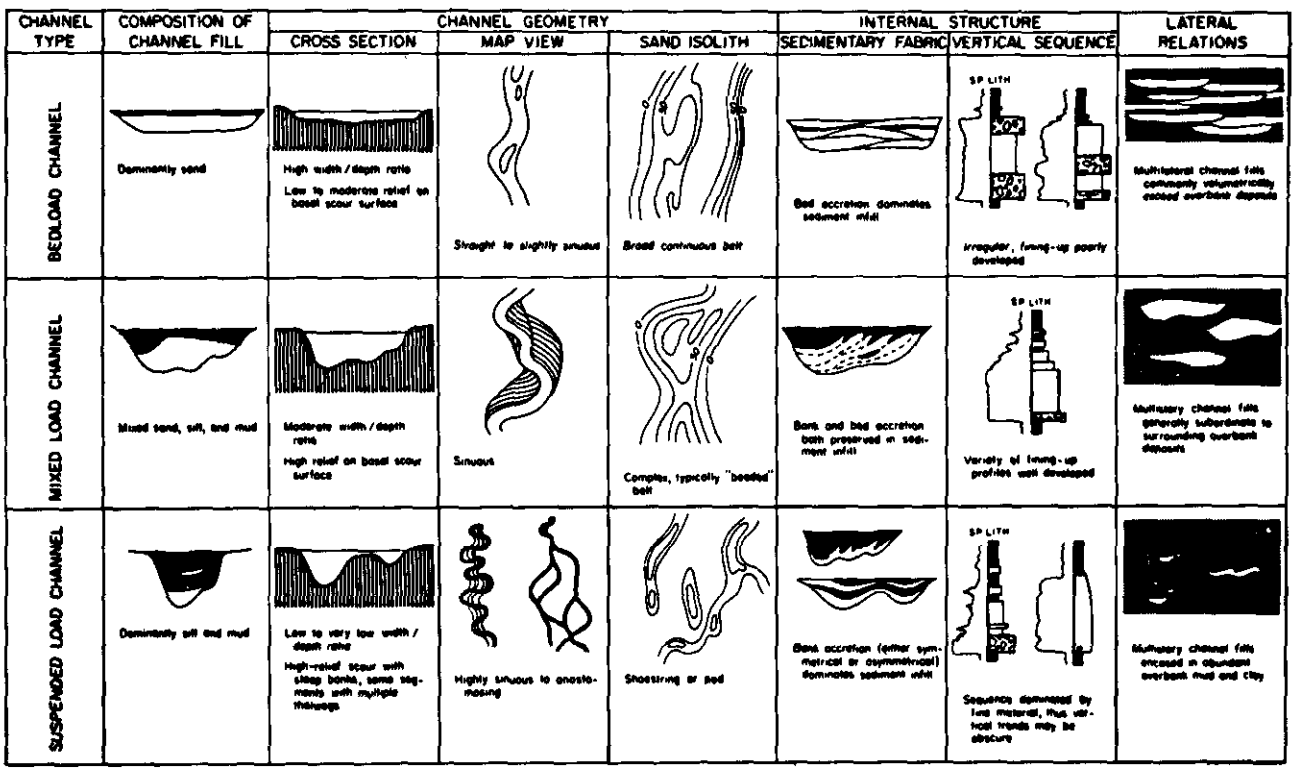

Fig. 6.4-8. - Geomorphological and sedimentary characteristics of bed-load, mixed-load, and suspended-load stream channel segments (from Galloway, 1977, and in Galloway & Hobday, 1983, Fig. 4-13).

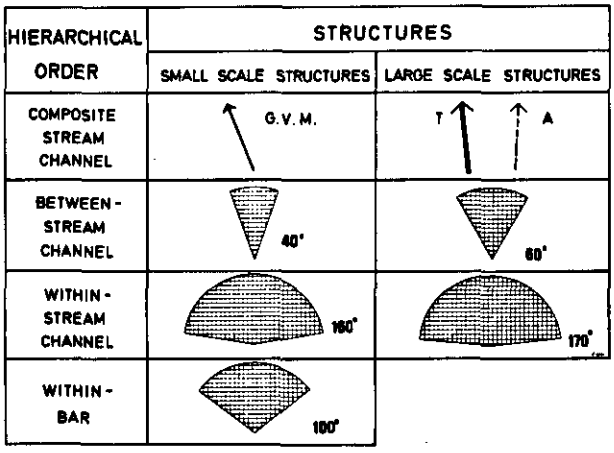

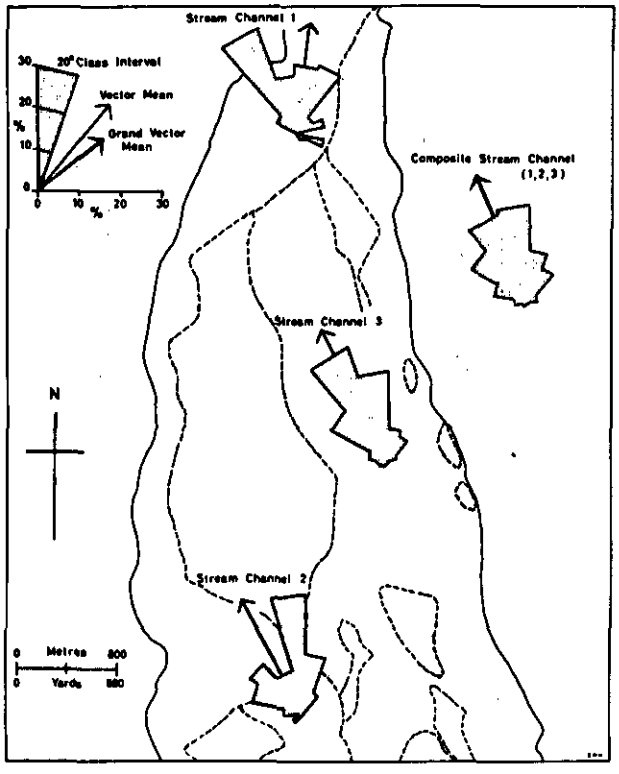

Fig. 6.4-9. - Dispersion of the azimuth of the directional current flow from the structures (from Williams & Rust, 1969, Fig. 28 & 23).

6.4.2.6. Directional Current flow Model

The ranges of directional current data for the hierarchical orders of small scale and large scale structures are summarized in Fig. 6.4-9. They show a characteristic unimodal azimuth distribution with a moderate to low scatter, along the down dip direction of the palaeoslope.

6.4.2.7. Reservoir Characteristics

Braided river deposits may constitute potentially good reservoir rocks with up to 30 % porosity and permeabilities of thousands of millidarcys. The

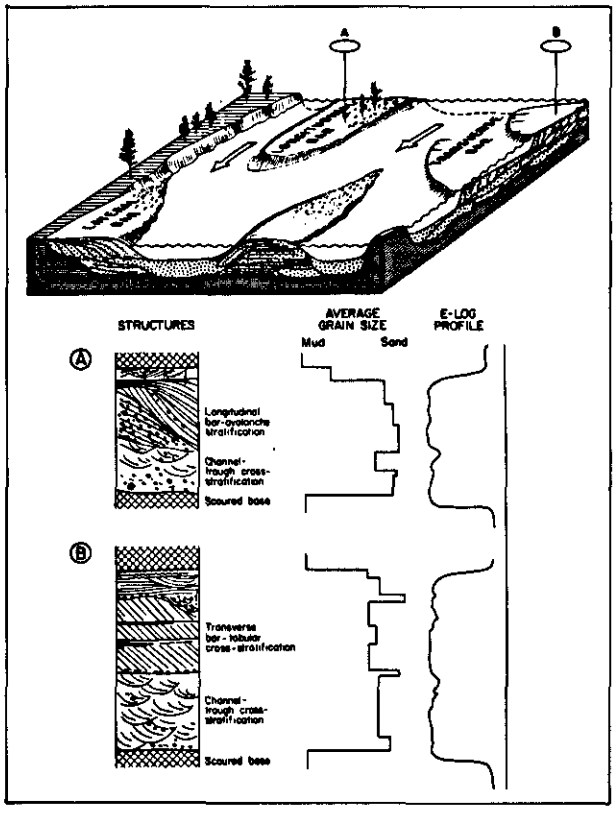

Fig. 6.4-10. - Generalized depositional model, vertical sequences of grain size and sedimentary structures, and S.P. log profiles produced by a low-sinuosity, braided channel. Sequence (A) is dominated by migration of a gravelly longitudinal bar. Sequence (B) records deposition of successive transverse bar cross-bed sets upon a braided channel fill (from Galloway & Hobday, 1983, Fig. 4-4).

shales are of limited lateral extend and do not play a major role in blocking fluid migration. They do not commonly form stratigraphic traps.

6.4.3. WELL-LOG RESPONSES AND CHARACTERISTICS

Galloway & Hobday (1983) proposed a generalized depositional model for a braided channel with theoretical S.P. log response (Fig. 6.4-10). The S.P. shape is typically a smooth cylinder. The responses and characteristics of the other logs will be illustrated by a case-study : The Upper Tipam Formation (Assam, India), the composite-log of which is represented by Fig. 6.4-11.

6.4.3.1. Electro-Lithofacies

A detailed study of the various crossplots was made in order to define the mineralogical composition of the formation.

The ρ_b vs ϕ_N crossplots (Fig. 6.4-12) with S.P. (Fig. 6.4-12b) and EATT (attenuation of the electromagnetic wave) (Fig. 6.4-12c) on the Z-axis

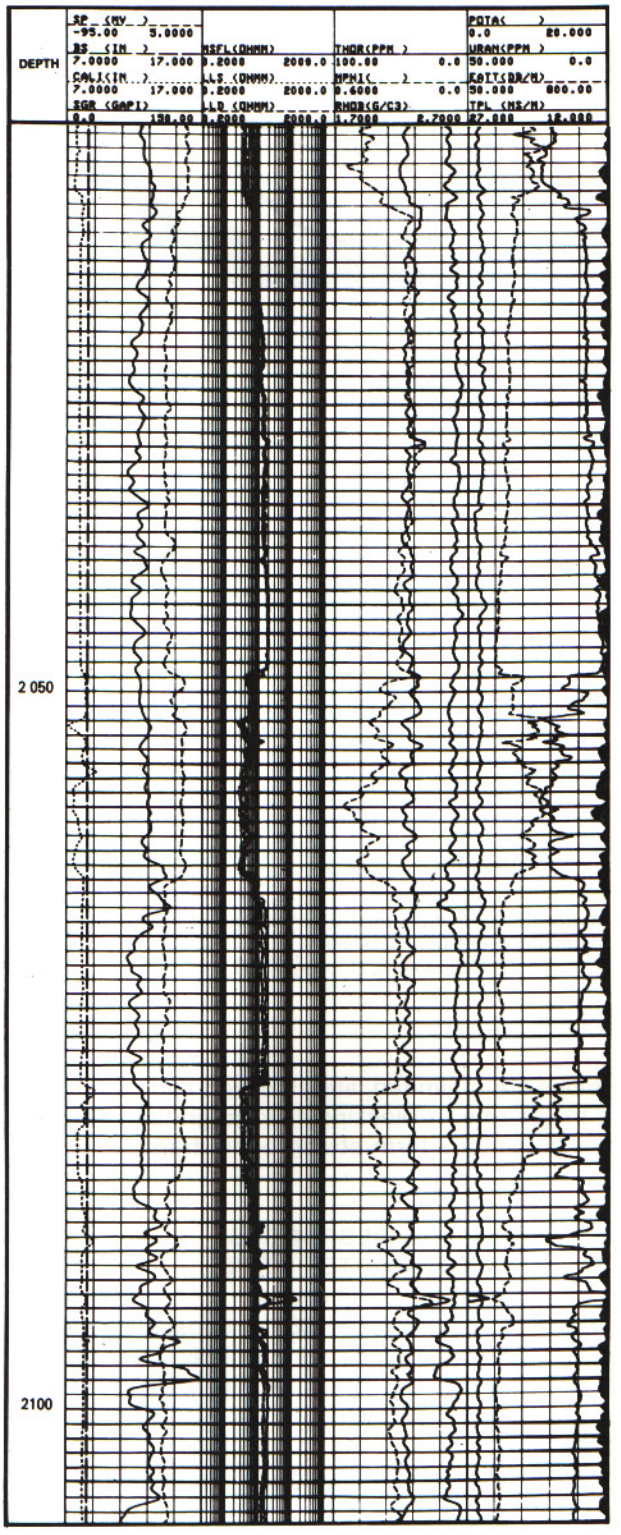

Fig. 6.4-11. - Typical log responses over a braided river system (from Schlumberger, Well Evaluation Conference, India, 1983).

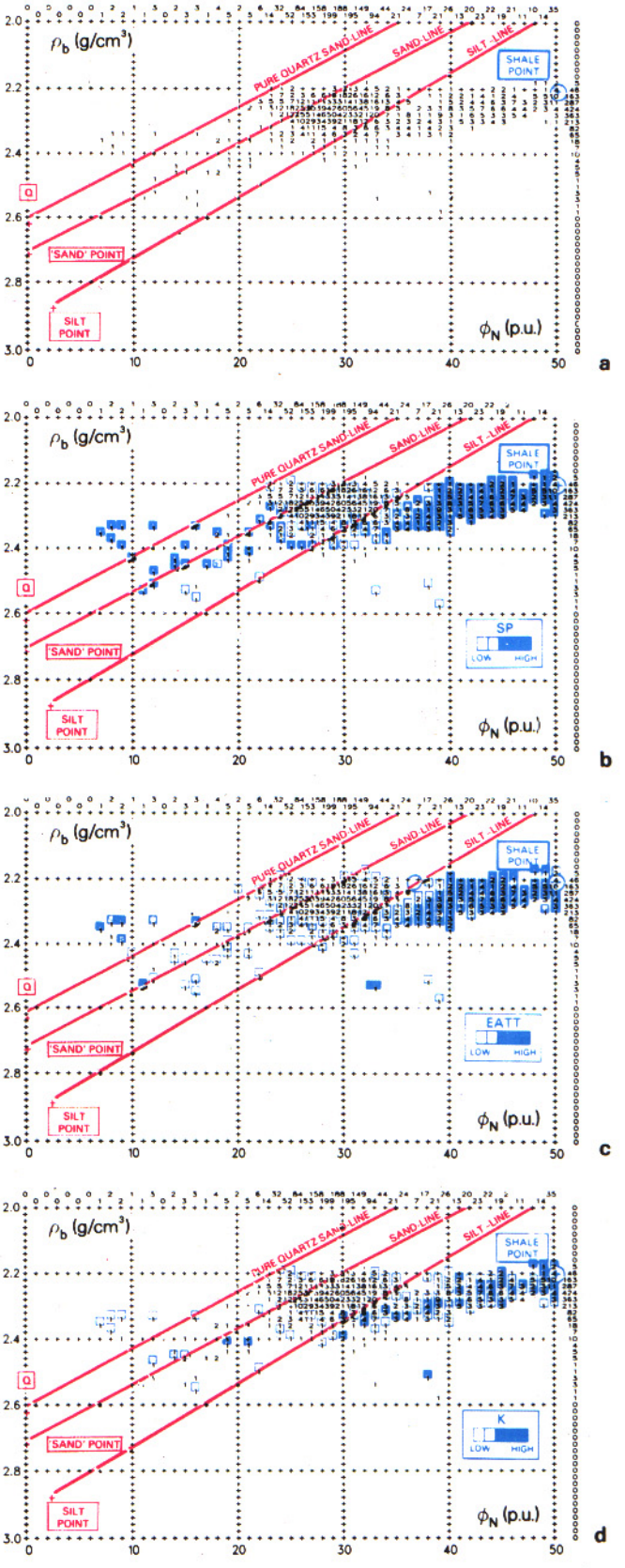

Fig. 6.4-12. - Density-neutron porosity crossplots with (a) frequency,(b) SP, (c) EATT and (d) potassium content on Z-axis (interpretation from Serra, in Schlumberger, Well Evaluation Conference, India, 1983).

show, very clearly, the change of grain size in the sands. The sandstone line corresponds to the line from the fluid point (ρ_b = 1., ϕ_N = 100 %) going through the most north-westerly points with low SP and EATT values. Similarly, the siltstone line

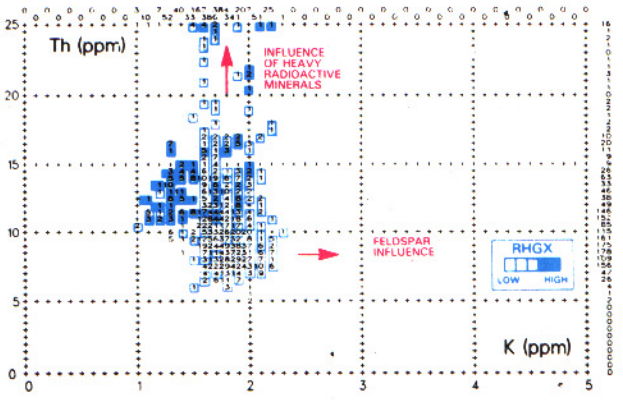

Fig. 6.4-13. - Thorium vs potassium with grain density on the Z-axis (interpretation from Serra, in Schlumberger, Well Evaluation Conference, India, 1983).

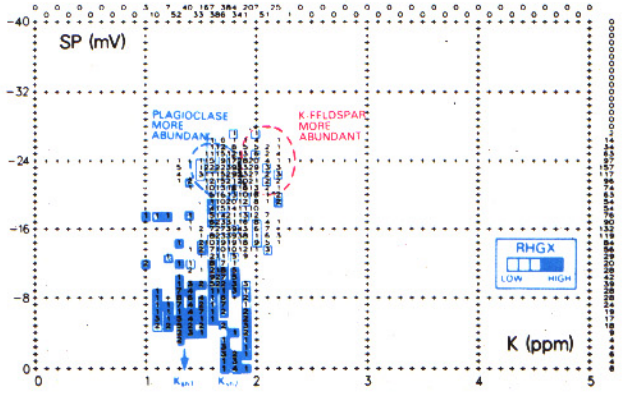

Fig. 6.4-14. - SSP vs potassium with grain density on the Z-axis (interpretation from Serra, in Schlumberger, Well Evaluation Conference, India, 1983).

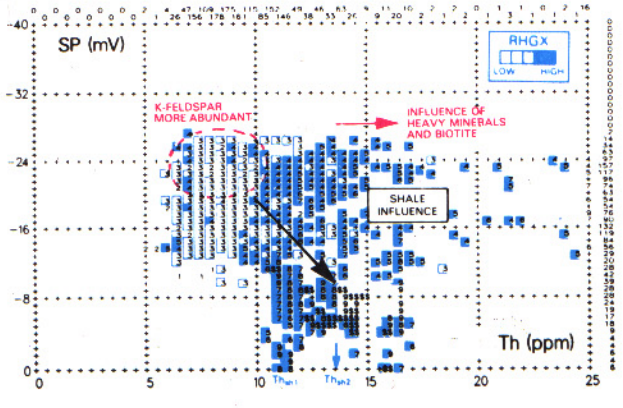

Fig. 6.4-15. - SSP vs thorium with grain density on the Z-axis (interpretation from Serra, in Schlumberger, Well Evaluation Conference, India, 1983).

can be drawn from the fluid point through the lowermost points with low to moderate SP and EATT values. The "sand point" corresponds to $\phi_N = 0$ on the sandstone line, and the "silt point" is obtained from the intersection of the siltstone line with a line drawn from the sand point parallel to the equiporosity line for the sand-silt mixture.

The moderately high and constant potassium values on the corresponding density-neutron crossplot (Fig. 6.4-12d) for all the sand and silt points suggest an *immature rock* composed of quartz, feldspar and plagioclase with mica and heavy radioactive minerals (e.g. zircon).

The potassium vs thorium crossplot (Fig. 6.4-13) confirms the presence of feldspar and also highlights the high thorium concentration from heavy radioactive minerals such as zircon.

The variation in the feldspar and biotite concentration in the sands can be recognized by analysing the evolution of the potassium content with respect to grain density ($(\rho_{ma})_a$) on the Z-axis (Fig. 6.4-14). The cluster of points with a high SSP deflection corresponds to sand. Within this cluster, plagioclases are more abundant when the potassium contentis lower (1.5 to 1.8 %) and the density higher, while K-feldspar concentration increases with higher potassium content (1.8 to 2.2 %) and lower density. The shale trend is clearly observed toward the low SSP values and high grain densities. In fact, over the interval studied, it is possible to identify two types of shale, one which appears in thick beds, and the other which is present as thin intercalations around 2260 and 2180 m. The corresponding K_{sh} can be selected for each shale from this crossplot.

On the SSP vs thorium (Th) crossplot (Fig. 6.4-15) the K-feldspar is more abundant in the sand cluster with lower thorium values (6.5 to 10 ppm) and lower densities (2 to 3 on the Z-axis). The increase in the content of biotite and heavy radioactive minerals corresponds to higher thorium values (10 to 18 ppm) and higher densities. The presence of the two type of shale is confirmed, and the general shale trend is clearly indicated. Core analysis confirmed the mineralogical composition deduced from the study of the crossplots.

6.4.3.2. Dipmeter curve Shape and Dip Patterns

From the GEODIP analysis (Fig. 6.4-16) the following conclusions can be done :

- Each sand starts with an abrupt lower contact, often non planar (four dip computation or no dip on GEODIP display). This feature could be related to possible erosional scoured surfaces.
- The sands are massive, apparently homogeneous, but with a few randomly distributed highly resistive peaks appearing only on 1, 2 or 3 curves. The resistive intervals show low GR, t_{pl} and hydrogen content, and high density. The mineralogy associated with such levels is not obvious, but chert or hydrated silica (opal) could possibly be present. If $(\rho_{ma})_a$ is higher than 2.65 a late diagenetic calcite formation may be involved.

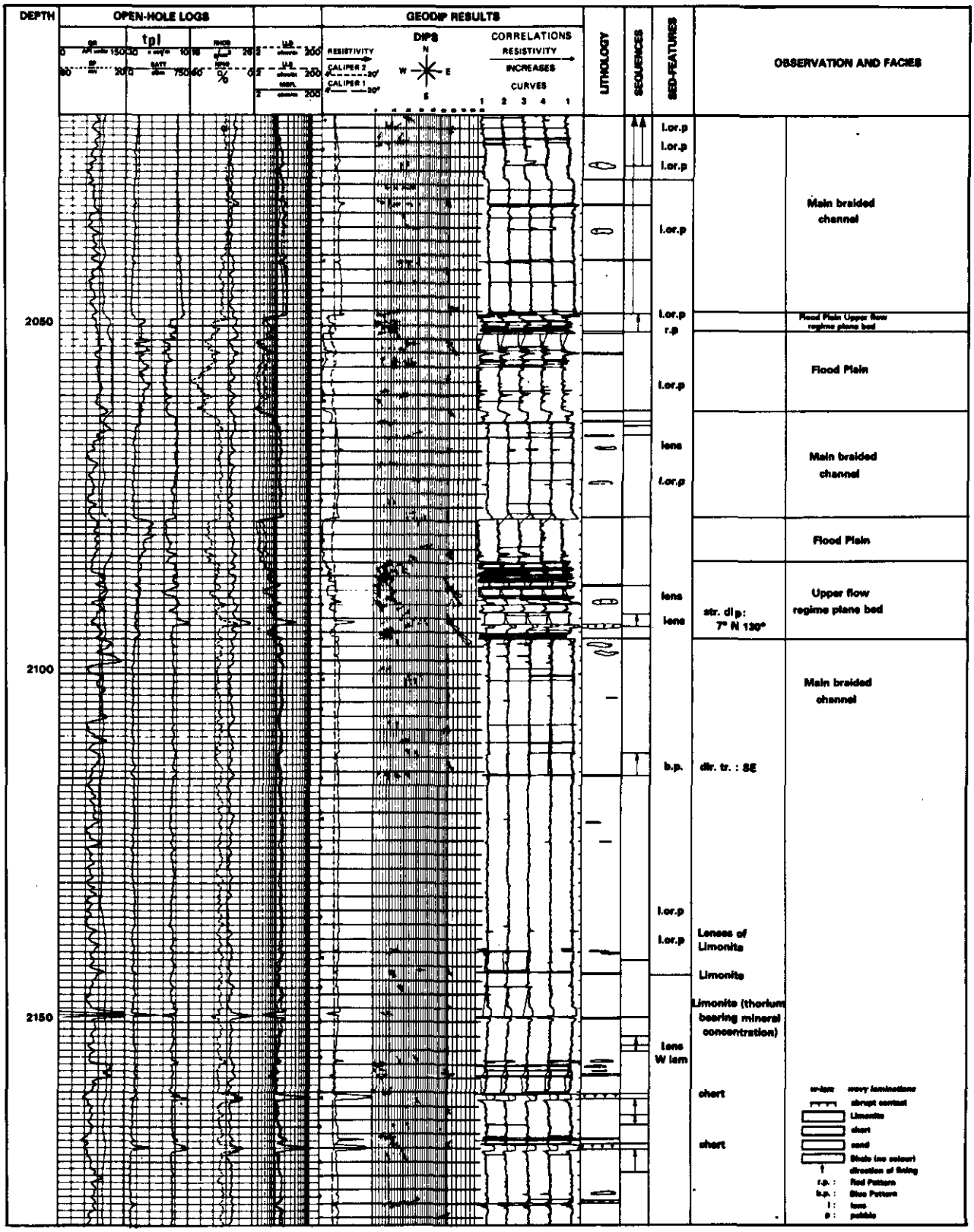

Fig. 6.4-16. - GEODIP arrow-plot on the same well and its interpretation (interpretation from Serra, in Schlumberger, Well Evaluation Conference, India, 1983).

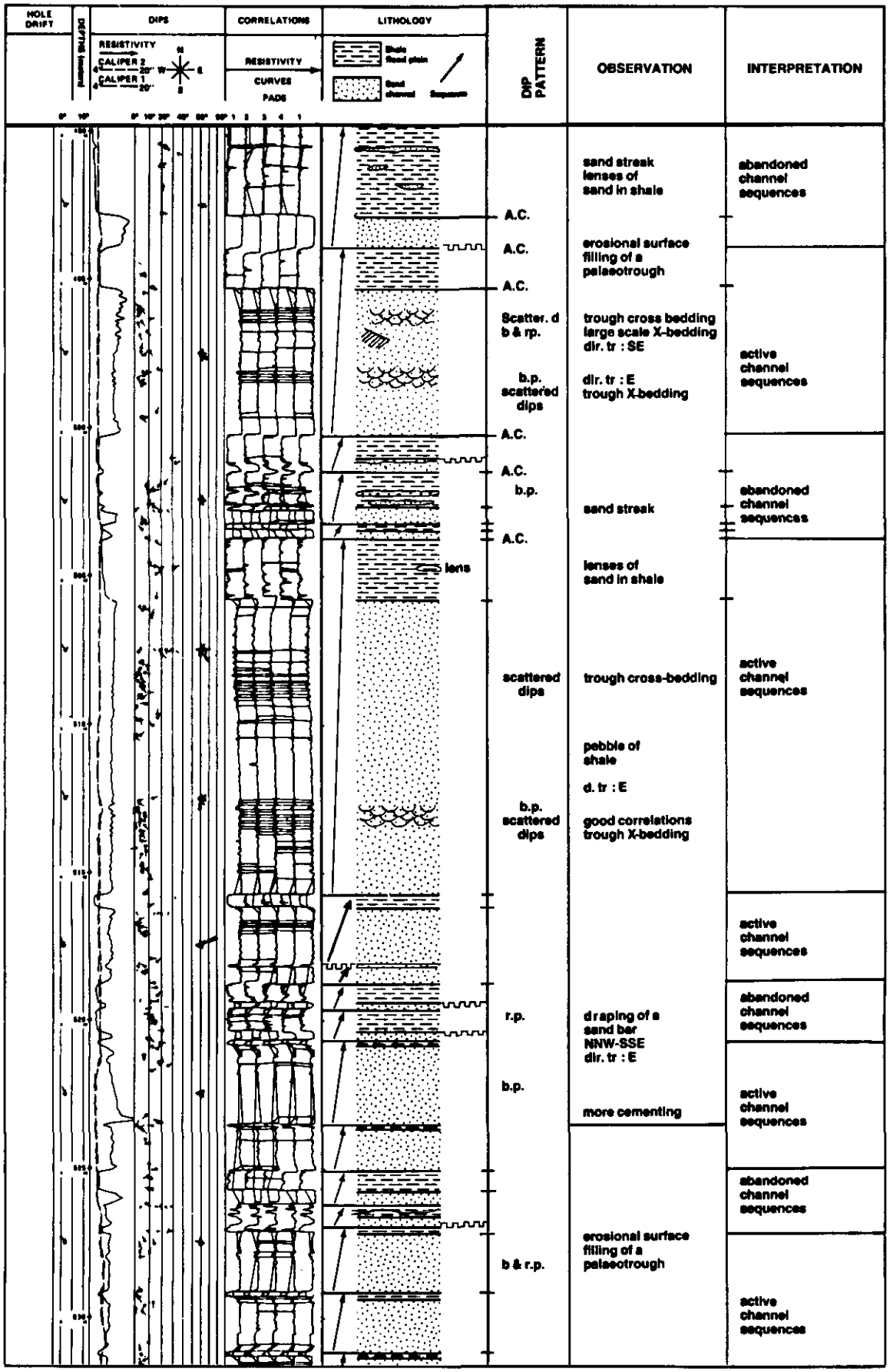

Fig. 6.4-17. - Other example of a braided river system from Africa as can be interpreted from GEODIP.

- Some thin, very conductive spikes are seen within the sands. Such features have high density, hydrogen content, EATT, t_{pl} and GR values. This could be limonite with concentration of thorium-bearing minerals (zircon).
- The sand-shale ratio is high.
- The general tendency within the sands appears to be fining upward.
- The upper intervals of the different sands show thin laminations.
- Few blue patterns can be seen. They generally indicate a S to SE direction of transport.

6.4.3.3. Boundaries

As it can be easily seen on the dipmeter resistivity curves the lower and upper sand boundaries are sharp or abrupt giving a general cylindrical shape.

6.4.3.4. Electro-Sequences

The general evolution of the resistivity curves indicates a fining upward sequence in the sands.

6.4.3.5. Thickness

Thickness of sand bodies is variable, but generally important in this example.

Another example from Africa, illustrated by Fig. 6.4-17 shows very variable thicknesses. As can be observed from the GEODIP analysis, all the other features are similar to the Tipam ones.

6.4.3.6. Confusion with other Environments

Cylinder shape of braided channels can be confused with the same features found in chute-bars (see Fig. 6.5-11).

6.5. FLUVIAL ENVIRONMENT : MEANDERING SYSTEM

6.5.1. DEFINITION

A continental environment characterized by deposits resulting from a river system of high sinuosity channels generated by a mature stream swinging from side to side accross its flood plain on a gentle slope. The style of a meandering river system is shown in Fig. 6.5-1, and a representative vertical section in Fig. 6.5-2.

Fig. 6.5-1. - Aerial photograph of meander bed and floodplain of the Animas River a few miles above Durango, Colorado (from Shelton, 1966, in Press & Siever, 1978, Fig. 7-26).

6.5.2. GEOLOGICAL FACIES MODEL

6.5.2.1. Lithology

Two parameters must be considered separately.

6.5.2.1.1. *Composition*

The main minerals are quartz, more or less altered feldspars and micas, and the sandstones range from quartzitic to lithic arenites due to their low to moderate chemical maturity. The most common cements are siliceous or calcareous. In the bedload of the channels, clay pebbles can occur; they come from levees slumping. Glauconite is absent. Peat and coal are present as beds (flood plain) and small fragments (channels). Carbonate and iron concretions may be formed in areas with a high rate of evaporation (flood plain). Clays are generally kaolinitic but other types may be present depending on the climatic conditions and the distance from the source area. During diagenesis fluids circulating in the subsurface may react with the detrital unstable minerals resulting in clay cementation. Calcite cement can also precipitate.

6.5.2.1.2. *Texture (see Table 6.5-1)*

Meandering river deposits show normal grading and are typically composed of sands, silts and shales with a sand-shale ratio generally lower than

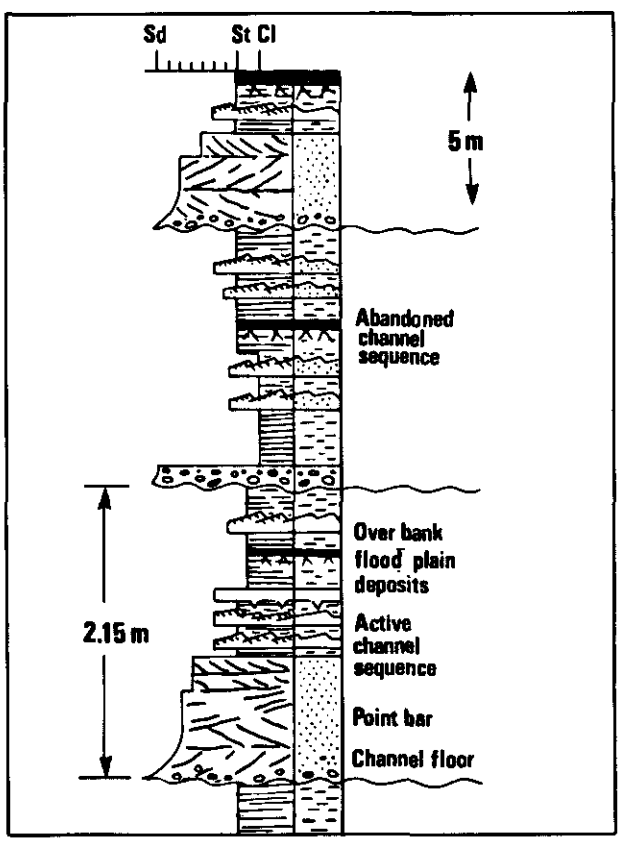

Fig. 6.5-2. - Generalized section of fining-upward sequence in a meandering system in Devonian Catskill facies, U.S.A. and south Wales (from Selley, 1976, Fig. 99).

Table 6.5-1
Physical characteristics of fluvial or valley-fill model. Line weight is suggestive of abruptness of transition between units
(adapted from Visher, 1965).

	MEAN GRAIN SIZE	SORTING	GRAIN SIZE RANGE	SEDIMENTARY STRUCTURES	GEOMETRY	SEDIMENTS
CHANNEL FILL	FINE	POOR-FAIR	SILT-CLAY	HORIZONTAL LAMINATION MUD CRAKS PLANTS-ROOTS	IRREGULAR (P)	
BACK SWAMP	VERY FINE	POOR	SILT-CLAY	HORIZONTAL LAMINATION PLANTS-ROOTS-COAL	IRREGULAR	
FLOOD PLAIN			SILT-CLAY	HORIZONTAL LAMINATION SLUMP STRUCTURES MUD CRAKS NEAR TOP	ARCUATE	
NATURAL LEVEE			FINE SAND-SILT	SMALL SCALE X-BEDS HORIZONTAL LAMINATED	WEDGE SHAPED (P)	
RIPPLE X-BED ZONE			FINE SAND-SILT	CLIMBING RIPPLES RIPPLE X-BEDDING	WIDTH TO 30 MI	
LAMINATED ZONE			SAND-SILT	HORIZONTAL BEDDING OR LAMINATION	WIDTH TO 30 MI	
MEGA-RIPPLE ZONE		VERY-GOOD	SAND	FESTOON OR PLANAR X-BEDDING	WIDTH TO 30 MI	
BEDLOAD ZONE	COARSE	POOR-GOOD	CLAY CHIPS PEBBLES COARSE SAND	POORLY BEDDED	WIDTH TO 30 MI	

1. The basal zone is poorly sorted and grain size ranges from conglomerates to coarse grained sands. It grades upward to a well sorted medium to fine sands. The upper zone is generally composed of very fine sands, silts and some clays and may be poorly to fairly sorted (Visher, 1965; Selley, 1972).

6.5.2.2. Structure

Table 6.5-1 summarizes the principal sedimentary structures found in a meandering system deposit in relation to the main facies. Sedimentary structures are related to the flow regime and consequently organized in sequences. The sequence starts with an erosional surface with scour troughs, followed by medium-scale cross-bedding; parallel laminations which are related to upper flow regime; foreset bedding in point bar or chute bar with small trough sets (Fig. 6.5-3 and 6.5-4, Mc Gowen & Garner, 1970). Flood plain deposits show horizontal or convolute bedding, generally destroyed by bioturbation. Rootlets may also be present.

6.5.2.3. Boundaries

Abrupt, sharp, erosional lower and lateral contacts are observed; they are gradational toward the top.

6.5.2.4. Sequences

Fundamentally, the sequence is fining upward (Fig. 6.5-5 from Allen, 1970). It consists of in-

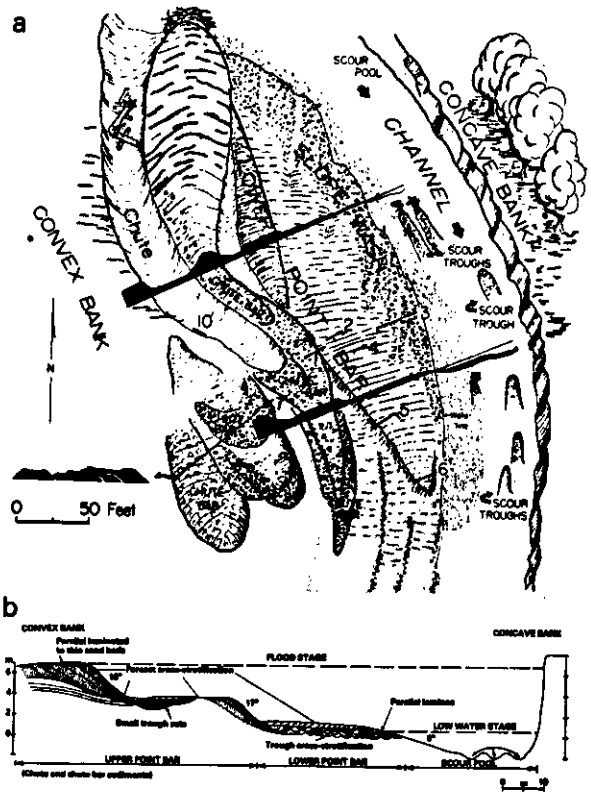

Fig. 6.5-3. - Topographic features and internal structure of a coarse-grained point bar. (a) Plan, (b) cross-section (after McGowen & Garner, 1970).

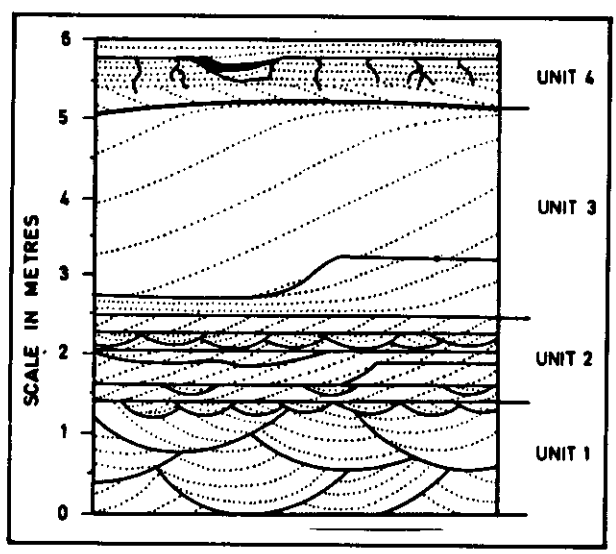

Fig. 6.5-4. - Vertical sequence of coarse-grained point bar deposits, showing various bedding features. Four units can be distinguished : Unit 1 - scour pool deposit; unit 2 - lower point bar deposit; unit 3 - chute bar deposit; unit 4 - flood plain deposit (from McGowen & Garner, 1970).

channel deposits (lateral accretion) followed by overbank fines (vertical accretion). The lag deposits cover a near-horizontal erosional surface and are capped by trough cross-bedding (sands), which, in turn, is overlain by small-scale trough

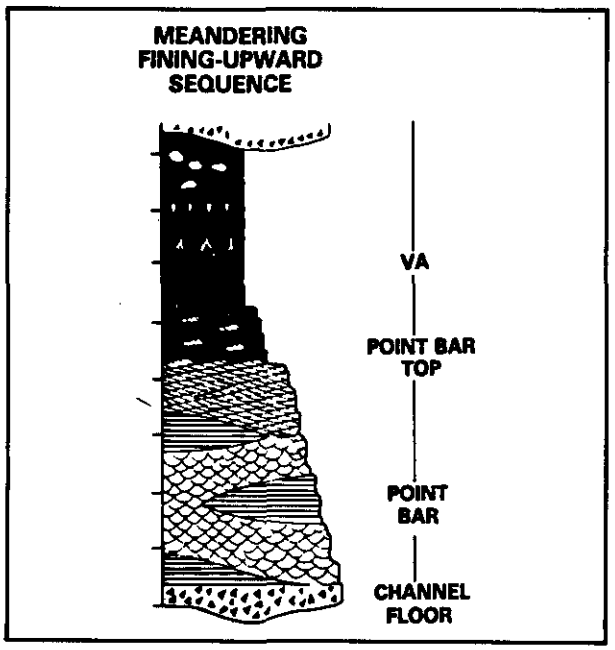

Fig. 6.5-5. - Theoretical sequence of facies in a meandering system. VA = vertical accretion (from Allen, 1970).

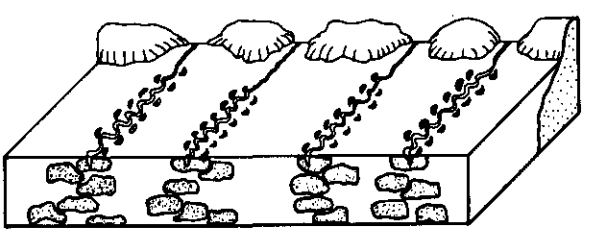

Fig. 6.5-6. - Conceptual models of fluvial channel geometry (adapted from Allen, 1965, by Visher, 1977).

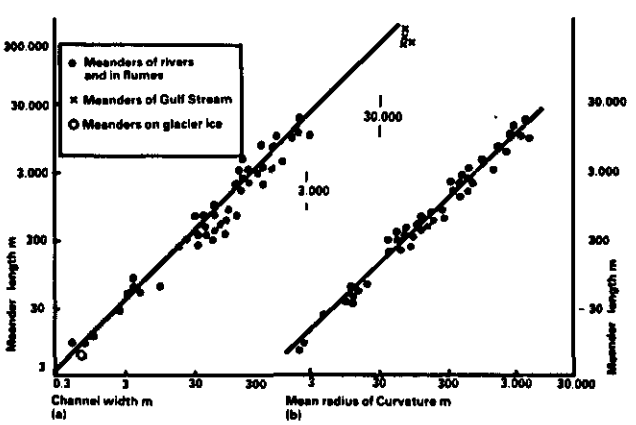

Fig. 6.5-7. - Relationship between meander length and (a) channel width, (b) mean radius of curvature (from Leopold & Wolman, 1960, in Leet *et al.*, 1978).

cross-laminations (silts). Horizontal laminations can occur at several places within this sequence. After the lateral channel migration, the sequence continues with vertical accretion deposits (silts and muds) introduced at the flood stage. Root traces and dessication cracks can be observed. In some humid climates, vegetation may grow sufficiently to form coal seams. In semi-arid or arid climates, the fluctuating water table and drying at the surface favour the formation of caliche-like concretions.

6.5.2.5. Geometry of the Bodies

Fundamentally a shoestring geometry is observed. Although, depending on the relationship between lateral and vertical accretion, tabular sand units may be developed (Fig. 6.5-6).

The length of the meander increases with the widening meandering stream and the mean radius of curvature of the meander (Fig. 6.5-7).

The width of sand bodies tends to be up to 10 times more than the channel width and up to 200 times more than the thickness. The overall thickness of one genetic sand unit compares closely to the water depth of the channel during flood (3 to 30 m). The coal beds are commonly 1.5 to 8 km in lateral extend and split by crevasse splay which thicken toward the meander belt.

6.5.2.6. Directional Current flow Model

In the meanders a spiral or helicoidal flow is created by the heaping up of water against outside shores of the bends. This mechanism is responsible for the lateral accretion of point bars (Fig.

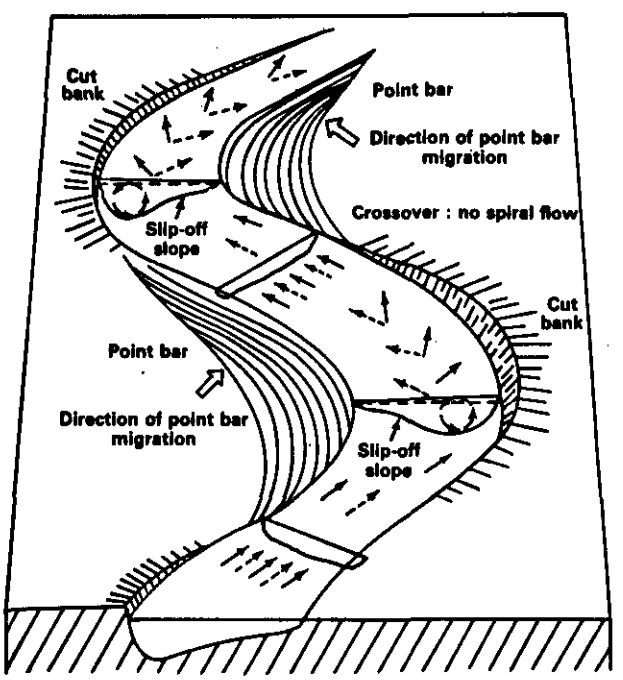

Fig. 6.5-8. - Downstream schematic block diagram of two meander bends and intervening crossover. Solid arrows indicate direction of surface current; dashed arrows indicate bottom current along; circular arrows with one barb, direction of spiral flow in plane of shaded transverse sections (from Friedman & Sanders, 1978, based on Friedkin, 1945).

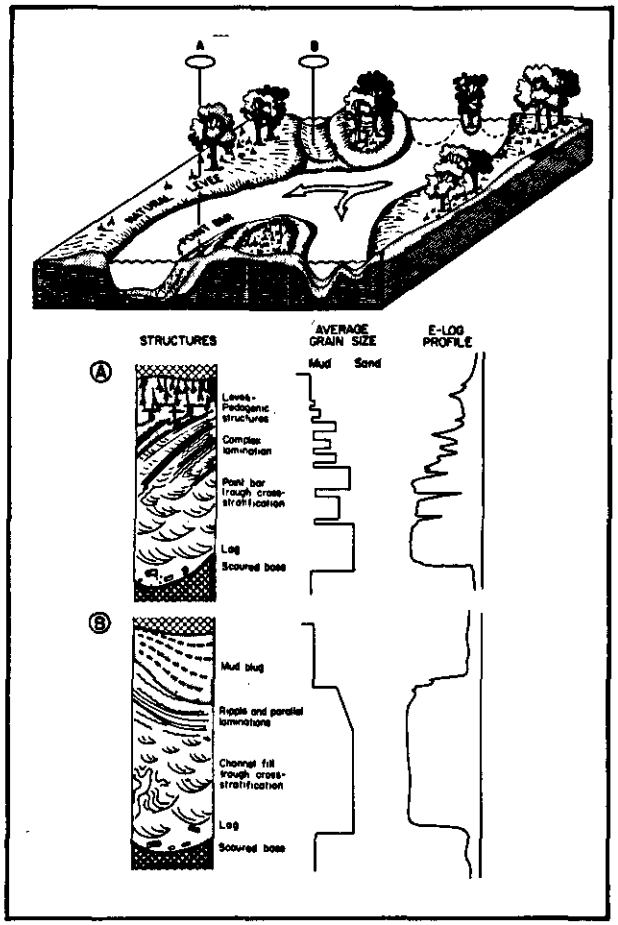

Fig. 6.5-9. - Generalized depositional model, representative vertical sequences, and idealized S.P. log profiles through laterally accreting (A) and symmetrically-filling channel segments (B) of an anastomosed channel system (from Galloway & Hobday, 1983, Fig. 4-5).

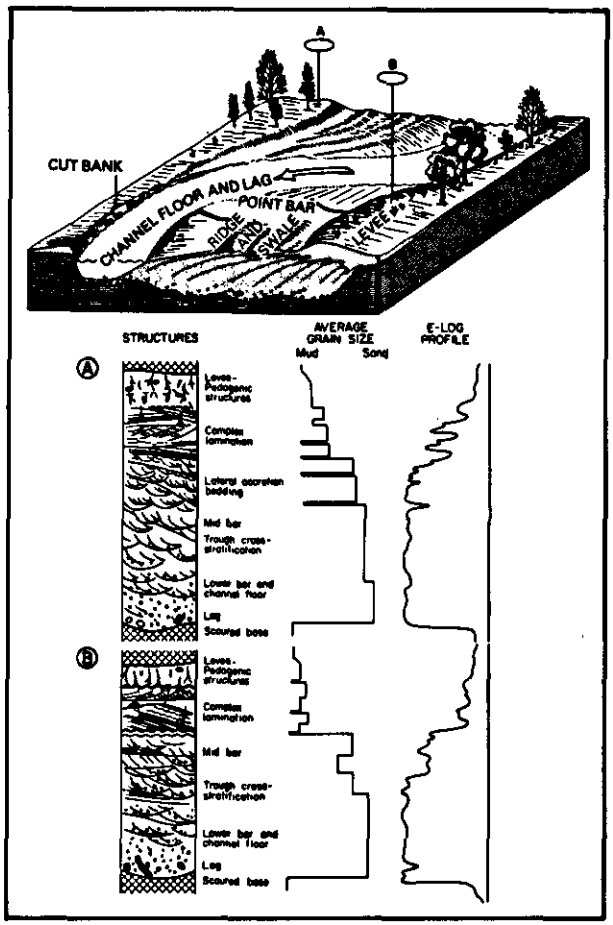

Fig. 6.5-10. - Generalized depositional model, representative vertical sequences, and idealized S.P. log profiles of a meanderbelt sand body produced by a high-sinuosity channel. Sequence (A) illustrates a complete fining-upward sequence typical of the mid- or downstream point bar. Section (B) illustrates the truncated vertical sequence commonly found in the upstream end of the bar (from Galloway & Hobday, 1983, Fig. 4-6).

6.5-8). Whereas, between meanders the flow is straight. The scour and fill in the channel generates down dip stream foresets in the direction of the flow. The helicoidal flow generates foresets in the point bars whose down dip direction is oblique to the channel direction, giving a bimodal azimuth frequency distribution in one sequence. The general azimuth frequency distribution shows a very large dispersion.

6.5.2.7. Reservoir Characteristics

Sand bodies potentially form good reservoir rocks with porosities up to 30 % and permeabilities up to several thousands of millidarcys, but they are laterally restricted. Shales beds or laminae can create permeability barriers. In such environments, the abundant impermeable floodplain shales can form stratigraphic traps. They often contain their own source rocks (plant debris and peat, lignite or coal), and, due to that, they are commonly considered more likely to contain gas than oil.

6.5.3. WELL-LOG RESPONSES AND CHARACTERISTICS

Galloway & Hobday (1983) proposed idealized S.P. log profiles for the main subenvironments found in meandering channels. They are represented by Fig. 6.5-9 to 6.5-11. A more complete description of log responses and characteristics will be now given.

6.5.3.1. Electro-Lithofacies

The radioactivity is medium to high depending on the importance of chemical maturity. Potassium percentage is generally less than 1 % if the rock is relatively mature, or between 1 and 2 % if immature (with feldspars, micas). Th/K ratio tends to be higher than 10. Uranium is often very low (oxidizing conditions), except in flood plain deposits rich in organic matter. On a ρ_b - ϕ_N crossplot, representative points fall between the sandstone and shale region. A few points may indicate

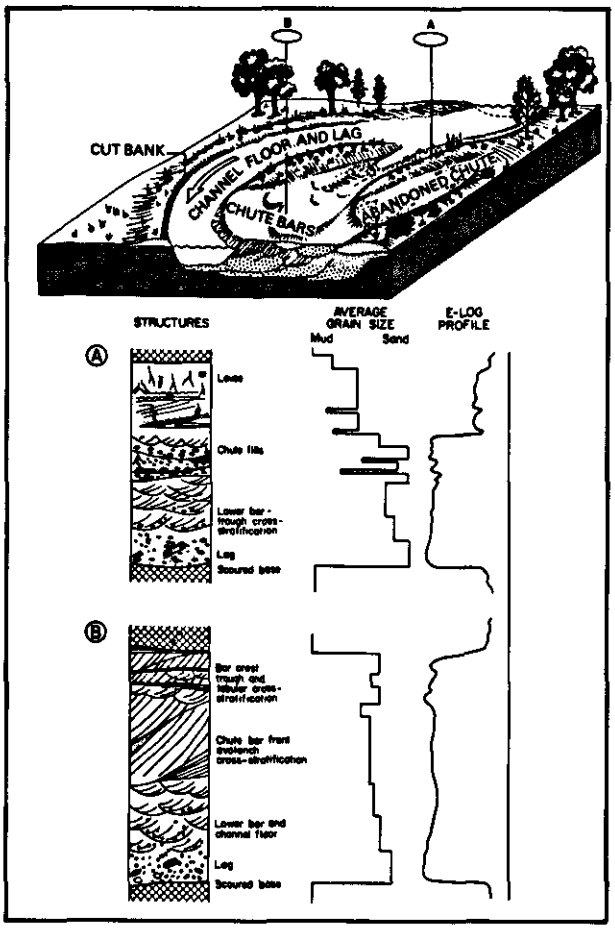

Fig. 6.5-11. - Generalized depositional model, representative vertical sequences, and idealized S.P. log profiles of a chute-modified point bar. Upstream portions of the point bar are capped by chute-channel deposits (A). Downstream, the channel and lower point bar deposits are capped by chute-bar sediments (B) (from Galloway & Hobday, 1983, Fig. 4-7).

carbonates (caliche-like). Points with high density and Pe may correspond to the presence of laterite or limonite. Pe generally does not exceed 3, unless heavy minerals (limonite, pyrite) are abundant. Sand-shale ratio is generally lower than 1. Coal beds are well identified by their well log responses. Two examples of meandering channels are represented in Figs. 6.5-12 and 6.5-14.

6.5.3.2. Dip Patterns

Most of the time, GEODIP or LOCDIP result displays (Fig. 6.5-13 and 6.5-15) show no dip or scattered dips (trough cross-bedding). Blue and red patterns may be present, sometimes with the same azimuth (Fig. 6.5-15, unit 3), indicating foreset beds, sometimes separated by a 90° azimuth. This last type of red patterns corresponds to channel fill; those patterns are perpendicular to the channel axis and indicate the direction of the thickest sand.

6.5.3.3. Boundaries

Generally one can observe a sharp contact at the bottom of the sand bed (Fig. 6.5-12 and 6.5-14), which is better seen on a resistivity microdevice (microlog) or on dipmeter curves (Fig. 6.5-13 and 6.5-15). Erosion can be detected by different thicknesses of the underlying unit on each pad. A gradational contact toward the top is observed.

6.5.3.4. Electro-Sequences

A general "bell shape", often serrated, for each individual sedimentary sequence is observed (Fig. 6.5-12 and 6.5-14; see also Fig. 4-2), which reflects

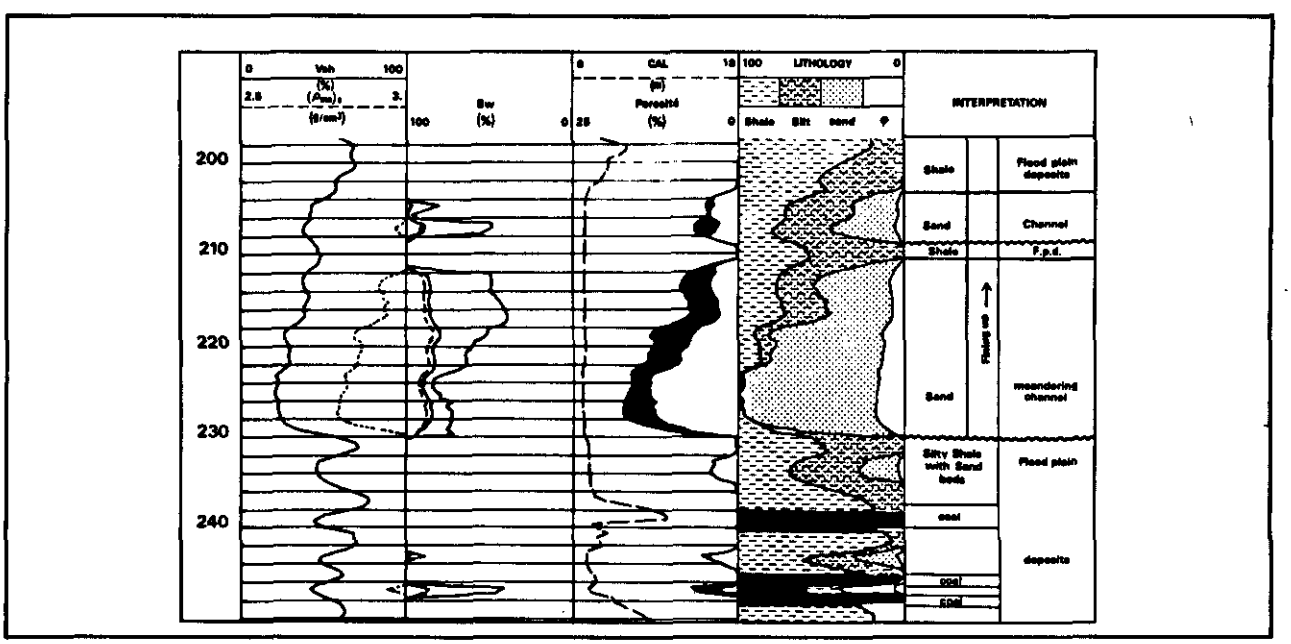

Fig. 6.5-12. - One meandering channel as illustrated by a SARABAND result display.

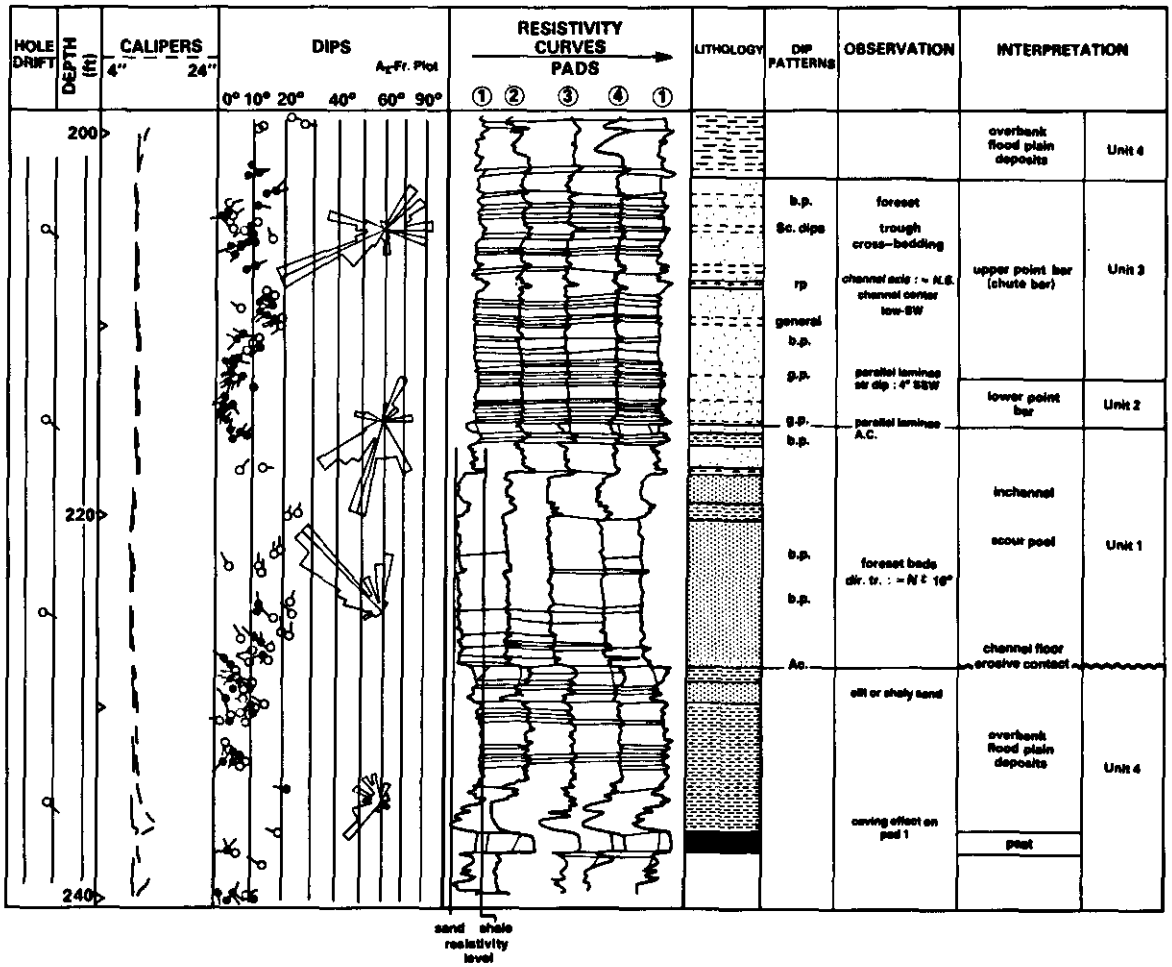

▲ Fig. 6.5-13. - GEODIP display on the same interval shown in Fig. 6.5-12, and its interpretation in terms of facies.

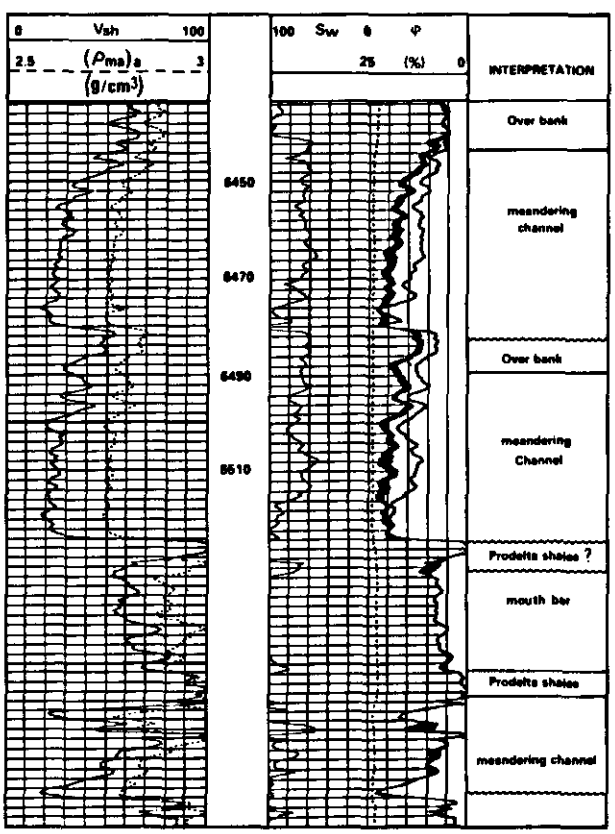

◀ Fig. 6.5-14. - Three meandering channels as they can be recognized from a SARABAND result display.

a general fining upward sequence. A succession of "bell shape" features with variable thicknesses is the rule.

6.5.3.5. Thickness

It ranges from several decimetres to several metres for one sequence. Shale beds also have various thicknesses.

6.5.3.6. Confusion with other Environments

In some cases fluvial deposits can be confused with turbidite deposits formed by stacking of several incomplete Bouma sequences (A, B and C units). Cylinder shapes corresponding to chute-bars can be also confused with braided channels.

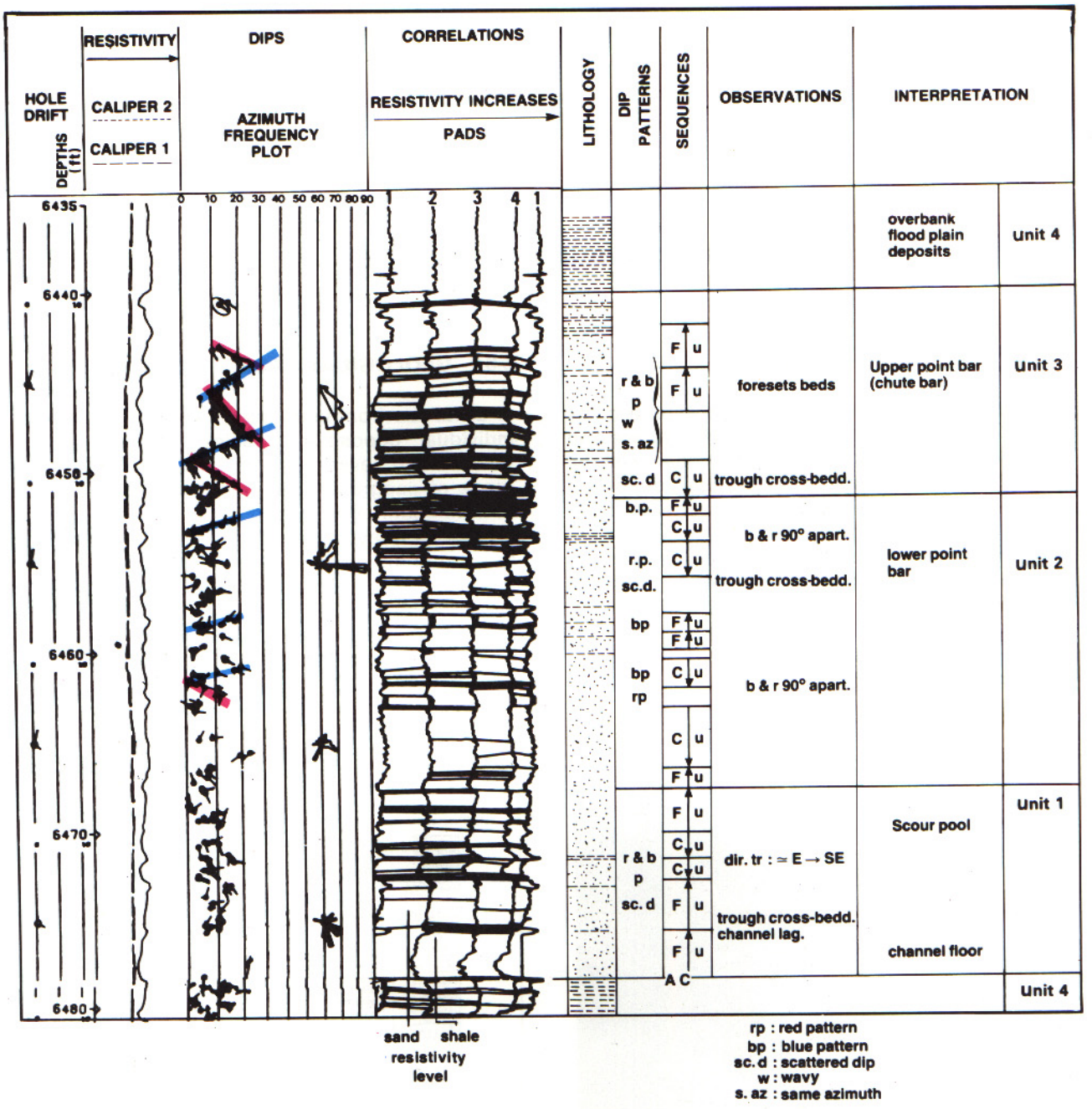

Fig. 6.5-15. - GEODIP display on the upper meandering channel shown in Fig. 6.5-14, and its interpretation in terms of facies.

6.6. DELTAIC ENVIRONMENT

6.6.1. DEFINITION

A transitional environment characterized by "sediments that have been transported to the end of a channel, (or a set of bifurcating channels), by a current of continental water, and deposited mostly subaqueously but partly subaerially, at the margin of the standing water into which the channel(s) discharged or is (are) still discharging (lake, sea, ocean)" (Friedman & Sanders, 1978). A satellite photograph of the modern Mississippi delta is shown in Fig. 6.6-1, and theoretical vertical cross-sections of the three types of deltas are reproduced in Fig. 6.6-2.

6.6.2. GEOLOGICAL FACIES MODEL

Delta environments have a wide variety of individual depositional facies. This complexity results from several factors : they exist in a wide range of geographic settings; they form in zones of interaction between fresh water and marine processes; they carry large volumes of sediments; the rate of deposition is often rapid resulting in the formation of extremely weak foundations, with a wide variety of mass-movement processes. Thus, these deposits display a large variety of geometries and vertical sequence characteristics (Coleman & Prior, 1982).

Fig. 6.6-1. - Aerial photograph of the modern Mississippi river delta. (Photo from NASA, extracted from Friedman & Sanders, 1978).

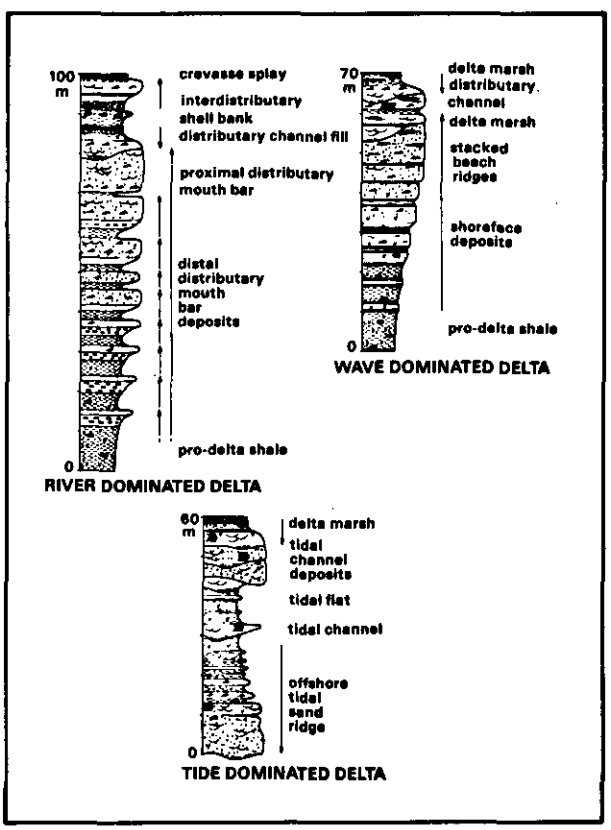

Fig. 6.6-2. - Theoretical vertical cross-sections in the three types of deltas (from Walker, 1979).

6.6.2.1. Subenvironments

In general terms, a delta can be subdivided into several subenvironments.

6.6.2.1.1. *The Delta Plain*

This is the subaerial, lowland part of the delta, which comprises active and abandoned channels separated by shallow water environments and emergent or near emergent surfaces. It includes :

- *Upper delta plain* or the part of a delta above the area of significant tidal or marine influences. Its deposits are essentially composed of :

a) migratory distributary channel deposits (braided or meandering; natural levee and point bar deposits);

b) lacustrine delta fill, interdistributary flood plain-deposits.

- *Lower delta plain* which lies within the realm of river-marine interaction and extends landward from the low-tide mark to the limit of tidal influence. Deposits include :

a) bay fill deposits (interdistributary bay, natural levee, marsh, crevasse splay-);

b) abandoned distributary-fill deposits.

6.6.2.1.2. *Subaqueous Delta Plain*

This is that part of the delta plain lying below low-tide level and extending seaward to that area actively receiving fluvial sediments.This area ranges in water depths from 10 to 300 m. It can be subdivided into two parts.

- *The Delta Front*

A high energy subenvironment, where the sediments are constantly reworked by tidal currents, marine longshore currents and wave action (10 m or less water depth). It includes delta front sheet sands, distributary mouth bar, river-mouth tidal range deposits, near shore, longshore and stream mouth bar deposits. The delta front is represented by a relatively large-scale coarsening upward sequence which records the vertical upward facies change from fine-grained offshore or prodelta facies into shoreline facies which is usually sandstone dominated. These sequences result from progradation of the delta front and may be truncated by fluvial-or tidal-distributary channel sequences as progradation continues.

- *The Prodelta*

A transitional subenvironment between the delta front and normal marine shelf deposits. It is the part of a delta that is below the effective depth of wave erosion, lying beyond the delta front and sloping gently down to the floor of the basin into which the delta is advancing. The sediments found in that part of the delta are composed of the finest material deposited from suspension.

6.6.2.2. Lithology

Two parameters must be considered separately.

6.6.2.2.1. *Composition*

Siliciclastic deposits, with a relatively good chemical and textural maturity, are the dominant lithofacies. Mica and lenses of heavy minerals are frequently described. Coal beds and detrital coal fragments are common. Glauconite and phosphates may be present, depending on marine influence. Shell debris and thin limestones are present. Siderite, pyrite, limonite and other iron-rich compounds are normally present in small amounts. Thin layers of evaporites would be present if climatic conditions favour them.

6.6.2.2.2. *Texture*

Grain size is mainly medium sand to clay. Conglomerates and coarse sands are rare, except for intraformational types (soft-clasts, slumped blocks or clay galls), or deltas resulting from alluvial fans penetrating the water mass (Fig. 6.6-3). Sorting is medium to well developed. Grain size tends to alternate in cyclic sequences. Roundness tends to be moderate to good. Each of the alternative sub models will leave their impressions on textural parameters.

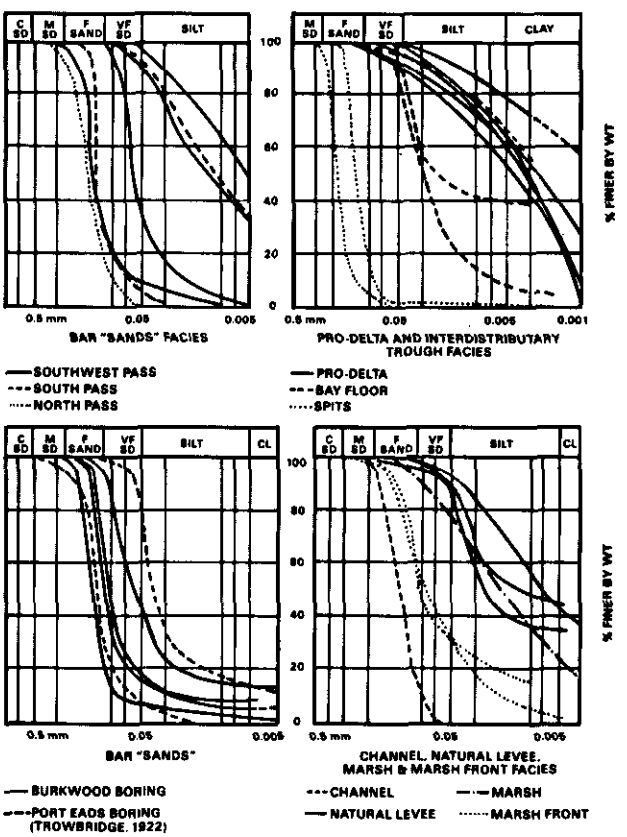

Fig. 6.6-3. - Cumulative size frequency curves of selected surface and subsurface samples representative of various sedimentary facies from the bird-foot delta (from Fisk *et al.*, 1977).

Table 6.6-1
Factors influencing deltaic sedimentation
(from Morgan, 1970).

RIVER REGIME (Variations influence sediment load and transport capacity)	Flood stage	Sediment load	Quantity of suspended load and bed load (that is, stream capacity) increases during flood
		Particle size	Particle size of suspended load and bed load (that is, *stream competence*) *increases during flood*
	Low river stage	Sediment load	Stream capacity diminishes during low river stage
		Particle size	Stream competence diminishes during low river stage
COASTAL PROCESSES	Wave Energy		High wave energy with resulting turbulence and currents erode, rework, and winnow deltaic sediments
	Tidal range		High tidal range distributes wave energy across an extende *littoral zone and creates tidal currents*
	Current strength		Strong littoral currents, generated by waves and tides, transport sediment alongshore, offshore, and inshore
STRUCTURAL BEHAVIOR (With respect to sea level datum)	Stable area		Rigid basement precludes delta subsidence and forces deltaic plain to build upward as it *progrades*
	Subsiding area		Subsidence through structural downwarping coupled wit sediment compaction allows delta to construct over-lapping sedimentary lobes as it progrades
	Elevating area		Uplift of land (or lowering of sea level) causes river distributaries to cut downward and rework their sedimentary deposits
CLIMATIC FACTORS	Wet area	Hot or warm	High temperature and humidity yield dense vegetative cover, which aids in trapping sediment transported by fluvial or tidal *currents*
		Cool or cold	Seasonal character of vegetative growth is less effective in sediment trapping; cool winter temperature allows seasonal accumulation of plant debris to form delta plain peats
	Dry area	Hot or warm	Sparse vegetative cover plays minor role in sediment trapping and allows significant aeolian processes in deltaic plain
		Cool or cold	Sparse vegetative cover plays minor role in sediment trappings; *winter ice interrupts fluvial processes;* seasonal thaws and aeolian processes influence sediment transportation and deposition

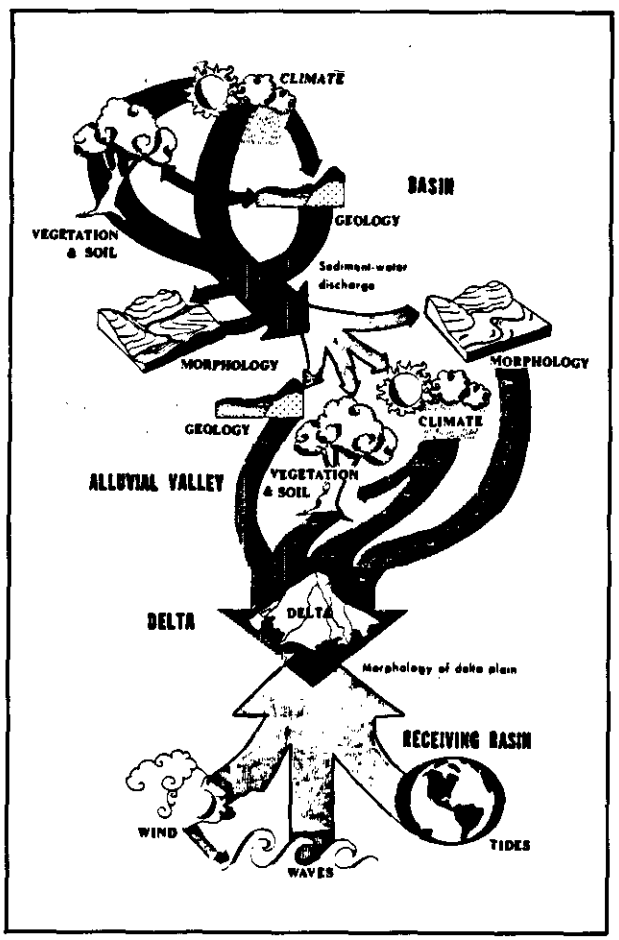

Fig. 6.6-4. - Major process controls on river systems (from Coleman & Prior, 1980).

Table 6.6-2
Characteristics of deltaic depositional sequences
(from Galloway, 1975).

	RIVER DOMINATED	WAVE DOMINATED	TIDE DOMINATED
GEOMETRY	ELONGATE TO LOBATE	ARCUATE	ESTUARINE TO IRREGULAR
CHANNEL TYPE	STRAIGHT TO SINUOUS DISTRIBUTARIES	MEANDERING DISTRIBUTARIES	FLARING STRAIGHT TO SINUOUS DISTRIBUTARIES
BULK COMPOSITION	MUDDY TO MIXED	SANDY	VARIABLE
FRAMEWORK FACIES	DISTRIBUTARY MOUTH BAR AND CHANNEL FILL SANDS, DELTA MARGIN SAND SHEET	COASTAL BARRIER AND BEACH RIDGE SANDS	ESTUARY FILLAND TIDAL SAND RIDGES
FRAMEWORK ORIENTATION	PARALLELS DEPOSITIONAL SLOPE	PARALLELS DEPOSITIONAL SLOPE	PARALLELS DEPOSITIONAL SLOPE

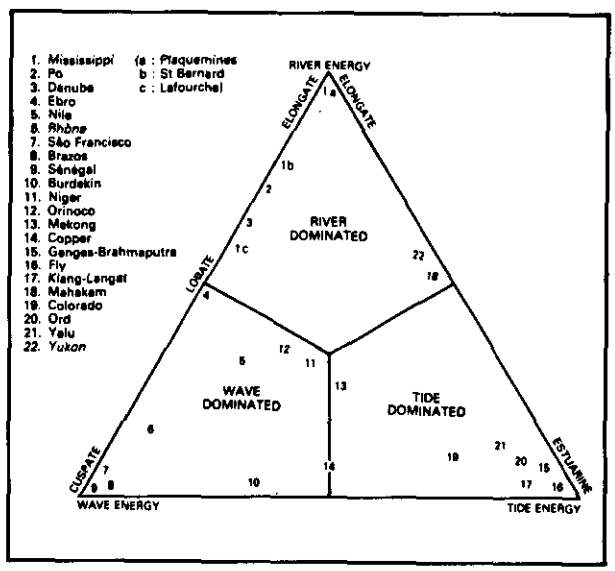

Fig. 6.6-5. - Triangular classification of deltaic depositional sequences (completed from Galloway, 1975).

6.6.2.3. Classification

The distribution, orientation and internal geometry of deltaic deposits are controlled by a variety of factors (Table 6.6-1 and Fig. 6.6-4) which include climate, morphology, vegetation, water discharge, sediment load, river-mouth processes, waves, tides, winds, currents, shelf slope and the tectonics and geometry of the receiving basin (Wright *et al.*, 1974).

To accomplish this complex set of variables, the deltas will be classified according to Galloway, 1975 (Table 6.6-2 and Fig. 6.6-5).

River-dominated deltas are referred to as "high-constructive" and wave- and tide-dominated deltas as "high-destructive" deltas, in the literature (for example Fisher *et al.*, 1969).

Structure, boundaries, geometry and directional flow models will be presented according with the classification.

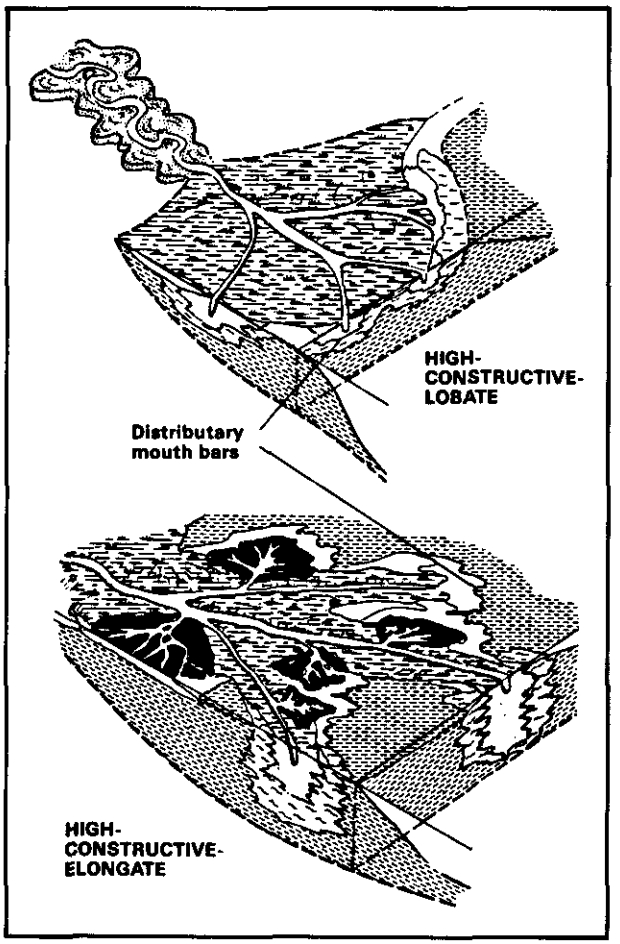

Fig. 6.6-6. - Block diagrams of the two types of river-dominated deltas (from Fisher *et al.*, 1969).

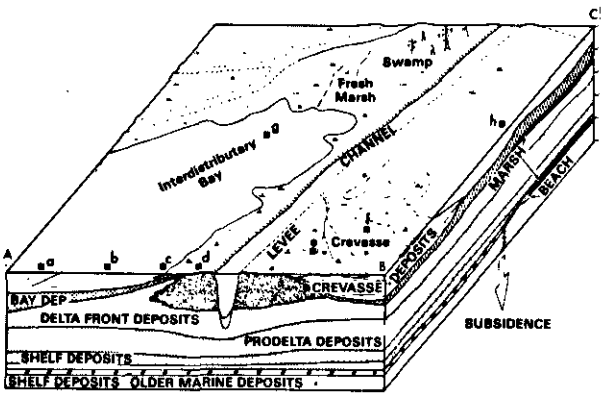

Fig. 6.6-7. - Block diagram showing subenvironments and facies relationship of a river-dominated elongate delta (from Coleman & Prior, 1980).

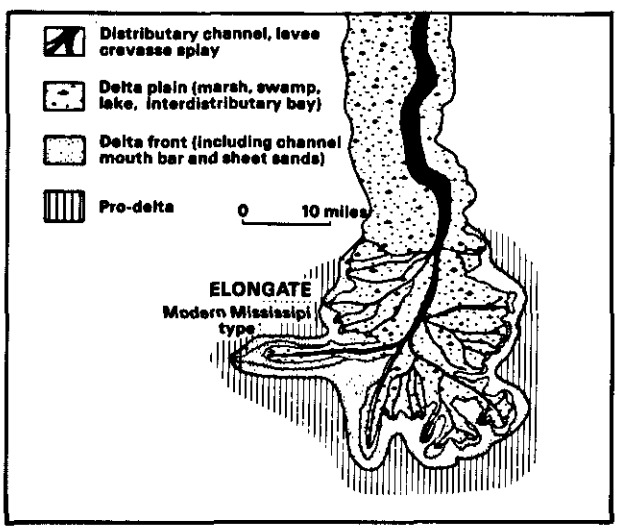

Fig. 6.6-8. - Surface distribution of facies in a bird-foot type river-dominated delta (from Fisher *et al.*, 1969).

6.6.2.4. River-Dominated Deltas

If waves, tidal and longshore currents are weak, and if the volume of sediments carried by the river is high, rapid seaward progradation takes place, and a variety of characteristic river-dominated depositional environments develops. At the mouth of each distributary channel *subaqueous levees* may form as the jet of the river water enters the sea. The main sediment load is deposited in a *distributary mouth bar*, in which the grain size becomes finer seaward. As progradation proceeds, the river slope is flattened and flow becomes less competent. At this stage a breach in the subaerial levee may occur upstream during a period of high discharge. Such a breach is termed a *crevasse*. The shorter route it offers to the sea via an *interdistributary bay* is generally the cause of a major flow diversion, and a subdelta *crevasse splay* deposit may develop rapidly. Eventually, the crevasse may become a major distributary and the process is repeated.

These are, in summary, the main mechanisms occurring in a river-dominated delta and generated subenvironments.

But there are two main subtypes in this delta category.

- The river discharge can be steady, generally with a high suspension load. This generates *bird-foot, elongate* type deltas with few distributaries, shoestring sands and discrete mouth bar deposits (Fig. 6.6-6 to 6.6-8).

- The river discharge can fluctuate, with, typically, a higher proportion of bedload in the transported sediments. This generates a *lobate* shape in outline; there are a greater number of distributaries, each of which tends to be more ephemeral, and the sediments are coarser grained and the mouth bar deposits merge laterally into sheet sands.

6.6.2.4.1. *Structure*

Massive bedding with general erosional surface; lenses, thin bedding up to laminations, parallel or wavy, of clay or interbedded silt and

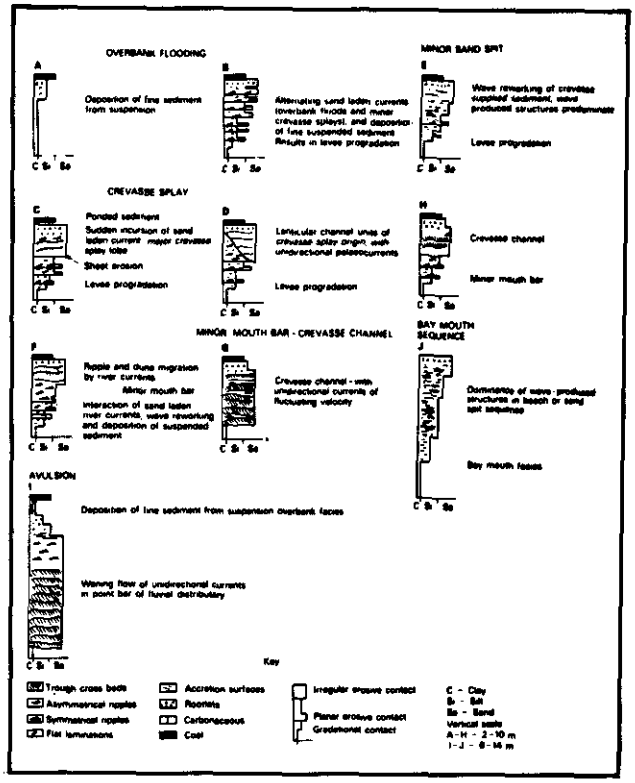

Fig. 6.6-9. - Vertical sequences of sedimentary structures in river-dominated interdistributary areas (from Elliot, 1974, in Reading, 1978).

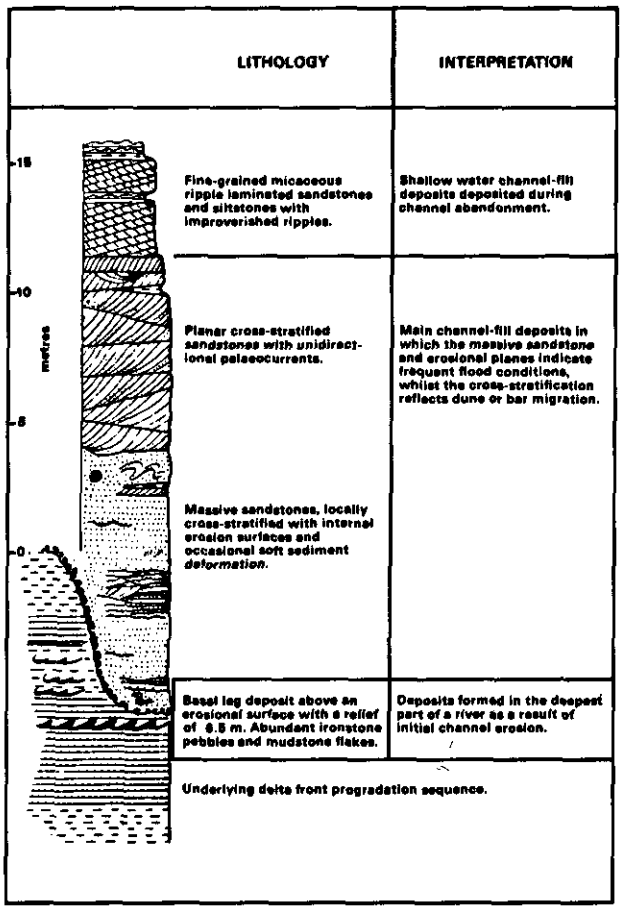

◀ Fig. 6.6-10. - Boundaries and sedimentary structures of a fluvial-distributary channel (from Reading, 1978, after Kelling & George, 1971).

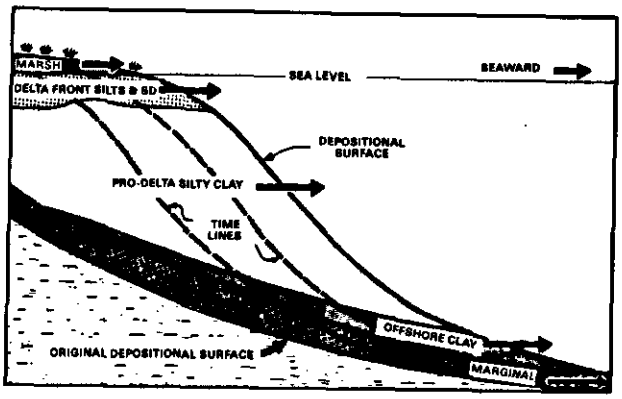

Fig. 6.6-11. - The "constructional" phase of the delta cycle (from Scruton, 1960).

clay; small to large symmetrical and asymmetrical ripples, abundant planar and trough cross-beds, generally high angle with unimodal current distribution, are the most common bedding types. Distorted bedding grades from load marks to convolute, mud lumps, diapiric and slumps (growth faults), generally related to prodelta clays. Bioturbations are moderate to high, including flora and related fauna. Shell beds may be present. Concretions of iron-rich minerals, scours, cut-and-fill and lag deposits are also sedimentary features commonly found (Fig. 6.6-9).

6.6.2.4.2. *Boundaries*

Large units tend to show basal gradational contacts with abrupt tops. Internally, gradational or sharp contacts are randomly distributed with tendency to be similar to the large units (Fig. 6.6-10).

6.6.2.4.3. *Sequences*

River-dominated deltas generate a large cyclical deposition (Fig. 6.6-11). Lithology, thickness and grain size evolution are illustrated by Fig. 6.6-12.

The rapid seaward progradation of these deltas gives rise to the most characteristic feature of deltaic sediments : the coarsening upward sequence. The complete cycle of a delta lobe (typically 50 to 100 m thick), and the distributary and crevasse cycles, which are its component parts, are summarized in Fig. 6.6-13.

Scruton (1960) pointed out that the growth of a delta is cyclic. He recognized two phases :

- *Constructional phase :* active seaward progradation causes prodelta muds to be overlain by delta-front silts and sands, these in turn by distributary-mouth bar deposits, mainly sands, and finally top-set delta marsh sediments, possibly including peat beds (Fig. 6.6-11).

- *Destructional phase : a delta lobe is even-*

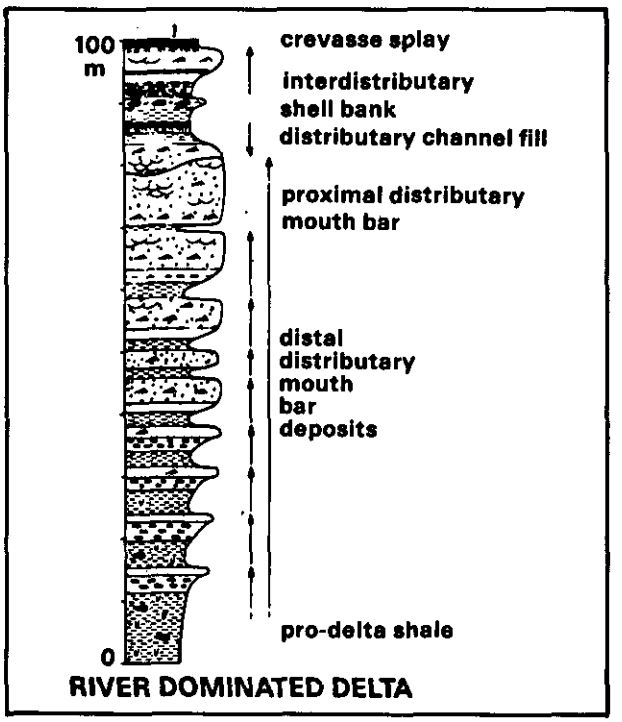

Fig. 6.6-12. - Vertical sequential evolution in a river-dominated delta (from Walker, 1979).

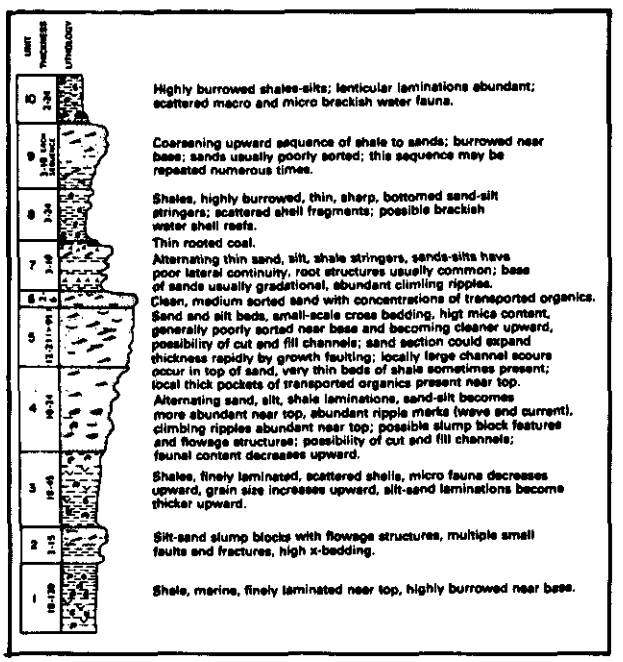

Fig. 6.6-13. - Composite stratigraphic sequence of depositional environments in the Mississippi River delta (from Coleman & Prior, 1980).

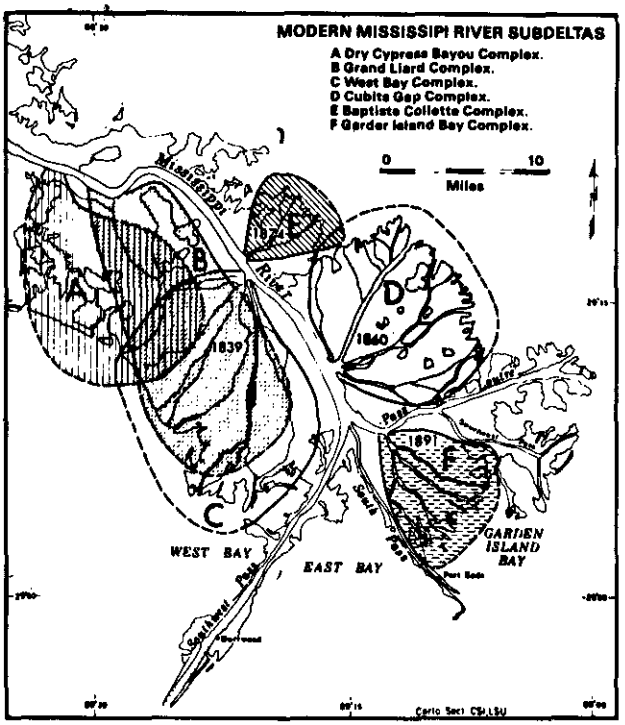

Fig. 6.6-14. - Sub-deltas infilling interdistributary bays of the modern Mississippi delta (from Coleman & Gagliano, 1964).

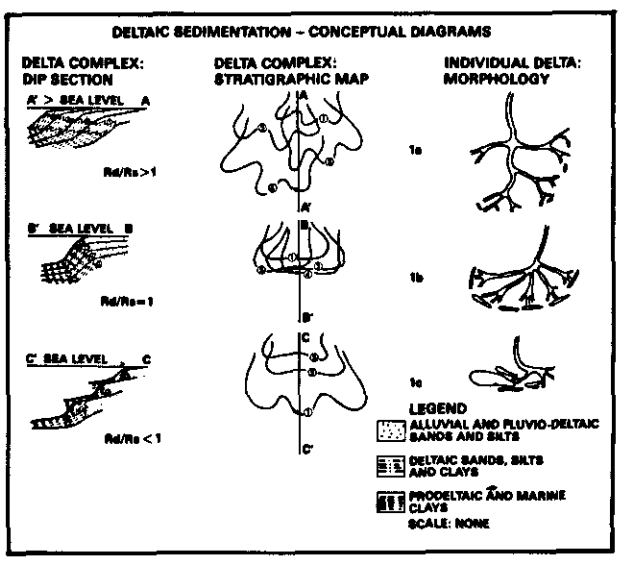

Fig. 6.6-15. - Conceptual diagrams of variations in delta characteristics resulting from variations in ratio between rate of deposition and rate of subsidence (Rd/Rs). (From Curtis, 1970).

tually abandoned if crevassing generates a shorter route to the sea. The topmost beds are then attacked by waves and current activity, and may be completely reworked. Compaction may allow a local marine transgression to occur.

This cycle is of course idealized. The complete delta cycle (sometimes termed a megacycle) may generate a stratigraphic succession between 50 and 150 m, or more, in thickness, but it may contain, or pass laterally into, numerous smaller cycles representing the progradation of individual distributaries or crevasse splays (Fig. 6.6-14).

These smaller cycles range from 2 to 14 m as shown by Coleman & Gagliano (1964) and by Elliot (1974). As in larger cycles, they tend to coarsen upward. The manner in which cyclic deltaic se-

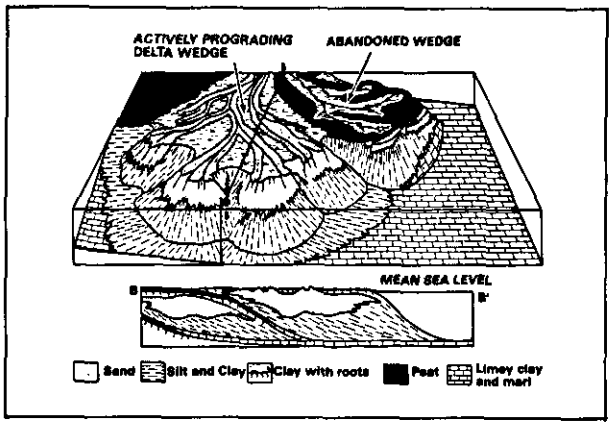

Fig. 6.6-16. - Cyclical active and abandonment evolution of Carboniferous deltas in the United States (from Ferm, 1970).

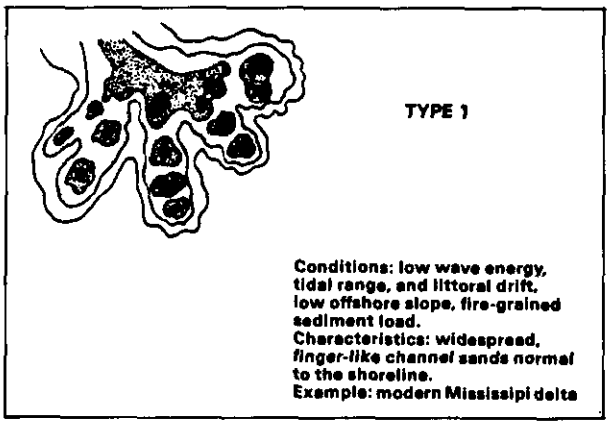

Fig. 6.6-17. - Sand distribution pattern (modified from Coleman & Wright, 1975).

Table 6.6-3

Geometrical and other geological parameters to identify deltaic subenvironments.

	BAY FILL	MARSH SWAMP	DISTRIBUTARY MOUTH-BAR	POINT BAR	CHANNEL	OVERBANK
TYPE OF DEPOSIT	DETRITAL	CHEMICAL	DETRITAL	DETRITAL	DETRITAL	DETRITAL
DOMINANT ROCK TYPE	Shale & siltyl shale.	Seatrock, clay, coal.	Medium to fine sandstone with shale lenses.	Coarses to medium sandstone.	Medium sandstone occasional conglomerats. Shale bands.	Silty shale, siltstone Fine micaceous sandstone.
GRAIN SIZE TREND	Generally coarsening upward.	No specific trend.	Coarsening upward.	Fining upward.	Highly variable in the middle. Generally fining upward.	Cyclic, each cycle fining upward.
NATURE OF BASAL CONTACT	Generally not seen.	Gradational to sharp.	Gradational to sharp.	Highly scoured wavy.	Sharp truncation. Highly erosive.	Gradational.
VERTICAL THICKNESS	1.5 to 15 ft.	0.3 to 1.8 m.	1.5 to 4.5 m.	6 to 14 m.	3 to 4.5 m.	0.9 to 4.5 m.
LATERAL EXTENT	60 m to 73.2 Km.	In kilometres.	0.4 m to 4.8 Km.	90 m to 0.4 Km.	19 m or less, to 120 m.	Very variable.
SHAPE OF UNIT	Rectangular in Cross section.	Elongated.	Sheet-like.	Hedge shapped lenticular.	Biconvex, planeconvex.	Thin, sheet-like.
BEDDING THICKNESS	Thinly bedded laminated.		Medium bedded. 0.3 to 9 m.	Thick bedded 1.5 to 2.0 m.	Medium to thinly bedded.	Thin bedded, laminated.
SEDIMENTARY STRUCTURES	Parallel and wavy lamination.		Planar cross-beds. Composit sets common Climbing ripples on lateral extremities.	Multi-directional trough cross-beds. Solitary cross-strats common.	Small scale scour and fill.	Parallel lamination, current Ripples. Small scale cross-bed.
NATURE AND DISTRIBUTION OF ORGANIC FRAGMENTS	Small leaves and twigs along bedding planes. Brachiopods.	Macerated plant material.	Small rounded organic fragments distributed at random.	Large leaves and stem on bedding planes. Rafted Coal lenses at base.	Oriented large stem at the base.	Small leaves and twigs along bedding planes.
MICACEOUS MINERAL	Coarse mica flakes along bedding planes.		Generally distributed at random. Some beds show unusually high concentration.	Mica distributed at random. Coarse flakes segregated along bedding planes.	Distributed at random.	Segregated along bedding planes.
POST DEPOSITIONAL MODIFICATIONS	Rooting on top only cone-in-cone burrowing.	Rooting.	Gas heave. Structure.	Convolute, laminations.	Slump features.	Rooting.
NODULES	Siderite nodules present.		Not seen.	Large disc, shaped nodules present .	Not seen.	Not seen.
PRIMARY HUES	Dark grayish, black.	Black grayish, black.	Light whitish, gray.	Dark gray.	Light gray.	Dark greenish gray grayish black.

quences are superimposed upon each other depends on the relative rates of sedimentation and subsidence (including compaction). If the two rates are in approximate balance a delta will tend to build vertically; if subsidence is faster the delta will prograde seaward, and, as each part of the depositional basin becomes filled, successive progradational events will move laterally. The mechanisms are described by Curtis, 1970 (Fig. 6.6-15).

6.6.2.4.4. *Geometry of the bodies*

The main bodies are lobate features with a strong lateral accretion mechanism which generates lenticular units (Fig. 6.6-16). Sandstone bodies tend to be lenticular to tabular for the distributary-mouth bars, grading to sand sheets. Near the top, finger- or shoestring-shapes are described. River-dominated delta geometry can be mapped most readily in the subsurface by measuring the

total sand content or the sand/shale ratio in a given stratigraphic unit. Areas of high sand content may outline lobate areas perpendicular to the basin margin, corresponding to the principal paths of delta progradation.

Fig. 6.6-17 shows this approach correlated with a present-day model.

Table 6.6-3 summarizes geometrical criteria for this kind of deltas.

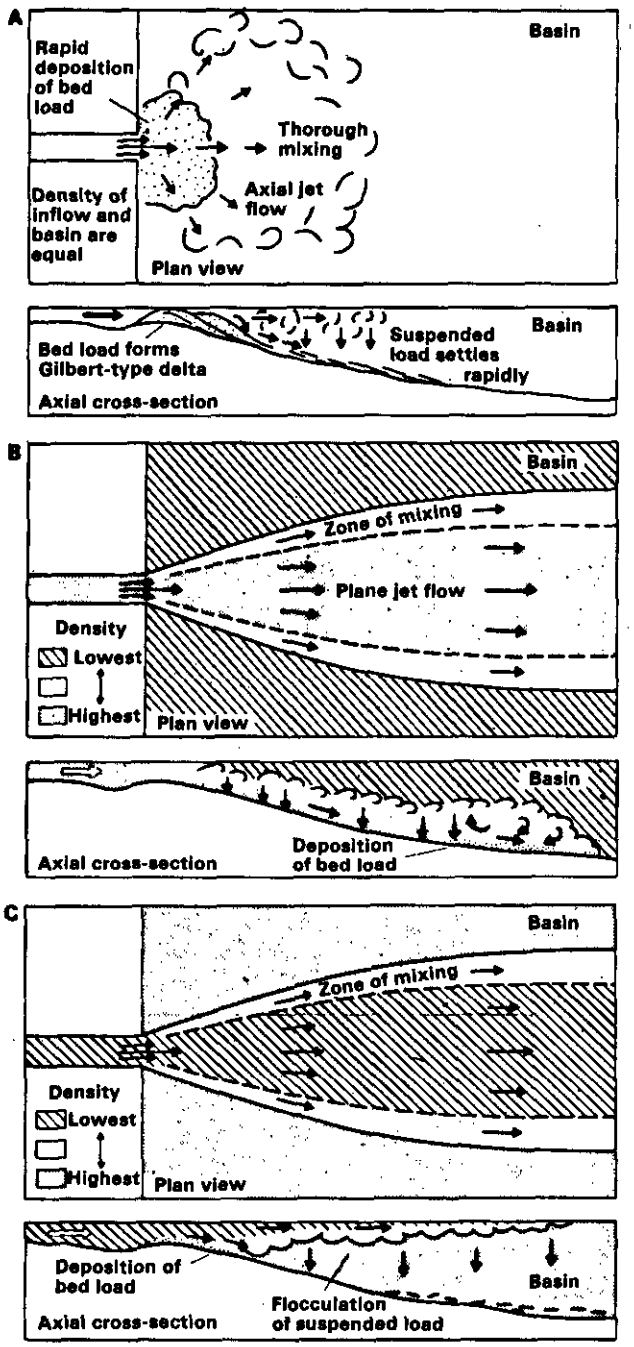

Fig. 6.6-18. - Contrasted modes of interaction between sediment-laden river waters and basin waters, determined by the relative density of the water bodies : (A) homopycnal flow; (B) hyperpycnal flow; (C) hypopycnal flow (from Fisher *et al.*, 1969; originally from Bates, 1953).

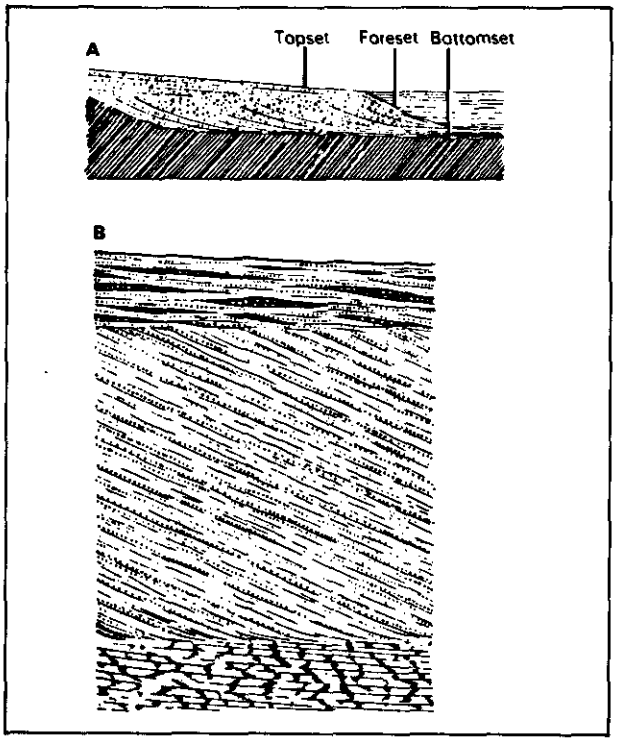

Fig. 6.6-19. - Lateral and vertical cross-sections of a delta, showing topset, foreset and bottomset developping as delta grows (from Reineck & Singh, 1975; and from Reading, 1978).

6.6.2.4.5. *Directional current flow model*

The radial change in hydraulic conditions at the distributary mouth causes the out flow to expand and decelerate, thus decreasing outflow competence and causing the sediment load to be deposited. Basinal processes either assist in the dispersion and eventual deposition of sediment, or rework and redistribute sediment deposited directly as a result of outflow dispersion.

Of prime importance in this part of the delta is the precise manner in which the outflow and basin waters mix at the distributary mouth. In an early example of the application of hydrodynamic principles to essentially geological problems, Bates (1953) contrasted situations in which the river waters were equally dense, more dense and less dense than the basin waters (homopycnal, hyperpycnal and hypopycnal flow respectively, Fig. 6.6-18). If the water bodies are of equal density, immediate three dimensional mixing occurs at the river mouth causing appreciable sediment deposition at this point. High density outflow tends to flow beneath the basin waters as density currents, causing sediment to by-pass the shoreline and thus restricting the development of a delta. If the outflow is less dense than the basin waters it enters the basin as a buoyantly supported surface jet or plume. This latter situation has been observed off the Mississippi and Po deltas (Scruton, 1956; Nelson, 1970) and is considered to operate wherever river outflow enters marine basins as sea water is slightly denser than freshwater. Other

important factors include inertial processes related to outflow velocity, and frictional processes which result from the outflow interacting with the sediment surface at the distributary mouth (Wright & Coleman, 1974).

In relation with the main progradational process, the mouth bars develop foreset beds, in which dips are generally downslope - as flow does - ranging in magnitude from 10° to 25° (Fig. 6.6-19). The dip azimuths show an unimodal distribution with moderate scattering around 90° (Coleman & Prior, 1980).

6.6.2.5. Wave-Dominated Deltas

In environments of strong wave activity mouth bar deposits are continually reworked into a series of superimposed coastal barriers. These may completely dominate the final sedimentary succession, and the internal geometry of the deposits will be quite distinctive. Sand bodies will tend to parallel the coastline, in contrast to those of river-dominated deltas, which are more nearly perpendicular to the coast (Fig. 6.6-20).

The surface facies distribution shows a strong reworking of the sand, creating more *cuspate* subaerial forms (Fig. 6.6-21).

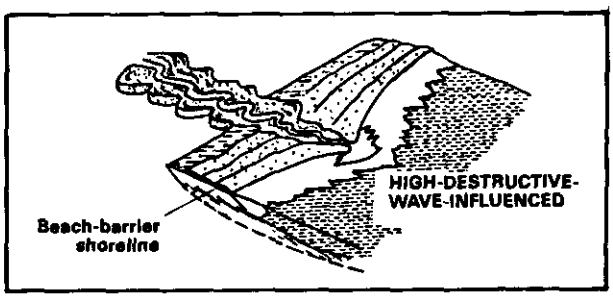

Fig. 6.6-20. - Block diagram of wave-dominated deltas (from Fisher *et al.*, 1969).

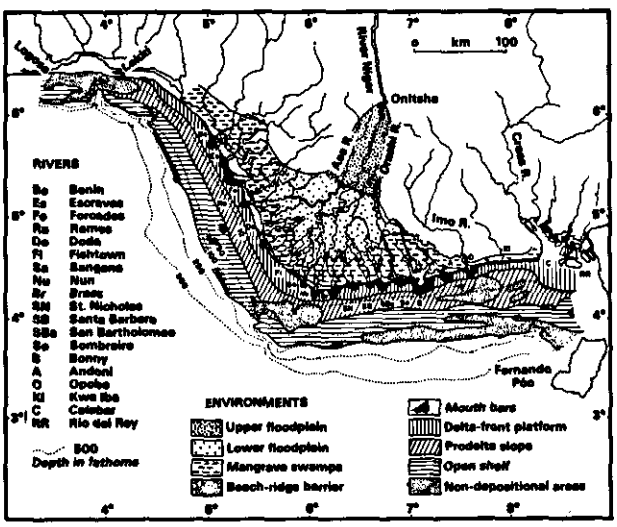

Fig. 6.6-21. - Principal sedimentary environments of the Niger delta (from Allen, 1970).

6.6.2.5.1. *Structure*

Laminations, thin bedding, parallel stratification, large and small scale, low and high angle cross-bedding, are the distinctive bedding features of this delta. Barrier and shoreface sands generally contain low-angle cross-bedding, representing wave accretion surfaces. Palaeocurrent distributions are bimodal or random (Fig. 6.6-22).

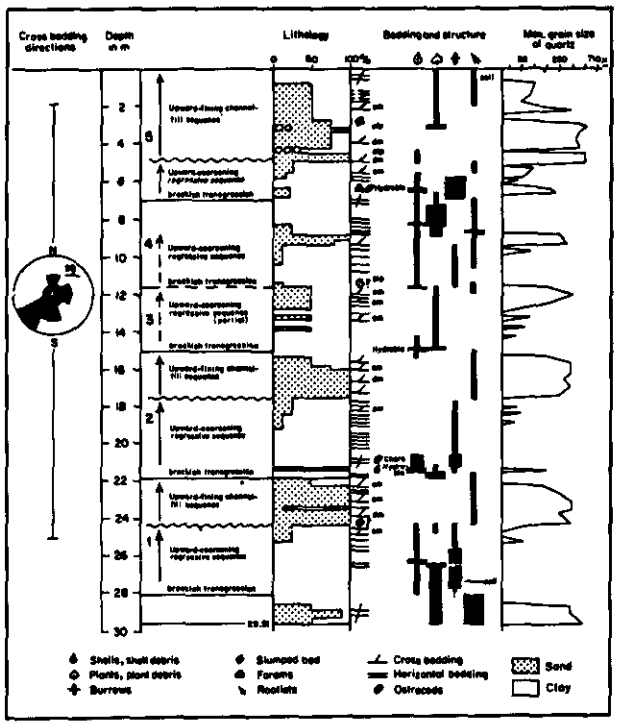

Fig. 6.6-22. - Typical example of deltaic coastal plain sedimentation, Rhône delta. Five upward coarsening sequences, of which three (1, 2 and 5) are overlain by upward fining channel-fill sequence, can be recognized in this core-log (from Oomkens, 1970).

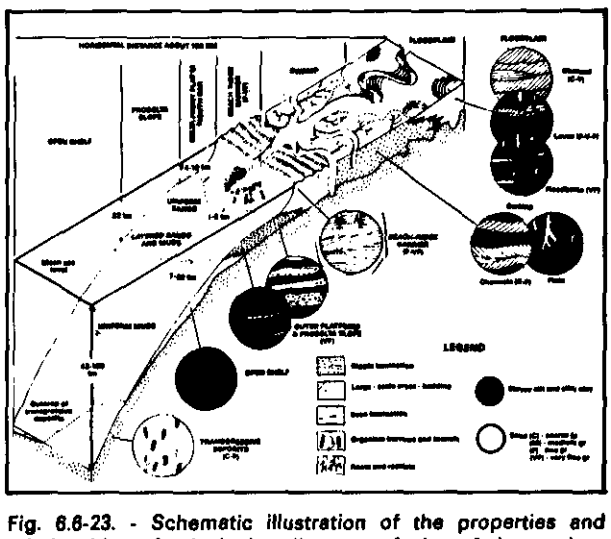

Fig. 6.6-23. - Schematic illustration of the properties and relationships of principal sedimentary facies of the modern Niger Delta (from Allen, 1970).

Table 6.6-4
Characteristics of sediments of Guadalupe delta and its beach-ridge plain
(from Donaldson *et al.*, 1970).

ENVIRONMENT		BASAL CONTACT		AVERAGE GRAIN SIZE					VERTICAL TEXTURAL GRADATION		GEOMETRY					PREDOMINATE TREND (if elongate)		SEDIMENTARY STRUCTURES			FOSSILS		
		sharp	gradational	sand	sandy silt	sand, silt, clay	clayey silt	silty clay	coarse to fine upward	fine to coarse upward	sheet	tabular	sheeting	pod	wedge	parallel regional slope	parallel shoreline	point bar	dunes and/or ripples	burrows	plant fragments including	ostracods and forams	low salinity -molusks
MEANDERING STREAM	INCREASING MARINE INFLUENCE ↑	×		×					×			×	×	×		×		×	×		×		
DISTRIBUTARY CHANNEL (not migrating)		×		active ×	×		aband. ×	×	×				×	×		×			×		×	×	
DISTRIBUTARY-MOUTH BAR			×	×	×					×	×	×	×	×		×			×	×	×	×	×
NATURAL LEVEE AND CHEVASSE			×				×	×			×	×	×	×	×	×				×	×		
MARSH AND LAKE			×					×			×	×	×	×	×	×				×	×	×	
PRODELTA			×				×	×			×				×		×		×		×		
INTERDISTRIBUTARY BAY			×					×							×	×				×	×	×	×
POORLY DEVELOPED SPITS AND BEACH RIDGE OF INTERDISTRIBUTARY BAY			×				×	×					×	×			×			×	×		×
TIDAL CHANNEL CONNECTING LAKE TO BAY		×				×	×	×	×				×	×		×			×	×	×	×	×
TIDAL FLAT			×					×			×	×			×		×			×		×	×
BEACH-RIDGE ON BEACH-RIDGE PLAIN	↓ INCREASING RIVER INFLUENCE		×	×	×					×			×	×			×			×			×

Stringers and partings of sand, shale, coal, evaporites, shell beds and heavy minerals may be present. Sands and shales tend to be burrowed and rooted, the last near tops of banks. Prodelta clays are rich in mud pellets. Fig. 6.6-23 summarizes structures and subenvironments in one of these deltas.

6.6.2.5.2. *Boundaries*

The base of megasequences shows gradational contacts. Parallel boundaries dominate in external as well as internal units. Distributary channels cut delta marshes showing small scours at the base (Fig. 6.6-22 and Table 6.6-4).

6.6.2.5.3. *Sequences*

Coarsening-upward mega- to micro-sequences are well developed. They are noticeable through grain size, sorting, thickness of bedding and fossil content (Fig. 6.6-24). Stacked beach-ridges obscure the effect (Fig. 6.6-25).

Beach-ridge sequences can develop in nondeltaic settings as a result of longshore drift and therefore additional criteria are necessary in order to identify a specific sequence as deltaic in origin. Bars forming on nondeltaic coastlines are commonly backed by lagoons, the sediments of which may cap the bar sequence, whereas in deltaic settings the bars develop in front of swamps and

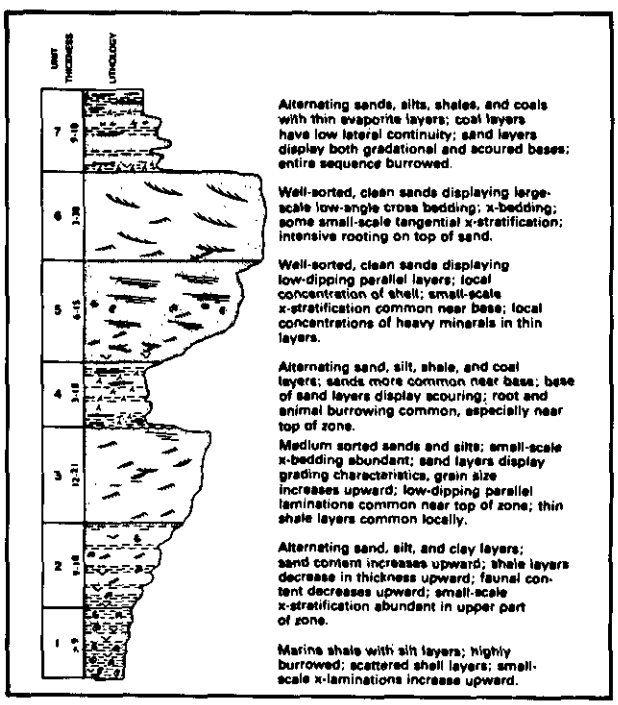

Fig. 6.6-24. - Composite stratigraphic sequence of depositional environments in the Senegal River delta (from Coleman & Prior, 1980).

fluvial channel complexes, the deposits of which should be quite distinctive. Coal may be an important constituent.

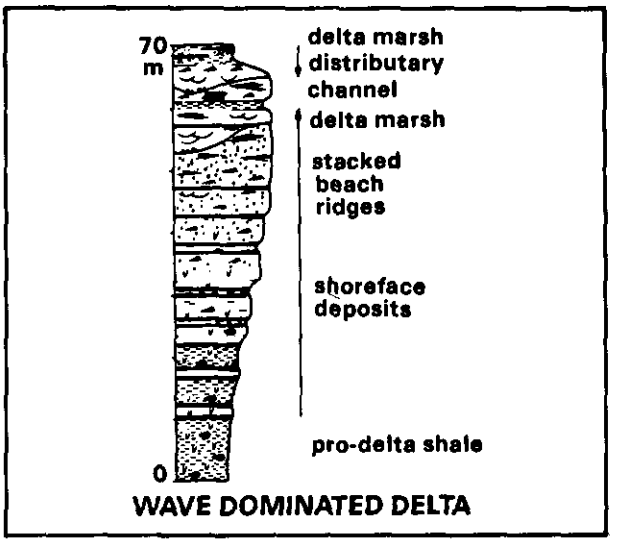

Fig. 6.6-25. - Vertical sequence distribution in wave-dominated delta (from Walker, 1979).

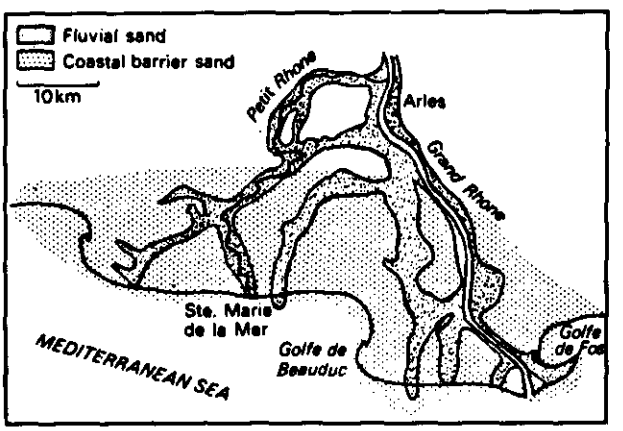

Fig. 6.6-26. - Distribution of sand bodies following their origin in the Rhône delta (from Oomkens, 1970).

6.6.2.5.4. *Geometry of the bodies*

The geometry of wave-dominated delta deposits is quite different from those where wave influence is low. Beach-ridge sands form linear sand masses sub-parallel to the basin margin, ideally forming a convex-seaward, arc-cusp-, or chevron-shaped body (Fig. 6.6-26). Associated fluvial sands will trend subperpendicular to the basin margin. The classic delta - that of the Nile -is a good example of a wave-dominated type delta.

Sand body geometries are strongly dependant on river-wave relationships (Fig. 6.6-27), giving cuspate to arcuate deltas.

6.6.2.5.5. *Directional current flow model*

Due to the wave action the current flow pattern tends to be bimodal with large scattering. The azimuth pattern may be modified because of longshore current activity and this will be reflected by the sand body geometry (Fig. 6.6-27).

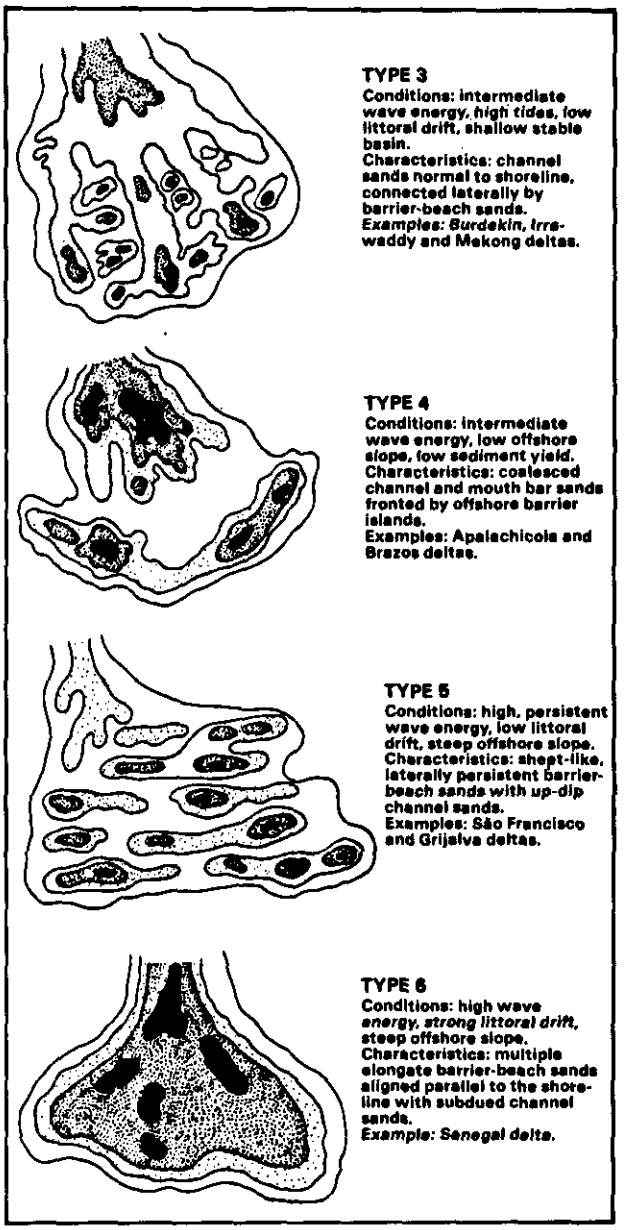

Fig. 6.6-27. - Sand bodies in modern wave-dominated deltas (from Coleman & Wright, 1975).

6.6.2.6. Tide-Dominated Deltas

Where the tidal range is high the reversing flow that occurs in the distributary channels during flood and ebb may become the principal source of sediment dispersal energy. Within, and seaward of the distributary mouths, the sediments can be reworked into a series of parallel, linear or digitate ridges parallel to the direction of tidal currents (Fig. 6.6-28 and 6.6-29).

Deltas of this type may be difficult to recognize in ancient sedimentary deposits. The coarser sediments are dispersed by tidal currents into offshore sand ridges parallel to the direction of the tide with low littoral drift. In high littoral drift the linear tidal ridges tend to parallel the shoreline

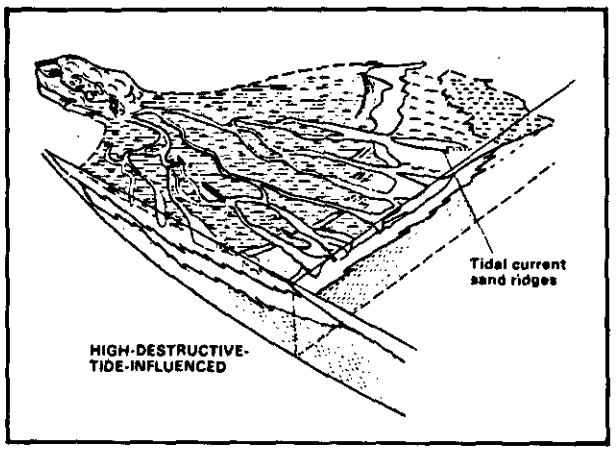

Fig. 6.6-28. - Block diagram of a tide-dominated delta (from Fisher *et al.*, 1969).

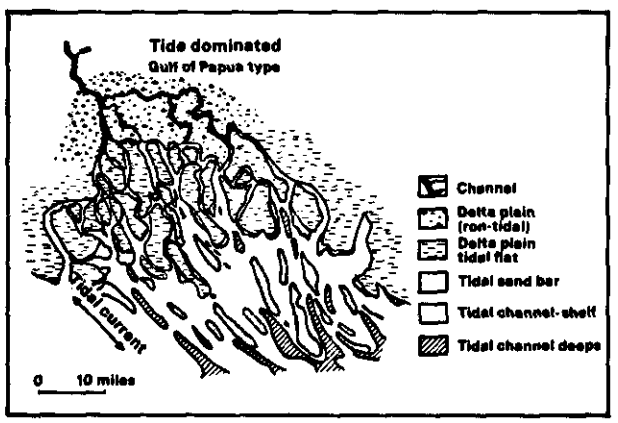

Fig. 6.6-29. - Surface distribution of facies and subenvironments in a modern tide-dominated delta : Gulf of Papua (from Fisher *et al.*, 1969).

(Coleman & Prior, 1980). The subaerial part of the delta consists largely of tidal flats comprising mainly fine-grained deposits. The distributary may contain well-sorted sands, and large quantities of clay and silt will tend to be flushed into the delta marsh environment by overbank flooding during high tides. A typical modern tide-dominated delta is that of the Klang-Langat Rivers in Malaysia (Coleman *et al.*, 1970).

6.6.2.6.1. *Structure*

Thin bedding, parallel to oblique laminations, small and large bidirectional (herringbone) and unidirectional trough cross-bedding; flaser structure; small scours and scour-and-fill; slumps; algal structures; intense bioturbation of sand tops and shales; mudcracks in shales, are the main features of these deltas (Fig. 6.6-30).

6.6.2.6.2. *Boundaries*

Due to permanent bidirectional flow, abrupt, planar to scoured contacts dominate the sequences (Fig. 6.6-31).

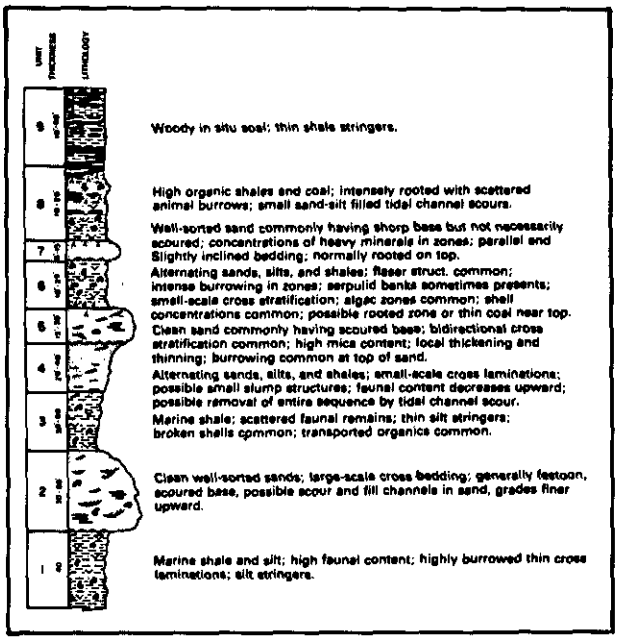

Fig. 6.6-30. - Composite stratigraphic sequence of depositional environments in the Klang-Langat Rivers delta (from Coleman & Prior, 1980).

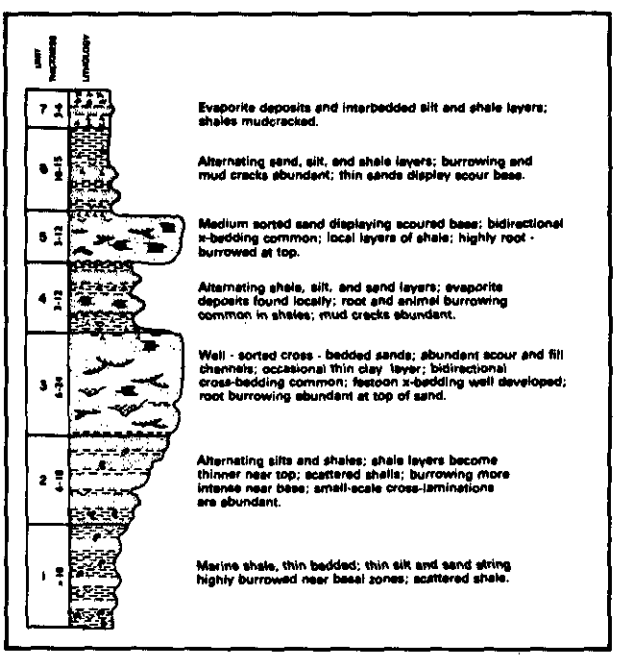

Fig. 6.6-31. - Composite stratigraphic sequence of depositional environments in the Ord River delta, Australia (from Coleman & Prior, 1980).

6.6.2.6.3. *Sequences*

They tend to show definite coarsening-upward, followed eventually by fining-upward, without a well defined boundary, depending on the position in the delta (Fig. 6.6-31).

6.6.2.6.4. *Geometry of the bodies*

Relative thick, elongated sand bodies in the direction of the tide, formed by tidal current ridge

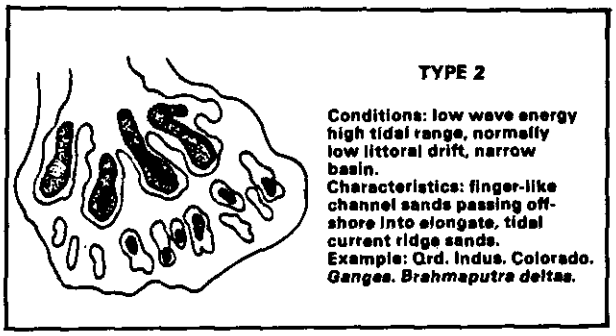

Fig. 6.6-32. - Sand distribution in a tide-dominated delta (from Coleman & Wright, 1975).

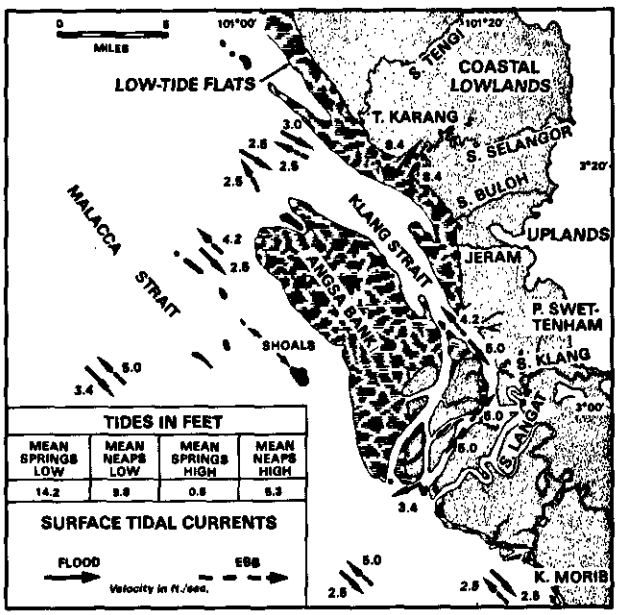

Fig. 6.6-33. - Major physiographic areas, tides, and tidal currents of the Klang-Langat Rivers delta. Tides refer to the British Admiralty data for the Malacca Strait (from Coleman *et al.*, 1970).

sands and shoals, comprising a complex of minor channels and megaripple sands (Fig. 6.6-32), are the main geometrical features observed in this type of delta.

Average measurements of the Ord River ridges gave 2 km long, 300 m wide and 10-22 m high.

6.6.2.6.5. *Directional current flow pattern*

Tidal streams play a dual role : flood and ebb currents tend to generate bimodal distribution. But, the influence of rivers, which renforce tidal action, tends to generate ebb currents stronger than flood, creating an umbalance in the distribution and allowing the system to prograde seaward (Fig. 6.6-33).

6.6.2.7. Reservoir Characteristics

Deltaic sands have, generally, good reservoir characteristics : porosity up to 35 %, permeability *up to thousands of millidarcys in mouth bar* deposits in relation to the good sorting. These properties decrease seaward. In distributary channel sands, the porosity is lower due to poorer sorting, but the permeability is still good in relation to the coarser grains. Due to the general coarsening up sequence the reservoir characteristics (porosity and permeability) are better developed towards the top of each marine deposited reservoir; on the contrary, in fluvial deposits they are better developed at the bottom of each fining up sequence. They constitute a multitude of reservoirs *of limited lateral and vertical extent.* They have the advantage of being in close proximity to potential source rocks. In this environment, growth faulting being common, tectonic and stratigraphic traps are abundant.

6.6.3. WELL-LOG RESPONSES AND CHARACTERISTICS

For more than thirty years, SP and resistivity log shapes (bell, funnel and cylinder shapes) have been used intensively by geologists to recognize sedimentary facies in deltaic deposits. Coleman & Prior (1982) have represented, by summary diagrams including SP and resistivity logs, the major characteristics of the main deposits. They are reproduced in Fig. 6.6-34 to 6.6-41. They can be used to give a rough idea of the facies (by combining curve shapes and thicknesses). Other attemps have been made, earlier by Fisher (1969), and, more recently, by Galloway & Hobday (1983). Hereafter in more detail, actual well-log responses and characteristics are described, as observed in ancient deltas all around the world.

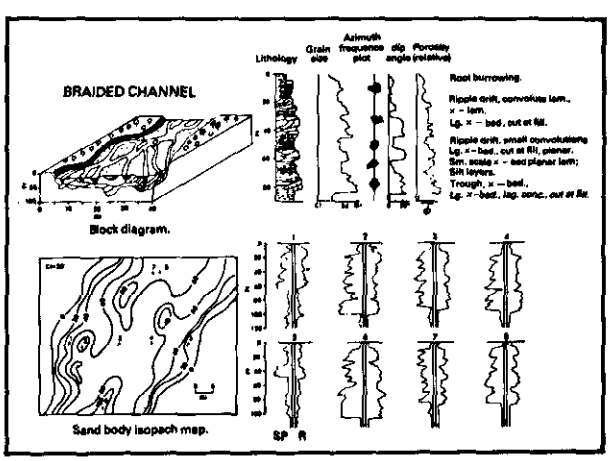

Fig. 6.6-34. - Summary diagrams illustrating the major characteristics of braided channel deposits (from Coleman & Prior, 1982).

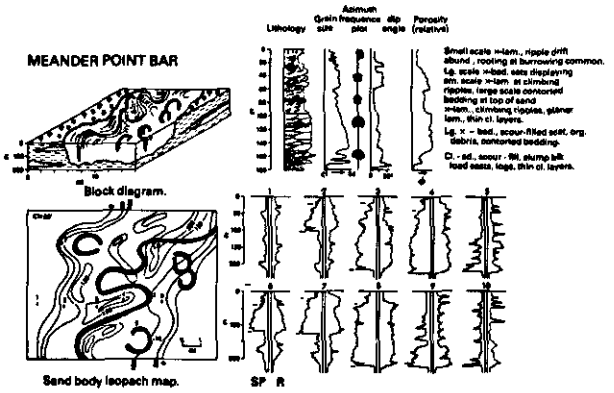

Fig. 6.6-35. - Summary diagrams illustrating the major characteristics of meandering point-bar deposits (from Coleman & Prior, 1982).

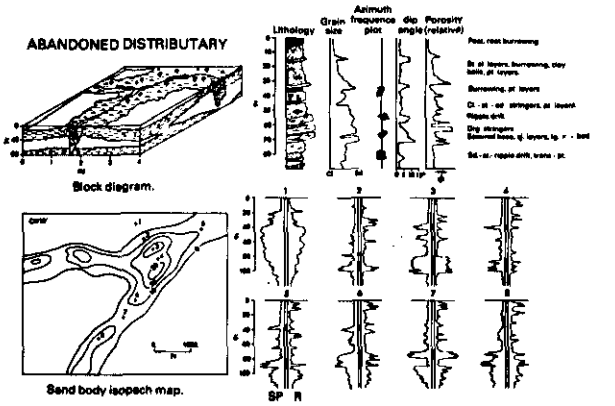

Fig. 6.6-38. - Summary diagrams illustrating the major characteristics of abandoned distributary deposits (from Coleman & Prior, 1982).

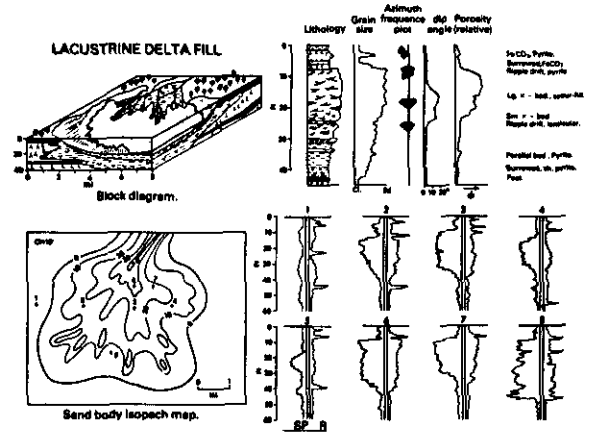

Fig. 6.6-36. - Summary diagrams illustrating the major characteristics of lacustrine delta-fill deposits (from Coleman & Prior, 1982).

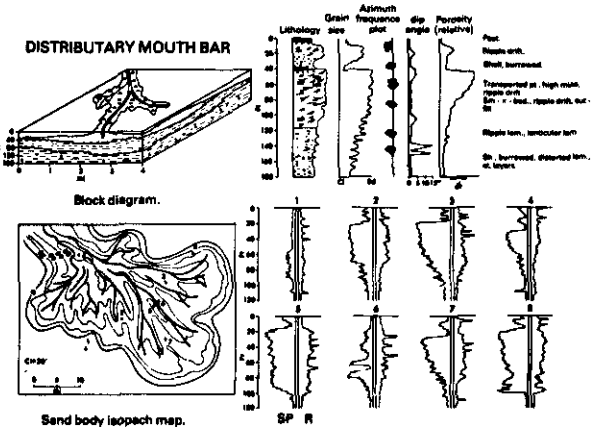

Fig. 6.6-39. - Summary diagrams illustrating the major characteristics of the distributary-mouth bar deposits (from Coleman & Prior, 1982).

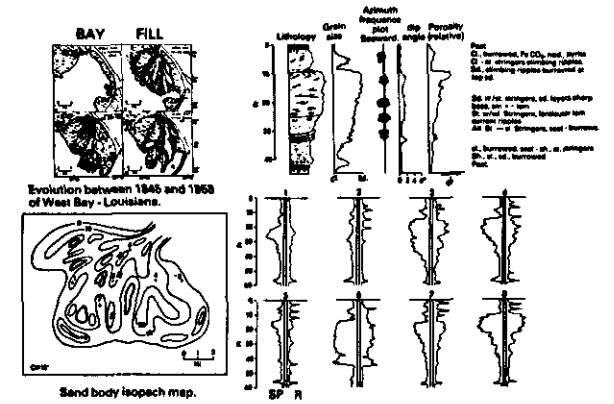

Fig. 6.6-37. - Summary diagrams illustrating the major characteristics of the bay-fill deposits (from Coleman & Prior, 1982).

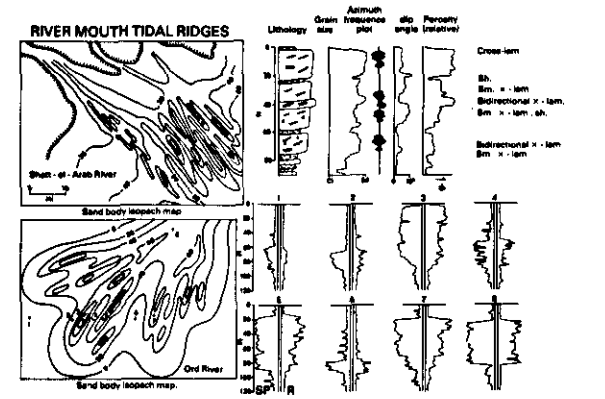

Fig. 6.6-40. - Summary diagrams illustrating the major characteristics of river-mouth tidal ridge deposits (from Coleman & Prior, 1982).

6.6.3.1. Electro-Lithofacies

The mineralogical composition is obtained by log and crossplot analysis. For instance, very low radioactive intervals can correspond to : (a) coarse grained or well washed sands, (b) coal (peat or lignite), or (c) limestone beds (accumulation of shell fragments). The separation between those facies is obtained with the help of the ρ_b vs ϕ_N crossplot, or of the Pe or $(U_{ma})_a$ values (Fig. 6.6-42).

Low to moderately radioactive intervals are representative of medium to fine sands.

Radioactive intervals can correspond to : (a) silt deposits rich in thorium bearing minerals (i.e.

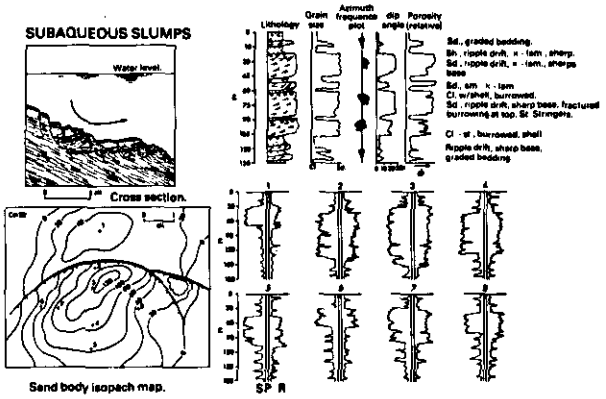

Fig. 6.6-41. - Summary diagrams illustrating the major characteristics of slump deposits (from Coleman & Prior, 1982).

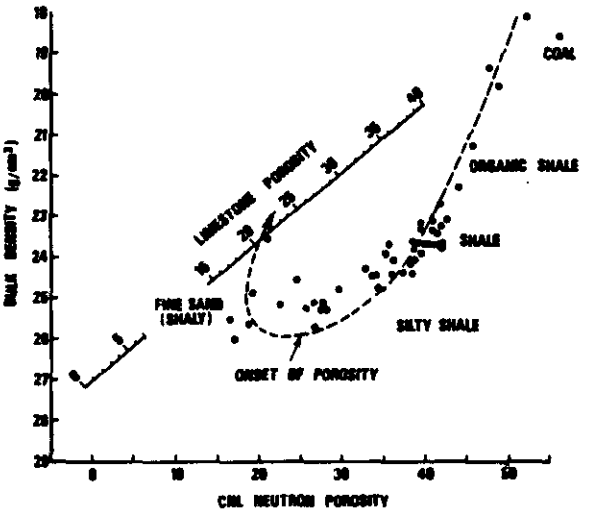

Fig. 6.6-42. - Location of facies on a ρ_b vs ϕ_N crossplot (from Rider & Laurier, 1979).

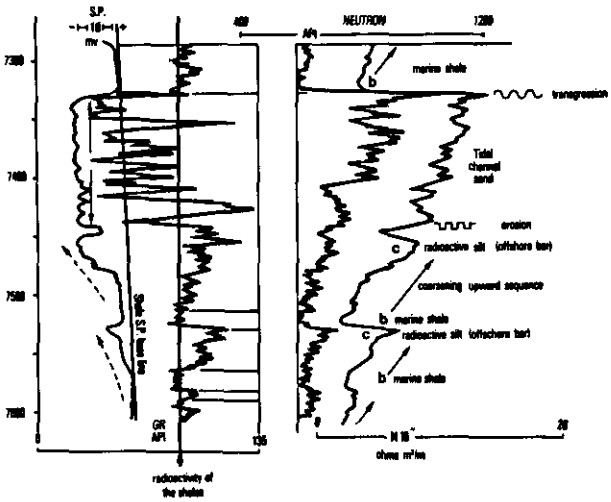

Fig. 6.6-43. - Example of silt more radioactive than the shale. Silt beds are easily located on the SP and neutron curves (levels c) (from Serra & Sulpice, 1975).

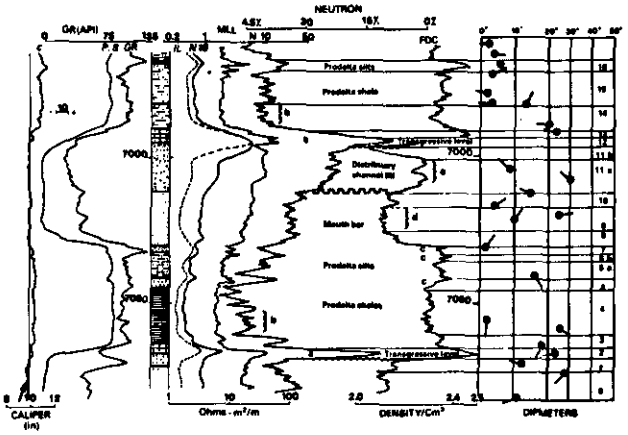

Fig. 6.6-44. - The analysis of the gamma ray, neutron, density and resistivity curves indicates clearly two types of sand : the deepest (d) is finer, a little radioactive due to small amount of silt, well sorted (high porosity 35 %); the sand above (e) is coarser (low radioactivity), moderately sorted (ϕ_{CP} = 22 %). This figure is an enlargement of an interval of Fig. 6.6-49 (see below).

zircon), and often heavy minerals (i.e. siderite, pyrite, micas), or (b) shales. The lithofacies recognition will be based on the ρ_b vs ϕ_N crossplots with SP, Pe, thorium (Th) and potassium (K) on Z axis. In the example of Fig. 6.6-43 the silty bed, *well differentiated on the SP and neutron curves* (level c), is more radioactive than the surrounding shales. Thorium and potassium help to define the predominant clay mineral type, and uranium correlates with the percentage of organic material.

Textural information can be extracted from the porosity level and its evolution in combination with gamma ray and SP analysis (Fig. 6.6-44). High porosity (between 30 and 40 %) suggests well sorted sand, the level of radioactivity and the position on the ρ_b vs ϕ_N crossplot indicating the *mean grain size (finer if more radioactive and* dense); medium porosity (from 15 to 25 %) may correspond to poorly to moderately sorted sand or to quartz cemented sand if the representative points fall on the sandstone or silstone line on a ρ_b vs ϕ_N crossplot with no change of Pe, or to a calcareous cemented sand, if the representative points move toward the limestone line and if the Pe value increases.

6.6.3.2. *Dip Patterns*

Several features can be observed in shale intervals : no or few dips reflect homogeneous, or heterogeneous, or bioturbated shales (Fig. 6.6-46b between 1362 and 1372 m), whereas numerous dips with approximately the same azimuth and small changes in magnitude (Fig. 6.6-46b between 1301 and 1317 m) indicate laminated silty shales without strong bioturbation, sometimes with small scale ripple marks. Blue patterns characterize foreset beds and can be used to define the

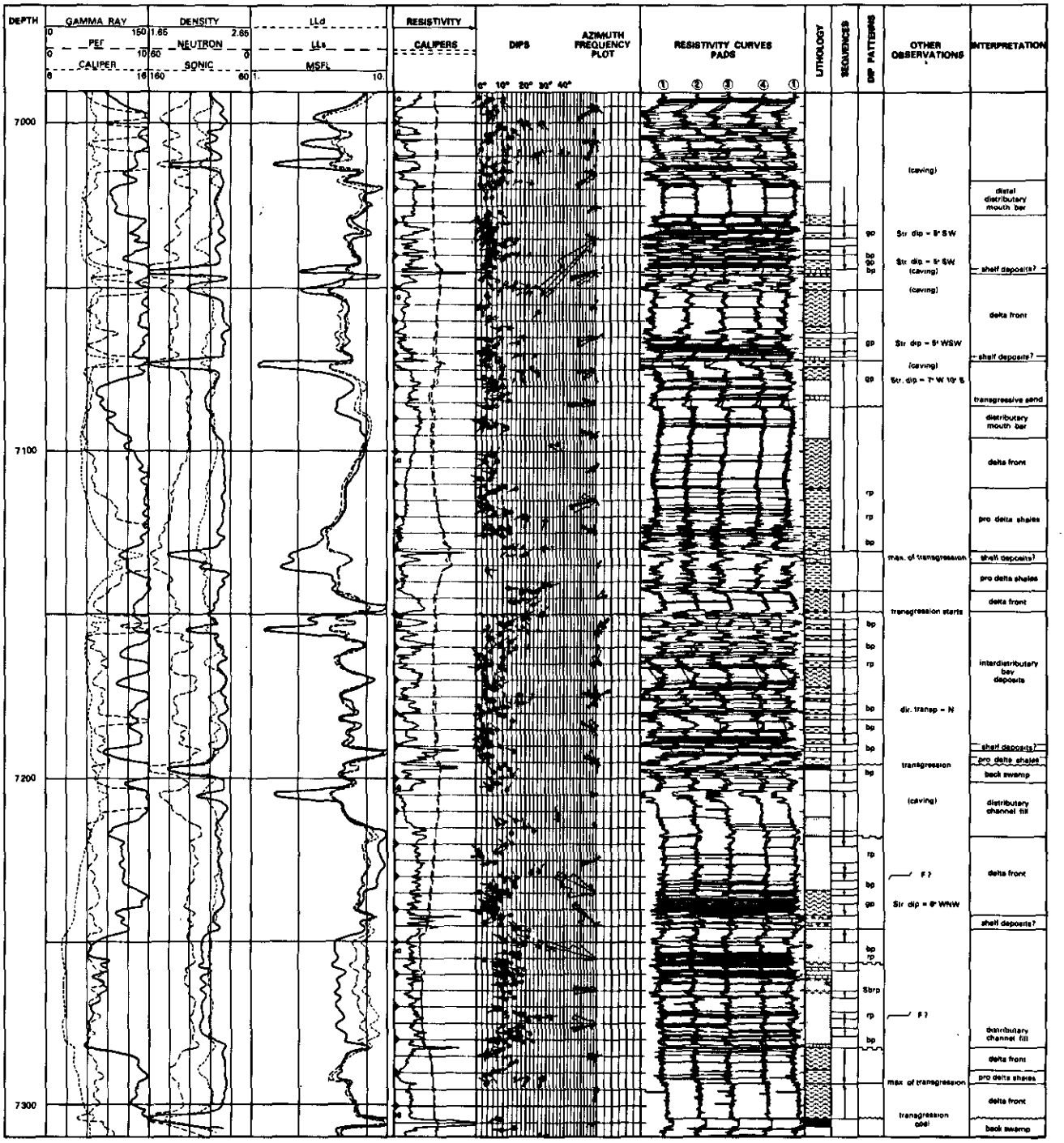

Fig. 6.6-45. - Composite-log with GEODIP results and their interpretation, illustrating a deltaic environment.

direction of transport. They indicate progradation processes. Isolated red patterns above a sand bed correspond to draping over the previous deposit (i.e. barrier bar).

In sandy intervals several dip patterns can be recognized. No or scattered dips reflect bioturbation or cross-bedding. Blue patterns correspond to foreset beds (Fig. 6.6-46b from 1276 to 1278 m). Red patterns can reflect filling of a channel (Fig. 6.6-45 from 7248 to 7273 m). Numerous dips with more or less the same azimuth and small changes in dip angle may correspond to ripple marks (Fig. 6.6-46b from 1296 to 1301 m).

FMS images can be useful to recognize typical sedimentary features such as foresets, flaser and wavy beddings, slumps, burrows... Those features have been illustrated in the chapter on structure. Herringbone cross-bedding which can indicate tidal influences can also be detected on FMS images as shown by Fig. 6.6-47.

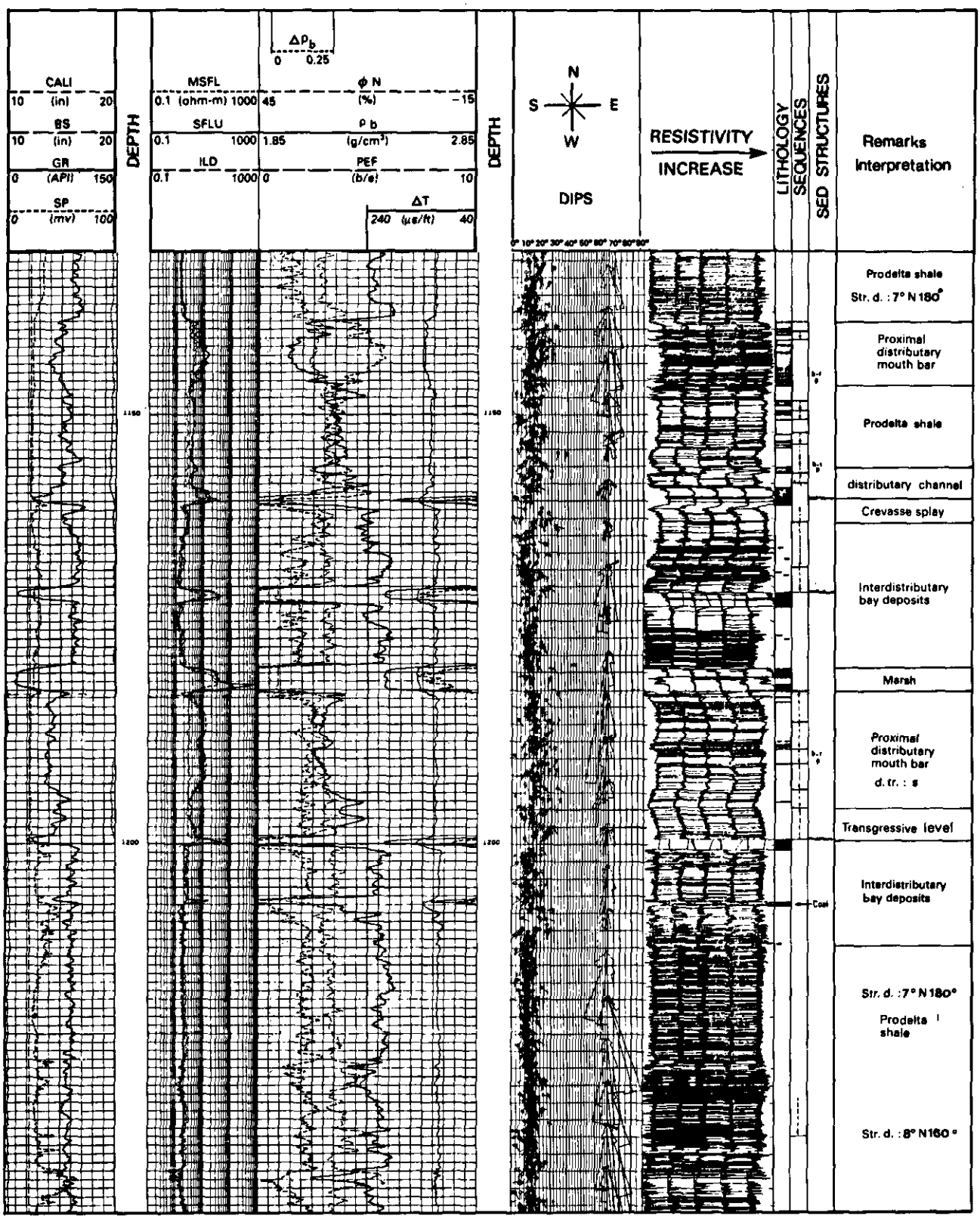

Fig. 6.6-46a. - Another example of a composite-log with its interpretation.

6.6.3.3. Boundaries

They are generally very well defined by dipmeter. Abrupt, sharp lower contact is the rule as well as gradational contact toward the top.

Fig. 6.6-46b. - Another example of a composite-log with its ▶ interpretation.

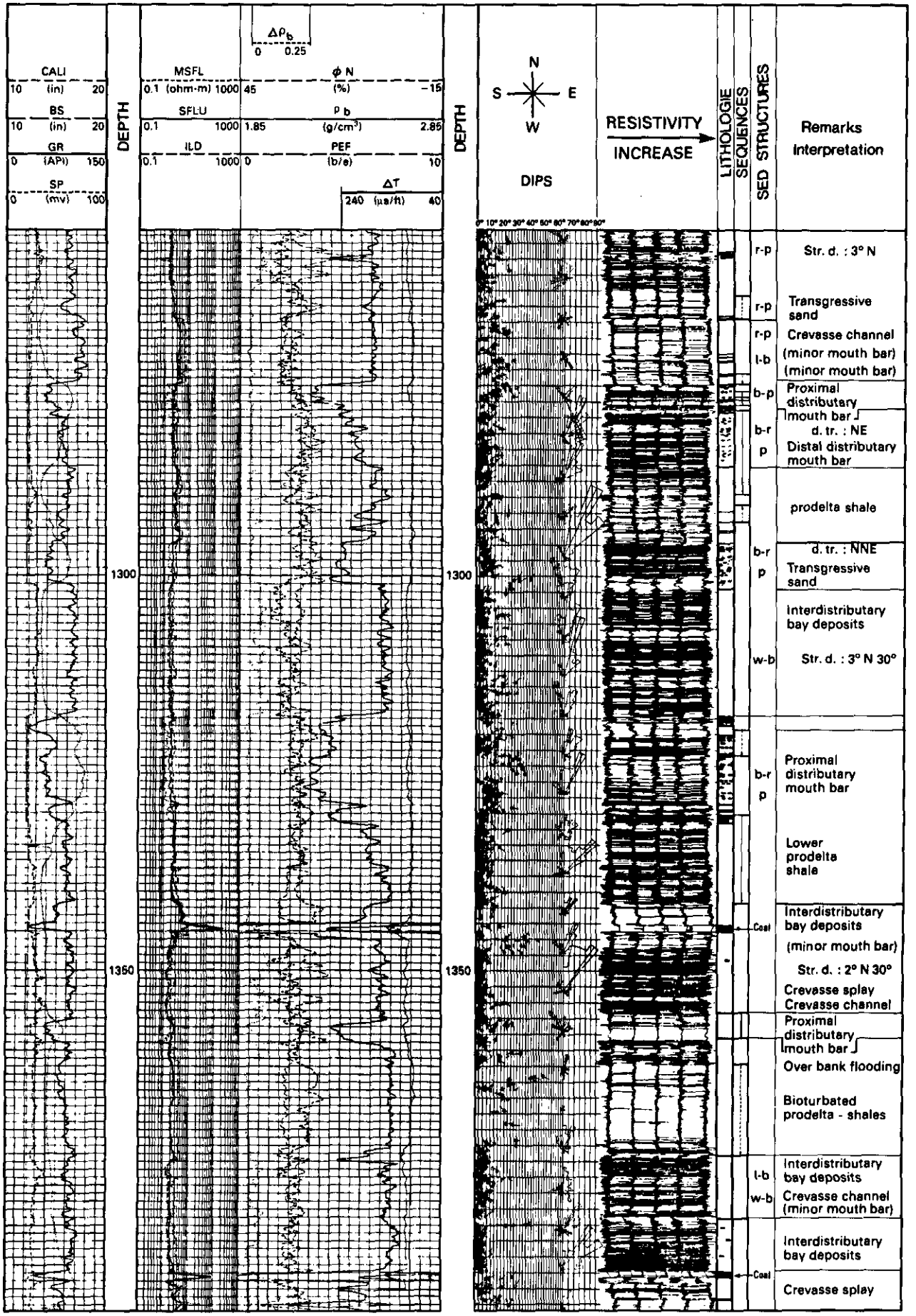
CALI
10 (in) 20
BS
10 (in) 20
GR
0 (API) 150
SP
0 (mv) 100
DEPTH
MSFL
0.1 (ohm-m) 1000
SFLU
0.1 1000
ILD
0.1 1000
Δρb
0 0.25
φN
45 (%) -15
ρb
1.85 (g/cm³) 2.85
PEF
0 (b/e) 10
ΔT
240 (μs/ft) 40
1300
1350
N
S
E
W
DIPS
RESISTIVITY
INCREASE
LITHOLOGIE
SEQUENCES
SED STRUCTURES
Remarks
Interpretation
r-p
Str. d. : 3° N
r-p
Transgressive sand
r-p
Crevasse channel
l-b
(minor mouth bar)
(minor mouth bar)
b-p
Proximal distributary mouth bar
d. tr. : NE
b-r
p
Distal distributary mouth bar
prodelta shale
d. tr. : NNE
b-r
p
Transgressive sand
Interdistributary bay deposits
w-b
Str. d. : 3° N 30°
b-r
p
Proximal distributary mouth bar
Lower prodelta shale
Coal
Interdistributary bay deposits
(minor mouth bar)
Str. d. : 2° N 30°
Crevasse splay
Crevasse channel
Proximal distributary mouth bar
Over bank flooding
Bioturbated prodelta - shales
l-b
w-b
Interdistributary bay deposits
Crevasse channel (minor mouth bar)
Interdistributary bay deposits
Coal
Crevasse splay

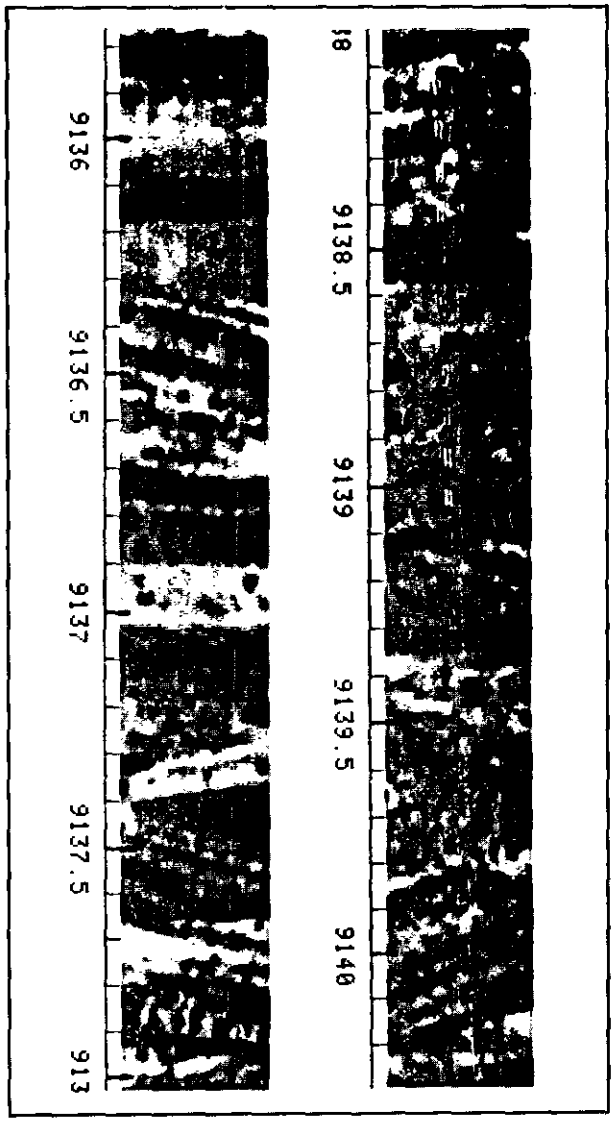

Fig. 6.6-47. - Example of herringbone cross-bedding as it can be observed on a FMS image (courtesy of Schlumberger).

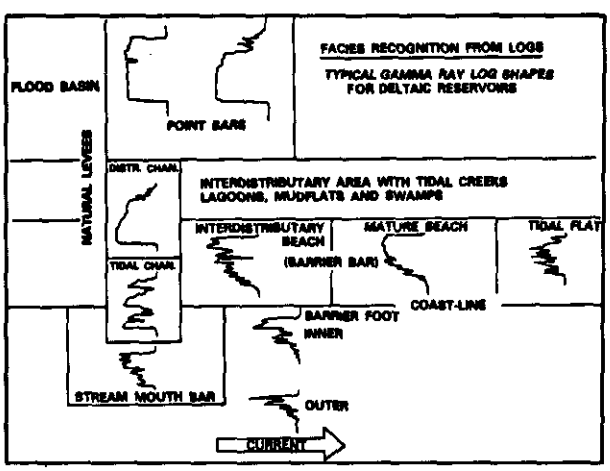

Fig. 6.6-48. - Interpretation of gamma ray curve shapes in *terms of facies in deltaic deposits (from Schlumberger, Well* Evaluation Conference. Nigeria, 1985).

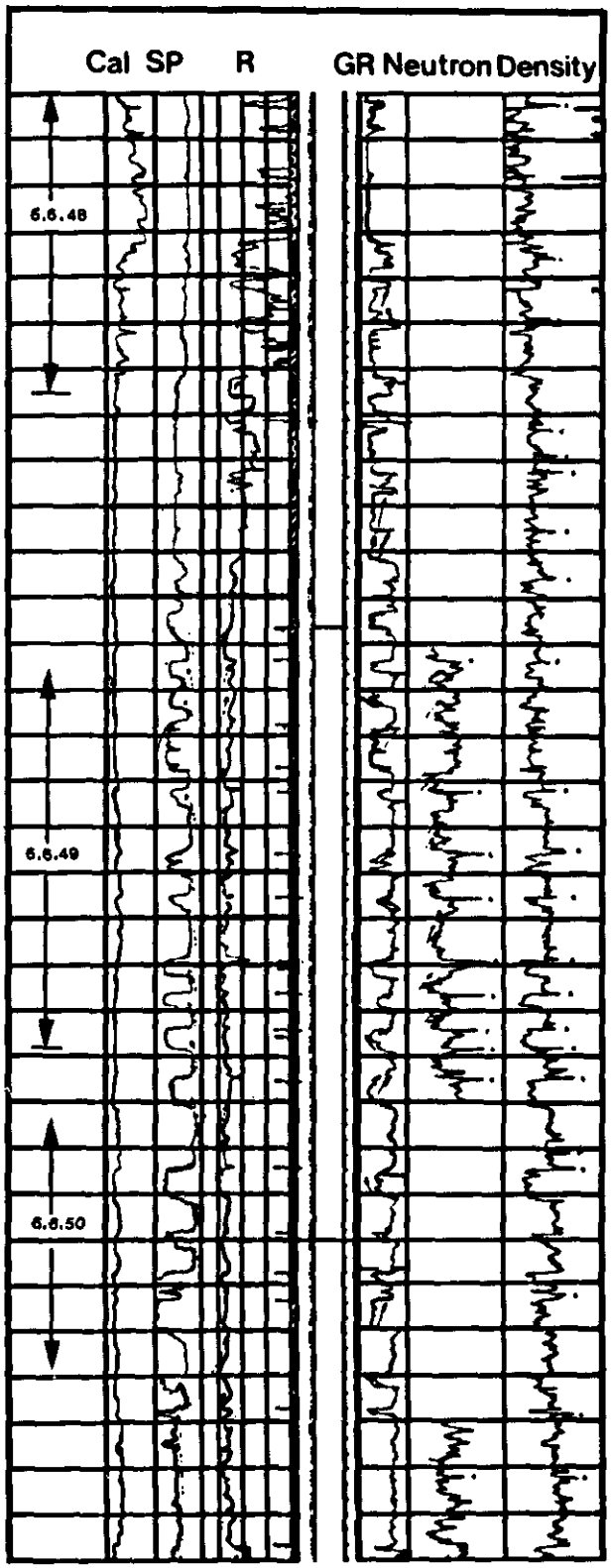

Fig. 6.6-49. - Composite-log from a Nigerian well giving *another example of a deltaic environment (adapted from Serra* & Sulpice, 1975).

6.6.3.4. Electro-Sequences

They are well known and have been used intensively in Gulf Coast to recognize the nature of the

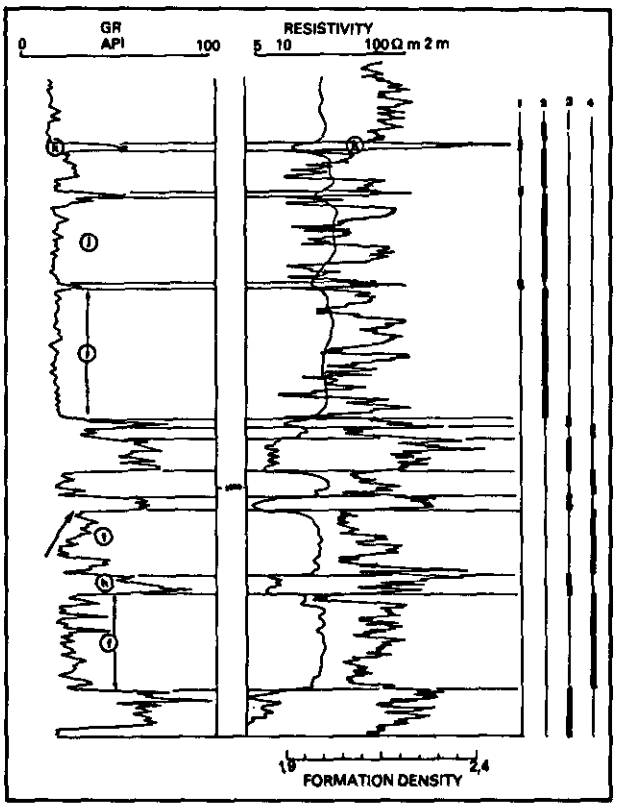

sand body (bell, funnel and cylinder shapes described by SHELL geologists thirty years ago). They are usually easily, and sometimes better, detected on open-hole logs than on dipmeter curves except when the elementary sequences are too thin, in that case dipmeter curves allow a more precise recognition of the polarity (fining or coarsening upward). In many cases, the shape of the SP or gamma ray curves can be directly interpreted in terms of facies as illustrated in Fig. 6.6-48.

Funnel shape corresponds to coarsening upward sequence and consequently to progradation process and subaqueous delta plain deposits (cf. Fig. 6.6-45 between 7130 and 7080 ft, and Fig. 6.6-46b between 1290 and 1276 m). Bell shape

◀ Fig. 6.6-50. - Enlargement of the upper interval of Fig. 6.6-49, illustrating bell shape (f) and cylinder shape (j) which may correspond respectively to meandering channel and braided channel deposits (from Serra & Sulpice, 1975).

Fig. 6.6-51. - Enlargement of the middle interval of Fig. 6.6-49, illustrating several funnel shapes and a succession of cylinder shapes constituting a general bell shape (interval f toward the top); this last interval may correspond to tidal channel deposits intercalated with tidal flats (from Serra & Sulpice, 1975). ▼

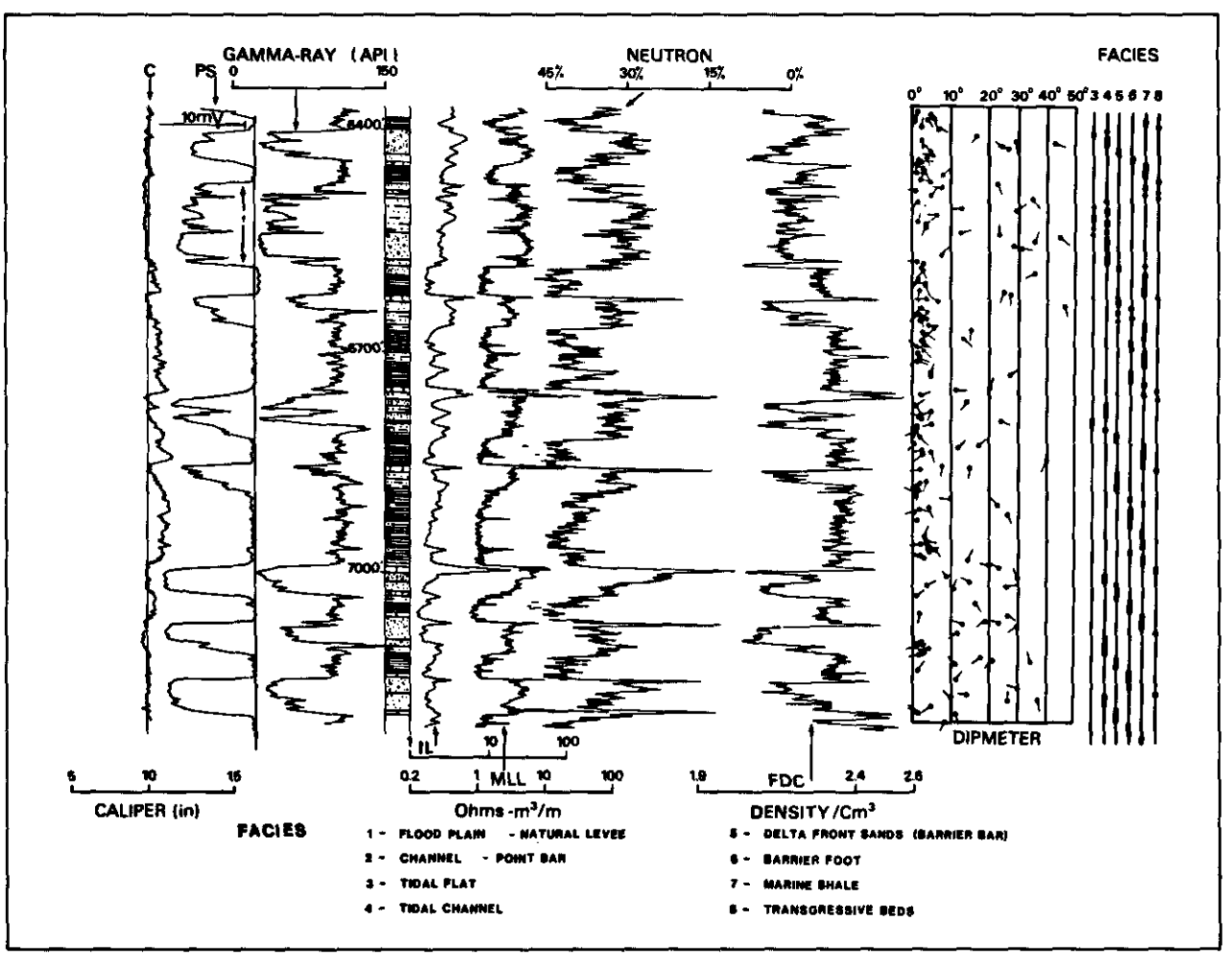

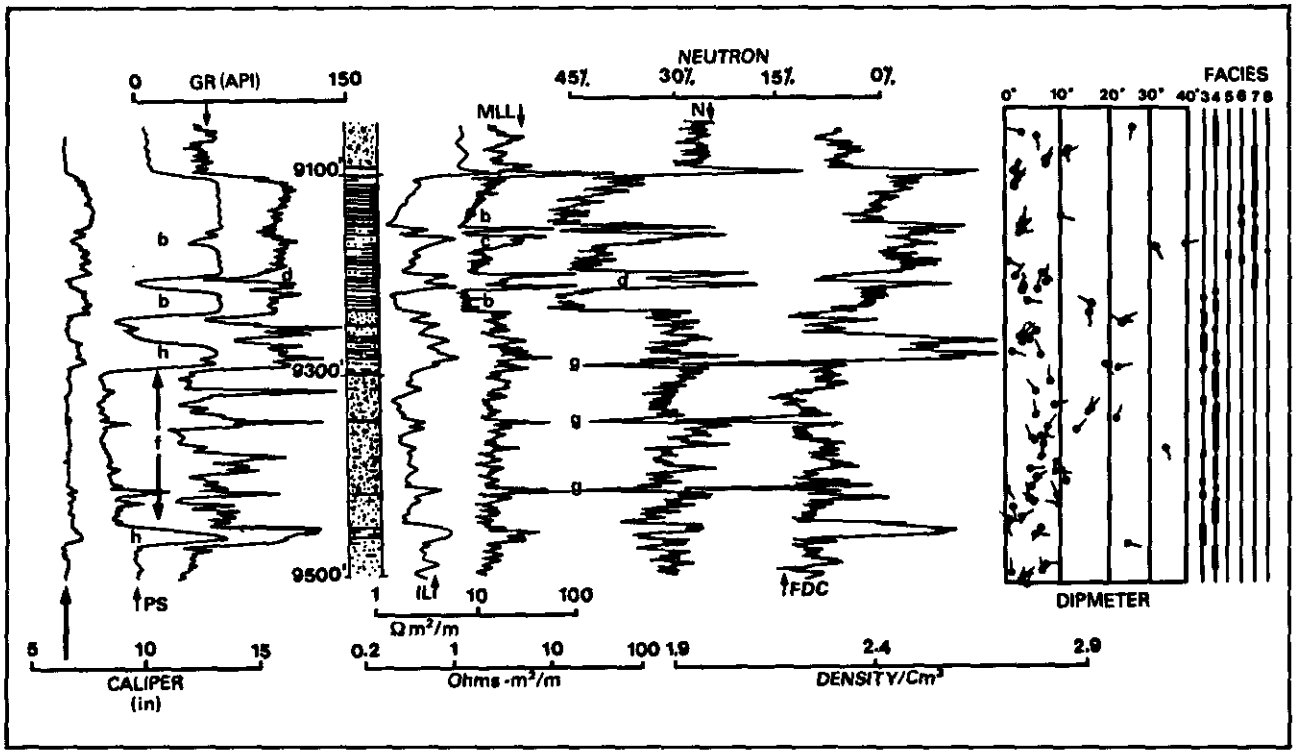

Fig. 6.6-52. - Enlargement of the lower interval of Fig. 6.6-49, showing two cylinder shapes one at the bottom, the other at the top. The deepest cylinder may correspond to a tidal channel interbedded with tidal flat deposits (lignite beds). The top cylinder starts with a very resistive and compact bed (i) which may correspond to an accumulation of shell debris mixed with coarse sand, often described at the bottom of tidal channels (from Serra & Sulpice, 1975).

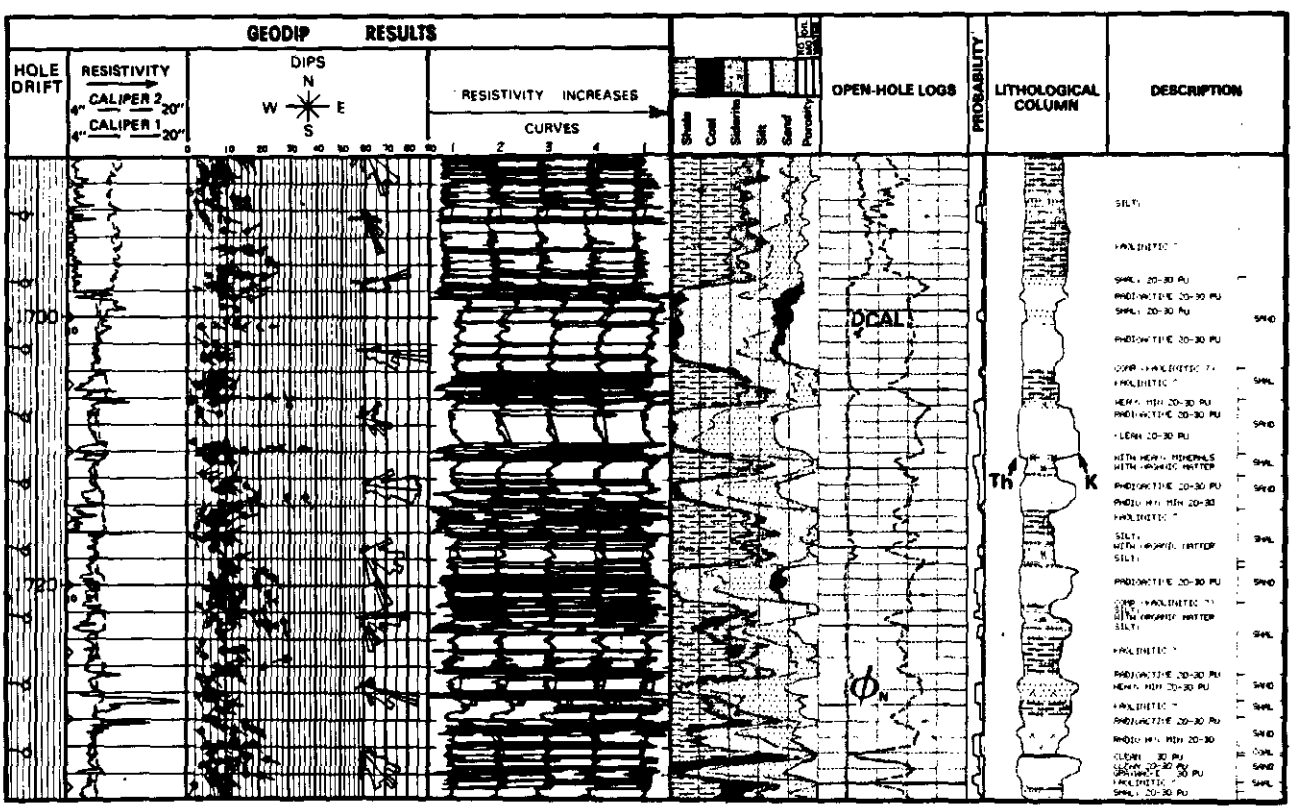

Fig. 6.6-53. - Composite-log with LITHO and GLOBAL results and a GEODIP arrow-plot at the same scale (from Schlumberger, Well Evaluation Conference. India, 1983).

corresponds to fining upward sequence which can be interpreted as distributary channel fill (Fig. 6.6-45 between 7283 and 7248 ft, and Fig. 6.6-46a between 1160 and 1155.5 m), meandering channel deposits, or transgressive level (Fig. 6.6-46b between 1301 and 1296 m). Cylinder shape, often serrated, may correspond to braided channel deposits (Fig. 6.6-49 and Fig. 6.6-50), tidal channel deposits (Fig. 6.6-51), subaqueous slump deposits. Dip patterns and FMS images can help to distinguish between those deposits.

Another typical log response in deltaic deposits is given with its interpretation. It comes from the Jotana Formation, India (Fig. 6.6-53 and 6.6-54). It illustrates several characteristic features which can be observed both on open-hole logs and dipmeter in deltaic environment.

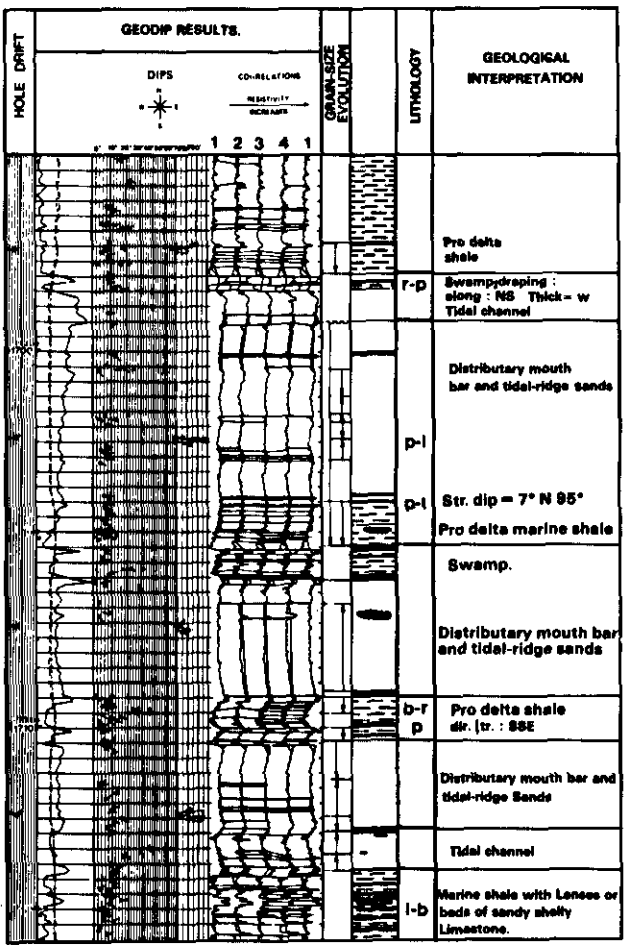

Fig. 6.6-54. - Detailed GEODIP interpretation of the lower ▶ interval of Fig. 6.6-53 (1720-1690 m) in a deltaic formation : Jotana Formation, India (from Schlumberger, Well Evaluation Conference. India, 1983).

l	: lens	dir. tr.	: direction of transport
p-lam	: parallel laminations	str. dip	: structural dip
l-b	: lenticular bedding		: sandy limestone (shell debris)
	: direction of fining		: marine transgression
	: peat		: erosional surface
	: coal fragment		: sand and silt
w.b.	: wavy bedding		: shale
b-r	: blue and red pattern.		

6.7. SHALLOW SILICICLASTIC SEA ENVIRONMENT

6.7.1. DEFINITION

Environments characterized by detrital deposits in moderate water depth (10-200 m), or on nearshore continent (at the exclusion of deltas), under tides, waves, wind, longshore currents, or storms as dominant sediment-moving forces. They include deposits such as : estuarine, tidal ridges, tidal flats, sand waves, sand ribbons, intertidal sand bars, strand plains, barrier islands, beach ridges, cheniers, shorelines, storm deposits ("tempestites" as defined by Ager, 1974), offshore bars.

6.7.2. GEOLOGICAL FACIES MODEL

Because of the difficulties to recognize all of these environments in ancient records, only three main environments will be described and illustrated hereafter.

6.7.2.1. Tidal sand Ridges

6.7.2.1.1. *Definition*

Tidal sand ridges are elongated sand bodies formed by tidal currents.

6.7.2.1.2. *Composition*

Detrital quartz is dominant and the sand is mineralogically mature; argillaceous rock fragments, skeletal shell debris can occur especially as a basal lag conglomerate. Some glauconite and authigenic feldspar are mentioned. Peat, clay galls and wood fragments are common. Detrital and authigenic cement can be present.

6.7.2.1.3. *Texture*

Well-sorted (Fig. 6.7-1), medium-grained sand is the dominant feature, with moderate to high grain-matrix ratio. Grain size distribution across the ridges is relatively uniform. Grain size may decrease upward within a ridge, and on a regional scale in the direction of net tidal current transport.

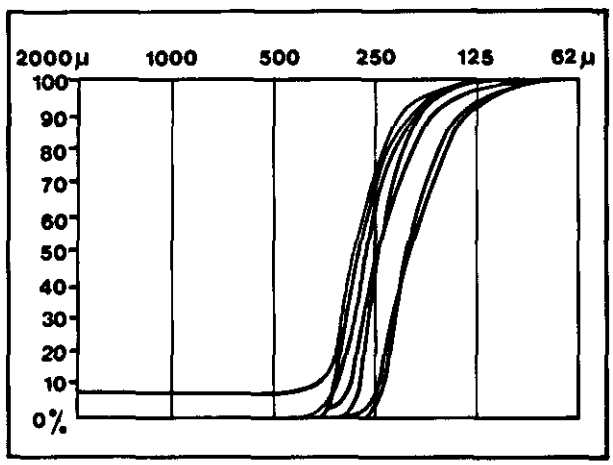

Fig. 6.7-1. - Example of grain size distribution curves from North Sea tidal sand ridges (from Houbolt, 1968).

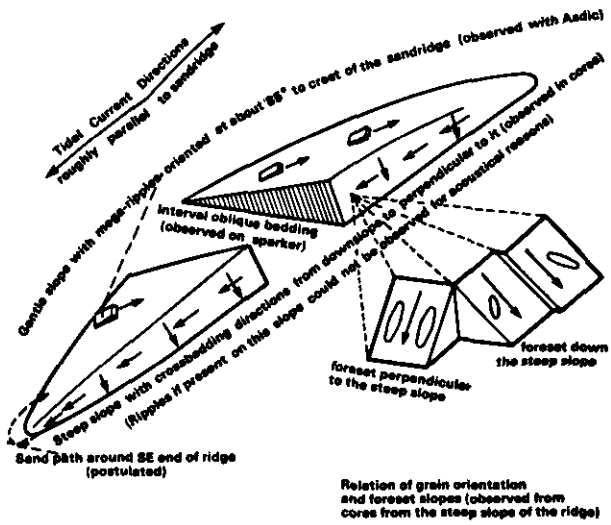

Fig. 6.7-2. - Schematic diagram of sedimentary features of a tidal ridge in the North Sea (from Houbolt, 1968).

6.7.2.1.4. *Structure*

Tidal ridges are composed of large-scale foreset beds with flanks dipping at angle of repose (30°), parallel to the steep ridge flank (Fig. 6.7-2). These cross sets are commonly draped by clay

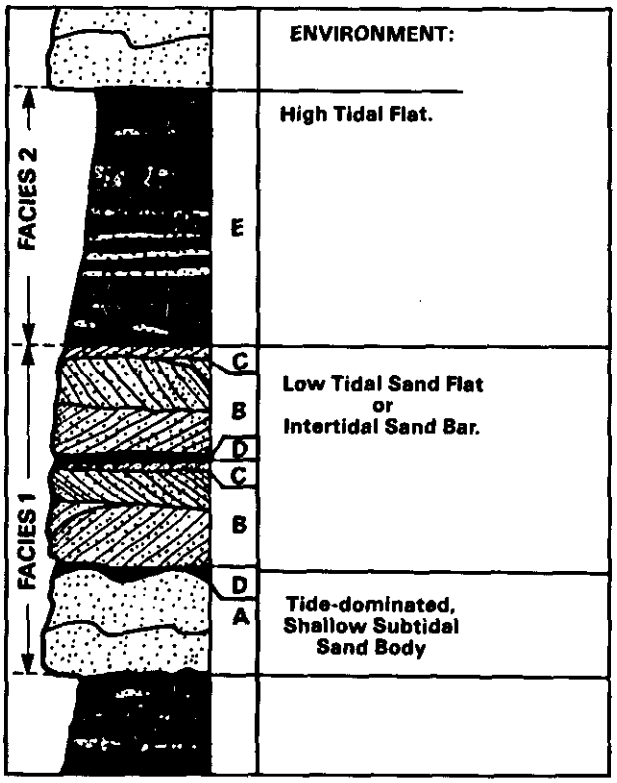

Fig. 6.7-3. - A fining upward sequence and its interpretation. This sequence includes alternation of facies 1 and 2, comprising tide-dominated shallow, subtidal sand body (massive sandstone of interval A) with basal lag conglomerate, grading into a low tidal sand flat or low tidal intertidal sand bar (cross-stratified sandstone of interval B) which has been reworked by late-stage, sheet-runoff tidal flow (sandstone of interval C), draped by clay produced by mud suspension settlement during slack water (interval D) occurring on top of both intervals A and C. Interval E consists of mudstone and silstone with lenticular bedding, tidal bedding, and burrowing structures, all deposited in a high tidal flat environment (adapted from Klein, 1970).

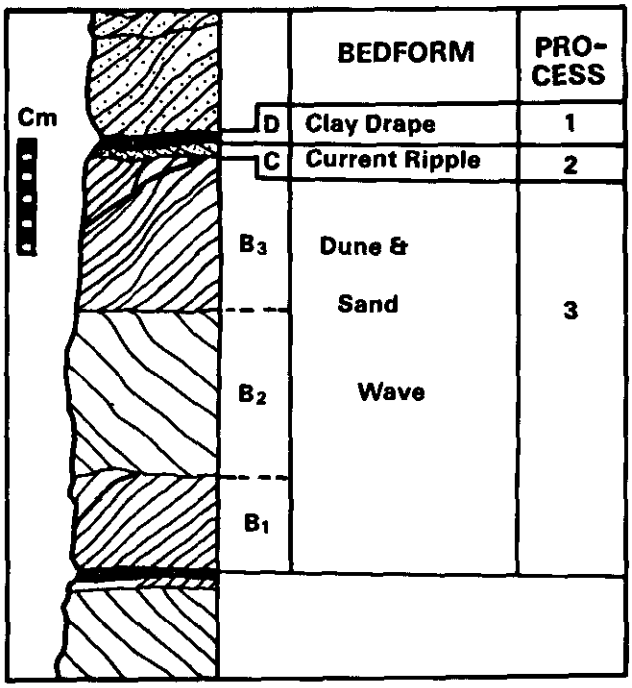

Fig. 6.7-4. - Sequence in facies 1 (see Fig. 6.7-3) showing vertical change from cross-stratified sandstone (interval B) into micro-cross-laminated sandstone with dips oriented at 90° to 180° to underlying cross-stratification dip orientation (interval C) and clay drape (interval D). Depositional processes are indicated on the side (from Klein, 1970).

laminae (mud suspension settlement during slack water : Fig. 6.7-3). Small foreset strata (sand waves) on the gentle ridge slope overlie the large cross sets. Asymmetrical ripples overlie the sand wave cross sets. Tracks, trails and burrows are abundant. A strong vertical decrease in grain size and bed thickness is generally observed.

6.7.2.1.5. *Boundaries*

An abrupt, erosional lower contact is the rule. Gradational contact toward the top is frequently observed.

6.7.2.1.6. *Sequences*

Vertical sequences within a tidal sand ridge may include (Spearing, 1971) : (1) a thin, basal lag conglomerate, rich in shell fragments, separating sand from underlying older marine clays; (2) large scale cross sets composed of well sorted sand; (3) thin, short silty-clay laminae draped over the cross sets; (4) upward grain size reduction; (5) sand wave cross sets near the top overlain by (6) asymmetrical ripple stratification. Klein (1970) recognizes sharp-based, fining upward sequences, which he interprets as shallow subtidal, tide-dominated facies which grade upward into low-tidal sand flat or low-tidal sand bar facies (Fig. 6.7-3 and 6.7-4).

6.7.2.1.7. *Geometry of the bodies*

Present day tidal sand ridges in the North Sea (Fig. 6.7-5) are long and straight, up to 40 m high, 65 km long and 5 km wide. Ridges are asymmetric in cross section with a steep lee slope and gentle stoss slope (Fig. 6.7-2).

Other associated sand bodies may exist. They are described hereafter.

Sand waves are much smaller and are oriented normal to tidal current directions. They are between 1 and 10 m high, asymmetrical, and spaced a few hundred metres apart.

Sand ribbons are elongated bodies that run parallel to the strongest tidal current flow. They are up to 15 km long, 200 m wide and not greater than 1 m thick.

Intertidal sand bars are linear, asymmetrical, about 5 to 6 km long, 1 km wide, and 6 to 10 m high. The steep slopes average 8° and gentle slopes 2°. Texture is fine to medium sand on steep bar faces. Bed forms are dominantly current ripples and dunes. Texture is medium to coarse sand on gently sloping bar faces. Bed forms are simple and complex dunes and sand waves.

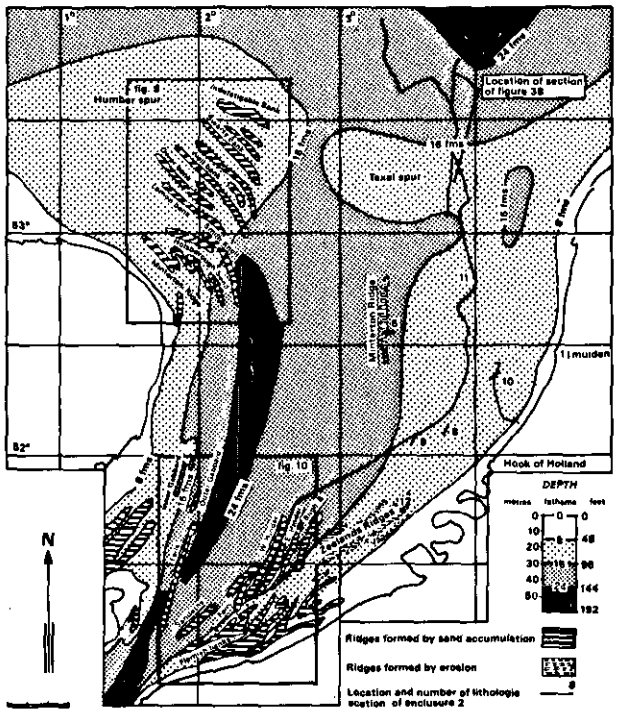

Fig. 6.7-5. - Tidal sand ridges location in the southern North Sea (from Houbolt, 1968).

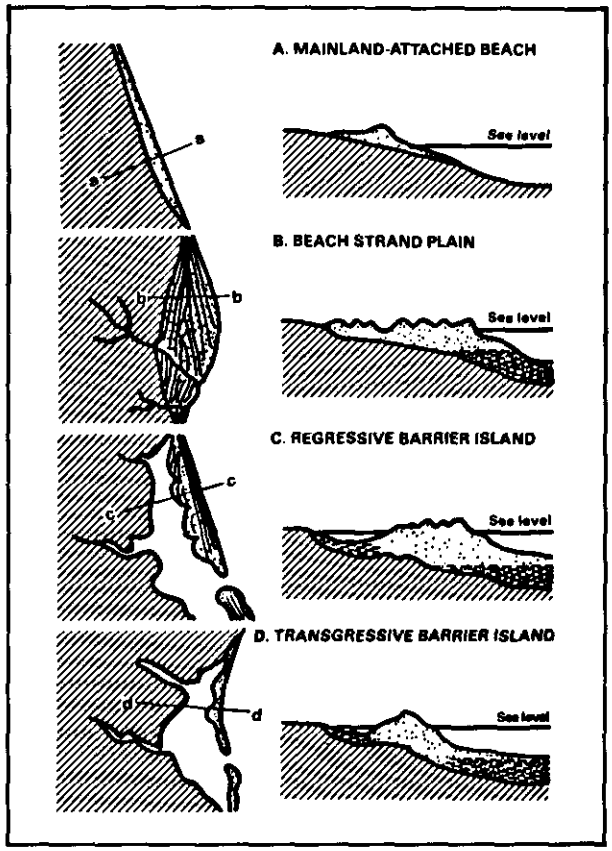

Fig. 6.7-6. - Generalized diagram illustrating the morphological relationship between beaches, strand plains and barrier islands (from Reinson, 1984).

6.7.2.1.8. *Directional current flow*

The long axis of tidal sand ridges is roughly parallel to the tidal current directions (Fig. 6.7-2).

6.7.2.1.9. *Surrounding facies*

Tidal sand ridges and other associated sand bodies (sand waves, sand ribbons and intertidal sands) may be surrounded by marine muds, tidal-flat silts and muds, barrier island, beach, or fluvial-estuarine deposits.

6.7.2.2. Clastic Shoreline, Barrier Island, and Associated Systems

6.7.2.2.1. *Definition*

According to Reinson (1984) "wave-dominated sandy shorelines in interdeltaic and non-deltaic coastal regions are characterized by elongated, shore-parallel sand deposits. These can occur as a single mainland-attached beach, a broader beach-ridge strand plain consisting of multiple parallel beach ridges and intervening swale zones or as barrier islands partially or wholly-separated from the mainland by a lagoon, estuary or marsh (Fig. 6.7-6)".

Considering a barrier island system three major geomorphic elements can be recognized (Fig. 6.7-7) : (1) the sandy barrier island chain itself; (2) the enclosed body of water behind it (lagoon or estuary); (3) the channels which cut through the barrier and connect the lagoon to the open sea (tidal inlets). They correspond to three major subenvironments : (1) the sub-tidal to sub-aerial barrier-beach complex; (2) the back-barrier region or subtidal-intertidal lagoon; and (3) the subtidal-intertidal delta and inlet-channel complex (Reinson, 1979). These subenvironments can in turn be subdivided into several zones. Their main characteristics (composition, texture, sedimentary features) are summarized in Fig. 6.7-8 and illustrated by the vertical profiles of Fig. 6.7-9 to 6.7-11.

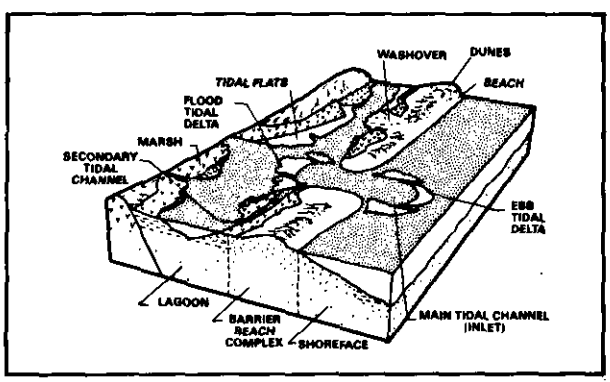

Fig. 6.7-7. - Block diagram illustrating the various subenvironments in a barrier-island system (from Reinson, 1979).

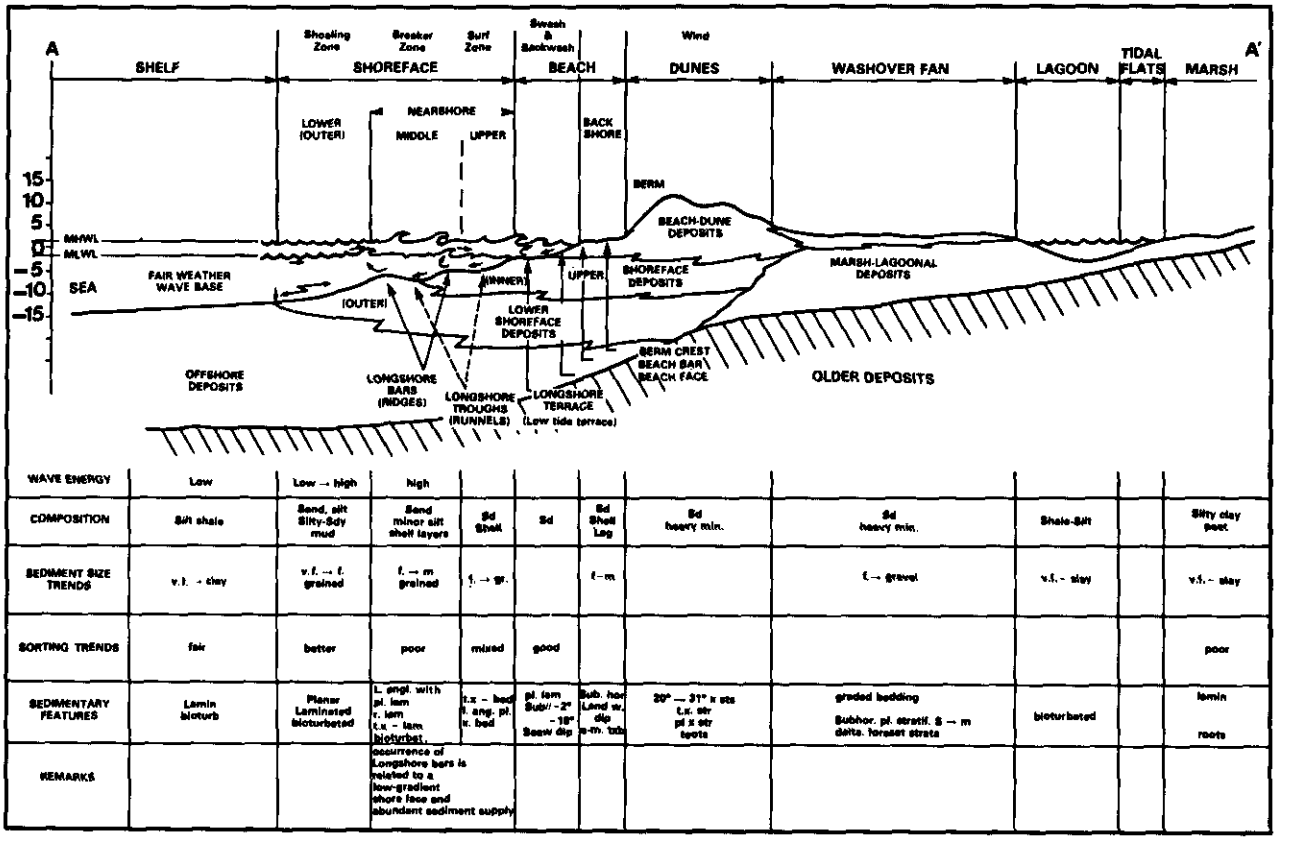

Fig. 6.7-8. - Schematic cross-section through a barrier-island system with indications of the main characteristics.

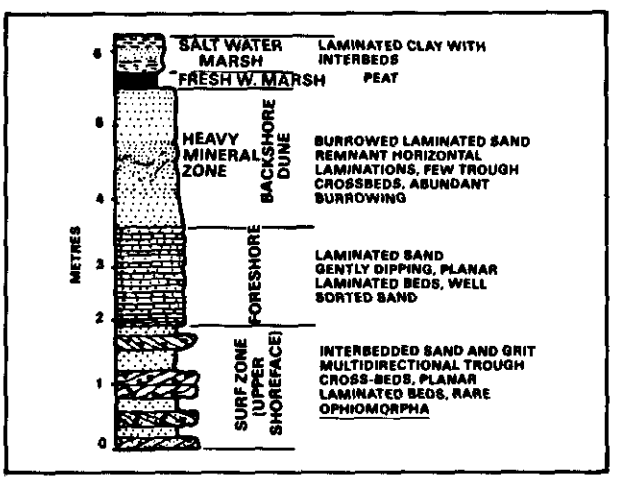

Fig. 6.7-9. - Generalized vertical profile in a barrier-island system from observations made in the Upper Tertiary Cohansey Sand of New Jersey (modified from Carter, 1978).

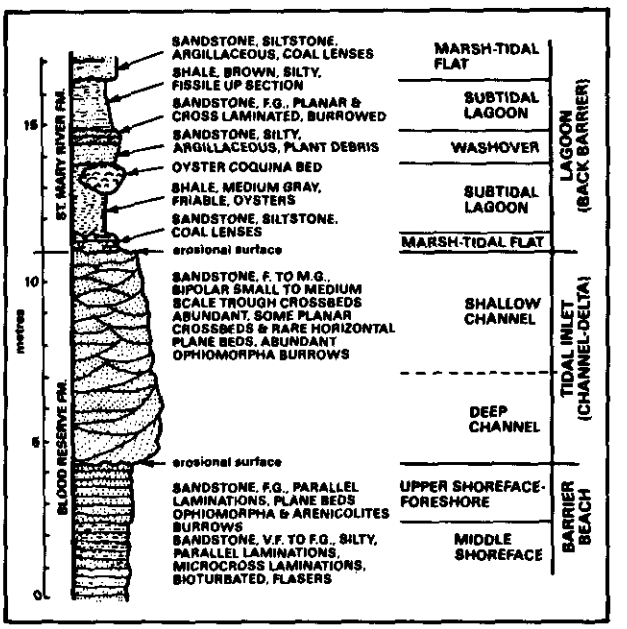

Fig. 6.7-10. - Composite stratigraphic section of the Upper Cretaceous Blood Reserve - St. Mary River Formations, Alberta, illustrating a sequence of barrier beach, tidal inlet and lagoonal deposits (from Young & Reinson, 1975).

6.7.2.2.2. *Sequences*

The general trend of barrier bar sands is coarsening upward. But following the subenvironments several more detailed lithologic, textural and sedimentary feature sequences have been described in several papers from which are extracted Fig. 6.7-12 to 6.7-16. Those figures are sufficiently explanatory to have not to develop sequence description by a long text.

6.7.2.2.3. *Geometry of the bodies*

The geometries of the bodies are schematically represented in the block diagram of Fig. 6.7-7.

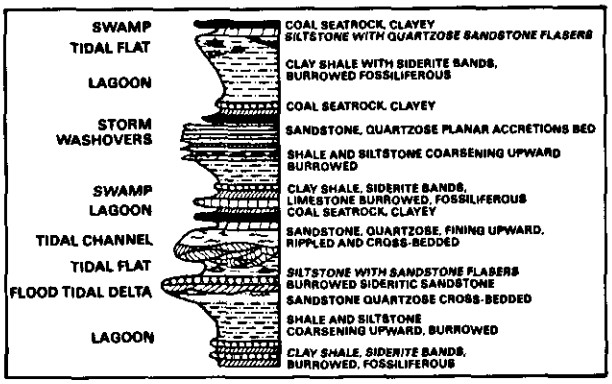

Fig. 6.7-11. - Generalized lagoonal sequence as illustrated by Carboniferous deposits of eastern Kentucky and southern Virginia (from Horne & Ferm, 1978).

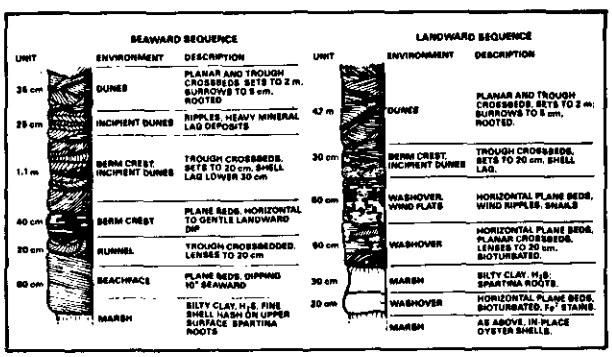

Fig. 6.7-12. - Lithological sequences observed on the landward and seaward edges of a Kiawah Island (South Carolina) beach *ridge (from Barwis, 1978).*

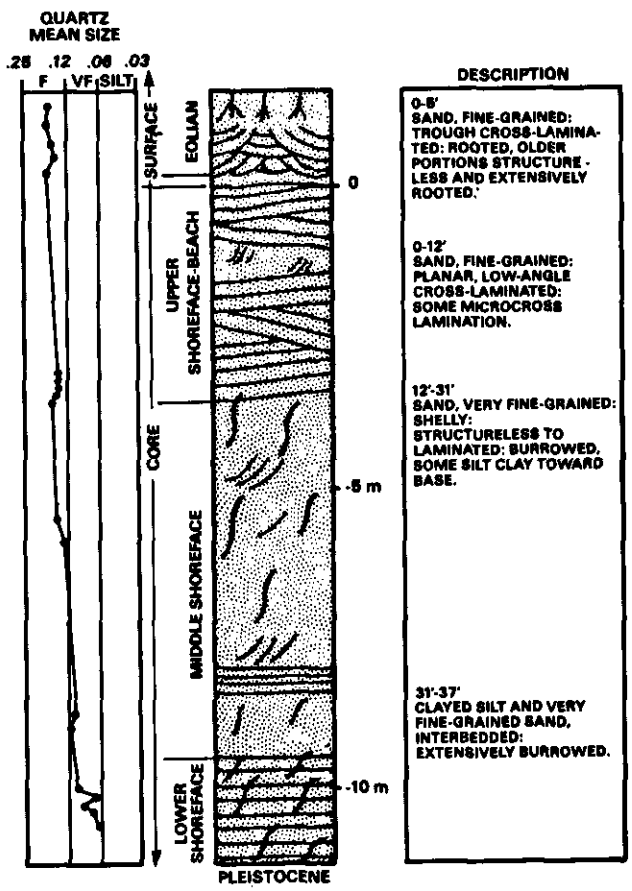

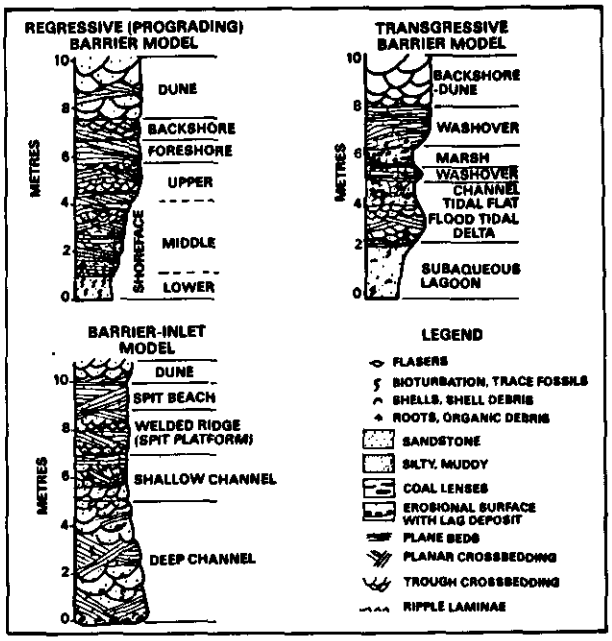

Fig. 6.7-14. - Three "end-member" facies models of barrier island stratigraphic sequences (from Reinson, 1979).

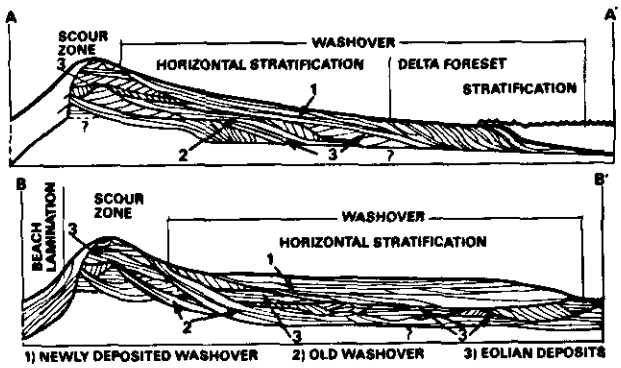

Fig. 6.7-15. - Two sequences of sedimentary structures through washover fans (from Schwartz, 1973).

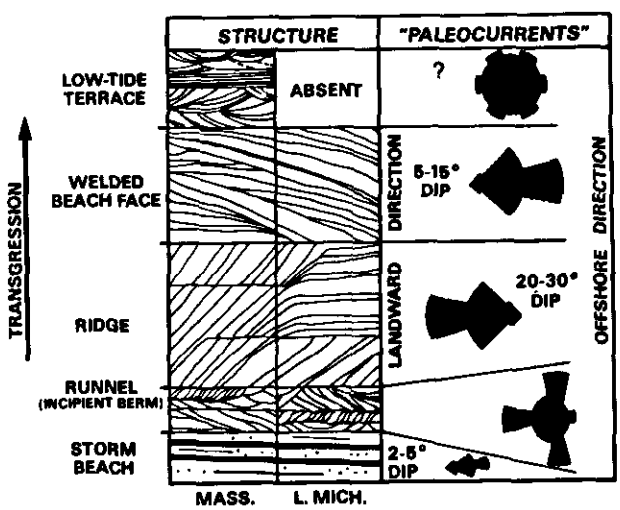

Fig. 6.7-16. - Transgressive sequence formed by the landward migration of ridge-and-runnel during beach construction phase. Vertical sequence would be about 1 m thick (from *Davis et al.*, 1972).

◀ Fig. 6.7-13. - Sequences of sedimentary structures, textures and lithology in a core through Galveston Island (from Davies *et al.*, 1971).

6.7.2.3. Linear Submarine sand Bars

6.7.2.3.1. *Definition*

They correspond to isolated elongated sand ridge, in a shallow marine environment (subtidal), occurring at some distance from, and extending generally parallel with, the shoreline, built chiefly by tidal, oceanic, storm- or wave-generated currents (Fig. 6.7-17).

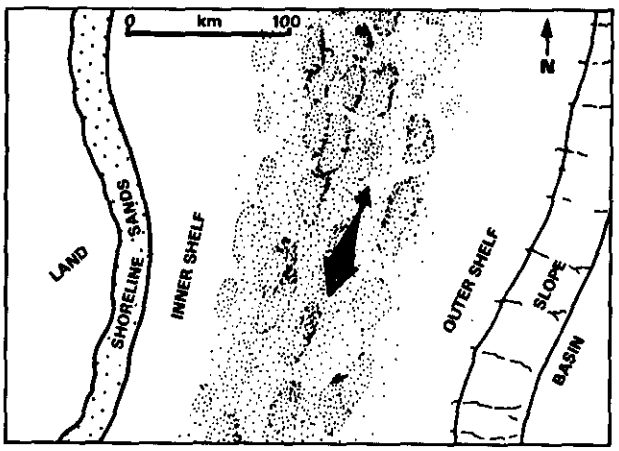

Fig. 6.7-17. - Hypothetical palaeogeographic reconstruction showing Shannon sand patches migrating south-southwest parallel to the shoreline (from Spearing, 1976).

6.7.2.3.2. *Composition*

Sand deposits of this environment are composed of quartz, shell debris, glauconite, chamosite (iron silicate) associated with limonite (or haematite) oolites or siderite, and phosphates.

6.7.2.3.3. *Texture*

The deposits have a textural maturity due to long periods of transport with winnowing of fines. Consequently the sands are well sorted.

6.7.2.3.4. *Structure*

Sedimentary structures are rarely environmentally diagnostic. Lenticular, wavy and flaser bedding, cross laminations, cross- and horizontal bedding are described. Bioturbation is minor.

6.7.2.3.5. *Boundaries*

The lower contact of the sequence is abrupt.

6.7.2.3.6. *Sequence*

The general sequence is coarsening upward (Fig. 6.7-18). It is composed of bioturbated mudstone and silty sandstone at the base, overlain by ripple cross-laminated fine-grained sandstone, capped by large-scale festoon cross-bedded, medium-grained sandstone. Bioclastic rich units form thin sheetlike units with erosional bases.

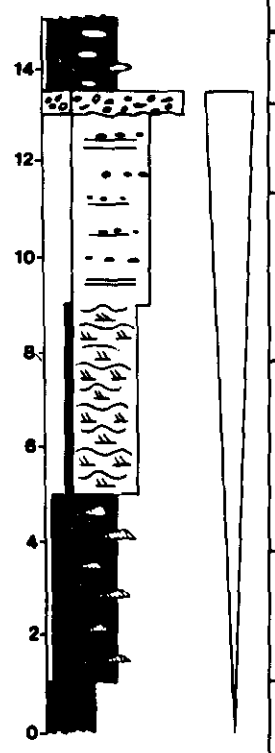

Units of Berg, 1975	Thickness	Description	Interpretation of the Facis	Interpretation of the Sequence
1	1.5-2.5 m	Bioturbated muds with reworked sand & granules. Horizontal bedding	Shelf muds with storm deposited sand layers.	Sudden cessation of active sand transport. Shelf muds blanket the linear sand bars.
2	0.30-1.0 m	Pebbly sandstone with chert & mudstone pebbles. Chert pebbles concentrated in top layer.	Wave reworked sands. Related to wave processes concentrated on bar crest.	Gradual increase in wave & current activity in response to a prograding linear tidal (?) sand body. Elongate geometry of several sand bodies parallel to shoreline & to current transport path suggests they may represent linear tidal (?) sand ridges which formed topographic highs. Coarsening upward sequence reflects both progradation & preferential reworking of bar crest & flanks.
3	1.5-5.5m	Cross bedded & flat bedded sandstone. Cross bed sets ca. 5-20 cm thick. Numerous mudfakes & occasional mud-drapes. Rare cross-laminated sands.	SE (?) migration of dunes in response to tidal currents, possibly enhanced by storms. Abundant penecontemporaneous erosion of mud. Sands deposited on upper bar flanks.	
4	1.0-5.0 m	Cross laminated fine grained sandstone with numerous mud-drapes. Occasional mudflakes & cross-bed sets. Minor bioturbation.	Deposition by current ripples in response to tidal (?) currents. Currents of fluctuating strength. Abundant fine grained suspended sediment. Deposition on lower bar flanks & troughs.	
5	0.9-4.0 m	Muds with rippled sandstone lenses & sandstone interbeds 1-5 cm thick. Minor bioturbation.	Suspension deposition of muds alternating with periodic sand influxes (? distal storm layers). Deposition downcurrent of the sand bars.	
		Massive marine muds but with little bioturbation.	Shelf muds.	

Fig. 6.7-18. - Description and interpretation of the Upper Cretaceous Sussex Sandstone, Wyoming (from Berg, 1975).

6.7.2.3.7. *Geometry of the body*

The sandstone bodies are elongate, between 3-30 m thick, 4-60 km wide and up to 160 km long, have planar bases and convex-upward tops.

6.7.2.3.8. *Direction of current transport*

The current is generally unidirectional parallel to the bar crest.

6.7.2.3.9. *Surrounding facies*

The linear sand bars are either surrounded by, or interfinger with, marine muds.

6.7.2.4. Reservoir Characteristics

Sand bodies have, generally, good reservoir characteristics but their volume is limited.

6.7.3. WELL-LOG RESPONSES AND CHARACTERISTICS

It is not always easy to distinguish between the shallow siliciclastic and the deltaic environments. Consequently, only some of the previously described deposits will be illustrated by examples of composite-logs and dipmeter results.

The first example is taken in the Muddy Formation, Granerous Group, Powder River Basin, Wyoming. This formation is sometimes and somewhere (Bell Creek Field, Montana) described as a typical ancient barrier island (Davies *et al.*, 1971). The composite-log (including gamma ray, neutron and density logs) of one well (no location reference) is given in Fig. 6.7-19b. From the shape of traditional open-hole logs a coarsening upward sequence followed by a fining upward seems quite evident. Now, by looking at in detail the LOCDIP arrow-plot (obtained from SHDT, Fig. 6.7-20b), several abrupt lower contacts followed by fining upward sequences appear clearly. An interpretation of the dipmeter has been done following the barrier island hypothesis. But some of the observations which can be done on the dipmeter (abrupt lower contacts, fining upward sequences, thin shale drapes) do not fit completely with the general continuous coarsening upward trend described in barrier island. Consequently, another interpretation, based on a tidal sand ridge hypothesis (Klein, 1970), can be proposed (compare with Fig. 6.7-3).

A second example is from the Shannon Sandstone in the Hartzog Draw Field, Powder River Basin, Wyoming. The composite-log (including SP, gamma ray, neutron, density, sonic, DIL-SFL and GEODIP arrow-plot) is reproduced in Fig. 6.7-21 alongside the core description and the interpretation in terms of facies and subenvironments. A general coarsening upward sequence is observed as expected in a linear submarine sand bar. Low ϕ_D peaks (9387, 9395 ft) correspond to levels richer in

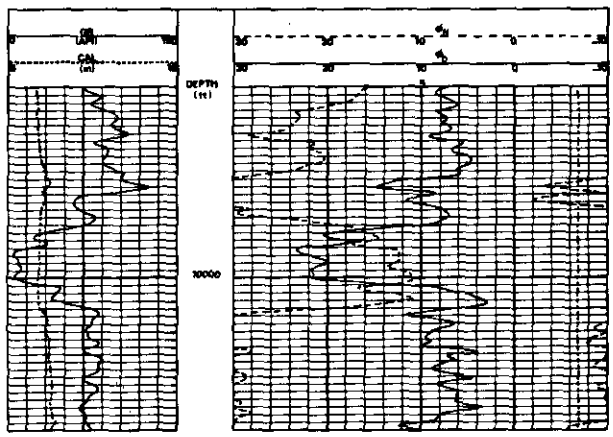

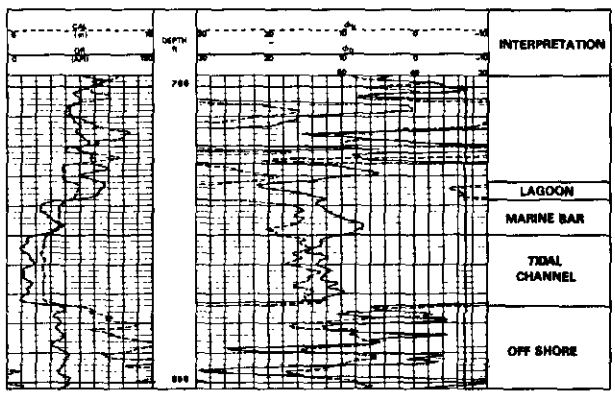

Fig. 6.7-19. - Two composite-logs of the Muddy Formation, Powder River Basin.

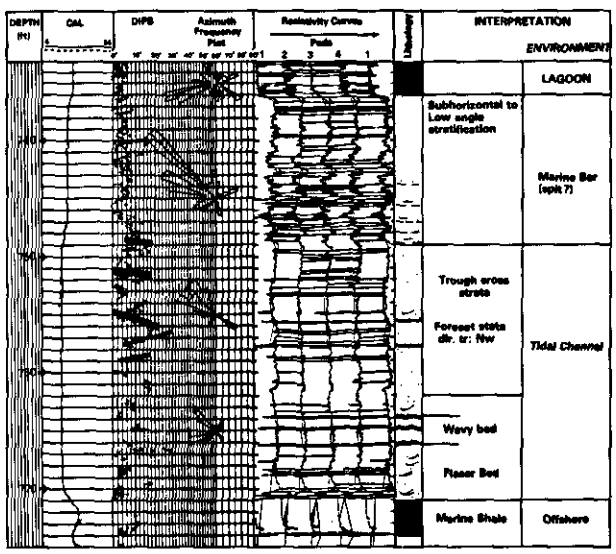

Fig. 6.7-20a. - GEODIP arrow-plot of the Muddy Formation in the well represented by the composite-log 6.7-19a, and its interpretation in terms of facies and environment.

siderite and glauconite (confirmed by core analysis). The analysis of the GEODIP arrow-plot (low sand character option) at an expanded scale (Fig. 6.7-22 to 6.7-24) permits a more detailed observation. The lower interval (9443-9412.5 ft) is very

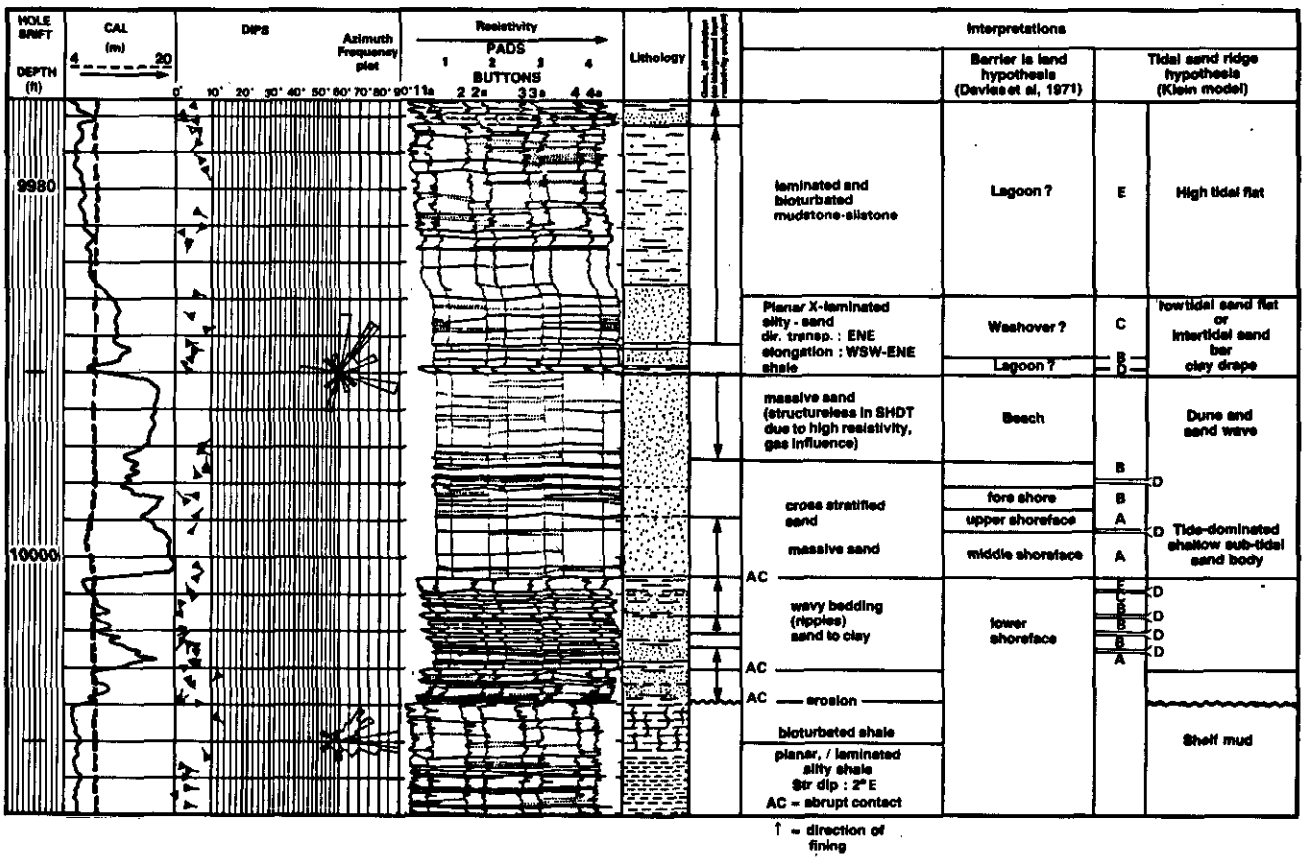

Fig. 6.7-20b. - LOCDIP arrow-plot of the Muddy Formation in the well represented by the composite-log 6.7-19b, and its interpretation in terms of facies and environment.

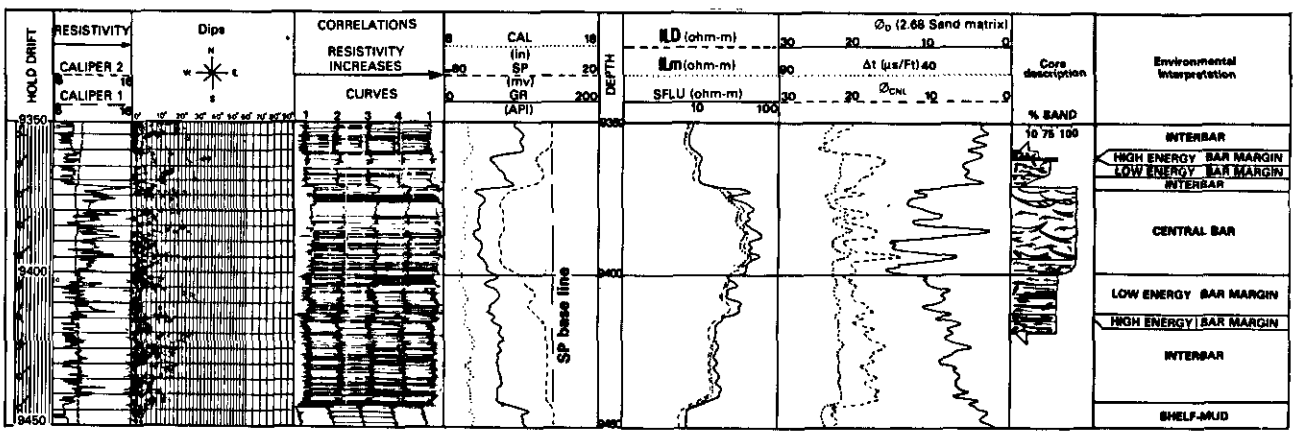

Fig. 6.7-21. - Composite-log of the Shannon Sandstone in the Hartzog Draw Field.

laminated on the HDT resistivity curves (a lot of very thin events) at a medium resistivity level, generating a lot of dips with scattered azimuth (observe the azimuth frequency plots), with low SP deflection, moderate radioactivity. In some places an erratic aspect of the curves can be observed. It could reflect some bioturbations. All these observations suggest a very thinly laminated, sometimes bioturbated interval, with small lenses (uncorrelated events seen only on one or two curves), with a relatively high clay percentage. Consequently one can deduce numerous intercalations of thin silt or sand beds (corresponding to more resistive continuous events) in the shale. This is confirmed by core photographs (Fig. 6.7-22). The following interval (9413-9400 ft) is more resistive, with a higher SP deflection (lower shale content), and slightly less radioactivity. On the dipmeter resisti-

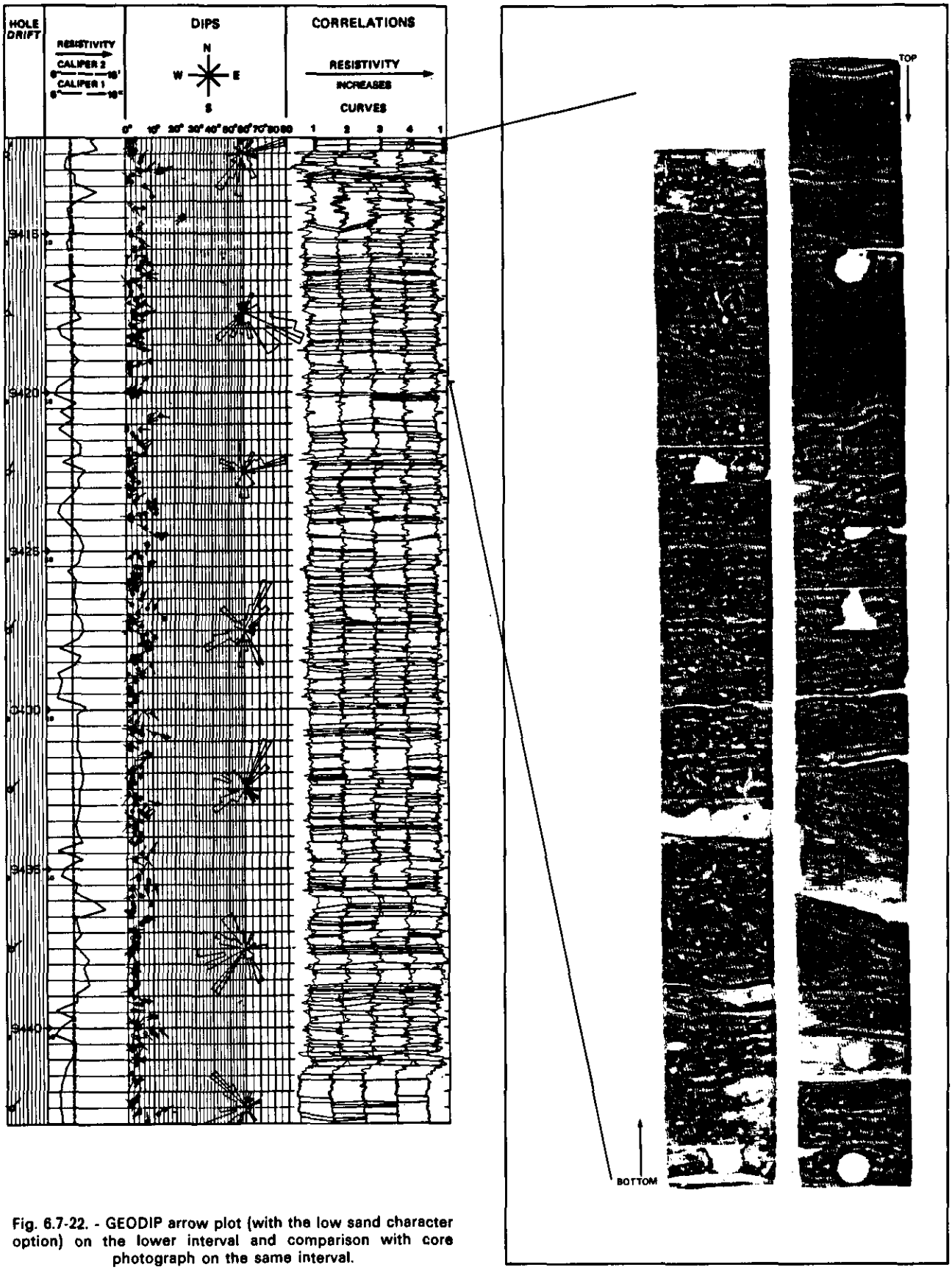

Fig. 6.7-22. - GEODIP arrow plot (with the low sand character option) on the lower interval and comparison with core photograph on the same interval.

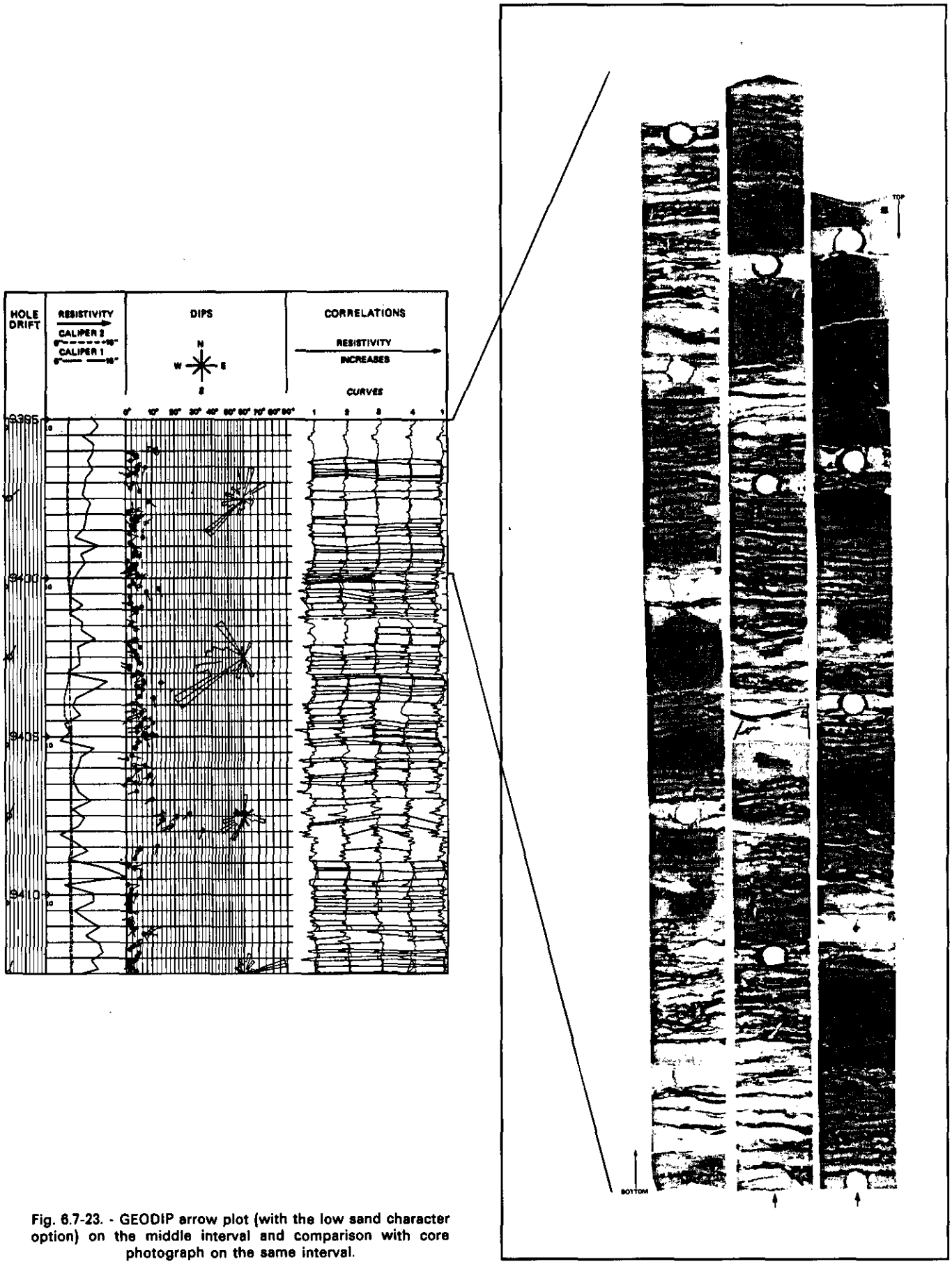

Fig. 6.7-23. - GEODIP arrow plot (with the low sand character option) on the middle interval and comparison with core photograph on the same interval.

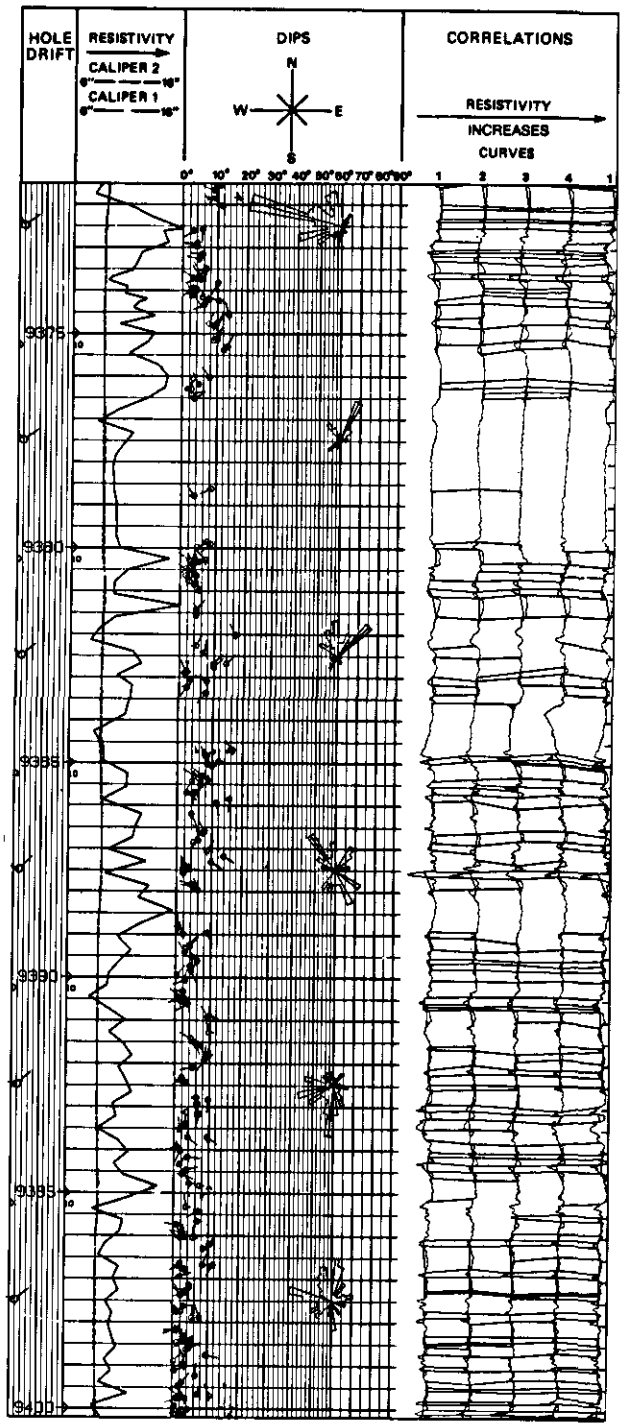

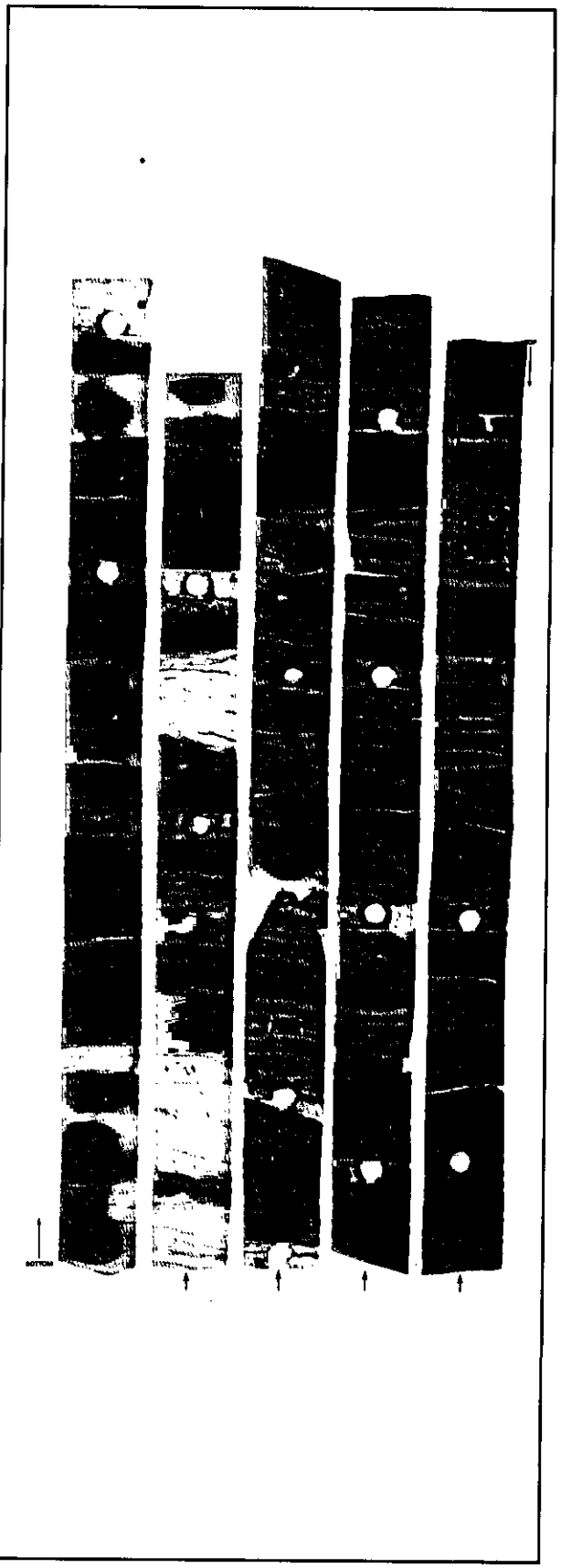

Fig. 6.7-24. - GEODIP arrow plot (with the low sand character option) on the upper interval and comparison with core photograph on the same interval.

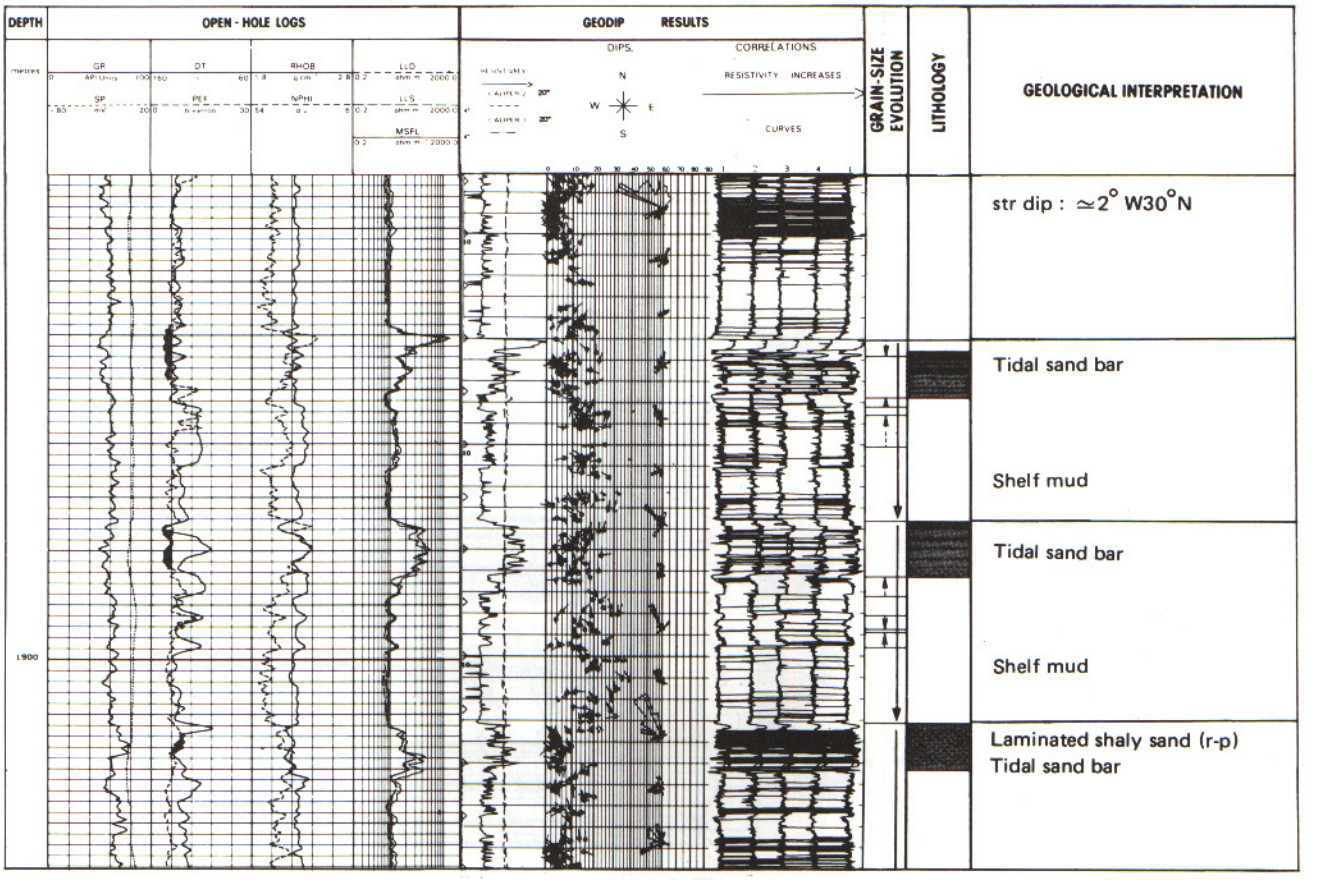

▲ Fig. 6.7-25. - Composite-log of three submarine sand bars in the Godavari Basin, India, and its interpretation (from Schlumberger, Well Evaluation Conference. India, 1983).

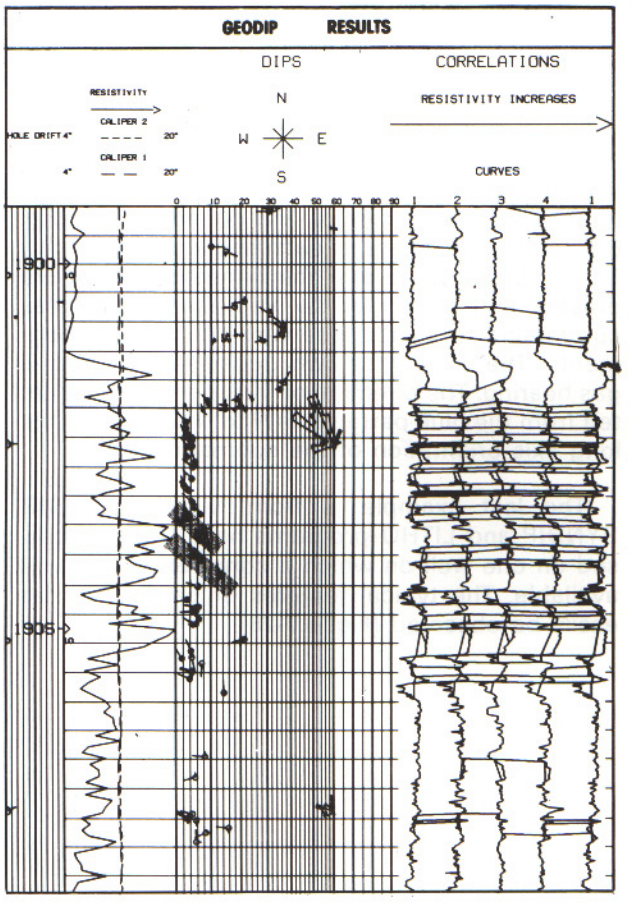

◀ Fig. 6.7-26. - GEODIP arrow plot of the lower sand at an expanded scale (from Schlumberger, Well Evaluation Conference. India, 1983).

Fig. 6.7-27. - Crossplot ρ_b vs ϕ_N showing the shale-silt-sand trend (boomerang shape) and the sandstones rich in shell fragments (from Schlumberger, Well Evaluation Conference. India, 1983). ▼

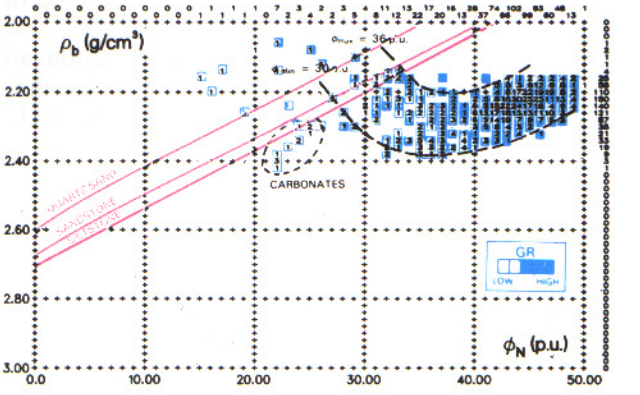

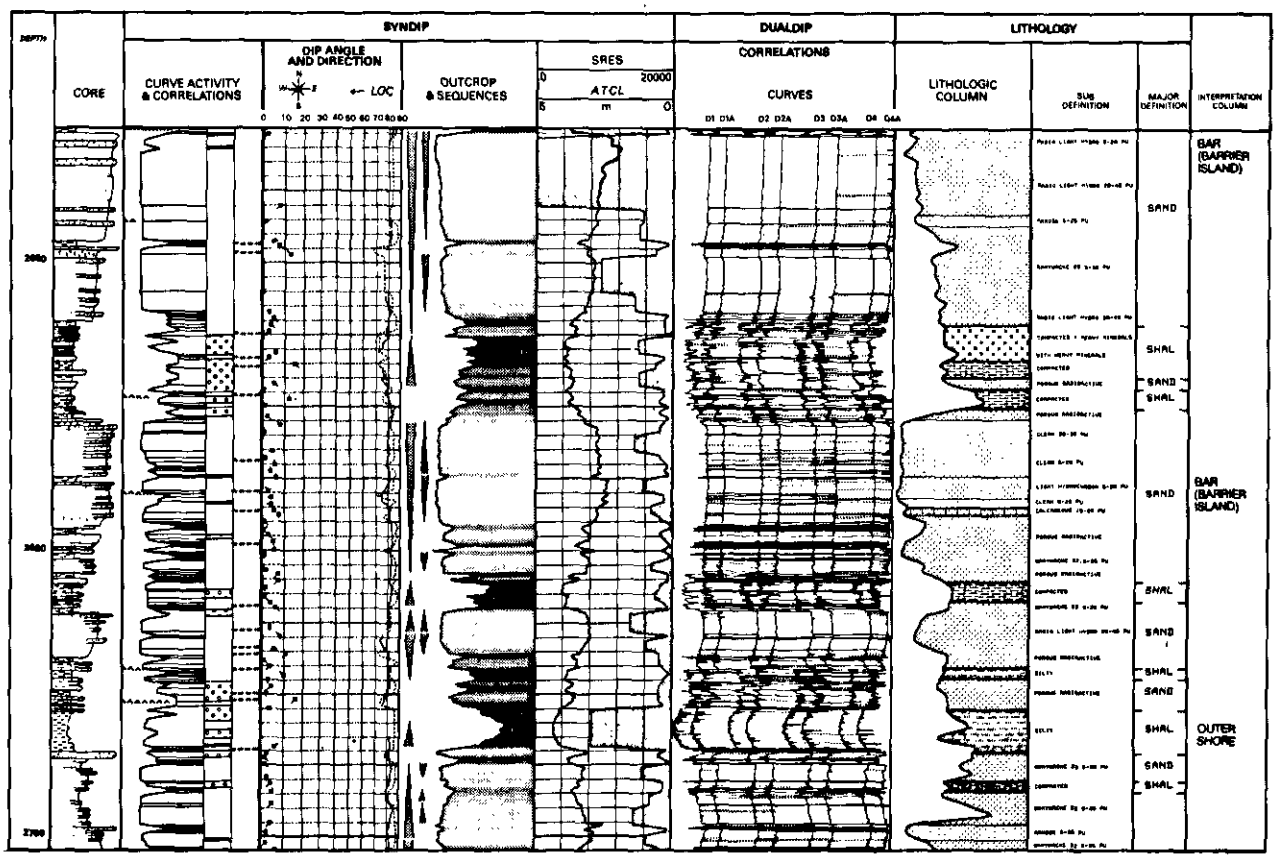

Fig. 6.7-28. - Interpretation of the studied sequences from LITHO, LOCDIP and SYNDIP results (from Schlumberger, Well Evaluation Conference. Nigeria, 1985).

vity curves, resistive beds are thicker and more continuous, with very thin conductive levels (shale laminae), which, when they are correlated, generate dips with variable magnitude (between 0° and 14°) and scattered azimuth, suggesting wavy bedding and sometimes flaser bedding when events are not seen on all curves (Fig. 6.7-23). Some blue and red patterns occur which can correspond to foresets or cut and fill features. The overlying interval (9400-9372 ft) is characterized by thicker resistive beds, with less frequent conductive levels, high SP deflection and lower radioactivity (Fig. 6.7-24). The top interval is more resistive (cemented) and is overlapped by gradually less resistive thin levels. The dips suggest a draping of the previous deposit (bar).

Another example is extracted from the Godavari Basin (India) and represented by the composite-log of Fig. 6.7-25 (GR-LDT-CNL-BHC-DLL-MSFL-SP and GEODIP at 1/200 scale), and the enlarged GEODIP arrow-plot on the lower interval (Fig. 6.7-26). Log evolutions suggest three coarsening upward sequences from shale to sand as interpreted from the ρ_b vs ϕ_N crossplot (Fig. 6.7-27). The thickness of each sequence is roughly 17 to 18 metres. Some thin limestone beds are present and confirmed by Pe values. They may correspond to sandstones very rich in shell fragments. The top of the two upper sand bodies is gas bearing. The direction of transport, as interpreted from the blue patterns, is N to NNW, giving the long axis orientation of the submarine bar.

The last example is from Nigeria. LOCDIP, SYNDIP and LITHO programs have been processed on one well on which a core description was available. The typical features of barrier bar can easily be observed (Fig. 6.7-28).

6.8. SHALLOW WATER CARBONATE ENVIRONMENT

6.8.1. DEFINITION

Environments characterized by carbonate deposits generated by biochemical processes in shallow water (< 100 m), but sometimes resulting from reworking and redistribution of those sediments by currents. According to Sellwood (in Reading, 1978), five major environmental zones can be recognized in shallow water carbonate environments : Supratidal Zone; Shore Zone; Marine Platform; Reef Belt; and Shelf Slope. They are located in the schematic block diagram (Fig. 6.8-1). Each of these zones can in turn be subdivided in subenvironments.

6.8.2. GEOLOGICAL FACIES MODEL

6.8.2.1. Generalities

Lithology, depositional texture, bedding and sedimentary structures observed in the various environments are summarized in the scheme and the table of Fig. 6.8-2 adapted from Wilson (1975).

6.8.2.2. Lithology

Two parameters must be considered separately.

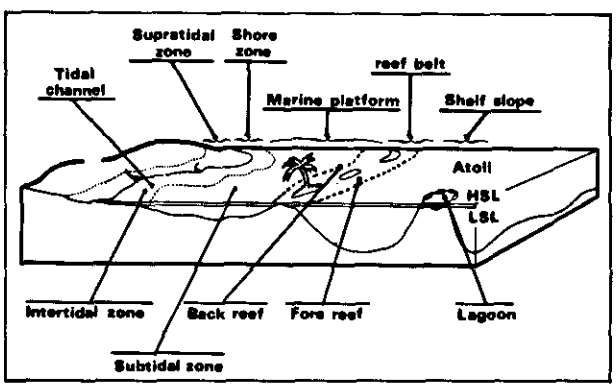

Fig. 6.8-1. - Schematic block diagram illustrating the location of shallow water carbonate environments.

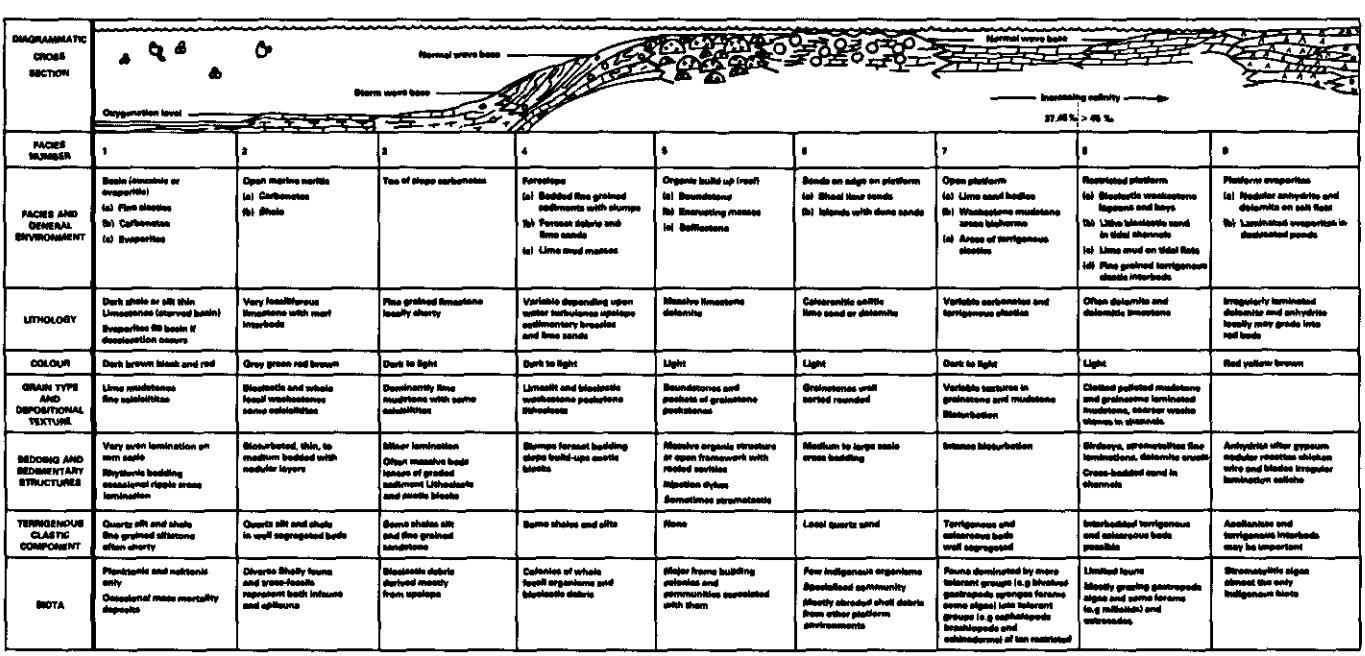

Fig. 6.8-2. - The scheme of standard facies belts (adapted from Wilson, 1975).

6.8.2.2.1. *Composition*

The dominant mineral is calcite, but dolomite, gypsum and anhydrite can be present and abundant in intertidal and supratidal zones. Terrigenous clastic materials may be interbedded with previous deposits, if the platform is connected to a continent, or if they are transported by wind storms. Iron-oolites and sideritic ironstones may be present on shoal (swell) areas. Phosphates and glauconite may occur.

6.8.2.2.2. *Texture*

Depositional textures (following the Dunham classification) are typical of the facies within the environment and are described in Fig. 6.8-2, but they can be obscured by diagenesis.

6.8.2.3. Structure

As texture, sedimentary structures generally define clearly the environment and are listed in Fig. 6.8-2.

6.8.2.4. Boundaries

Due to the general sequential evolution (both vertical and lateral) the boundaries are often not well marked.

6.8.2.5. Sequences

The most frequent sequence type observed is a shallowing-upward sequence. James (1979) stated that "this is because carbonate sediments are produced mainly in the environment of deposition - especially in shallow water where conditions for the biological and physicochemical fixation of carbonate are optimum - . As a result, carbonate accumulations repeatedly build up to sea level and above, resulting in a characteristic sequence of deposits, in which each unit is deposited in progressively shallower water. This shallowing-upward sequence is repeated many times in a succession of shallow water deposits" (in Walker, 1979). The units composing the sequence are illustrated in Fig. 6.8-3.

As indicated by the flow diagram of Fig. 6.8-4, various possible environmental transitions may be present in a carbonate shallowing-upward sequence.

Block diagrams of Fig. 6.8-5, adapted from James, in Walker (1979), show the location of sub-, inter- and supra-tidal zones in two typical conditions : very arid desert (similar to the modern Persian Gulf), and humid climate (similar to the modern Bahamas).

Several theoretical sequences corresponding to the various possible transitions are shown in Fig. 6.8-6. Letters on the side refer to the subenvironments of Fig. 6.8-3.

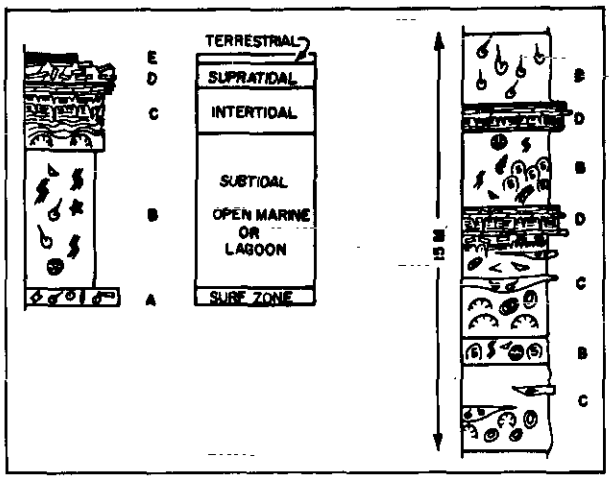

Fig. 6.8-3. - The five divisions of the shallowing-upward sequence model for carbonate (from James, in Walker, 1979).

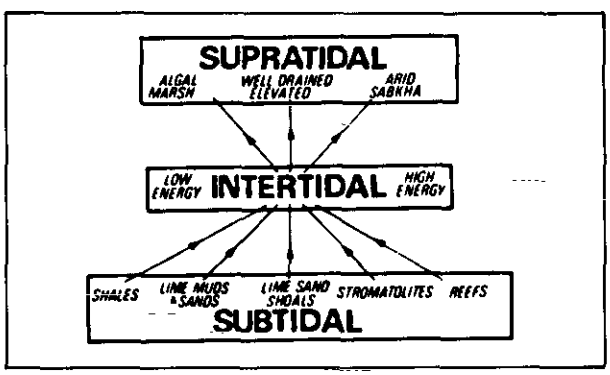

Fig. 6.8-4. - A flow diagram indicating the various possible environmental transitions present in a carbonate shallowing-upward sequence (from James, in Walker, 1979).

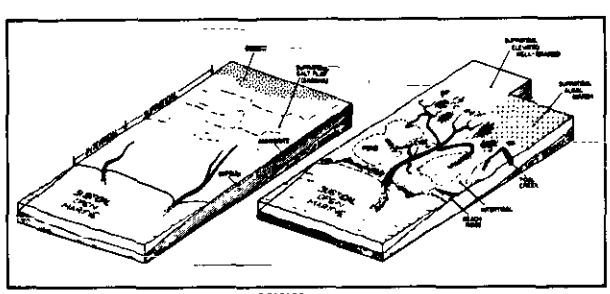

Fig. 6.8-5. - Block diagrams showing the major morphological elements of a tidal flat; (a) a hypersaline tidal flat with few tidal channels bordering a very arid desert; (b) a normal marine tidal flat with many tidal channels and ponds bordering an elevated well-drained area of low swamp algal marsh in a humid climate (from James, in Walker, 1979).

Deepening-upward sequences can also exist. They correspond to a transgressive phase related either to subsidence or to eustatic changes. Fig. 6.8-7 shows two examples of such cycles.

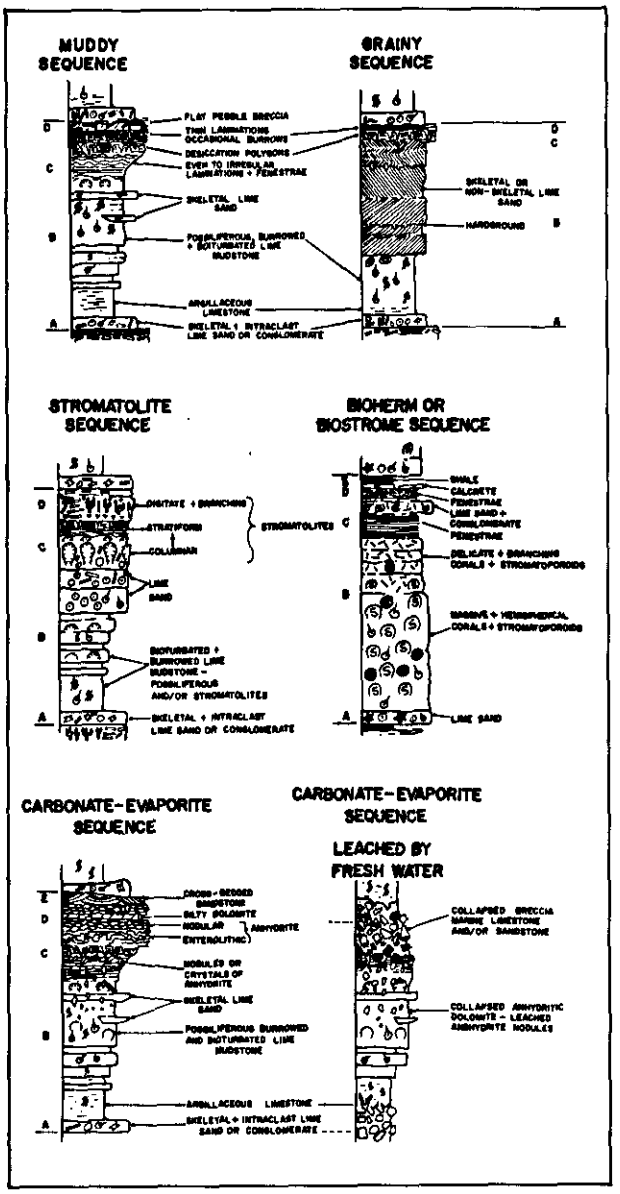

Fig. 6.8-6. - Theoretical sequences in different transitions from sub- to supra-tidal subenvironments (from James, in Walker, 1979).

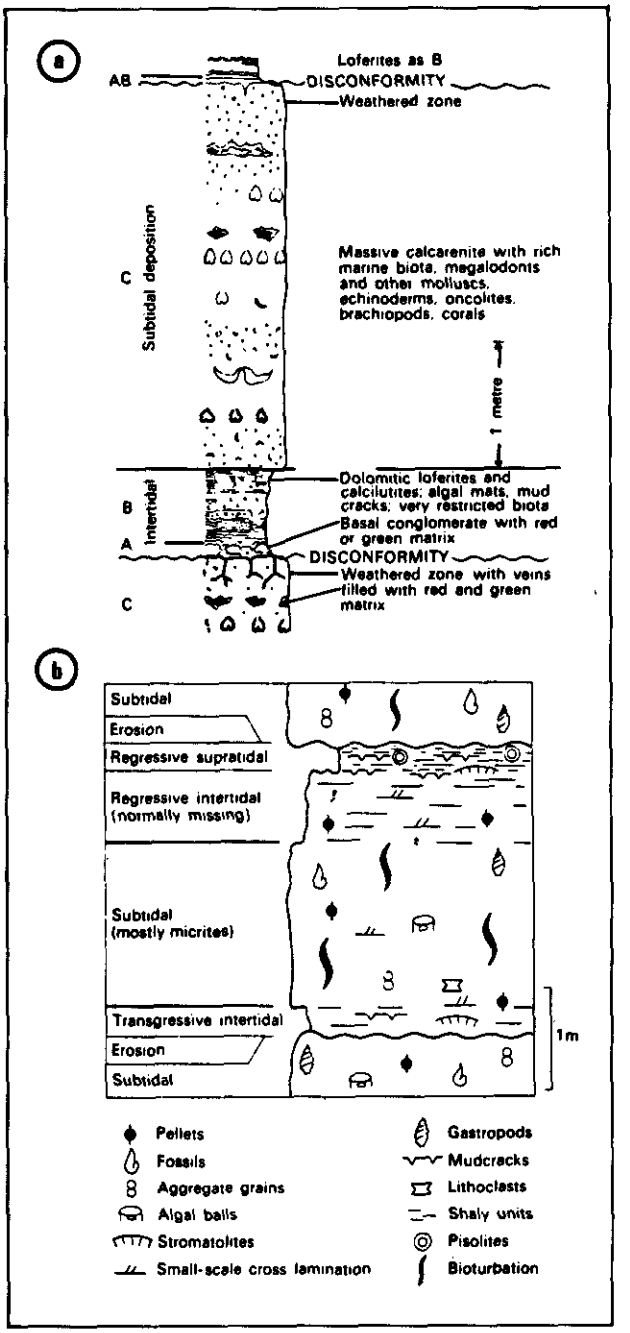

Fig. 6.8-7. - Two examples of deepening-upward sequences : (a) an idealized Lofer cyclothem (after Fisher, 1964, 1975); an idealized cycle for the Calcare Massiccio, Italy (after Colacicchi *et al.*, 1975).

6.8.2.6. Geometry of the Bodies

Facies related to shallow water carbonate environments can be distributed as successive belts, parallel to the coast line, or as atolls or pinacles (reef facies). Associated channel deposits (channel fill, levees) are present in inter- and supra-tidal zones.

6.8.2.7. Reservoir Characteristics

Carbonate rocks can have good reservoir characteristics depending on the importance of diagenetic effects. When dissolution has occurred, the porosity and the permeability are very high. Other diagenetic effects reduce the porosity. The permeability is often related to the presence of fractures which occur frequently in such rocks. Carbonate reservoirs can be very thick and have a large extension. Source rocks are often close to the reservoir rocks. Cap rocks are composed of either shale or anhydrite beds.

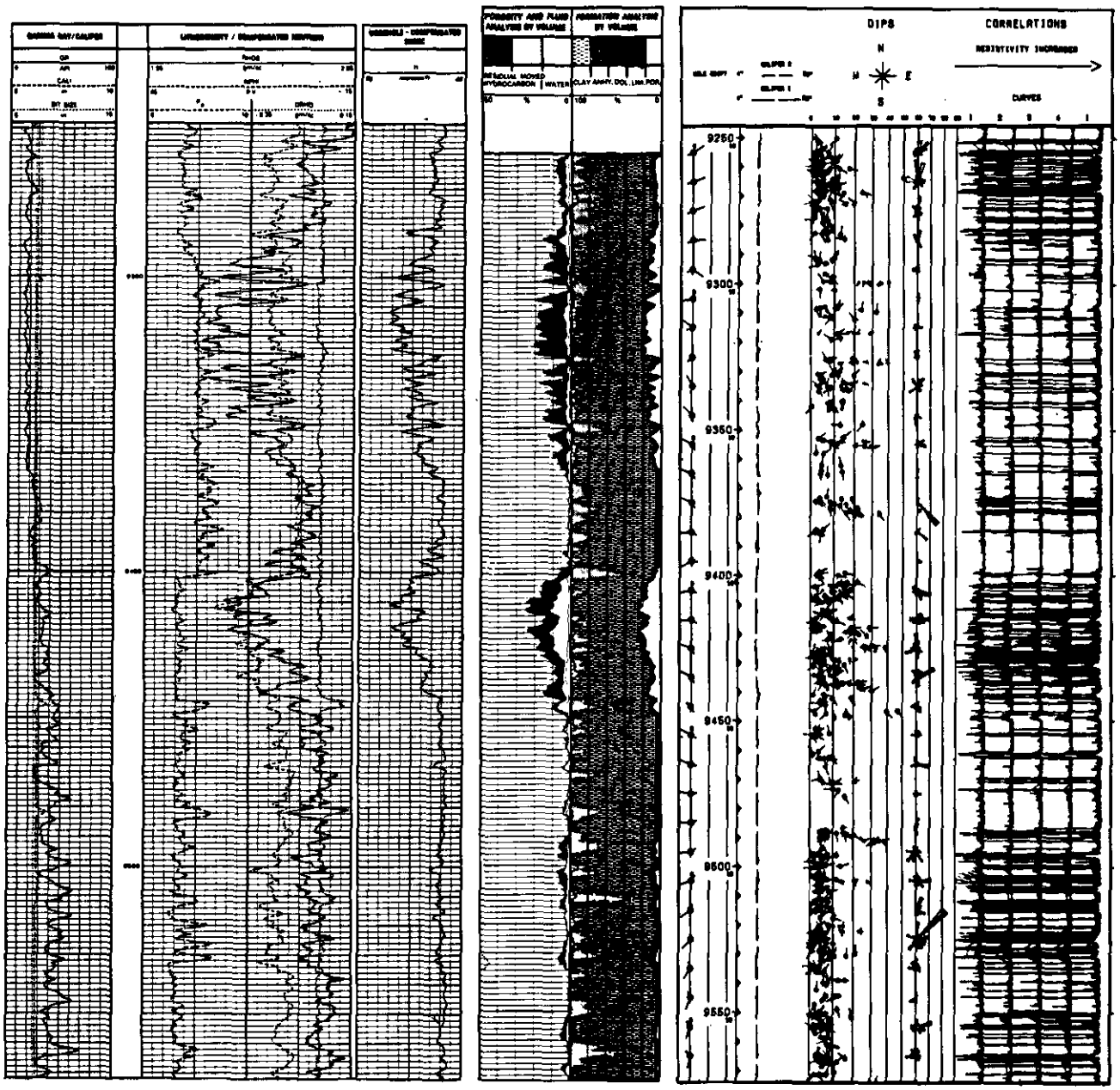

Fig. 6.8-8. - Composite-log combining open-hole logs, GLOBAL results and GEODIP (from Schlumberger, Well Evaluation Conference, Emirates/Qatar, 1981).

6.8.3. WELL-LOG RESPONSES AND CHARACTERISTICS

6.8.3.1. Electro-Lithofacies

Typical log responses are represented by the composite-log from the Khuff Formation in the southern Persian Gulf (Fig. 6.8-8). Representative points plot on, or below, the limestone line on the ρ_b vs ϕ_N *crossplot (Fig. 6.8-9a), - if the formation is* not gas bearing - following the calcite, dolomite, anhydrite, heavy mineral (pyrite or siderite), or shale content. Radioactivity is generally low except in shaly intervals in which thorium, potassium and uranium curves will deflect, or if organic matter or phosphates are present in the formation. In that case only uranium will deflect significantly. Use of the Pe curve (Fig. 6.8-9b), or better still the derived $(\rho_{ma})_a$ vs $(U_{ma})_a$ crossplot (Fig. 6.8-9c), allows definition of mineral composition.

6.8.3.2. Dipmeter curve Shape and Dip Patterns

As previously mentioned the dipmeter reflects essentially the texture, and sometimes the structure, of the limestone. Several resistivity features

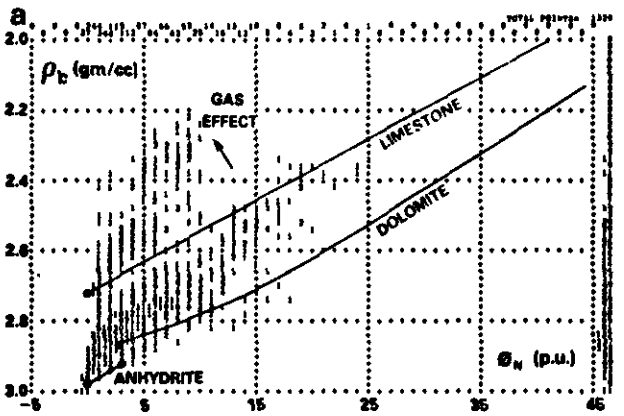

Density vs. Neutron

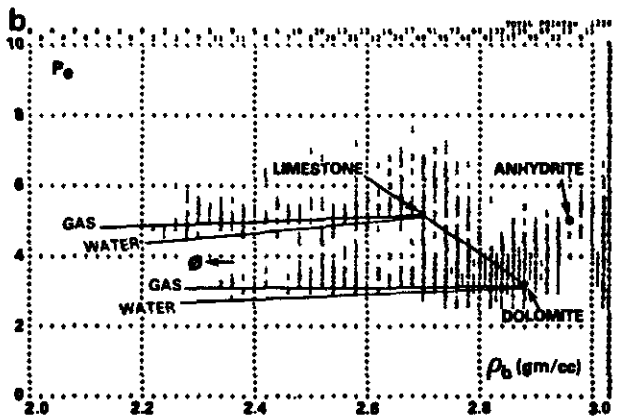

Photoelectric factor vs. Density

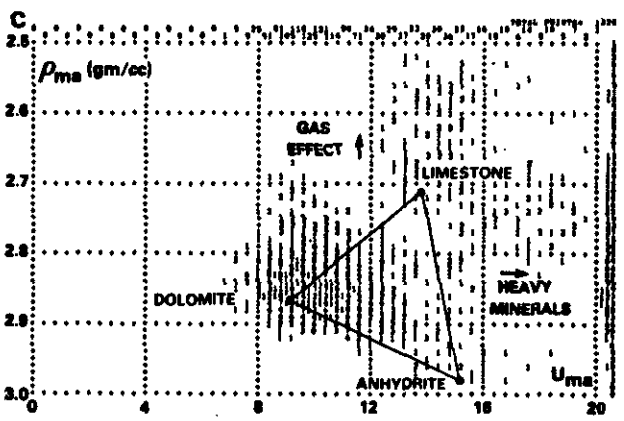

Fig. 6.8-9. - Crossplots (a) : density-neutron; (b) : photoelectric factor-density; (c) : $(\rho_{ma})_a$ - $(U_{ma})_a$ (from Schlumberger, Well Evaluation Conference, Emirates/Qatar, 1981).

and dip patterns can be observed. They will be illustrated by GEODIP or LOCDIP examples coming from Arab Formation, Abu Dhabi.

- Dipmeter resistivity curves show no events in a medium to high resistivity range recognized on the other open-hole logs as a limestone. This type of response can be interpreted as a mudstone

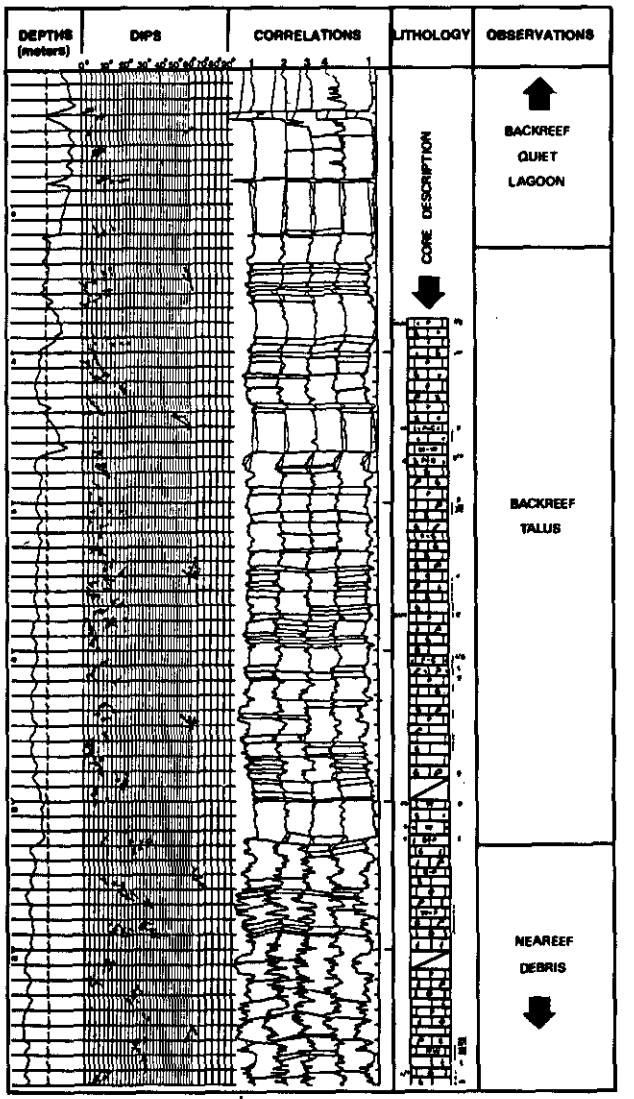

Fig. 6.8-10. - Typical GEODIP responses in reef, backreef and lagoon subenvironments (from Theys *et al.*, 1983).

which corresponds to backreef-lagoonal deposits (Fig. 6.8-10).

- Dipmeter resistivity curves show no events in a very high resistivity level. This corresponds to a tight limestone or dolomite, or anhydrite. The open-hole logs will indicate the lithology (6.8-11).

- Dipmeter resistivity curves show low to medium activity with small and thin events, not always easily correlated from pad to pad but well correlated from button to button (Fig. 6.8-12). This kind of feature can be interpreted as grainstone to packstone. Sometimes dips show blue patterns (Fig. 6.8-11 to 6.8-13), which can be interpreted as foreset beds on a backreef talus, or in a tidal channel point bar; or red patterns which can correspond to tidal channel fill deposits.

- Dipmeter resistivity curves show medium to high activity with events often uncorrelated, or wrongly correlated, and so generating few dips.

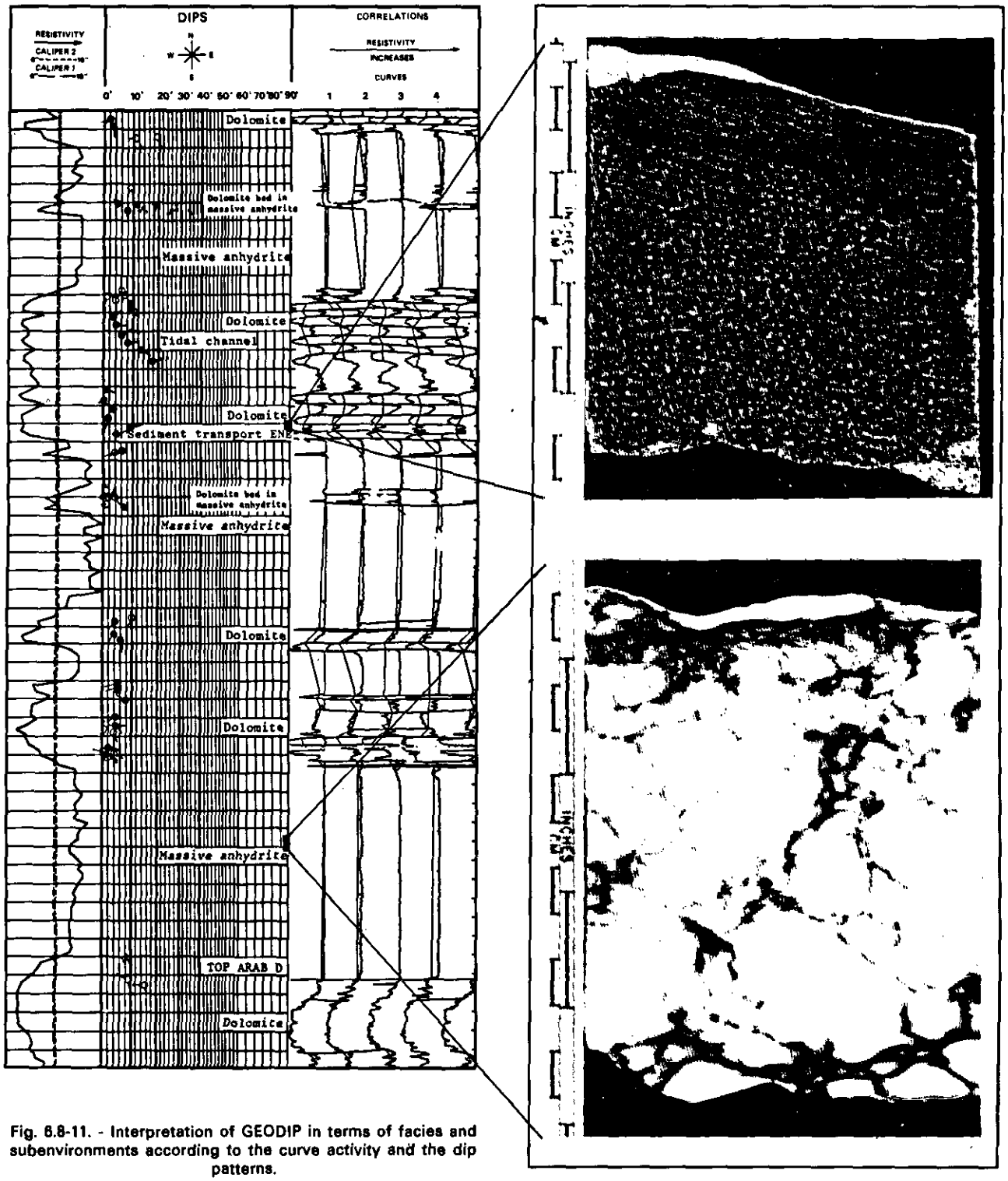

Fig. 6.8-11. - Interpretation of GEODIP in terms of facies and subenvironments according to the curve activity and the dip patterns.

This kind of response corresponds to wackestone or boundstone, often vuggy, if the open-hole logs indicate limestone or dolomite (Fig. 6.8-14), or to dolomite with nodules of anhydrite (Fig. 6.8-15).

- Dips consistent in magnitude and azimuth reflect either laminations of shaly limestone, or even of shale, if the thorium and potassium curves deflect, or intercalations of mudstone with grainstone or packstone if the thorium and potassium contents are very low (Fig. 6.8-16).

Another example, coming from Desert Creek, Paradox Basin, illustrates the same kind of environment. The composite-log (including gamma ray, neutron and density tools) is shown in Fig.

Fig. 6.8-12. - Interpretation of LOCDIP in terms of facies and subenvironments according to the curve activity and the dip patterns. ▶

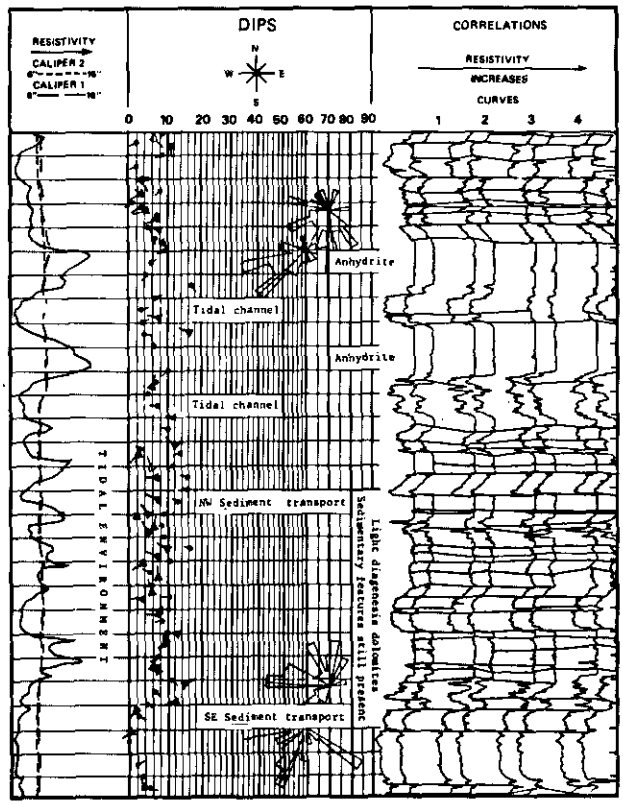

Fig. 6.8-13. - Another example of GEODIP and its interpretation. The blue patterns indicate a direction of transport toward ESE. ▼

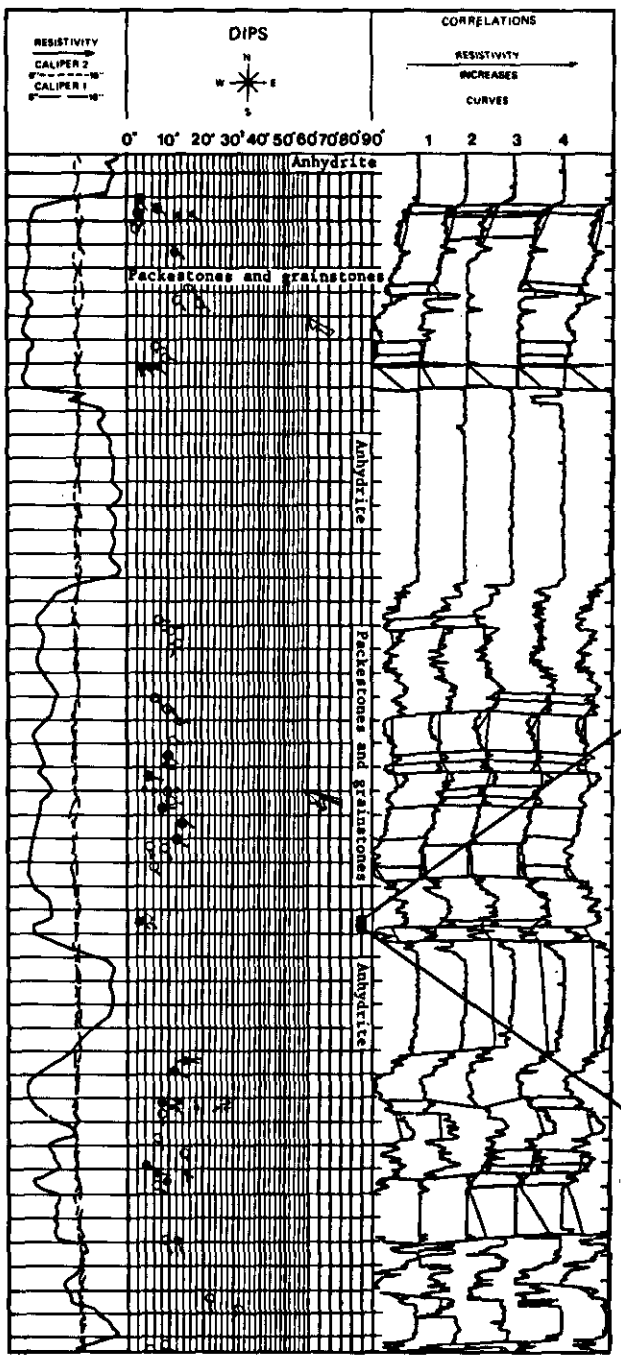

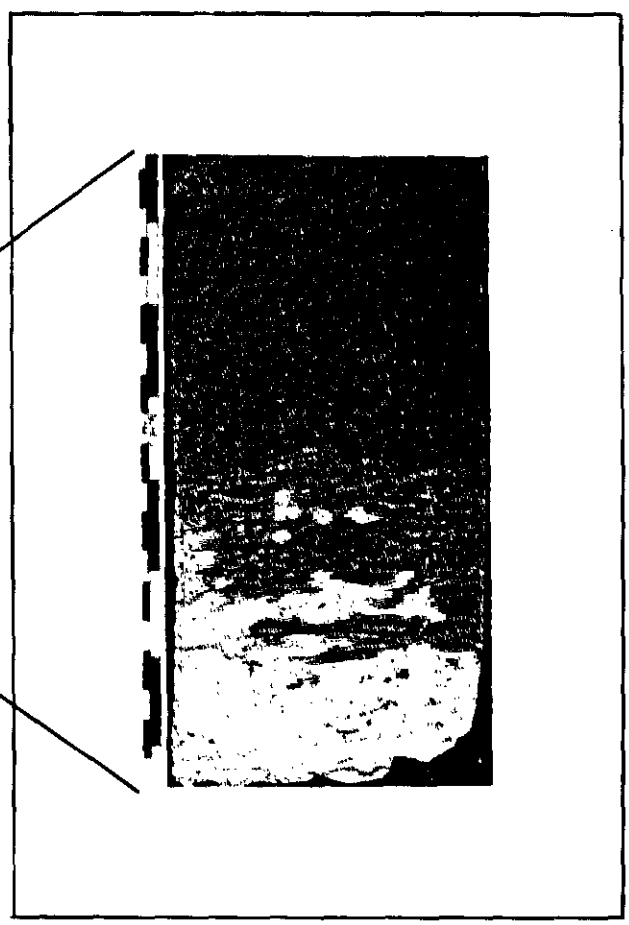

Fig. 6.8-15. - Typical curve activity in anhydritic dolomite to ▶
dolomitic anhydrite (nodules of anhydrite in dolomite).

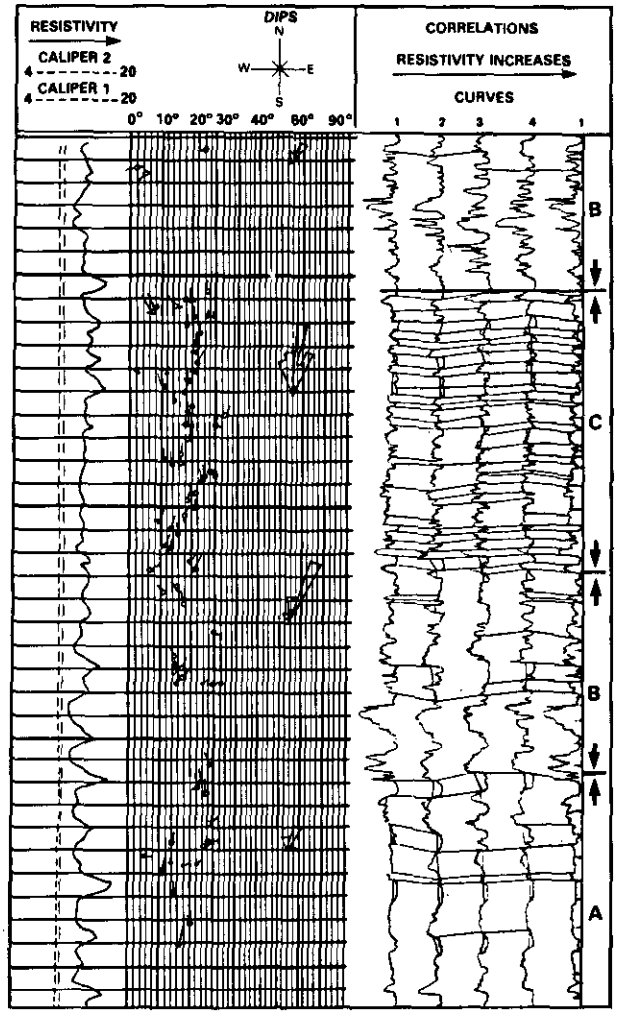

Fig. 6.8-14. - Three types of curve activity reflecting three main *limestone textures and facies; (a) : mudstone to wackestone;* (b) : boundstone (reef build up); (c) : packstone to grainstone (from Theys *et al.*, 1983). ▼

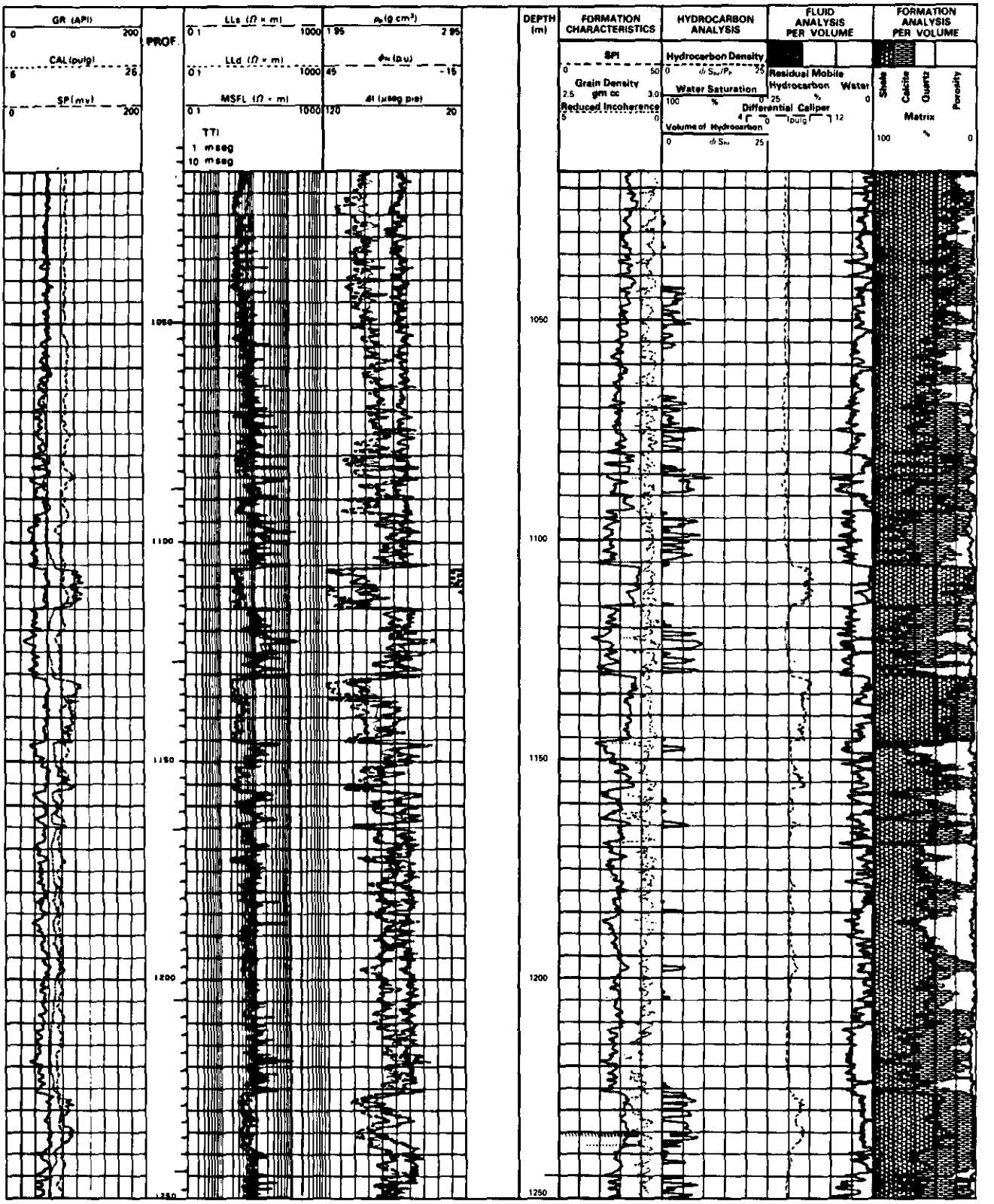

a

Fig. 6.8-16. - Example of very thin laminations, sometimes shaly, in a limestone-dolomite formation, a) Composite-log (from Schlumberger, Evaluacion de formaciones en Mexico, 1984).

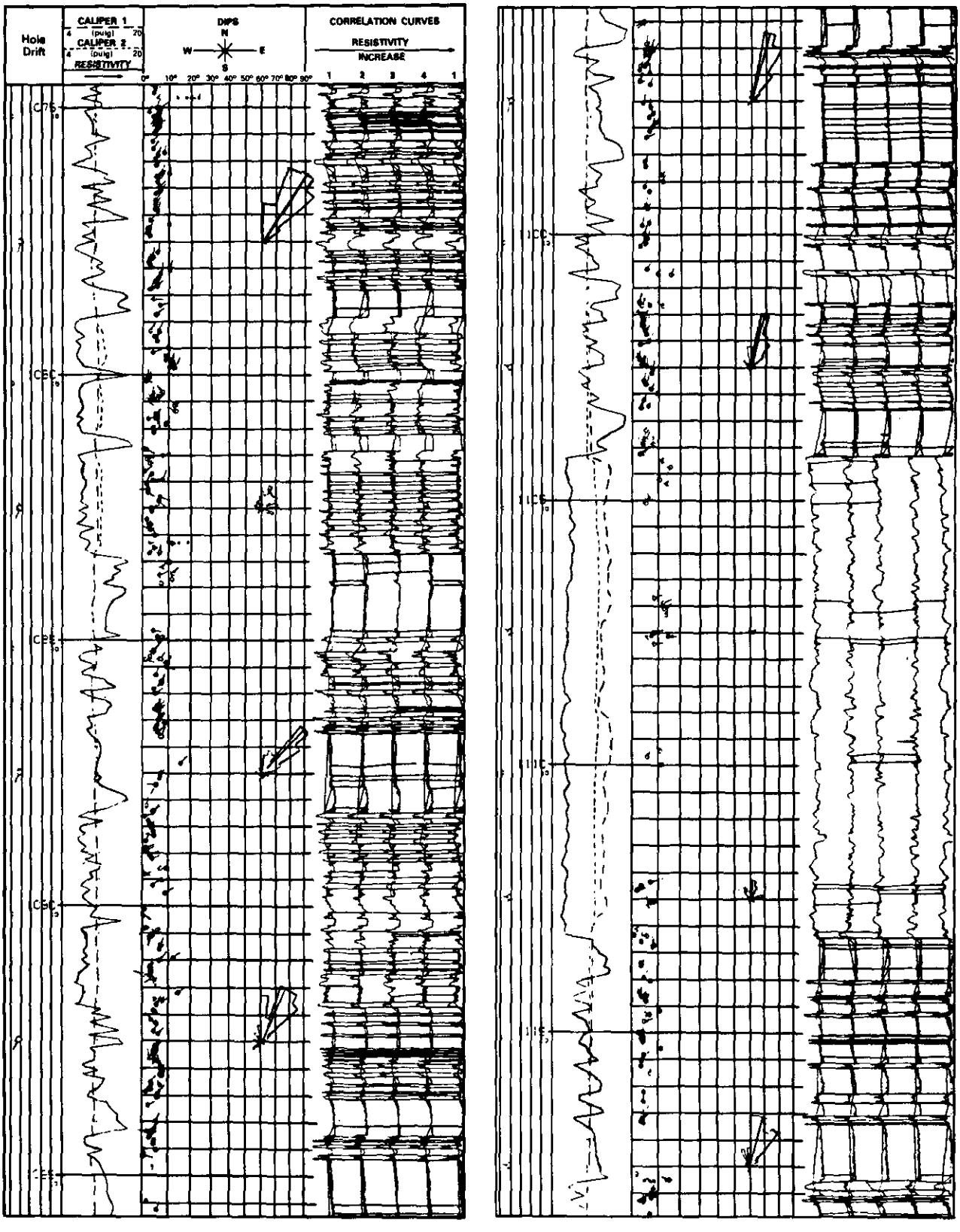

b

Fig. 6.8-16. - Example of very thin laminations, sometimes shaly, in a limestone-dolomite formation, b) GEODIP display on a short interval (from Schlumberger, Evaluacion de formaciones en Mexico, 1984).

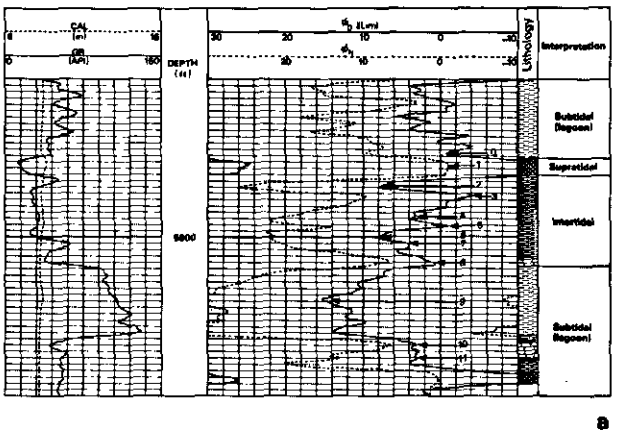

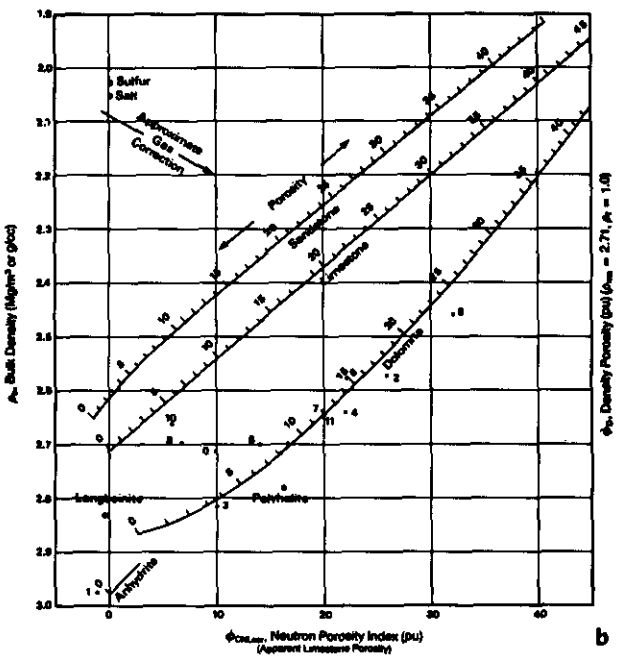

Fig. 6.8-17. - a) Composite-log, b) Crossplot ρ_b vs ϕ_N on Desert Creek Formation, Paradox Basin.

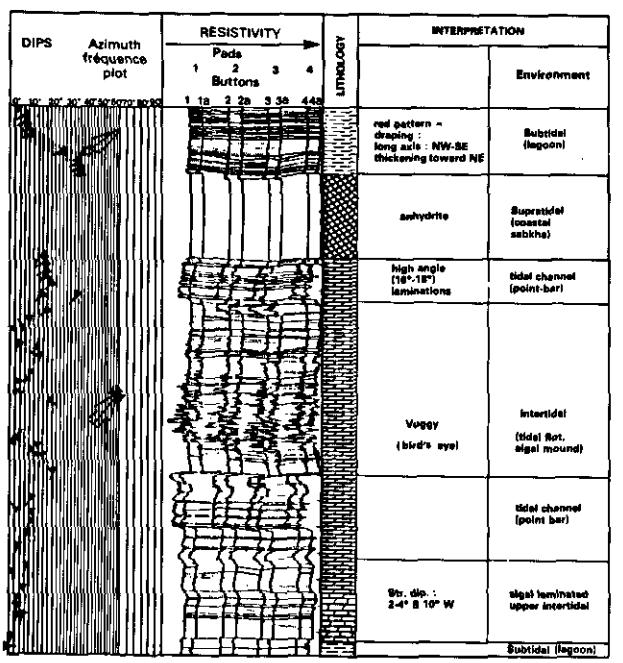

◀ Fig. 6.8-18. - LOCDIP on the same interval and its interpretation.

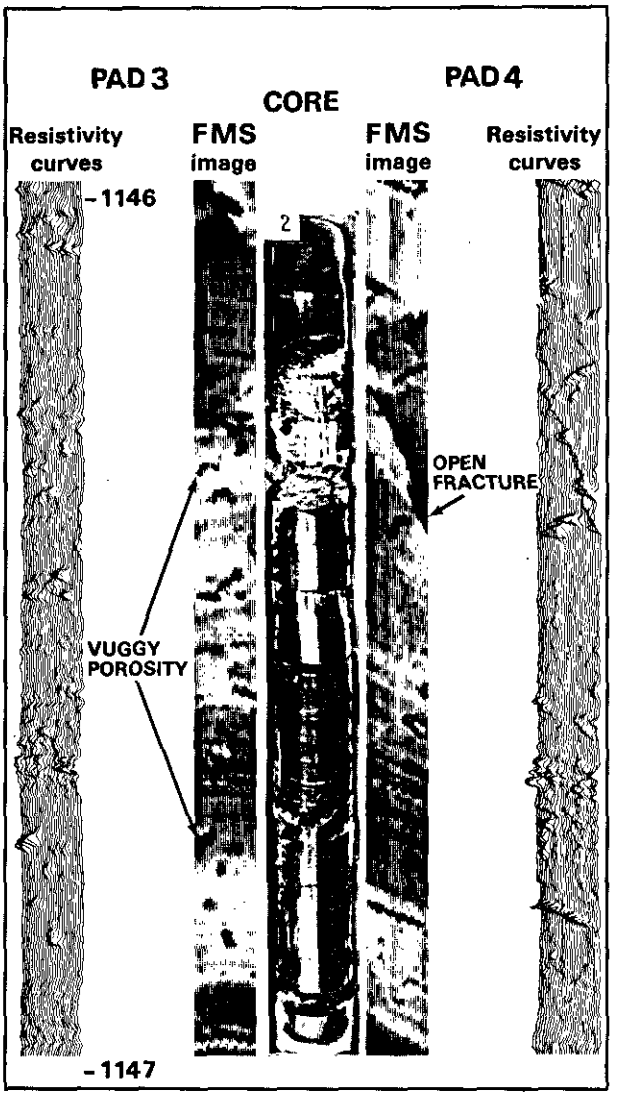

Fig. 6.8-19. - Example of FMS image in a vuggy limestone

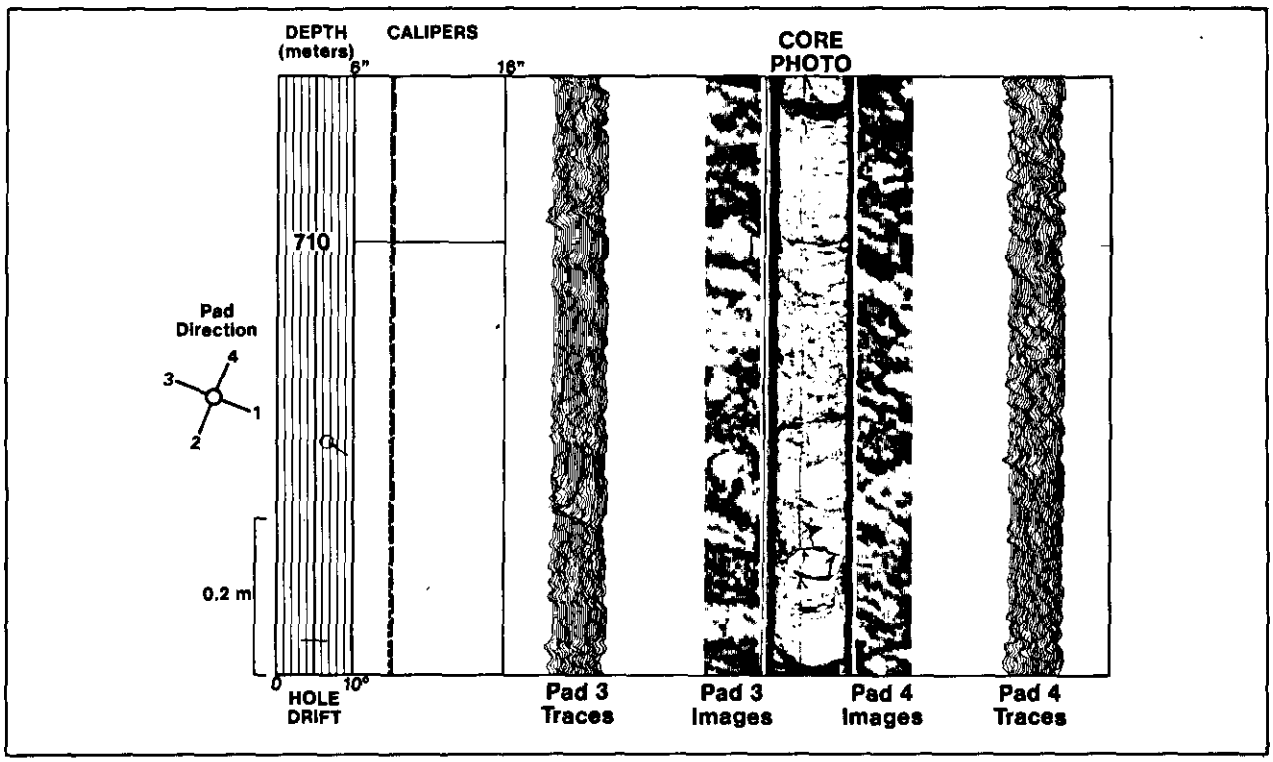

Fig. 6.8-20. - Example of anhydritic nodules clearly observed on a FMS image

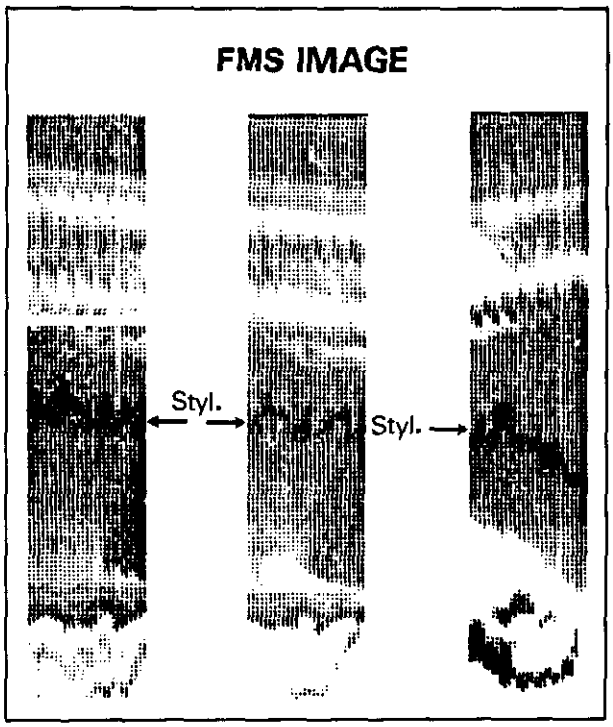

Fig. 6.8-21. - Example of stylolites recognized on a FMS image

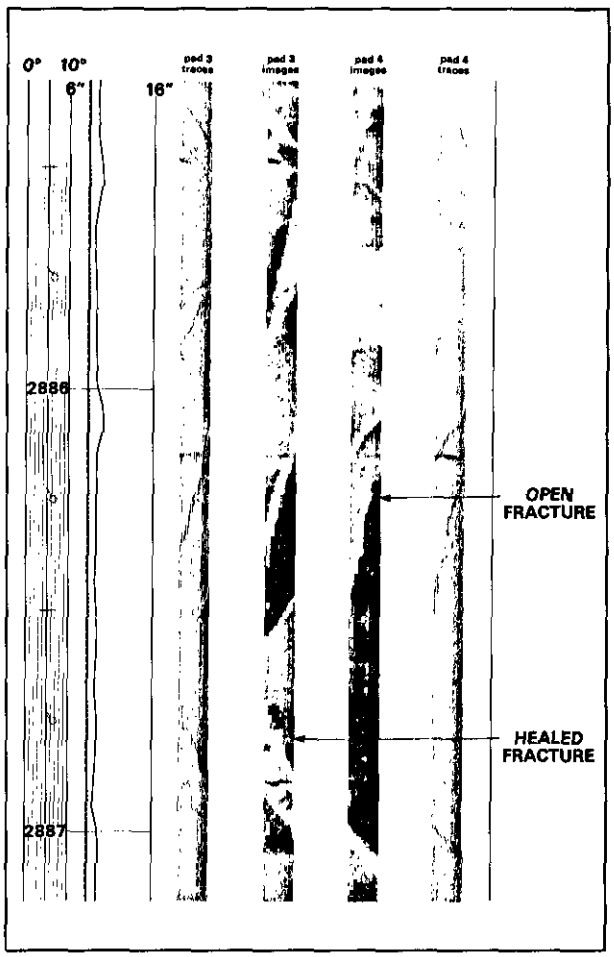

Fig. 6.8-22. - Example of fractures detected on a FMS image. ▶
One can separate between open and healed fractures

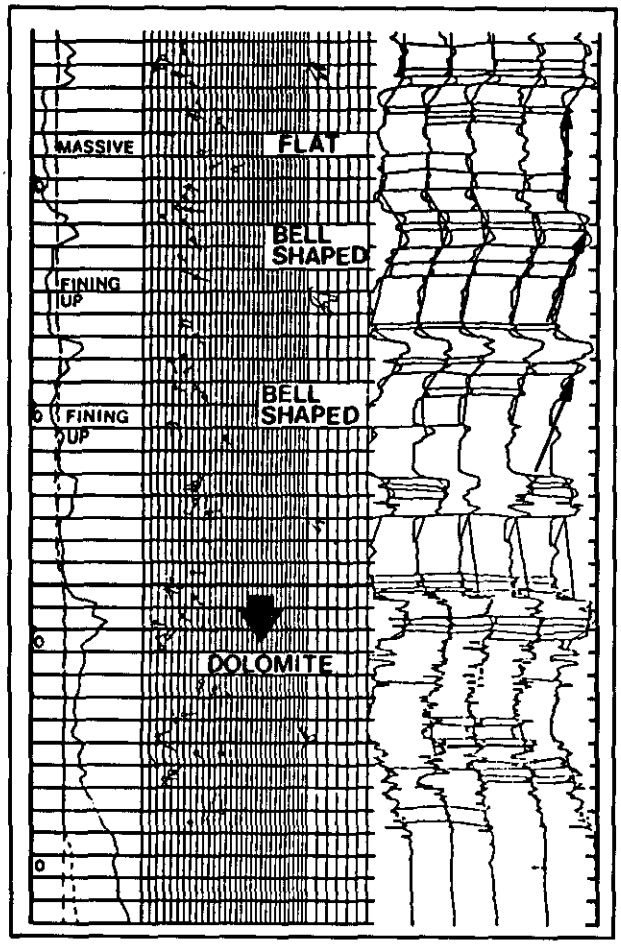

6.8-17, and the interpreted LOCDIP in Fig. 6.8-18.

FMS images are very useful to identify typical diagenetic features such as vuggy porosity (Fig. 6.8-19), anhydrite nodules (Fig. 6.8-20), and stylolites (Fig. 6.8-21), or fractures (Fig. 6.8-22).

6.8.3.3. Boundaries

They are not easily detected except when they correspond to an abrupt change of lithology.

6.8.3.4. Electro-Sequences

Sequential evolution in composition and in sedimentary features can be observed, as well as a "bell" or "funnel" shape on the dipmeter resistivity curves (Fig. 6.8-23), which permit the interpretation of the interval in terms of sequences and depositional environments (see previous figures).

◀ Fig. 6.8-23. - Example of resistivity evolution in carbonate formation (from Theys *et al.*, 1983).

6.9. DEEP-SEA CLASTIC ENVIRONMENT

6.9.1. DEFINITION

Environments characterized by sediments deposited in a large body of water below the action of waves, resulting from sediment gravity flow mechanisms. They are illustrated in the block diagram of Fig. 6.9-1. A theoretical vertical cross-section in a submarine fan sequence is reproduced Fig. 6.9-2.

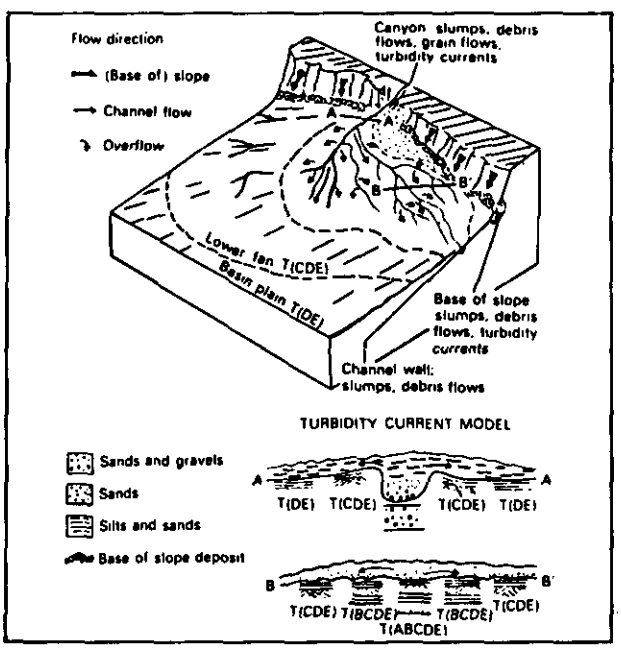

Fig. 6.9-1. - Theoretical illustration of a deep-sea clastic environment showing bi-modal channel and overbank deposition by turbidity currents across a turbidite fan. The model is largely based on the Astoria Fan (from Nelson & Kulm, 1973). Letters refer to the divisions of the Bouma sequence.

Fig. 6.9-2. - Vertical cross-section showing a hypothetical submarine fan stratigraphic sequence produced by fan progradation. C.T. = classical turbidite. M.S. = massive sandstone. P.S. = pebbly sandstone. D.F. = debris flow. Arrows show thickening- (T.U.) and coarsening-upward sequences (C.U.) and thinning- (Th.U.) and fining-upward sequences (F.U.). (Adapted from Walker, 1975). ▶

6.9.2. GEOLOGICAL FACIES MODEL

6.9.2.1. Lithology

Two parameters must be considered separately.

6.9.2.1.1. *Composition*

Generally, the main minerals are quartz, potassium feldspars, plagioclases, and micas. Rock fragments are also present. Consequently the sandstones range from subgraywackes to graywackes. But, depending on the source of the feeder sediments, they also can be made up of pure quartz (orthoquartzite sands), of pure carbonates, or even of volcanic debris sands. Skeletal debris are present and can generate concretions

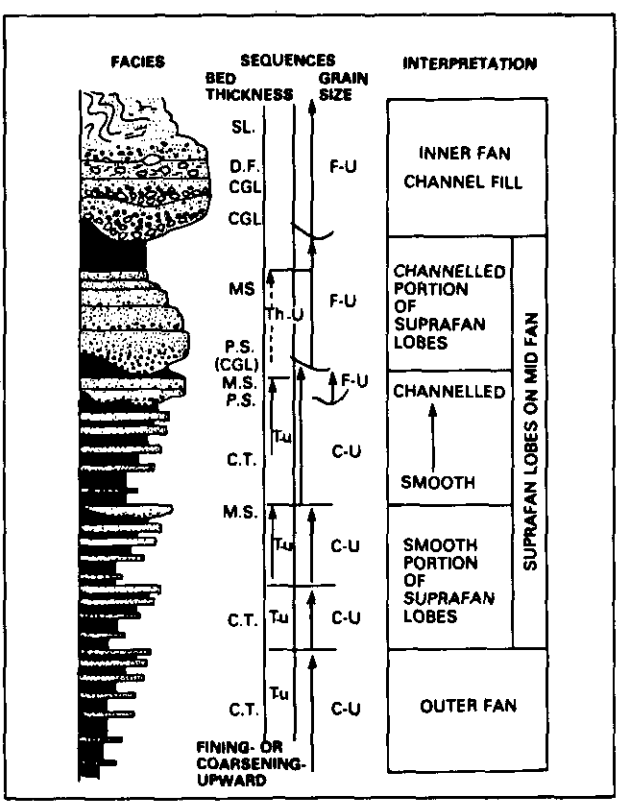

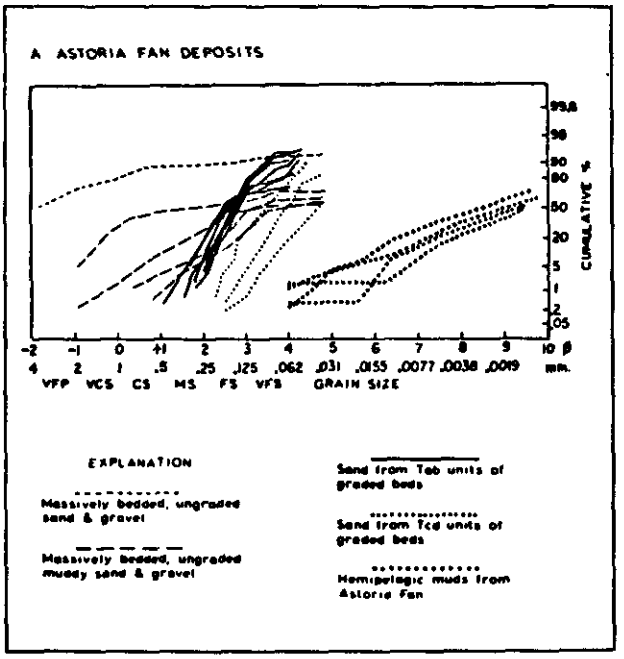

Fig. 6.9-3. - Log-probability plots of grain size distribution of representative sediment types of Astoria Fan. Massive clean sands and gravels, and massive muddy sands and gravels are from upper fan valleys. Bouma AB and CD sands are from the middle and lower fan, and hemipelagic muds are from throughout the fan. (From Nelson & Kulm, 1973).

(or cemented balls or nodules) by dissolution, diffusion and reprecipitation of calcite in the pore space. Carbonaceous fragments and shale clasts are also present. Clay is the principal matrix and cement. Glauconite, if available, may be present.

6.9.2.1.2. *Texture*

Grain size can vary between gravel to clay range. Sorting is very poor to fair (Fig. 6.9-3). Low grain-matrix ratio. Intraformational conglomerates are present due to reworking of previous deposits by the new sediment flow. Grain size decreases from the proximal to the distal ends of turbidite deposits.

6.9.2.2. Structure

Graded beds are rhythmically interbedded with shale. Absence of large-scale cross-beds. Sole marks, asymmetrical ripple marks, laminated and convoluted beds are common. Trails and tracks are generally present (Pettijohn *et al.*, 1972).

6.9.2.3. Boundaries

Sharp, sometimes erosional, lower contact is observed; the upper contact is gradational toward the top and the outer fan.

6.9.2.4. Sequences

Vertical and lateral grain size sequence of one flow is fundamentally fining. Sequences can be also recognized in sorting, sedimentary structures, and thickness variations. This is illustrated by the Bouma sequence, (1962), which applies to the typical turbidite (Fig. 6.9-4).

With regard to the proximity of the feeder channel, different vertical and lateral sequences -incomplete and truncated, compared to the Bouma sequence - can be described (Fig. 6.9-5 and 6.9-6).

This bed thickness evolution is noticeable by comparing proximal and distal deposits (Table 6.9-1).

Depending on the main active process, the sequence can be modified as shown in Fig. 6.9-7.

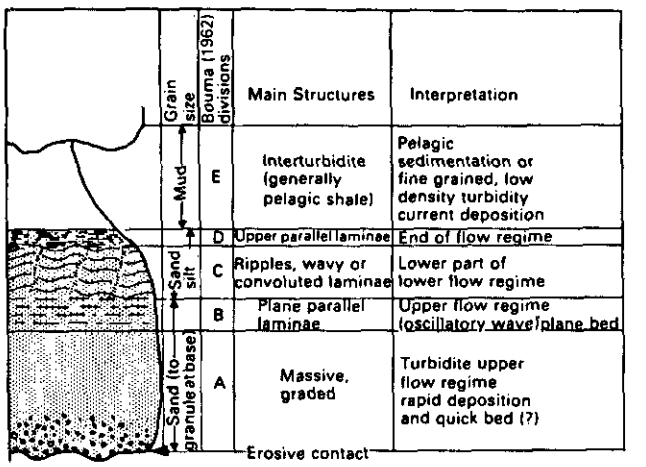

Fig. 6.9-4. - The Bouma sequence of structural divisions in a turbidite bed and its flow regime interpretation (modified from Middleton & Hampton, 1976).

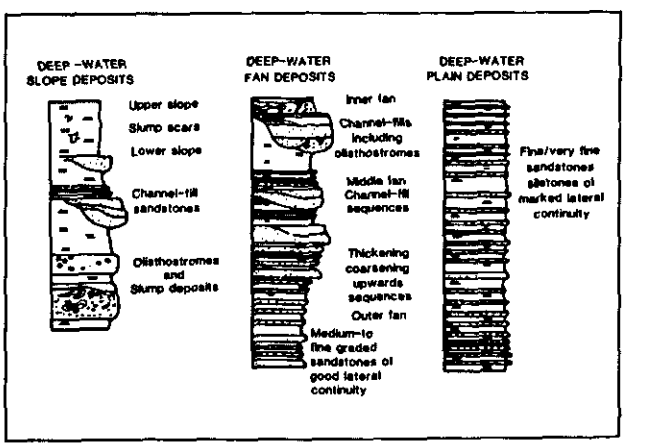

Fig. 6.9-5a. - Sequences characteristic of slope, fan and basin plain deposits (from Mutti & Ricci-Lucchi, 1972).

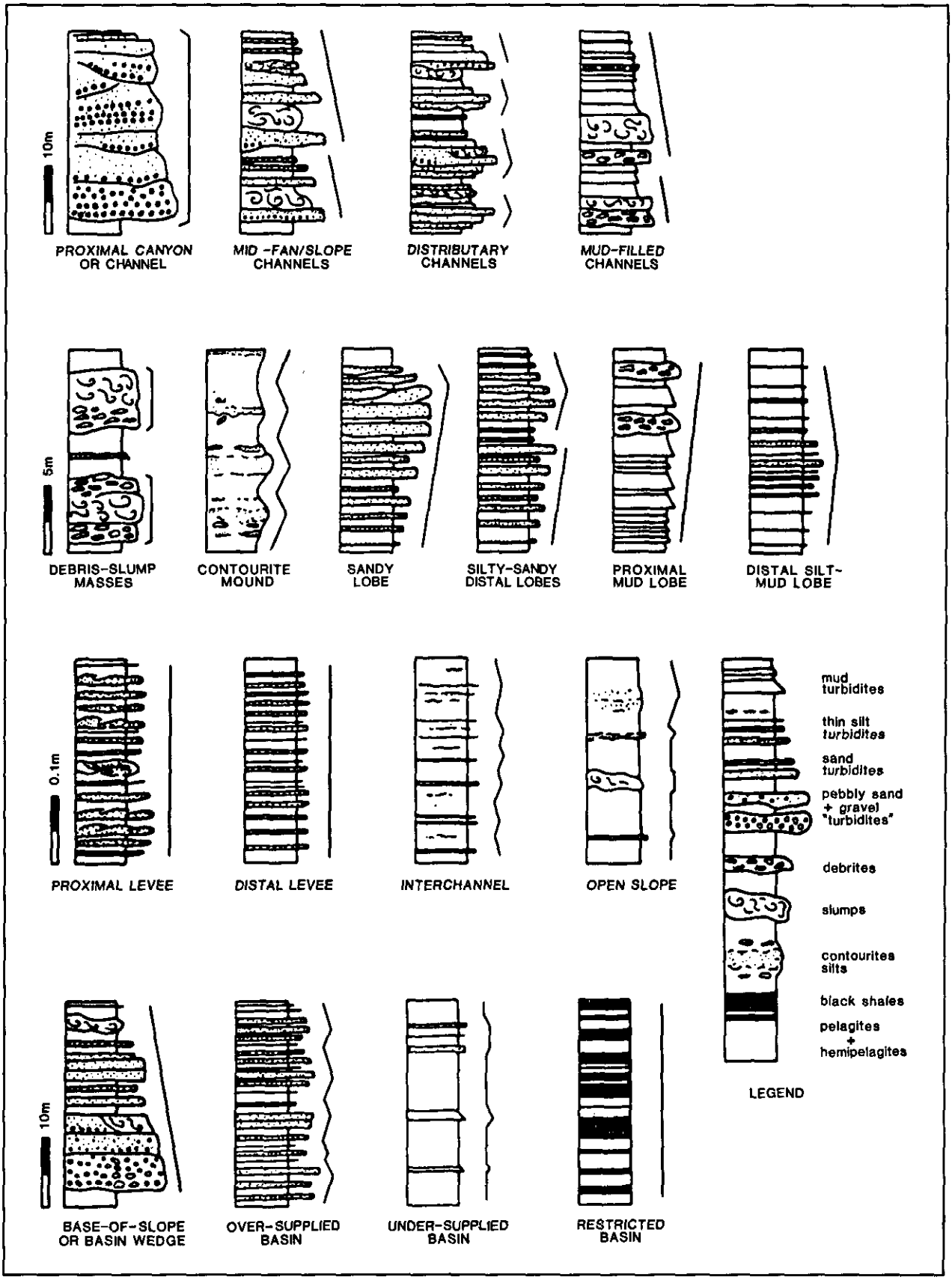

Fig. 6.9-5b. - Typical vertical sequences of turbidite and associated sediments from various morphological elements in the different *deep-sea environments. Fining-upward, coarsening-upward, blocky, symmetrical and irregular sequence types are indicated* by the lines to the right of lithological columns (from Stow, 1985).

Table 6.9-1
Comparison of proximal and distal turbidite sequences
(from Walker, 1967).

	PROXIMAL	DISTAL
A	Beds thick	Beds thin
B	Beds coarse grained	Beds fine grained
C	Individual sandstones often amalgamate to form thick beds	Individual sandstones rarely amalgamate
D	Beds irregular in thickness	Beds parallel-sided regularly bedded
E	Scours, washouts and channels common	Few small scours, no channels
F	Mudstone partings between sandstones poorly developed or absent. Sand/mud ratio high	Mudstone layers between sandstones well developed. Sand/mud ratio low
G	Beds ungraded or crudely graded	Beds well graded
H	Base of sand always sharp, top often sharp, many AE sequences	Base of sand always sharp, top grades into finer sediment, AE sequences rare
I	Laminations and ripples occur infrequently	Laminations and ripples very common
J	Scour marks occur more frequently than tool marks	Tool marks occur more frequently than scour marks

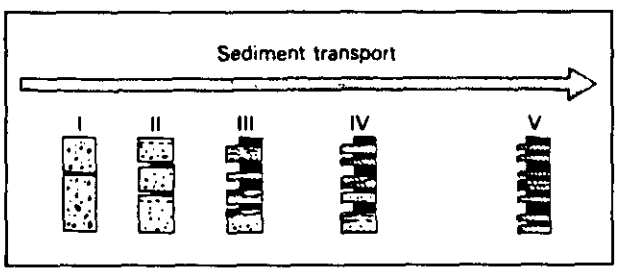

Fig. 6.9-6. - Schematic illustration of the downcurrent decrease of bed thickness, grain size and sand-shale ratio in a turbidite sequence (from Einsele, 1963).

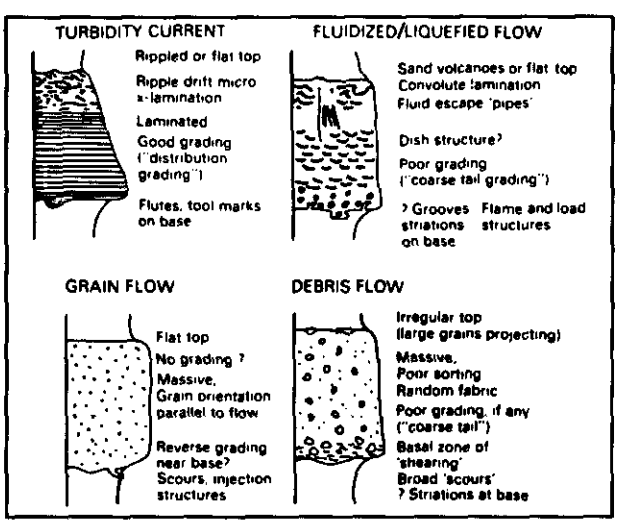

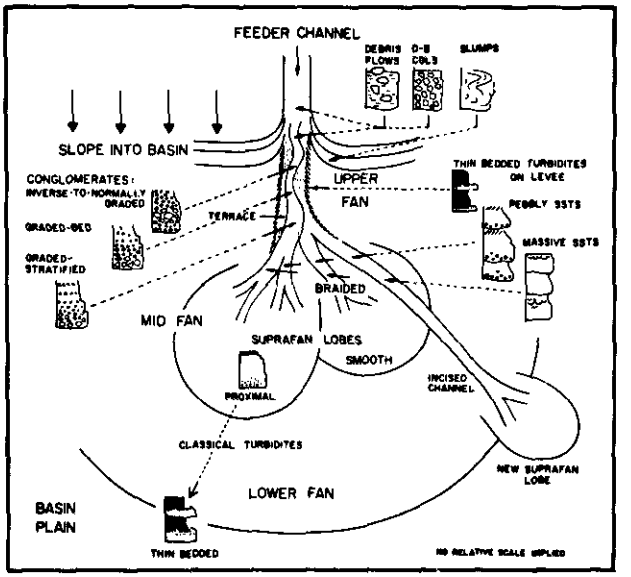

Fig. 6.9-8. - Subaqueous fan environmental model (from Walker, 1975).

6.9.2.5. Geometry of the Body

Turbidite bodies can be separated into three main groups (Fig. 6.9-8 to 6.9-10).

- Channel or subaqueous canyon deposits : they are elongate fills up to several miles long, truncating subjacent strata. They occur on the upper slopes, close to canyon mouths (*upper fan* and *upper mid fan*). Although they can be fairly straight, they may also be dendritic and bifurcating.

- Subaqueous fan deposits : they tend to be more sheetlike. They show a broad radial sedimentation pattern (fan shaped) and occur in the *lower mid fan* and *lower fan*.

- Basin floor deposits : They are thin sheet-type deposits, covering a large area compared to the first two groups.

Each elementary sequence thickness ranges from a few centimetres to more than 3 metres. A megasequence is composed of 10 to more than 100 elementary sequences. It can be subdivided in several mesosequences marked by successive thickening up sequences. The growth of the megasequence is due to both progradation and lateral avulsion of active suprafan lobes and channels (Fig. 6.9-11).

◀ Fig. 6.9-7. - Structures and textures of deposits from single mechanism mass-gravity flows. No vertical scale is implied (from Middleton & Hampton, 1976).

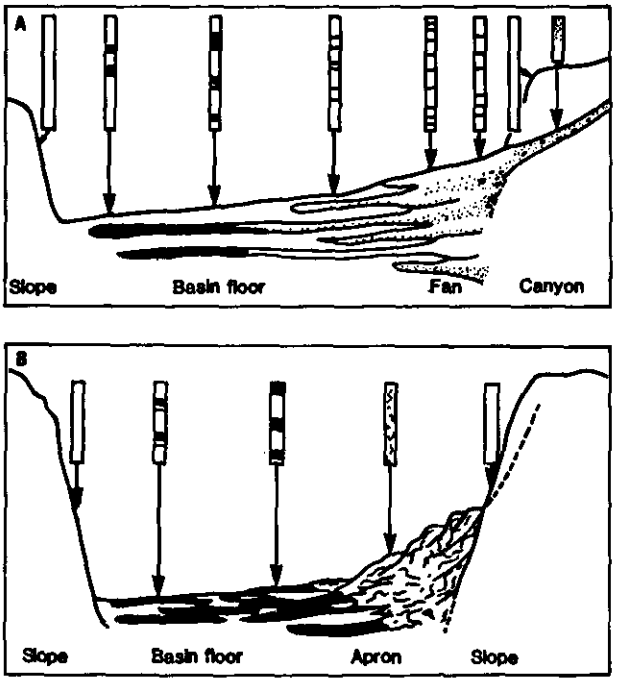

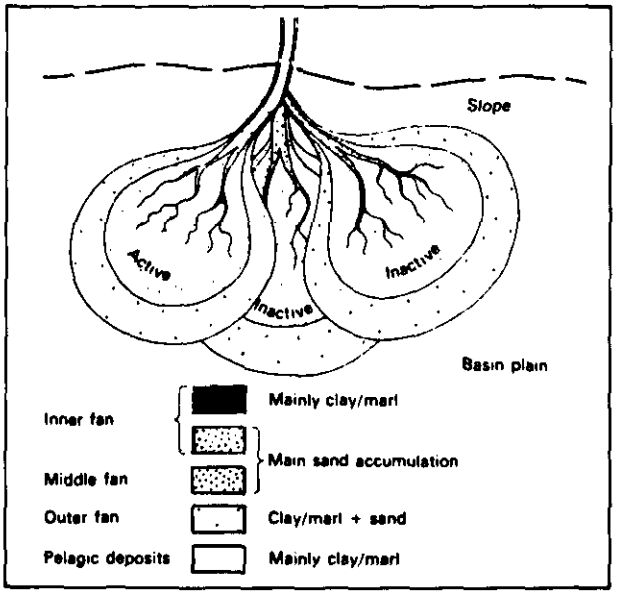

Fig. 6.9-11. - Model of fan growth by progradation and lateral avulsion of an active, major fan lobe (from Kruit *et al.*, 1975).

◀ Fig. 6.9-9. - Cross-section showing the basin margins (canyon-fan and slope-apron) and basin floor relationship (from Gorsline & Emery, 1959).

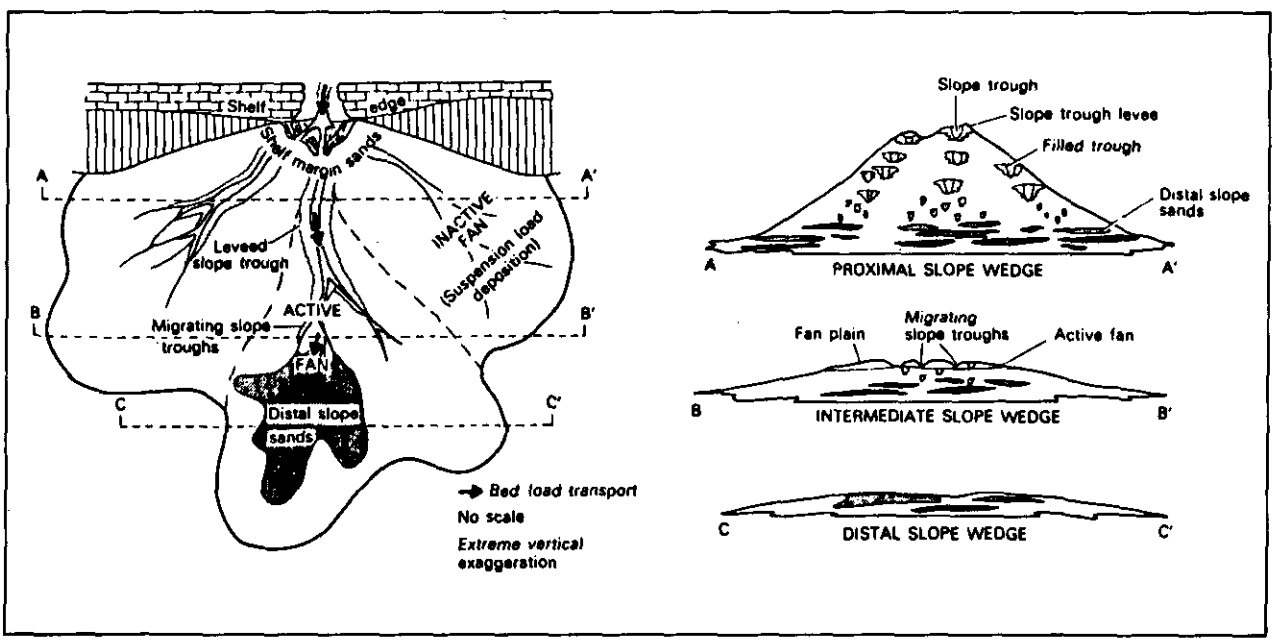

Fig. 6.9-10. - Fan model for the Upper Pennsylvanian Cisco Group, north-central Texas (from Galloway & Brown, 1973).

6.9.2.6. Directional Current flow Model

The flow is generated by gravity and is down-slope. Different processes (Fig. 6.9-12) may occur producing different types of deposits. In a turbidity current different flow paths and velocity profiles can be recognized (Fig. 6.9-13) in relation to the cohesiveness of the supporting bed (Fig. 6.9-14).

In mass flow, when the gravity motion starts, the whole flow compresses the water mass which

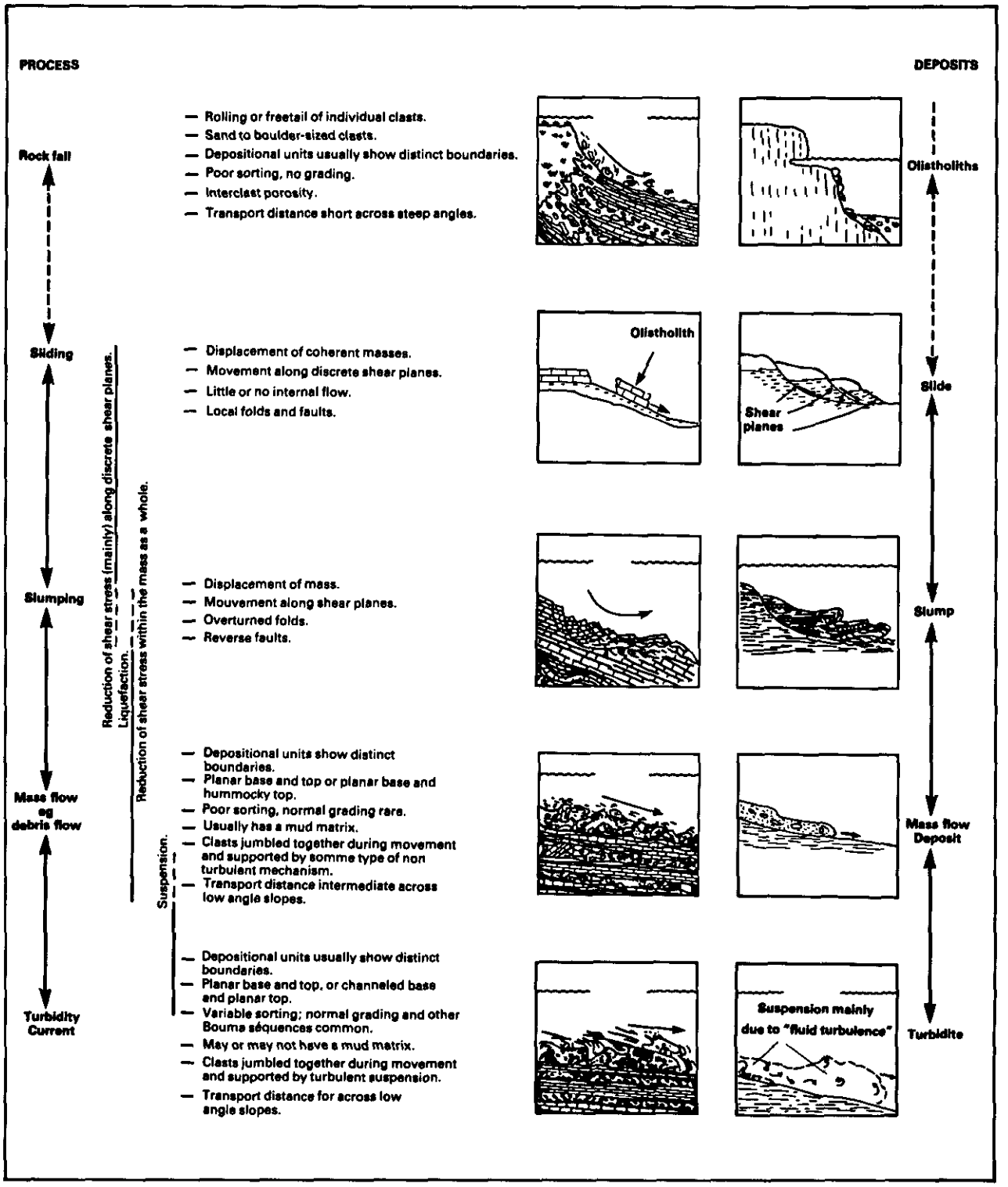

Fig. 6.9-12. - Major types of gravity transport processes (adapted from Dott, 1963).

in turn reacts generating an oscillatory wave which decays in energy with time (dispersive pressure).

With respect to its decreasing energy this wave generates (Fig. 6.9-4) : parallel laminae (B unit of the Bouma's sequence), ripples (C unit), and fine upper parallel laminae (D unit). An interpretation of the interrelation of different processes which occur in a single event of mass-gravity transport is shown in Fig. 6.9-15.

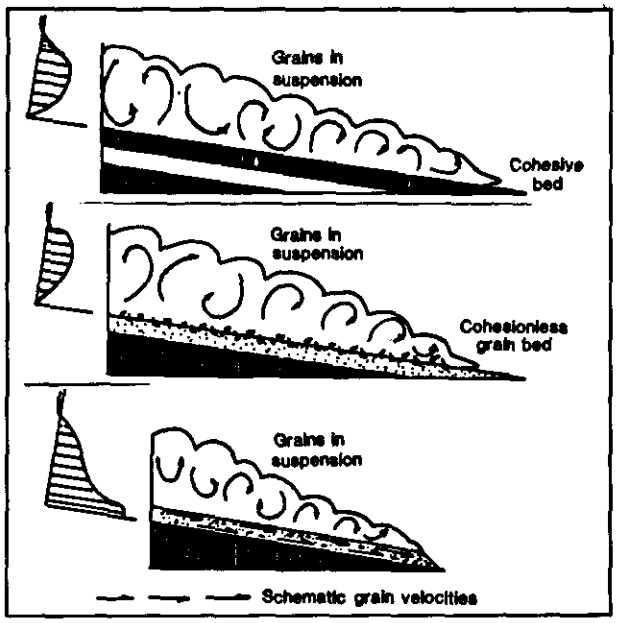

Fig. 6.9-13. - Different turbidity current motions following the cohesiveness of the underlying bed (from Friedman & Sanders, 1978).

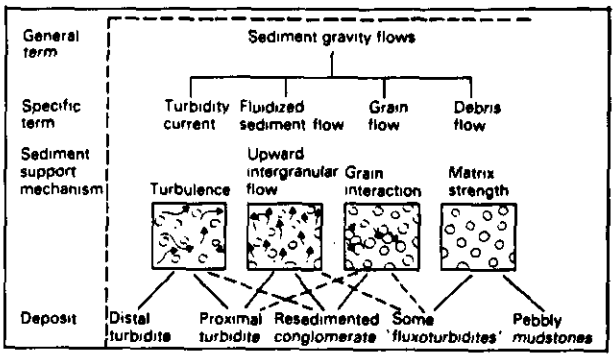

Fig. 6.9-14. - Classification of sediment gravity flow based on the mechanism of grain support (from Middleton & Hampton, 1973).

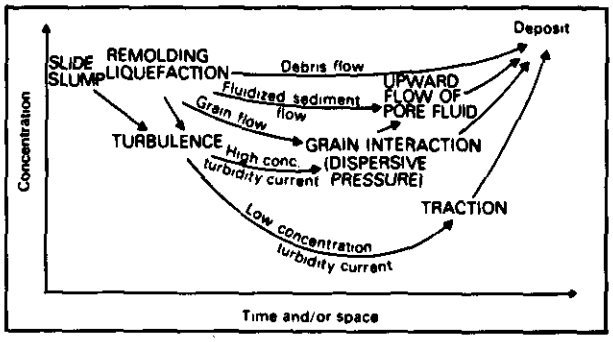

Fig. 6.9-15. - Interrelation of different processes in a single event of mass-gravity transport (adapted from Middleton & Hampton, 1973).

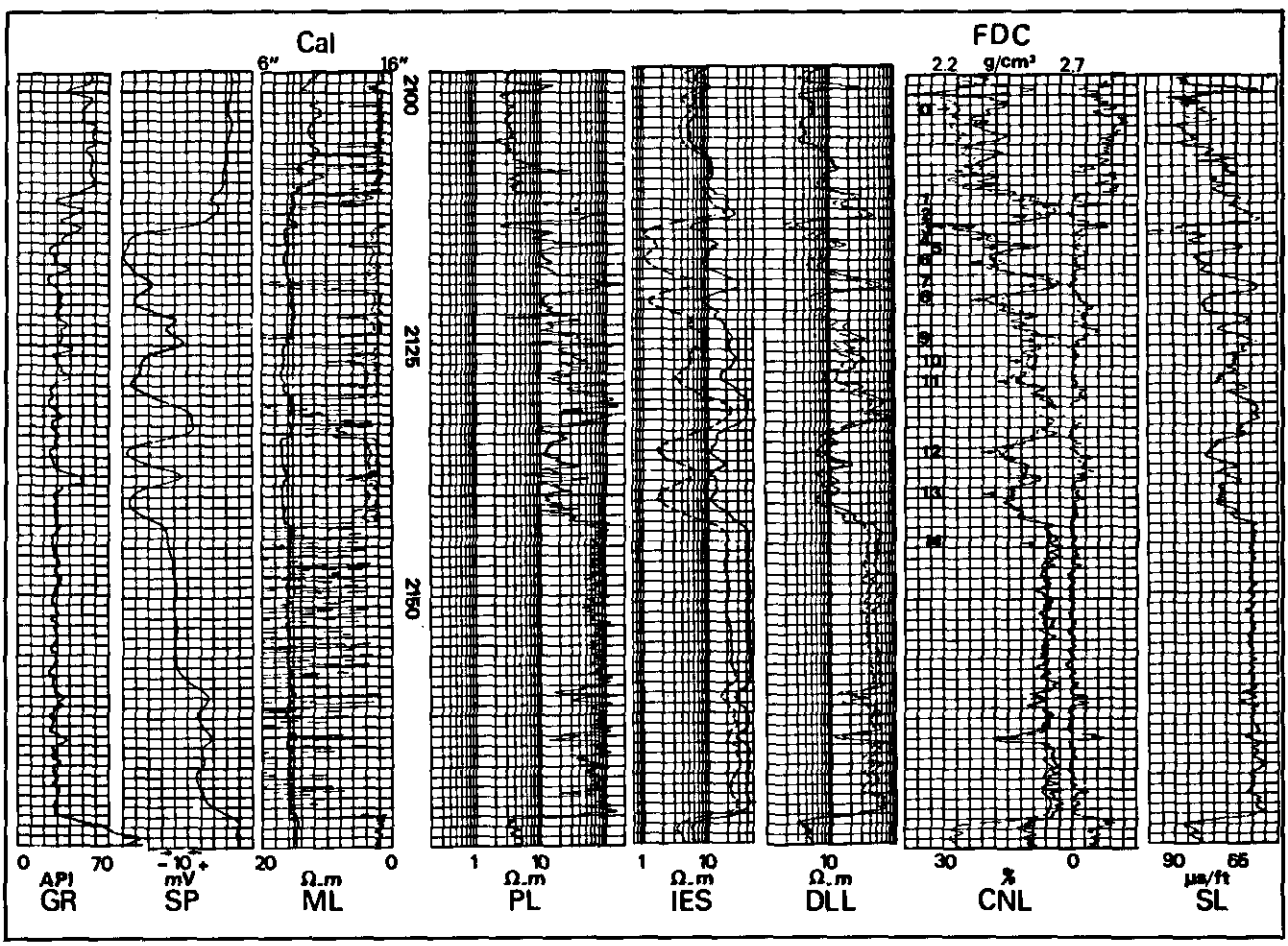

Fig. 6.9-16. - Composite-log in a flysch and turbidite deposit (from Payre & Serra, 1979). From that it is not obvious that it corresponds to a turbidite. Only dipmeter shows evidence of turbidite deposit (see Fig. 6.9-22).

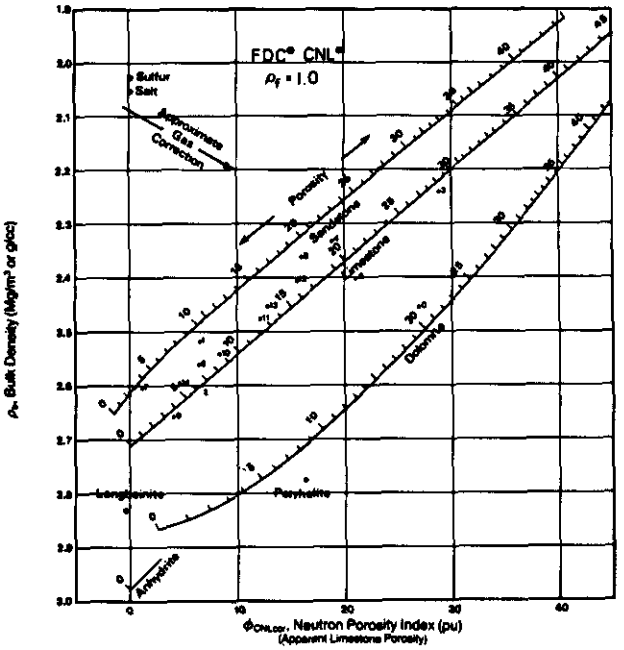

Fig. 6.9-17. - Density-neutron crossplot showing the position of some of the readings from Fig. 6.9-16 (from Payre & Serra, 1979).

6.9.2.7. Reservoir Characteristics

Due to the general immaturity of the sands, their characteristics are often moderate to poor. The permeability increases from distal to proximal fans. Distal sands constitute numerous sheet-like beds with no vertical permeability. Proximal sands can be thick, with good vertical permeability, with a shoestring shape. Overpressures are often observed.

6.9.3. WELL-LOG RESPONSES AND CHARACTERISTIC

6.9.3.1. Electro-Lithofacies

Following the type of turbidites (siliciclastic or bioclastic) two kinds of well-log responses must be considered.

6.9.3.1.1. *Composition*

- *Siliciclastic turbidites*

Thorium and potassium content, and hence the level of radioactivity can vary considerably in turbidite deposits, depending on the mineralogical maturity of the materials extracted from the parent source rocks. Fig. 6.9-16 gives an example of mature material with relatively low radioactivity (20 to 35 API). Fig. 6.9-18, on the contrary, shows a very high radioactivity reflecting an immature material rich in potassium feldspar and micas as pointed out from interpretation of crossplots of Fig. 6.9-19. On ρ_b vs ϕ_N crossplot representative

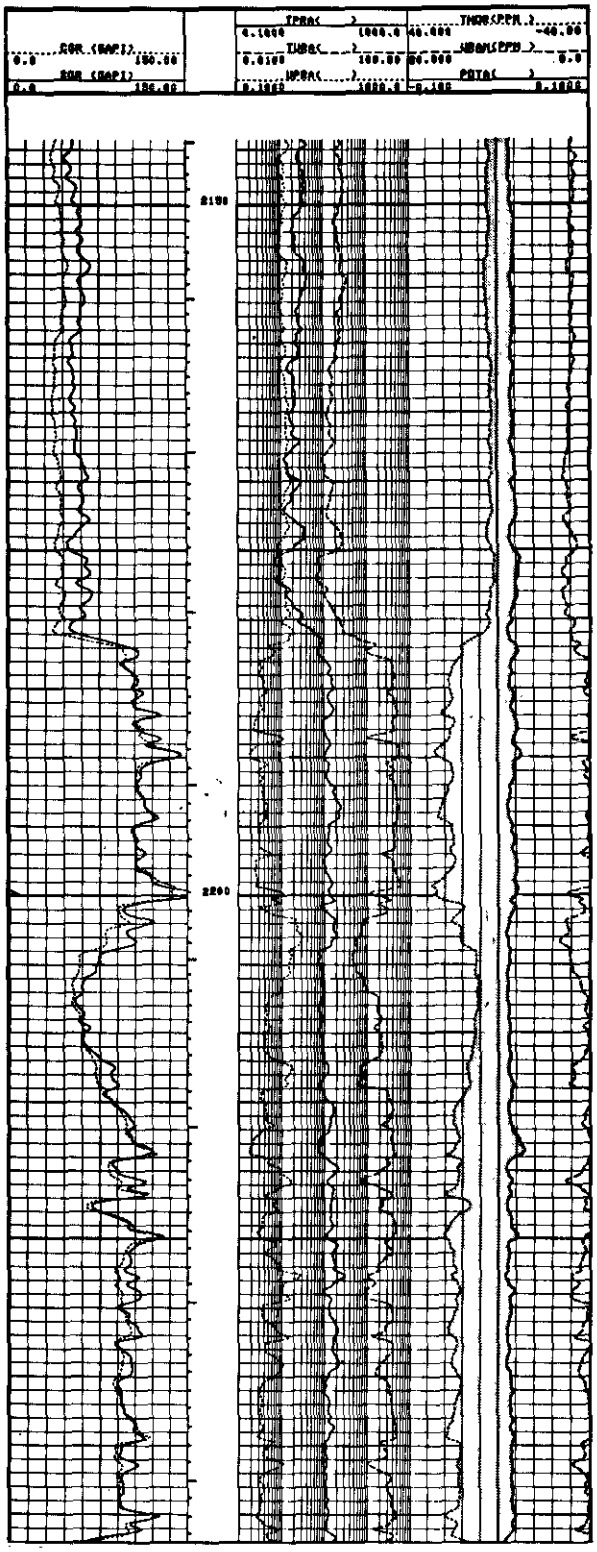

Fig. 6.9-18. - NGS log over the sandstone formations of North Palk Bay, India (from Schlumberger, Well Evaluation Conference, India, 1983).

points fall between the quartz sand and the limestone lines, generally closer to the latter (Fig. 6.9-17 and 6.9-19). Some points, close to the shale region, correspond to pelagic shale deposits (E unit of the Bouma sequence).

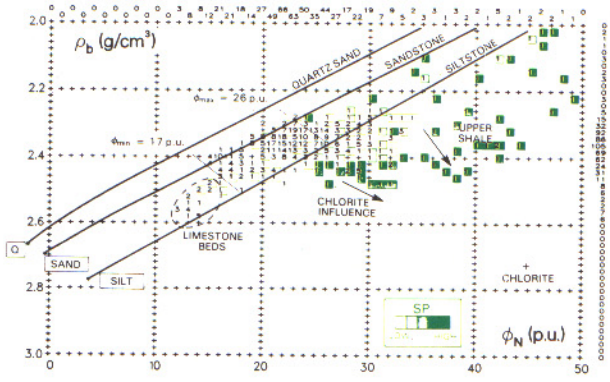

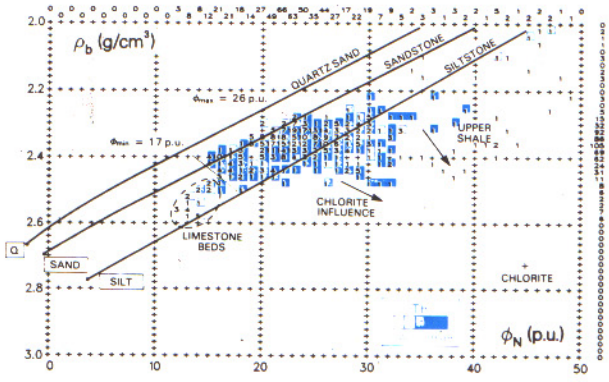

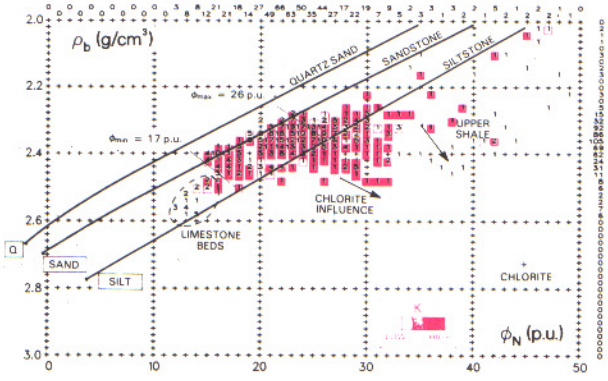

Fig. 6.9-19. - Set of crossplots showing the mineralogy of the formations of Fig. 6.9-18 (from Schlumberger, Well Evaluation Conference. India, 1983).

Fig. 6.9-20. - Composite-log in a carbonate turbidite (from Payre & Serra, 1979). The well-log responses do not indicate a turbidite deposit. Interpretation of the GEODIP display (see Fig. 6.9-26) will show the sequences and other features which will indicate the origin of the deposit.

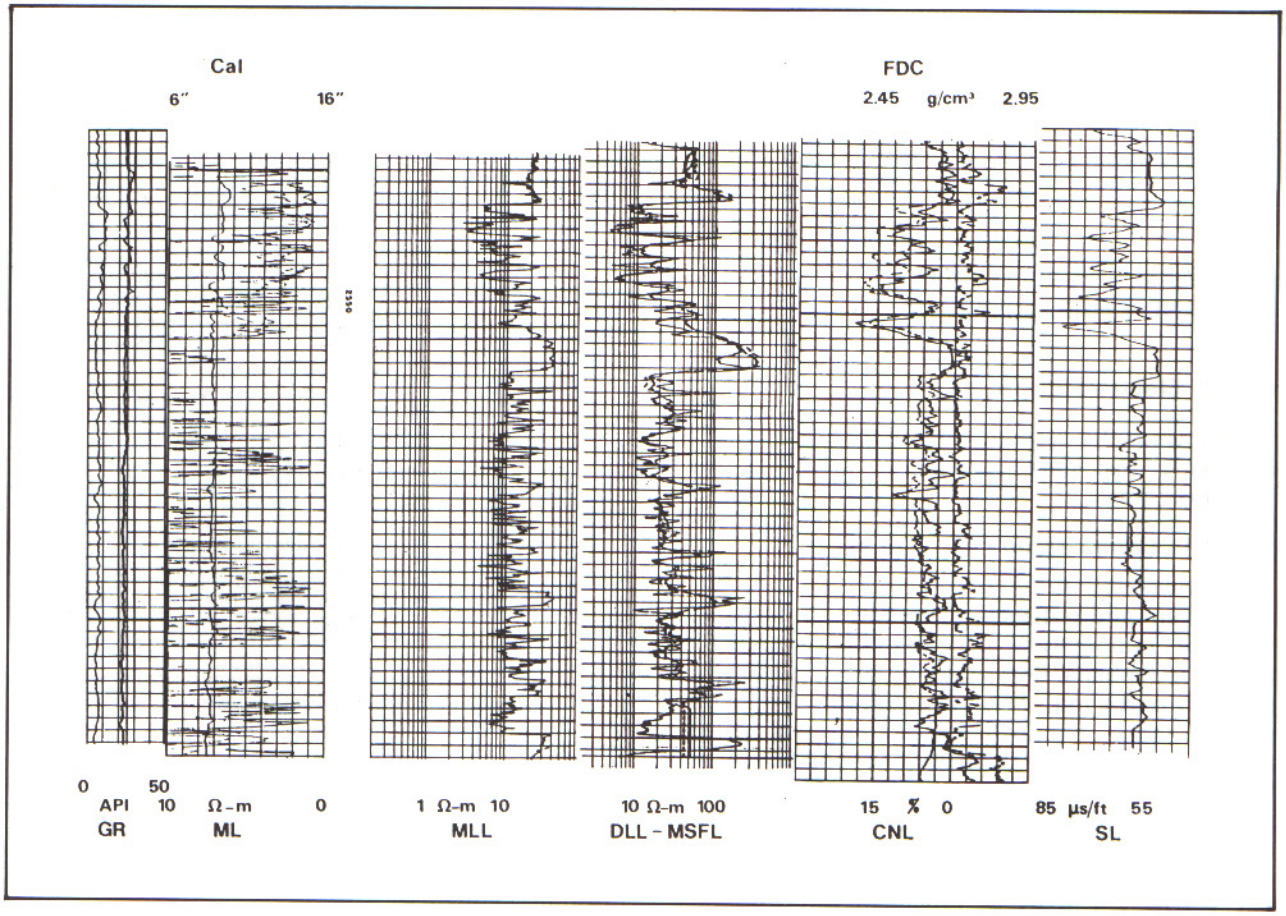

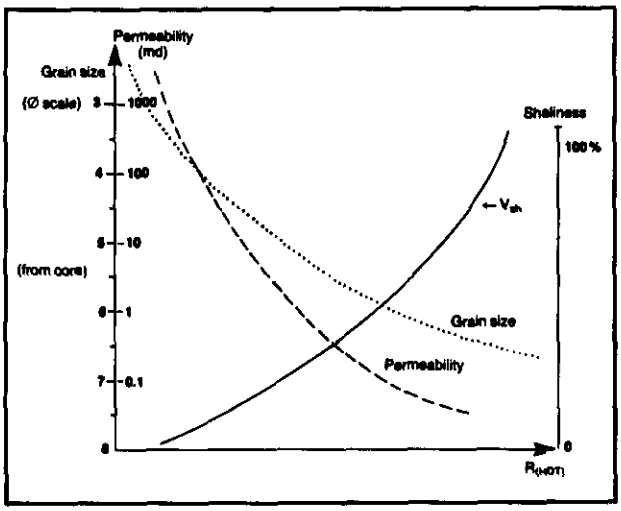

Fig. 6.9-21. - Example of relationship between dipmeter resistivity curve on the one hand, and grain size and permeability on the other hand.

- Bioclastic (carbonate) turbidites

Radioactivity is generally low (less than 10 API in the example of Fig. 6.9-20) in relation to a very low thorium and potassium content. Potassium content may be higher in pelagic muds. On a ρ_b vs ϕ_N crossplot, representative points are very close to the limestone line. Pe values indicate calcite as the main mineral.

6.9.3.1.2. *Texture*

In siliciclastic turbidites an idea of the relative grain size can be obtained from the study of crossplots (Fig. 6.9-19), or, better, from the dipmeter resistivity evolution, after calibration from core analysis (Fig. 6.9-21). In carbonate turbidite the shape of dipmeter resistivity curves may help in recognizing mudstone, grainstone or boundstone or breccia.

6.9.3.2. Dip Patterns

As illustrated by Fig. 6.9-22, in case of a proximal fan, amplitudes of variations in dip magnitude and changes in azimuth reflect the relative posi-

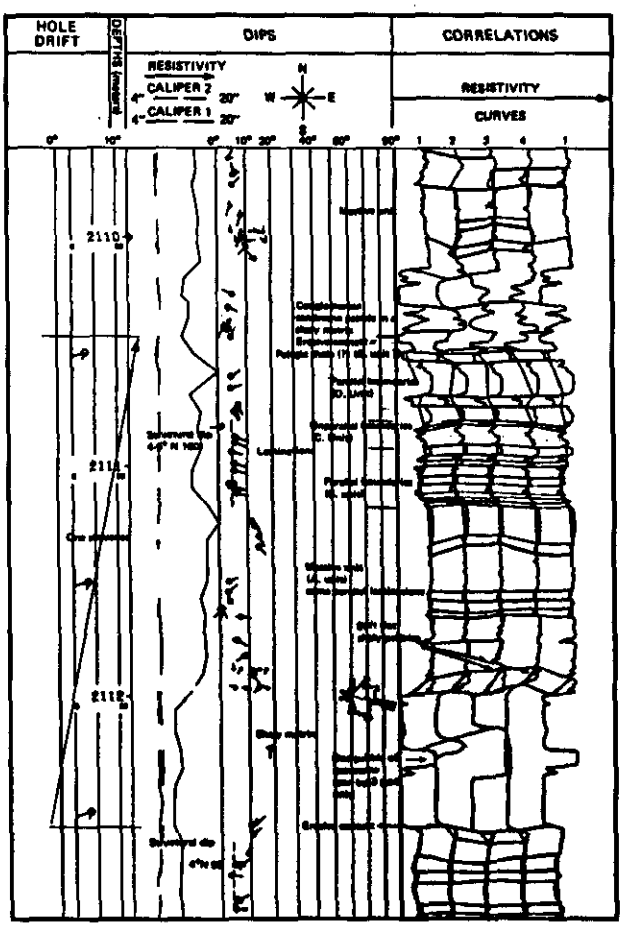

Fig. 6.9-22. - A Bouma sequence as seen by the dipmeter (a) and its interpretation; (b) core photograph of the same interval (from Payre & Serra, 1979).

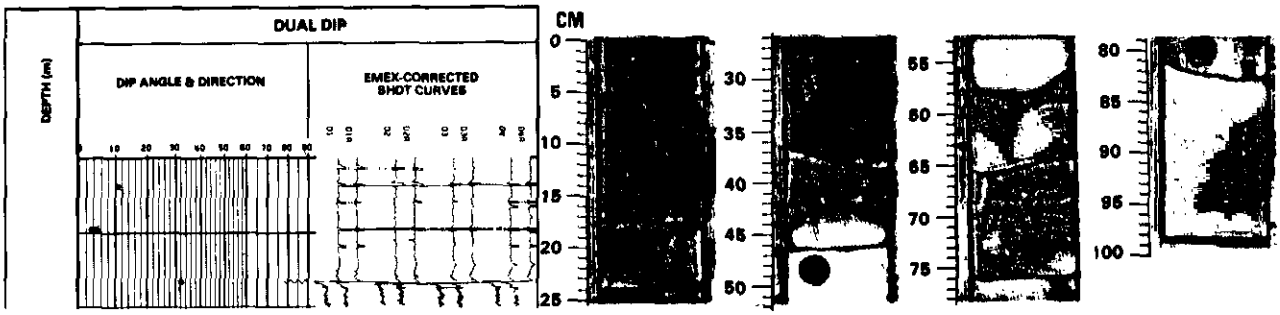

Fig. 6.9-23. - Isolated resistive events in a massive sandstone corresponding to cemented balls as seen by LOCDIP (a), confirmed by photograph of core (b) (from Delhomme & Serra, 1984).

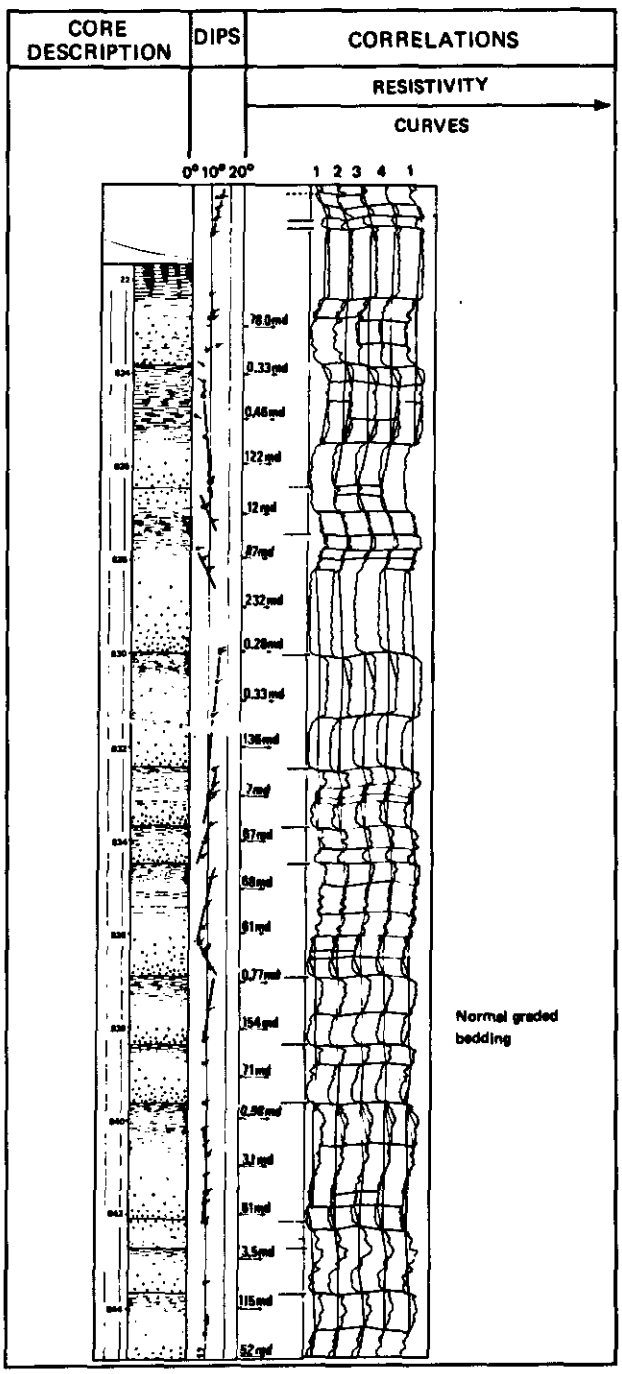

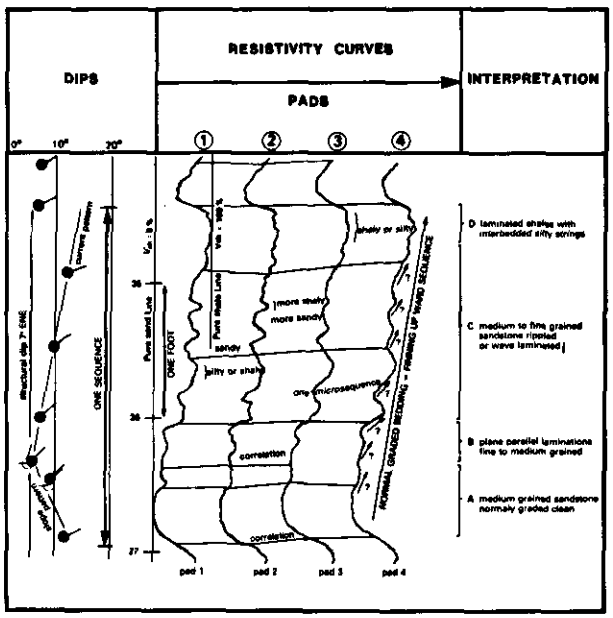

Fig. 6.9-24b. - Enlargement of one sequence of the previous example.

tion in the Bouma sequence : scattered dips or no dip in the A unit; none or low variations (green *pattern) in the B or D units; higher variations* with changes in azimuth in the C unit. Isolated thin conductive events in the massive sands (A unit) may correspond to flat shale clasts. Isolated resistive events in the massive sands can correspond to cemented balls created by dissolution of bioclasts and reprecipitation of the calcite as cement in the surrounding pore space (Fig. 6.9-23). Such events indicate diagenetic effects.

Several isolated resistive events on dipmeter resistivity curves reflect matrix supported conglo*merates, if they are observed at the bottom of a*

◀ Fig. 6.9-24a. - Example of several turbidite sequences detected by the dipmeter. Resistivity evolutions allow detection of fining and coarsening upward sequences as well as thickening or thinning upward megasequences.

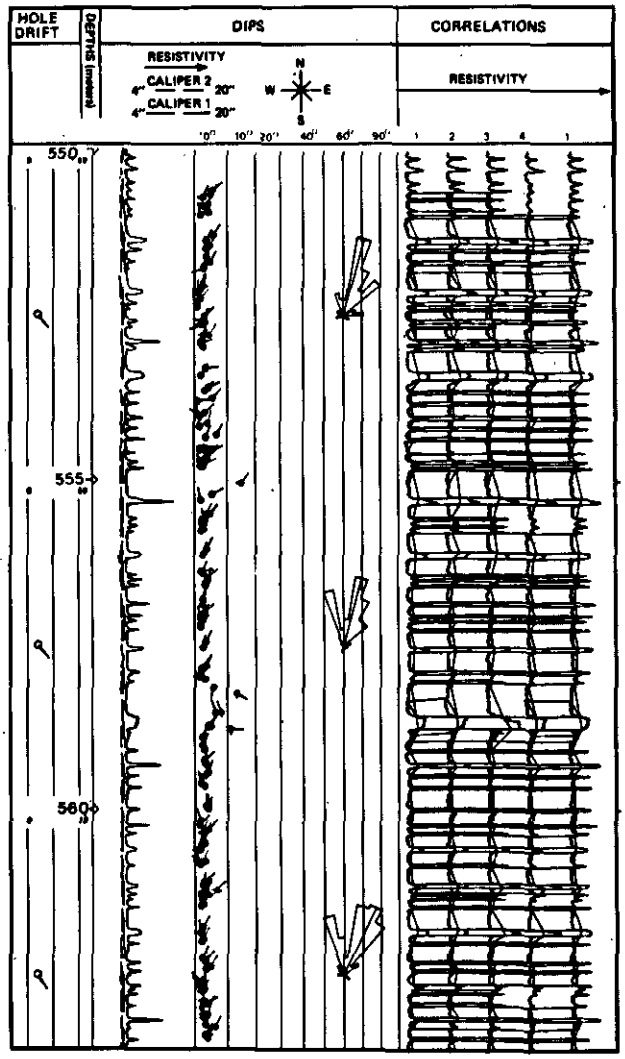

Fig. 6.9-25a. - Example of dipmeter responses in distal turbidites (GEODIP arrow-plot).

sequence. They can correspond to an erosion of the top of the previous deposit by the front of the turbidite flow and mixing of D or C unit sandstones with E unit pelagic shales. When the isolated resistive events are observed anywhere in a massive sand they correspond, generally, to cemented balls. Some blue patterns can be observed, they possibly reflect progradation of the fan. Red patterns may be present and could correspond to draping of previous deposits or filling of channels (Fig. 6.9-24b). Azimuth variations observed on a long interval, including several sequences, can give an idea of the broad shape of the fan due to lateral avulsion.

In mid fan (Fig. 6.9-24a) and distal fan (Fig. 6.9-25) dips are more consistent in magnitude and azimuth.

In mass flow deposits (Fig. 6.9-26) very few correlations are found generating scarce dips with random azimuth.

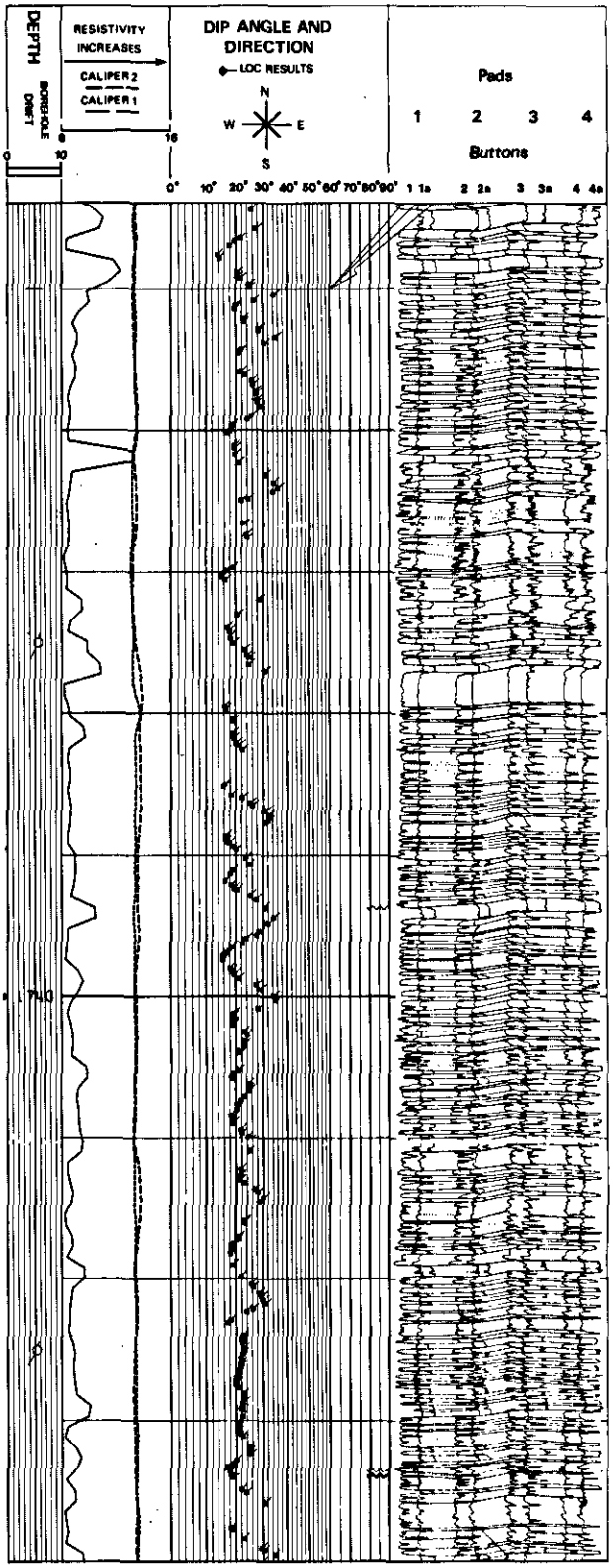

Fig. 6.9-25b. - Example of dipmeter responses in distal turbidites (LOCDIP arrow-plot). This last example shows a lot of blue and red patterns which suggest fan progradation with direction of transport towards NE, and draping of the previous fan by the following one.

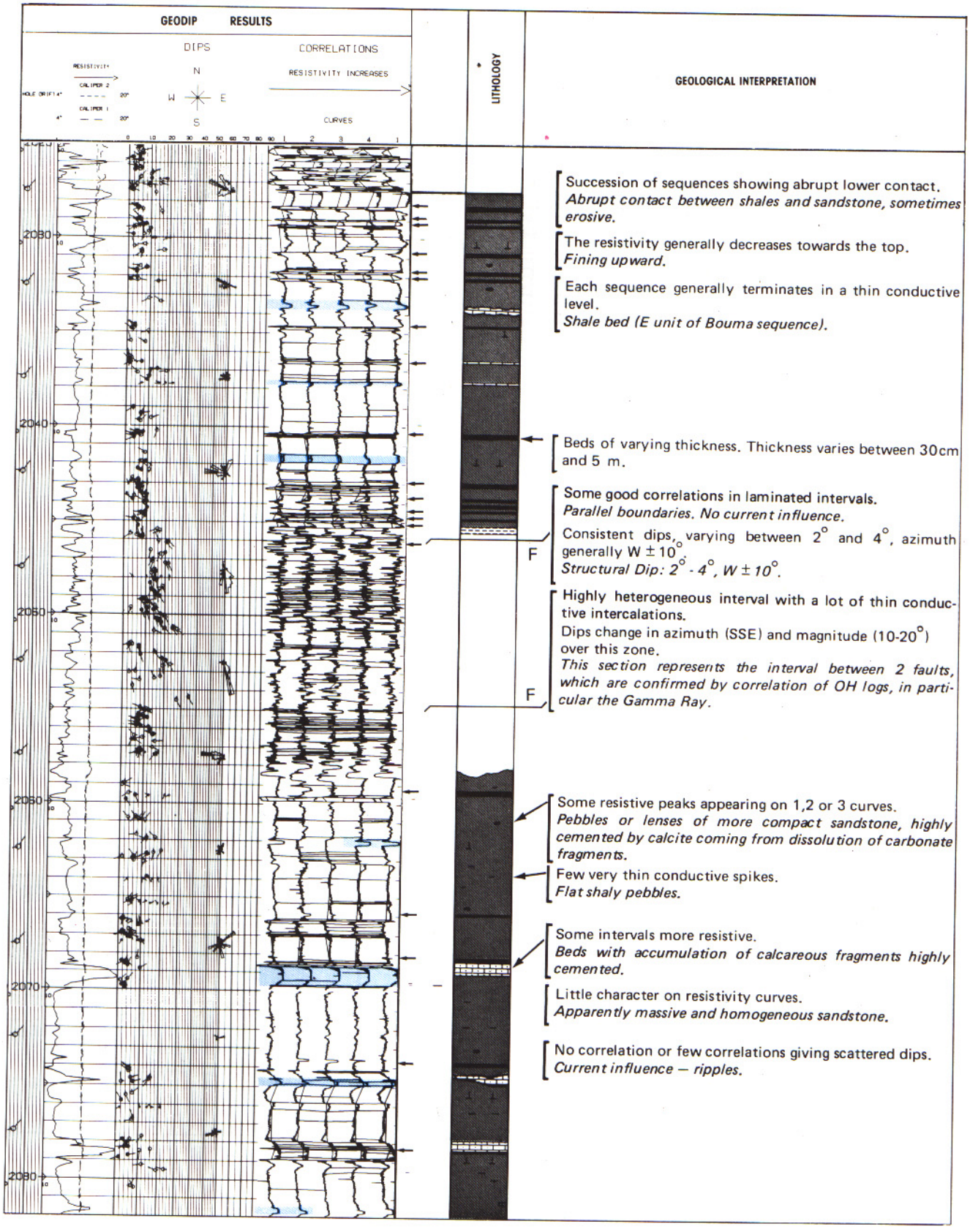

Fig. 6.9-26. - Example of dipmeter response in mass flow deposit (from Schlumberger, Well Evaluation Conference. India, 1983).

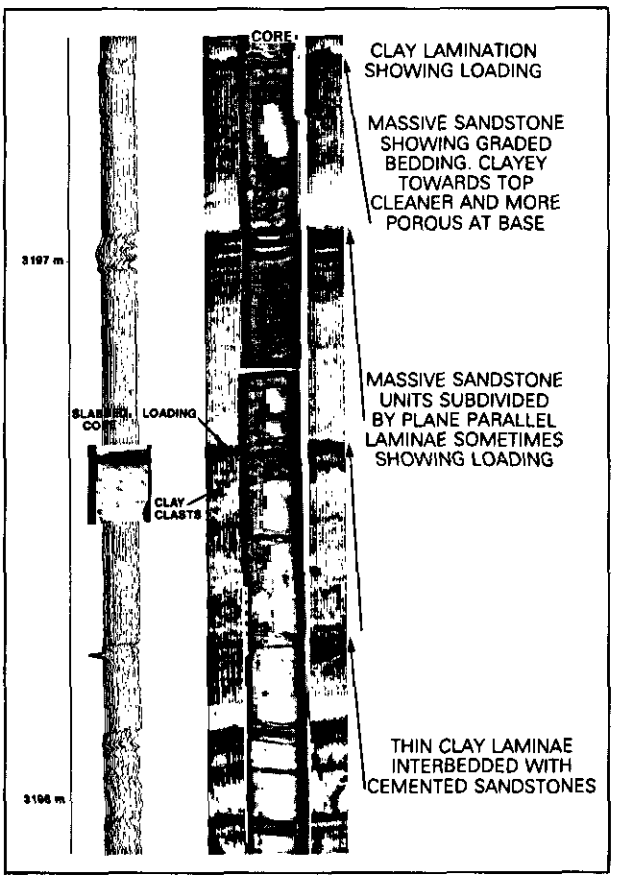

In this kind of environment FMS images enable the recognition of several features such as load casts, clay galls, slumps. Of course, thin laminations, planar or wavy, can easily be observed (Fig. 6.9-27 and 6.9-28).

6.9.3.3. Boundaries

One generally observes abrupt, sharp lower contacts, that are better seen on dipmeter resistivity curves. The lower contact appears to be sometimes non planar (4 dip computation in GEODIP display; wavy symbol in LOCDIP or SYNDIP presentation). The upper boundary may be gradational in the mid fan, or abrupt in the distal fan. Limits between consecutive sequences are not always easy to detect in mass flow deposits.

Comparison of dip patterns with oriented core measurements (Fig. 6.9-29) shows that LOCDIP and CSB give correct answers which can be interpreted.

◀ Fig. 6.9-27. - FMS traces and images showing all the typical features encountered in turbidite deposits : loading features, thin laminations, graded bedding, clay clasts

Fig. 6.9-28. - Very thin laminations detected on FMS traces and images in a distal turbidite ▼

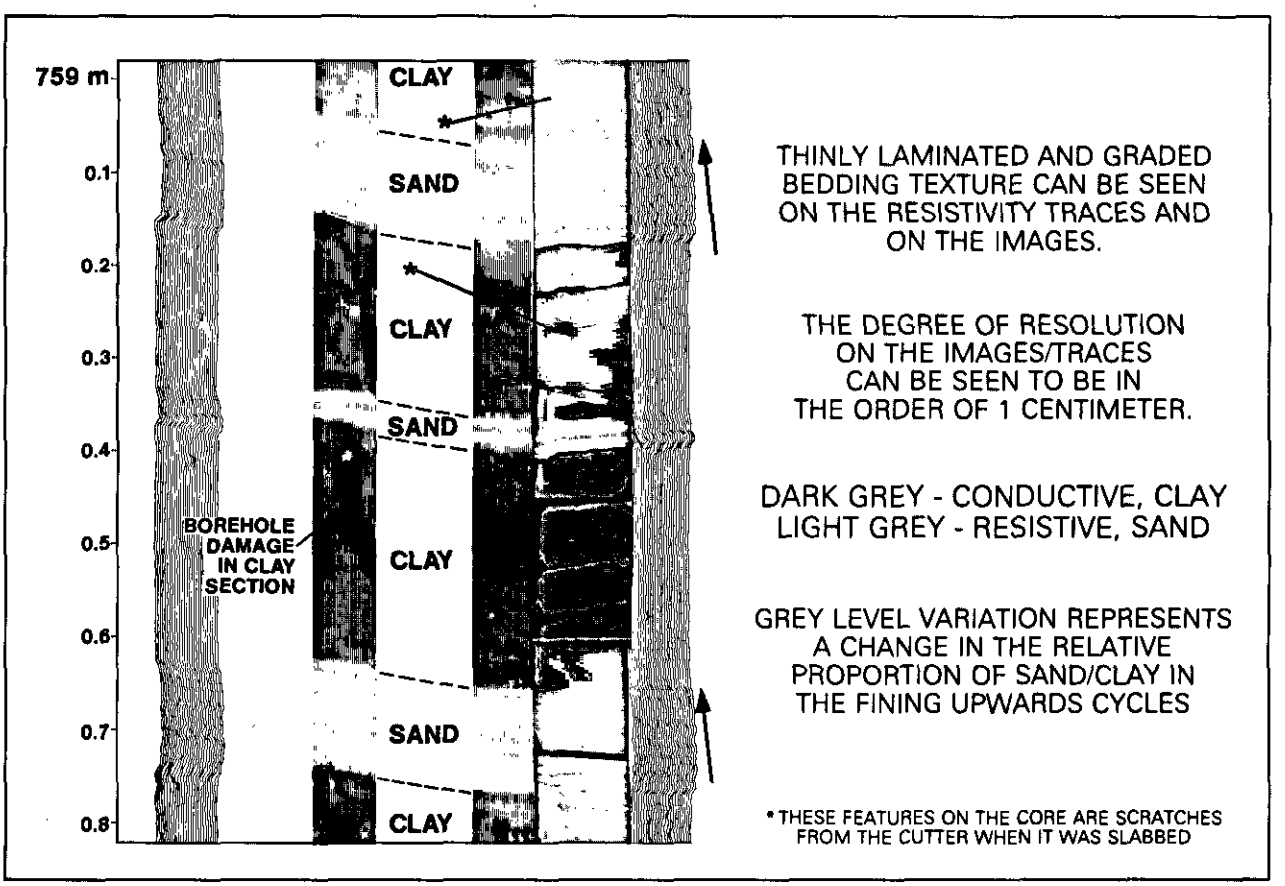

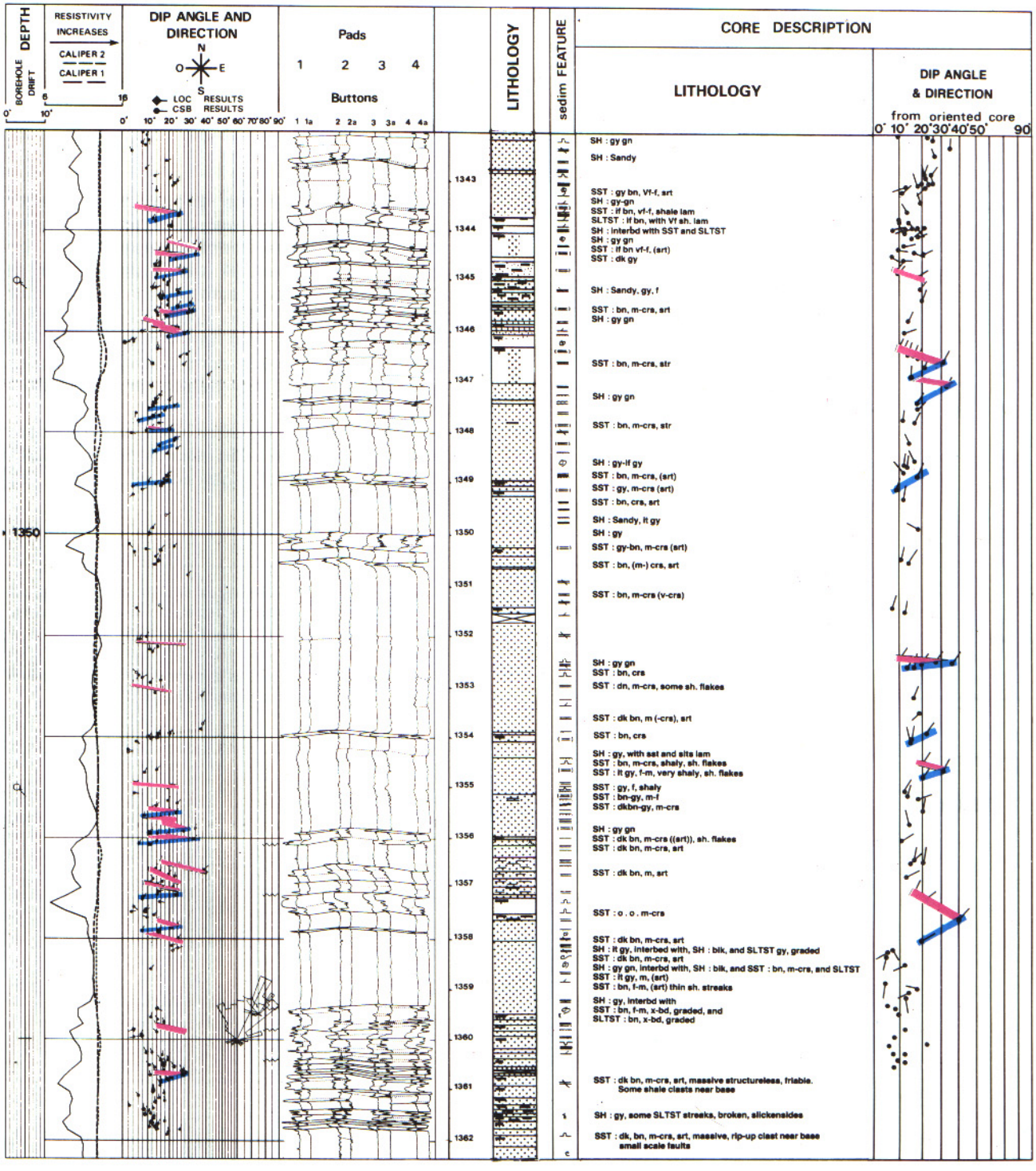

Fig. 6.9-29. - Comparison of LOCDIP and CSB arrow plots with oriented core measurement illustrating the very good fit between the two types of information.

6.9.3.4. **Electro-Sequences**

Numerous similar sequences can be observed (Fig. 6.9-25). Dipmeter resistivity curves (Fig. 6.9-24a and 6.9-30) very often show continuous evolutions which reflect, most of the time, fining upward sequences. But coarsening upward sequences may be present too. Megacoarsening and thickening upward sequences are easily detected (Fig. 6.9-24a and 6.9-31).

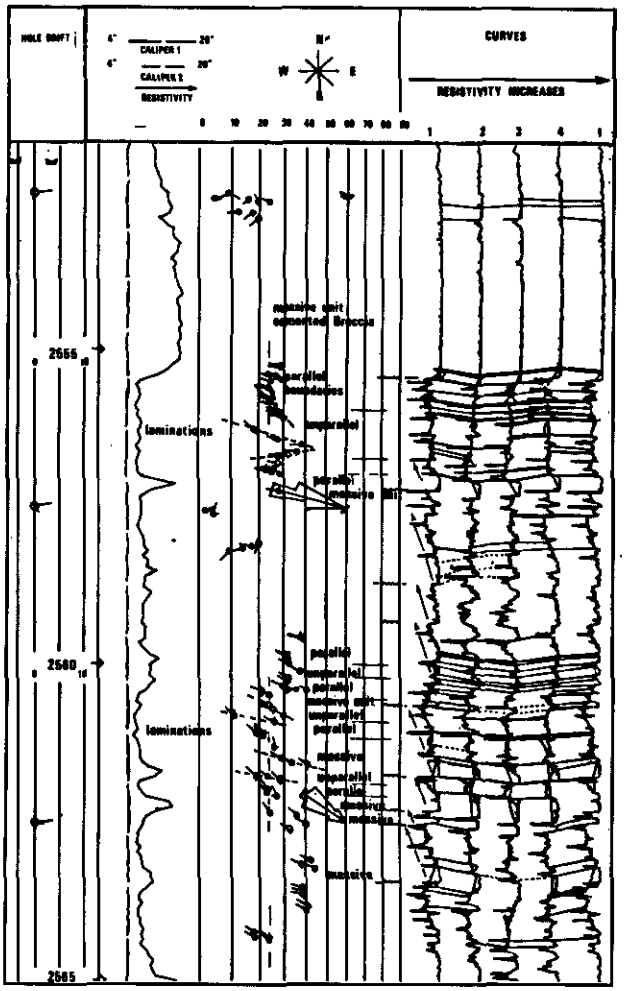

Fig. 6.9-30. - Example of dipmeter response in carbonate turbidite (from Payre & Serra, 1979).

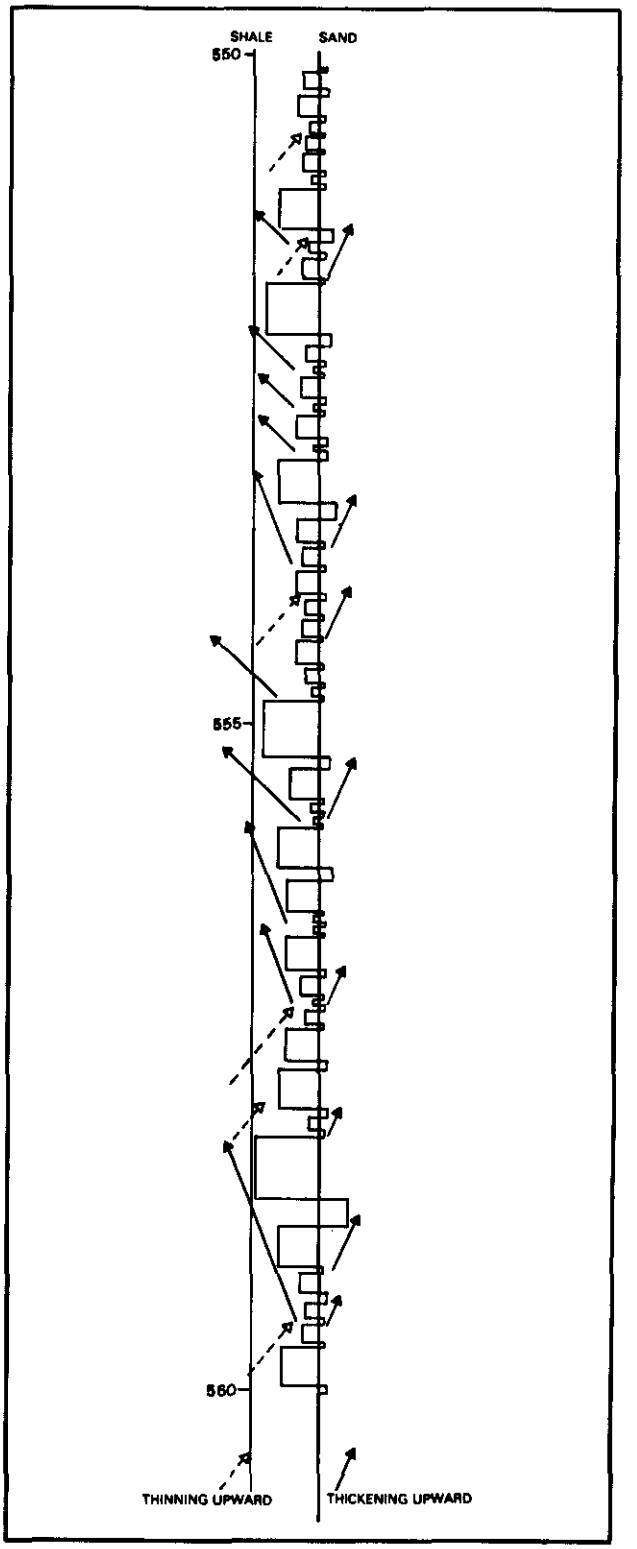

Fig. 6.9-31. - Thickness evolution of shale and sand beds of Fig. ▶ 6.9-26.

6.9.3.5. Thickness

The thickness of individual sequences can vary between a few decimetres to 3-4 metres. A general thickening upward is observed (Fig. 6.9-31 and 6.9-32).

The interval, shown in Fig. 6.9-33, illustrates a megasequence in a turbidite environment. The lower section corresponds to the distal fan with thin sands and shales (the interval is recognized as shaly sands by LITHO). The intermediate section corresponds to the mid fan. One can observe that

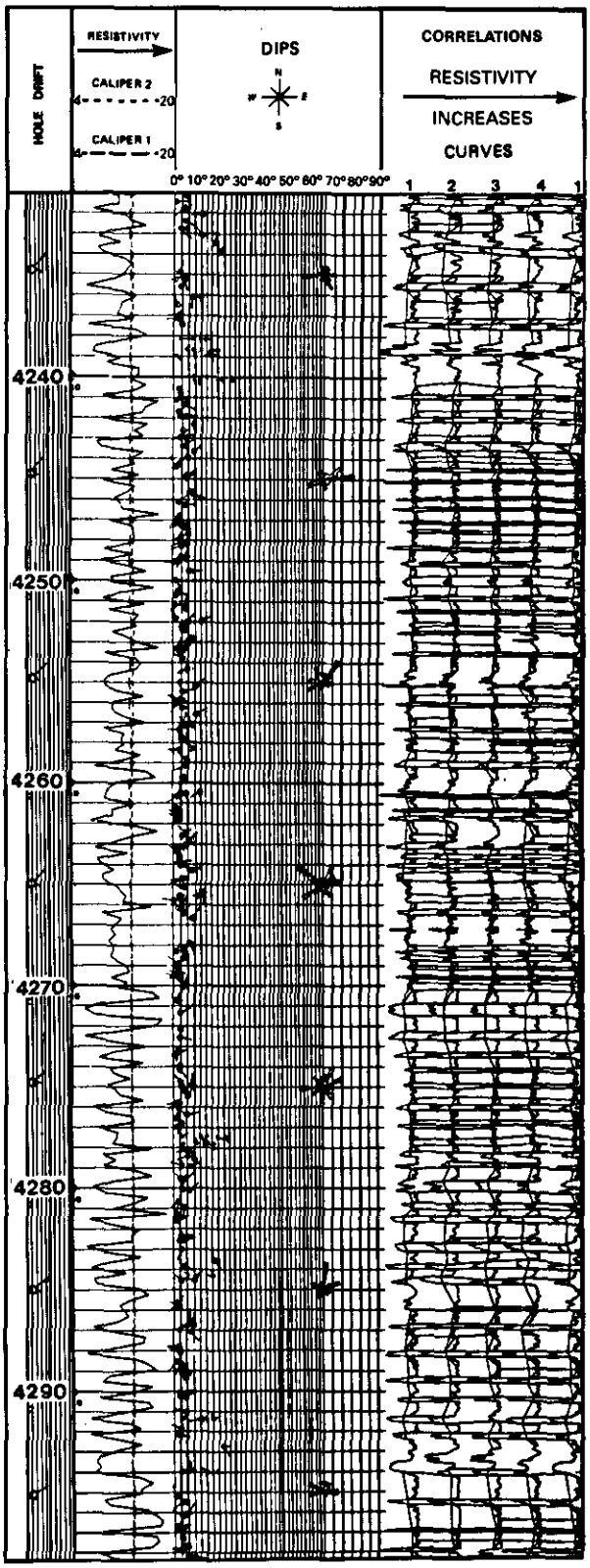

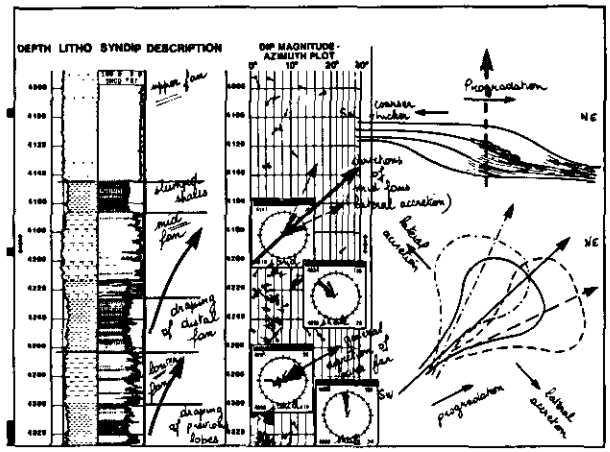

Fig. 6.9-33. - LITHO, SYNDIP, and azimuth frequency plots in a turbidite environment, with their interpretation.

the sands are thicker and "cleaner". The upper section corresponds to the upper fan. The sands are stacked, and constitute a very thick bed. One can conclude that, in this example, the grain size and the bed thickness increase from bottom to top. The interpretation of the azimuth frequency plots in sands and in shales indicates the general direction of transport and the draping of the lobes by shale deposits.

◀ Fig. 6.9-32. - Another example of dipmeter responses in a carbonate turbidite. Observe the rhythmic sedimentation and the thickness of each sequence.

6.10. "DEEP" WATER EVAPORITIC ENVIRONMENT

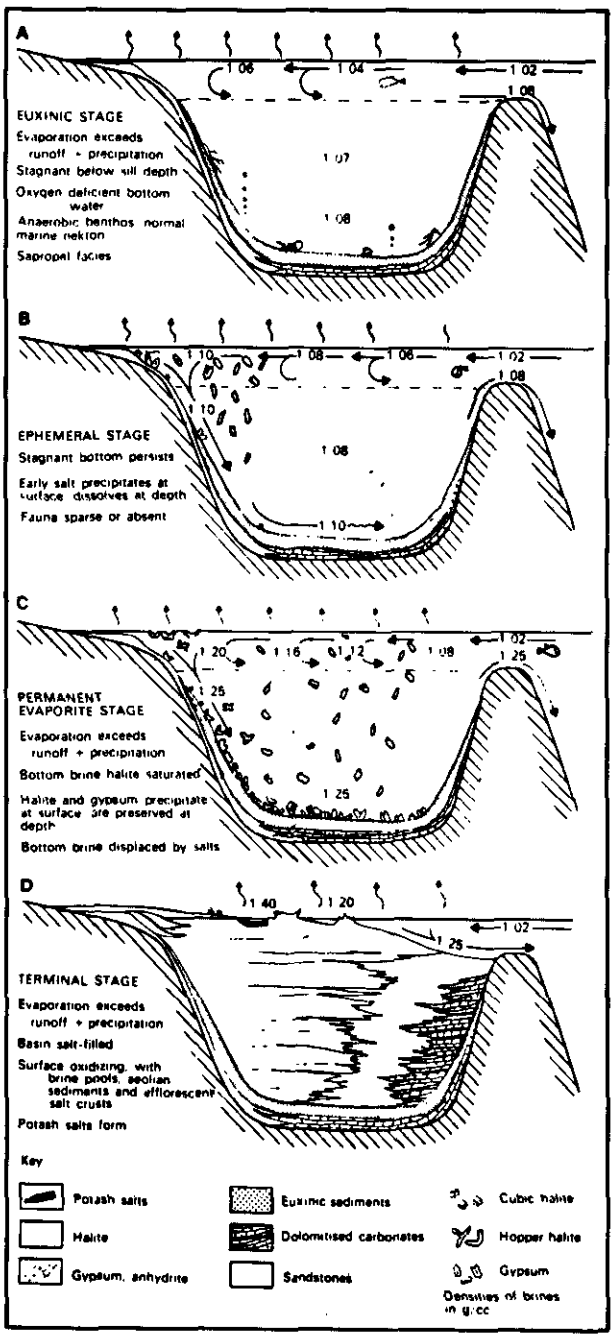

6.10.1. DEFINITION

Environment characterized by precipitation of minerals by evaporation of a body of water (saline brine), and density segregation within this body continuously or periodically maintained by sea water (marine inflow) entering across a shallow barrier into a restricted, enclosed or confined basin, not necessarily very deep (Fig. 6.10-1).

6.10.2. GEOLOGICAL FACIES MODEL

6.10.2.1. Composition

The main minerals present in this environment are sulphates (predominantly gypsum or anhydrite; secondarily polyhalite or langbeinite), chlorures (predominantly halite; secondarily carnallite,

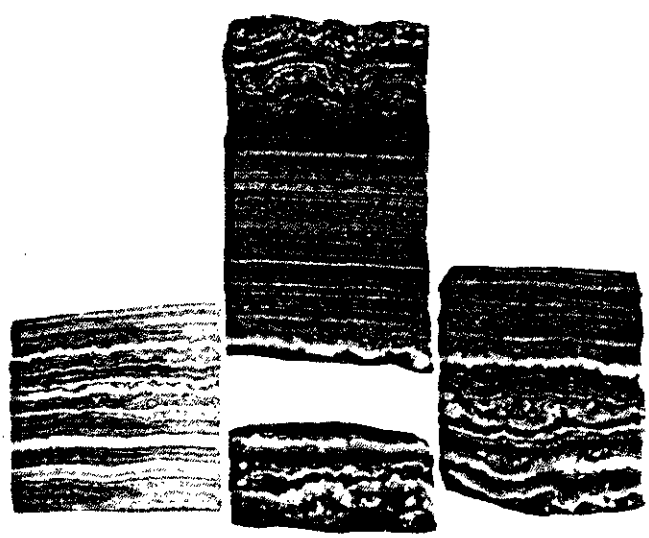

Fig. 6.10-2. - Example of carbonate-anhydrite laminae which can be correlated over several kilometres (from Kendal, 1984).

◀ Fig. 6.10-1. - A model for deep-water evaporite deposition (after Schmalz, 1969).

a

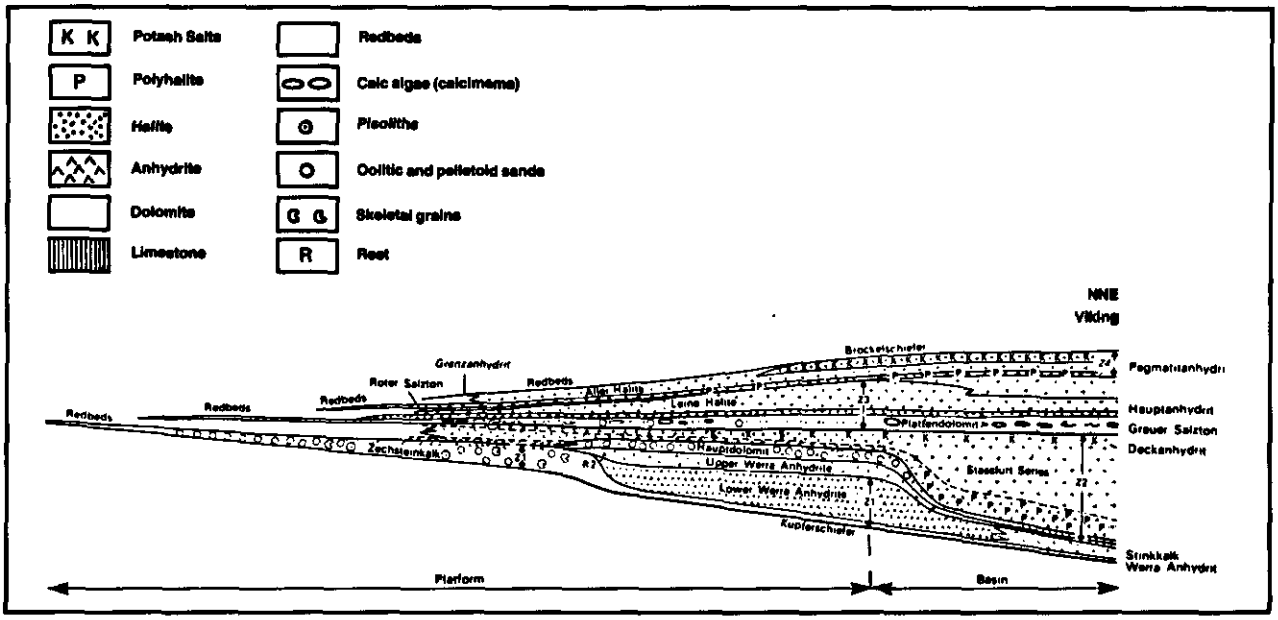

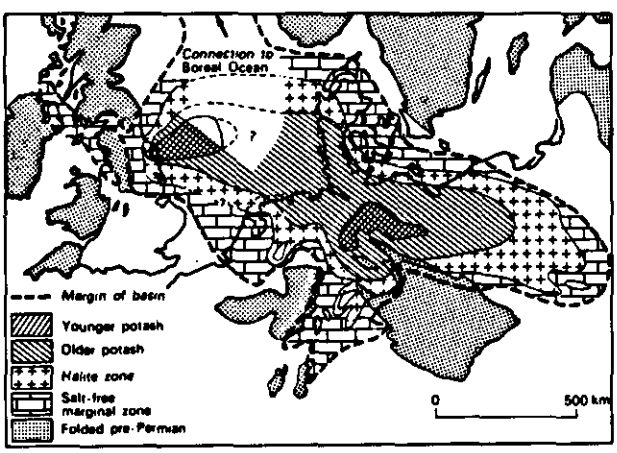

b Fig. 6.10-3. - Generalized cross-section through the Zechstein Basin in North Sea showing the cycles (from Taylor & Colter, 1975) with repartition of the facies (from Borchert & Muir, 1964).

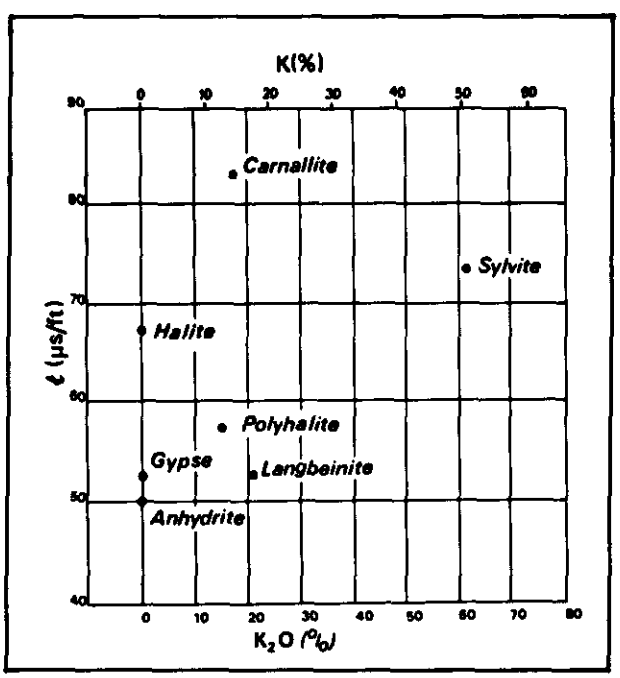

◀ Fig. 6.10-4. - Several crossplots showing the position of the main evaporite minerals.

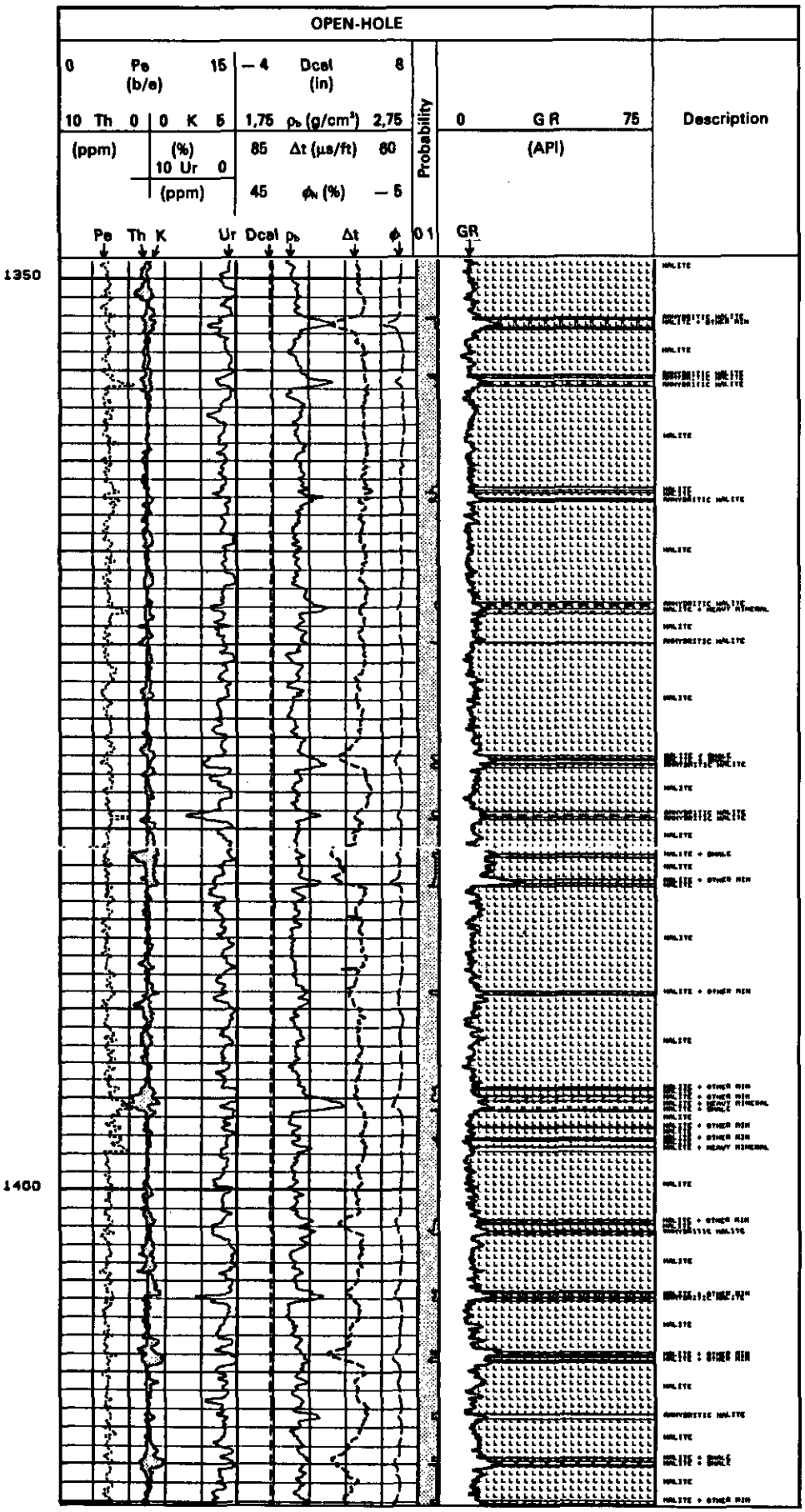

Fig. 6.10-5. - (a) Sonic-gamma ray crossplots showing the main minerals present in the interval (halite, anhydrite and polyhalite) and to compute their percentage. (b) The corresponding composite-log from the Lower Zechstein in North Sea (from Serra, 1980).

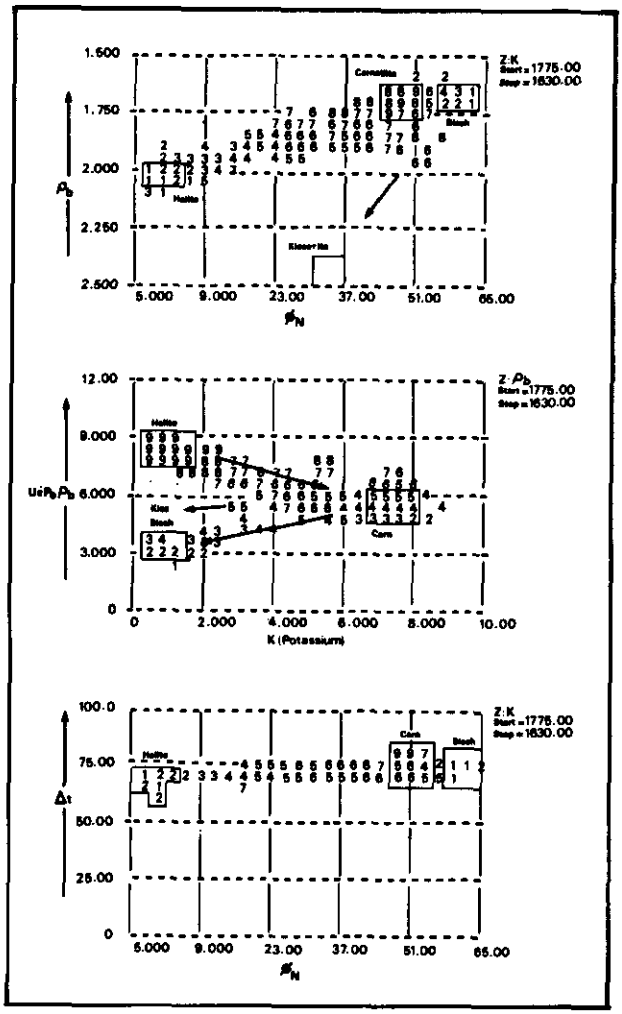

Fig. 6.10-6. - Several crossplots showing the presence of halite, carnallite, bischofite and kieserite in the Upper Zechstein (Z3) in northern Netherlands (from Haile & Blunden, 1984).

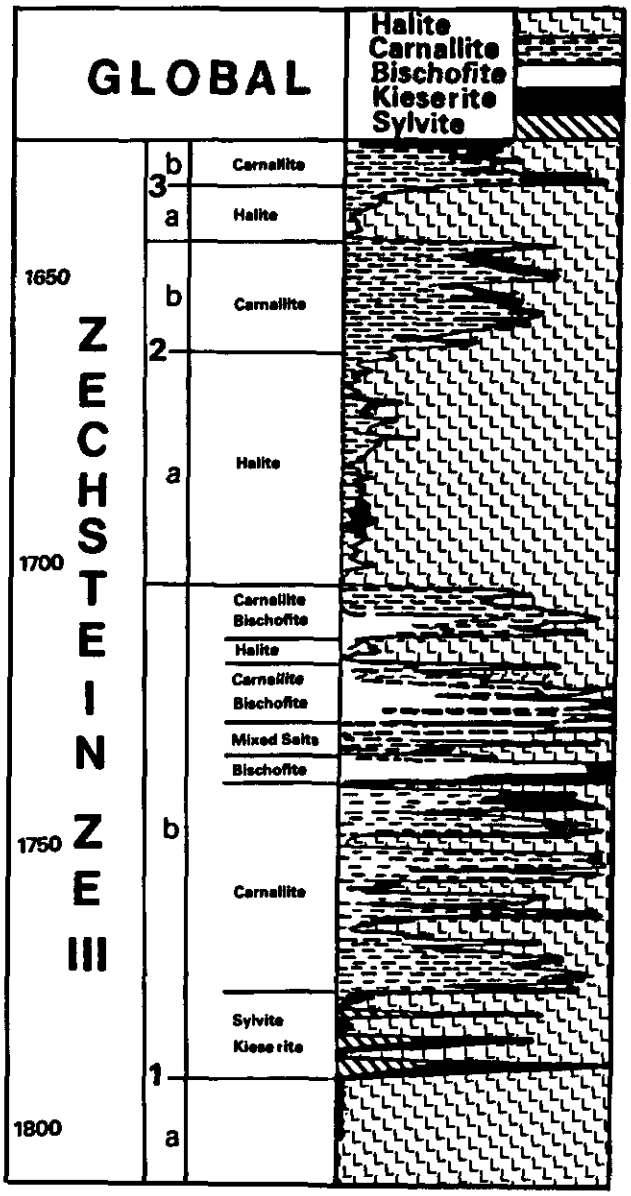

Fig. 6.10-7. - Results of the mineral percentage computation by the GLOBAL program and comparison with core analysis results (from Haile & Blunden, 1984).

sylvite, tachydrite, or bischofite); and sometimes, in small amount, carbonates, clays, organic matter, and quartz.

Original textures and structures are not well known because early diagenetic processes of crystallization, dissolution, re-crystallization occur masking them. However at least three main facies are described for halite : detrital halite, crustal or chevron halite, displacive halite cubes.

6.10.2.2. Sequences

Anhydrite-carbonate laminae are often present in halite (Fig. 6.10-2), as well as clay or silty quartz bands, generating thin cycles or sequences reflecting "regression" or "transgression" conditions (more or less confined, decreased or increased brine-recharge).

On a larger scale cycles have been described (North Sea Zechstein Fig. 6.10-3, Prairie or Muskeg in Saskatchewan-Alberta) starting with dolomites, anhydrite, sometimes with polyhalite, halite and potash deposits as the final precipitates in more localized bitterns. This kind of sequence is toward more restricted or confined conditions.

6.10.2.3. Geometry of Bodies

This type of evaporites can constitute very thick deposits up to 1200 m with very wide extension (Fig. 6.10-3).

6.10.3. WELL-LOG RESPONSES AND CHARACTERISTICS

It is well known that the well-logs can be used to identify the evaporitic minerals. This is due to

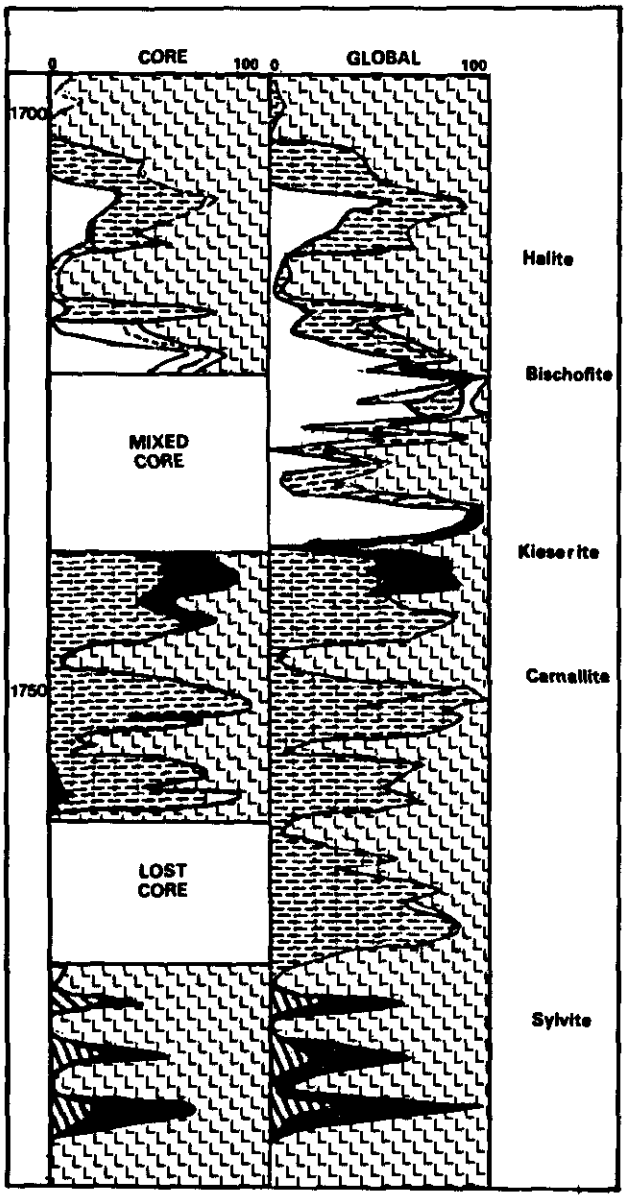

b

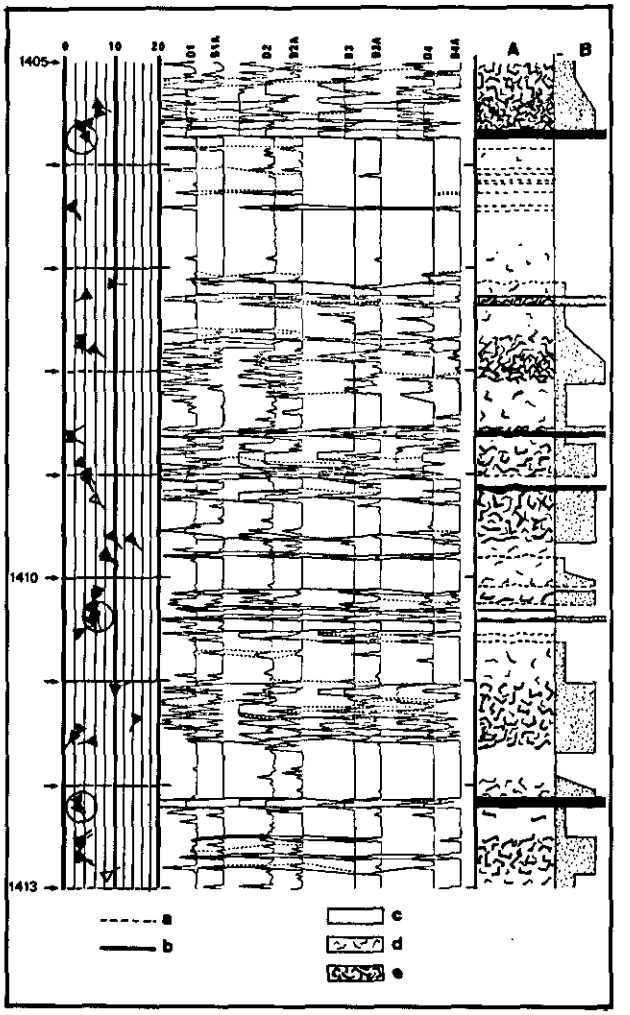

Fig. 6.10-8. - Example of SHDT response in evaporite (mainly halite) illustrating very thin laminations of carbonates-anhydrite mixtures or even shale with organic matter.

the fact that those minerals have the same general composition and are non-porous. Consequently each of them has the same characteristic set of log responses, worldwide, which allows their identification on any type of crossplot.

6.10.3.1. Electro-Lithofacies

The mineral identification can be realized by analysing crossplots (Fig. 6.10-4). If only one pure mineral is present (halite or anhydrite) representative points fall close to the ideal position. If the rock is made up of two or more minerals the representative points will fall on or near the line joining the representative points of the two pure minerals, or inside the surface or volume delimited by the representative points of the minerals present in the mixture (Fig. 6.10-5). A quantitative interpretation using the GLOBAL program can be used to compute the percentage of each mineral (Fig. 6.10-6 and 6.10-7). Potassium evaporites are recognized by their very high radioactivity, or by their potassium content, obtained by a NGS tool. Shale layers are differentiated by their thorium and uranium content.

6.10.3.2. Dipmeter curve Shape and Dip Patterns

The resistivity of the evaporites is very high but with the SHDT tool and the automatic EMEX control the curves show variations with sufficient contrast to reflect some thin laminations of more conductive materials (carbonates, shales), and hence allow computation of dips (Fig. 6.10-8).

6.11. REFERENCES

AGER, D.V. (1974). - Storm deposits in the Jurassic of the Moroccan High. *Palaeogeography, palaeoclimatology, palaeoecology,* **15**, *p. 83-93.*

AHLBRANDT, T.S., & FRYBERGER, S.G. (1982). - Introduction to Eolian Deposits. *In : Scholle, P.A., & Spearing, D. (eds.) : Sandstone Depositional Environments; Amer. Assoc. Petroleum Geol., Mem.* **31.**

ALLEN, J.R.L. (1963). - The classification of cross-stratified units, with notes on their origin. *Sedimentology,* **2**, *p. 93-114.*

ALLEN, J.R.L. (1965). - A review of the origin and characteristics of recent alluvial sediments. *Sedimentology, special issue,* **5**, *p. 89-191.*

ALLEN, J.R.L. (1965). - Late Quaternary Niger Delta and adjacent areas : Sedimentary environments and lithofacies. *Bull. Amer. Assoc. Petroleum Geol.,* **49**, *p. 547-600.*

ALLEN, J.R.L. (1965). - Coastal geomorphology of Eastern Nigeria : beach ridges, barrier island and vegetated tidal flats. *Geol. en Mijnbouw,* **44.**

ALLEN, J.R.L. (1968). - Current Ripples. *North-Holland, Amsterdam.*

ALLEN, J.R.L. (1970). - Sediments of the modern Niger Delta : a summary and review. *In : Deltaic Sedimentation, Modern and Ancient, SEPM special pub.* **15**, *p. 138-151.*

ALLEN, J.R.L. (1970). - Physical Processes of Sedimentation. *Elsevier, New York.*

ALLEN, J.R.L. (1984). - Sedimentary structures. Their character and physical basis. *Developments in sedimentology,* **30**, *Elsevier, Amsterdam.*

Amer. Assoc. Petroleum Geol. (1971). - Origin of Evaporites. *Amer. Assoc. Petroleum Geol., reprint series* **2.**

Amer. Assoc. Petroleum Geol. (1972). - Continental Shelves - Origin and Significance. *Amer. Assoc. Petroleum Geol., reprint series* **3.**

Amer. Assoc. Petroleum Geol. (1973). - Sandstone Reservoirs and Stratigraphic Concepts, I, & II. *Amer. Assoc. Petroleum Geol., reprint series* **7**, **& 8.**

Amer. Assoc. Petroleum Geol. (1974). - Facies and the Reconstruction of Environments. *Amer. Assoc. Petroleum Geol., reprint series* **10.**

Amer. Assoc. Petroleum Geol. (1976). - Modern Deltas. *Amer. Assoc. Petroleum Geol., reprint series* **18.**

Amer. Assoc. Petroleum Geol. (1976). - Ancient Deltas. *Amer. Assoc. Petroleum Geol., reprint series* **19.**

Amer. Assoc. Petroleum Geol. (1976). - Deltaic and shallow marine sandstones : sedimentation, tectonics and petroleum occurrences. *Continuing Education Course Note Series* **2**, *by WEIMER, R.J.*

ASQUITH, G.B. (1979). - Subsurface carbonate depositional models - a concise review. *Penn Well, Tulsa.*

ASQUITH, G.B. (1982). - Basic Well Log Analysis for Geologists. *Amer. Assoc. Petroleum Geol., Methods in Exploration Series.*

BAGNOLD, R.A. (1941). - The physics of blow sand and desert dunes. *Methuen (London).*

BARWIS, J.H. (1978). - Stratigraphy of Kiawah Island beach ridges. *Southeastern Geology,* **19**, *p. 111-122.*

BATES, C.C. (1953). - Rational theory of delta formation. *Bull. Amer. Assoc. Petroleum Geol.,* **37**, *p. 2119-2162.*

BATHURST, R.G.C. (1976). - Carbonate Sediments and their Diagenesis. *Developments in Sedimentology,* **12**, *Elsevier, Amsterdam.*

BEARD, D.C., & WEYL, P.K. (1973). - Influence of texture on porosity and permeability of unconsolidated sand. *Bull. Amer. Assoc. Petroleum Geol.,* **57**, *p. 349-369.*

BERG, R.R. (1968). - Point-bar origin of Fall River Sandstone Reservoirs, Northeastern Wyoming. *Bull. Amer. Assoc. Petroleum Geol.,* **52**, *11, p. 2116-2122.*

BERG, R.R. (1975). - Depositional environment of Upper Cretaceous Sussex Sandstone, House Creek Field, Wyoming. *Bull. Amer. Assoc. Petroleum Geol.,* **59**, *p. 2099-2110.*

BERNARD, H.A., MAJOR, C.F., PARROTT, B.S., & LeBLANC, R.J., Sr., (1970). - Recent sediments of southeast Texas. *Texas Bur. Econ. Geol. Guidebook,* **11**, *Austin, Texas.*

BIGARELLA, J.J. (1972). - Eolian Environments -their Characteristics, Recognition, and Importance. In : *"Recognition of Ancient Sedimentary Environments", edited by RIGBY, J.K., & HAMBLIN, W.K., SEPM, special publication* **16.**

BIGELOW, E.L. (1985). - Making more intelligent use of Log derived Dip measurements. Parts I to V. *The Log Analyst,* **26**, *1 to 5.*

BLATT, H. (1979). - Diagenetic processes in Sandstones. *SEPM, Special Paper* **26.**

BLATT, H., MIDDLETON, G., & MURRAY, R. (1972, 1980). - Origin of Sedimentary Rocks. 1st and 2nd ed. *Prentice-Hall Inc., Englewood Cliffs, New Jersey.*

BLISSENBACH, E. (1954). - Geology of alluvial fans in semiarid regions. *Geol. Soc. America Bull.,* **65,** *p. 175-189.*

BOERSMA, J.R., MEENE, E.A. van de, & TJALSMA, R.C. (1968). - Intricated cross-stratification due to interaction of a mega ripple withits lee-side system of backflow ripple (upper point bar deposits, lower Rhine). *Sedimentology,* **11,** *p. 147-162.*

BOUMA, A.H. (1962). - Sedimentology of some Flysch Deposits. *Elsevier, Amsterdam.*

BOUMA, A.H., & BROUWER, A. (eds) (1964). -Turbidites. *Elsevier, Amsterdam.*

BOUMA, A.H., & HOLLISTER, C.D. (1973). -Deep ocean basin sedimentation. *SEPM, Pacific Section, Short Course, Anaheim.*

BOUMA, A.H., MOORE, G.T., & COLEMAN, J.M. (1978). - Framework, Facies, and Oil-Trapping Characteristics of the Upper Coninental Margin. *Amer. Assoc. Petroleum Geol., Studies in Geology,* **7.**

BOUMA, A.H., BERRYHILL, H.L., BRENNER, R.L., & KNEBEL, H.J. (1982). - Continental Shelf and Epicontinental Seaways. *In : Scholle, P.A., & Spearing, D. (eds.) : Sandstone Depositional Environments; Amer. Assoc. Petroleum Geol., Mem.* **31.**

BORCHERT, H., & MUIR, R.O. (1964). - Salt deposits. The origin, metamorphism and deformation of Evaporites. *Van Nostrand, London.*

BROUSSARD, M.L. (ed.) (1975). - Deltas. Models for exploration. *Houston Geological Society.*

BULL, W.B. (1960). - Geometry of alluvial fans in western Fresno County, California. *Geol. Soc. America Bull.,* **71,** *p. 1836-1837.*

BULL, W.B. (1963). - Alluvial fan deposits in western Fresno County, California. *J. Geol.,* **71,** *p. 243-251.*

BULL, W.B. (1972). - Recognition of Alluvial-Fan Deposits in the Stratigraphic Record. In : *"Recognition of Ancient Sedimentary Environments", edited by RIGBY, J.K., & HAMBLIN, W.K., SEPM, special publication* **16.**

BULL, W.B. (1977). - The alluvial fan environment. *Progress in Physical Geography,* **1,** *p. 224-270.*

BURKE, J.A., CAMPBELL, Jr. R.L., & SCHMIDT, A.W. (1969). - The Litho-Porosity Cross Plot. *SPWLA, 10th Ann. Log. Symp. Trans., paper Y.*

BUSCH, D.A. (1974). - Stratigraphic Traps in Sandstones - Exploration Techniques. *Amer. Assoc. Petroleum Geol., Mem.* **21.**

CAMPBELL, C.V. (1967). - Lamina, Laminaset, Bed and Bedset. *Sedimentology,* **8,** *p. 7-26.*

CAMPBELL, R.L. (1968). - Stratigraphic applications of dipmeter data in Mid-Continent. *Bull. Amer. Assoc. Petroleum Geol.,* **52,** *9, p. 1700-1719.*

CANT D.J. (1982). - Fluvial facies models and their application. *In : Scholle, P.A., & Spearing, D. (eds.) : Sandstone Depositional Environments; Amer. Assoc. Petroleum Geol., Mem.* **31.**

CAROZZI, A.V. (Ed.) (1975). - Sedimentary Rocks. *Benchmark Papers in Geology,* **15,** *Dowden, Hutchinson, & Ross, Inc., Stroudsburg, Pennsylvania.*

CARTER, C.H. (1978). - A regressive barrier and barrier-protected deposit : depositional environment and geographic setting of the Late Tertiary Cohansey Sand. *Jour. sediment. Petrology,* **48,** *p. 933-950.*

Chambre Syndicale de la Recherche et de la Production du Pétrole et du Gaz naturel (1966). -Essai de normalisation, & caractérisation des principales structures sédimentaires. *Ed. Technip, Paris.*

Chambre Syndicale de la Recherche et de la Production du Pétrole et du Gaz naturel (1974). -Méthodes modernes de géologie de terrain. 1 -Principes d'analyses sédimentologiques. *Ed. Technip, Paris.*

CHAUVEL, Y. (1984). - Applications of the SHDT stratigraphic high resolution dipmeter to the study of depositional environments. *SPWLA, 25th Ann. Log. Symp. Trans., New Orleans.*

CHILINGARIAN, G.V., & WOLF, K.H. (Eds) (1975). - Compaction of Coarse-Grained Sediments. *Developments in Sedimentology,* **18A, & 18B,** *Elsevier, Amsterdam.*

CHOQUETTE, P.W., & PRAY, L.C. (1970). -Geological nomenclature and classification of porosity in sedimentary carbonates. *Bull. Amer. Assoc. Petroleum Geol.,* **54,** *p. 207-250.*

CLARKE, F.W., & WASHINGTON, H.S. (1924). -The composition of the Earth's Crust. *U. S. Geol. Survey, Profess. Paper 127.*

CLAVIER, C., & RUST, D.H. (1976). - MID-PLOT : a new Lithology Technique. *The Log Analyst, 17, 6.*

CLIFTON, H.E. (1982). - Estuarine Deposits. *In : Scholle, P.A., & Spearing, D. (eds.) : Sandstone Depositional Environments; Amer. Assoc. Petroleum Geol., Mem.* **31.**

COLACICCHI, R., PASSERI, L., & PIALLI, G. (1975). - Evidences of tidal environment deposition in the Calcare Massiccio Formation (Central Apennines-Lower Lias. In : *Tidal Deposits : a Casebook of Recent Examples and Fossil Counterparts (Ed. by GINSBURG, R.N.), p. 345-353. Springer, Berlin.*

COLEMAN, J.M., & GAGLIANO, S.M. (1964). -Cyclic Sedimentation in the Mississippi river deltaic plain. *Gulf-Coast Ass. Geol. Socs. Trans.,* **14,** *p. 67-80.*

COLEMAN, J.M., GAGLIANO, S.M., & SMITH, W.G. (1970). - Sedimentation in a Malaysian high tide tropical delta. *In : Deltaic Sedimentation Modern and Ancient. (Ed. by Morgan, J.P.) SEPM, special publ.* **15.**

COLEMAN, J.M., & PRIOR, D.B. (1980). - Deltaic Sand Bodies. *Amer. Assoc. Petroleum Geol., Continuing Education Course Note Series* **15.**

COLEMAN, J.M., & PRIOR, D.B. (1982). - Deltaic Environments. *In : Scholle, P.A., & Spearing, D. (eds.) : Sandstone Depositional Environments; Amer. Assoc. Petroleum Geol., Mem.* **31.**

COLEMAN, J.M., & WRIGHT, L.D. (1975). -Modern river deltas : variability of processes and sand bodies. *In : Delats, Models for Exploration. (Ed. by Broussard, M.L.), Houston Geol. Soc., p. 99-149.*

COLLINSON J.D., & THOMPSON, D.B. (1982). -Sedimentary Structures. *George Allen & Unwin Publ. Ltd., London.*

CONYBEARE, C.E.B. (1976). - Geomorphology of oil and gas Fields in sandstone bodies. *Elsevier, Amsterdam.*

COOK, H.E., & ENOS, P. (eds) (1977). - Deep-Water Carbonate Environments. *SEPM, special publication* **25.**

COOK, H.E., & MULLINS, H.T. (1983). - Basin Margin Environment. *In : Scholle, P.A. et al.,* (eds.) : Carbonate Depositional Environments; Amer. Assoc. Petroleum Geol., Mem. **33.**

CROSBY, E.J. (1972). - Classification of Sedimentary Environments. In : *"Recognition of Ancient Sedimentary Environments", edited by RIGBY, J.K., & HAMBLIN, W.K., SEPM, special publication* **16.**

CURRY, W.H., & CURRY, W.H. III (1972). - South Glenrock Oilfield, Wyoming : Prediscovery, Thinking and Post-Discovery Description. *In Stratigraphic Oil and Gas Fields - Classification, Exploration Methods, and Case Histories, Amer. Assoc. Petroleum Geol., Memoir* **16,** *p. 415-427.*

CURTIS, D.M. (1970). - Miocene deltaic sedimentation, Louisiana Gulf Coast. In : *Deltaic sedimentation modern and ancient (Ed. by MORGAN, J.P. & SHAVER, R.H.) SEPM, special pub.* **15.**

CURTIS, D.M. (1976). - Sedimentary Processes : Diagenesis. *SEPM, Reprint series* **1.**

DAPPLES, E.C. (1967). - Silica as an Agent in Diagenesis. In : *Diagenesis in Sediments, LARSEN, G., & CHILINGAR, C.V., Eds, p. 91-125, Elsevier,Amsterdam.*

DAPPLES, E.C. (1972). - Some concepts of Cementation and Lithification of Sandstones. *Bull. Amer. Assoc. Petroleum Geol.,* **56,** *p. 3-26.*

DAVIES, D.K., ETHRIDGE, F.G., & BERG, R.R. (1971). - Recognition of barrier environments. *Bull. Amer. Assoc. Petroleum Geol.,* **55,** *p. 550-566.*

DAVIS, R.A., & ETHINGTON, R.L. (eds) (1976). -Beach and Nearshore Sedimentation. *SEPM, special publication* **24.**

DAVIS, R.A. Jr., FOX, W.T., HAYES, M.O., & BOOTHROYD, J.C. (1972). - Comparison of ridge-and-runnel systems in tidal and non-tidal environments. *J. sediment. Petrol.,* **32,** *p. 413-421.*

DEAN, W.E., & FOUCH, T.D. (1983). - Lacustrine Environment. *In : Scholle, P.A. et al.,* (eds.) : Carbonate Depositional Environments; Amer. Assoc. Petroleum Geol., Mem. **33.**

DELFINER, P., PEYRET, O., & SERRA, O. (1984). - Automatic determination of Lithology from Well Logs. *59th Ann. Techn. Conf. SPE of AIME, Houston, Texas; paper n° SPE 13290.*

DELHOMME, J.P., & SERRA, O. (1984). - Dipmeter-derived Logs for Sedimentological Analysis. *SPWLA, 9th Europ. Intern. Format. Eval. Trans., paper 50.*

DICKEY, P.A. (1979). - Petroleum Development Geology. *Petroleum Publishing Co., Tulsa.*

DICKINSON, K.A., BERRYHILL, H.L., Jr., & HOLMES, C.W. (1972). - Criteria for Recognizing Ancient Barrier Coastlines. In : *"Recognition of Ancient Sedimentary Environments", edited by RIGBY, J.K., & HAMBLIN, W.K., SEPM, special publication* **16.**

DICKINSON, W.R. (ed) (1974). - Tectonics and Sedimentation. *SEPM, special publication* **22.**

DOEGLAS, D.J. (1962). - The structure of sedimentary deposits of braided rivers. *Sedimentology,* **1,** *p. 167-190.*

DONALDSON, A.C., MARTIN, R.H., & KANES, W.H. (1970). - Holocene Guadalupe delta of Texas Gulf Coast. *In : Deltaic Sedimentation Modern and Ancient. (Ed. by Morgan, J.P.) SEPM, special publ.* **15.**

DOTT, R.H. (1963). - Dynamics of gravity depositional processes. *Bull. Amer. Assoc. Petroleum Geol.,* **47,** *p. 104-108.*

DOTT, R.H. Jr., & SHAVER, R.H. (eds) (1974). -Modern and Ancient Geosynclinal Sedimentation. *SEPM, special publication* **19.**

DUFF, P. McL. D., HALLAM, A., & WALTON, E.K. (1967). - Cyclic Sedimentation. *Developments in Sedimentology,* **10,** *Elsevier, Amsterdam.*

DUNHAM, R.J. (1962). - Classification of Carbonate Rocks according to Depositional Texture. *Amer. Assoc. Petroleum Geol., Mem.* **1,** *p. 108-121.*

DZULYNSKI, S., & WALTON, E.K. (1965). -Sedimentary Features of Flysch and Greywackes. *Developments in Sedimentology,* **7,** *Elsevier, Amsterdam.*

EASTERBROOK, D.J. (1982). - Glacial sediments. In : *Sandstone Depositional Environments (Ed. by SCHOLLE, P.A., & SPEARING, D.) Amer. Assoc. Petroleum Geol.*

EDMUNDSON, H., & RAYMER, L.L. (1979). -Radioactive parameters for Common Minerals. *SPWLA, 20th Ann. Log. Symp. Trans., paper O.*

EDWARDS, M.B. (1978). - Glacial Environments. *In : Sedimentary Environments and Facies. (Ed. by Reading, H.G.) Blackwell Scientific Publications, Oxford.*

EINSELE, G. (1963). - Über Art und Richtung der Sedimentation im klastischen rheinischen Oberdevon (Famenne). *Abhandl. Hess. Landesamtes Bodenforsch,* **43,** *60.*

ELLIOTT, T. (1974). - Abandonment facies of high-constructive lobate deltas, with an example from the Yoredale Series. *Proc. Geol. Assoc.*, **85**, *p. 359-366.*

ELLIOTT, T. (1974). - Interdistributary bay sequences and their genesis. *Sedimentology*, **21**, *p. 611-622.*

ELLIOTT, T. (1978). - Clastic Shorelines. *In : Sedimentary Environments and Facies. (Ed. by Reading, H.G.) Blackwell Scientific Publications, Oxford.*

ELLIOTT, T. (1978). - Deltas. *In : Sedimentary Environments and Facies. (Ed. by Reading, H.G.) Blackwell Scientific Publications, Oxford.*

ENOS, P. (1983). - Shelf Environment. *In : Scholle, P.A. et al., (eds.) : Carbonate Depositional Environments; Amer. Assoc. Petroleum Geol., Mem.* **33.**

ENOS, P., & MOORE, C.H. (1983). - Fore-reef Slope Environment. *In : Scholle, P.A. et al., (eds.) : Carbonate Depositional Environments; Amer. Assoc. Petroleum Geol., Mem.* **33.**

ETHRIDGE, F.G., & FLORES, R.M. (eds) (1981). -Recent and Ancient Nonmarine Depositional Environments : Models for Exploration. *SEPM, special publication* **31.**

FAIRBRIDGE, R.W. (1967). - Phases of Diagenesis and Authigenesis. In : *Diagenesis in Sediments, LARSEN, G., & CHILINGAR, G.V., Eds, p. 19-89, Elsevier, Amsterdam.*

FERM, J.C. (1970). - Allegheny deltaic deposits. *In : Deltaic Sedimentation Modern and Ancient. (Ed. by Morgan, J.P.) SEPM special publ.* **15.**

FISCHER, A.G. (1964). - The Lofer cyclothems of the Alpine Triassic. *In : Symposium on Cyclic Sedimentation (Ed. by MERRIAM, D.F.), p. 107-149. Bull. geol. Surv. Kansas,* **169.**

FISCHER, A.G. (1975). - Tidal deposits, Dachstein Limestone of the North Alpine Triassic. In : *Tidal Deposits : a casebook of recent examples and fossils counterparts (Ed. by GINSBURG, R.N.), p. 235-242, Springer, Berlin.*

FISHER, W.L., & McGOWEN, J.H. (1969). -Depositional systems in Wilcox Group (Eocene) of Texas and their Relation to Occurrence of Oil and Gas. *Bull. Amer. Assoc. Petroleum Geol.*, **53**, *p. 30-54.*

FISHER, W.L., BROWN, L.F., SCOTT, A.J., & McGOWEN, J.H. (1969). -Delta systems in the exploration for oil and gas. *Bur. econ. Geol., Univ. Texas, Austin.*

FISHER, J.H. (ed.) (1977). - Reefs and Evaporites - Concepts and Depositional Models. *Amer. Assoc. Petroleum Geol., Studies in Geology* **5.**

FLINT, R.F. (1971). - Glacial and Quaternary Geology. *John Wiley & Sons, New York.*

FOLK, R.L. (1959). - Practical Petrographic Classification of Limestones. *Bull. Amer. Assoc. Petroleum Geol.*, **43**, *p. 1-38.*

FOLK, R.L. (1962). - Spectral subdivision of Limestone Types. *Amer. Assoc. Petroleum Geol., Mem.* **1**, *p. 64-84.*

FONS, L. Sr. (1969). - Geological application of well logs. *SPWLA, 10th Ann. Log. Symp. Trans.*

FOUCH, T.D., & DEAN, W.E. (1982). - Lacustrine Environments. *In : Scholle, P.A., & Spearing, D. (eds.) : Sandstone Depositional Environments; Amer. Assoc. Petroleum Geol., Mem.* **31.**

FRASER, H.J. (1935). - Experimental study of porosity and permeability of clastic sediments. *J. Geol.*, **43**, *p. 910-1010.*

FRIEDMAN, G.M. (1964). - Early diagenesis and lithification in carbonate sediments. *J. sediment. Petrol.*, **34**, *p. 777-813.*

FRIEDMAN, G.M. (ed.) (1969). - Depositional Environments in Carbonate rocks. *Soc. econ. Paleont. Mineral., special publication* **14.**

FRIEDMAN, G.M., & ALI, S.A. (1981). - Diagenesis of Carbonate Rocks : Cement-Porosity Relationships. *SEPM Reprint series* **10.**

FRIEDMAN, G.M., & SANDERS, J.E. (1978). -Principles of Sedimentology. *John Wiley, & Sons, New York.*

FROST, S.H., WEISS, M.P. & SAUNDERS, J.B. (1977). - Reefs and related Carbonates - Ecology and Sedimentology. *Amer. Assoc. Petroleum Geol., Studies in Geology* **4.**

FRYBERGER, S.G. (1979). - Dune forms and wind regimes. In : *A Study of Global Sand Seas (Ed. by McKEE, E.D.), U.S. Geol. Surv. Prof. Paper 1052.*

FRYBERGER, S.G. (1979). - Eolian-Fluviatile (continental) origin of ancient stratigraphic trap for petroleum in Weber Sandstone, Rangely oil field, Colorado. *Mountain Geologist*, **16**, *p. 1-36.*

FÜCHTBAUER, H. (1967). - Influence of different types of diagenesis on sandstone porosity. *Proc. 7th Wld Petrol. Cong., Mexico, p. 353-369.*

GALLOWAY, W.E. (1975). - Process framework for describing the morphologic and stratigraphic evolution of deltaic depositional systems.

GALLOWAY, W.E. (1977). - Catahoula formation of the Texas Coastal Plain : Depositional systems, composition, structural developement, ground-waterflow history, and uranium distribution. Bur. Geol. Univ. Texas, Austin, Rept. Invest. N° 87.

GALLOWAY, W.E. (1981). - Depositional architecture of Cenozoic Gulf Coastal Plain Fluvial Systems. *SEPM, special publication* **31.**

GALLOWAY, W.E, & BROWN, L.F. Jr. (1973). -Depositional systems and shelf-slope relations on cratonic basin margin, Uppermost Pennsylvanian of north-central Texas. *Bull. Amer. Assoc. Petroleum Geol.*, **57**, *p. 1185-1218.*

GALLOWAY, W.E., & HOBDAY, D.K. (1983). -Terrigenous Clastic Depositional Systems. *Springer, New York.*

GARRELS, R.M., & MACKENSIE, F.T. (1971). -Evolution of Sedimentary rocks. *Norton, W.W., & Co, New York.*

GARY, M., McAFEE, R.Jr., & WOLF, C.L. (1972). - Glossary of Geology. *Amer. Geol. Institute, Washington, D.C.*

GERSIB, G.A., & McCABE, P.J. (1981). - Continental coal-bearing sediments of the Porthood Formation (Carboniferous), Cape Linzee, Nova Scotia, Canada. *SEPM, special publication* **31**, *p. 95-108.* GIGNOUX, M. (1950). - Géologie stratigraphique. *Masson, Paris.*

GILREATH, J.A., & MARICELLI, J.J. (1964). -Detailed Stratigraphic Control through dip Computations. *Bull. Amer. Assoc. Petroleum Geol.*, **48**, *12, p. 1904-1910.*

GILREATH, J.A., HEALY, J.S., & YELVERTON, J.N. (1969). - Depositional Environments Defined by Dipmeter Interpretation. *Gulf Coast Assoc. Geol. Soc. Trans.*, **19**, *p. 101-111.*

GILREATH, J.A., & STEPHENS, R.W. (1971). -Distributary Front Deposits Interpreted from Dipmeter Patterns. *Gulf Coast Assoc. Geol. Soc. Trans.*, **21**, *p. 233-243.*

GILREATH, J.A., & STEPHENS, R.W. (1975). -Interpretation of Log Responses in a Deltaic Environment. *Amer. Assoc. Petroleum Geol. Marine Geology Workshop, Dallas, Texas.*

GINSBURG, R.A. (1975). - Tidal Deposits. *Springer, New York.*

GLENNIE, K.W. (1970). - Desert Sedimentary Environments. *Developments in Sedimentology*, **14**, *Elsevier, Amsterdam.*

GLENNIE, K.W. (1972). - Permian Rotliegendes of Northwest Europe interpreted in light of Modern Desert Sedimentation Studies. *Bull. Amer Assoc. Petroleum Geol.*, **56**, *6.*

GOETZ, J.I., PRINS, W.J., & LOGAR, J.F. (1977). - Reservoir Delineation by Wireline Techniques. *paper presented at 6th Ann. Conv. Indonesia Petroleum Assoc., Jakarta, May 1977.*

GORSLINE, D.S., & EMERY, K.O. (1959). -Turbidity-current deposits in San Pedro and Santa Monica basins off southern California. *Bull. geol. Soc. Amer.*, **70**, *p. 279-290.*

GRABAU, A.W. (1903). - Paleozoic coral reefs. *Bull. Geol. Soc. Amer.*, **14**, *p. 337-352.*

GRANDVILLE, B.F. de la (1981). - Appraisal and Development of a Structural and Stratigraphic Trap Oil Field with Reservoirs in Glacial to Periglacial Clastics. *Middle East Oil Technical Conference of SPE, Bahrain, March 9-12, 1981.*

GRIM, R.E. (1958). - Concept of diagenesis in argillaceous sediments. *Bull. Amer. Assoc. Petroleum Geol.*, **42**, *p. 246-253.*

GRIM, R.E. (1968). - Clay Mineralogy. 2nd ed. *McGraw Hill, New York.*

HAILE, P.M., & BLUNDEN, H.A. (1984). - Zechstein Magnesium rich Evaporite Deposits of northern Netherlands and their volumetric analysis by GLOBAL. *SAID-SPWLA, 9th International Log Symp. Trans., Paris, paper 37.*

HALLEY, R.B., HARRIS, P.M., & HINE, A.C. (1983). - Bank Margin Environment. *In : Scholle, P.A. et al., (eds.) : Carbonate Depositional Environments; Amer. Assoc. Petroleum Geol., Mem.* **33.**

HECKEL, P.H. (1972). - Recognition of Ancient Shallow Marine Environments. In : *"Recognition of Ancient Sedimentary Environments", edited by RIGBY, J.K., & HAMBLIN, W.K., SEPM, special publication* **16.**

HEPP, V., & DUMESTRE, A.C. (1975). - CLUSTER - A method for selecting the most probable dip results from dipmeter survey. *SPE of AIME, 50th Ann. Fall Mtg., Dallas, Paper SPE 5543.*

HOBSON, G.D., & TIRATSOO, E.N. (1975). -Introduction to Petroleum Geology. *Scientific Press Ltd, Beaconsfield, England.*

HOOKE, R. LEB. (1967). - Processes on arid-region alluvial fans. *J. Geol.*, **75**, *p. 438-460.*

HORNE, J.C., & FERM, J.S. (1978). - Carboniferous depositional environments : eastern Kentucky and southern West Virginia. *Department of Geology, University of South Carolina.*

HOUBOLT, J.J.H.C. (1968). - Recent sediments in the southern bight of the North Sea. *Geol. Mijnb.*, **47**, *p. 245-273.*

HOWELL, D.G., & NORMARK, W.R. (1982). -Sedimentology of Submarine Fans. *In : Scholle, P.A., & Spearing, D. (eds.) : Sandstone Depositional Environments; Amer. Assoc. Petroleum Geol., Mem.* **31.**

HUTTON, J. (1788). - Theory of the earth. *Royal Soc. Edinburgh, Trans.*, **1**, *p. 209-304.*

INDEN, R.F., & MOORE, C.H. (1983). - Beach Environment. *In : Scholle, P.A. et al.,* (eds.) : Carbonate Depositional Environments; Amer. Assoc. Petroleum Geol., Mem. **33.**

INGRAM, R.L. (1954). - Terminology for the thickness of stratification and parting units in sedimentary rocks. *Bull. Geol. Soc. Amer.*, **65**, *p. 937-938.*

JAMES, N.P. (1979). - Shallowing-upward Sequences in Carbonates. *In : Facies Models. (Ed. by Walker, R.G.). Geoscience Canada Reprint Series 1.*

JAMES, N.P. (1979). - Reefs. *In : Facies Models. (Ed. by Walker, R.G.). Geoscience Canada Reprint Series 1.*

JAMES, N.P. (1983). - Reef Environment. *In : Scholle, P.A. et al., (eds.) : Carbonate Depositional Environments; Amer. Assoc. Petroleum Geol., Mem.* **33.**

JOPLING, A.V., & McDONALD, B.C. (eds) (1975). - Glacio fluvial and Glaciolacustrine Sedimentation. *SEPM, special publication* **23.**

KEIGHIN, C.W., & FOUCH, T.D. (1981). - Depositional environments and diagenesis of some non marine upper Cretaceous Reservoir rocks, Uinta Basin, Utah. *SEPM, special publication* **31.**

KENDALL, A.C. (1984). - Evaporites. *In : Walker, R.G. ed. : Facies Models 2d ed., Geoscience Canada.*

KLEIN, G. deVries (1970). - Depositional and dispersal dynamics of intertidal sand bars. *J. sedim. Petrol.*, **40**, *p. 1095-1127.*

KLEIN, G. deVries (1980). - Sandstone Depositional Models for Exploration for fossils fuels. 2nd ed. *CEPCO. Div., Burgess Publishing Co.*

KRUEGER, W.C. (1968). - Depositional environments of sandstones as interpreted from electrical measurements. An introduction. *Trans. Gulf Coast Assoc. Geol. Soc., 18th ann. Mtg.*, **18.**

KRUIT, C., BROUWER, J., KNOX, G., SCHÖLLNBERGER, W., & VLIET, A. van (1975). -Une excursion aux cônes d'alluvions en eau profonde d'âge Tertiaire près de San Sebastian (province de Guipúzcoa, Espagne). *9th Int. Congr. Sedimentol., Nice, excursion* **23.**

KRUMBEIN, W.C. (1942). - Physical and Chemical Changes in Sediments after Deposition. *J. sediment. Petrol.*, **12,** *p. 111-117.*

KRUMBEIN, W.C., & SLOSS, L.L. (1963). -Stratigraphy and Sedimentation. 2nd ed. *W.H. Freeman, & Co., San Francisco.*

KRYNINE, P.D. (1948). - The megascopic study and field classification of sedimentary rocks. *J. Geol.*, **56,** *p. 130-166.*

KUENEN, Ph. H. (1953). - Graded bedding, with observations on Lower Paleozoic rocks of Britain. *Verhandel. koninkl. Ned. Akad. Wetenschap., Afdel. Natuurk., Sect. I,* **20,** *3, p. 1-47.*

KUENEN, Ph. H. (1953). - Significant features of graded bedding. *Bull. Amer. Assoc. Petroleum Geol.*, **37,** *p. 1044-1066.*

KUKAL, Z. (1970). - Geology of recent sediments. *Academia, Prague.*

LANDES, K.K. (1951). - Petroleum Geology. *John Wiley, & Sons, New York.*

LAPORTE, L.F. (ed) (1974). - Reefs in Time and Space. *SEPM, special publication* **18.**

LARSEN, G, & CHILINGAR, G.V. (1967). - Diagenesis in Sediments. *Elsevier, Amsterdam.*

LeBLANC, R.J., Sr., (1972). - Geometry of sandstone reservoir bodies. *Amer. Assoc. Petroleum Geol., Memoir* **18,** *p. 133-177.*

LEE, C.H. (1919). - Geology and groundwaters of the western part of San Diego County, California. *Wat.-Supply Irrig. Pap. Wash.*, **446,** *121 p.*

LEET, L.Don, JUDSON, S., & KAUFFMAN, M.E. (1978). - Physical Geology. 5th ed. *Prentice-Hall Inc., Englewood Cliffs, New Jersey.*

LEOPOLD, L.B., & WOLMAN, M.G. (1960). -River meanders. *Bull. Geol. Soc. Amer.*, **71,** *p. 769-793.*

LINK, P.K. (1982). - Basic Petroleum Geology. *OGCI Publications, Tulsa.*

LOMBARD, A. (1956). - Géologie Sédimentaire. Les séries marines. *Masson, Paris.*

LOMBARD, A. (1972). - Séries sédimentaires. Genèse - Evolution. *Masson, Paris.*

LONGMAN, M.W. (1980). - Carbonate diagenetic textures from nearsurface diagenetic environments. *Bull. Amer. Assoc. Petroleum Geol.*, **64,** *p. 461-487.*

LUCIA, F.J. (1972). - Recognition of Evaporite-Carbonate Shoreline Sedimentation. In : *"Recognition of Ancient Sedimentary Environments", edited by RIGBY, J.K., & HAMBLIN, W.K., SEPM, special publication* **16.**

MATTHEWS, R.K. (1974). - Dynamic Stratigraphy. An introduction to Sedimentation and Stratigraphy. *Prentice-Hall Inc., Englewood Cliffs, New Jersey.*

MAYER, C., & SIBBIT, A. (1980). - GLOBAL, a new Approach to Computer-processed Log Interpretation. *SPE of AIME, ann. Fall Mtg., Dallas, SPE 9341.*

McCUBBIN, D.G. (1982). - Barrier-Island and Strand-Plain Facies. *In : Scholle, P.A., & Spearing, D. (eds.) : Sandstone Depositional Environments; Amer. Assoc. Petroleum Geol., Mem.* **31.**

McGOWEN, J.H., & GARNER, L.E. (1970). -Physiographic features and stratification types of coarse-grained point bars : Modern and ancient examples. *Sedimentology,* **14,** *p. 77-111.*

McGOWEN, J.H., & GROAT, C.G. (1971). - Van Horn Sandstone, West Texas : An alluvial fan model for mineral exploration. *Bur. Econ. Geol. Univ. Tex., Rept. Invest. 72, 57 p.*

McKEE, E.D. (1957). - Flume experiments on the production of stratification and cross-stratification. *J. sediment. Petrol.*, **27,** *p. 129-134.*

McKEE, E.D. (1966). - Structures of dunes at White Sands National Monument, New Mexico (and comparison with structures of dunes from other selected areas). *Sedimentology,* **7,** *p. 1-69.*

McKEE, E.D., & WARD, W.C. (1983). - Eolian Environment. *In : Scholle, P.A. et al., (eds.) : Carbonate Depositional Environments; Amer. Assoc. Petroleum Geol., Mem.* **33.**

McKEE, E.D., & WEIR, G.W.(1953). - Terminology for stratification and cross-stratification in sedimentary rocks. *Bull. geol. Soc. Amer.*, **64,** *p. 381-390.*

MIALL, A.D. (1977). - A review of the braided-river depositional environment. *Earth Sci. Rev.*, **13,** *p. 1-62.*

MIALL, A.D. (ed.) (1978). - Fluvial Sedimentology. *Canad. Soc. Petroleum Geol., Mem.* **5.**

MIALL, A.D. (1979). - Deltas. *In : Facies Models. (ed. by Walker, R.G.). Geoscience Canada Reprint Series 1.*

MIALL, A.D. (1984). - Principles of Sedimentary Basin Analysis. *Springer, New York.*

MIDDLETON, G.V. (ed.) (1965). - Primary sedimentary structures and their hydrodynamic interpretation. *SEPM, Spec. Pub.* **12.**

MIDDLETON, G.V. (1976). - Hydraulic interpretation of sand size distributions. *J. Geology,* **84,** *p. 405-426.*

MIDDLETON, G.V., BOUMA, A.H. *et al.*, (1973). -Turbidites and deep-water sedimentation. *SEPM, Pacific Section, Short Course, Anaheim.*

MIDDLETON, G.V., & HAMPTON, M.A. (1973). -Sediment gravity flow : Mechanics of flow and deposition. *SEPM, Pacific Section, Short Course, Anaheim.*

MIDDLETON, G.V., & HAMPTON, M.A. (1976). -Subaqueous sediment transport and deposition by sediment gravity flows. In : *Marine Sediment Transport and Environmental Management (Ed. by STANLEY, D.J., & SWIFT, D.J.P.), p. 197-218. Joh Wiley, New York.*

MILLOT, (1970). - Geology of clays. *Springer, Berlin.*

MONS, F., & BABOUR, K. (1981). - Vertical Seismic Profiling : Recording, Processing, Applications.

MOORE, R.C. (1949). - Meaning of facies. *Geol. Soc. Amer., Mem.* **39**, *p. 1-34.*

MORGAN, J.P. (ed.) (1970). - Deltaic Sedimentation Modern and Ancient. *SEPM, Spec. Pub.* **15.**

MUTTI, E., & RICCI-LUCCHI, F. (1972). - Le torbiditi dell'Appennino settentrionale : introduzione all'analisi di facies. *Mem. Soc. Geol. Ital.*, **11**, *p. 161-199.*

NELSON, B.W. (1970). - Hydrography, sediment dispersal, and recent historical development of the Po river delta, Italy. *In : Deltaic Sedimentation, modern and ancient. (Ed. by Morgan, J.P.). SEPM special publ.* **15.**

NELSON, C.H., & KULM, V. (1973). - Submarine fans and channels. *SEPM, Pacific Section, Short Course, Anaheim.*

NILSEN, T.H. (1969). - Old red sedimentation in the Buelandet-Vaerlandet Devonian district, western Norway. *Sediment. Geol.*, **3**, *p. 35-57.*

NILSEN, T.H. (1982). - Alluvial Fan Deposits. *In : Scholle, P.A., & Spearing, D. (eds.) : Sandstone Depositional Environments; Amer. Assoc. Petroleum Geol., Mem.* **31.**

NORWOOD, E.M. Jr., & HOLLAND, D.S. (1974). - Lithofacies mapping. A descriptive tool for ancient delta systems of the Louisiana outer continental shelf. *Trans. Gulf Coast Assoc. Geol. Soc.*, **24.**

NURMI, R.D. (1978). - Use of well logs in evaporite sequences. *In : Marine Evaporites (Ed. by Dean, W.E, & Schreiber, B.C.). SEPM, short course* **4**, *p. 144-176.*

NURMI, R.D. (1984). - Geological evaluation of stratigraphic high resolution dipmeter data. *SPWLA, 25th Ann. Log. Symp. Trans., New Orleans.*

OOMKENS, E. (1970). - Depositional sequences ans sand distribution in the postglacial Rhône delta complex. *In : SEPM, special pub.* **15.**

OTTO, G.H. (1938). - The sedimentation unit and its use in field sampling. *J. Geol.*, **46**, *p. 569-582.*

PAYRE, X., & SERRA, O. (1979). - A case study - Turbidites recognized through dipmeter. *SPWLA, 6th Europ. Log. Symp. Trans., London, paper K.*

PERRIN, G. (1975). - Comparaison entre des structures sédimentaires à l'affleurement et les pendagemétries de sondages. *Bull. Centre Rech. Pau, SNPA,* **9**, *p. 147-181.*

PETTIJOHN, F.J. (1930). - Imbricate arrangement of pebbles in apre-Cambrian conglomerate. *Jour. Geol.*, **38**, *p. 568-573.*

PETTIJOHN, F.J. (1975). - Sedimentary Rocks. 3rd ed. *Harper, & Row, Publishers, New York.*

PETTIJOHN, F.J., & POTTER, P.E. (1964). - Atlas and Glossary of Primary Sedimentary Structures. *Springer, New York.*

PETTIJOHN, F.J., POTTER, P.E., & SIEVER, R. (1972). - Sand and Sandstone. *Springer, New York.*

PICARD, M.D., & HIGH, L.R. (1972). - Criteria for Recognizing Lacustrine Rocks. In : *"Recognition of Ancient Sedimentary Environments", edited by RIGBY, J.K., & HAMBLIN, W.K., SEPM, special publication* **16.**

PIRIE, G. (1982). - Geology and log study of tight gas sandstones : Cotton Valley Group. *Gulf Coast Assoc. Geol. Soc. Trans.*, **32**, *p. 77-88.*

PIRSON, S.J. (1977). - Geologic Well Log Analysis. 2nd ed. *Gulf Publishing Co., Houston.*

POTTER, P.E., & PETTIJOHN, F.J. (1977). -Paleocurrents and Basin Analysis. 2nd ed. *Springer, New York.*

POWERS, M.C. (1967). - Fluid release mechanisms in compacting marine mudrocks and their importance in oil exploration. *Bull. Amer. Assoc. Petroleum Geol.*, **51**, *p. 1240-1253.*

PRAY, L.C., & MURRAY, R.C. (Eds) (1965). -Dolomitization and Limestone Diagenesis. *SEPM, Special Publication* **13.**

PRESS, F., & SIEVER, R. (1982). - Earth. 3rd ed. *W.H. Freeman, & Co, San Francisco.*

RAAF, J.F.M. de (1968). - Turbidites et associations sédimentaires apparentées, I and II. *Kon. Ned. Akad. Wetensch., Amsterdam, Verh.,series B,* **71**, *p. 1-23.*

RAAF, J.F.M. de, READING, H.G., & WALKER, R.G. (1965). - Cyclic sedimentation in the Lower Westphalian of north Devon, England. *Sedimentology,* **4**, *p. 1-52.*

READING, H.G. (Ed.) (1978). - Sedimentary Environments and Facies. *Blackwell Scientific Publications, Oxford.*

REINECK, H.E. (1972). - Tidal Flats. In : *"Recognition of Ancient Sedimentary Environments", edited by RIGBY, J.K., & HAMBLIN, W.K., SEPM, special publication* **16.**

REINECK, H.E., & SINGH, I.B. (1971). - Der Golf von Gaeta/Tyrrhenisches Meer. 3. Die Gefüge von Vorstrand-und Schelfsedimenten. *Senckenbergiana maritima,* **3**, *p. 185-201.*

REINECK, H.E., & SINGH, I.B. (1975, 1980). -Depositional Sedimentary Environments. 1st and 2nd ed. *Springer, New York.*

REINSON, G.E. (1979). - Barrier-Island Systems. *In : Walker, R.G. ed. : Facies Models, 1st ed., Geoscience Canada.*

REINSON, G.E. (1984). - Barrier-Island and Associated Strand-Plain Systems. *In : Walker, R.G. ed. : Facies Models, 2d ed., Geoscience Canada.*

RIDER, M.H., & LAURIER, D. (1979). - Sedimentology using a computer treatment of well logs. *SPWLA, 6th Europ. Symp. Trans., paper J.*

RIEKE, H.H. III, & CHILINGARIAN, G.V. (1974). -Compaction of Argillaceous Sediments. *Developments in Sedimentology,* **16**, *Elsevier, Amsterdam.*

RIGBY, J.K., & RAMBLIN, W.K. (eds) (1972). -Recognition of Ancient Sedimentary Environments. *SEPM, special publication* **16.**

RUSSELL, W.L. (1951). - Principles of Petroleum Geology. *McGraw-Hill Book Co., New York.*

RUST, B.R. (1972). - Structure and process in a braided river. *Sedimentology,* **18,** *p. 221-246.*

RUST, B.R. (1972). - Pebble orientation in fluvial sediments. *J. sediment. Petrol.,* **42,** *p. 384-388.*

SABINS, F.F. (1972). - Comparison of Bisti and Horseshoe Canyon Stratigraphic Traps, San Juan Basin, New Mexico. *In Stratigraphic Oil and Gas Fields - Classification, Exploration Methods, and Case Histories, Amer. Assoc. Petroleum Geol., Memoir* **16,** *p. 610-622.*

SALLEE, J.E., & WOOD, B.R. (1982). - Use of the Dipmeter to Improve Formation Evaluation in Thin-Bedded Sand/Shale Sequences. *Offshore South East Asia 82 Conference, 9-12 Feb., Singapore.*

SCHEIDEGGER, A.E., & POTTER, P.E. (1971). -Downcurrent decline of grain size and thickness of single turbidite beds : a semi-quantitative analysis. *Sedimentology,* **17,** *p. 41-49.*

Schlumberger Ltd (1970). - Fundamentals of Dipmeter Interpretation.

Schlumberger Ltd (1972). - Log Interpretation. Volume I - Principles.

Schlumberger Ltd (1974). - Log Interpretation. Volume II - Applications.

Services Techniques Schlumberger (1974). -Well Evaluation Conference. North Sea.

Schlumberger (1979). - Well Evaluation Conference. Algeria.

Schlumberger Ltd (1981). - Dipmeter Interpretation. Volume 1 - Fundamentals.

Schlumberger Middle East S.A. (1981). - Well Evaluation Conference. United Arab Emirates/ Qatar.

S.P.E. Schlumberger (1982). - Well Evaluation Developments. Continental Europe.

Schlumberger Technical Services, Inc. (1982). -Essentials of Natural Gamma ray Spectrometry Interpretation.

Schlumberger (1983). - Well Evaluation Conference. Afrique de l'Ouest.

Schlumberger Technical Services, Inc. (1983). -Well Evaluation Conference. India.

Schlumberger Middle East S.A. (1984). - Well Evaluation Conference. Egypt.

Schlumberger Offshore Services (1984). - Evaluacion de Formaciones en Mexico.

SCHMALZ, R.F. (1969). Deep-water evaporite deposition : a genetic model. *Bull. Amer. Assoc. Petroleum Geol.,* **53,** *p. 798-823.*

SCHOLLE, P.A., & SPEARING, D. (Ed.) (1982). -Sandstone Depositional Environments. *Amer. Assoc. Petroleum Geol., Mem.* **31.**

SCHOLLE, P.A., ARTHUR, M.A., & EKDALE, A.A. (1983). - Pelagic Environment. *In : Scholle, P.A. et al.,* (eds.) : Carbonate Depositional Environments; Amer. Assoc. Petroleum Geol., Mem. **33.**

SCHWARTZ, M.L. (ed.) (1973). - Barrier islands. *Stroudsburg, PA., Dowden, Hutchinson and Ross, 451 p.*

SCHWARZACHER, W. (1953). - Cross-bedding and grain size in the Lower Cretaceous sands of East Anglia. *Geol. Mag.,* **90,** *p. 324-330.*

SCOTT, K.M. (1966). - Sedimentology and dispersal pattern of a Cretaceous flysch sequence, Patagonian Andes, southern Chile. *Bull. Amer. Assoc. Petroleum Geol.,* **50,** *p. 74-107.*

SCRUTON, P.C. (1956). - Oceanography of Mississippi delta sedimentary environments. *Bull. Amer. Assoc. Petroleum Geol.,* **40** *p. 2864-2952.*

SCRUTON, P.C. (1960). - Delta building and the deltaic sequence. *In : SHEPARD et al.,* (ed.), Recent sediments, northwest Gulfof Mexico : Tulsa, Okla., Amer. Assoc. Petroleum Geol.

SELLEY, R.C. (1966). - Petrography of the Torridonian rocks of Raasay and Scalpay, Inverness-shire. *Proc. geol. Ass. London,* **77,** *p. 293-314.*

SELLEY, R.C. (1970). - Studies of sequence in sediments using a simple mathematical device. *J. geol. Soc. London, Quart. Jour.,* **125,** *p. 557-581.*

SELLEY, R.C. (1970, 1978). - Ancient Sedimentary Environments. 1st and 2nd ed. *Chapman, & Hall, London.*

SELLEY, R.C. (1972). - Diagnosis of marine and non-marine environments from the Cambro-Ordovician sandstones of Jordan. *J. geol. Soc. London,* **128,** *p. 135-160.*

SELLEY, R.C. (1976). - An Introduction to Sedimentology. *Academic Press, London.*

SELLEY, R.C. (1978). - Concepts and methods of subsurface facies analysis. *Amer. Assoc. Petroleum Geol., Continuing Education Course Note Series* **9.**

SELLEY, R.C. (1979). - Dipmeter and log motifs in North Sea submarine-fan sands. *Bull. Amer. Assoc. Petroleum Geol.,* **63,** *6, p. 905-917.*

SELLWOOD, B.W. (1978). - Shallow-water Carbonate Environments. *In : Sedimentary Environments and Facies. (Ed. by Reading, H.G.) Blackwell Scientific Publications, Oxford.*

Society of Economic Paleontologists and Mineralogists (1975). - Depositional environments as interpreted from primary sedimentary structures and stratification sequences. *SEPM short course* **2.**

SERRA, O. (1972). - Diagraphies, & Stratigraphie. In : *Mém. B.R.G.M.,* **77,** *p. 775-832.*

SERRA, O. (1973). - Interprétation Géologique des diagraphies en Séries Carbonatées. *Bull. Centre Rech. Pau - SNPA,* **7,** *1, p. 265-284.*

SERRA, O. (1974). - Interprétation géologique des Séries deltaïques à partir des diagraphies différées. *Rev. A.F.T.P.,* **227,** *Oct., p. 9-17.*

SERRA, O. (1977). - Méthode rapide d'analyse faciologique par diagraphies différées. *SPWLA, 5th Europ. Symp. Trans., Paris, paper 9.*

SERRA, O. (1980). - Aspects diagraphiques des Evaporites. *Bull. Centre Rech. Pau - SNPA,* **4,** *1, p. 411-431.*

SERRA, O. (1984). - Fundamentals of Well-Log Interpretation. Volume 1 : The Acquisition of Logging Data. *Developments in Petroleum Science*, **15A**, *440 p., Elsevier, Amsterdam.*

SERRA, O., & ABBOTT, H. (1980). - The Contribution of Logging data to Sedimentology and Stratigraphy. *55th Ann. Fall Techn. conf. SPE of AIME, paper SPE 9270, and in SPE J., Feb. 1982.*

SERRA, O., BALDWIN, J., & QUIREIN, J. (1980). - Theory, Interpretation and practical Application of Natural Gamma ray Spectroscopy. *SPWLA, 21st Ann. Log. Symp. Trans., paper Q.*

SERRA, O., & SULPICE, L. (1975). - Sedimentological Analysis of shale-sandseries from well logs. *SPWLA, 16th Ann. Log. Symp. Trans., paper W.*

SERRA, O., & SULPICE, L. (1975). - Apports des diagraphies différées aux études sédimentologiques des séries argilo-sableuses traversées en sondage. *9th Cong. Intern. Sédiment., Nice, thème 3, p. 86-96.*

SHARP, R.P. (1960). - Glaciers. *The Condon Lectures, Oregon State system of education, Eugene, Oregon.*

SHELTON, J.S. (1966). - Geology Illustrated. *Freeman, & Co., New York.*

SHELTON, J.W. (1967). - Stratigraphic models and general criteria for recognition of alluvial, barrier-bar, and turbidity current sand deposits. *Bull. Amer. Assoc. Petroleum Geol.*, **5**, *12, p. 2441-2461.*

SHINN, E.A. (1983). - Tidal Flat Environment. *In : Scholle, P.A. et al.,* (eds.) : Carbonate Depositional Environments; Amer. Assoc. Petroleum Geol., Mem. **33.**

SHIRLEY, M.L. (ed.) (1966). - Deltas in their geologic framework. *Houston Geological Society.*

SHROCK, R.R. (1948). - Sequence in Layered Rocks. *McGraw-Hill Book Co., Inc., New York.*

SPEARING, D.R. (1971). - Summary sheets of Sedimentary Deposits. *Published by Geol. Soc. America.*

SPEARING, D.R. (1976). - Upper Cretaceous Shannon Sandstone : an offshore, shallow-marine sand body. *Wyoming Geol. Ass. Guidebook, 28th Field Conf., p. 65-72.*

STEEL, R.J., MAEHLE, S., NILSEN, H., ROE, S.L., & SPINNANGR, A. (1977). - Coarsening upward cycles in the alluvium of Hornelen Basin (Devonian), Norway. Sedimentary response to tectonic events. *Bull. Geol. Soc. Amer.*, **88**, *p. 1124-1134.*

STEINMETZ, R. (1967). - Depositional history, primary sedimentary structures, cross bed dips, and grain size of an Arkansas river point bar at Wekiwa, Oklahoma. *Rep. F67-G-3 (In : REINECK, & SINGH, 1975).*

STOKES, W.L. (1968). - Multiple parallel truncation bedding planes - a feature of wind-deposited sandstone formations. *J. sediment. Petrol.*, **38**, *p. 510-516.*

STOW, D.A.V. (1985). - Deep-sea clastics : where are we and where are we going ? *In : Sedimentology. Recent developments and Applied Aspects. Ed by P.J. Brenchley & B.P.J. Williams. Blackwell Scientific Publications, Oxford.*

TAYLOR, J.C.M., & COLTER, V.S. (1975). -Zechstein of the English Sector of the southern North Sea Basin. *In : Petroleum and the Continental Shelf of North-West Europe. Vol. 1. Geology. (Ed. by A.W. Woodland). Applied Science Publishers, London.*

THEYS, P., LUTHI, S., & SERRA, O. (1983). - Use of dipmeter in Carbonates for detailed sedimentology and reservoir engineering studies.

VATAN, A. (1954). - Pétrographie sédimentaire. *Ed. Technip, Paris.*

TIXIER, M.P., & ALGER, R.P. (1967). - Log Evaluation of Non-Metallic Mineral Deposits. *SPWLA, 8th Ann. Log. Symp. Trans., paper R.*

VINCENT, P., GARTNER, J., & ATTALI, G. (1979). - GEODIP - An approach to detailed dip determination using correlation by pattern recognition. *J. Petroleum Technol., Feb. 1979, p. 234-240.*

VISHER, G.S. (1965). - Use of vertical profile in environmental reconstruction. *Bull. Amer. Assoc. Petroleum Geol.*, **49**, *p. 41-61.*

VISHER, G.S. (1969). - How to distinguish barrier bar and channel sands. *World Oil, May.*

VISHER, G.S. (1972). - Physical Characteristics of Fluvial Deposits. In : *"Recognition of Ancient Sedimentary Environments", edited by RIGBY, J.K., & HAMBLIN, W.K., SEPM, special publication* **16.**

WALKER, R.G. (1967). - Turbidite sedimentary structures and their relationship to proximal and distal depositional environments. *J. sedim. Petrol.*, **37**, *p. 25-43.*

WALKER, R.G. (1975). - Generalized facies models for resedimented conglomerates of turbidite association. *Bull. geol. Soc. Amer.*, **86**, *p. 737-748.*

WALKER, R.G. (1976). - Facies Models. Turbidites and associated coarse clastic deposits. *Geoscience Canada*, **3**, *p. 25-36.*

WALKER, R.G. (Ed.) (1979, 1984). - Facies Models. 1st and 2nd ed. *Geoscience Canada, reprint series 1, published by Geol. Assoc. Canada.*

WALKER, R.G., & MUTTI, E. (1973). - Turbidite facies and facies association. *SEPM, Pacific Section, Short Course, Anaheim.*

WALKER, T.R., & HARMS, J.C. (1972). - Eolian origin of Flagstone beds, Lyons sandstone (Permian), type area, Boulder County, Colorado. *Mountain Geologist*, **9**, *p. 279-288.*

WEBER, K.L. (1971). - Sedimentological aspects of oil fields in the Niger delta. *Amer. Assoc. Petroleum Geol. Bull.*, **49**, *6.*

WEIMER, R.J. (1976). - Deltaic and shallow Marine sandstones. Sedimentation, tectonics and Petroleum occurrences. *Amer. Assoc. Petroleum Geol., Continuing Education Course Note Series* **2.**

WIDDICOMBE, R.E., & NOON, P. (1984). -Multiwell FACIOLOG evaluation, Hartzog Draw Field, Powder River Basin, Wyoming. *SPWLA, 25th Ann. Log. Symp. Trans., New Orleans.*

WILLIAMS, P.F., & RUST, B.R. (1969). - The sedimentology of a braided river. *J. sediment. Petrol.*, **39**, *2, p. 649-679.*

WILSON, J.L. (1975). - Carbonate Facies in Geologic History. *Springer, New York.*

WILSON, J.L., & JORDAN, C. (1983). - Middle Shelf Environment. *In : Scholle, P.A. et al.,* (eds.) : Carbonate Depositional Environments; Amer. Assoc. Petroleum Geol., Mem. **33.**

WRIGHT, L.D., & COLEMAN, J.M. (1972). - River delta morphology, wave climate, and the role of the subaqueous profile. *Science*, **176**, *p. 284-288.*

WRIGHT, L.D., & COLEMAN, J.M. (1973). -Variations in morphology of major river deltas as functions of ocean wave and river discharge regimes. *Bull. Amer. Assoc. Petroleum Geol.*, **57**, *p. 370-398.*

WRIGHT, L.D., & COLEMAN, J.M. (1974). -Mississippi River mouth processes : effluent dynamics and morphologic development. *J. Geol.*, **82**, *p. 751-778.*

YOUNG, F.G., & REINSON, G.E. (1975). - Sedimentology of Blood Reserve and adjacent formations (Upper Cretaceous), St. Mary River, Southern Alberta. *In : Shawa, M.S., ed., Guidebook to selected sedimentary environments in south western Alberta, Canada. Can. Soc. Petroleum Geol., Field Conference.*

ZOBELL, C.E. (1942). - Changes produced by Microorganisms in Sediments after Deposition. *J. sediment. Petrol.*, **12**, *p. 127-136.*

Photocomposition et impression
IMPRIMERIE LOUIS-JEAN
BP 87 — 05002 GAP
Tél. : 92.51.35.23
Dépôt légal : 502 — Juillet 1989
Imprimé en France